A FUNDAMENTAL EVALUATION OF THE ATMOSPHERIC PRE-LEACHING SECTION OF THE NICKEL-COPPER MATTE TREATMENT PROCESS

by

RODRICK MULENGA LAMYA

Dissertation presented for the Degree

of

DOCTOR OF PHILOSOPHY

(Extractive Metallurgical Engineering)

in the Department of Process Engineering at the University of Stellenbosch, South Africa

Promoter

Prof. L. Lorenzen

STELLENBOSCH

March 2007

DECLARATION

I the undersigned, hereby declare that the work contained in this dissertation is my own original work and that I have not previously in its entirety or in part submitted it at any university for a degree.

Signature: .....

Date: .....

SYNOPSIS

Nickel-Copper sulphide ores are the most important Platinum Group Metal bearing ores. The South African deposits are exceptionally rich in the platinum group metals (PGMs) and production of the PGMs is the primary purpose of treating these ores. The methods used in the recovery of the PGMs from the nickel-copper ores generally consists of ore concentration by physical techniques, pyrometallurgical concentration and hydrometallurgical extraction of the base metals followed by the PGMs. Pyrometallurgical concentration produces Ni-Cu matte, which is treated by hydrometallurgical processes to recover the nickel, copper, cobalt and the precious metals.

In this study, the leaching behaviour of a Ni–Cu matte in $CuSO_4$–H_2SO_4 solution during the repulping (pre-leach) stage at Impala Platinum Refineries was studied. The repulping stage is basically a non–oxidative atmospheric leach stage, in which nickel, iron and cobalt are partially dissolved, while the copper is precipitated. To understand the nature of the leaching process during this stage of the base metal refining operation, the effects of variations in the key process variables such as temperature, stirring rate, particle size, pulp density, residence time, initial copper and acid concentrations were investigated. The pre-leached matte was then pressure leached to ascertain the effect of process conditions in the pre-leach stage on the subsequent pressure leach stage.

It was found that the leaching mechanism entails dissolution of metal alloys out of sulphide minerals with transformation of Ni_3S_2 to NiS. Aqueous copper precipitates as metallic copper and as chalcocite. The matte is leached by both acid and the cementation process, especially in the early stage when the Cu^{2+} ions are present. Galvanic interaction of the sulphide minerals and/or the Ni alloy also enhances the leaching process. The leaching kinetics of Ni was characterized with the shrinking core model and was found to be controlled by diffusion through surface layer. An activation energy of 31 kJ/mol was obtained, which also suggested a diffusion controlled leaching reaction. Atmospheric leaching tests indicated that Ni

extraction increased slightly in the temperature range 50 – 60 ^{o}C, however no significant increase was observed from 60 to 80 ^{o}C, probably because the leaching process was found to be diffusion controlled. The slight increase in nickel dissolution at higher temperatures (>60 ^{o}C) may be attributed to the transformation of Ni_3S_2 to NiS, which is easier to leach. Co extraction appeared to be insensitive to temperature changes, while Fe extraction was low at 50 ^{o}C but increased significantly at 60 – 80 ^{o}C. The Ni extraction increased gradually with increase in the stirring rate from 145 to 400 rpm while Co and Fe extractions were insensitive at 145 and 205 rpm, but increased substantially at 400 rpm. This was probably due to increased mass transfer rate and transformation of Ni_3S_2 to NiS. With pulp density, Ni and Co extractions appeared to be insensitive to changes in the pulp density as only a slight increase in extractions was observed when the density was reduced from 1.7 kg/L to 1.6 kg/L. Similar iron extractions were achieved at 1.7 and 1.75 kg/L but increased significantly at 1.6 kg/L. It was found that Ni and Co extractions were not significantly affected by changes in the particle size, probably because metal alloys were liberated and hence exposed to the leaching solution. Iron extraction could not be determined accurately because of iron precipitation at pH above 3. Generally the leaching of metals did not depend on the initial copper concentration in the investigated range of 25 - 48 g/L Cu. It was also observed that initial acid concentration did not have an effect on Ni extraction, probably due to the fact that most of the nickel was leached by the process of cementation. However, Co and Fe extractions increased when the acid increased from 90 g/L to 110 g/L, but no further increase was noted at 125 g/L. A residence time of 5 hours was found to be adequate as there was no significant increase in metal extractions when the residence time was increased beyond 5 hours. As much as 20% Ni, 40% Co and 80% Fe can be extracted from the Ni-Cu matte during the repulping stage of the leaching process studied, provided the investigated conditions prevail.

Generally the rate of Cu cementation increased with increasing temperature and pulp density, but decreased with an increase in particle size, acid and copper

concentrations. The rate of stirring did not affected Cu cementation. It was found that aqueous copper precipitated from the solution within 90 minutes when the temperature was raised to 80 ^{o}C. However, under the present pre-leach temperature of about 60 ^{o}C complete Cu cementation can only be achieved after about 5 hours. The cementation reaction was found to follow a mixed control mechanism, with two distinct activation energies namely 18.2 kJ/mol at 70 – 80 ^{o}C and 74.6 kJ/mol at 50 – 70 ^{o}C. This suggested that the rate of cementation reaction is probably controlled by a boundary layer diffusion mechanism at higher temperatures. At low temperatures the rate is probably controlled by a surface reaction mechanism.

The pressure leaching experiments, which were aimed at investigating the response of pre-leached matte to the subsequent pressure leaching process, showed that Ni extractions were similar for the investigated pre-leach temperature of 50 – 80 ^{o}C and stirring rate of 145 – 400 rpm. For the pre-leach stage conditions of 60 – 80 ^{o}C and 205 – 400 rpm Ni_3S_2 was transformed into NiS, which is easier to leach in the pressure leaching stage. However, because of the aggressive conditions prevailing in the pressure leaching stage, all the nickel minerals were leached at about the same rate. In the case of pulp density, Ni extraction was comparable for all the investigated pulp densities (1.6 – 1.75 kg/L). This was probably due to the fact that Ni_3S_2 transformed to NiS in the pre-leach stage. It was found that Ni extraction increased with increasing residence time for the investigated time of 1 hour to 9 hours, probably due to the changes in the mineral phases of the matte as indicated above. The copper minerals (Cu_2S and $Cu_{1.96}S$) transformed into Cu_2S and $Cu_{1.8}S$ with aqueous copper being precipitated, and were not leached under the applied conditions. All the cobalt and iron dissolved in the pressure leaching stage.

A semi-empirical kinetic model was developed for the pre-leaching stage. A comparison of the model predictions and the experimental data for the dissolved species during the batch leaching process showed that the model can satisfactorily fit the trends in the leaching of the metals.

OPSOMMING

Nikkel-koper-sulfiederts is die belangrikste platinum-groep metaaldraende erts. Die Suid-Afrikaanse afsetting in die platinum-groep metale (PGM's) is buitengewoon ryk en die produksie van die PGM's is die hoofdoel vir die behandeling van hierdie erts. Die metodes wat gebruik word om die PGM's van die nikkel-koper-erts te herwin, bestaan hoofsaaklik uit ertskonsentrasie deur fisiese tegnieke, pirometallurgiese konsentrasie en hidrometallurgiese ekstraksie van die basismetale, gevolg deur die PGM's. Pirometallurgiese konsentrasie produseer Ni-Cu swaelmetaal, wat deur hidrometallurgiese prosesse behandel word om die nikkel, koper, kobalt en edelmetale te herwin.

In hierdie studie is die uitlogingsgedrag van 'n Ni–Cu swaelmetaal in 'n $CuSO_4$–H_2SO_4-oplossing gedurende die herverpulping- (vooruitlogings-)fase by Impala Platinum Refineries ondersoek. Die herverpulpingsfase is basies 'n nie-oksidatiewe atmosferiese uitlogingsfase, waartydens nikkel, yster en kobalt gedeeltelik opgelos word terwyl die koper gepresipiteer word. Ten einde die aard van die uitlogingsproses gedurende hierdie fase van die basismetaal-affineringsproses te verstaan, is die uitwerking van die variasies in die hoofprosesveranderlikes, soos temperatuur, roertempo, partikelgrootte, pulpdensiteit, verblyftyd en aanvanklike koper- en suurkonsentrasies ondersoek. Drukuitloging is daarna op die vooruitgeloogde swaelmetaal toegepas om die uitwerking van die proses se toestande in die vooruitlogingsfase op die daaropvolgende drukuitlogingsfase te bepaal.

Daar is gevind dat die uitlogingsmeganisme oplossing van metaallegerings uit sulfiedminerale met transformasie van Ni_3S_2 na NiS behels. Waterkoper presipiteer as metaalkoper en as chalkosiet. Die swaelmetaal word deur sowel die suur as die sementasieproses uitgeloog, veral in die vroeë fase wanneer die Cu^{2+}-ione teenwoordig is. Galvaniese interaksie van die sulfiedminerale en/of die Ni-legering versterk ook die uitlogingsproses. Die uitlogingskinetika van Ni is deur die krimpende kernmodel gekenmerk en daar is gevind dat dit deur diffusie deur die

bolaag beheer is. 'n Aktiveringsenergie van 31 kJ/mol is verkry, wat ook 'n diffusiebeheerde uitlogingsreaksie aan die hand doen. Atmosferiese uitlogingstoetse het aangedui dat Ni-ekstraksie effens in 'n temperatuur van 50 °C tot 60 °C toegeneem het. Geen beduidende toename is egter tussen 60 °C en 80 °C waargeneem nie, waarskynlik omdat daar gevind is dat die uitlogingsproses diffusiebeheerd is. Die effense toename in nikkel-dissolusie teen hoër temperature (>60 °C) kan aan die transformasie van Ni_3S_2 na NiS toegeskryf word, wat makliker is om uit te loog. Co-ekstrasie blyk nie sensitief vir temperatuurveranderinge te wees nie, terwyl Fe-ekstraksie laag was teen 50 °C maar aansienlik teen 60 °C tot 80 °C verhoog het. Die Ni-ekstraksie het geleidelik verhoog met toename in die roertempo van 145 rpm tot 400 rpm, terwyl Co en Fe nie teen 145 rpm en 205 rpm sensitief was nie, maar wesenlik teen 400 rpm verhoog het. Dít is heel moontlik weens die verhoogde tempo van massa-oordrag en transformasie van Ni_3S_2 na NiS. Wat pulpdensiteit betref, blyk Ni- en Co-ekstraksies nie sensitief vir veranderinge in die pulpdensiteit te wees nie, aangesien slegs 'n effense verhoging van ekstraksies waargeneem is toe die densiteit van 1.7 kg/L tot 1.6 kg/L verminder is. Soortgelyke yster-ekstraksies is teen 1.7 kg/L en 1.75 kg/L bereik, maar het beduidend teen 1.6 kg/L vermeerder. Daar is gevind dat Ni- en Co-ekstraksies nie wesenlik deur veranderinge in die partikelgrootte beïnvloed is nie, heel moontlik omdat metaallegerings vrygestel is en dus aan die uitlogingsoplossing blootgestel is. Yster-ekstraksie kon weens yster-presipitering by pH bo 3 nie akkuraat bepaal word nie. Oor die algemeen het die uitloging van metale nie afgehang van die aanvanklike koper-konsentrasie in die reeks van 25 g/L tot 48 g/L Cu wat ondersoek is nie. Daar is ook gemerk dat aanvanklike suurkonsentrasie geen uitwerking op Ni-ekstraksie gehad het nie, heel moontlik weens die feit dat die meeste van die nikkel deur die sementasieproses uitgeloog is. Co- en Fe-ekstraksies het egter vermeerder toe die suur van 90 g/L tot 110 g/L toegeneem het, maar geen verdere toename is teen 125 g/L waargeneem nie. 'n Verblyftyd van vyf uur blyk genoegsaam te wees, aangesien daar geen beduidende toename van metaalekstraksies was toe die verblyftyd langer as vyf uur was nie. Soveel as 20% Ni, 40% Co en 80% Fe kan van die Ni-Cu-swaelmetaal tydens die

herverpulpingsfase van die uitlogingsproses wat ondersoek is, uitgeloog word, mits die toestande wat ondersoek is, teenwoordig is.

Oor die algemeen het die tempo van Cu-sementasie met ’n toename in temperatuur en pulpdensiteit toegeneem, maar met ’n toename in partikelgrootte en koper- en suurkonsentrasies afgeneem. Die roertempo het nie Cu-sementasie beïnvloed nie. Daar is gevind dat waterkoper binne 90 minute uit die oplossing gepresipiteer het toe die temperatuur tot 80 ^{o}C verhoog is. Onder die huidige vooruitlogingstemperatuur van ongeveer 60 ^{o}C kan volledige Cu-sementasie egter slegs ná ongeveer vyf uur verkry word. Daar is gevind dat die sementasiereaksie op ’n gemengde kontrolemeganisme volg, met twee duidelike aktiveringsenergieë, naamlik 18.2 kJ/mol teen 70 ^{o}C tot 80 ^{o}C en 74.6 kJ/mol teen 50 ^{o}C tot 70 ^{o}C. Dit suggereer dat die tempo van die sementasiereaksie heel moontlik deur ’n grenslaag-diffusiemeganisme teen hoër temperature beheer word. Teen lae temperature word die tempo moontlik deur ’n oppervlak-reaksiemeganisme beheer.

Die drukuitlogingseksperimente, wat daarop gemik was om die reaksie van vooruitgeloogde swaelmetaal op die daaropvolgende drukuitlogingsproses te ondersoek, het aangetoon dat Ni-ekstraksies soortgelyk was by die vooruitlogingstemperatuur van 50 ^{o}C tot 80 ^{o}C wat ondersoek is en ’n roertempo van 145 rpm tot 400 rpm. By die toestande in die vooruitlogingsfase van 60 ^{o}C tot 80 ^{o}C en 205 rpm tot 400 rpm is Ni_3S_2 na NiS getransformeer, wat makliker is om in die drukuitlogingsfase uit te loog. Weens die aggressiewe toestande wat tydens die drukuitlogingsfase heers, is al die nikkelminerale egter teen ongeveer dieselfde tempo uitgeloog. Ni-ekstraksies was vergelykbaar vir al die pulpdensiteite wat ondersoek is (1.6 kg/L tot 1.75 kg/L). Dit is heel moontlik toe te skryf aan die feit dat Ni_3S_2 in die vooruitlogingsfase na NiS getransformeer het. Daar is gevind dat Ni-ekstraksie met verhoogde verblyftyd in die ondersoektyd van een tot nege uur vermeerder het, moontlik weens die veranderinge in die mineraalfases van die swaelmetaal soos hier bo aangedui. Die koperminerale (Cu_2S en $Cu_{1.96}S$) het na Cu_2S en $Cu_{1.8}S$ getransformeer, met waterkoper wat gepresipiteer het, en is nie

onder die toegepaste toestande uitgeloog nie. Al die kobalt en yster het in die drukuitlogingsfase opgelos.

'n Semi-empiriese kinetiese model is vir die vooruitlogingsfase ontwikkel. 'n Vergelyking van die model-voorspellings en die eksperimentele data vir die opgeloste spesies tydens die lot-uitlogingsproses het aangetoon dat die model bevredigend by die neigings in die uitloging van die metale kan inpas.

DEDICATION

To my dear wife Kezia, my sons Mulenga, Mulasha and Mwewa for your tolerance, patience and understanding.

ACKNOWLEDGEMENTS

I wish to thank my supervisor Professor Leon Lorenzen for his invaluable support, guidance and encouragement throughout the course of this study. The financial support I received from him is also greatly appreciated. I would like to thank Dr Johan Rademan of Crusader Systems (Pty) Ltd for the helpful discussion and advice on the aim of this study.

In the Department of Process Engineering at the University of Stellenbosch, I wish to thank all the staff for providing a friendly environment; and for their cooperation and support while I was in Stellenbosch.

This work was also performed at Impala Base Metals Refinery (BMR). I would therefore like to acknowledge and thank the personnel at the BMR for providing me with the Laboratory, material and the equipment, in particular Mr T. Spandiel (BMR Manager), Ms R. Ramkumar, Mr V. Nkomo, Mr D. Hall and Mr H. Ramagwede. I am thankful to Mr Z. Mthethwa, Mr E. Mabunda, Mr P. Montso and Mrs S. Phochana for the helpful advice on the Impala BMR process. The assistance I received from the staff of the Base Metals Laboratory is also acknowledged, in particular the help rendered by Mr G. Langenhoven and Mr N. Halwindi is sincerely appreciated. Special thanks to the Laboratory Manager of School of Chemical and Metallurgical Engineering at the University of Witwatersrand for allowing me to use the pressure reactor.

I wish to gratefully thank Impala Platinum Refineries for providing the material and financial support. The support and encouragement I got from Mr M. Fox (Technical Manager) and Mr E. Orellana (R&D Manager) is sincerely acknowledged. Many thanks to Mrs E. Lategan and Mrs W. Harvey of the Impala Technical Library for their assistance in providing the information on time.

Finally, Thanks to my family and all my friends in Johannesburg and Cape Town for their support and encouragement.

LIST OF ABBREVIATIONS

ASTM	American Society for Testing Materials
BET	Brunauer-Emmett-Teller
BMs	Base Metals
BMR	Base Metals Refinery
BML	Base Metals Laboratories
D2EHPA	Di (2-ethyl hexyl) phosphoric acid
EF	Electric Furnace
EDX	Energy-Dispersive X-ray
EPL	Eastern Platinum Limited
FSF	Flash Smelting Furnace
ICP	Inductively Coupled Plasma
IRS	Impala Refining Services
LG-1	Lower Group 1
LG-2	Lower Group 2
LG-3	Lower Group 3
LCD	Liquid Crystal Display
MG-1	Middle Group 1
MG-2	Middle Group 2
MG-3	Middle Group 3
MEC	Magnetic Concentrates
NCM	Non-Magnetic Concentrates
PGE	Platinum-Group Element
PGM	Platinum Group Metals
PMR	Precious Metals Refinery
PLC	Programmable Logic Controller
RBMR	Rustenburg Base Metals Refiners
SCM	Shrinking Core Model
SEM	Scanning Electron Microscope
UG-2	Upper Group 2

WPL	Western Platinum Limited
WPR	Western Platinum Refinery
XRD	X-ray diffraction

LIST OF SYMBOLS

A	Surface area of matte particles (cm^2)
A	frequency factor
A_s	the surface area factor that accounts for the effect of variation in the effective surface area of the matte particles
C_M	Initial concentration of M in the initial volume of leaching solution (g/L)
$C_{M,j}$	the concentration of M in sample j (g/L)
c_m	the wt % of M in the solids added into the reactor
$[Cu^{2+}]_t$	copper concentration at time t (g/L)
$[Cu^{2+}]_0$	initial copper concentration at t = 0 (g/L)
C_A	concentrations of reactant species A in solution
C_B	concentrations of reactant species B in solution
E_a	activation energy of a reaction (kJ/mol)
f_{O2}	oxygen fugacity
i	the i^{th} reaction
j	the j^{th} sample taken during leaching
J	the total number of samples taken
K	reaction rate constant
M	the exact mass of the solids added into the reactor (g)
M	molality of species used to draw Potential – pH diagrams
N_A	moles of species A (mol)
n_A	stoichiometric coefficient of species A in the reaction rate expression

r_A	reaction rate of species A based on the unit volume of solution (mol/L.min^{-1})
R	gas constant
t	reaction time (S, min or hr)
T	temperature (^{o} C)
V	the volume of the solution (cm^3 or L)
V_j	the volume of the solution sample j (L)
Vr	reaction volume (L)
X_{Mi}	the percent extraction of M at the time t_i
X	is the fraction reacted during the leaching process
Z	the term that accounts for the shrinking core leaching effect

Greek symbols

α	kinetic constant used in the Shrinking Core Model

TABLE OF CONTENTS

LIST OF FIGURES

LIST OF TABLES

CHAPTER 1

1.0 INTRODUCTION

The nickel-copper sulphide ores of South Africa are among the most important Platinum Group Metal (PGM) bearing ores, and contain the world's largest reserves of platinum. The nickel-copper sulphide ores are also found in other regions such as Canada, Russia, Austraria, Zimbabwe, Botswana and the Pacific Ocean belt, to mention a few. The South African deposits are exceptionally rich in the platinum group metals and production of the platinum group metals is the primary purpose of treating the nickel-copper sulphide ores, which also have some cobalt. The methods used in the recovery of the Platinum Group Metals (PGMs) from the nickel-copper ores generally consist of three main unit processes, namely ore concentration by physical techniques (e.g. flotation and gravity), pyrometallurgical concentration and hydrometallurgical extraction of base metals followed by the PGMs. Pyrometallurgical concentration entails smelting of the nickel-copper concentrates obtained from the flotation/gravity concentration step. This is a thermal treatment of the concentrates to melt them and bring about physical and chemical changes that enable recovery of base metals, PGMs and other valuable metals in crude form. It allows separation of valuable metals from the bulk of unwanted constituents. In the smelting process, the general practice is to eliminate the unwanted material (gangue) and substantially all of the iron sulphide and to concentrate the metal values into a high-grade converter matte. Matte refers to the intermediate product that is produced from the smelting process. It is the product that contains metal values, which is further processed to recover the contained metals. The matte is further treated by hydrometallurgical processes to produce marketable metal values such as nickel, copper, cobalt and precious metals, in the case of PGM bearing nickel-copper mattes. The principal objective of hydrometallurgical extractive

processes is to leach the desired elements selectively into an aqueous phase so as to separate them from the bulk of the unwanted material.

The first step in the hydrometallurgical processing of the Ni-Cu matte is the leaching stage in which the metal values are first dissolved in a solution and later recovered as final products in the subsequent stages. Conventionally, two process routes are employed for leaching the Ni-Cu mattes, especially those containing platinum group metals. The first process involves both atmospheric and pressure leaching in acidic copper–nickel sulphate solution, with oxygen being the oxidizing agent. In this process the matte is first leached under atmospheric conditions followed by a pressure leach step, and in both steps O_2/air is sparged into the leaching vessels. During atmospheric leaching substantial quantities of nickel and cobalt are dissolved while copper and iron are precipitated from the solution, and any PGM present remains in the solids. The precipitated copper and any unleached nickel and cobalt are dissolved in the subsequent pressure leach step or, in some cases, fed to a smelter. The other leaching process route employs a pre-leach step, which is essentially a matte repulping step, prior to a pressure leach step. The repulping process may be considered to be basically a non–oxidative atmospheric leach stage since leaching of the matte starts immediately it comes into contact with the $CuSO_4$ –H_2SO_4 repulping solution. During the pre-leach stage nickel, iron and cobalt are partially dissolved, while the copper is precipitated. In both of these Ni-Cu matte process route alternatives, nickel and cobalt can be recovered from the solution as metal by electrowinning or hydrogen reduction, or they may be recovered as sulphate crystals. Copper can be recovered as metal by electrowinning from the sulphate solution or by electrorefining if the precipitated copper was treated by the smelting process.

The pre-leach stage in the second process route alternative, described above, is the subject of this study. The study investigates the leaching behaviour of a Ni–Cu matte in H_2SO_4-$CuSO_4$ solution during the pre-leaching (repulping) stage at

Impala Platinum Refinery. Impala Platinum Ltd is currently the second largest producer of platinum in the world. It operates two separate refineries at Springs east of Jonnesburg, South Africa: the Base Metals Refinery and the Precious Metals Refinery. The pre-leaching stage is an important stage of the process as some leaching of the matte takes place at this stage.

The Base Metal Refinery employs the Sherrit Gordon acid pressure leaching technology, which involves successive stages of acid-oxidation leaching. The base metals are first leached out while the Platinum Group Metals (PGMs) are leached in subsequent series of leaching stages. In the base metal recovery process, nickel and cobalt are first leached. The nickel and cobalt are then recovered as metallic powder by hydrogen pressure reduction in autoclaves. The solids are further leached in the next stage to solubilise copper which is recovered by electrowinning. At this stage the leach residue is basically the PGM concentrate that is fed to the Precious Metal Refinery, after impurity removal. A more detailed description of the Sherritt Gordon process is given in chapter 3, and can be found in literature (Burkin, 1987; Boldt and Queneau, 1967).

1.1 Motivation

At Impala Base Metals Refinery, the repulping (pre-leach) section is the first stage in the leaching process of nickel-copper matte to produce a high grade Platinum Group Metal (PGM) concentrate. Therefore, knowledge of all aspects of the leaching process taking place at this stage will lead to a better understanding of the entire nickel-copper matte leaching process, including the pressure leaching process. Consequently, this will in turn lead to an efficient process and increased production efficiency of a high grade PGM concentrate. It was thus the aim of this work to study the leaching behaviour of the nickel-copper matte at the pre-leaching stage. The study also investigated the response of the pre-leached matte to the subsequent pressure leaching stage.

Objectives

The objectives of this study were to:

i. Study the chemical processes, leaching mechanism and kinetics of the leaching process that occurs in the repulping stage during the refining of the nickel-copper matte, with a view of improving efficiency of the leaching process.

ii. Investigate the response of the pre-leached matte to the subsequent pressure leaching operation and quantify the influence that pre-leached matte has on the subsequent pressure leaching operation.

iii. Study mineralogical transformations that may occur during the matte repulping stage.

iv. Develop a model that can simulate the leaching process taking place in the repulping stage.

The application of the knowledge gained in this study and the implementation of recommendations to improve the efficiency of the process were not part of the scope of this study.

1.2 Outline of the Dissertation

The first part of this study (chapter 2) is essentially a review of the literature on the geology/mineralogy of the Platinum Group Metal (PGM) bearing ores of South Africa; and a review of the methods employed in the recovery of the platinum group metals from the ores, starting from milling to smelting of the ore resulting in the production of nickel-copper matte that contains the metal values. A few examples of commercial operations that treat Ni-Cu mattes have been presented, and the chemistry of the leaching processes of the matte has been described. The chapter has also presents a short literature review of the kinetics of leaching processes.

In chapter 3, a short description of the operations of the Impala Platinum Refineries has been presented, in particular the operations of the Impala Base

Metals Refinery whose pre-leach section was studied. An overview of the base metal hydrometallurgical refining process has been described, highlighting the major unit processes.

Chapter 4 has described the nature of experiments conducted in this study. It has presented the material used in the experiments, and the process parameters investigated. Two sets of laboratory scale experiments were conducted, namely atmospheric leaching experiments that were designed to investigate the effect of variations in the operating conditions of the matte repulping stage; and pressure leaching tests on the leach residue from the atmospheric leaching experiments. These tests were aimed at investigating the response of the pre-leached matte to the subsequent pressure leaching operations.

In chapter 5, results of the atmospheric leaching experiments have been discussed on the basis of the thermodynamics and mechanisms of the leaching system studied. The first section (section 5.1) discussed the thermodynamics of the Ni-Cu matte – H_2SO_4 leaching system using the Potential-pH (Eh–pH) equilibrium diagrams (Pourbaix diagrams). Section 5.2 discussed the leaching mechanism of the matte, based on the mineralogical investigations of the matte as well as on the chemistry of the leaching process, while section 5.3 discussed the leaching of the matte due to galvanic interaction between the mineral phases. Chapter 6 has presented and discussed in detail the results of the atmospheric leaching experiments, outlining the effects of variations in the process parameters. Chapter 7 has presented and discussed results of the pressure leaching experiments that were conducted to investigate the response of pre-leached matte to pressure leaching. The chapter has also presented the thermodynamics of the Ni-Cu-H_2SO_4 pressure leaching system using the Eh-pH diagrams.

A semi-empirical kinetic model has been developed on the basis of the leaching mechanism and chemical reactions of the leaching system investigated. This is presented in chapter 8.

CHAPTER 2

2.0 LITERATURE REVIEW

This chapter reviews the literature on the geology and mineralogy of the Platinum Group Metal (PGM) bearing ores of the Bushveld Complex of South Africa. It describes the geology and mineralogy of economically significant platiniferous horizons of the Bushveld Complex, namely the Merensky reef, the UG-2 chromitite, the platreef and the Dunit pipes. The chapter also describes the methods employed in the recovery of Platinum Group metals (PGMs) from the ores, starting from milling to smelting of the ore resulting in the production of nickel-copper matte that contains PGMs. Examples of commercial hydrometallurgical processes for treating the Ni-Cu matte are also presented, and the chemistry of the leaching processes of the matte has been described. Finally, the chapter presents literature on the kinetics of leaching processes.

2.1 Geology and Mineralogy of the Bushveld Complex

In this section a short description of the geology and mineralogy of the Bushveld Complex of South Africa is presented. The Bushveld Complex is found in the Northwest, Limpopo, Gauteng and Mpumalanga provinces of South Africa and is said to be the largest stratiform Platinum-Group Metals (PGM) ore body known, measuring about 66 000 km^2 (von Gruenewaldt,1977). Impala Platinum Mines, from which the material used in this study originated, are located the Bushveld Complex, except for some mines that are located in Zimbabwe. The Bushveld Complex has been extensively studied; and reviews and investigations on the geology and mineralogy have been presented by several researchers, for example Wagner (1973) published a book that gives a comprehensive description of the platinum deposits and Mines of South Africa. The Bushveld Complex can be divided into four units (Figure 2.1): the Lebowa Granite Suite, the Rashoop

Granophyre Suite, the Rooiberg Group and the Rusternburg Layered Suite (Lindsay, 1988 and Boerst, 2001). The Lebowa Granite Suite consists of a series of different granite types, the Rashoop Granophyre Suite consists of predominantly homogeneous granophyre as well as associated granophyric granite, graphyre porphyry and pseudogranophyre. The Rusternburg Layered Suite is a large, thick layered body of ultramafic to mafic intrusive rocks, which make up the bulk of the bushveld complex (Hochreiter et al., 1985).

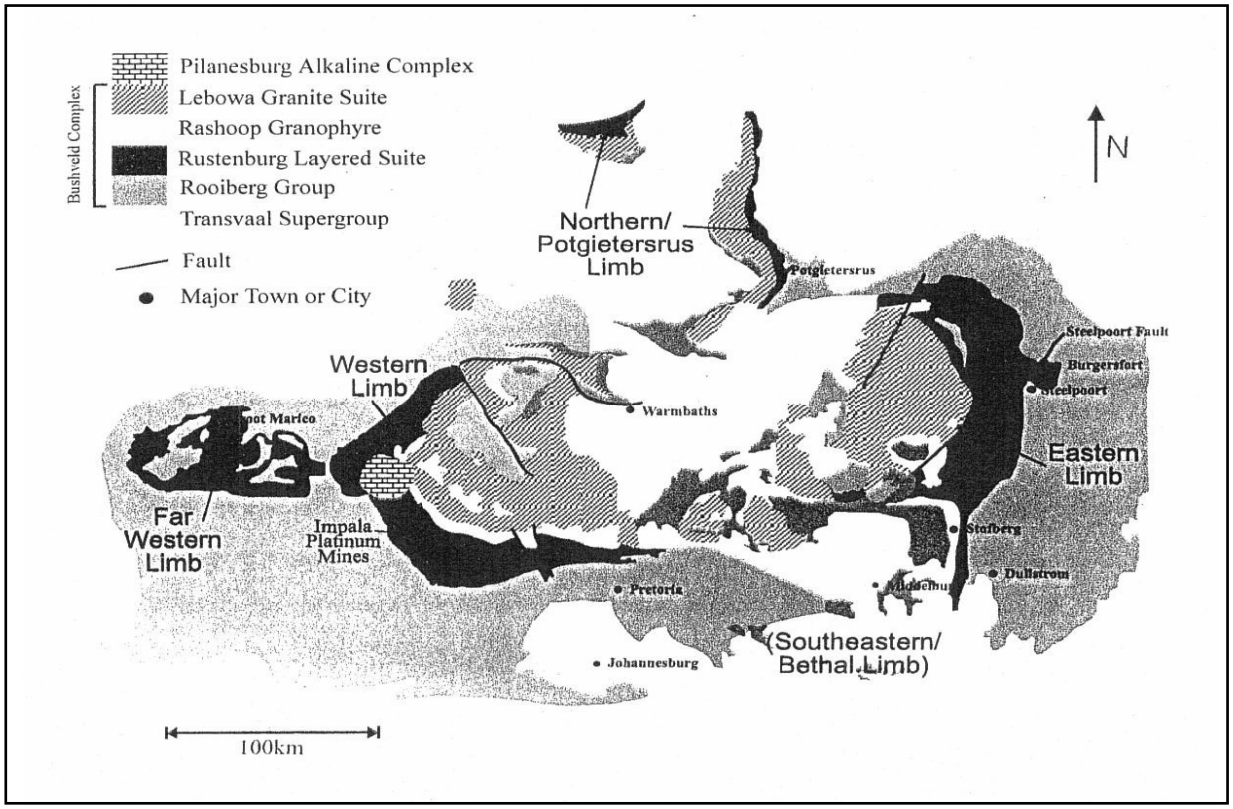

Figure 2.1: Generalised geological bedrock map of the Bushveld Complex with selected host rocks (Boerst, 2001)

The Rusternburg Layered Suite is further subdivided into five zones from bottom to top (Figure 2.2). These are the marginal zone, the lower zone, the critical zone, the main zone and the upper zone. The marginal zone is a skin between the older Transvaal sequence rocks and the layered rocks of the Bushveld Complex.

The lower zone is a thick sequence of alternating basic/ultrabasic rocks which lies above the marginal zone, but below the critical zone. The critical zone consists of a series of layered rocks. In terms of the Platinum-Group Element (PGE) mineralization, it is the most important unit, which consists (in its lower part) of a series of chromitite layers within pyroxenite, and in its upper part of a series of cyclically repetitive triplets of chromitite, pyroxenite and norite (Hochreiter et al., 1985). The critical zone is divided according to the chromitite layer into the Lower Group, Middle Group and Upper Group (Figure 2.3). The basal chromitite of each unit is identified by being numbered according to its group from the bottom upwards, e.g. LG-1, LG-2, LG-3, etc for Lower Group chromitite, MG-1, MG-2. MG-3, etc for Middle Group and so on. Of the chromitites only the UG2 is said to carry significant PGE values throughout the Bushveld complex (Hochreiter et al., 1985). Near the top of the critical zone is the Merensky Reef, above of which occurs the final chromitite-pyroxenite called the Bastard Reef.

In the upper critical zone of the Rusternburg Layered Suite, four economically significant platiniferous horizons occur: the Merensky reef, the UG-2 chromitite, the Platreef and the platiniferous ultramafic pipes. Of the above platiniferous horizons, the Merensky reef is the most exploited horizon for platinum group metals followed by the UG-2, despite higher grades and large reserves due to difficulties encountered in recovering the PGMs from UG-2 (Bryson, 2004a and Green et al., 2004). Naldrett (1981) also noted that the Platinum Group Element (PGE) mineralization of economic importance on the Bushveld Complex occurs in four distinct settings, namely the Merensky Reef, the UG-2 chromitite layer, the Platreef of the Potgietersrus (Mokopane) area and the Discordant Dunite Pipes of the Eastern limb. von Gruenewaldt (1977) studied the the geology and mineralogy of the Bushveld Complex and published a paper on the mineral resources of the Bushveld Complex. He studied the three types of deposits namely the Merensky Reef, the UG-2 chromitite layer and the Platreef, and

identified the most important mineral deposits of the Bushveld Complex as the sulphide ores.

Some of the work that has been published on the other horizons includes a study by Sharpe (1982) who studied and presented data on the concentrations of noble metals (Ir, Rh, Pt, Pd and Au) from representatives of the major units of the marginal rocks of the Bushveld Complex. From these data, an estimate was made of a possible liquid composition from which the UG-2 layer and the Merensky Reef crystallized. This estimate was used to calculate values of the silicate/sulphide melt distribution co-efficient for the mineralized layers. Hulbert and von Gruenewaldt (1982) published a review of nickel, copper and platinum mineralization of the Lower Zone of the Potgietersrus limb of the Bushveld Complex. They noted that the Lower Zone of the Potgietersrus limb consists of a succession of ultramafic rocks, and that two significant horizons of sulphide and platinum group element mineralization were known within the Lower Zone of the area.

Kinloch (1982) conducted a study on the regional trends in the platinum-group mineralogy of the Critical zone and noted that the platinum-group minerals of the UG-2 chromitite and overlying Merensky Reef show close similarities in the mineral types in any one area. For example, if in one particular area the Merensky Reef contains abundant Pt-Pd sulphides, the underlying UG-2 layer is also enriched in Pt-Pd sulphides. This is also the case for Pt-Fe alloy. In contrast, the distribution of Pt-Pd tellurides displays no pattern in the complex. Three main categories of mode of occurrence of the platinum-group minerals (PGMs) were identified:

1. PGMs associated with base metal sulphides.
2. PGMs associated with chromite or other oxides.
3. PGMs enclosed in silicates.

Categories 1 and 2 can be further subdivided into PGMs enclosed in base metal sulphides/chromite, and PGMs attached to base metal sulphides/chromite

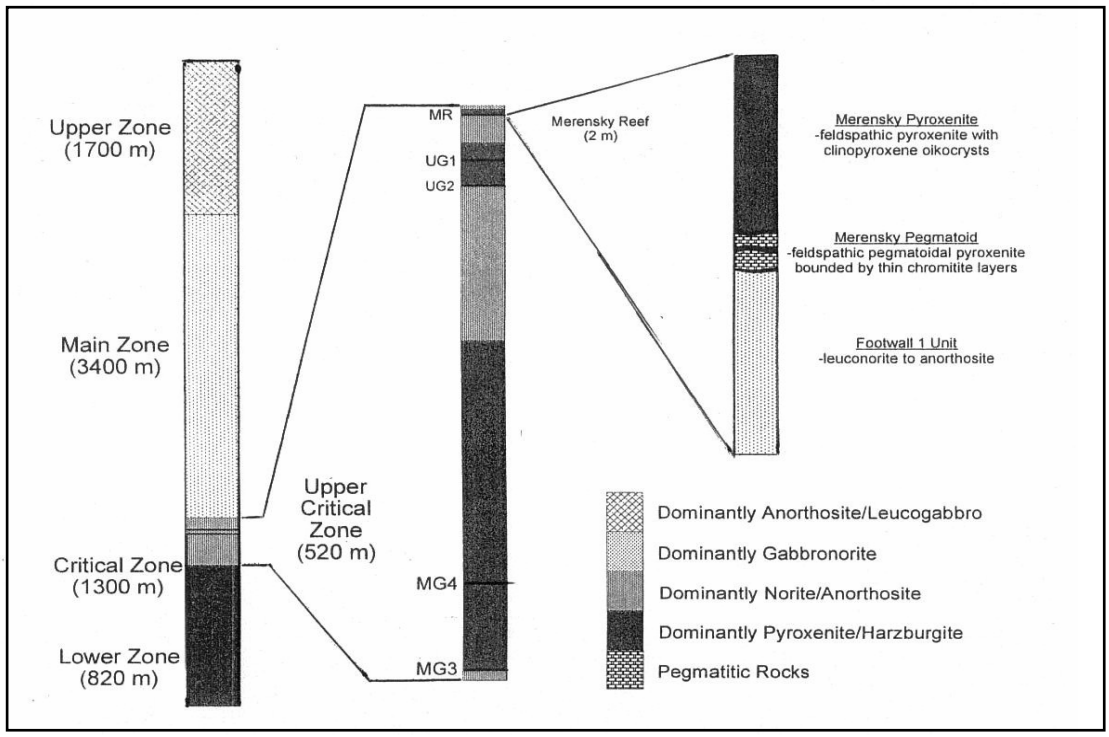

Figure 2.2: Generalized stratigraphic column of the Rustenburg Layered Suit, showing location and lithology of the Merensky Reef (Boerst, 2001).

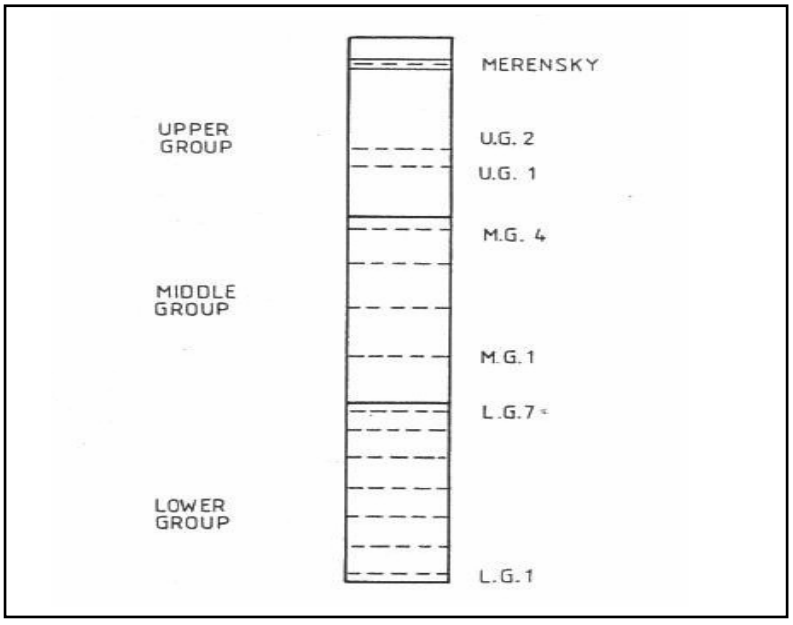

Figure 2.3: Stratigraphy of the Critical Zone (Naldrett, 1981)

2.1.1 The Merensky Reef

The Merensky Reef was discovered in 1924 by Dr Hans Merensky (Wagner, 1973 and Hochreiter et al., 1985). In a review of the platinum-group element deposits of the Bushveld Complex, Naldrett (1981) noted that the term "Reef" was inherited from Witwatersrand gold mines, where it refers to the ore zone. In the Merensky Reef the major base metal sulphides are (in order of decreasing abundance) pyrrhotite, pentlandite, chalcopyrite and pyrite. These occur interstitially between cumulus and intercumulus silicates (orthopyroxene and plagioclase respectively) commonly as multimineralic aggregates. The PGMs are normally found in association with the sulphides as inclusions or along sulphide/silicate grain boundaries. They also occur, to some extent, as inclusions in silicate and in close association with chromite. The dominant PGMs are cooperite (PtS) and braggite (Pt,Pd,Ni)S with subordinate amounts of sperrylite ($PtAs_2$), Pt-Pd tellurides, laurite (RuS_2) and Pt-Fe alloy (Lindsay, 1988).

Vermaak and Hendriks (1976) published a review of the mineralogy of the Merensky Reef, and defined the Merensky Reef as the economically valuable pegmatoidal layer bounded by thin chromite seams or stringers. According to these authors the Merensky consists of a cumulate orhopyroxene-chromite pegmatoid containing post cumulus feldspar and clinopyroxene, although local olivine-rich or quartz-bearing facies occur. The orthopyroxene is bimodal, with separate coarse and fine fractions present. The base metal sulphides occur as a temporal sequence typical of magmatic assemblages with a host of rare minor minerals. They noted the main base metal sulphides as pyrrhotite, pentlandite, pyrite and chalcopyrite. The precious minerals are predominantly associated with the base metal sulphides, with the major discrete platinoid minerals being idiomorphic braggite, cooperite and laurite with minor sperrylite. Another main platinoid constituent is Pt-Fe alloy, which most commonly occurs as complex intergrowths with other minerals, principally base metal sulphides.

Schwellnus et al. (1976) conducted a study of the Merensky Reef at a mine called Atok Platinum Mine, located in the north-eastern sector of the Bushveld Complex. They observed that at this particular locality the Merensky Reef zone mineralization composed platinoid and other metal values, which were almost invariably associated with chromitite seams and porphyritic pyroxenite, though portions of pegmatoid were also frequently mineralised. Sulphide minerals such as chalcopyrite, pentlandite, pyrite and pyrrhotite were also noticed in the porphyritic pyroxenite and pegmatoid. The sulphide minerals which were found only in trace amounts included mackinawite, bravoite and galena. In the ores that were slightly oxidised, violarite was observed as an alteration product of pentlandite. In conclusion Schwellnus et al. (1976) pointed out that the platinum group minerals are preferentially associated with the sulphides and tend to occur at the boundaries of sulphides grains.

Brynard et al. (1976) carried out a mineralogical investigation of the Merensky Reef at the Western Platinum Mine. They described the geology of the Merensky Reef as generally consisting of pegmatitic pyroxenite and porphyritic pyroxenite, situated between two thin chromitite bands (Figure 2.4). In the western portion of the complex, the lower chromitite band is in contact with a band of anorthosite. In the eastern portion the lower chromitite band is in contact with pegmatitic pyroxenite, and the interval between the two chromitite bands usually consists of porphyritic pyroxenite. The interval of the reef above the upper chromitite band consists of porphyritic pyroxenite grading into anorthosite. The authors compared the character of the reef within the western portion of the complex at different localities and found that at Western Platinum Mine the reef consisted of porphyritic melanorite, whereas at Rustenburg it consisted of pegmatitic pyroxenite. The mineralisation of platinum-group elements occurs near the upper chromitite band at Western Platinum, whereas it occurs between the two bands at Rustenburg. The most abundant minerals phases at Western Platinum Mines are sperrylite and Pt-Pd bismuthotellurides together with Pt-Pd sulphides, whereas at Rustenburg the most abundant phases are braggite and cooperite.

They concluded that the platinum-group mineralogy of the Merensky Reef was different for every locality that had been investigated.

Kingston and El-Dosuky (1982) studied platinum-group mineralogy of the Merensky Reef at the Rustenburg Platinum Mine. Their study indicated that the main platinum-group minerals (PGMs) at this particular location, in decreasing order of abundance, are braggite (Pt,Pd,Ni)S, cooperite (PtS), moncheite ((Pt,Pd,Ni)(Te,Bi,Sb)$_2$), laurite (RuS_2), kotulskite (Pt,Pd,Ni)(Te,Bi,Sb), merenskyite (Pd,Pt,Ni)(Te,Bi,Sb)$_2$, Pt-Fe alloy, palladian electrum (Au,Ag,Pd,Cu) and sperrylite ($(Pt,Rh)As_2$). The remainder (< 1%) include atokite [$(Pd,Pt)_3Sn$], paolovite [$(Pd,Pt)_2Sn$], rustenburgite [$(Pt,Pd,Bi)_3Sn$] and a palladium arsenide. They noted that cooperite and braggite were nearly always found at or near the pentlandite-silicate contact of the base metal sulphide aggregates. Laurite also occurs in the base metal sulphide aggregates, it appears as small crystals enclosed particularly by pentlandite and chalcopyrite, and close to or in contact with the silicate boundaries. Laurite was also found to occur on veins within the silicates and within chromite. Sperrylite was very rare and occurred as crystals in chalcopyrite and pyrrhotite. Platinum-group Tellurides, for example moncheit, kotulskite, merenskyite etc, were found to occur in three main forms:

a) as large laths situated at the base metal sulphide-silicate contacts and predominantly associated with pentlandite.

b) Both as small grains and crystals enclosed by chalcopyrite and rarely by pentlandite.

c) As pockets of small grains closely associated and often intergrown with chalcopyrite remote from the main base metal sulphide aggregates.

The platinum-iron alloy was found to occur as four main intergrowth types with the base metal sulphides and other PGMs: Type 1 occurs predominantly with

pyrrhotite, occurrences in pentlandite and chalcopyrite are minor. Type 2 occurrences consist of aggregates of small crystals of Pt-Fe alloy that are intergrown most commonly with pyrrhotite matrix, and rarely pentlandite and chalcopyrite. Type 3 occurrences include fine spong to graphic intergrowths of Pt-Fe alloy with cooperate; and type 4 occurrences of the Pt-Fe alloy are large and often occur as homogenous grains with cooperite in the PGM concentrates. The Pt-Pd-Sn compounds (paolovite, atokite, etc) occur as large laths enclosed by chalcopyrite at its contact with the silicates, or may occur within the silicates away from the base metal sulphide aggregates. No rhodium mineral occurrences were located in the samples examined from the Rustenburg mine.

The platinum-group mineralogy of the Merensky Reef at the Impala Platinum mines in Rustenburg was investigated by Mostert et al. (1982). They reported that the Merensky Reef in the Impala area is typically a coarse-grained to pegmatoidal pyroxene with either one or two thin chromite layer (Figure 2.4). The platinum-group element – bearing zone is associated with the footwall chromitite layer in the pyroxenitic reef and with the upper chromitite layer in the pegmatoidal reef. The chromitite layers of the reef consist of chromite and interstitial plagioclase with minor sulphides, biotite and rutile. Orthopyroxene, sulphides, rare chromite and olivine, together with interstitial plagioclase and clinopyroxene, as well as minor hornblende, talc and biotite, constitute the silicate part of the reef in this area.

The main base metals sulphides, in decreasing order of abundance, were found to be pyrrhotite (41%) pentlandite (37%), chalcopyrite (18%) and pyrite (4%). The sulphides occur as blebs interstitial to silicate and chromite. Of the PGMs, cooperite (PtS) is by far the most abundant mineral (44%) followed by laurite (RuS_2) at 21%, moncheite (17%) and braggite (12%). The rare minerals were grouped together and constituted about 6% (Table 2.1). It was found that most of the PGMs associated with the base metal sulphides and most of these minerals were found to associate with chalcopyrite, although chalcopyrite is not the most

abundant base metal sulphide. However, this distribution pattern is not followed by laurite, which tends to occur more frequently with pentlandite. It should be noted that cooperite and laurite occur preferentially in the chromitite layers, whereas moncheite was most commonly found in the silicate part of the Merensky Reef. The investigation showed that cooperite, laurite, moncheite and braggite are the most abundant platinum-group minerals in the Merensky Reef in the Impala area of Rustenburg.

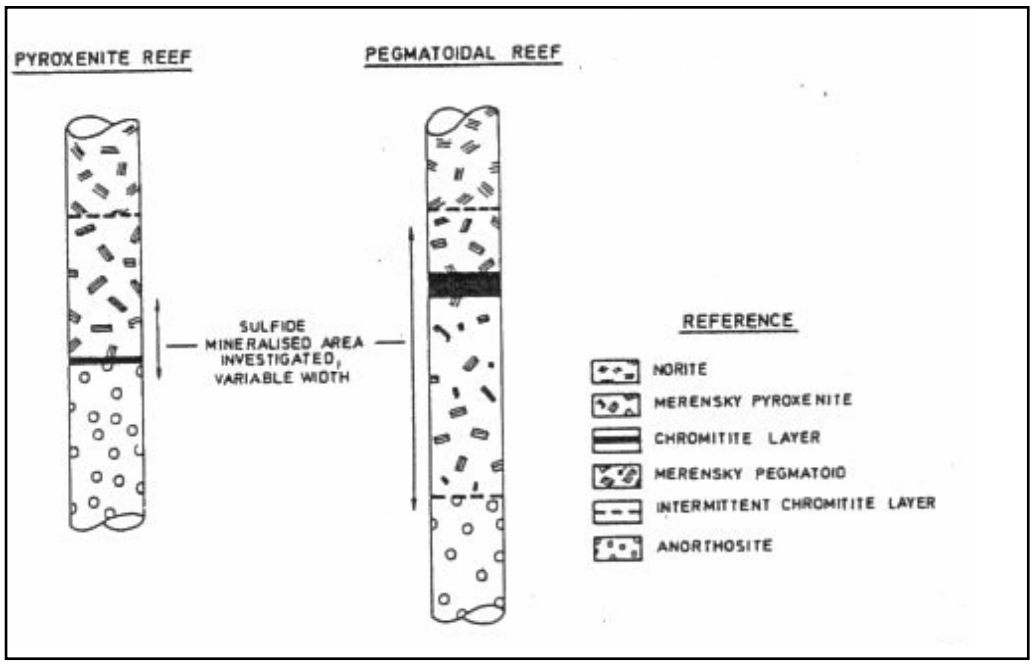

Figure 2.4: Schematic diagram of the two main types of Merensky Reef petrology (pyroxenite and pegmatoid reefs) occurring in the Impala Platinum Mines (Mostert et al., 1982).

Table 2.1: Platinum-Group Metals of the Merensky Reef at the Impala Platinum Mines near Rustenburg (Mostert et al., 1982).

	Ideal formula	Average abundance (vol. %)
Cooperite	PtS	44
Laurite	RuS_2	21
Moncheite	$Pt(Te, Bi)_2$	17
Braggite	(Pt, Pd, Ni)S	12
Pt-Fe alloy	Pt_3Fe	6
Electrum	Au, Ag	
Sperrylite	$PtAs_2$	
Merenskyite	$PdTe_2$	
Niggliite	PtSn	
Hollingworthite	RhAs	
Michenerite	PdBiTe	
Pt-Pd alloy	Pt, Pd	
Unnamed	Pt, Rh, S	
Pt metal	Pt	
Pt-Ni-Cu alloy	Pt, Ni, Cu	
Rustenburgite?	$(Pt, Pd)_3Sn$	
Atokite?	$(Pd, Pt)_3Sn$	

2.1.2 The Upper-Group-two (UG-2) Reef

The UG-2 Chromitite layer is 30 – 50 m below the Merensky Reef in the northwestern sector of the Bushveld Complex, 140 – 180m below in the southwestern sector and as much as 400m below in the northeastern sector (Naldrett, 1981). The UG-2 chromitite is a layer of well-packed cumulate chromites found below the Merensky Reef in the upper Critical Zone. The PGMs and base metal sulphides occur interstitially, long chromite grain boundaries and locked in chromites. The base metal sulphides include pentlandite, pyrrhotite, chalcopyrite and pyrite; as well as several minor species. The most common PGMs are Os, Ir-bearing laurites, which are often locked in chromite. Other species present in significant quantities include cooperite, braggite and the Rh sulphides (hollingworthite and an unnamed Pt-Rh-Ir-Cu sulphide species). These are generally found in close association with interstitial base metal sulphides (Lindsay, 1988).

McLaren (1978) stated that PGE values in the UG-2 layer are mainly in the basal and middle portion of the main chromitite over the northwestern, southwestern and southeastern sectors. In the southwestern sector, the most common minerals are laurite (RuS_2), cooperite (PtS), braggite ((Pt,Pd,Ni)S) and unnamed minerals which were simply given as Pt-Rh-Cu-S, Rh-S and Pt-Pd-Cu-S. In the northwest braggite, laurite, cooperite, Pt-Fe alloy and an unnamed Pt-Rh-Ir-Cu-S mineral are the main species. In the southeast, laurite, braggite, vysotskite, cooperite and an unnamed mineral Pt-Rh-Ir-Cu-S mineral predominate; while in the northeastern sector sulphides of the PGE were revealed to be predominant in the UG-2 layer.

McLaren and De Villiers (1982) studied the chemistry and mineralogy of the platinum-group metals of the UG-2 chromitite layer of the Bushveld complex. They noted that the most abundant PGMs were laurite, cooperite, an unnamed Pt-Ir-Rh-Cu sulphide, vysotskite (PdS), braggite, a Pt-Fe alloy, gold and electrum (Au,Ag), as well as intermetalloids such as Pt-Fe, Pd-Cu, Pd-Pb and Pd-Hg. All the PGMs were observed as discrete grains that are predominantly associated with the base metal sulphides; they also occur along grain boundaries in silicates or in chromite. The main base metal sulphides associated with the PGMs are pentlandite, chalcopyrite, pyrrhotite and pyrite.

2.1.3 The Platreef and Dunite pipes

The platreef and Dunite pipes are other horizons containing economically significant quantities of PGEs (Figure 2.1). The platreef occurs in the Potgietersrus limb of the Bushveld Complex where the Critical Zone is not well developed and the base metal sulphide and PGE mineralization are erratic. The platinum-group mineral assemblage is made up mostly of Pt-Pd tellurides, cooperite, braggite and Pt-Fe alloy, which tend to be associated with the base-metal sulphides along grain boundaries and enclosed in silicate (Lindsay, 1988

and Kinloch, 1982). Dunite pipes (PGE-bearing ultramafic pipes) occur in both the western and eastern sectors of the Bushveld Complex (Lindsay, 1988; Kinloch, 1982 and Naldrett, 1981). The mineralogy of the pipes differ from that of the Merensky reef or UG-2 ore zones in that there are no Bi tellurides, and sulphides of the PGE are rare (Naldrett, 1981). The PGM mineralogy is dominated by Pt-Fe alloy and various PGE sulpharsenides, arsenides and antimonides, which mainly occur interstitially with the silicates (Lindsay, 1988).

2.1.4 The Great Dyke of Zimbabwe

Impala Platinum Holdings Limited obtains some of the PGE concentrates from its mines in Zimbabwe. Platinum-group mineral occurrences in Zimbabwe are confined to the Great Dyke of Zimbabwe. The PGEs are associated with base-metal sulphides, namely pentlandite, pyrrhotite, chalcopyrite and pyrite. The major PGMs are sperrylite, moncheite, merenskyite and hollingworthite (Lindsay, 1988). More information on the geology-mineralogy of the Great Dyke of Zimbabwe, and problems associated with the processing of nickel ores can be found in a paper published by Mashanyane and Storey (1986).

2.2 PROCESSING OF PGM BEARING MINERALS

The processing of Platinum Group-Minerals (PGMs) generally comprises several steps, the major steps being the following:

1) Comminution (crushing and grinding).
2) Concentration of ore by physical techniques such as flotation and gravity concentration.
3) Pyrometallurgical concentration, which involves smelting and converting to produce a PGM-rich nickel-copper sulphide matte.
4) Hydrometallurgical extraction of base metals. This includes leaching and recovery of individual base metals (BMs), and production of PGM concentrate.

5) Refining of the PGM concentrate to produce individual platinum group elements (PGE).

A simplified block flow diagram of the Platinum-Group Mineral (PGMs) refining process is shown in Figure 2.5, and each of the steps is briefly described below. However, the refining of the PGM concentrate to produce individual platinum-group elements (step 5) has not been described, as it is not in the scope of this study. The Pyrometallurgical operations have been described in general terms, as the description fits most of the current commercial operations. However, one operation that differs slightly from the general process description is the Outokumpu Nickel Smelting Process (DON process), which does not use a converter after the smelting furnace (Knuutila et al., 1997). Most of the other nickel-copper smelting processes make use of a matte converter. A brief description of the Outokumpu smelting process is given in section 2.2.3. The hydrometallurgical processes of most platinum producers differ considerably, hence only a few examples of the process routes that are employed commercially have been presented. Reviews of the PGMs recovery routes include papers by Edwards (1976, 1984), Newman (1973), Corrans et al. (1982), Mostert and Roberts (1973) and Hochreiter et al. (1985).

2.2.1 Comminution (crushing and grinding)

Comminution serves to reduce the ore to manageable size fractions and liberate the ore minerals. The run-of-mine ore is first crushed to reduce the size and fed to the milling circuit where it is ground to further reduce the size and liberate the ore minerals from the gangue. The milled ore is classified and the desired size fraction is transferred to the flotation circuit to separate the gangue from ore minerals. Because of their different metallurgical properties, ores mined from the Merensky and UG-2 reefs are usually treated in separate milling and flotation circuits up until the smelting stage.

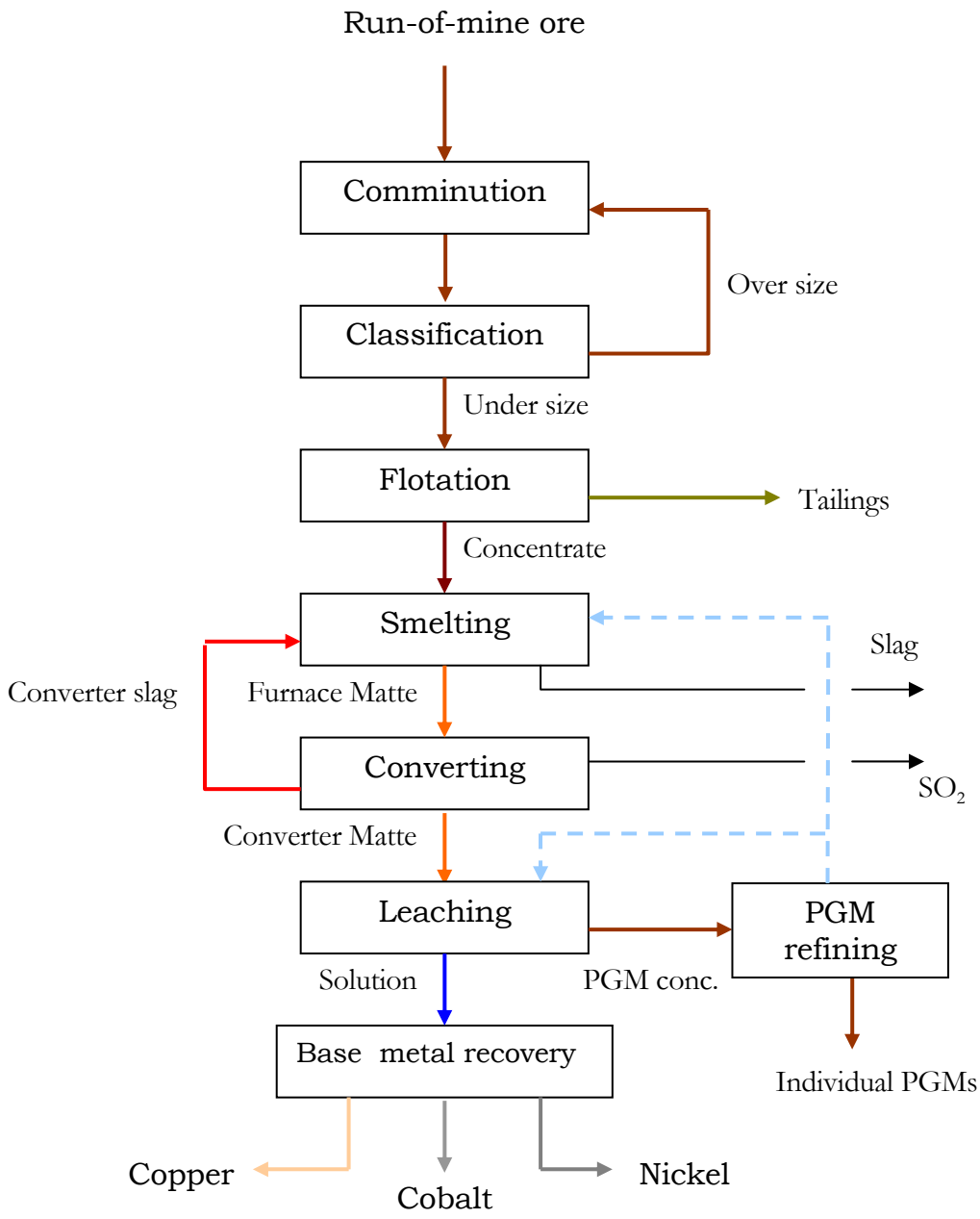

Figure 2.5: Simplified generic flow diagram of platinum-group mineral refining process

2.2.2. Flotation / Gravity separation

The process of flotation separates gangue from ore minerals by making use of surface properties of the individual minerals. The surface properties of the ore and gangue minerals may be modified by the addition of reagents, for example collectors that render the surfaces of selected particles hydrophobic, frothers which stabilize and strengthen bubble walls, and modifiers may be added to enhance or inhibit the floatability of specific mineral species. Base metal sulphides are mainly recovered by the flotation process. Gravity separation is used to remove PGMs by virtue of their characteristically high density, it reduces losses of PGMs and reduces the flotation head grade which helps in lowering the overall grade of the tailings (Corrans et al., 1982).

The distribution of PGEs in different mineral phases is an important factor in the beneficiation process (Bryson, 2004b and Cabri, 1981). Kinloch (1982), Kingston and El-Dosuky (1982), Mostert et al. (1982) and Peyerl (1983) have shown that the PGEs occur in several forms, such as discrete PGMs, in base metal sulphides and oxides and/or silicates. Platinum, Ruthinium, Osmium and Iridium as well as some Palladium form discrete PGMs which are usually amenable to concentration by gravity and flotation. Palladium and rhodium mostly occur in base metal sulphides and are therefore, recoverable mainly by flotation (Lindsay, 1988).

Textures of the minerals are also important, euhedral-subhedral PGMs such as sperrylite, laurite, Pt-Pd sulphides (cooperite-Braggite –Vysotskite) and portion of Pt-Fe alloy are usually readly liberated and recovered by flotation and/or gravity. PGMs such as the Pt-Pd bismuthotellurides often occur as thin veinlets and plates and are not readily recovered by gravity as they have relatively low densisty and are flaky in habit. Thus, they show a tendency to follow the base metal sulphides into the flotation circuit; this behaviour applies also to small, reatively light laurite particles. PGMs that are intimately intergrown with gangue

and which are not easily liberated may be lost to the tailings. PGMs such as Pt-Fe alloy, which are either intergrown with base metal sulphides or locked in them end up in the flotation circuit and are recovered by the flotation of the host base-metal sulphides. Thus, in general, the PGMs most commonly found in the flotation concentrate are braggite, laurite and sperrylite with minor cooperite and Pt-Pd tellurides (Kinloch, 1982). However, the most contributor of PGEs to the flotation concentrate are the base metal sulphides, therefore, losses of base metal sulphides constitutes a big loss of PGEs. Chalcopyrite and pentlandite float well, however, pyrrhopytite is a notoriously slow floater that mostly reports to the flotation tailings and constitutes the greatest source of PGE losses (Corrans et al., 1982). The PGE bearing minerals that are most successfully recovered by gravity techniques are cooperite and isoferroplatinum.

The alteration of minerals is another contributing factor to the losses of PGEs. PGE losses are enhanced when a reef whose mineralogy has been altered is processed. Altered minerals, both silicates and base metal sulphides, have been found to report mostly to the tailings during flotation (Lindsay, 1988). Alteration of base metal sulphides can cause changes to their surface chemistry resulting in partial loss of hydrophobic properties, which inhibits their ability to flotation. Common altered sulphides include mackinawite covellite, violarite and valleriite. Oxidation of sulphide minerals also has adverse effects on flotation. For example oxidation of sulphides may occur during milling, possibly enhanced by galvanic reactions (Adam et al., 1984) to form Fe-oxide, hydroxide and/or sulphate oxidation rims on the Fe – sulphides surfaces. The oxidation products may coat other base-metal sulphides and interfer with their surface hydrophobic properties, resulting in them reporting to the flotation tailings together with the PGEs.

2.2.3 Pyrometallurgical concentration: Smelting and Converting

The next major step in the processing of PGE bearing minerals is the smelting-converting stage. During this stage, the base metals and PGEs are concentrated into sulphide matte to enhance grades to 400 –800 ppm PGE, 16 – 18% Ni and 8 – 11% Cu in the furnace matte, and in the subsequent converting stage the metals are upgraded to 1500 – 2500 ppm PGE, 45 – 50% Ni and 25 – 35% Cu in the converter matte (Impala reports, 2003-2005, Hochreiter et al., 1985, and Mostert and Roberts, 1973).

(i) Smelting

During the smelting process the sulphides form a molten matte in which valuable metals are concentrated while the silicates and oxides form a slag phase, which contains most of the gangue minerals. Losses of metals to the slag may occur by matte entrainment, or dissolution of the metals in the slag as oxides.

The furnace feed consists of dried and pelletised flotation concentrate blended with flux (lime), low grade reverts and occasionally iron ore. Miscellaneous additions may include recycled furnace matte/slag containing metal values, especially those emanating from barrens/effluent treatment processes in the Precious Metals Refineries. In addition, molten converter slag, which is mostly fayalite with some magnetite, is recycled back to the furnace. The concentrate consists of base metal sulphides with traces of PGMS, and gangue minerals. The predominant minerals are chalcopyrite, pentlandite, pyrrhotite and pyrite. The gangue component of the feed is normally predominantly bronzite (pyroxene) with subordinate plagioclase (Ca- feldpar) and some amounts of biotite–phlogopite (Fe, Mg–mica) serpentine, talc (hydrated Mg-Silicate) and chlorite (hydrated Mg, Fe, Ca silicate) (Lindsay, 1988).

The smelting is carried out in electric arc furnaces. During smelting the furnace electrodes make contact with the slag to form a circuit, this result in heat generation by the electrical resistance of the slag. Temperature control can be effected by varying the input voltage and electrode depth into the slag. During smelting the average matte temperature can be as high as 1200 ^{o}C and that of slag as high as 1400 ^{o}C. The difference in the temperature of the matte and slag creates a temperature gradient which may induce thermal convection and slow matte setting, as well as cause erosion of furnace refractories (Newman, 1973). As melting proceeds, the charge gradually smelts and separates into immiscible silicate and sulphides liquid phases. The silicate forms slag layer, which overlies the denser matte layer. The slag is tapped continuously and cooled down or granulated in water, after which it may be milled and subjected to flotation to recover entrained sulphides before it is transferred to the slag dump. The furnace matte is tapped periodically and transferred by laddle to converters.

Lindsay (1988) described the smelting of the furnace feed components, in particular the silicates, sulphides and PGMs of the flotation concentrate as follows:

Smelting of Silicates

During the smelting process the minor hydrated silicates such as serpentine, talc, chlorite, biotine – phlogopite are first to react by a series of dehydration reactions within the temperature range 600 – 900 ^{o}C. Most of these silicates decompose to forsterite, enstatite and/or a silica-rich melt. The dominant silicates, particularly bronzite and plagioclase decompose and melt at higher temperatures (1000 – 1500 ^{o}C). However, the melting point can be lowered by adding CaO to the system. Bronzite is a pyroxene which melts at about 1240 ^{o}C and undergoes a number of solid –state transformations to form ferriferous wollastonite (Deers et al., 1978). Plagioclase, feldspar in the Merensky reef flotation concentrates start to smelt at 1400-1440 ^{o}c and finishes at 1480 – 1520 ^{o}C. However, the combination of diopside and plagioclase forms a ternary system

which lowers the melting point of the mixture. In a diopside – dominant mixture which is the case with the flotation concentrate, the mixture would start melting at 1250 – 1275^{o}c and complete melting by 1391 ^{o}C.

Smelting of Base Metal Sulphides

The predominant base sulphides in the flotation concentrate are chalcopyrite, pyrrhotite and pentlandite. The melting of these base metal sulphides involves a series of solid – state reactions and transformations. Phase equilibria of the Cu-Fe-S system at various temperatures have been presented by Barton (1973). A more detailed discussion of the Cu-S, Ni-S, Cu_2S-Ni_3S_2 systems and general pyrometallurgy of sulphide ores of nickel can be found in the paper by Terry (1987). The transformations of these minerals at temperatures below 650 ^{o}C have been described by Lindsay (1988). At a temperature of 547 ^{o}C, chalcopyrite ($CuFeS_2$) breakdowns to form intermediate solid solution ($CuFeS_2$-$CuFe_2S_3$-$Cu_3Fe_4S_6$), pyrite (FeS_2) and sulphur. In the presence of pyrrhotite the chalcopyrite breaks down at temperatures of 334 ^{o}C – 450 ^{o}C. The intermediate solid solution is stable over a large composition and temperature range. Pentlandite becomes unstable at 610 ^{o}C to form monosulphide solid solution ($Fe_{1-X}S.Ni_{1-X}S$) and heazlewoodite solid solution $(Ni,Fe)_{3\pm X}S_2$. The heazlewoodite solid solution melts at 806 – 862 ^{o}C to form $(Ni,Fe)S_2$ and sulphide liquid, the NiS_2 phase melts at 991 ^{o}C. The monosulphide solid solution melts at 635 ^{o}C and forms a Ni – S composition, and as the temperature increases to 912 ^{o}C the Fe – S liquid appears. The last of the solid phases, Fe-rich monosulphide solid solution melts at 1192 ^{o}C. Reviews and investigations on the smelting of base metal sulphides have been published by many authors, including Robiette (1973), Biswas and Davenport (1976), Boldt and Queneau (1967), Rosenqvist (1974), Nagamori (1974) and Celmer et al. (1987).

Smelting of Platinum-Group Minerals

Lindsay (1988) has given the decomposition temperatures of the platinum-group minerals as follows:

Laurite (RuS_2) decomposes at >1000 ^oC
Kotulskite (PdTe) decomposes at 720 ^oC
Merenskyite ($PdTe_2$) decomposes at 740 ^oC
Vysotskite (PdS) decomposes at 912 ^oC
Moncheite ($PtTe_2$) decomposes at 1150 ^oC
Cooperrite (PtS) decomposes at 1175 ^oC
Sperryrite ($PtAS_2$) decomposes at 1400 ^oC

Braggite (Pt, Pd, Ni)S starts to decompose at temperatures as low as 600 ^oC. At temperatures above 1000 ^oC, braggite decomposes to form Pt–Pd alloy and sulphur. Isoferroplatinum (Pt_3 Fe) decomposes to form Pt – Fe alloy, which melts according to melting points of Pt (1769 ^oC) and Fe (1535 ^oC). These temperatures are in excess of those found in the smelter. The addition of lime (CaO) to the furnace feed brings down the melting temperature. It also decreases the melt viscosity which assists slag/matte separation. In addition, CaO decreases the holding capacity of the slag for Fe oxide which can result in the precipitation of magnetite (Lindsay, 1988). The other source of magnetite is the converter slag that is recycled to the furnace. Magnetite has the effect of cooling the matte and excess amounts precipitate out to form a viscous layer between the matte and slag layers, although some of it dissolves in the matte and slag (Robiette, 1973; Biswas and Davenport, 1976, and Lindsay, 1988). This magnetite interface may inhibit matte settling although it tends to be dispersed by convection and the magnetite eventually settles and accretes on the bottom of the furnace (Boldt and Queneau, 1967 and Lindsay, 1988). The magnetite content can be controlled by the addition of silica (SiO_2) (reaction 2.11) or providing extra heat to the furnace. This prevents magnetite settling and favours the reaction with FeS according to reactions 2.15 and reverse of 2.13 (Lindsay, 1988).

(ii) Converting

The transformation that takes place and reactions involved in the conversion of furnace matte to converter matte have been described by Kellogg (1986), Boldt and Queneau (1967), Lindsay (1988), Terry (1987) and Alcock (1976). Conversion of furnace matte is performed in Pierce Smith converters. During the operation silica, high-grade reverts and oxygen (as air) are added. The converting process serves to eliminate iron and sulphur from the matte by oxidation, and to create a metal-rich matte that contains alloy phases into which the precious metals can concentrate. This is achieved by blowing air through the molten matte. Oxygen reacts with the sulphides to oxidise Fe and S to FeO and SO_2, respectively. The FeO then reacts with SiO_2 to form fayalite slag which can be skimmed off.

The oxidation of Fe-Ni-S furnace matte is accompanied by desulphurisation according to reaction 2.1. Thermodynamically, the iron oxidation reaction (reaction 2.1) is the most favoured reaction at temperatures and oxygen fugacities of the converter (T = 1300 ^{o}C, f_{O2} = 10^{-8} to 10^{-7}). This fact was observed by Robiette (1973) and Alcock (1976) who used Ellingham-type diagrams for the oxidation and sulphurization of metals to show that, with respect to Cu and Ni, Fe forms the most stable oxide and the least stable sulphide. Terry (1987) illustrated the principles behind the conversion or oxidation of copper-nickel-iron mattes by referring to the diagram of standard free energies of formation of the oxides and sulphides of copper, nickel and iron as a function of temperature. He concluded that in the temperature range 1250 – 1350 ^{o}C, typical of converting temperatures:

- The sulphides of copper, nickel and iron have comparable thermodynamic stabilities.
- In the presence of oxygen each of the oxides is considered more stable than the sulphide.
- Iron forms the most stable oxides; sulphur and nickel oxides have comparable stabilities and copper forms the least stable oxides.

$$FeS + 1½O_2 = FeO + SO_2 \quad (2.1)$$

Other important converter reactions involve the formation of Cu and Ni sulphides:

$$2(Fe, Ni)_9S_8 + 13O_2 = 6Ni_3S_2 + 18FeO + 4SO_2 \quad (2.2)$$

$$2Cu_5FeS_4 + 4O_2 = 5Cu_2S + 2FeO + 3SO_2 \quad (2.3)$$

$$3NiS + O_2 = Ni_3S_2 + SO_2 \quad (2.4)$$

$$2CuS + O_2 = Cu_2S + SO_2 \quad (2.5)$$

At higher oxygen fugacities and/or higher temperatures, the oxidation of nickel and copper can occur, generally towards the end of the final blow:

$$Ni_3S_2 + 3½O_2 = 3NiO + 2SO_2 \quad (2.6)$$

$$NiS + 1½O_2 = NiO + SO_2 \quad (2.7)$$

$$2Cu_2S + 3O_2 = 2Cu_2O + 2SO_2 \quad (2.8)$$

The NiO is thermodynamically more stable and forms more readily than Cu_2O, whereas Ni-sulphide is less stable than Cu-sulphide. The oxidation of Ni and Cu is undesirable as their oxidic forms are soluble in slag.

It is believed that the Cu-Ni alloy found in the converter matte is initiated in the furnace with the iron component being oxidized and replaced by Ni and Cu in the converter. The Ni and Cu metallic components are generated during converting by reactions such as the following:

$$Ni_3S_2 + 2O_2 = 3Ni + 2SO_2 \quad (2.9)$$

$$Cu_2S + O_2 = 2Cu + SO_2 \quad (2.10)$$

These metals are completely miscible with each other and are stable in the matte at converter temperatures.

The Converter slag is formed by reaction between ferrous oxide and silica (reaction 2.11), and is removed periodically by slagging.

$$2FeO + SiO_2 = Fe_2SiO_4 \quad (2.11)$$

The other function of the slag forming reaction (2.11) is to control the generation of magnetite, which is produced by reactions such as:

$$3FeO + \tfrac{1}{2}O_2 = Fe_3O_4 \quad (2.12)$$

$$4FeO + \tfrac{1}{2}S_2 = FeS + Fe_3O_4 \quad (2.13)$$

$$3FeS + 5O_2 = Fe_3O_4 + 3SO_2 \quad (2.14)$$

Magnetite is stable and generally inert at smelting temperatures, with low solubility in the molten slag. On cooling, solubility decreases and dissolved magnetite is expelled from the iron silicate to form myrmekitic intergrowths. Its presence in the liquid silicate is problematic as converter slag is returned to the furnace where it contributes to magnetite problems such as inhibiting matte-slag separation, reducing furnace volume (Robiette, 1973; Biswas and Davenport, 1976, and Lindsay, 1988). The formation of Cu oxides and Ni oxides (reactions 2.6 - 2.8) may be reversed in the presence of excess FeS by reactions such as the following:

$$3Fe_3O_4 + FeS + 5SiO_2 = 5Fe_2SiO_4 + SO_2 \quad (2.15)$$

$$NiO + FeS = NiS + FeO \quad (2.16)$$

$$Cu_2O + FeS = Cu_2S + FeO \quad (2.17)$$

In the newly formed slag, matte separates out as an immiscible liquid rich in slag-incompatible components such as Ni_2S_3, Cu_2S, Cu-Ni alloy, platinum group elements and unreacted FeS. The slag is rich in matte-incompatible components such as Fe-silicate with dissolved Cu and Ni oxides, and magnetite. This is returned to the furnace to recover valuable components. The final converter matte consists of molten Cu and Ni sulphides, and significant quantities of Cu-Ni alloy. The matte is either poured out and allowed to cool slowly or granulated in water. Slow cooled matte facilitates the crystallization of a metallic Ni-Cu-Fe alloy containing most of the PGMs, and a PGM-free nickel-copper matte, which is non magnetic (Hofirek and Halton, 1990; Hochreiter et al., 1985). However, slow cooled matte results in the formation of undesirable trevorites ($NiO.Fe_2O_3$) and magnetite ($FeO.Fe_2O_3$) which are insoluble in the subsequent base metal leaching stages and report to the PGM concentrate; while granulation prevents this from happening and is therefore preferred (Steenekamp and Dunn, 1999). Sulphur dioxide produced during the smelting process is used to make sulphuric acid, which is used in the hydrometallurgical processes.

The Direct Outokumpu Nickel Smelting Process (DON process)

The direct Outokumpu Nickel Smelting Process (DON process) differs slightly from the smelting process described in the preceding section in that it does not make use of a converter to clean the smelting furnace matte. The Don process produces two types of matte: a low iron matte in the flash smelting furnace (FSF), and a high iron matte produced by cleaning the flash furnace slag in an electric furnace (EF) (Knuutila et al., 1997). Figure 2.6 is a simplified flow sheet of the DON process.

The primary feed for the DON process is a blend of various concentrates, nickel containing secondary materials and iron precipitate from the electric furnace matte leaching circuit. The chemistry of the base metal sulphide smelting has been described earlier in this section. Matte from the flash furnace is granulated

and fed to the flash smelting furnace matte leaching circuit, while the slag is tapped into the electric furnace for cleaning. Hot gas from the flash furnace is cooled down in a waste heat boiler and fed to an acid plant. In the electric furnace coal is used as a reductant and dry nickel concentrate as a sulphidizing agent to produce a desired quality of matte and slag. The matte is granulated and fed to the EF matte leaching plant. The slag from the electric furnace is also granulated and stored in slag dumps.

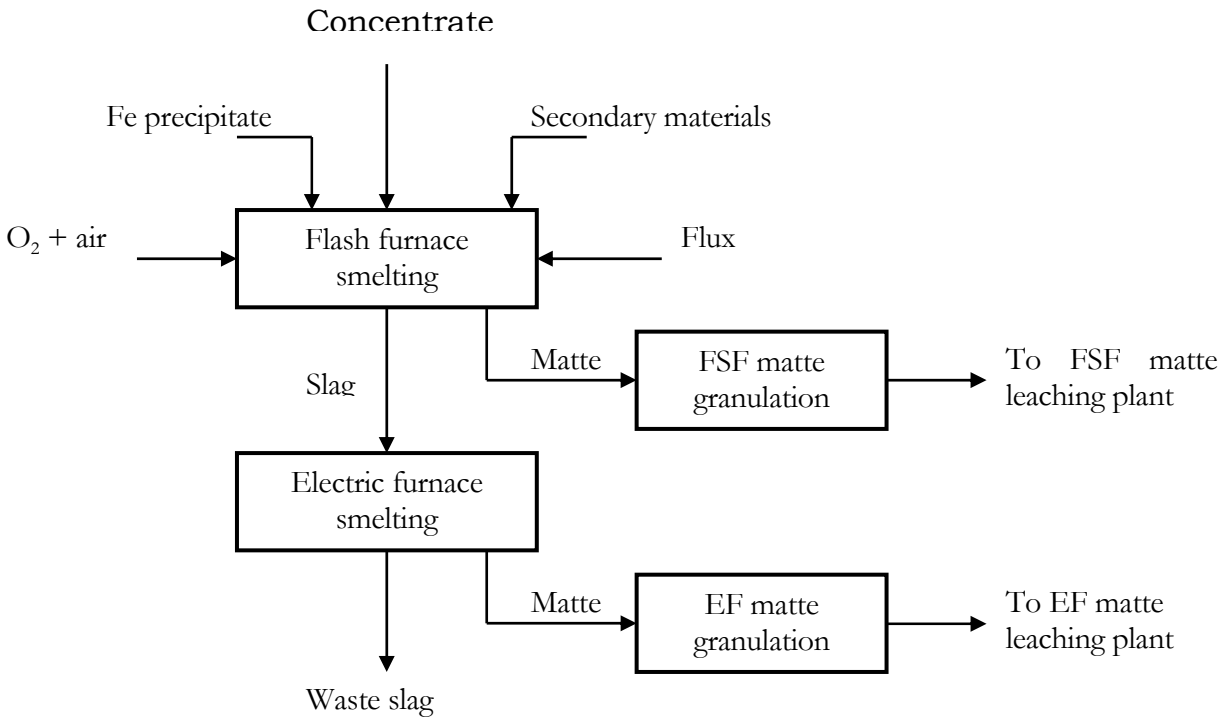

Figure 2.6: Simplified flowsheet of the direct Outokumpu Nickel Smelting Process (DON process).

2.2.4 Hydrometallurgical Processing of nickel-copper matte

The converter matte is hydrometallurgically treated to recover valuable base metals, (e.g. Cu, Ni, Co), remove base metal impurities and produce PGM concentrate. At this stage of the PGM recovery process, the process routes of the various platinum producers start to differ. The following are examples of the process routes employed by some operations in South Africa. Description of the process at Impala Platinum Refineries is given in chapter 3.

The operations at Rustenburg Base Metals Refinery

Rustenburg Base Metals Refiners (RBMR) is part of a large integrated mining and metallurgical complex, the Rustenburg Platinum Mines, situated near Rustenburg town about 120 km northwest of Johannesburg. It is the world's largest producer of platinum. The operations of the RBMR have been described by many authors, including Hofirek and Halton (1990); Hofirek and Nafal (1995); Hofirek and Kerfoot (1992); Anonymous, (1981).

The Rustenburg Base Metals Refinery comprises a platinum-group element (PGE) enrichment plant that produces PGE concentrate, and a base metal refinery. It treats nickel-copper converter matte for the recovery of nickel metal, copper metal, cobalt sulphate crystals and production of PGE concentrates. The converter matte is first crushed and milled. The milled product undergoes magnetic separation; the magnetic separation removes the alloy from the sulphides to produce magnetic (MEC) and non-magnetic (NCM) concentrates, respectively. The NCM is transferred to the Base Metal Refinery to recover nickel, copper and cobalt. The PGE rich magnetic concentrate undergoes three leaching steps to remove base metals. The primary leach is performed in an oxidising medium of concentrated Sulphuric acid, which removes most of the Ni, Co and some Cu into solution. The solution is filtered and transferred to the Base Metal Refinery. The PGE-Cu-Fe residue undergoes a reducing secondary leach under atmospheric conditions, in which ferric iron (Fe^{3+}) is reduced to ferrous iron (Fe

$^{2+}$) to facilitate its removal. The third stage leach is similar to the primary leach but is performed under more severe conditions to dissolve copper, which is returned to the primary leach stage. The residue at the end of this stage contains ± 60 % PGE + Au and is sent to Precious Metals Refinery (Hofirek and Halton, 1990, and Lindsay, 1988).

The solutions from the primary leach of the magnetic concentrate and the non-magnetic sulphide fraction (NCM) containing large quantities of nickel and copper with cobalt, is fed to the Base Metals Refinery to recover the valuable metals. A simplified block flow diagram of the Base Metals Refinery is shown in Figure 2.7. In the base metals refinery, the NCM is initially fed to the copper removal stage (atmospheric leach) where it is contacted with the primary pressure leach discharge solution (Figure 2.7). All the dissolved copper and iron is rejected into the residue producing virtually Cu, Fe and acid free solution, while stoichiometrically equivalent amounts of nickel are dissolved (Hofirek and Halton, 1990). After thickening the solids are fed to the primary pressure leach whilst the nickel rich solution undergoes further purification. The copper removal stage residue is subjected to a pressure leach in Sherritt Gordon horizontal autoclaves, with copper spent electrolyte from copper tank house being used as the leaching solution. Only the leading two compartments of the autoclave are aerated at a controlled rate to ensure maximum nickel dissolution; the last 2 compartments are operated without air in order to re-precipitate part of the copper, which was either dissolved in the oxidizing phase or supplied with the copper spent electrolyte. After thickening and filtration, the primary leach residue then undergoes secondary copper leaching. In this stage all the autoclave compartments are aerated to ensure almost complete dissolution of copper and the residue nickel, whilst large proposition of iron is re-precipitated in the form of jarosite or hematite. The slurry is then filtered and the residue is treated in a small Pyrometallurgical section for the recovery of the residual PGEs, which are recycled to the converters. The copper-rich filtrate is treated with sodium sulphite solution to precipitate selenium. After filtration the

selenium-rich cake is combined with the secondary leach residue (Figure 2.7). The purified copper solution goes to copper electrowinning. Copper spent electrolyte is recycled to both pressure leach stages where it is used as lixiviant.

The solution from the atmospheric leach is subjected to further purification to remove lead and cobalt prior to nickel electrowinning. The lead is precipitated from the solution by barium hydroxide. The lead removal cake obtained is recycled to the smelter. Cobalt is removed from the Ni-rich solution by precipitation with nickelic hydroxide. The cobalt removal cake is initially leached at a controlled pH in nickel spent electrolyte to dissolve the nickel hydroxides, followed by a reducing leach in sulphuric acid to dissolve the remaining nickel with the cobalt. After further impurity (Cu, Fe and Pb) removal the cobalt is separated from the nickel by solvent extraction with D2EHPA. Pure cobalt solution is crystallized to saleable $CoSO_4.7H_2O$ whilst the nickel-rich raffinate is transferred to the Sulphur removal stage (Hofirek and Halton, 1990).

The Ni-rich solution from the cobalt removal stage is transferred to nickel tankhouse for electrowinning. Any sulphides, sulphur oxidized in the leaching stages is removed at the end of the nickel circuit in the “sulphur removal” stage (Figure 2.7). After this stage, part of the nickel spent electrolyte is neutralized with sodium hydroxide, generating a sodium sulphate solution, which is used to form crystals.

Western Platinum Base Metals Refinery

Western Platinum Base Metals Refinery (BMR) is situated about 70 km northwest of Johannesburg and is owned by Lonrho Platinum, which comprises Western Platinum Limited (WPL) and Eastern Platinum Limited (EPL). A simplified block flow diagram of the Base Metals Refinery is shown in Figure 2.8. The converter matte can either be crushed or water granulated. According to Steenekamp and Dunn (1999), water granulation of the matte was preferred to pouring it into moulds and allowing it to cool down before crushing. This is due

to the fact that during the mould cooling process some of the sulphides in the matte are oxidised to form magnetite ($FeO.Fe_2O_3$) and trevorite ($NiO.Fe_2O_3$). These ferrite species are insoluble in the BMR leaching stages and report to the PGM concentrate. To reduce ferrite formation during the cooling period, and hence prevent contamination of the PGM concentrate, water granulation of the matter was implemented. The granulated matte was found to be more reactive than the crushed matte with more copper and PGM precipitation from the solution.

The converter matte is ball milled in a closed circuit. After thickening the matte slurry is pumped to the first stage leach, which is an atmospheric leach consisting of a number of agitated tanks in series. Both sulphuric acid and copper spent electrolyte are used as leaching solution, and oxygen is sparged into the first two tanks. More than 50 % Ni extraction is achieved at this stage while copper is precipitated from solution (Steenekamp and Dunn, 1999; Brugman and Kerfoot, 1986). The slurry is then fed to a thickener to obtain a nickel-rich overflow solution from which nickel sulphate hexahydrate is crystallized. The underflow slurry is fed to the second stage pressure leach step conducted in horizontal autoclaves. Oxygen and copper spent electrolyte and sulphuric acid are added to the autoclave to extract most of the remaining nickel and copper. The autoclave discharge slurry is filtered to obtain a PGE concentrate. The concentrate is further upgraded by leaching, dried and dispatched to Western Platinum Refinery (WPR) in Brakpan, Johannesburg, about 150 km from the BMR. The filtrate is heated and mixed with aqueous sulphur dioxide solution to precipitate selenium and tellurium as copper selenide and telluride. Some of the PGEs that also dissolved into solution are co-precipitated. The residue is then processed to recover some of the valuable metals (Figure 2.8). Solution from the selenium removal stage is fed to copper electrowinning circuit to recover copper as cathodes.

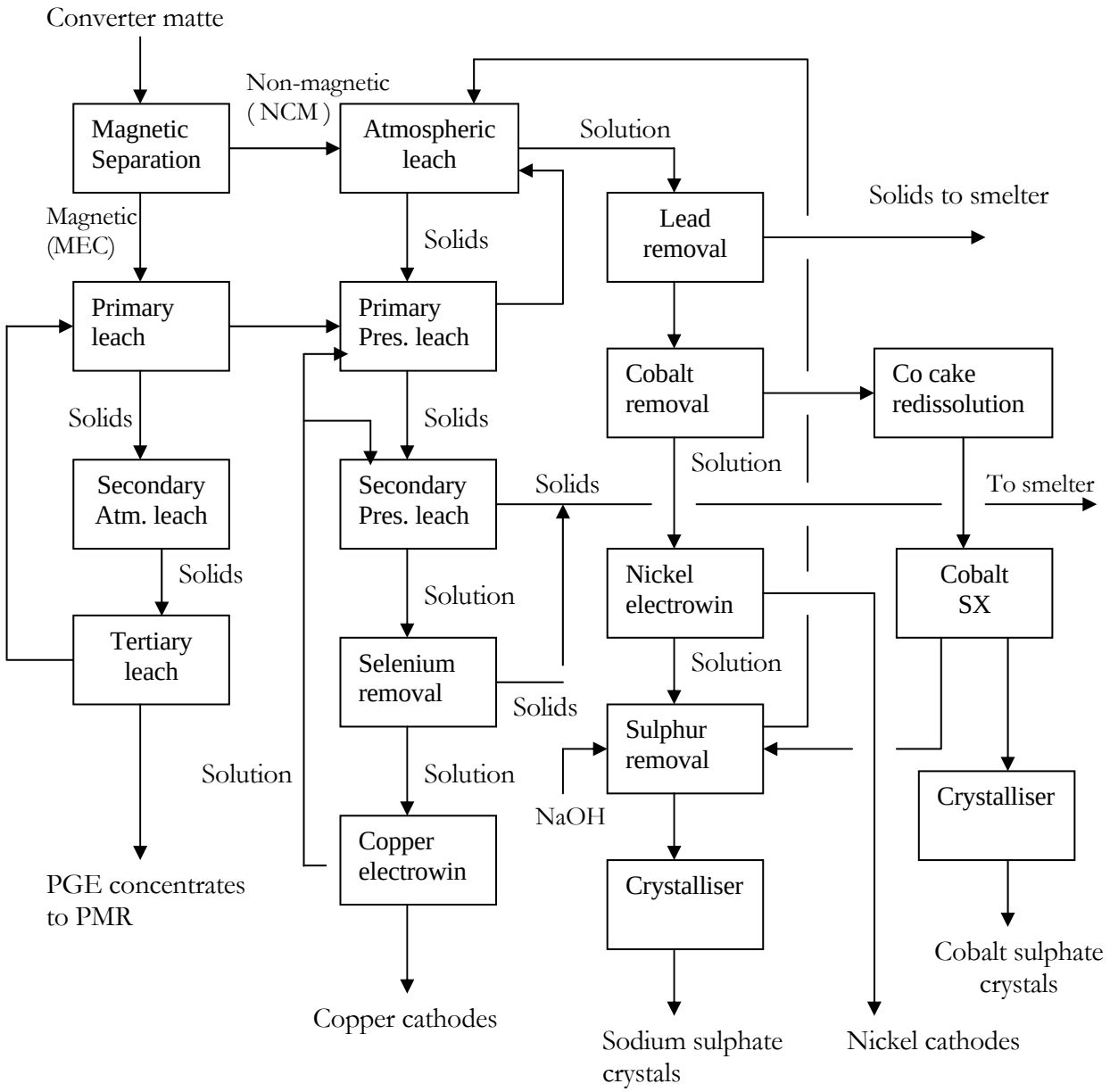

Figure 2.7: Simplified block flow diagram of the Rustenburg Base Metals Refining process.

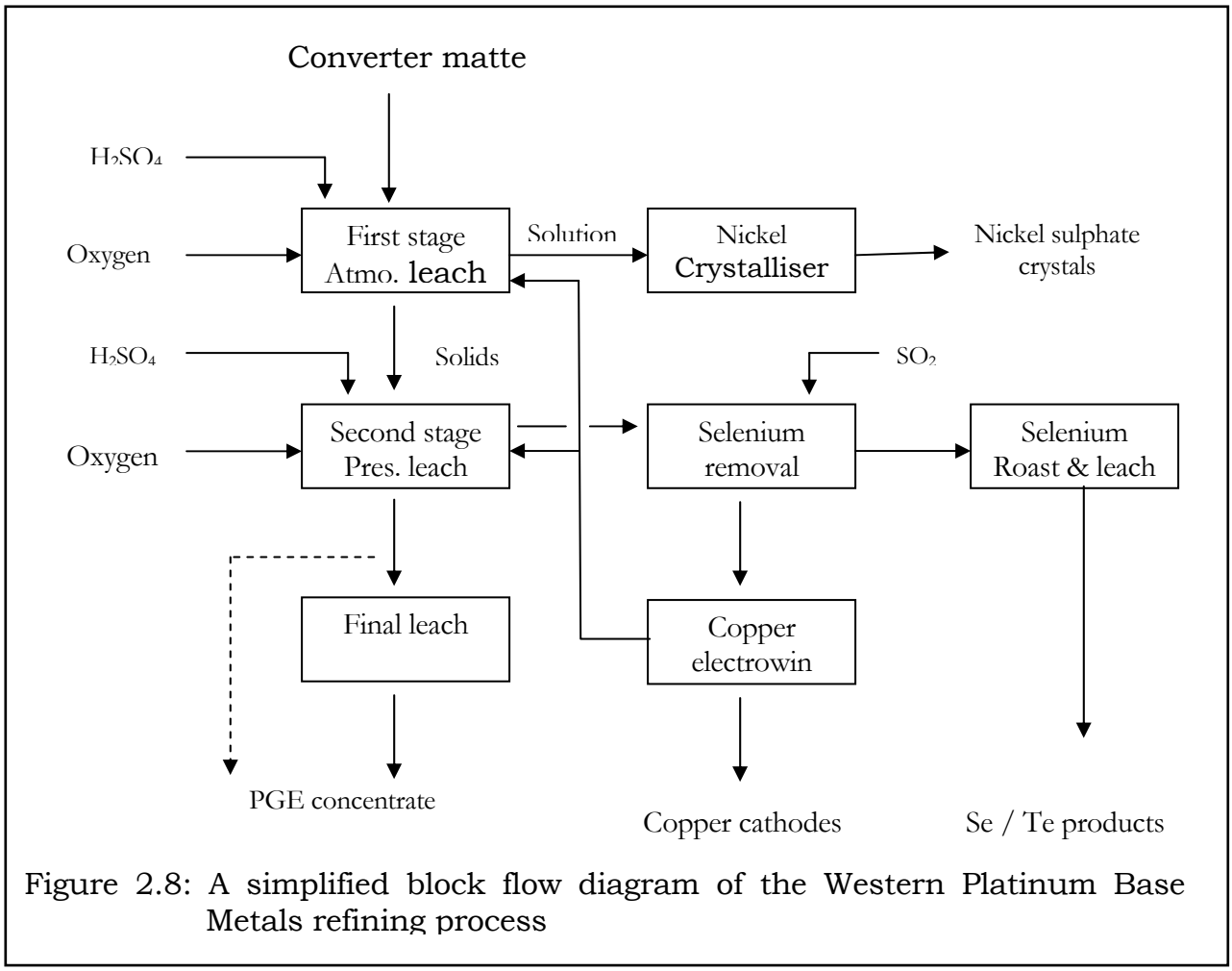

Figure 2.8: A simplified block flow diagram of the Western Platinum Base Metals refining process

Outokumpu nickel-copper matte leaching process

The Outokumpu nickel-copper matte leaching process has been described by Knuutila et al. (1997), Fugleberg et al. (1995) and Nyman (1992). The process consists of both atmospheric and pressure leach stages. Two types of matte are produced, namely matte obtained from a flash smelting furnace (FSF) and matte obtained after cleaning the flash furnace slag through an electric furnace (EF). Detailed description of the smelting process is given in section 2.3. Prior to leaching, the two types of matte are wet ground in ball mills to reduce the

granulated particle size followed by leaching in separate circuits (Figure 2.5). The main leaching agents are sulphuric acid and oxygen.

The Flash Smelting Furnace (FSF) matte leaching circuit

The FSF matte leaching circuit consists of three stages connected counter-currently. The first stage is the atmospheric copper removal stage whose objective is to produce a nickel-cobalt sulphate solution with low concentrations of iron, copper, arsenic and other impurities. The leaching is conducted in mechanically agitated reactors with oxygen inlet below the stirrer. The leaching solution is sulphuric acid and recycled streams (Figure 2.9). The product solution from the copper removal stage is separated from solids by a thickener and passed through a press filter before it goes to the cobalt and nickel recovery circuits. The leach residue is fed to the next stage, the nickel atmospheric leach, where more nickel and cobalt are leached while Cu, Fe, As, Sb and Bi are kept to the minimum. After solid-liquid separation, using a thickener, the solution is recycled to the copper removal stage while the thickener underflow is fed to the nickel pressure leach stage.

The aim of the nickel pressure leach is to bring unleached or precipitated nickel and iron into solution and produce an outlet for copper in the form of copper sulphide. This stage consists of a selective nickel leaching part where no or little oxygen is used and a total leaching part with efficient oxidation. Most of the nickel is leached at this stage, while the copper is precipitated as sulphide. After solid-liquid separation the solution is routed to the Electric Furnace (EF) matte leach circuit. The leach residue, consisting mostly of copper sulphide, is split into two portions: one portion goes to the copper smelter and the other portion is an outlet for precious metals. This last portion is fed to the total pressure leach where the residual base metal sulphides are leached almost completely to produce precious metal concentrates.

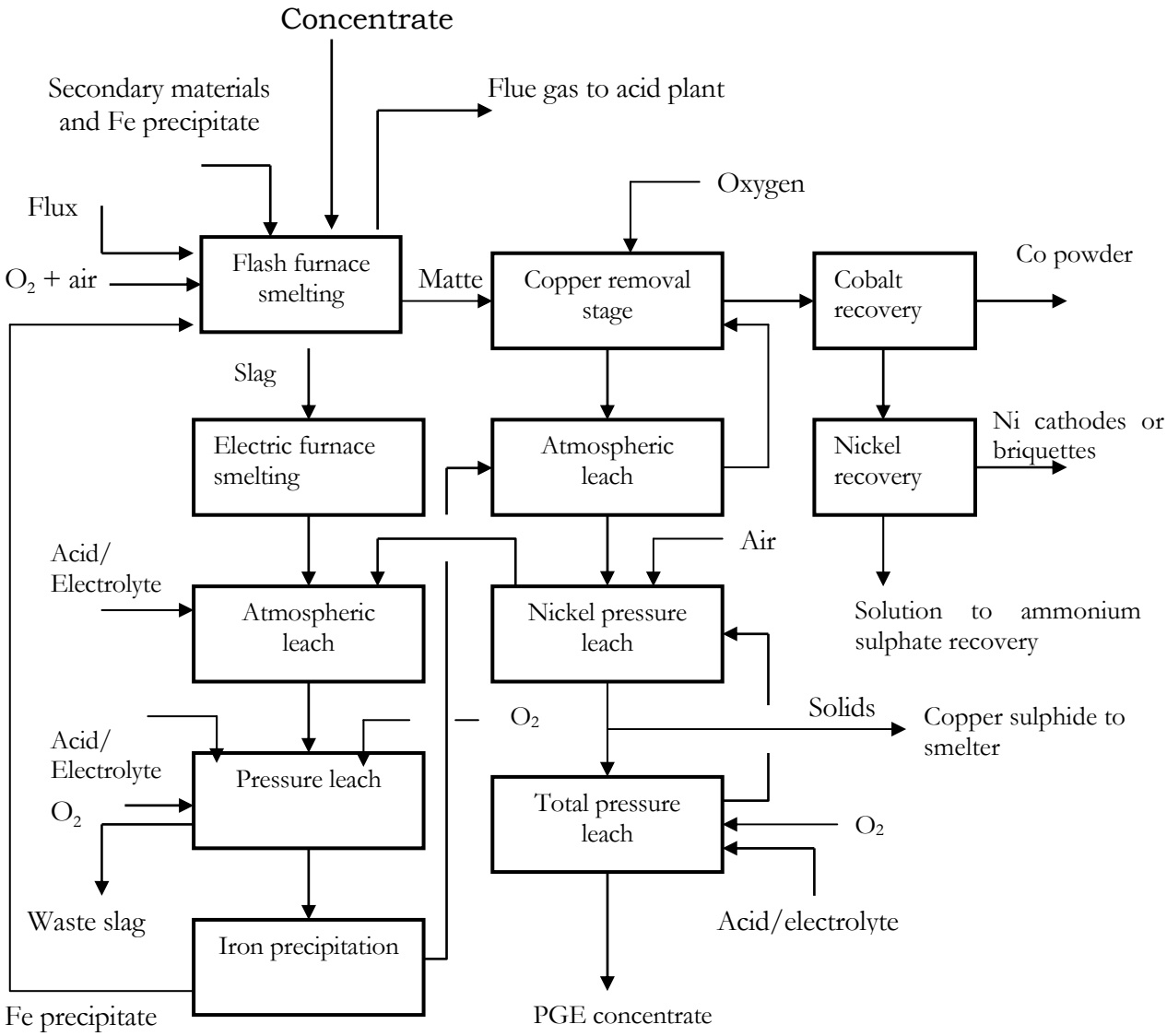

Figure 2.9: Block flow diagram of the Outokumpu nickel-copper smelter and matte leaching process

The Electric Furnace (EF) matte leaching circuit

The objective of the electric furnace matte leaching circuit is to leach nickel, copper and cobalt from the cleaned FSF slag (EF matte), and precipitate the iron as goethite-hematite. The main component of the EF matte is metallic alloy (Ni-Fe alloy), copper may also be present in the alloy. Pentlandite is the major sulphide component of the matte. The EF matte is leached in two stages: firstly an atmospheric leach followed by a pressure leach stage (Figure 2.9). High recoveries of nickel, cobalt and copper are achieved and also iron precipitation is optimised. The iron is precipitated as goethite in the atmospheric leach and as hematite in the pressure leach stage. Solid-liquid separation is carried out in thickeners. After thickening the solution from the pressure leach stage goes to an iron removal autoclave where iron is precipitated and recycled to the flash smelting furnace.

2.3 Chemistry of Nickel-Copper Matte Leaching Processes

Knuutila et al. (1997) described the processing of nickel-copper matte at Outokumpu Harjavalta Metals Oy in Finland, and presented an overview of the matte leaching chemistry. The process consisted of both atmospheric and pressure leaching of matte in sulphuric acid/nickel sulphate solution, with oxygen being the oxidizing agent (see section 2.2.4). Two types of matte were produced namely matte obtained from a flash furnace and that obtained after cleaning the flash furnace slag through an electric furnace. Both types of matte were first atmospherically leached prior to pressure leach stage (Figure 2.9).

The main minerals in the blast furnace matte were heazlewoodite (Ni_3S_2), Copper Sulphide (Cu_2S) and a Ni-Cu alloy. Of these minerals the most reactive phase was noted to be the metallic alloy followed by Ni_3S_2 and then by Cu_2S. The main component of the electric furnace matte was a metallic alloy (Ni-Fe) which may

be mixed with copper; while pentlandite $(Ni,Fe)_9S_8$ was the major sulphide component of the matte.

The atmospheric leaching of the blast furnace matte was carried out in two stages, with the important reactions in the first stage being the precipitation of copper and the simultaneous leaching of nickel. The most important net reactions were the following:

$$CuSO_4 + Ni\text{-}Cu + 0.5O_2 \rightarrow Cu_2O + NiSO_4 \quad (2.18)$$

$$2CuSO_4 + 2Ni_3S_2 + 0.5O_2 \rightarrow Cu_2O + 2NiSO_4 + 4NiS \quad (2.19)$$

$$3CuSO_4 + 2Ni_3S_2 + O_2 + 2H_2O \rightarrow Cu_3SO_4(OH)_4 + 2NiSO_4 + 4NiS \quad (2.20)$$

$$2CuSO_4 + Ni\text{-}Cu + O_2 + 2H_2O \rightarrow Cu_3SO_4(OH)_4 + NiSO_4 \quad (2.21)$$

Any iron in the leaching solution was virtually Fe^{2+}, and was oxidized and precipitated as FeOOH:

$$FeSO_4 + Ni_3S_2 + 0.75O_2 + 0.5H_2O \rightarrow FeOOH + NiSO_4 + 2NiS \quad (2.22)$$

However, some $Fe(OH)_3$ was also formed. Other elements present in the matte like arsenic, antimony and bismuth were mainly precipitated together with iron in poorly soluble ferric compounds similar to ferric arsenate, $FeASO_4$.

In the second stage of the atmospheric leaching of the flash furnace matte, the objectives were to leach remaining Ni_3S_2 as completely as possible leaving NiS as the secondary phase prior to pressure leach and to mimimise Cu, Fe, As, Sb, and Bi levels in the solution.

The main reaction was the leaching of Ni_3S_2 according to reaction (2.23):

$$Ni_3S_2 + H_2SO_4 + 0.5O_2 \rightarrow NiSO_4 + 2NiS + H_2O \quad (2.23)$$

Copper sulphide (Cu_2S) also reacted, but more slowly than heazlewoodite (Ni_3S_2). A small amount of copper was leached, but the bulk of it was converted into more oxidized sulphide species; with the most common species being $Cu_{1.8}S$ and CuS (reactions 2.24 and 2.25).

$$Cu_2S + 0.2H_2SO_4 + 0.1O_2 \rightarrow Cu_{1.8}S + 0.2CuSO_4 + 0.2H_2O \quad (2.24)$$

$$Cu_{1.8}S + 0.8H_2SO_4 + 0.4O_2 \rightarrow CuS + 0.8CuSO_4 + 0.8H_2O \quad (2.25)$$

Iron was again precipitated as FeOOH (reaction 2.22).

The atmospheric leach residue was then fed to the nickel pressure leach section to solubilise unleached or precipitated nickel and iron, and produce an outlet for copper in the form of copper sulphide.

The pressure leaching section consisted of a two stage selective nickel leaching process. In the first stage no or little oxygen was added; NiS and eventually remaining Ni_3S_2 were converted into digenite ($Cu_{1.8}S$) according to the following reactions:

$$6NiS + 9CuSO_4 + 4H_2O \rightarrow 5Cu_{1.8}S + 6NiSO_4 + 4H_2SO_4 \quad (2.26)$$

$$8Ni_3S_2 + 27CuSO_4 + 4H_2O \rightarrow 15Cu_{1.8}S + 24NiSO_4 + 4H_2SO_4 \quad 2.27)$$

NiS reacted very fast, whereas the leaching rate of Ni_3S_2 was much slower. CuS and Cu^{2+} ions also reacted to form $Cu_{1.8}S$ and sulphuric acid according to reaction (2.28):

$$6CuS + 3CuSO_4 + 4H_2O \rightarrow 5Cu_{1.8}S + 4H_2SO_4 \quad (2.28)$$

As the solution was acidic, Fe^{3+} in solution was reduced by the sulphide:

$$Fe_2(SO_4)_3 + 1.25Cu_{1.8}S \rightarrow 2FeSO_4 + 1.25CuS + CuSO_4 \quad (2.29)$$

When Fe^{3+} was removed from the solution, dissolution of FeOOH, $FeASO_4$ as well as Sb and Bi compounds proceeded as long as free acid and reducing sulphide were available. On the contrary, Se was precipitated from the solution in this step.

In the second stage of the pressure leaching process where oxygen was added and efficient oxidisation occurred, any remaining Ni_3S_2 was leached according to reaction (2.23) whereas NiS and CuS were leached according to reaction (2.30):

$$MeS + 2O_2 \rightarrow MeSO_4, \text{ where Me = Ni, Cu} \quad (2.30)$$

Thus, the sulphides of the matte were leached almost completely, and the leach residue from the pressure leach stage was composed mainly of precious metals.

The leaching circuit for the electric furnace matte also consisted of atmospheric and pressure leach stages (Figure 2.9). The electric furnace matte can react vigorously with sulphuric acid to form hydrogen and hydrogen sulphide if mixing and supply of oxygen are not adequate, especially at high temperatures. The formation of these unwanted products was prevented by providing excess oxygen into the solution and by vigorous agitation. The metallic alloys were leached in the atmospheric leach stage whereas the sulphides were leached under high pressure. High recoveries of nickel, copper and cobalt were achieved with iron precipitation. The leaching of this matte whose main minerals were a metallic alloy (Ni-Fe) which may be mixed with copper and pentlandite $(NiFe)_9S$ can roughly be described by the following overall reactions.

$$Me + H_2SO_4 + 0.5O_2 \rightarrow MeSO_4 + H_2O \quad \text{where Me = Ni, Cu, Fe} \qquad (2.31)$$

The pentlandite reacts according to reaction (2.32)

$$(NiFe)_9S_8 + H_2SO_4 + 16.5O_2 \rightarrow 9(Ni,Fe)SO_4 + H_2O \qquad (2.32)$$

Hydrogen can be produced according to reaction (2.33), while hydrogen sulphide may be formed by reaction (2.34):

$$Ni\text{-}Fe + 2H_2SO_4 \rightarrow NiSO_4 + FeSO_4 + 2H_2 \qquad (2.33)$$

$$(NiFe)_9S_8 + 4H_2SO_4 \rightarrow 5NiS + 4FeSO_4 + 3H_2S + H_2 \qquad (2.34)$$

Iron was mainly precipitated as goethite in the atmospheric leach (reaction 2.35), but can also be precipitated as jarosite at pH values < 2. In the pressure leach it was precipitated as hematite according to reaction (2.36):

$$2FeSO_4 + 3H_2O + 0.5O_2 \rightarrow 2FeOOH + 2H_2SO_4 \qquad (2.35)$$

$$2FeSO_4 + 2H_2O + 0.5O_2 \rightarrow Fe_2O_3 + 2H_2SO_4 \qquad (2.36)$$

Fugleberg et al. (1995) also presented an overview of the chemistry of matte leaching at the Harjavalta operations in Finland. They also noted that in the oxidative acid leaching of nickel-copper matte the metallic phase was the most reactive, followed by heazlewoodite (Ni_3S_2). Chalcocite (Cu_2S) was the most stable phase. In the atmospheric leach, the metallic phase reacts first according to the following reactions:

$$Ni^o + H_2SO_4 + 0.5O_2 \rightarrow NiSO_4 + H_2O \qquad (2.37)$$

$$2Cu^o + 0.5O_2 \rightarrow Cu_2O \qquad (2.38)$$

$$3Cu^{o} + H_2SO_4 + H_2O + 1.5O_2 \rightarrow CuSO_4.2Cu(OH)_2 \quad (2.39)$$

The copper forms either cuprite (Cu_2O) or basic copper sulphate antlerite ($CuSO_4.2Cu(OH)_2$) depending on pH and availability of oxygen. When the metallic phase has reacted, heazlewoodite will be leached followed by chalcocite according to reactions (2.23) – (2.25).

Under certain conditions, with excessive oxidation, millerite (NiS) can be converted to polydymite (Ni_3S_4):

$$4NiS + H_2SO_4 + 0.5O_2 \rightarrow Ni_3S_4 + NiSO_4 + H_2O \quad (2.40)$$

Fugleberg et al. (1995) indicated that studies conducted at Outokumpu showed that:

- Cu^{2+} will react with Ni_3S_2, NiS and Ni_3S_4, and the resulting copper sulphides will be $Cu_{1.96}S$, $Cu_{1.8}S$ and $Cu_{1.8}S$ respectively.
- The reaction rate for NiS is very fast, but the rate for both Ni_3S_2 and Ni_3S_4 are least one order of magnitude lower.

The overall leaching reactions for heazlewoodite and polydymite would be given by reaction (2.41) and (2.42), respectively.

$$8Ni_3S_2 + 27CuSO_4 + 4H_2O \rightarrow 15\ Cu_{1.8}S + 24NiSO4 + 4H_2SO_4 \quad (2.41)$$

$$8Ni_3S_4 + 45CuSO_4 + 28H_2O \rightarrow 25Cu_{1.8}S + 24NiSO_4 + 28H_2SO_4 \quad (2.42)$$

It was found that the ideal feed to the pressure leach should contain only millerite, the formation of polydymite should be avoided.

Llanos et al. (1974) carried out a study of the atmospheric leaching response of Ni-Cu mattes with varied composition at the Port Nickel Refinery, Louisiana, USA. The major phases in the matte were Ni_3S_2, Cu_7S_4 and Ni-Cu alloy, with

traces of cobalt and iron. It was observed that contact of the matte with the lixiviant (H_2SO_4/Ni-Cu solution) caused a rapid rise in nickel concentration in solution due to the cementation reaction:

$$Ni^o + Cu^{2+} \rightarrow Ni^{2+} + Cu^o \quad (2.43)$$

However, with matte high in copper and sulphur, high concentration of copper was observed in the early leaching stages probably due to the oxidation and dissolution of metallic copper from the Ni-Cu alloy, according to reactions (2.44) and (2.45):

$$2Cu^o + \tfrac{1}{2}O_2 \rightarrow Cu_2O \quad (2.44)$$

$$Cu_2O + 4H^+ + \tfrac{1}{2}O_2 \rightarrow 2Cu^{2+} + 2H_2O \quad (2.45)$$

It was believed that during the first minutes of leaching, more copper was generated by reaction (2.45) than was consumed by reaction (2.43). When the solution pH rose to a value of 2, the rate of reaction (2.45) decreased sharply. Copper oxide then accumulated on the unreacted matte particles and almost completely prevented further oxidation.

In high-sulphur mattes, most of the nickel was present as Ni_3S_2 and the solubilization of one atom of nickel from the sulphide takes place according to reaction (2.46):

$$Ni_3S_2 + 2H^+ + \tfrac{1}{2}O_2 \rightarrow Ni^{2+} + 2NiS + H_2O \quad (2.46)$$

Reaction (2.46) was believed to be controlled by the rate of oxygen transfer from the gas to the aqueous phase when leaching high sulphur mattes, but that it was unimportant for low-sulphur mattes because of the much greater effect of reaction (2.43). This is because the Ni_3S_2 to alloy weight ratio, depends on the

matte sulphur content, with the ratio becoming smaller as sulphur content decreases. Aqueous copper also reacts with Ni_3S_2 in the absence of oxygen according to the following reaction:

$$Ni_3S_2 + 2Cu^{2+} \rightarrow Cu_2S + NiS + 2Ni^{2+} \quad (2.47)$$

In the presence of oxygen, the interaction between Ni_3S_2 and Cu^{2+} probably occurs as in reaction (2.48):

$$Ni_3S_2 + 2Cu^{2+} + \tfrac{1}{2}O_2 \rightarrow 2NiS + Ni^{2+} + Cu_2O \quad (2.48)$$

At high pH values, aqueous copper precipitates in the form of basic copper sulphates:

$$3Cu^{2+} + SO_4^{2-} + 4H_2O \rightarrow CuSO_4.2Cu(OH)_2 + 4H^+ \quad (2.49)$$

The degree and the rate of this hydrolysis reaction are said to be dependent on temperature. Increasing the leaching temperature increases the extent of copper hydrolysis and chemical reaction rates, as well as diffusion rates. It also lowers the solubility of oxygen in the leach. The hydrolysis of Cu^{2+} becomes rate controlling above pH 3.9, particularly during leaching of low-sulphur mattes. The acid generated during hydrolysis further reacts with Ni_3S_2 and Cu_2O as in reactions (2.45) and (2.46). These reactions continue until all aqueous copper is either precipitated as basic sulphate or consumed via either reaction (2.43) or reaction (2.48).

The $Cu_{1.75}S$ initially present in the matte undergoes a transformation into $Cu_{1.95}S$, the transformation is thought to proceed as in reactions (2.50) and (2.51:

$$10Cu_{1.75}S + 3Cu^{2+} + 4H_2O \rightarrow 9Cu_{1.95}S + SO_4^{2-} + 8H^+ \quad (2.50)$$

Cathodic conversion of $Cu_{1.75}S$ into $Cu_{1.95}S$ is also possible via reaction (2.51):

$$Cu_{1.75}S + 0.2Cu^{o} \rightarrow Cu_{1.95}S \quad (2.51)$$

The mineral CuS was also observed in the leach residue, it was probably formed by reaction of dissolved Cu^{2+} with the hydrogen sulphide gas produced as an intermediate product (reaction 2.52)

$$Cu^{2+} + H_2S \rightarrow CuS + 2H^{+} \quad (2.52)$$

In conclusion Llanos et al. (1974) noted that the time required to effectively reject copper from solution and leach the matte in question is inversely proportional to the sulphur content in the matte, but almost insensitive to the matte Ni/Cu ratio. The rate of nickel dissolution is controlled by the rate of copper cementation on nickel during the first few minutes of leaching until a pH value of 3.9 is attained; thereafter oxygen transfer between gas and liquid phase controls the rate of dissolution. At higher pH values hydrolysis of Cu^{2+} and subsequent precipitation of basic copper sulphate dictates the time required to attain a final pH of 5.3. The Ni/Cu ratio of the matte at one sulphur level has little effect on the relative ratio of Ni_3S_2 to Ni^{o} in the matte. They observed also that if the molar amount of copper plus acid per mole of nickel in the matte remains constant, variations in the Cu^{2+} / H_2SO_4 ratio of the leaching solution have little effect on the total nickel dissolution from the matte. The higher the molar ratio of aqueous copper plus free acid to nickel in the matte, the longer the leaching time and the greater the nickel extraction. Generally, the leaching time was inversely proportional to the pulp density, the higher the pulp density the faster the leaching kinetics. Iron concentration in either the matte or the lixiviant has adverse effect on the leaching kinetics, the higher the iron content the longer the leaching time.

Other studies on the atmospheric leaching of Ni-Cu matte include investigations by Filmer (1981) and Symens et al. (1979). Symens et al. (1979) studied the atmospheric leaching of matte at the Port Nickel Refinery. Their work investigated special measures necessary in operating the atmospheric leach circuit to process mattes containing in excess of 2% iron. High iron concentrations in leach systems have been reported to cause unfavourable leach response, for example they increase total leaching time (Llanos et al. (1974), and Dutrizac and Chen (1987). Two types of matte were studied, which were categorized as high sulphur (19.6% S) and low sulphur (15.2% S). The mattes composed of Ni_3S_2, Cu_2S containing exsolved CuS, Ni–Fe alloy, entrapped slag particles, some copper and minor cobalt. Like other studies done after Llanos et al. (1974), this study also found that sulphur content in the matte has an effect on the leaching characteristics of the matte in that the lower the sulfur, the faster copper is rejected from solution regardless of the electrolyte ratio of H_2SO_4 to aqueous copper in the lixiviant. Conversely, the rate at which iron is rejected from solution is faster the higher the sulphur content of the matte and the lower the H_2SO_4/Cu ratio of the leaching solution. It was also found that fast oxidation and precipitation of iron from the nickel leach liquor is favoured by low temperatures. On the other hand, the lower the leach temperature the slower copper is rejected from solution. Copper is removed from the leach system as Cu^o and Cu_2O according to reactions (2.43), and reactions (2.44), (2.48), (2.18) and (2.19), respectively. It can also be precipitated as CuO via reaction 2.53:

$$Cu_2O + ½O_2 \rightarrow 2CuO \qquad (2.53)$$

The study showed that the precipitation of copper between pH 1.5 and 4.0 is accelerated by operating under one or a combination of the following conditions:

- High H_2SO_4 /Cu^{2+} ratio in the leaching solution.
- Low sulphur matte feed (i.e. high amount of Ni-Fe alloy phase).
- High leaching temperature.

- Under the above conditions copper removal is mainly attributable to its cementation by the alloy phase of the matte. Copper precipitation above pH 4 is believed to be mainly due to hydrolysis according to reaction (2.49).

Dissolution of copper also occurs above pH 4 when either too much oxygen or oxygen at too high a partial pressure is introduced into the system. Perhaps excess oxygen accelerates conversion of Cu^o to Cu_2O by reaction (2.44) and perhaps to CuO which is relatively soluble (reaction 2.53). This redissolution is reduced or avoided by decreased agitation and /or oxygen partial pressure, or by increasing the solution temperature.

Aqueous iron was removed via the following reactions:

$$2Fe^{2+} + 2H^+ + \tfrac{1}{2}O_2 \rightarrow 2Fe^{3+} + H_2O \qquad (2.54)$$

$$Fe^{3+} + 3H_2O \rightarrow Fe(OH)_3 + 3H^+ \qquad (2.55)$$

Symens et al. (1979) noted that precipitation of iron started after the first hour of leaching. In general the rate of iron oxidation is directly proportional to the oxygen partial pressure; hence the rate of oxygen dissolution becomes the controlling step such that an increase in agitation and decrease in solution temperature accelerate iron rejection. However, when catalysts are available in sufficient quantities, the reaction becomes independent of oxygen pressure. Copper is an effective catalyst for oxidation of ferrous iron, thus if aqueous copper is rapidly rejected from the leach solution during the early stage of leaching, the rejection of iron will be inhibited.

Dutrizac and Chen (1987) carried out a mineralogical study of the phases formed during the leaching of Nickel – Copper matte by the Sherrit Gordon process. The study identified the changes occurring in the sulphide phases during the leaching of the matte in $CuSO_4 – H_2SO_4 – O_2$ solutions. In this process, milled

Ni-Cu matte is mixed with H_2SO_4 and recycled copper spent electrolyte in feed tanks. Recycled copper cementation solids are added too. The pulp is then subjected to a number of pressure leaching stages. In the first stage leach nickel is selectively leached with $CuSO_4$-H_2SO_4-O_2 media while copper is precipitated as copper sulphides. In the second stage leach the pulp is reacted with O_2 and H_2SO_4 to dissolve the copper sulphides and residual nickel sulphides. The copper solution from the second stage leach is purified prior to copper recovery by electrolysis, while the nickel-rich solution from the first stage leach undergoes hydrogen reduction to recover nickel as powder and/or briquettes. The Sherrit Gordon process is described in detail in chapter 3.

The feed to the leaching circuit consists of mostly of Ni_3S_2, Cu_2S and $Cu_{1.96}S$ and Ni alloy. In the feed tanks both the Ni alloy in the matte and the recycled copper cementation product react rapidly according to the following reactions:

$$Ni^o + H_2SO4 + ½\ O_2 \rightarrow NiSO_4 + H_2O \qquad (2.56)$$

$$Ni^o + CuSO_4 \rightarrow Cu^o + NiSO_4 \qquad (2.57)$$

$$Cu^o + H_2SO_4 + ½O_2 \rightarrow CuSO_4 + H_2O \qquad (2.58)$$

A small amount of the Ni_3S_2 may also react, but this was not observed by the investigators (Dutrizac and Chen, 1987).

In the first stage leach circuit the Ni is completely leached according to reactions (2.56), (2.57) and (2.58); the Cu_2S or $Cu_{1.96}S$ originally present in the matte is oxidized to digenite and is complete within this stage:

$$Cu_2S + 0.1O_2 + 0.2H_2SO_4 \rightarrow Cu_{1.8}S + 0.2CuSO_4 + 0.2O_2 \qquad (2.59)$$

The reaction between the Ni_3S_2 and $CuSO_4 - H_2SO_4 - O_2$ leaching system also occurs in this stage:

$$2Ni_3S_2 + 3/2\ O_2 + 3H_2SO_4 \rightarrow 3NiSO_4 + Ni_3S_4 + 3\ H_2O \quad (2.60)$$

$$3Ni_3S_2 + 2CuSO_4 + 2O_2 + 4H_2SO_4 \rightarrow\ 6NiSO_4 + Ni_3S_4 + 2CuS + 4H_2O \quad (2.61)$$

Reaction (2.60) is believed to be initially more predominant than reaction (2.61). In the last section of the first stage leach circuit, Ni_3S_2 disappears and covellite (CuS) is the major phase. This suggests that equation (2.61) becomes more important and that digenite is attacked to some extent:

$$Cu_{1.8}S + 0.4O_2 + 0.8H_2SO_4 \rightarrow CuS + 0.8CuSO_4 + 0.8H_2O \quad (2.62)$$

However, work conducted by Plasket and Romanchuk (1978) on a similar process indicated that the leaching of Ni_3S_2 proceeds through NiS intermediary rather than Ni_3S_4, this was observed in this study too.

The discharge from the first stage leach, consisting of $Cu_{1.8}S$, CuS and Ni_3S_2 with various oxide and silicate phases, is further treated in the second stage leach circuit where the sulphides are further attacked by $H_2SO_4 - O_2$ (Dutrizac and Chen, 1987):

$$Cu_{1.8}S + 0.40_2 + 0.8\ H_2SO_4 \rightarrow CuS + 0.8CuSO_4 + 0.8H_2O \quad (2.63)$$

$$CuS + 2O_2 \rightarrow CuSO_4 \quad (2.64)$$

$$Ni_3S_4 + H_2O + 15/2\ O_2 \rightarrow 3NiSO_4 + H_2SO_4 \quad (2.65)$$

At this point, the leach residues contain oxide, silicate, sulphate or hydroxy – sulphate phases. Iron is present in the original matte both as oxide grains and as trace constituent of the Ni_3S_2, Cu_2S, or Ni alloy. Part of the iron is present as

magnetite and nickel ferrite. These were observed to report to the leach residue. Part of the iron dissolves, and this is variously precipitated and redissolved. It was suggested that iron precipitated mostly as ammonium jarosite (reaction 2.66), although some iron may also have precipitated as amorphous ferric arsenate (reaction 2.67).

$$NH_4^+ + 3Fe^{3+} + 2SO_4^{2-} + 6\ H_2O \rightarrow NH_4Fe_3(SO_4)_2\ (OH)_6 + 6H^+ \quad (2.66)$$

$$Fe^{3+} + AsO_4^{3-} + 2H_2O \rightarrow FeAsO_4 + 2H_2O \quad (2.67)$$

Dissolution of the ammonium jarosite occurs with the concomitant release of iron to the solution, especially when fresh acid is added to the circuit:

$$NH_4Fe_3(SO_4)_2(OH)_6 + 6H^+ \rightarrow\ NH_4^+ + 3Fe^{3+} + 2SO_4^{2-} + 6H_2O \quad (2.68)$$

Dutrizac and Chen (1987) concluded that during the pressure leaching of matte consisting predominantly of heazlewoodite (Ni_3S_2), chalcocite (Cu_2S) and a Ni alloy phase in $CuSO_4$-H_2SO_4-O_2 media, the Ni alloy is rapidly dissolved. The Cu_2S is oxidized to digenite ($Cu_{1.8}S$) and the Ni_3S_2 is dissolved and/or altered to soluble $NiSO_4$ and a mixture of polydymite (Ni_3S_4) and covellite (CuS). The resulting residue (from the first stage leach) consisting of $Cu_{1.8}S$, CuS and Ni_3S_4 is then re-leached in H_2SO_4-O_2 media to dissolve copper and residual nickel. The $Cu_{1.8}S$ is oxidized to CuS, and both the CuS and Ni_3S_4 are further oxidized to soluble sulphates. The oxide minerals pass through the leach circuit largely unaffected, although extensive dissolution of silicate particles occurs. Iron present in the sulphides or in the Ni alloy is dissolved and is subsequently precipitated as ammonium jarosite. The ammonium jarosite itself seems to dissolve to a limited extent in various parts of the circuit.

The chemistry of matte leaching process at Rustenburg Base Metals Refiners (RBMR) has been published by many workers (Hofirek and Halton, 1990; Hofirek

and Nafal, 1995; Hofirek and Kerfoot, 1992). The RBMR operations have been described in section 2.2.4 in this thesis. The work published by Hofirek and Kerfoot (1992) is of most interest and is reviewed below:

Chemistry of the nickel–copper matte leaching as well as its application to process control and optimisation at RBMR was extensively studied at laboratory and pilot-plant scales. The study evaluated chemical and mineralogical changes occuring during the leaching of non-magnetic sulphide fraction of the converter matte. The RBMR operations consist of a first stage atmospheric leach followed by a two – stage pressure leach in Sherritt Gordon horizontal autoclaves at temperatures in excess of 130 ^{o}C. Initially, the converter matte is separated magnetically into a PGM – containing metalic fraction and a non magnetic sulphide fraction (Figure 2.7). The non–magnetic material does not contain any Ni–Fe alloy but has two major mineralogical species present, namely heazlewoodite (Ni_3S_2) and djurleite ($Cu_{1.96}S$). Minor species which were identified included pentlandite $(Ni,Fe)_9S_8$, godlevskite (Ni_7S_6), bornite (Cu_5FeS_4) and idaite (Cu_5FeS_6).

In the atmospheric leach the non-magnetic is leached in a mixture of copper-nickel sulphate solution at a pH of about 2.5, temperature of 75-80 ^{o}C and an overall residence time of 12 hours. A detailed analysis of the atmospheric leach tests revealed three characteristic leaching steps defined by the pH of the leach slurry:

- Copper cementation (metathesis) up to a pH of 2.5 accompanied by the formation of $Cu_{1.96}S$ and NiS (Ni_7S_6).
- Iron hydrolysis in the pH range 2.5 – 4.5 accompanied by the formation of ferric hydroxide $Fe(OH)_3.x\ H_2O$ or basic ferric sulphate $Fe(OH)SO_4$.
- Copper hydrolysis in the pH range of 4.5 - 6 accompanied by the formation of basic cupric sulphate $Cu_3(OH)_4SO_4$ (antlerite).

The individual reaction steps may or may not be present, or may proceed simultaneously, depending on the initial conditions. According to the initial acidity three modes of atmospheric leach operation were characterised:

- An atmospheric leach in moderate or high acid solution of >10g/L, acid/matte ratio of >0.1w/w is distinguished by a rapid and complete copper rejection from solution during cementation, followed by iron hydrolysis. Copper hydrolysis is generally absent.

- An atmospheric leach in low acid solutions of 1 – 10g/L, acid/matte ratio of <0.1 w/w is characterised by a separate occurrence of all three reaction steps in the order of: cementation, iron hydrolysis and copper hydrolysis.

- An atmospheric leach in acid-free solutions of pH >2.5 is characterised by an absence of cementation. Iron hydrolysis and copper hydrolysis proceed simultaneously.

The chemical reactions proposed in this study were similar or identical to those described by Llanos et al. (1974) and Symens et al. (1979). The overall reaction of copper cementation (metathesis) is generally presented as

$$Ni_3S_2 + 2Cu^{2+} \rightarrow Cu_2S + NiS + 2Ni^{2+} \quad (2.69)$$

This reaction is said to proceed only in the presence of hydrogen ions and accelerates with increasing acid concentration. In excess acid, Heazlewoodite decomposes according to reaction (2.23), which is believed to proceed stepwise through the initial formation of godlevskite Ni_7S_6:

$$3Ni_3S_2 + 4H^+ + O_2 \rightarrow Ni_7S_6 + 2Ni^{2+} + 2H_2O \quad (2.70)$$

$$Ni_7S_6 + 2H^+ + \tfrac{1}{2}O_2 \rightarrow 6NiS + Ni^{2+} + H_2O \quad (2.71)$$

Any ferric ion present in the solution is reduced to ferrous state through reaction (2.72). It is assumed that the dissolved iron acts as an electron carrier and enhances the leaching rate:

$$Ni_3S_2 + 2Fe^{3+} \rightarrow 2Fe^{2+} + 2NiS + Ni^{2+} \quad (2.72)$$

At pH values above 2-2.5 iron dissolution and its reduction to ferrous state ceases and the ferrous ion is oxidised to the ferric ion by the oxygen in air:

$$2Fe^{2+} + 2H^{+} + 0.5O_2 \rightarrow 2Fe^{3+} + H_2O \quad (2.73)$$

At pH values above 3.5 ferric iron begins to hydrolyze to ferric hydroxide or basic ferric sulphate (parabutlerite):

$$Fe^{3+} + 3H_2O \rightarrow Fe(OH)_3 + 3H^{+} \quad (2.74)$$

$$Fe^{3+} + HSO_4^{-} + H_2O \rightarrow Fe(OH)SO_4 + 2H^{+} \quad (2.75)$$

At this pH value copper cementation ceases. Under normal operating conditions iron hydrolysis is almost complete in the pH range of 4.5 - 5. When a leach is done at pH values above 2.5, where iron and copper hydrolyze simultaneously at an Fe/Cu ratio above 1, the copper hydrolysis is completed prior to iron hydrolysis and iron concentration in solution (up to 1g/L) persists to pH 6 (Hofirek and Kerfoot, 1992). This residual iron is present in a non-hydrolysable ferrous state probably due to lack of cupric ions which is known to have a catalytic effect on the rate of ferrous ion oxidation (Burkin, 1966). Yuhua and Xianxuan (1990) also found that the rate of iron oxidation and hydrolysis was affected by the concentration of copper ions in the iron removal stage of the nickel purification circuit at Jinchuan Non-ferrous Metals Company in China. They noted that when the nickel solution was very low in copper the rate of iron removal was very slow. When the copper concentration was increased, the rate of

iron oxidation and hydrolysis increased significantly. They attributed the increase in the rate of iron oxidation to the fact that Cu^{2+} ions can oxidize Fe^{2+} ions in solution, according to reaction (2.76):

$$Fe^{2+} + Cu^{2+} \rightarrow Cu^{+} + Fe^{3+} \quad (2.76)$$

Cu^{2+} ions are reduced to Cu^{+} ions which are then re-oxidised to Cu^{2+} by air/oxygen.

The lack of cupric ions during iron hydrolysis was believed to be a probable reason for long reaction times required for complete iron rejection in moderate or high acid solutions (Hofirek and Kerfoot, 1992). At pH values above 4.5 the cupric ion hydrolyses to form basic cupric sulphate $Cu3(OH)_4SO_4$ (antlerite):

$$3Cu^{2+} + HSO_4^{-} + 4H_2O \rightarrow Cu_3(OH)_4SO_4 + 5H^{+} \quad (2.77)$$

Reaction (2.77) releases acid, which is consumed by the unreacted Ni_3S_2 or Ni_7S_6 according to reactions (2.70) and (2.71) and shift the equilibrium of reaction (2.77) in favour of basic cupric sulphate precipitation. If the pH rises above 6.5, basic nickel sulphate may start to precipitate.

The residue from the atmospheric leach (Figure 2.3), composing of heazlwodite (Ni_3S_2), godlevskite (Ni_7S_6), millerite (NiS), djurleite ($Cu_{1.96}S$) and antlerite ($Cu_3(OH)_4SO_4$), is first repulped with copper spent electrolyte prior to pressure leach. In the repulping tank reactions (2.69), (2.70) and (2.71) proceed to a significant extent, as well as dissolution of antlerite (reaction 2.78) and precipitated iron species.

$$Cu_3(OH)_4SO_4 + 5H^{+} \rightarrow 3Cu^{2+} + HSO_4^{-} + 4H_2O \quad (2.78)$$

After repulping and preheating of the slurry, the solids are essentially a mixture of millerite (NiS) and djurleite ($Cu_{1.96}S$) which are leached in the initial phase of

the oxidative pressure leach operation to produce polydymite (Ni_3S_4) and covellite (CuS) by reactions (2.79) and (2.80), respectively:

$$4NiS + 2H^+ + ½\ O_2 \rightarrow Ni_3S_4 + Ni^{2+} + H_2O \quad (2.79)$$

$$*^1Cu_2S + 2H^+ + ½\ O_2 \rightarrow CuS + Cu^{2+} + H_2O \quad (2.80)$$

However, it was found that a substantial part of the nickel (about 30%) was dissolved by direct oxidation of millerite to nickel sulphate:

$$NiS + 2O_2 \rightarrow Ni^{2+} + SO_4^{2-} \quad (2.81)$$

The authors observed that the rate of copper precipitation in the form of $Cu_3(OH)_4SO_4$ (reaction (2.77), and dissolution from the sulphide phase (reaction 2.80) were in a dynamic equilibrium, resulting in no pH and solution copper concentration changes. The iron redissolved in the feed preparation tank is reprecipitated again, but now most probably as jarosite or haematite.

In the non–oxidizing phase of the first stage pressure leach, significant nickel dissolution (up to 20%) and sulphur oxidation (up to 10%) occurred despite absence of oxygen and acid. A large quantity of copper was also precipitated from solution by metathesis:

$$NiS + Cu^{2+} \rightarrow CuS + Ni^{2+} \quad (2.82)$$

Copper is also precipitated as digenite (Cu_9S_5), with a minor amount of covellite (CuS). According to Hofirek and Kerfoot (1992) the mechanism of the reaction between polydymite (Ni_3S_4) and the cupric ion that forms digenite involves a

*1Djurleite ($Cu_{1.96}S$) in equation 2.80 is susbtituted with Cu_2S for the sake of simple stoichiometric co-efficients

range of non-stochiometric metal sulphides. The overall reaction can be represented by the following equation:

$$4Ni_3S_4 + 9Cu^{2+} + 8H_2O \rightarrow Cu_9S_5 + 9NiS + 3Ni^{2+} + 2SO4^{2-} + 16H^+ \quad (2.83)$$

It was also observed that polydymite remnants showed a high nickel deficiency, Ni : S ratio of 0.45. This was probably due to nickel substitution by copper prior to the formation of the discrete digenite phase (reaction 2.84):

$$Ni_3S_4 + xCu^{2+} \rightarrow Ni_3\text{-}xCu_xS_4 + xNi^{2+} \quad (2.84)$$

The solid residue from the first stage of the pressure leach (primary leach) is fed to the second stage of the pressure leach operation, the secondary leach (Figure 2.3). This stage is operated at 140-145 ^oC, pressure of 1050 kPa and 8 hours residence time. Air is sparged into all compartments of the autoclave at controlled rates (Hofirek and Kerfoot, 1992). The feed to the secondary pressure leach stage is composed of polydymite (Ni_3S_4 with Cu), Millerite (NiS), Digenite (Cu_9S_5), Covellite (CuS) and Antlerite ($Cu_3(OH)_4SO_4$). Contact of the feed solids with the spent electrolyte in the feed preparation tank results in redissolution of basic copper, iron and nickel sulphates (if present). In the autoclave, the major reaction in the initial phases of the leach is the decomposition of digenite:

$$Cu_9S_5 + 8H^+ + 2O_2 \rightarrow 5CuS + 4\ Cu^{2+} + 4H_2O \quad (2.85)$$

The generated covellite (CuS) is either directly oxidized to copper sulphate according to reaction (2.64), or can be decomposed to elemental sulphur by the leaching of copper from the covellite lattice:

$$CuS + 2H^+ + \tfrac{1}{2}O_2 \rightarrow Cu^{2+} + S^o + H_2O \quad (2.86)$$

Reaction (2.85) and (2.64) proceed simultaneously, oxidized covellite being substituted by covellite generated from digenite, so initially no change in covellite content occurs until digenite is depleted. The reaction sequence for the dissolution of the polydymite (Ni_3S_4) or copper – containing polydymite is obsecure, but the overall stoichiometry can be described by equation (2.87):

$$Ni_3S_4 + 7½O_2 + H_2O \rightarrow 3Ni^{2+} + 4SO_4^{2-} + 2H^+ \quad (2.87)$$

The millerite (NiS) is partially converted to polydymite (equation 2.79) as well as directly oxidized to nickel sulphate (equation 2.81).

At this high temperature (140 -145 ^oC) the ferric ion hydrolysis commences at a moderate acid concentration of about 30 g/L. Depending on the conditions, iron precipitates either as the sodium jarosite (reaction 2.88) or as haematite (reaction 2.89):

$$3Fe^{3+} + Na^+ + 2SO_4^{2-} + 6H_2O \rightarrow NaFe_3(OH)_6(SO_4)_2 + 6H^+ \quad (2.88)$$

$$2Fe^{3+} + 3H_2O \rightarrow Fe_2O_3 + 6H^+ \quad (2.89)$$

Both reactions release a considerable quantity of acid which is either consumed in the digenite decomposition (reaction 2.85) or results in acid concentration increase in the terminal phases of the leach. The residue from this stage is composed predominantly of iron precipitates.

The chemistry of Ni-Cu matte leaching at Lonrho Platinum's Base Metals Refinery was described by Steenekamp and Dunn (1999). Detailed description of the leaching process is given in section 2.2.4. The leaching process basically consisted of a two-stage operation (Figure 2.8). In the first stage the ground matte was leached in tanks in series at atmospheric pressure, with oxygen sparging into the first two tanks. Both concentrated H_2SO_4 and recycled tankhouse copper spent electrolyte were used as leaching solutions. Nickel and small quantities of cobalt were leached while copper and PGMs were precipitated

from solution. After thickening the copper free overflow solution was fed to the nickel sulphate crystalliser, while the underflow slurry was routed to the pressure leach stage. Oxygen and sulphuric acid were added to the autoclave to extract the majority of the remaining nickel and copper.

The atmospheric leach chemistry of nickel-copper mattes has been published by various workers, including Hofirek and Kerfoot (1992), Hofirek and Nofal (1995), Hofirek and Halton (1990), Knuutila et al. (1997), Fugleberg et al. (1995), Dutrizac and Chen (1987), Llanos et al. (1974). The reactions in the first atmospheric stage leach essentially comprise of oxidising rections of the type represented by equations (2.33), (2.46), (2.56) and metathesis reactions represented by (2.47) and (2.90).

$$5NiS + 2CuSO_4 \rightarrow Cu_2S + 2NiSO_4 + Ni_3S_4 \quad (2.90)$$

Steenekamp and Dunn (1999) presented a break-down of the principle reactions occurring in the pressure leach stage into two categories. First the dissolution of atmospheric leach hydrolysis products:

$$Cu(OH)_2CuSO_4 + H_2SO_4 \rightarrow 2CuSO_4 + 2H_2O \quad (2.91)$$

$$2Fe(OH)SO_4 + H_2SO_4 \rightarrow Fe_2(SO_4)_3 + 2H_2O \quad (2.92)$$

And secondly the oxidation of sulphide minerals according to reactions (2.23), (2.64), (2.81) and (2.93).

$$Cu_2S + H_2SO_4 + 2½O_2 \rightarrow 2CuSO_4 + H_2O \quad (2.93)$$

These reactions are exothermic and the heat released is almost proportional to the amount of sulphur being oxidised.

The hydrometallurgical operations at Impala Base Metals Refinery (BMR) have been described in chapter 3 of this document. The chemistry of the Ni-Cu leaching process of the BMR is similar to that of other Ni-Cu processing operations described earlier, especially those processes utilizing the Sherritt Gordon process. Detailed description of the chemistry of the Impala base metals refinery has been published by Plasket and Romanchuk (1978), Rademan et al. (1999), Forbes (1999), Plasket and Dunn (1986a) and Plasket and Dunn (1986b).

2.4 Kinetics of leaching process

Several models have been developed, and more are still being developed, that are used to evaluate the dissolution kinetics of metals during the leaching process. One of the commonly used model type is the shrinking core model (SCM, which applies to monosized spherical particles. Depending on the chemical-physical process controlling the leaching process, different equations can be applied. These equations, which are presented below, have been extensively discussed in the literature (Ahmed et al., 2000; Gbor et al., 2000; Herreros et al., 2002; Sato and Lawson, 1983).

For a surface chemical reaction controlled process:

$$1 - (1 - X)^{1/3} = K_1 t \qquad (2.94)$$

For a product layer/ash diffusion controlled process:

$$1\text{-}3(1\text{-}X)^{2/3} + 2(1\text{-}X) = K_2 t \qquad (2.95)$$

For mixed (surface and product layer/ash) controlled process:

$$[1\text{-}3(1\text{-}X)^{2/3} + 2(1\text{-}X)] + \alpha[1\text{-}(1\text{-}X)^{1/3}] = K_3 t \qquad (2.96)$$

Where X is the fraction reacted, K_1 and K_2 and K_3 reaction rate constants and t is the time. Detailed derivation of the equations for various controlling conditions in the SCM can be found in Levenspiel (1972), Sohn and Wadsworth (1979) and Szekely et al. (1976).

Gbor et al., 2000 carried out an investigation into the behaviour of Co and Ni during aqueous sulphur dioxide leaching of a nickel smelter slag. They used the shrinking core model to explain the behaviour of Co and Ni, and found that Co extraction was limited by both ash layer diffusion and surface chemical reaction; whereas Ni extraction was limited only by ash layer diffusion. In another investigation, the same authors (Ahmed et al. 2000) studied the dissolution behaviour of Co, Cu, Fe, Ni and Zn from smelter slag in aqueous sulphur dioxide. It was found that dissolution kinetics of Co, Fe, Zn, and Ni, could be described using the shrinking core model. The equation based on the assumption of ash layer control gave the best fit to the data.

A study was conducted of the dissolution kinetics of enargite (Cu_3AsS_4) with chlorine generated in solution by the reaction between sodium hypchlorite and hydrochloric acid (Herreros et al., 2002). The kinetics of the dissolution were characterized by two sequential stages: relatively fast reaction initially, while later the reaction become very slow. In the first stage, the fraction of Cu extracted (α) varied linearly with time according to $\alpha = K_1 t$, whereas in the second stage, the dissolution was represented by the shrinking core model controlled by diffusion through a porous product layer (equation 2.95). Colussi et al. (1983) carried out a study to obtain kinetic models for the leaching of Zinc – containing slags with sulphuric acid. They analyzed the data obtained according to the shrinking core models represented by equations 2.94 and 2.95. The dissolution kinetic mechanism was divided into two stages: The first was chemically controlled and the second diffusion controlled. Dutrizac and Chen (1995) investigated the leaching of galena (PbS) in the ferric sulphate media and found that relatively slow kinetics were observed in most instances, with the shrinking

core model for a diffusion - controlled reaction (equation 2.94) being closely obeyed. The diffusion controlled kinetics were attributed to the formation of a tenacious layer of $PbSO_4$ and S^o on the surface of the galena. Other authors who have used the shrinking core model (SCM) to describe the dissolution kinetics of materials/metals during the leaching process include Mulak (1985), Colek et al. (1987), Yu et al. (1973), and Youzbashi and Dixit (1991).

Dry and Bryson (1987) investigated the kinetics of leaching of a low-grade Fe-Ni-Cu-Co matte in ferric sulphate solution. They used the shrinking – particle surface area model to represent the change during leaching of the mineral surface area. This was combined with an electrochemical surface-reaction mechanism to represent the dissolution reactions. It was found that the surface reaction was rate-limiting and electrochemical in nature. Filippou and Demopoulos (1992) developed a reaction kinetic model for the leaching of industrial zinc ferrite particulates in sulphuric acid media. They found that the grain model for surface reaction control (Szekely et al. 1976) exhibited the best fit to the experimental data, as long as the rate equation was expressed as a function of the activity of H^+, instead of the concentration of H_2SO_4. Ma and Ek (1991) used a modified grain model to explain test results and to predict the relationship between conversion and leaching time (or other process variables) in a study conducted to investigate the leaching of a manganese carbonate ore in sulphuric acid. It was found that the rate controlling steps included diffusion in the porous residue layers and reaction within the mineral grains. Provis et al. (2003) developed a semi-empirical mathematical model for the acid-oxygen pressure leaching of Ni-Cu matte from Impala Platinum Refineries, based on data from batch leaching experiments conducted by Rademan (1995). The primary controlling factor in the leaching process was found to be galvanic inhibition of the more highly oxidized copper and nickel sulphide species by less oxidized species, particularly Ni alloy and Ni_3S_2. The kinetic model was based on first-order chemical reaction controlled rate expressions, as the reactions occurring were electrochemical in nature.

Several other kinetic models have been developed to describe the leaching process taking place in various leaching systems. Among these models are those developed for the non-oxidative dissolution of sphalerite (Crundwell and Verbaan, 1987) and for the pressure oxidation of pyrite in sulphuric acid media (Long and Dixon, 2004). Others have been developed for the leaching of pentlandite in acidic ferric sulphate solutions (Corrans and Scholtz, 1976) and for leaching of calcined magnesite using ammonium chloride (Raschman, 2000).

2.5 Summary

This chapter has reviewed the literature on the geology and mineralogy of the Platinum Group Metal (PGM) bearing ores of the Bushveld Complex of South Africa. The Bushveld Complex can be divided into four units namely the Lebowa Granite Suit, the Rashoop Granophyre Suite, the Rooiberg Group and the Rustenburg Layered Suite. In terms of the Platinum Group Element (PGE) mineralization, the Rustenburg Layered Suite is the most important unit. Within this unit there are four PGE mineralization of economic importance, namely the Merensky Reef, the Upper Group 2 (UG-2) chromitite layer, the Platreef and the Discordant Dunite Pipes. The most important mineral deposits of the Bushveld Complex are the sulphide ores (pyrrhotite, pentlandite, chalcopyrite and pyrite). In the Merensky Reef the base metal sulphides are found in association with Platinum Group Metals (PGMs). In the UG-2 chromitite the PGMs and base metal sulphides occur interstitially along chromite grain boundaries and locked in chromites.

The chapter has also describes the methods employed in the recovery of the Platinum Group metals (PGMs) from the ores; starting from milling to smelting of the ore, resulting in the production of nickel-copper matte that contains PGMs. The general process route for the platinum group metal ores consists of three

main unit processes, namely ore concentration by physical techniques (flotation and gravity), pyrometallurgical concentration and hydrometallurgical extraction of base metals and Platinum Group Metals (PGMs). The pyrometallurgical process employed by commercial PGM producers is generally the same. However, different hydrometallurgical processes are used, although most of them employ both atmospheric and pressure leaching of the Ni-Cu matte in the initial stages. A few examples of commercial hydrometallurgical processes for treating the Ni-Cu matte have been presented, and the chemistry of the leaching processes of the matte has been described in detail. Literature on the leaching kinetics of different materials has also been included.

CHAPTER 3

In this chapter a short description of the operations of the Impala Platinum Ltd is presented, in particular the operations of the Impala Base Metals Refinery. The Precious Metals Refinery was not in the scope of this study, and therefore has not been discussed. An overview of the base metal hydrometallurgical refining process has been presented, highlighting the major unit processes.

3.0 HYDROMETALLURGICAL OPERATIONS AT IMPALA PLATINUM REFINERIES

Impala platinum Refineries commenced production operations in 1969, and is currently the second largest producer of platinum in the world. It operates two separate refineries at springs in Jonnesburg, South Africa: the Base Metals Refinery (BMR) and the Precious Metals Refinery (PMR). The hydrometallurgical process of the BMR has been described by many authors, including Plasket and Dunn (1986a), Plasket and Romanchuk (1978), Plasket and Dunn (1986b), Rademan et al. (1999) and Forbes (1999). Therefore only a brief description/overview of the BMR operations will be presented in this study. Moreover, emphasis has been placed on the pre-leach stage (matte repulping stage) as this was the part of the Ni-Cu matte refining process that has been investigated in this study. Information on the PMR operations is confidential and is not available in the public domain; therefore it has not been discussed in this study. Impala Platinum Ltd gets ore from the Merensky reef and the UG2 reef at its mines situated near Rustenburg about 100 km Northwest of Johannesburg. In addition it also gets ore from its mines located in the Limpompo province in the Eastern limb of the Bushveld complex, and from its mines in Zimbabwe. The other source of raw material is the Impala Refining Services (IRS), which is a subsidiary company responsible for sourcing PGE-bearing materials for toll-refining by the Impala operations. The ore is processed and concentrated at the

mineral processing plants on the mine sites to obtain a concentrate, which is transported to the Impala Smelter in Rusternburg. The concentrate is smelted and converted to produce a matte consisting mostly of nickel and copper sulphides with small amounts of iron and cobalt sulphides, and a small percent of PGMs. The matte is transported by trucks from Rustenburg, where the smelter is located, to the Base Metals Refinery (BMR) in Springs, Johannesburg. At the BMR the converter matte is treated to produce nickel, copper, cobalt and ammonium sulphate as a by-product. The residue, which is the Precious metals concentrate, is sent to the Precious Metals Refinery (PMR) where the PGEs and small quantities of gold and silver are recovered.

3.1 Impala Base Metals Refinery (BMR)

The Sherritt Gordon Technology

The Impala Base Metals Refinery (BMR) employs the Sherritt Gordon acid pressure leaching technology, which involves successive stages of acid-oxidation leaching. Nickel is leached and removed in the first stage and the Ni solution is reduced by hydrogen to recover nickel in a powder form. Copper is removed in the second stage and recovered by electrowinning. The residue from the second stage is further leached under acid conditions to produce a PGM rich final residue that constitutes the feed to the Precious Metals Refinery.

In the Sherritt Gordon process, the objective of the first stage leach is to achieve as high as possible nickel extraction, while at the same time precipitating copper out of the solution. After thickening, the thickener overflow is treated with either fresh matte (or NaHS) and $NiSO_4$ to precipitate the rest of the copper from solution. The copper free solution is further treated to remove iron and other impurities, after which it is treated with ammonia and ammonium sulphate. The adjusted nickel solution is then fed into an autoclave in which the nickel is reduced with hydrogen under pressure and precipitated as nickel powder. The remaining nickel barren solution is treated with ammonium sulphate and fed to

the cobalt circuit to recover cobalt in a powder form. The cobalt barren solution goes to the ammonium sulphate plant to recover ammonium sulphate as crystals.

The thickener underflow from the first stage leach goes to the second stage leach after adjusting the pulp density. The second stage leach extracts almost all of the copper and any residual nickel from the first stage leach solids. The solids from the second stage leach are transferred to the third stage then to the fourth stage and finally to the fifth stage. The last three stages serve as PGM concentrating stages. The solution from the second stage is first treated to remove impurities before going to the copper electrowinning circuit where copper is recovered as cathode copper.

The last three leaching stages (third, fourth and fifth) extract the remaining small amounts of nickel, copper and iron from the second stage leach solids, and recycle the solution. Therefore, the solids from the fifth stage leach are very rich in platinum group metals (1.6 – 2.1 kg/ton) and are transferred to the Platinum Metals Refinery.

3.2. Impala Base Metals Refinery (BMR) process description

3.2.1 The pre-leach stage (Pulp density adjustment stage)

This section presents a short description of the leaching process as well as that of the other stages of the base metal refining process. More information on the BMR process can also be found in papers published by Plasket and Dunn (1986a), Plasket and Romanchuk (1978), Plasket and Dunn (1986b), Rademan et al. (1999) and Forbes (1999). The matte generally comprises primarily heazlewoodite (N_3S_2), chalcocite (Cu_2S) and/or djurleite ($Cu_{1.96}S$) and a nickel-rich alloy. Typically, the matte fed to the BMR circuit is composed of the following: 25 – 32% Cu, 46 – 51% Ni, 0.2 – 0.5% Co, 0.2 - 1.5% Fe and 19 – 23% S. The matte is repulped in demineralised water to a density of about 3.0 kg/L and milled to ±50% minus 45µm particle size using a ball mill. The slurry from the ball mill is then combined with solids from copper cementation and spent

electrolyte from the copper electrowinning circuit in the pre-leach tanks to obtain a pulp density of 1.6 - 1.8kg/L prior to pressure leaching (Figure 3.1). The spent electrolyte typically contains 24 - 26g/L Ni, 24 - 25g/L Cu, 0.4 - 0.8g/L Fe, 0.2 – 0.3g/L Co and 90 - 110g/L H_2SO_4, depending on the operation of the copper electrowinning circuit. The temperature in the pre-leach stage (pulp density adjustment stage) is in the range of 50 – 65 ^oC.

The matte feed rate to the ball mill is in the range of 7 – 8 ton/hr and is controlled by a weightometer on the conveyor belt. The demineralised water flowrate is controlled by a manual valve. The ball mill is operated in a batch process, which is determined by the level in tank 2100, such that milling starts when the level is below 50% and stops after it is full. The mill product is controlled by measuring the pulp density at regular intervals while milling. The pulp from the ball mill and solids from the copper cementation circuit are transferred to tank 2100 where the pulp density is adjusted with copper spent electrolyte solution to about 3.0 kg/L (Figure 3.1). From tank 2100 the pulp is transferred through a splitter box to tank 2102 where the pulp density is further adjusted with the copper spent electrolyte to a density of 1.6 - 1.8kg/L. The splitter box controls the pulp flowrate to tank 2102 as well as the spent electrolyte flowrate to both tanks 2100 and 2102, which are set according to the pulp densities in these tanks. Both tanks 2100 and 2102 have level indicators, which are connected to the programmable logic controller (PLC) system in the control room. The copper spent electrolyte is stored in tank 2107 from where it is pumped to tanks 2100 and 2102 and then directly to the first stage leach autoclave.

3.2.2 First stage pressure leach

The first stage pressure leaching operation is performed in a four-compartment autoclave. The pulp from tank 2102 is fed to the first compartment using a special air pump. The air pump setting is usually kept constant at a

predetermined flowrate to maintain the matte throughput. Steam is used to heat and maintain the temperature at 135 – 150 ^{o}C in the first compartment. Temperatures in the second compartment are kept within the range 150 – 160 ^{o}C, while temperatures in the third and fourth compartments are 155 – 165 ^{o}C and 130 – 150 ^{o}C, respectively. Air or oxygen (oxidant) pressure is maintained at about 450 kPa through out the autoclave. The desired temperature and pressure are maintained by adding steam directly into the autoclave and by bubbling air/oxygen through the pulp, respectively. Both the temperature and pressure are automatically controlled by the PLC. The autoclave is vented at constant intervals to prevent build-up of gases and to ensure proper flow of oxygen through the pulp. Spent electrolyte is used to maintain the pH in the range 1.8 - 2.5 in the autoclave. pH of the pulp is an important controlling parameter, depending on the pH, the spent electrolyte flowrate into the autoclave is varied or the pulp feed flowrate is adjusted. Samples are taken at specific intervals from the first and fourth compartments of the autoclave to determine the pH and analyse for Ni, Cu and Fe content. All the leach process inputs are added in the first compartment. The discharge from the autoclave goes to a thickener where the solids are separated from the solution; the solids are fed to the second stage leach while the solution is transferred to the copper cementation and other impurity removal stages prior to nickel recovery in the form of powder or briquette (Figure 3.2).

3.2.3 Second stage pressure leach

In the second stage solids from the first stage leach are leached in sufficient sulphuric acid to meet the requirements of the non-stoichiometric sulphides. The objective here is to dissolve the remaining nickel and most of the copper from the first stage leach solids, as well as complete oxidation of the sulphide sulphur to sulphate with minimal dissolution of the PGMs. Typical leaching conditions are: temperature in the range 130 – 140 ^{o}C, 550 - 600 kPa total pressure and about 4 hours residence time. At this stage almost all the nickel and copper (> 95%) are

extracted from the matte. Approximately 94% of the matte is leached in the second stage. The leach residue is separated from solution by thickening, and the copper-rich solution undergoes impurity removal prior to copper recovery by electrowinning. Copper spent electrolyte from the electrowinning cells, containing some nickel, copper and regenerated sulphuric acid is recycled to the first stage leach circuit (Figure 3.2).

3.2.4 Third stage pressure leach

The second stage leach residue is repulped and mixed with sulphuric acid before charging it into the third stage leaching autoclave. The third stage leach is operated batchwise and is used to remove the remaining iron impurities from the Platinum-Group Metals (PGM) concentrate. The leach solution is separated from the leach solids by filtration. The leach solids, which are now rich in PGM, but contains also some copper, selenium, tellurium, arsenic and sulphur impurities, are routed to the fourth stage leach. The solution containing mostly iron and copper is recycled to the first stage leach.

3.2.5 Fourth stage Pressure leach

The fourth stage leach is also operated as a batch process and is used to remove residual copper from the PGM concentrate. The third stage leach residue, rich in PGM, is repulped in sulphuric acid and fed to the fourth stage autoclave. After leaching the slurry is filtered and the solution is routed to the copper recovery circuit where it joins the spent electrolyte. The PGM-rich solids, containing trace elements such selenium, arsenic, tellurium and sulphur impurities are routed to the firth stage pressure leach for further impurity removal.

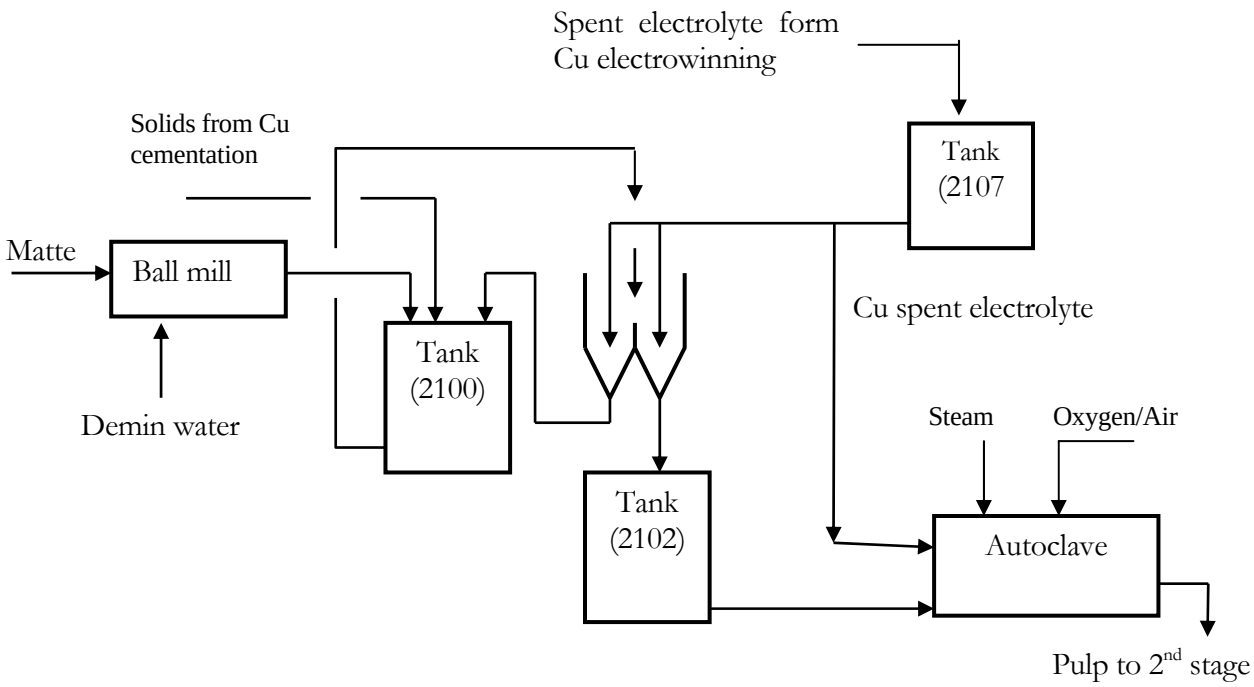

Figure 3.1: Simplified block flow diagram of the pre-leach/first stage leach process

3.2.6 Fifth stage Pressure leach

The fifth stage leach serves to remove selenium, arsenic, tellurium and sulphur from the PGM concentrate. The concentrate is repulped in water, then mixed with sodium hydroxide and fed into the autoclave, which is also operated as a batch process. The autoclave is operated at high temperatures (175 – 195 ^{o}C) with addition of oxygen. The total pressure in the autoclave is in the range 1750 – 1850 kPa so as to dissolve Se, Te, As and S. After leaching the PGM concentrate is separated from the solution by filtration. The solution containing small quantities of dissolved PGMs is transported to the Precious Metals Refinery (PMR) to recover the PGMs via the barren solution circuit. The PGM concentrate

is dried in a steam drier prior to dispatching it to the PMR for PGM recovery. At this stage the PGM concentrate has been upgraded to about 25% PGM.

3.2.7 Nickel and cobalt recovery circuit

The nickel - cobalt solution from the first stage leach process is first fed to a copper removal stage where copper is precipitated by cementation with matte or nickel. The resulting solution is then fed to an autoclave where oxygen and ammonia are added to oxidize and precipitate out iron, arsenic and lead. Ferrous iron is oxidised to the ferric state and reacts with ammonium sulphate to form ammonium jarosite. The arsenic precipitates as ferric arsenate, while lead is precipitated as plumbojarosite.

The iron, arsenic and lead precipitates are filtered off using filter presses and the purified nickel-rich solution is transferred to the next stage where ammonia and ammonium sulphate are added to obtain desired concentrations of nickel and cobalt diamine sulphates. The adjusted nickel solution is then pumped to nickel reduction autoclaves where hydrogen is added to reduce nickel and precipitate it as powder (Figure 3.2). The powder is discharged from the autoclaves, washed and dried or it is briquetted. Steam is used to heat and maintain temperature at about 200°C, while the pressure is kept at about 2800 kPa.

Solution from the nickel reduction autoclaves is taken to the next stage where it is cooled and acidified with sulphuric acid, which results in the precipitation of a mixed double salt containing nickel and cobalt ammonium sulphate. Small quantities of iron, copper, manganese and arsenic are also precipitated along with the mixed double salt. After filtration the pH of the filtrate is adjusted to neutral and heated before a portion of it is recycled to the nickel solution purification circuit, and the remainder is pumped to ammonium sulphate fertilizer plant. The mixed double salt is repulped in solution/water to which ammonia is added to precipitate iron and arsenic as goethite and ferric arsenate

respectively. After filtration, ammonia is added to the iron-arsenic-free solution to provide the desired molar ratio of ammonia to total nickel plus cobalt. The cobaltous ammines are then oxidized to the stable cobaltic aquapentammine. After cobalt oxidation sulphuric acid is added to the solution and cooled to below 30 ^{o}C to precipitate nickel ammonium sulphate. The nickel salt is redissolved in aqueous ammonia and recycled to recover the nickel. Any remaining copper and manganese are then precipitated out of the cobalt-rich solution, after which the cobaltic cobalt is converted back to the cobaltous state by reacting the solution with cobalt powder. The purified cobaltous ammine sulphate solution is then reduced with hydrogen at elevated temperature and pressure to cobalt powder in an autoclave. The slurry is filtered and the filtrate is recycled to the mixed double salt circuit.

3.2.8 Copper recovery circuit

The solution from the second stage leach, which is now rich in copper, goes through a thickener and filter presses prior to selenium and tellurium removal step, where sulphurous acid is added to precipitate selenium and tellurium. The Se and Te precipitates are filtered off and the copper rich solution is directed to an electrowinning plant where copper is recovered as cathodes. The spent electrolyte containing some nickel, copper and regenerated sulphuric acid is recycled to the first leaching stage (Figure 3.2).

3.3 Summary

In this chapter a short description of the operations of the Impala Platinum Refineries has been presented, in particular the operations of the Base Metals Refinery whose pre-leaching section was studied. An overview of the base metal hydrometallurgical refining process has been described, highlighting the major unit processes. Impala Platinum Ltd obtains Platinum Group Metal (PGM) bearing ores from its mines situated in Rustenburg, in Limpopo Province and

Zimbabwe. The other raw material comes from different sources for toll-refining. The run-of-mine ore is concentrated and smelted in Rustenburg, about 100 km northwest of Johannesburg. The converter matte obtained from the smelter, containing mostly nickel and copper with minor amounts of cobalt and PGMs, is transported to Johannesburg where both the Base Metal Refinery and the Precious Metals Refinery are situated. The Base Metal Refinery employs the Sherrit Gordon acid pressure leaching technology, which involves successive stages of acid-oxidation leaching. The base metals are first leached out while the Platinum Group Metals (PGMs) are leached in subsequent series of leaching stages. In the base metal recovery process, nickel and cobalt are first leached. The nickel and cobalt are then recovered as metallic powder by hydrogen pressure reduction in autoclaves. The solids are further leached in the next stage to solubilise copper which is recovered by electrowinning. At this stage the leach residue is basically the PGM concentrate that is fed to the Precious Metal Refinery, after impurity removal.

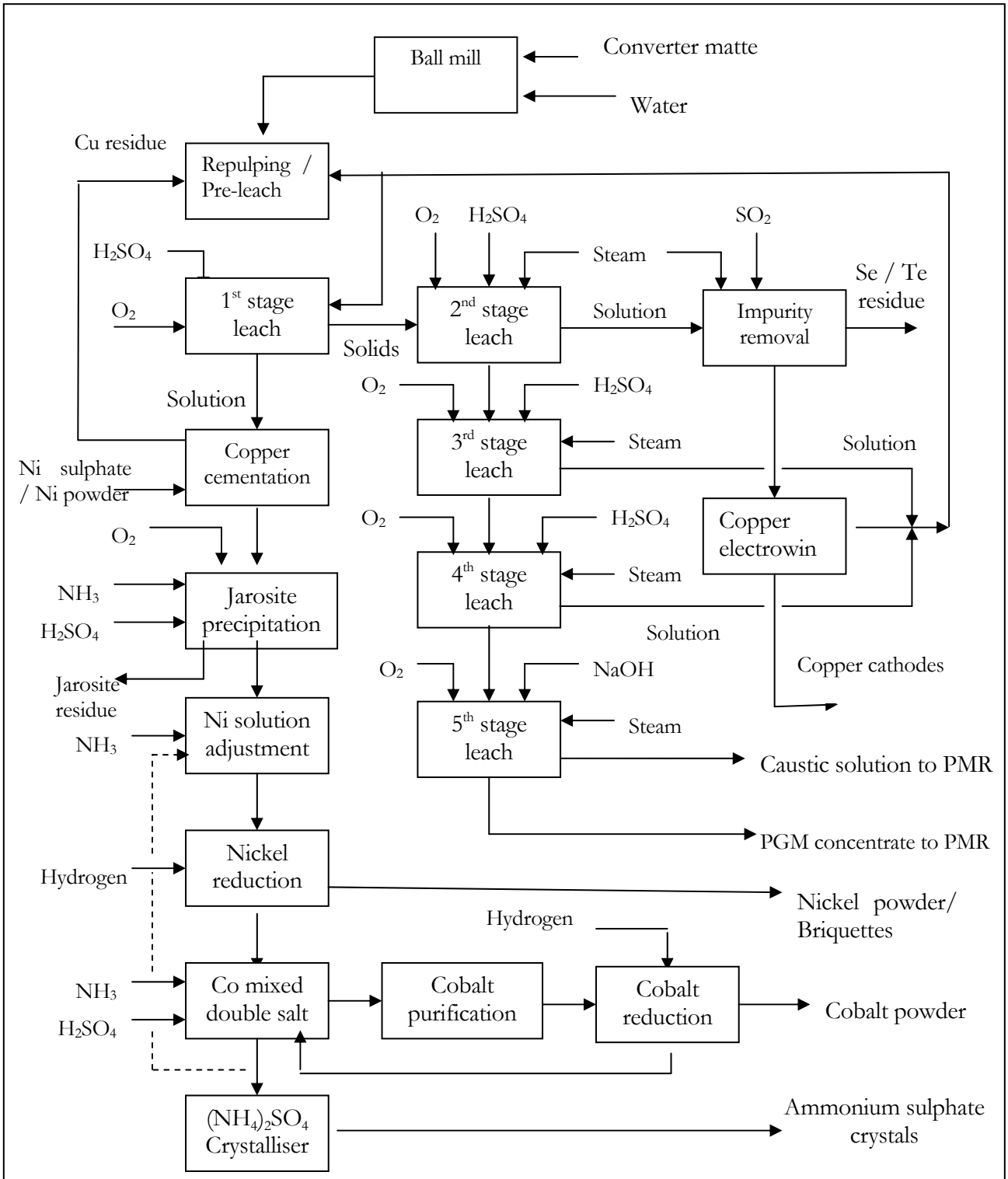

Figure 3.2: Simplified block flow diagram of the Impala Base Metals Refinery (BMR).

CHAPT ER 4

4.0 EXPERIMENTAL

The study was carried out to investigate the leaching behaviour of Ni – Cu matte in copper spent electrolyte during the matte repulping (pre-leaching) stage at Impala Base Metal Refinery (BMR). The study also investigated the response of the pre-leached matte to the subsequent pressure leaching operation. Therefore, two sets of laboratory scale experiments were conducted. The first set consisted of experiments that were designed to simulate the operating conditions of the matte repulping stage of the BMR plant. The second set of experiments consisted of pressure leach tests simulating the first stage pressure leach of the BMR process. The process parameters that influence the pre-leach process were identified as temperature, particle size, pulp density, stirring rate, acid and copper concentration; then effects of variations in these parameters on the pre-leach process were investigated. The experiments simulating the pre-leach stage of the Impala Base Metals Refinery (BMR) were conducted at the University of Stellenbosch, while pressure leach experiments were performed at Impala Base Metal Refinery. The materials used in the study were Ni–Cu converter matte and copper spent electrolyte obtained from Impala Base Metal Refinery. The matte sample (about 50kg) was taken before the milling section, and about 200 litres of the copper spent electrolyte were taken from tank 2107 and stored in a 200-litre plastic drum. Tank 2107 feeds into the pre-leach tank (tank 2102) via a spliter box (Figure 3.1). All the atmospheric pre-leach experiments were conducted using this batch of copper spent electrolyte, while the pressure leach experiments were performed using a new batch of the electrolyte solution.

Experimental methodology

In the experimental design employed in this study, the approach was to change the value of one variable at a time while keeping the other variables constant; this allowed for determination of the effect of that particular variable on the

leaching behaviour of the matte. It must be noted that the main purpose and objective of the study was to understand the chemical processes and reactions, as well as to determine the possible controlling mechanisms occurring in the matte repulping stage; and not the optimisation of the process. Modelling of the process was a secondary objective. It is understood that in complex leaching processes such as the one investigated in this study there are interactions between variables; but to try and understand the chemistry involved and get a general picture of the effects of the variables on the leaching process the approach of changing one variable and keeping others constant was applied. Thus, the interactions between the various variables during the leaching process were not evaluated.

It should be noted that the pre-leach stage at Impala Base Metals Refinery was a "black box" before this study, in that the leaching behaviour of the matte at this stage of the process was unknown. Therefore, this study was undertaken to investigate the leaching behaviour and gain some knowledge on how various process variables affect the leaching process. Although the factorial design approach could have been used, the method employed was considered to be adequate for this study.

4.1 Matte Preparation

The as-received matte was dry milled in a rubber-lined pilot plant scale ball mill. After milling the matte was thoroughly mixed using a pilot plant scale spiral mixer. The matte was then wet screened using ASTM standard sieves to obtain the desired particle size distribution, which was designed to simulate the BMR plant conditions. The matte was screened into the following particle size fractions: +300, -300+212, -212+150, -150+75, -75+45 and -45 microns (Table 4.1). Table 4.1 shows also the particle size distribution of the original matte sample before milling. Table 4.1 shows that about half (50.4%) of the milled matte had particle sizes less than 45 microns, which was the particle size distribution employed on the plant. Table 4.2 compares particle size analysis of

the plant-milled matte to that of the matte sample used in the present study. Note that only the –45 μm size fraction is determined on the plant.

Table 4.1: Particle size distribution of the matte sample before and after milling

Particle size (μm)	Matte sample before milling		Matte sample after milling	
	Wt (g)	Distribution (%)	Wt (g)	Distribution (%)
+300	429.2	85.8	38.6	9.8
-300+212	33.7	6.7	50.0	12.6
-212+150	14.9	3.0	39.2	9.9
-150+75	10.5	2.1	48.7	12.3
-75+45	1.4	0.3	19.8	5.0
-45	10.3	2.5	199.3	50.4
Total	500	100	395.6	100

Table 4.2: Comparison of particle size analysis of matte sample used in this study and matte used on the plant for 3 randomly selected days

Particle size (μm)	Particle size distribution (%)			
	Experimental matte	Plant matte		
		Day 1	Day 2	Day 3
+300	9.8	-	-	-
-300+212	12.6	-	-	-
-212+150	9.9	-	-	-
-150+75	12.3	-	-	-
-75+45	5.0	-	-	-
-45	50.4	51.6	56.0	48.1

It can be seen from Table 4.2 that the particle size of the – 45 μm size fraction of the matte prepared for the study was comparable with that of the matte milled on the plant. It was important that the particle size distribution of the matte used for the study was close to that of the matte employed on the plant, if not

same, this was because the study had to simulate the plant operating conditions in order to draw proper conclusions from the experimental results.

A portion of the milled matte sample was wet screened to get three different size fractions, namely -300+150, -106+45 and –45 μm (Table 4.3). These size fractions were used to investigate the effect of particle size on the leaching characteristics of the matte. Chemical composition of the three size fractions was determined and is also presented in Table 4.3. The specific surface area of the matte powder was also determined using the BET method (Table 4.4). Details about the BET theory and its application to measurement of surface area can be found in the book by Webb and Orr (1997). The surface area of the matte was used in the evaluation of kinetics of the copper cementation reactions (see chapter 6.0).

Table 4.3: Particle size distribution and chemical composition of size fractions used to investigate effects of particle size on leaching characteristics of the matte

Particle size (μm)	**Distribution (%)**	**Chemical composition (%)**			
		Ni	**Cu**	**Co**	**Fe**
+300	10.6	-	-	-	-
-300+150	21.4	49.1	30.4	0.33	0.70
-106+45	16.3	47.9	31.6	0.31	0.58
-45	51.7	48.8	30.5	0.35	0.61

Table 4.4: Specific surface area of the original matte and particle size fractions that was used in the evaluation of kinetics of the copper cementation reactions

Particle size fractions	**Specific surface area (Cm^2/g)**
Original matte	66982
-300+150 μm	36868
-106+45 μm	89247
-45 μm	82846

4.2 Chemical and Mineral composition of the matte

4.2.1 Chemical composition of the matte

Chemical analyses of the matte as provided by Impala Base Metals Refineries are shown in Table 4.5**,** together with the analyses obtained in this study. The analysis was performed by digesting the matte in aqua regia, and analyzing the solution using inductively coupled plasma (ICP). Sulphur content of the matte was analysed using a Leco sulphur analyzer. It can be seen that the discrepancy between the values provided by Impala and those obtained in this study was quite small. It was, however, decided to use the average values in all the work presented in this study. It should be noted that only base metals (major elements) of the matte were analysed and reported, the other elements, for example PGEs were not analysed. At this stage the PGEs were present in very small quantities (100 – 2000 ppm).

Table 4.5: Chemical composition of the matte

Element/chemical	**Matte chemical Composition (wt %)**		
	Analysis from Impala	**Analysis from this study**	**Average values**
Nickel	47.10	48.85	47.98
Copper	30.19	32.42	31.31
Cobalt	0.33	0.34	0.34
Iron	0.52	0.67	0.60
Sulphur	20.10	20.7	20.4

4.2.2 Mineral composition of the matte

Mineralogical analysis was performed on the matte sample to determine the mineral phases present. The analysis was performed by means of X-ray diffraction (XRD) and Scanning Electron Microscope (SEM) equipped with an

energy-dispersive X-ray (EDX) analyzer. The XRD analyses indicated presence of heazlewoodite (Ni_3S_2), djurleite ($Cu_{1.9}S$) and chalcocite (Cu_2S), this can be seen from the XRD graphs in Appendix C. Cobalt and iron phases could not be detected by the XRD analysis probably due to the small amounts of these elements in the matte (0.5 – 0.9% Fe and 0.3 – 0.4% Co). The SEM-EDX analysis indicated the presence of Ni-Fe alloy and Ni-Cu alloy (Figure 5.3, and also in appendix C), but did not detect any cobalt. However, information from Impala Base Metals Refineries indicated that cobalt in the Impala matte is present as Co_3S_2, and iron as Fe-Ni alloy phase, FeS in the Ni_3S_2 matrix and as FeAsS (Spandiel, 1996).

On the basis of the mineral phases present in the matte and the chemical analyses shown in Table 4.5, the major mineral phases in the matte were estimated as 54% Ni_3S_2, 33% Cu_2S-$Cu_{1.9}S$, 11% Ni-rich alloy and 2% other minerals (Figure 4.1). The method employed in determining the percent mineral composition is illustrated in Appendix D.

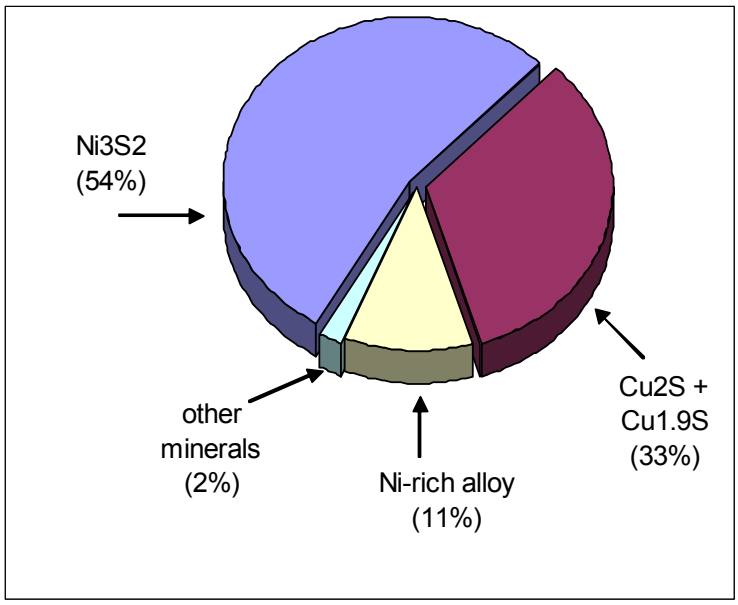

Figure 4.1: Mineral composition of the matte

4.3 Preparation of Leaching Solution

The leaching solution was copper spent electrolyte obtained from the copper electrowinning circuit at Impala Base Metals Refinery. The original copper spent electrolyte that was used in the pre-leach/atmospheric leaching experiments had the following chemical composition: 28 g/L Ni, 30 g/L Cu, 0.95 g/L Fe, 0.29 g/L Co and 95 g/L H_2SO_4. The second batch of the copper spent electrolyte, which was used for the pressure leaching experiments, had the following chemical composition: 25 g/L Ni, 30 g/L Cu, 0.90 g/L Fe, 0.26 g/L Co and 100 g/L H_2SO_4. To simulate the leaching conditions prevailing on the plant in both the pre-leach and pressure leach stages, it was necessary to determine the various ratios of matte, spent electrolyte solution and demineralized water which had to be mixed together for the variations in the pulp density. The calculations involved in the determination of the ratios are shown in Appendix D2. Therefore, before each experiment was conducted the quantities of copper spent electrolyte and demineralised water to be mixed together prior to heating up to the desired temperature were calculated. The chemical compositions of the leaching solutions used in the atmospheric pre-leach experiments and pressure leach experiments are shown in Table 4.6, which also shows typical composition range of the original copper spent electrolyte. The chemical compositions of the leaching solutions shown in Table 4.6 were obtained after mixing the original copper spent electrolyte with dematerialized water, according to predetermined solution /water ratio.

For the experiments conducted to investigate the effect of copper and acid concentrations of the leaching solution on nickel extraction and copper cementation, the required leaching solutions were prepared as follows:

- For effect of acid concentration, the acid concentration of the leaching solution was increased by adding concentrated sulphuric acid. The acid concentrations investigated were 90 g/L, 110 g/L and 125 g/L (see also Table 4.7).

- For effect of copper concentration, the copper concentration of the leaching solution was increased by adding copper sulphate crystals ($CuSO_4.5H_2O$). Copper concentrations investigated were 25 g/L, 36 g/L and 48 g/L (see also Table 4.7).

Table 4.6 Composition of copper spent electrolyte solution

Chemical	**Typical range of original solution (g/L)**	**Atmospheric leaching solution (g/L)**	**Pressure leaching solution (g/L)**
Nickel	25 – 30	24.6	21.9
Copper	25 – 30	25.0	26.2
Iron	0.5 – 1	0.67	0.75
Cobalt	0.15 – 0.30	0.18	0.17
H_2SO_4	90 - 100	90	99.4

4.4 Atmospheric leaching (Pre-leaching) experiments

4.4.1 Experimental equipment

The atmospheric leaching experiments were performed in a 3-litre stainless steel vessel provided with baffles, a cover, a thermometer, a pH electrode and equipped with a variable speed overhead stirrer (Figure 4.2). The stirrer had a flat-blade turbine type impeller and the rate of stirring was set by a tachometer. The set-up was placed in a water bath with temperature controls (Figure 4.3). The cover of the reaction vessel was fitted such that air ingression into the reactor during the experiments was minimal. This was done to simulate conditions existing in the pre-leach tank in the commercial plant. The cover of the vessel had ports for holding a thermometer, a pH electrode and for taking samples.

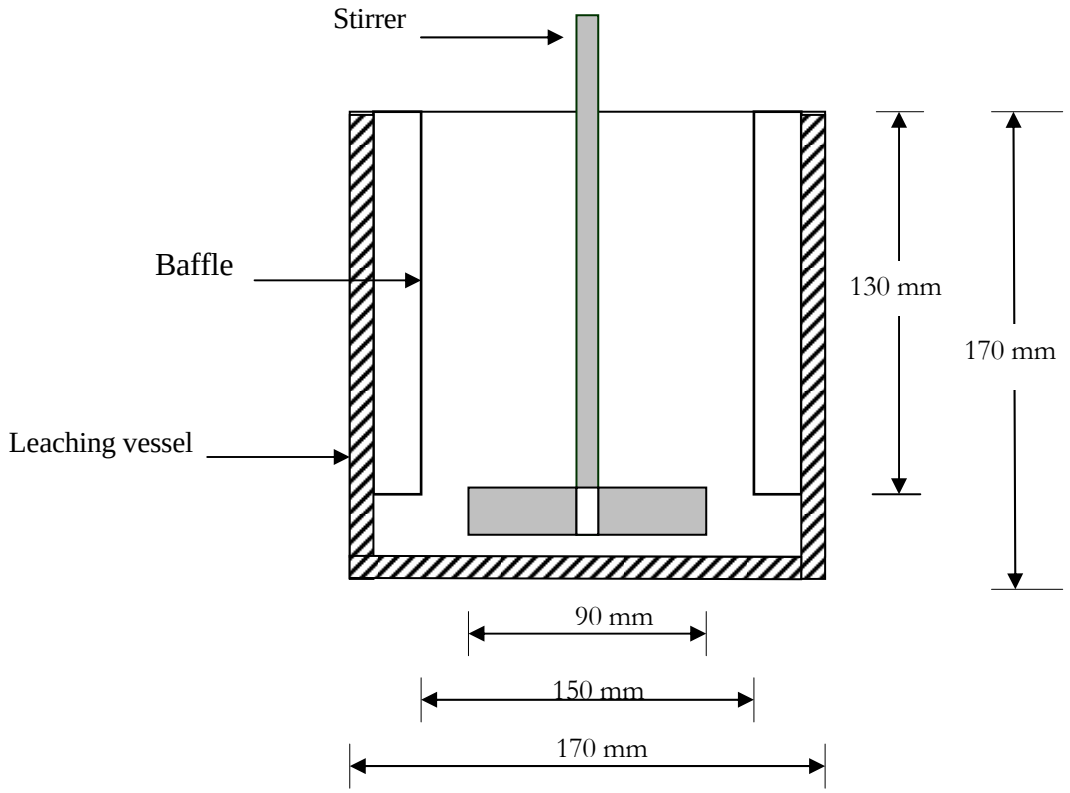

Figure 4.2: Cross section of the leaching vessel used for the atmospheric leaching experiments

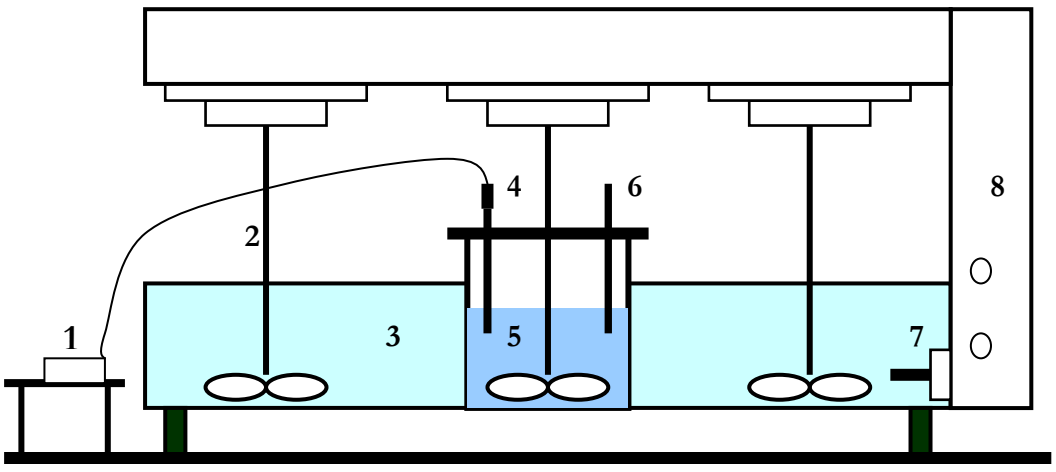

1. pH meter
2. Impeller
3. Water bath
4. pH probe
5. Leach reactor
6. Thermometer
7. Heating element
8. Heat and stirrer control panel

Figure 4.3: Schematic diagram of the atmospheric leaching experimental set-up

4.4.2 Experimental conditions

As was noted at the beginning of this chapter, the study was carried out to investigate the leaching behaviour of Impala nickel-copper matte in the copper spent electrolyte during the pre-leaching (repulping) stage at the Base Metals Refinery. To do this, effects of variations in the process parameters such as temperature, pulp density, stirring rate, residence time, matte particle size, solution acid and copper concentrations were studied. In order to obtain meaningful results the leaching conditions employed were aimed at simulating the actual conditions prevailing during the repulping (pre-leach) stage in tank 2102 in the plant, except for experiments conducted to investigate the effect of variation in the plant parameters. It should be noted that the conditions in the repulping tanks (tanks 2100 and 2102) are not strictly monitored and hence optimum conditions were not known. However, before this study was commenced the plant personnel were requested to carefully monitor the temperature and the pulp density in the tank that feeds the autoclaves (tank 2102), though the pulp density and pulp level in this tank were routinely monitored and recorded in the log sheets by the operators. Thus, the following values of the parameters were taken as optimum values, and most of the experiments were conducted at these values: temperature of 60 ^{o}C and pulp density of 1.7 kg/L. A stirring rate of 205 rpm was chosen on the basis that it was high enough to keep the matte particles in suspension; while a residence time of 5 hours was found long enough to cater for the time the matte takes to go through the repulping stage, i.e. to move from the ball mill to the 1st stage of pressure leaching. Table 4.6 shows the parameters that were investigated together with values, and plant parameter values. Conditions prevailing in the two tanks of the pre-leach stage, tanks 2100 and 2102 could not be simulated separately. Since the pre-leaching of the matte is understood to take place mostly in the autoclave feed tank (tank 2102), it was assumed that the conditions prevailing in tank 2100 would be reached very quickly in tank 2102 where most of the copper spent electrolyte is added (Figure 3.1).

Table 4.7: Atmospheric leaching parameter values that were investigated, with plant parameter values

Parameter	Experimental parameter value	Plant parameter value
Temperature (°C)	50, 60, 70, 80	50 – 65
Pulp density (kg/L)	1.6, 1.7, 1.75	1.6 – 1.8
Stirring rate (rpm)	145, 205, 400	-
Residence time (hrs)	1, 3, 5, 7, 9	4.5 - 5.5
Initial particle size (μm)	50% -45 μm, -300+150, -106+45, -45	~50% - 45 μm
Initial spent electrolyte copper concentration (g/L)	25, 36, 48	26 - 28
Initial spent electrolyte acid concentration (g/L)	90, 110, 125	90 - 100

4.4.3 Experimental procedure

Before each set of experiments were conducted stock leaching solution was prepared so as to simulate the actual plant leaching solution. This was done by determining the quantities of the copper spent electrolyte and demineralised water to be mixed together to form the required leaching solution. The predetermined volumes of copper spent electrolyte and demineralised water were thoroughly mixed together and a sample was taken for chemical analysis. The amount of matte to be mixed with the leaching solution to form pulp of the desired density was also calculated (Appendix D). The leaching solution was then poured into the leaching vessel and placed in the water bath with temperature set at the desired value. When the leaching solution reached the desired temperature, the predetermined quantity of matte was added and the stirrer was set to the required speed. At this point timing of the experiment started and was taken as time = 0 minutes. Detailed outline of the experimental procedure is given below:

1. 1537 mL of the leaching solution was added to the leaching vessel, which was then placed in a water bath and heated to the desired temperature.
2. When the desired temperature was reached, 1276 g of the matte was added and the stirrer was set to the desired stirring rate using a tachometer.

The first sample was taken 15 minutes after the experiment began and thereafter at 15-minute time intervals. The pH of the reaction mixture was also monitored at 15-minute time intervals. The samples, each of 25 mL, were taken using a pipette and were immediately filtered. The filter cake was washed with demineralised water and dried in an oven at about 100 ^{o}C overnight. The filtrate and the dried cake were kept in sample bottles for chemical analysis, and for free acid determination in some solution samples. At the end of each experiment the pulp was allowed to cool down to room temperature, filtered, washed with demineralised water and solids dried overnight. Both the solids and the filtrate were also kept for chemical analysis.

4.5 Pressure leaching experiments

4.5.1 Experimental equipment

The pressure leaching experiments were conducted at Impala Base Metals Refinery (BMR), and were aimed at investigating the response of pre-leached matte to the subsequent pressure leaching operations. The experiments were conducted in a 2-litre Paar Series 4520 bench top pressure reactor (autoclave) made of 316 stainless steel (Figure 4.4a). Leaching of the material takes place inside a reaction chamber called the bomb (Figure 4.4b), which is placed inside the shell of the reactor. The reaction chamber can be removed from the reactor when loading samples.

(a)

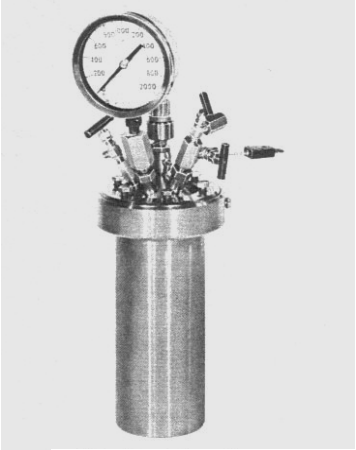

2 - litre bomb assembly

(b)

Figure 4.4: 2-litre Paar Series 4520 bench top pressure reactor

The autoclave is equipped with an agitator, dip pipe for sparging gas, sample port, vent valves and a pressure gauge; and is heated by an electric heater that is connected to an automatic temperature controller. The temperature controller regulates temperature in the autoclave by means of a thermocouple connected to it. The autoclave temperature and the agitator speed are displayed on an LCD monitor, which houses both the temperature and stirrer controllers. The speed of the stirrer is set manually on the LCD monitor, and the pressure in the autoclave is controlled manually by setting the pressure on the gas regulator of the gas cylinder and then by monitoring the pressure on the autoclave itself. The oxygen gas cylinder was connected to the autoclave by a flexible pressure hose.

4.5.2 Experimental conditions

As the objective of the pressure leaching experiments was to investigate the response of the pre-leached/atmospheric leached matte to the subsequent pressure leaching process, it was important to simulate the leaching conditions employed in this process. Therefore all the experiments were performed under

the same conditions, using the pre-leached matte samples obtained from the atmospheric leach experiments. The leaching conditions employed in the pressure leaching experiments simulated the first stage pressure leach conditions. Table 4.8 shows the experimental conditions as well as those of the plant.

Table 4.8: Experimental pressure leaching conditions, and plant leaching conditions

Parameter	Experimental parameter value	Plant parameter value
Temperature (^{o} C)	145 ± 3	135 – 150
Pulp density (kg/L)	1.4	1.35 – 1.5
Residence time (hrs)	3	-
Total pressure (kPa)	500 ± 2	450 – 600

4.5.3 Experimental procedure

The quantities of the leaching solution (copper spent electrolyte plus demineralised water) and matte to be mixed to obtain the desired pulp density (1.4 kg/L) were calculated prior to the experiments, as explained in section 4.4.3 (see Appendix D2). The calculated volume of the leaching solution (1167 mL) was first poured into the autoclave reaction chamber (bomb) and the matte was added. The autoclave bomb was then covered, placed into the autoclave shell and heated slowly. When the temperature was about 130 ^{o}C, the pressure relief valve was slightly opened for a few seconds to remove any air present inside the autoclave. Upon attaining a temperature of about 135 ^{o}C, the vapour pressure of the solution was noted, stirrer speed increased to about 900 rpm and oxygen admitted into the autoclave. The leaching was started at a temperature of about 135 ^{o}C, instead of the required temperature of 145 ^{o}C to avoid overshooting of temperature, as the reactions taking place during the leaching process were exothermic. The total pressure in the autoclave was then set at about 500 kPa.

At this point timing of the experiment started and was taken as the beginning of the pressure leaching process (time = 0 minutes), i.e. 25 minutes after starting heating the slurry. Upon addition of oxygen the temperature rose from 135 to 145 ^{o}C very fast and sometimes reached 148 ^{o}C before it came down within 10 – 15 minutes and stabilized at 145 ± 1 ^{o}C. Consequently the total autoclave pressure also rose to about 520 kPa before it stabilized at 500 ± 2 kPa. The first sample was taken after 15 minutes from commencement of the leaching process and thereafter every 15 minutes until the experiment was completed. After taking the sample (20 mL) the pH was measured and the sample was immediately filtered. The cake was washed with demineralised water and dried in an oven at 100 ^{o}C overnight. The dried cake and the filtrate were kept for chemical and total acid analysis. The residence time of all the experiments was 3 hours. At the end of each experiment the pulp was allowed to cool down to room temperature, filtered, washed with demineralised water and solids dried overnight. Both the solids and the filtrate were also kept for chemical analysis.

4.6 Chemical and mineralogical analysis

Chemical and mineralogical analysis of the samples from the atmospheric leaching experiments were done at University of Stellenbosch, however some of the samples were sent to independent Laboratories such as the Bemlab in Cape Town, to double check and verify the chemical analyses done at the University laboratories. The pressure leaching experiments were conducted at the Impala Platinum's Base Metals Refinery, therefore the chemical analysis was performed at Impala Base Metals Laboratories (BML), while mineralogical analysis was conducted at University of the Witwatersrand in Johannesburg. Some samples were also sent to Setpoint Laboratories to double-check the analyses from Impala's Base Metals Laboratories.

Solution samples were analysed for Ni, Cu, Co and Fe using inductively coupled plasma (ICP). Solid samples were analysed by XRF , although some sample were analysed by dissolving the solid sample in perchloric acid and/or aqua regia and

analyzing for the same elements using the ICP. Total sulphur was determined using a Leco furnace. Characterisation of the solid samples was done by means of a TOPCON ABT60 scanning electron microscope (SEM) quipped with an energy – dispersive X–ray (EDX) analyzer; and also by X-ray diffraction analysis using a Philips X-ray Diffractometer.

The percent extraction ($X_{M,i}$) of nickel, cobalt and iron at the time t_i during the leaching was evaluated using the following formula:

$$X_{M,i} = \frac{\left(V - \sum_{j=1}^{i=1} V_j\right) C_{M,j} + \sum_{j=1}^{i-1} V_j C_{M,j} - \left(V\ C_M\right)}{m(c_m/100)} \qquad (4.1)$$

Where:

X_{Mi} = the percent extraction of M at the time t_i (M= nickel, cobalt or iron)

V = the initial volume of the leaching solution (L)

C_M = Initial concentration of M in the initial volume of leaching solution (g/L)

V_j = the volume of the solution sample j (L)

$C_{M,j}$ = the concentration of M in sample j (g/L)

M = the exact mass of the solids added into the reactor (g)

c_m = the wt % of M in the solids added into the reactor

j = the j^{th} sample taken during leaching

J = the total number of samples taken

4.7 Summary

This chapter has described the nature of experiments conducted in this study. It has presented the material used in the experiments, and the process parameters investigated. Two sets of laboratory scale experiments were conducted, namely

atmospheric leaching experiments and pressure leaching experiments on the leach residue from the atmospheric leaching experiments. The approach was to change the value of one variable at a time while keeping the other variables constant; this allowed for determination of the effect of that particular variable on the leaching behaviour of the matte, in particular the chemistry of the leaching process. The main purpose and objective of the study was to understand the chemical processes and reactions, as well as to determine the possible controlling mechanisms occurring in the matte repulping stage; and not the optimisation of the process. Modelling of the process was a secondary objective. The pressure leaching tests were aimed at investigating the response of the pre-leached matte to the subsequent pressure leaching operations. The process parameters that were investigated in the atmospheric leach experiments were temperature, particle size, pulp density, stirring rate, acid and copper concentrations. In the pressure leaching experiments, plant conditions of the 1st stage leach were employed.

Chemical and mineralogical composition of the matte was determined. The mineralogical analysis indicated presence of heazlewoodite, djurleite, chalcocite and nickel alloy. Cobalt and iron mineral phases could not be identified due to the small amounts of these elements in the matte (0.34% Co and 0.6% Fe). The major mineral phases in the matte were estimated at 54% Ni_3S_2, 33% Cu_2S-$Cu_{1.9}S$, 11% Ni-rich alloy and 2% other minerals. The specific surface area of the matte powder was also determined and used in the evaluation of kinetics of the copper cementation reactions. The leaching solution was copper spent electrolyte obtained from the copper electrowinning circuit at Impala Base Metals Refinery.

CHAPTER 5

5.0 LEACHING CHARACTERISTIC OF Ni – Cu MATTE

5.1 Thermodynamics of the Ni-Cu matte-H_2SO_4 Leaching System

One of the most convenient techniques used to predict what species would be formed under particular conditions of redox potential and pH in a leaching system, such as the one investigated in this study, is to draw the potential – pH equilibrium diagrams (Pourbaix, 1966). These diagrams, which are known as Pourbaix diagrams, show predominance areas of species that may be thermodynamically stable in the system under study. They provide information on the tendency of a chemical reaction to occur in a particular direction, but do not provide information on the rate of the reaction. Many researchers have used Eh-pH diagrams to predict equilibrium stable species in leaching and solution treatment operations. Osseo-Asare and Fuerstenau (1978) investigated the application of activity-activity diagrams to ammonia hydrometallurgy, and presented Eh-pH diagrams for the system Cu-NH_3-H_2O, Ni-NH_3-H_2O and Co-NH_3-H_2O at a temperature of 25 ^oC. In a separate study, Osseo-Asare (1981) later studied the same systems at elevated temperatures. Ferreira (1975) presented high temperature Eh-pH diagrams for the systems S-H_2O, Cu-S-H_2O and Fe-S-H_2O; his study dealt with the oxides and sulphides of copper and iron, in particular the behaviour of the sulphide minerals of copper and iron during leaching or during geological formations.

In the present study predominance area diagrams have been used to predict the thermodynamically stable species in the Ni-Cu matte-H_2SO_4-$CuSO_4$ leaching system, under the investigated conditions. For the sake of clarity the discussion of the Eh-pH diagrams has been restricted to the regions applicable to this study, which are in the pH range of -1 to 4.5. Species which are not relevant to this study have been omitted. The diagrams were drawn using the HSC Chemistry

computer software program written by Roine (2002). The method and calculations involved in the development of the Pourbaix diagrams have been published by many authors, including Pourbaix (1966), Ferreira (1975), Osseo-Asare (1981). The thermodynamically stable species as predicted by the Eh-pH diagrams were in agreement with those expected from the chemistry of the leaching process (section 5.2.2) and XRD and SEM-EDX analysis of the solids obtained after leaching of the matte (Appendix C).

The Eh-pH diagrams for the atmospheric leaching of the Ni-Cu matte are presented in Figures 5.1 – 5.3, which show the stability regions of the species in the Ni-S-H_2O, Cu-S-H_2O and Fe-S-H_2O systems at temperatures of 50 ^oC and 80 ^oC. Figure 5.1 shows that during the atmospheric leaching of the matte, in the repulping stage of the leaching process under study, the possible stable species are aqueous nickel ions (Ni_2^+), metallic nickel (Ni^o) and nickel sulphides such as heazlewoodite (Ni_3S_2). Figure 5.1 (a) and (b) show that at both temperatures of 50 and 80 ^oC, pH values of less than 5 and under oxidizing conditions (redox potential of about zero and above), nickel can be leached from the matte. It can also be seen that under the investigated conditions, the potential range as well as pH range in which dissolved nickel seem to be stable does not change with temperature. This means that nickel can be leached in the same pH range at both lower temperatures (50 ^oC) and higher temperatures (80 ^oC), although the kinetics of the leaching process may not be the same. This was evident from the results of the leaching tests performed at 50 and 80 ^oC (section 6.1). The nickel species presented by the Eh-pH diagrams are comparable with the results obtained from the XRD analysis of the leach solids (Appendix C). It should however, be noted that the diagram for the temperature of 80 ^oC (Figure 5.1 (b)) does not show presence of millerite (NiS), although XRD analysis showed the presence of NiS in the leach solids. (see section 7.3.1, Table 7.1).

The stability regions of copper species are presented in Figure 5.2. It can be seen that the possible stable species of copper for pH values less than 4 are aqueous

copper ions (Cu^{2+}), metallic copper (Cu^{o}) and copper sulphides such as chalcocite. Any increase in pH above 4 will result in hydrolysis of aqueous copper to form basic copper sulphates ($Cu_3(OH)_4SO_4$) or copper oxides depending on the potential of the system. However, under the investigated leaching conditions (pH < 4.5) all the aqueous copper precipitated before the pH of the system reached 4. It should be noted that although the diagrams show only one type of copper sulphide mineral (Cu_2S), other minerals such as $Cu_{1.9}S$ and $Cu_{1.8}S$ may also be present as the chemical composition of these minerals are very close. Infact XRD analysis of the leach solids showed both Cu_2S and $Cu_{1.9}S$ as being present at both temperatures of 50 and 80 ^{o}C (see section 7.3.1, Table 7.1). The size of the stability regions of all the copper species is not affected by change in temperature under the investigated conditions.

Figures 5.3 (a) and 5.3 (b) show the stability regions of the iron species in the Fe-S-H_2O system at 50 ^{o}C and 80 ^{o}C, respectively. The possible stable iron species under the investigated conditions are aqueous iron (Fe^{2+} and Fe^{3+}), metallic iron (Fe^{o}) and iron hydroxide ($Fe(OH)_3$). Under the investigated conditions of pH < 4.5 aqueous ferrous iron (Fe^{2+}) is stable at redox potential of between 0.75V and –0.5V, however it undergoes hydrolysis to form ferric hydroxide ($Fe(OH)_3$) if the pH is raised from about 2 and the potential is decreased from about 0.75V to -0.5V. The Fe^{2+} is oxidized to Fe^{3+} as the potential increases from about 0.75V as long as the pH is less than 1. Figure 5.3 shows also that dissolved ferrous iron will precipitate as metallic iron if the potential is decreased to less than -0.5V. It should be noted that no iron compound was detected in the leach solids by the XRD analysis. This was probably due to the small amount of iron present in the matte (0.6 %) and leaching solution (0.67 g/L). However, precipitated solids from the leach solutions were examined by SEM- EDX analysis and revealed presence of Fe, which was most likely in the $Fe(OH)_3$ form. It can also be seen that increase in temperature from 50 to 80 ^{o}C does not significantly change the stability regions of the iron species, except that the pH range over which Fe^{2+} is stable decreases slightly from about 8 at 50 ^{o}C to about 7 at 80 ^{o}C.

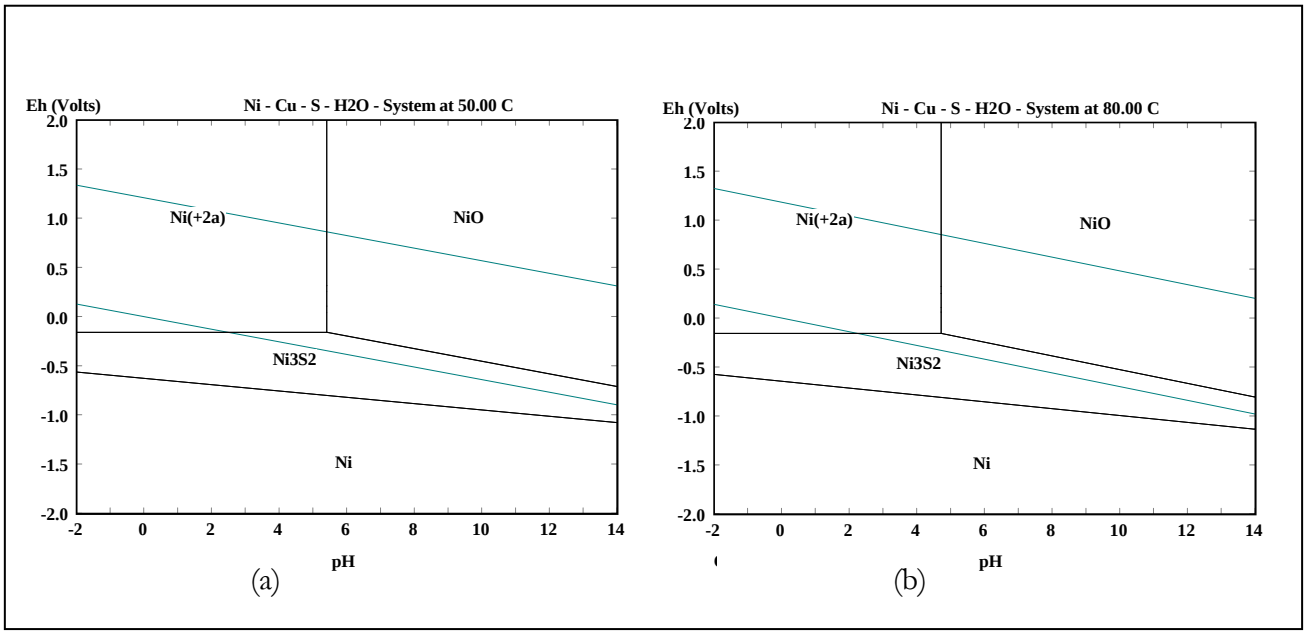

Figure 5.1: Eh-pH diagram for the Ni-S-H_2O system at (a) 50 ^oC, (b) 80 ^oC; [Ni] = 2.00 M, [S] = 2.00 M at atmospheric pressure. (M = molality)

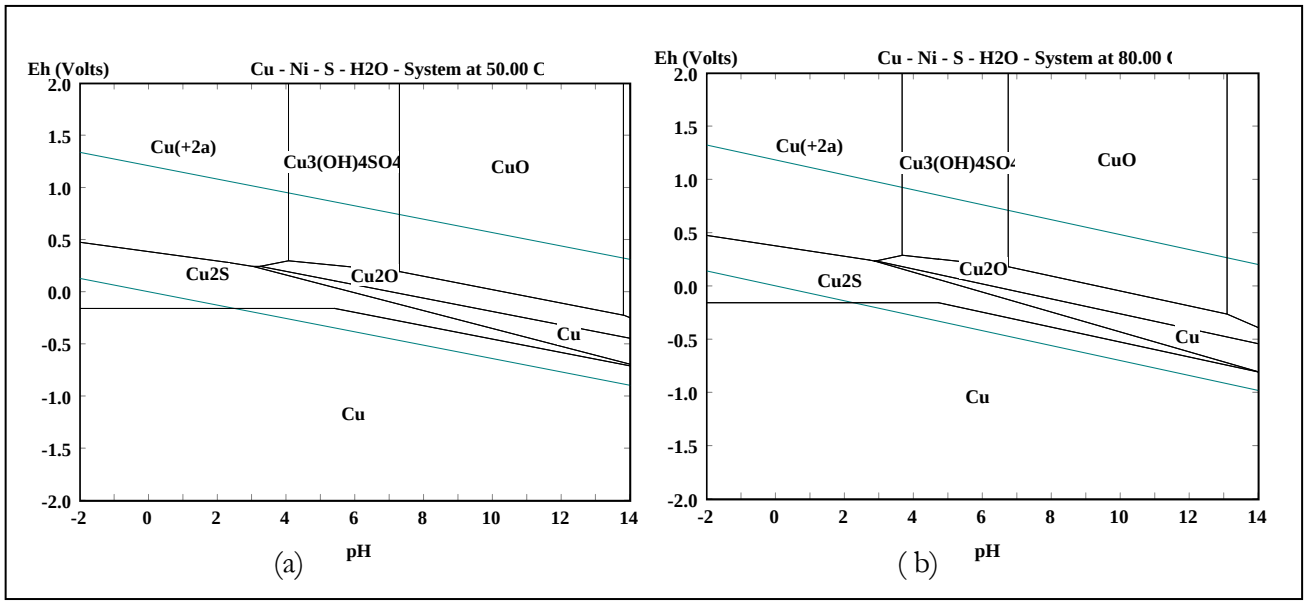

Figure 5.2: Eh-pH diagrams for the Cu-S-H_2O system at (a) 50 ^oC and (b) 80 ^oC; [Cu] = 1.50 M, [S] = 2.00 M at atmospheric pressure. (M = molality).

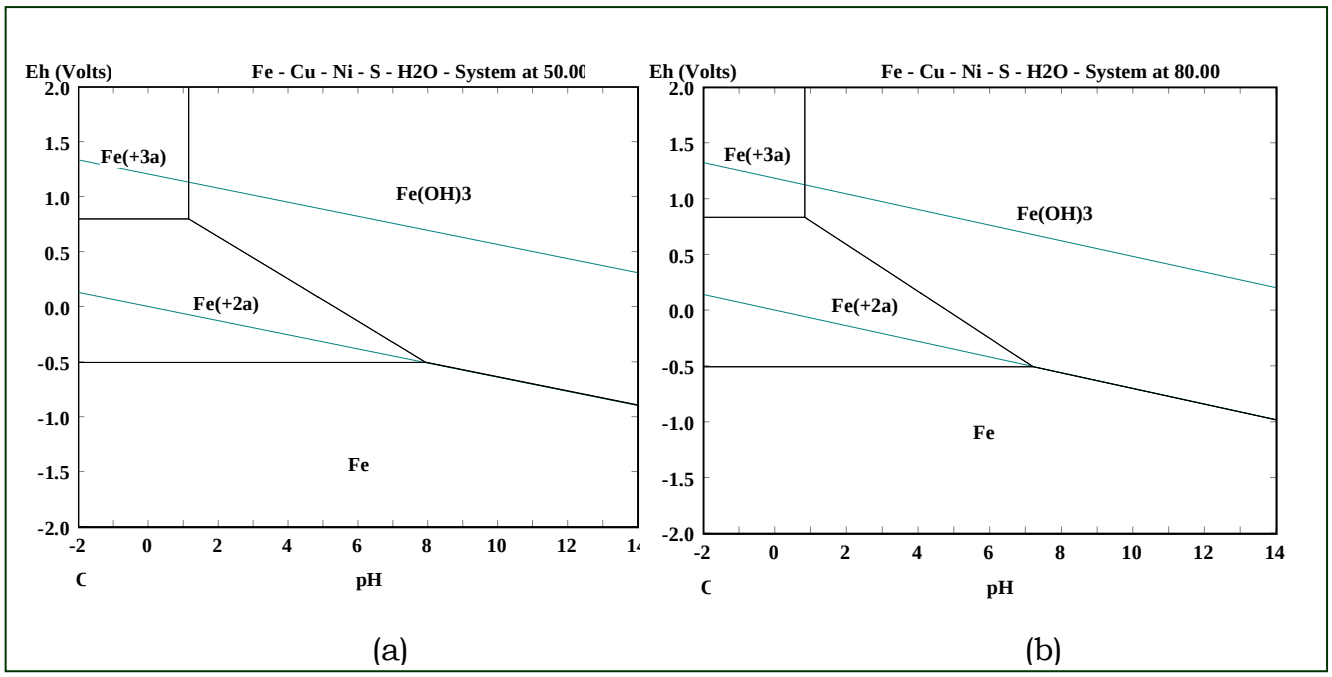

Figure 5.3: Eh-pH diagrams for the Fe-S-H_2O system at (a) 50 ^oC and (b) 80 ^oC; [Fe] = 0.50 M, [S] = 2.00 M at atmospheric pressure. (M = molality)

5.2 Mechanism of Atmospheric Leaching of Ni-Cu Matte

5.2.1 Leaching mechanism based on mineralogical investigations

Leaching kinetics of base metals from the Ni-Cu matte are dependent on the phases in which the metals are present. Therefore, changes in the mineral phase characteristics have an influence on the leaching mechanism of the matte. In the present study only changes in the minerals of nickel and copper were considered. This was because these minerals were the major components of the matte, estimated at 54% Ni_3S_2, 33% Cu_2S and 11% Ni alloy. Cobalt, iron and other minerals constituted about 2% of the matte.

Results of mineralogical investigations indicated the presence of heazlewoodite (Ni_3S_2), djurleite ($Cu_{1.96}S$) and chalcocite (Cu_2S). Cobalt and iron phases could not be detected by XRD analysis due to the small amounts of these elements in the matte (0.33 – 0.34% Co and 0.5 – 0.9% Fe). However, a discussion document from Impala Platinum Refineries (Spandiel, 1996) has indicated that cobalt in the

Impala converter matte is present as Co_3S_2 and iron as Fe in the nickel alloy phase, FeS in the Ni_3S_2 matrix and as FeAsS. Berezowsky (2003) suggested that some cobalt exists in metallic form; however, SEM-EDS analysis was not able to detect any cobalt phase but showed the presence of Ni-Fe alloy and Ni-Cu alloy. Figure 5.4 shows an SEM image of a particle of nickel alloy in the Ni-Cu sulphide matrix prior to leaching. SEM-EDS analysis also showed that nickel and copper mineral phases were intergrown, with copper minerals always present in nickel minerals and vice versa. Figure 5.5 shows images of a matte particle taken after 5 hours of leaching. It can be seen that the nickel alloy was leached out of the matte particle, leaving holes in the particle. This is evident from Figure 5.6, which shows holes created by the dissolution of the Ni-Cu alloy (spots 2, 3 and 4) and Ni-Fe alloy (spot 1). Figure 5.6 revealed also that the metal alloys were not completely dissolved after 5 hours of leaching. The metals in the alloy phase were leached out of the matte particles and no mineral matrix disintegration was observed.

The presence of Ni-Cu and Ni-Fe-Cu alloys in converter matte has been reported by other researchers, including Rademan et al. (1999), Llanos et al. (1974), and Hofirek and Kerfoot (1992). Mackinnon et al. (1971) stated that the preparation of mattes involves a slow cooling process during which a Ni-Cu alloy is formed. However, the Impala matte is granulated and not slow cooled; therefore it seems that both granulated and slow cooled matte may contain Ni-Cu-Fe alloy. Slow cooled matte facilitates the crystallisation of a metallic Ni-Cu-Fe alloy containing most of the PGMs, and a PGM-free nickel-copper matte (Hofirek and Halton, 1990 and Hochreiter et al., 1985). However, slow cooled matte results in the formation of undesirable trevorites ($NiO.Fe_2O_3$) and magnetite ($FeO.Fe_2O_3$) which are insoluble in the subsequent base metal leaching stages and report to the PGM concentrate. Granulation prevents this from happening and is therefore preferred (Steenekamp and Dunn, 1999). Rademan et al. (1999) carried out an extensive study of the pressure leaching process at Impala base metals refinery and noted the same mineral phases in the converter matte as those observed in

the present study. They reported that mineral structure of the nickel and copper sulphides can be visualized as layers of sulphides anions with nickel and copper cations filling some of the spaces in this layer, where the filling of the nickel and copper cations in the sulphides lattice will determine the crystal structure of the mineral and hence it's properties. Nickel and copper are gradually leached out of the sulphides lattice to form minerals with lower nickel and copper to sulphur ratio. Table 5.1 shows the mineralogical composition of the matte prior to leaching and that of the same matte after 5 hours of atmospheric leaching in the $CuSO_4$-H_2SO_4 solution.

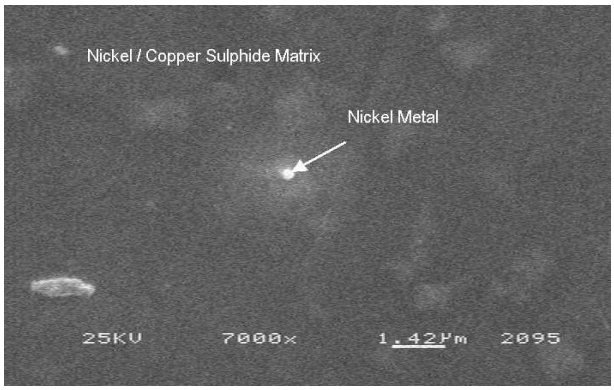

Figure 5.4: SEM image of matte particle before leaching showing a particle of nickel alloy in the Ni/Cu sulphide matrix at a magnification of 7000x.

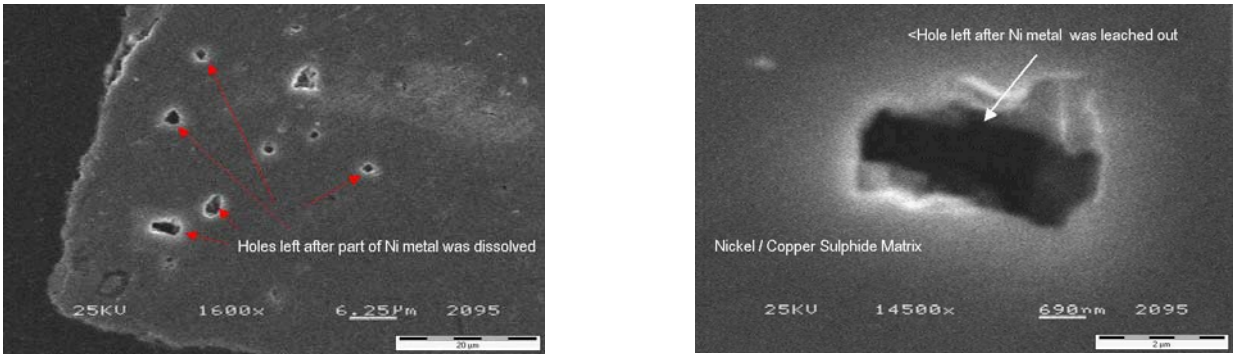

(a) (b)

Figure 5.5: SEM images of matte particle after 5 hours of leaching, showing holes formed in the particle after metal alloy was leached out: (a) 1600x magnification; (b) 14500x magnification,

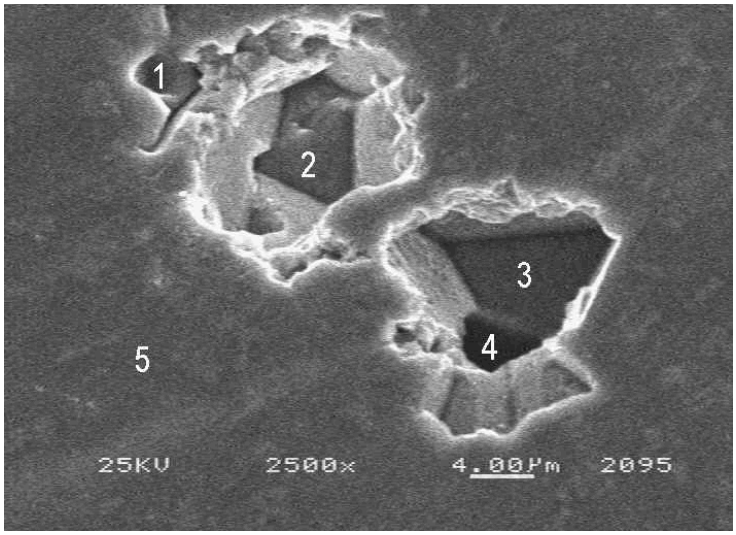

Figure 5.6: SEM image of matte particle after 5 hours of leaching, showing that the Ni-Cu alloy and Ni-Fe alloy were not completely dissolved: spot 1: Ni-Fe alloy; spots 2, 3 and 4: Ni-Cu alloy; Spot 5: Ni/Cu sulphides

Table 5.1: Mineralogical composition of the matte before and after leaching for 5 hours

Mineral composition of matte (%)	
Before leaching	**After leaching**
Heazlewoodite (Ni_3S_2)	Heazlewoodite (Ni_3S_2) Millerite (NiS)
Chalcocite (Cu_2S) Djurleite ($Cu_{1.96}S$)	Chalcocite (Cu_2S) Djurleite ($Cu_{1.96}S$ Chalcocite-Q
Ni-Cu alloy Ni-Fe alloy	Ni-Cu alloy Ni-Fe alloy

Table 5.1 shows that some of the heazlewoodite was leached and transformed into millerite, this is evident from the XRD analysis graphs given in Appendix C. However, most of the nickel was expected to be leached from the alloy. In the atmospheric leaching of Ni-Cu converter matte, with no air or/and oxygen

addition and under the conditions applied in this study, the copper sulphide minerals were not leached. Instead aqueous copper from the solution was precipitated and formed copper minerals, while nickel was leached from the matte. The copper was precipitated as metallic copper and as chalcocite or chalcocite-Q, although this could not be confirmed as there was already chalcocite in the original matte. It should be noted that these two copper minerals are difficult to distinguish as their XRD patterns and peaks overlap, besides their chemical compositions are very close. Hence these copper minerals are sometimes simply referred to as Cu_2S.

5.2.2 Leaching mechanism based on process chemistry

The leaching mechanism presented in this section was based on mineral phase changes discussed in the preceding section, chemical analysis and information from the literature. Under the conditions employed in this study, where no oxidant was added, the metals were not expected to be leached to any significant degree especially from the sulphide minerals. The leaching mechanism of the matte under the investigated conditions can be divided into two parts:

(a) Leaching of the matte with simultaneous precipitation of aqueous copper via the cementation process.
(b) Leaching of the matte by direct acid attack.

(a) Leaching of the matte with simultaneous precipitation of aqueous copper via the cementation process

The major mineral phases in the matte were Ni_3S_2, Cu_2S (Cu_2S plus $Cu_{1.96}S$) and Ni alloy. The nickel in the alloy was leached by the process of cementation according to reaction 5.1:

$$Ni^o + CuSO_4 \rightarrow Cu^o + NiSO_4 \qquad (5.1)$$

This reaction is substantiated by the fact that metallic copper was clearly visible on the sides of the leaching vessel and in the leach solids. The Ni alloy continued to be leached throughout the five-hour leaching period and was not dissolved completely, as is evident from Figure 5.6. The dissolution of metallic iron from the Ni–Fe alloy was believed to proceed according to the well-known reaction of cementation of copper by metallic iron:

$$Fe^{o} + CuSO_4 \rightarrow FeSO_4 + Cu^{o} \quad (5.2)$$

The ability of Ni-Cu matte to precipitate Cu^{2+} from solution with simultaneous leaching of Ni, is a well known fact (Llanos et al., 1974; Rademan et al., 1999; Hofirek and Kerfoot, 1992; Plasket and Romanchuk, 1978). Therefore, some of the aqueous copper may be precipitated by the heazlewoodite according to the following reactions:

$$Ni_3S_2 + CuSO_4 \rightarrow Cu^{o} + 2NiS + NiSO_4 \quad (5.3)$$

$$Ni_3S_2 + 2CuSO_4 \rightarrow Cu_2S + NiS + 2NiSO_4 \quad (5.4)$$

$$Ni_3S_2 + Ni + 4CuSO_4 \rightarrow 2Cu_2S + 4NiSO_4 \quad (5.5)$$

The formation of NiS was supported by the presence of this phase in the leach solids examined by XRD (see Appendix C). However, the formation of Cu_2S through reactions (5.4) and (5.5) could not be substantiated by means of XRD analysis as there was already Cu_2S in the original matte. No copper precipitation by hydrolysis (reaction 5.6) was expected to occur, since under normal operating conditions copper hydrolysis takes place above pH 4 (Hofirek and Kerfoot, 1992; and Symens et al., 1979). In all the experiments, it was observed that copper was completely rejected from the solution by reactions (5.1) – (5.5) before pH 4 was attained. This was why basic cupric sulphate $Cu_3(OH)_4SO_4$ (antlerite) was not detected in the leach solids.

$$3Cu^{2+} + SO_4^{2-} + 4H_2O \rightarrow Cu_3(OH)_4SO_4 + 4H^+ \quad (5.6)$$

(b) Leaching of the matte by direct acid attack

In the absence of an oxidant, such as air or oxygen, some of the nickel and iron from the alloy can be leached by the sulphuric acid according to reaction (5.7):

$$Ni–Fe + 2H_2SO_4 \rightarrow NiSO_4 + FeSO_4 + 2H_2 \quad (5.7)$$

The other possible reactions are the leaching of NiS and FeS by the sulphuric acid (reactions 5.8 and 5.9). FeS is reported to be in the Ni_3S_2 matrix (Spandiel, 1996), while NiS is formed during the leaching process by reactions (5.3) and (5.4).

$$NiS + H_2SO_4 \rightarrow NiSO_4 + H_2S \quad (5.8)$$

$$FeS + H_2SO_4 \rightarrow FeSO_4 + H_2S \quad (5.9)$$

Although the leaching vessel was covered during the experiments, some air may have entered the leaching system. Thus, in the presence of air some of the nickel, iron and a small portion of the heazlewoodite may have been leached by oxidative dissolution in the sulphuric acid according to the following reactions:

$$Ni^o + H_2SO_4 + ½O_2 \rightarrow NiSO_4 + H_2O \quad (5.10)$$

$$Fe^o + H_2SO_4 + ½O_2 \rightarrow FeSO_4 + H_2O \quad (5.11)$$

$$Ni_3S_2 + H_2SO_4 + ½O_2 \rightarrow NiSO_4 + 2NiS + H_2O \quad (5.12)$$

It was not possible to determine the form of cobalt in the matte, due to the small amount of this element present in the matte (0.33 – 0.34%). If it is assumed that some of it existed in metallic form, as reported by Berezowsky (2003), then it was leached as shown in reaction (5.13):

$$Co^{o} + H_2SO_4 + \tfrac{1}{2}\, O_2 \rightarrow CoSO_4 + H_2O \quad (5.13)$$

As the leaching vessel was not air tight, some of the matte may have been leached according to reactions (5.4a) and (5.5a), resulting in the production of H_2S as an intermediate product. According to Mulak (1987) Ni_3S_2 is unstable in acid oxidizing solutions and evolution of H_2S gas takes place spontaneously. The aqueous Cu^{2+} ions accept electrons from evolved hydrogen sulphide to form Cu_2S. Rademan et al. (1999) indicated that the formation of H_2S occurs through the oxidative (anodic half-cell) reaction of the cementation of copper with Ni_3S_2 and Ni alloy.

$$Ni_3S_2 + 2H^+ = NiS + 2Ni^{2+} H_2S + 2e^- \quad (5.4a)$$

$$Ni_3S_2 + Ni + 4H^+ = 4Ni^{2+} + 2H_2S + 4e^- \quad (5.5a)$$

$$2Cu^{2+} + H_2S + 2e^- = Cu_2S + 2H^+ \quad (5.4b)$$

$$4\, Cu^{2+} + 2H_2S + 4e^- = 2Cu_2S + 4H^+ \quad (5.5b)$$

The overall equation for reactions (5.4a) and (5.4b) is equation (5.4), while equation 5.5 represents the overall equation for reactions (5.5a) and (5.5b).

$$Ni_3S_2 + 2Cu^{2+} \rightarrow Cu_2S + NiS + 2Ni^{2+} \quad (5.4)$$

$$Ni_3S_2 + Ni + 4Cu^{2+} \rightarrow 4\, Ni^{2+} + 2Cu_2S \quad (5.5)$$

However, no smell of H_2S was detected during the leaching experiments, probably due to the fact that reactions (5.4b) and (5.5b) were as fast as reactions (5.4a) and (5.5a). Hence, H_2S was probably consumed as fast as it was produced.

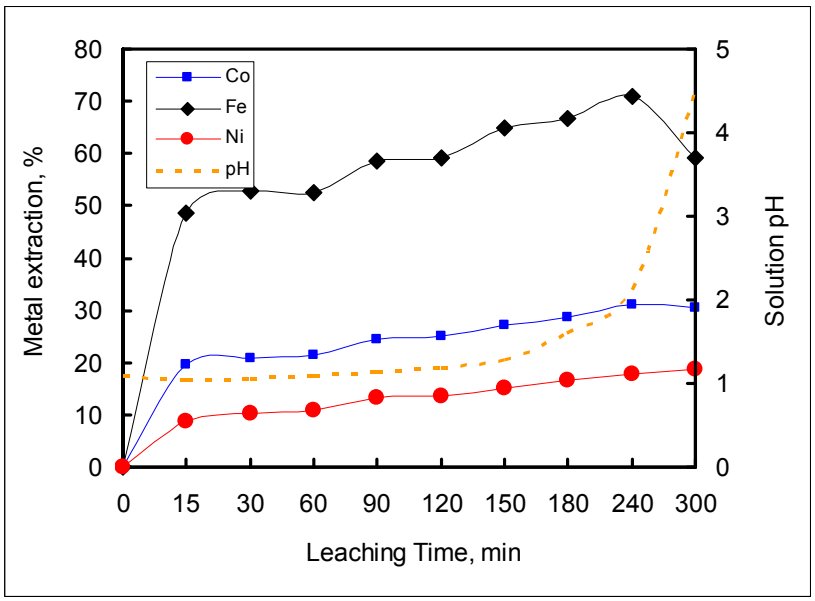

Figure 5.7: Variation of metal concentrations and pH of leach solution as a function of leaching time at 70 °C (Stirring rate: 205 rpm; Pulp density: 1.7kg/L)

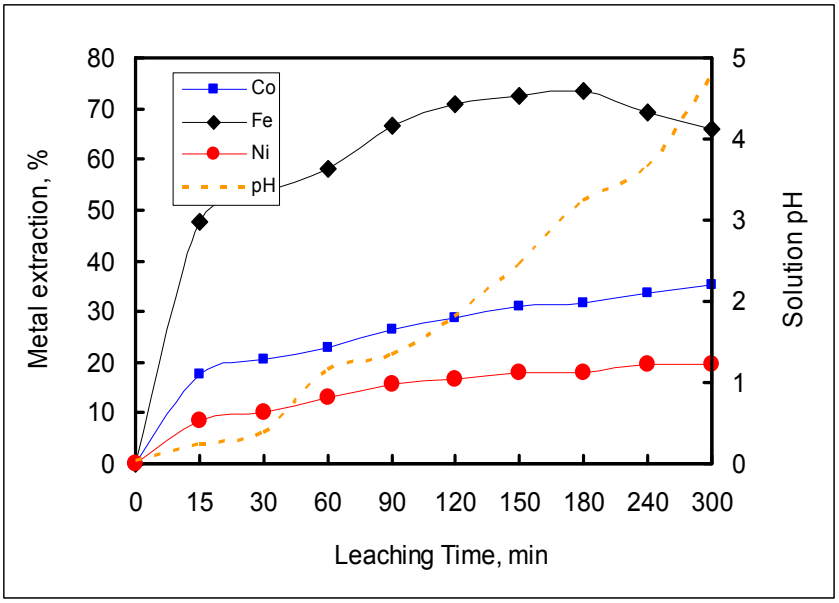

Figure 5.8: Variation of metal concentrations and pH of leach solution as a function of leaching time at 80 °C (Stirring rate: 205 rpm; Pulp density: 1.7kg/L)

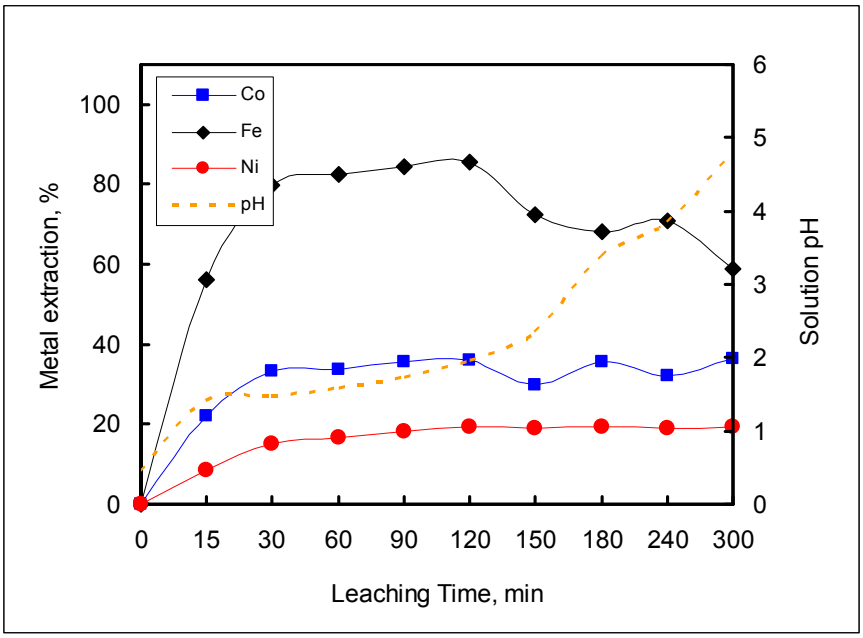

Figure 5.9: Variation of metal concentrations and pH of leach solution as a function of leaching time at a stirring rate of 400 rpm (Temp.: 60 ^{o}C; Pulp density: 1.7kg/L)

One interesting observation was that the pH of the solution increased sharply immediately after Cu^{2+} ions were completely precipitated out of solution as can be seen in Figures 5.10, 5.11 and 5.12, which also show metal concentrations of the leach solution as a function of leaching time at temperatures of 60, 70 and 80 ^{o}C, respectively. The reason for this behaviour was attributed to the fact that prior to complete copper cementation, part of the matte leaching process occurred via the cementation process (reactions 5.1 – 5.5) and by direct attack with H_2SO_4 (reactions 5.7 – 5.13). After complete copper rejection, the leaching process was mainly by direct reaction of the matte with H_2SO_4, which consumed most of the acid and hence raised the solution pH. The rise in the pH resulted in the precipitation of iron at pH values above 3 (see Figures 5.7, 5.8 and 5.9). It should be noted that the rise in pH to above 3 was only observed in the experiments where the Cu^{2+} ions were completely precipitated within 3 hours of leaching time. (Figures 5.11 and 5.12).

Iron can hydrolyse to form ferric hydroxide or basic ferric sulphate (parabutlerile) as shown in reactions (5.14) and (5.15):

$$Fe^{3+} + 3H_2O \rightarrow Fe(OH)_3 + 3H^+ \quad (5.14)$$

$$Fe^{3+} + HSO_4^- + H_2O \rightarrow Fe(OH)SO_4 + 2H^+ \quad (5.15)$$

Under the leaching conditions applied in this study, where the leaching vessel was covered and no air/oxygen was added, most of the iron was expected to be in the ferrous form. However, due to the fact that the leaching vessel was not air-tight some air from the atmosphere may have entered the system and oxidized some of the ferrous iron to ferric according to reaction (5.16):

$$2Fe^{2+} + 2H^+ + \tfrac{1}{2}O_2 \rightarrow 2Fe^{3+} + H_2O \quad (5.16)$$

It is also known that copper is an effective catalyst for oxidation of ferrous iron (Symens et al., 1979; and Hofirek and Kerfoot, 1992). The rate of iron oxidation and hydrolysis increases significantly in the presence of copper ions. If cupric ions are rejected from the leach solution, as was the case in this study, iron hydrolysis and precipitation required longer reaction time for complete precipitation. Yuhua and Xianxuan (1990) noted that the rate of iron oxidation increases because the Cu^{2+} ions can oxidize Fe^{2+} ions in solution according to reaction (5.17):

$$Fe^{2+} + Cu^{2+} \rightarrow Cu^+ + Fe^{3+} \quad (5.17)$$

The Cu^+ is then re-oxidized to Cu^{2+} by air.

Hofirek and Kerfoot (1992) indicated that the dissolved iron acts as an electron carrier and enhances the leaching rates according to the following reaction:

$$Ni_3S_2 + 2Fe^{3+} \rightarrow 2Fe^{2+} + 2NiS + Ni^{2+} \quad (5.18)$$

Symens et al. (1992), who conducted an atmospheric leach on a Ni-Cu matte with a higher iron content (1 – 3%), indicated that increase in the agitation and

decrease in solution temperature accelerate iron precipitation. This fact was also noted in the present study where more iron was precipitated at a higher stirring rate of 400 rpm in comparison with that at 205 rpm (see Figure 6.13). However, this phenomenon was not observed in the experiments where the effect of temperature was investigated (Figure 6.4).

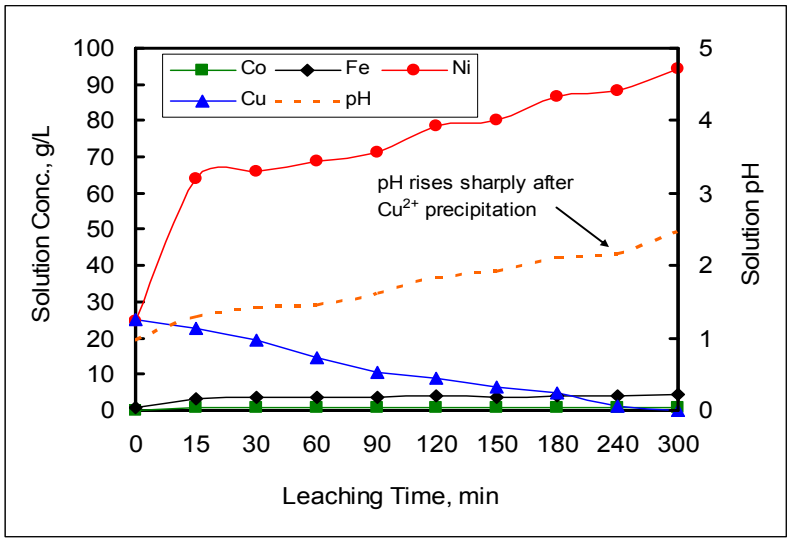

Figure 5.10: Variation of metal concentrations in leach solution as a function of leaching time at 60 °C (Stirring rate: 205 rpm; Pulp density: 1.7kg/L).

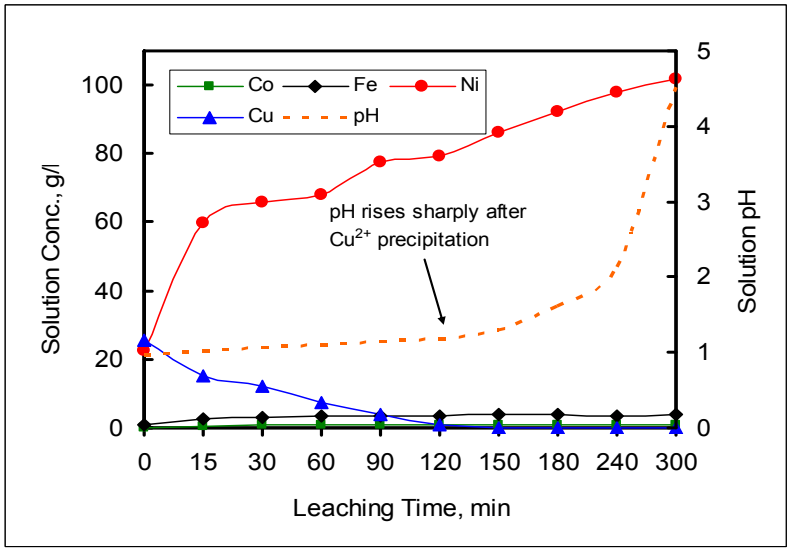

Figure 5.11: Variation of metal concentrations in leach solution as a function of leaching time at 70 °C (Stirring rate: 205 rpm; Pulp density: 1.7kg/L).

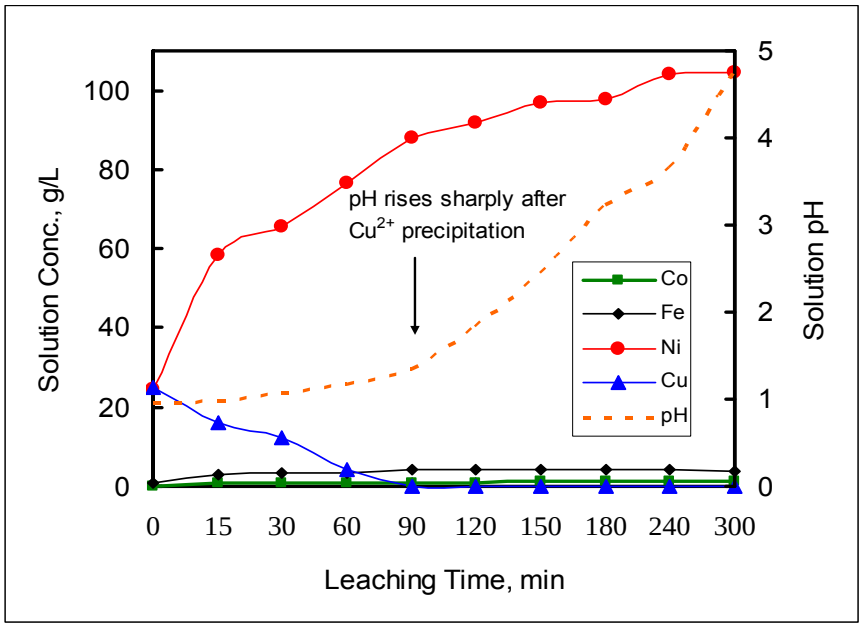

Figure 5.12: Variation of metal concentrations in leach solution as a function of leaching time at 80 °C (Stirring rate: 205 rpm; Pulp density: 1.7kg/L).

5.3 Galvanic interaction between mineral phases during leaching of the Ni-Cu matte

It is a well known fact that when conducting or semi conducting minerals in contact with each other are subjected to a leaching medium which facilitates charge transfer, galvanic interactions may occur which can enhance the leaching rate of one or more members of the electrochemically coupled minerals and retard the dissolution of other mineral members. In general, a galvanic couple is operative where two or more solid phases are in electrical contact, and each solid assumes either anodic or cathodic behaviour and has its own separate surface area for reaction. The galvanic interaction results in change of rates of anodic and cathodic half reactions that occur at the surface of each solid phase. Several investigators have published information on the electrochemical behaviour of sulphide minerals. Hiskey and Wadsworth (1981) published an extensive review of electrochemical processes that take place in the leaching of metal sulphides and oxides, and noted that a fundamental property of semi-conducting minerals is the characteristic “rest” potential. The rest potential, for interfacial electrode

processes, corresponds to the equilibrium (no net anodic or cathodic current) electrode potential. Generally the phenomenon of galvanic interaction is explained in terms of the rest potential of each mineral with respect to the standard hydrogen electrode (SHE). Minerals with more positive rest potentials (i.e. more noble minerals) act as cathodes, while minerals with less positive (or more negative) rest potentials act as anodes. For example, if chalcocite (Cu_2S) with rest potential of 0.44 V vs SHE is in contact with covellite (CuS) whose rest potential is 0.42 V vs SHE in the presence of a leaching medium the CuS will dissolve anodically and the rate of dissolution will increase, while Cu_2S will act as the cathode which will retard its dissolution. Berry et al. (1978) studied galvanic interaction between chalcopyrite (rest potential: 0.52 V vs SHE) and pyrite (rest potential: 0.63 V vs SHE) during bacterial leaching of low-grade chalcopyrite waste rock. They observed that during the leaching of these minerals as separate, non-contacting phases, the pyrite corroded more rapidly than the chalcopyrite. When the pyrite and chalcopyrite were in contact, the resulting galvanic interaction caused the chalcopyrite to corrode more rapidly than the pyrite; which was effectively passivated. Holmes and Crundwell (1995) studied the copper-pyrite galvanic couple in acidified ferric sulphate solution and the galena-pyrite galvanic couple in ferric nitrate solution. They developed a quantitative description of galvanic interactions between sulphide minerals based on thermodynamic and kinetic parameters; and used these parameters in a mathematical model to obtain a prediction of the magnitude of the galvanic interaction. Southwood (1985) carried out experiments on the acid leaching of nickel and copper from sulphidic ore in the presence of pyrite under atmospheric pressure and temperature (25 ^oC). The results obtained showed that the dissolution rate of nickel and copper from a pyrrhotite-pentlandite-chalcopyrite ore in a lixiviant of sulphuric acid was greatly enhanced in the presence of pyrite. He attributed the observed result to a probable galvanic mechanism. Leaching behaviour of gold in contact with associated minerals depends on the galvanic interaction between gold and the minerals and partially on the formation of a passivating film on the gold surface (Lorenzen and van Deventer, 1992). Gold in

contact with conducting minerals will passivate as a result of the enhanced magnitude of the cathodic current, resulting in decreased gold dissolution rates. The list of electrochemical studies of anodic dissolution of minerals is inexhaustible and includes investigations by Paul et al. (1978), Nicol et al (1975, Nicol, 1984), Jayasekera et al. (1995) and Reddy et al. (1987).

Although galvanic phenomenon could not be proved in the leaching system investigated in the present study, the Ni-Cu sulphide minerals and the Ni alloys were in intimate contact with one another in the matte, therefore it was possible that a galvanic couple existed between the Ni alloy and the sulphide minerals in which the Ni alloy had a lower rest potential and thus acted as an anode. This may have also contributed to the leaching of the nickel from the alloy, as depicted in Figure 5.13. The dissolution of nickel from the Ni alloy can occur through the anodic half cell reaction represented by equation (5.5a). It should be noted that equations 5.4a, 5.4b, 5.5a and 5.5b are given in section 5.2.2, but are repeated here for the sake of clarity.

$$Ni + Ni_3S_2 + 4H^+ = 2H_2S + 4Ni^{2+} + 4e^- \quad (5.5a)$$

The cathodic reaction is the reduction of aqueous copper ions by the H_2S onto the Ni_3S_2 surface (equation (5.5b)):

$$4Cu^{2+} + 2H_2S + 4e^- = 2Cu_2S + 4H^+ \quad (5.5b)$$

The other factor that may have contributed to the leaching of the nickel is the galvanic couple between the copper sulphide and nickel sulphide minerals. In this case, the anodic reaction is the leaching of the Ni_3S_2 according to reaction (5.4a):

$$Ni_3S_2 + 2H^+ = H_2S + NiS + 2Ni^{2+} + 2e^- \quad (5.4a)$$

The cathodic reaction is the reduction of copper ions by the H_2S:

$$2Cu^{2+} + H_2S + 2e^- = Cu_2S + 2H^+ \quad (5.4b)$$

The thermodynamic relationships of various solids in contact with aqueous solutions of specific composition can be illustrated by potential-pH diagrams (Pourbaix diagrams). These diagrams can be used to get a rough indication as to which galvanic couples in a leaching system are thermodynamically favoured to react anodically, and those that are thermodynamically likely to react cathodically. For example Figure 5.14 indicates that the potential of the Cu^{2+}/Cu_2S couple for the given conditions is more positive than that of the Ni^{2+}/Ni_3S_2 couple. This indicates that reactions involving the Ni^{2+}/Ni_3S_2 couple have lower half cell potentials than those of the Cu^{2+}/Cu_2S couple, and are therefore thermodynamically favoured to react anodically in the presence of copper ions. However, it should be noted that the sequence of reaction products does not necessarily correspond to those having the greatest thermodynamic drive, but relative reaction rates should also be taken into account (Hiskey and Wadsworth, 1981).

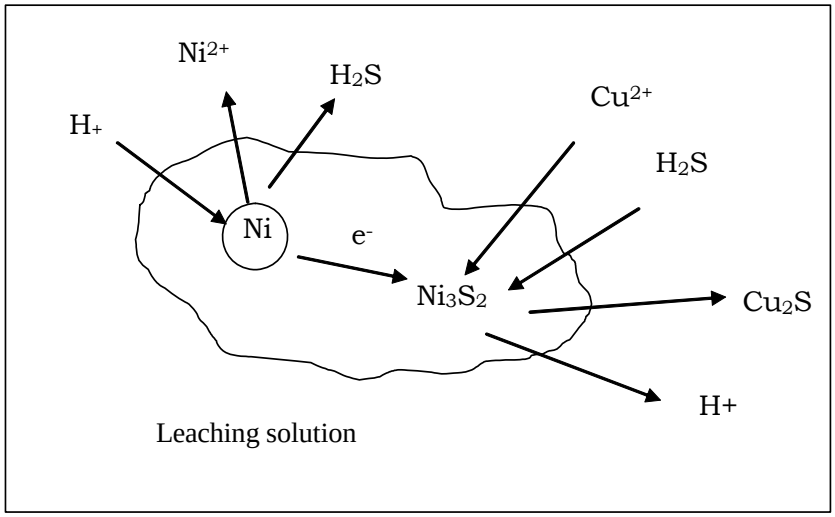

Figure 5.13: Schematic diagram of galvanic couple between nickel alloy and nickel sulphide minerals.

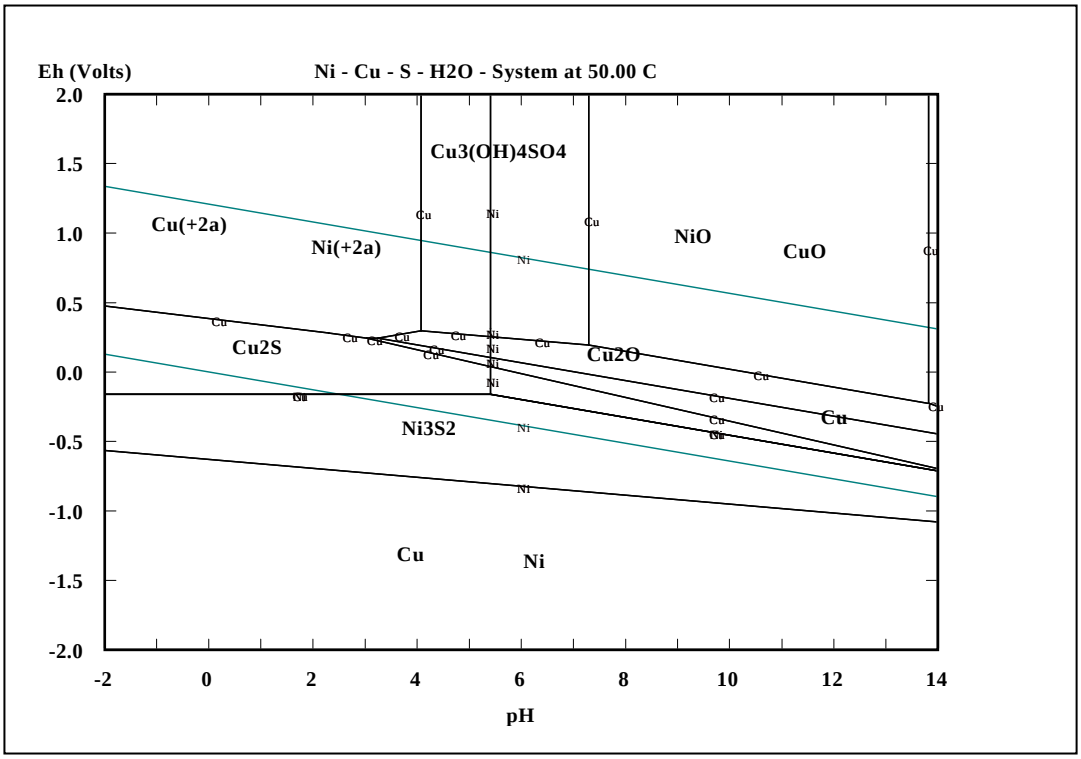

Figure 5.14: Eh-pH diagram for the Ni-Cu-S-H_2O system at 50 ^oC,; [Ni] = 2.00 M, [S] = 2.00 M and atmospheric pressure. (M = molality)

5.4 Mechanism of copper cementation during leaching of the Ni-Cu matte

Cementation is defined as an electrochemical reaction involving the precipitation of a more noble metal ion from solution by another more electropositive metal according to the overall reaction:

$$mN^{n+} + nM = nM^{m+} + mN \qquad (5.19)$$

Where N is the noble metal and M is the precipitant. Cementation is an important reaction in hydrometallurgical processes, for example it can be used to recover copper from acid leach solutions and gold from cyanide leach solutions. Many studies have been conducted on the process of cementation of copper, using precipitants such as Fe, Al, and Ni, to understand the mechanisms and kinetics involved. Nadkarni et al. (1967) carried out a study of copper precipitation on iron using a rotating disc. They correlated the rate of

cementation with such parameters as copper and hydrogen ion concentration, flowrate, geometric factors and temperature. Annamalai and Murr (1979) conducted a similar study to investigate the influence of deposit morphology on the kinetics of copper cementation on pure iron. Investigations on copper cementation on pure aluminum disc include kinetic studies carried out by Annamalai and Hiskey (1978), Mackinnon and Ingraham (1970), and Donmez et al. (1999). Mackinnon et al. (1971) studied copper cementation on pure nickel and nickel-copper alloy discs. According to their results, copper cementation on the Ni-Cu alloy was unsuccessful, and this was attributed to a lower potential difference between the copper solution and the surface of the nickel-copper alloy. However, satisfactory results were obtained in the present study in which the precipitant was also the nickel metal in the form of Ni-Cu alloy within the sulphide matte. Other authors who have carried out investigations on the cementation of various metals from different solutions include Anacleto and Carvalho (1996), Hsu and Tran (1996), Puvvada and Tran (1995), Sahoo and Srinivasa (1982), and Addy and Fletcher (1987).

Copper cementation reaction on a nickel precipitant can be represented by equation 5.20:

$$Ni^{o} + Cu^{2+} = Ni^{2+} + Cu^{o} \qquad (5.20)$$

During the leaching of the Ni-Cu matte some of the aqueous copper precipitated as Cu_2S (equations (5.4b) and (5.5b)) due to the presence of H_2S, which was generated during the leaching process, according to reactions (5.4a) and (5.5a).

However, as no oxidant was added to the system the reaction between the sulphide minerals and acid was considered insignificant. It was therefore assumed that reactions (5.4) and (5.5) did not have significant effect on the overall cementation process, and was not accounted for in the discussion of the kinetics of copper cementation presented in chapter 6.

The mechanism by which the over-all cementation reaction at the solid-liquid interface can occur is generally considered to go through a number of steps. For

cementation of aqueous copper ions onto solid Ni-Cu matte particles, the steps involved are:

1. Diffusion of Cu^{2+} ions to the solid matte surface,
2. Adsorption of the Cu^{2+} onto the surface,
3. Chemical reaction at the surface,
4. Desorption of Ni^{2+} from the matte surface, and
5. Diffusion of Ni^{2+} away from the surface.

Any one of the above steps may be rate controlling. Diffusion of the Cu^{2+} ions through the bulk solution may be eliminated by sufficiently increasing the stirring rate. However, diffusion through a boundary layer could still be the rate – controlling step.

5.5 Nature of the cemented deposit

The nature of the deposit, with regard to size and shape of the particles, could not be determined due to the small quantity of the deposit in comparison with the leach solid residue. Examination of the initial matte and the leach residue under a scanning electron microscope did not clearly show the difference in particle size and shape between the initial matte sample and the final leach residue, as the deposit was mixed with the residue (Figure 5.13).

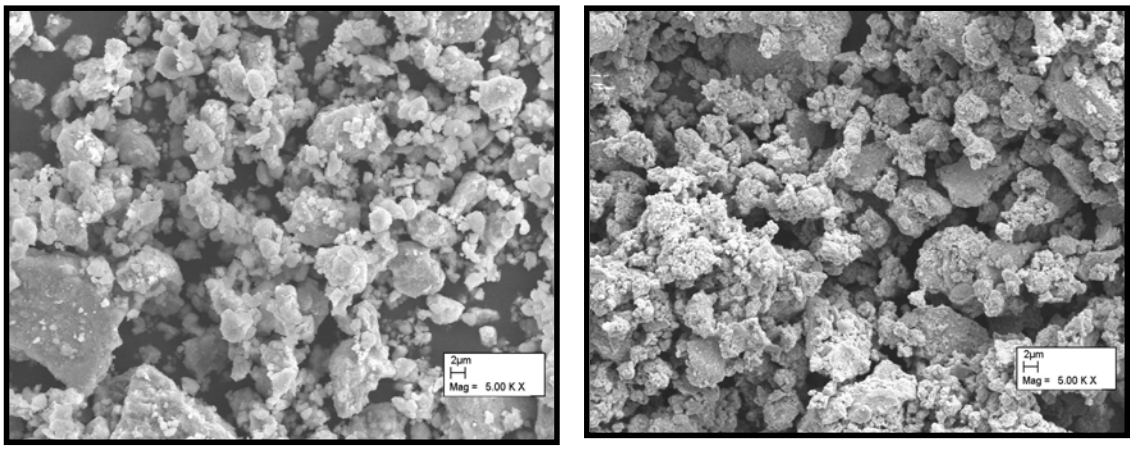

(a) **(b)**

Figure 5.13: SEM images of matte particles: (a) before leaching, (b) after 5 hours of leaching.

5.6 Summary

In this chapter results of the atmospheric leaching experiments have been discussed on the basis of the thermodynamics and mechanism of the leaching system studied. The first section (section 5.1) discussed the thermodynamics of the Ni-Cu matte – H_2SO_4 leaching system using the Potential-pH (Eh – pH) equilibrium diagrams (pourbaix diagrams). The pourbaix diagrams have predicted the possible thermodynamically stable species in the Ni-Cu matte – H_2SO_4 – $CuSO_4$ leaching system, under the investigated conditions, as aqueous nickel, metallic nickel, nickel sulphides (e.g. Ni_3S_2), aqueous copper, metallic copper and copper sulphides (e.g. Cu_2S). The species predicted by the Eh-pH diagrams were in agreement with the results obtained from the analysis of the leach solids and solutions.

Section 5.2 discussed the leaching mechanism of the matte, based on the mineralogical investigations of the matte as well as on the chemistry of the leaching process. It was noted that the leaching mechanism of base metals depends on the phases in which the metals are present. The metals in the alloy phase were leached out of the matte particles and no mineral matrix disintegration occurred. The results showed some millerite (NiS) in the leach solids indicating that heazlewoodite dissolved to some extent, and transformed into NiS. The aqueous copper precipitated as metallic copper and probably as chalcocite/chalcocite-Q, although this could not be confirmed by the XRD analysis as there was already chalcocite in the original matte. The leaching mechanism based on the process chemistry was supported by mineral phases found in the leach solids, solution analyses and information from the literature. In this mechanism the matte leaching occurred through the cementation process and direct attack of the matte by acid, especially in the early stages when the aqueous copper was still present. After copper was completely precipitated from the solution, the leaching process was by direct reaction of the matte with acid. The pH of the solution rose sharply after the Cu^{2+} ions were completely

precipitated, probably due to the rapid consumption of the acid by the leaching reactions. The sharp rise in the pH was only noted in the experiments where the copper ions were completely precipitated. The nickel sulphides may have been leached by the metathesis reaction and by acid due to presence of air, as the leaching vessel was not air tight. The nature of the copper deposit could not be characterised due to the small quantity of deposit in comparison with the leach solid residue.

In section 5.3 leaching of the matte due to galvanic interaction between the mineral phases has been discussed. It was postulated that because the Ni-Cu sulphide minerals and the Ni alloys were in intimate contact, they formed a galvanic couple in which the Ni alloy had a lower rest potential and thus dissolved anodically. The other factor that may have contributed to the leaching of the matte is the galvanic couple between the copper sulphide and nickel sulphide minerals. In this case, the nickel sulphide minerals dissolved anodically.

CHAPTER 6

6.0 ATMOSPHERIC LEACHING EXPERIMENTS OF Ni-Cu MATTE

Leaching behaviour of the nickel-copper matte in copper spent electrolyte during the repulping stage at Impala Base Metals Refinery (BMR) was studied in order to improve understanding of the process. Results of the dissolution of nickel, cobalt and iron as well as cementation of copper during the leaching process are presented and discussed in this chapter. As stated earlier (see chapter 3), the base metal refining process consists of a matte repulping stage prior to a series of pressure leaching stages. The repulping stage can be considered as a "non-oxidative" atmospheric leach stage, since leaching of the matte starts immediately it comes into contact with the $CuSO_4$-H_2SO_4 repulping solution.

It should be noted that the results are an indication of the degree of leaching that can be expected under the experimental conditions employed in this study. To show the trend in the dissolution behaviour of nickel, cobalt and iron during the leaching process the extractions were ploted against leaching time. Results obtained from solid analysis have been compared with those from the solution analysis. To show reproducibility of the results graphs of tests done in duplicate are also presented. The results are also depicted in bar graphs; the error bars on the graphs indicate a 5% error in the results.

Effect of variations in the process parameters such as temperatures, stirring rate, pulp density, matte particle size, initial copper and acid concentrations were studied. Leaching kinetics of the matte were characterized with the shrinking core model, which was done by using the dissolution kinetics of nickel in the experiments conducted at temperatures of 50, 60 and 70 ^oC using a portion of matte that was screened to –300+150 µm particle size fraction. Nickel dissolution kinetics was used because nickel was the most abundant element in

the matte (48%), and was one of the elements that dissolved. Iron and cobalt content of the matte was very low at 0.6 %Fe and 0.34% Co. Copper which was about 31% in the matte precipitated during the leaching process, and hence could not be used in the model. Depending on the chemical-physical process controlling nickel dissolution, different equations can be applied. The equations, which are also given in section 2.4 but repeated here for clarity, may be summarized as:

For a surface chemical reaction controlled process:

$$1-(1-X)^{1/3} = kt \qquad (6.1)$$

For a product layer/ash diffusion controlled process:

$$1-3(1-X)^{2/3} + 2(1-X) = kt \qquad (6.2)$$

For mixed (surface and product layer/ash) controlled process:

$$[1-3(1-X)^{2/3} + 2(1-X)] + \alpha[1 - (1-X)^{1/3}] = kt \qquad (6.3)$$

Where X is the fraction reacted, t is the time of leaching, k is the rate constant and α is a kinetic constant.

The kinetics of copper cementation was evaluated by measuring the rate of decrease of copper concentration in the solutions, as a result of precipitation onto the suspended matte particles of known surface area. Cementation reactions are first order processes with respect to the noble metal, which is copper in this case. The reactions are found to obey the first order kinetic law, in which data fit a first order rate equation. The rate of copper cementation onto Ni–Cu matte can be represented by the following first order rate equation:

$$\frac{d[Cu^{2+}]}{dt} = -KA\frac{[Cu^{2+}]}{V} \qquad (6.4)$$

By integration and rearrangement of Equation (6.4) one can obtain the following equation:

$$Log\ \frac{[Cu^{2+}]_t}{[Cu^{2+}]_0} = -\frac{KAt}{2.303V} \qquad (6.5)$$

Where $[Cu^{2+}]_t$ = copper concentration at time t (g/L)

$[Cu^{2+}]_0$ = initial copper concentration at t = 0 (g/L)

K = Cementation rate constant (cm/s)

V = Volume of solution (cm^3)

A = Surface area of matte particles (cm^2)

t = reaction time (s)

A plot of $\log[Cu^{2+}]_t / [Cu^{2+}]_0$ vs time would yield a straight line with a slope equal to -KA/2.303V, from which the cementation rate constant or mass transfer coefficient (cms^{-1}) can be determined.

Equation (6.5) shows that the rate of cementation is also a function of the depositing surface area (A), on which the copper ions are reduced and precipitated. At various reaction conditions the morphology of the deposits has been reported to be different (Annamalai and Hiskey, 1978 and Annamalai and Murr, 1979). This results in a change in the surface roughness and hence in the effective surface area of the deposit which may change the mass transfer conditions within the boundary layer. The rate of cementation is therefore, a function of all parameters that influence the morphology of the deposit and can be accelerated or retarded. Most cementation processes proceed through two distinct kinetic regions namely an initial slow period followed by a final enhanced period where the cementation rate is much higher. The enhanced rate of cementation is attributed to the enhancing effect of the surface deposit.

Annamalai and Murr (1979) explained the enhancement in terms of attaining a critical deposit mass which effectively increases the cathodic surface area, and alters the diffusion boundary layer by increased surface roughness. While the two-step mechanism was typical for most experiments in this study, it did not appear in a few cases in which the entire rate was slow.

The kinetics of copper cementation onto the Ni-Cu matte was analysed using the first-order rate law shown in Equation (6.5). The cementation reaction can be seen as consisting of two stages: the initial period of reaction (stage 1), and the subsequent period (stage 2). Stage 1 of the reaction is represented by the initial straight line portion of the $\log[Cu^{2+}]_t/[Cu^{2+}]_0$ vs time plot, and stage 2 is represented by the subsequent straight line of the graph (see Figure 6.8). It should be noted that each of the two stages on the graph has a different slope, and hence different value of the rate constant (K). However, due to the fact that no geometric correction was used for the change in the surface area of the matte during the reaction period, only the rate constant for the first stage was determined in all the tests. Thus, K refers to the first stage rate constant in the present study. It should be noted that lower values of the rate constants (K) were obtained in the present study (values ranged from 0.004 to 0.028 x 10^{-3} cm/s) in comparison with those obtained by MacKinnon et al. (1971), Annamalai and Hiskey (1978), MacKinnon and Ingraham (1970), and Nadkarni et al. (1967). MacKinnon et al. (1971) obtained rate constant values of more than 0.2 x 10^2 cm/sec in a study of copper cementation on nickel discs using rotating disc method. The comparatively low rate of cementation obtained in the present study was probably due to the fact that the total surface area of the matte, which was used in the calculation of the K values, was much larger than the surface area of nickel particles in the matte on which the cementation reaction takes place. In addition, much higher pulp densities and solution concentrations were employed in this study.

The activation energy (E_a) of both the leaching and cementation reactions were determined from the Arrhenius equation (Equation 6.6).

$$K = Ae^{-E_a/RT} \quad (6.6)$$

Where K is the reaction rate constant, A is called the frequency factor, R is the gas constant and E_a is the activation energy of the reaction.

6.1 Effect of temperature on the leaching behaviour of the Ni-Cu matte

6.1.1 Effect of temperature on the dissolution of nickel, cobalt and iron

The effect of temperature on the leaching behaviour of the matte was investigated by changing the value of the temperature while keeping the other variables constant. The experiments were conducted for the temperature range 50 – 80 ^oC at a pulp density of 1.7 kg/L and stirring rate of 205 rpm. The results obtained are presented in Table 6.1, and graphically illustrated in Figures 6.1 – 6.4. Figure 6.5 illustrates the reproducibility of the results, and shows similar leaching behaviour of the metals. Results obtained from solid analysis were also comparable with those from the solution analysis (Appendix A). It should be noted that the results obtained are an indication of the leaching that can be expected under the experimental conditions employed in this study. To show the trend in the dissolution behaviour of nickel, cobalt and iron during the leaching process the extractions were ploted against leaching time as shown in Figures 6.1, 6.2 and 6.3, respectively. Detailed data on the metal extractions and concentrations of the leach solutions during the atmospheric leaching process are presented in Appendix A.

The results indicated that increasing the temperature from 50 ^oC to 60 ^oC slightly increased both the rate and degree of nickel extraction; however no significant increase in the degree of nickel extraction was observed for the temperature

range 60 – 80 °C (Figure 6.1). Mineralogical analysis also indicated that more nickel was leached in the temperature range 60 – 80 °C as suggested by the fact that Ni_3S_2 transformed into NiS at 60 – 80 °C, whereas at 50 °C no mineral transformation occurred (see Table 7.1 in section 7.3.1)

In the case of cobalt, no clear trend was observed with regard to the effect of temperature variation as both the rate and degree of leaching appeared to be insensitive to temperature changes in the range 50 - 70 °C and only increased slightly at 80 °C (Figure 6.2). Figure 6.3 shows that at the low temperature of 50 °C relatively low iron extraction was achieved, however when the temperature was increased to 60 °C both the rate and degree of leaching increased. It also illustrates that increasing the temperature from 60 to 80 °C did not have effect on the iron dissolution as similar extractions were observed. However, it should be noted that iron extractions could not be determined with certainty due to iron hydrolysis and subsequent precipitation above pH 3.

Table 6.1: Ni, Co, and Fe extractions and final metal concentrations of the solution after atmospheric leaching of the matte at different temperatures

Temperature (°C)	**Metal extraction (%)**			**Final solution concentration (g/L)**			
	Ni	**Co**	**Fe ***	**Ni**	**Co**	**Fe**	**Cu**
50	13.2	27.5	45.8	76.6	0.9	4.2	7.9
60	16.9	28.7	70.4	85.8	1.0	4.3	0.0
70	18.6	30.4	70.8	101.6	1.1	3.6	0.0
80	19.5	35.3	73.4	104.6	1.2	3.9	0.0

*The value shows maximum extraction attained prior to Fe precipitation.
Leaching conditions: stirring rate: 205 rpm, pulp density: 1.7kg/L, residence time: 5 hours

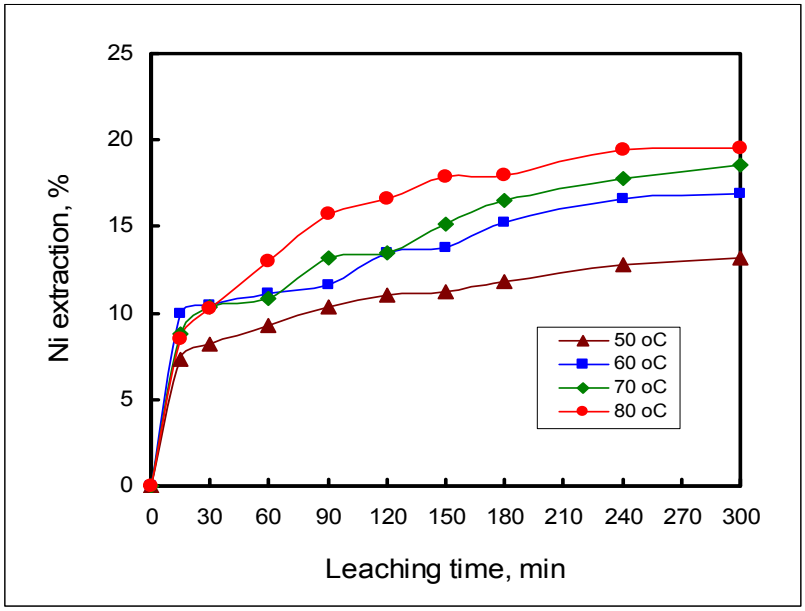

Figure 6.1: Nickel extraction as a function of leaching time at different temperatures (stirring rate: 205 rpm, pulp density: 1.7kg/L).

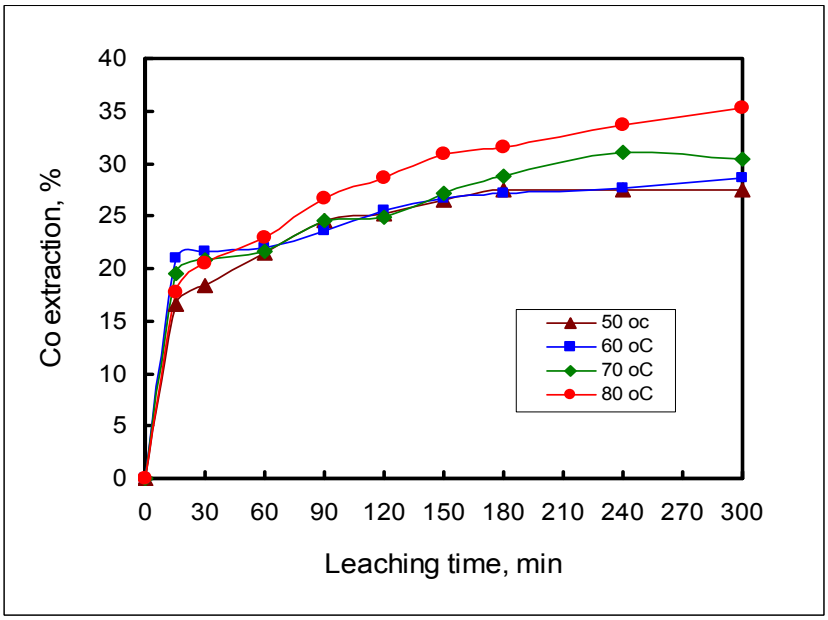

Figure 6.2: Cobalt extraction as a function of leaching time at different temperatures (stirring rate: 205 rpm, pulp density: 1.7kg/L)

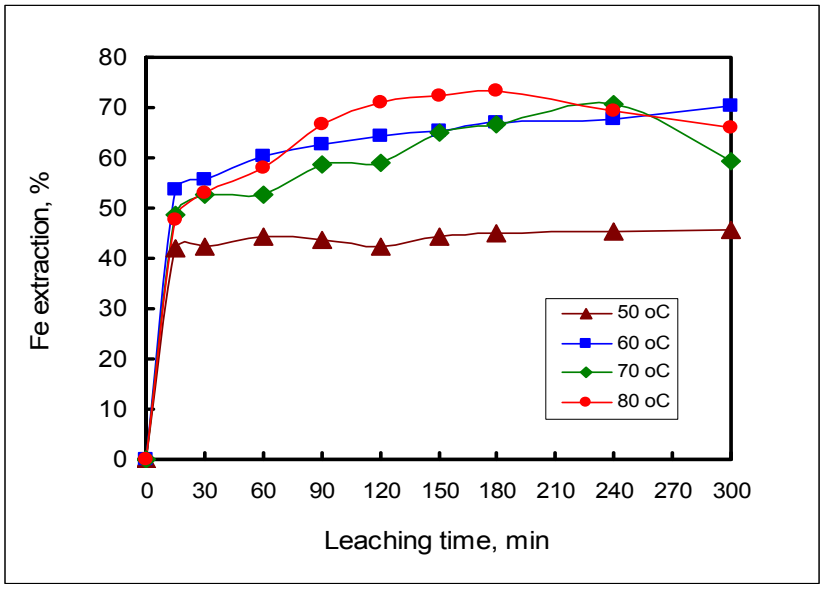

Figure 6.3: Iron extraction as a function of leaching time at different temperatures (stirring speed: 205 rpm, pulp density: 1.7kg/L)

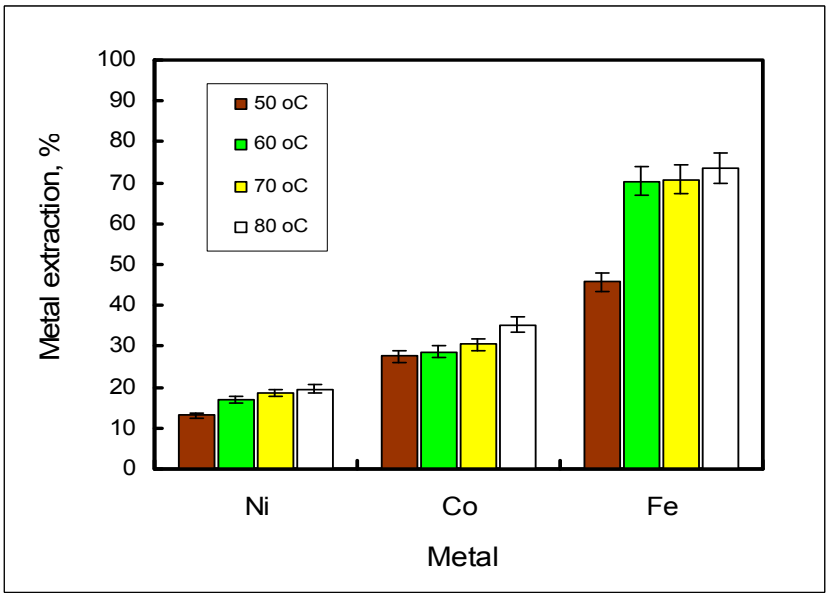

Figure 6.4: Metal extractions after atmospheric leaching of the Ni-Cu matte at different temperatures

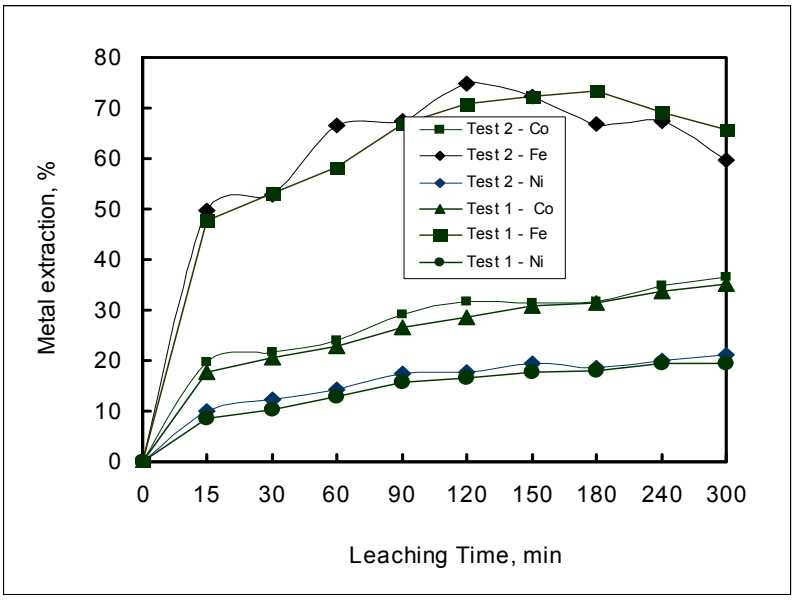

Figure 6.5: Comparison of metal extractions between two tests conducted at a temperature of 80 °C (stirring rate: 205 rpm, pulp density: 1.7kg/L).

The initial dissolution rates of all the three metals were relatively high during the first 15 minutes of leaching (Figures 6.1 – 6.3). The high rates of metal dissolution were probably due to the fast chemical reaction kinetics of the matte in the initial stages of leaching (0 – 15 min.) when fine particles were still present. About 50% of the "leacheable nickel" was extracted within the first 15 minutes, while more than 50% of leacheable cobalt and iron were solubilized. The term leacheable nickel (or leacheable metal) in this case refers to the maximum nickel that can possibly be leached under the leaching conditions employed in this study. The leacheable nickel is believed to leach mostly from the Ni alloy, the remainder originated from the nickel sulphide.

The results show different degrees of extraction for the three metals, iron extraction was the highest followed by that of cobalt; and nickel extraction was the lowest. This suggests that most of the iron in the matte probably occurred in an alloy form, probably as Ni-Fe alloy (Figure 5.6) which was leachable under the conditions employed in this study. Cobalt extraction was the second highest and

it is believed that part of it existed as an alloy and the rest as sulphide, as reported in a discussion document from Impala Platinum Refineries (Spandiel, 1996). However, it was difficult to detect it with the SEM-EDX and XRD analyses because the matte had very low cobalt content (0.3%). It is possible that the metallic cobalt was responsible for most of the cobalt dissolution observed in this study. As expected, the degree of nickel extraction was the lowest since most of the Ni in the Ni-Cu matte exists as heazlewoodite (54%) and little occurs as an alloy (11%), which is more likely to leach under the conditions employed where no oxygen was added.

As indicated earlier the dissolution kinetics of the metals were characterized with the shrinking core model using nickel dissolution kinetics data obtained from an experiment conducted on the -300+150μm size fraction of the matte. The equation describing reaction controlled by diffusion through surface layer (Equation 6.2), appeared to give the best fit (Figure 6.6a), in comparison with the equations describing reaction controlled by a surface chemical reaction (Equation 6.1) as shown in Figure 6.6b or the equation describing a mixed (chemical reaction and diffusion) controlled process (Equation 6.3) as shown in Figure 6.6c. Although the mixed controlled equation also appeared to give a good fit, the correlation coefficient values obtained were lower than those for the diffusion controlled reaction. The correlation coefficient values for the diffusion controlled reaction at the temperatures of 50, 60 and 70 ^{o}C were found to be 0.95, 0.91 and 0.96 respectively, while those of a mixed controlled reaction were 0.88, 0.84 and 0.91 at 50, 60 and 70 ^{o}C respectively. In view of the higher correlation coefficient values obtained for the diffusion controlled reaction, it is reasonable to conclude that the diffusion control equation gives the best representation of the leaching process.

$$1-(1-X)^{1/3} = kt \qquad (6.1)$$

$$1\text{-}3(1\text{-}X)^{2/3} + 2(1\text{-}X) = kt \quad (6.2)$$

$$[1\text{-}3(1\text{-}X)^{2/3} + 2(1\text{-}X)] + \alpha[1 - (1\text{-}X)^{1/3}] = kt \quad (6.3)$$

The variation of 1- $3(1\text{-}X)^{2/3}$ + 2(1-X) with time is shown in Figure 6.6a for three temperatures (50, 60 and 70 ^{o}C). The reaction rate constants (K) were obtained from the slopes of the 1-$3(1\text{-}X)^{2/3}$ + 2(1-X) Vs time lines (Figure 6.6a), and these rate constants were used in the Arrhenius equation (Equation 6.6) to determine the activation energy (E_a) of the reaction using Figure 6.6. Activation energy (E_a) of 31 kJ/mol was obtained from the Arrhenius plot of equation 6.6 (see Figure 6.7) and this value of the E_a suggested a diffusion-controlled leaching reaction. Detailed experimental data and calculations are presented in Appendix A.

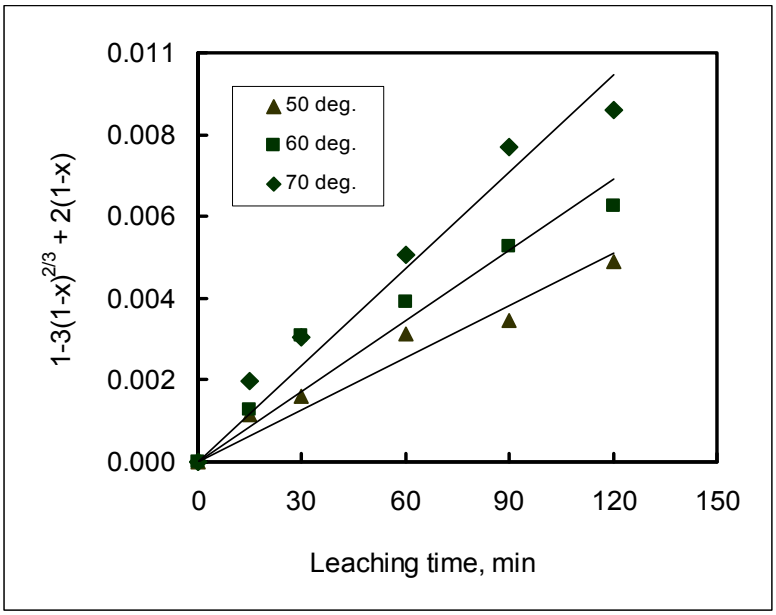

Figure 6.6a: Plot of 1-$3(1\text{-}X)^{2/3}$ + 2(1-X) vs time for the leaching of Ni at different temperatures for the diffusion controlled reaction.

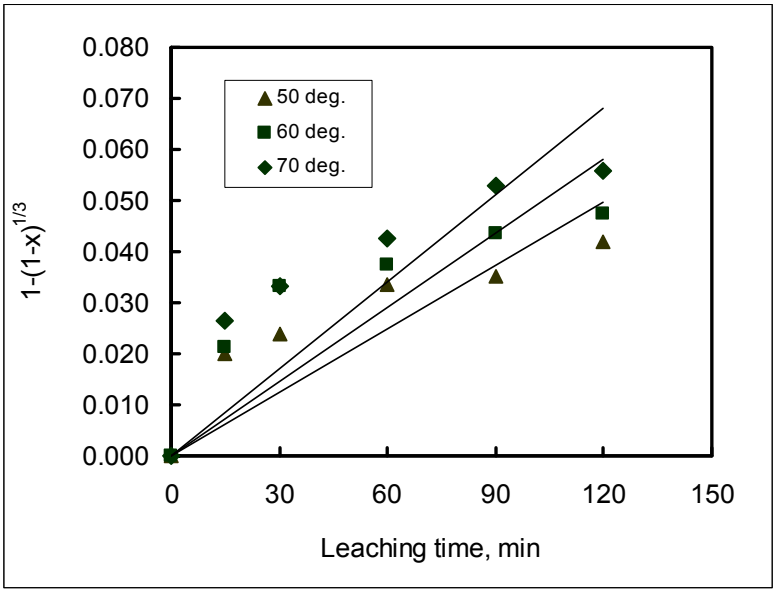

Figure 6.6b: Plot of $1-(1-X)^{1/3}$ vs time for the leaching of Ni at different temperatures for the chemically controlled reaction.

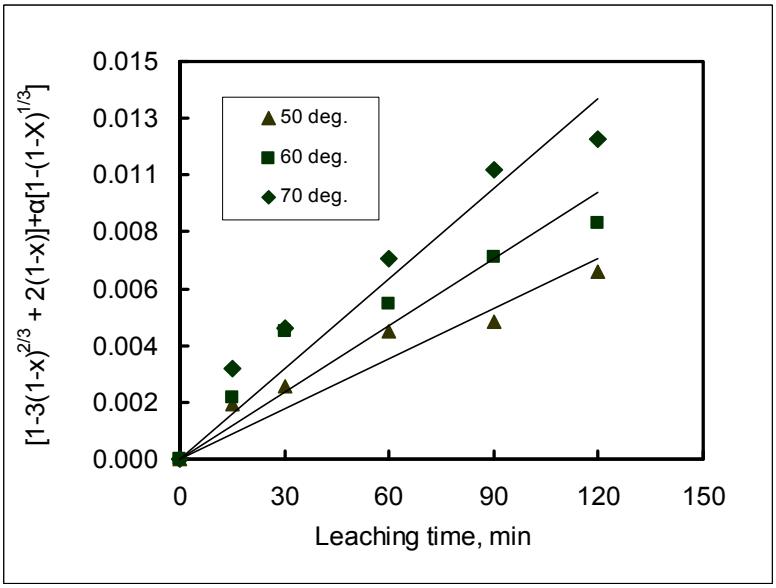

Figure 6.6c: Plot of $[1-3(1-X)^{2/3} + 2(1-X)] + \alpha[1 - (1-X)^{1/3}]$ vs time for the leaching of Ni at different temperatures for the mixed controlled reaction.

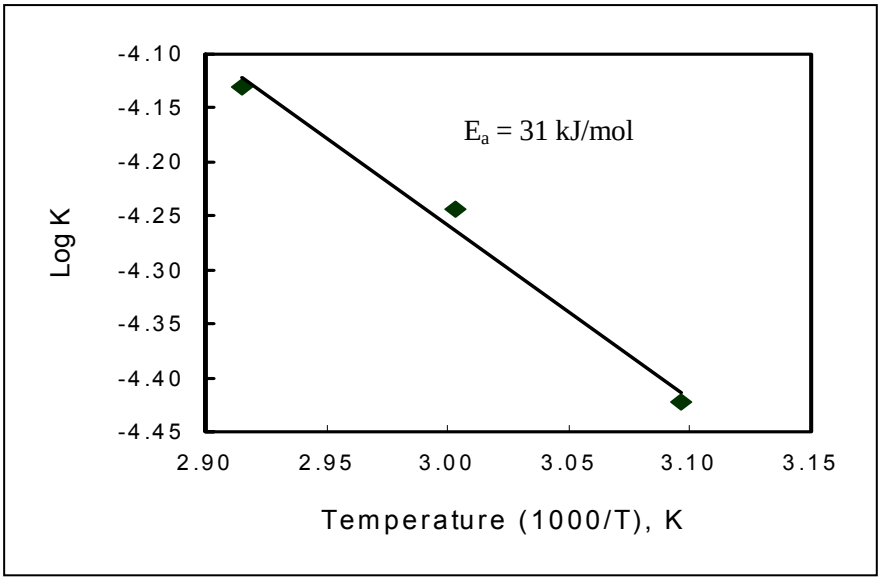

Figure 6.7: Arrhenius plot for the Ni leaching reaction at three different temperatures.

6.1.2 Effect of temperature on copper cementation

Effect of temperature on the cementation rate of copper during the atmospheric leaching of the matte in the temperature range 50 – 80 ^{o}C is illustrated in Figure 6.8, which shows the trend in the rate of copper precipitation. It can be seen that the rate of copper cementation increased substantially with increasing temperature in the range 50 – 70 ^{o}C, however when the temperature increased from 70 ^{o}C to 80 ^{o}C only a slight increase in the cementation rate was observed. At 80 ^{o}C all the aqueous copper was precipitated, whereas at 50 ^{o}C only 68% of the copper precipitated. The observed behaviour of copper suggested that if copper needs to be removed from the solution as fast as possible during the repulping stage (pre-leach stage), the temperature should be increased.

The effect of temperature on the copper cementation reaction kinetics is shown in Figures 6.9a and 6.9b. Figure 6.9a is a plot of $\log\{[Cu^{2+}]_t/[Cu^{2+}]_0\}$ against time at various temperatures, as explained earlier in this chapter (see equation 6.5). From the slopes of these plots, cementation rate constants (K) were determined and plotted against 1/T (Arrhenius plot) as presented in Figure 6.9b, which

shows the effect of temperature on the rate constant for the first period (stage 1) of the reaction (Figure 6.9a). It can be seen from Figure 6.9a that the cementation rate constant increased with increase in temperature. From the slopes of the plots in Figure 6.9b, the activation energy of the reaction (E_a) was calculated using the Arrhenius relationship (Equation 6.6). The results indicated that the reaction proceeded under two rate controlling mechanisms, as shown in Figure 6.9b. MacKinnon et al. (1971) obtained similar results in their studies of cementation of copper on nickel discs. Annamalai and Hiskey (1978) also observed the two rate controlling mechanisms in their study of copper cementation on pure aluminum.

Two distinct activation energies, namely 18.2 kJ/mol at high temperatures (70 – 80 ^oC) and 74.6 kJ/mol for lower temperatures (50 – 70 ^oC) were obtained. These values of the activation energy indicated that the rate of the reaction was probably controlled by a boundary layer ionic diffusion mechanism at higher temperatures. At low temperatures, the activation energy was quite high indicating that the rate was probably controlled by a surface reaction. This result agrees with the observed insensitivity of the cementation rate constants to variations in the stirring rates at a temperature of 60 ^oC (Figure 6.17), which suggests a surface reaction controlled cementation process. MacKinnon et al. (1971) observed similar cementation behaviour and obtained an activation energy of 7 kcal/mol (29 kJ/mol) for a temperature range of 59 ^oC - 84 ^oC, and 44 kcal/mol (184.2 kJ/mol) for a temperature range of 49 ^oC – 59 ^oC, for copper cementation on nickel discs. They attributed their results to the presence of an oxide film on the surface of the disc, which retarded the cementation reaction. High temperatures help breakdown the oxide layer and therefore the reaction proceeds at a faster rate. The high value of the activation energy and low rate of cementation observed at low temperatures in the present study may be attributed to the small surface area of nickel particles that was exposed to the aqueous copper ions, since most of the matte particles consisted of Ni-Cu

sulphide minerals. The presence of an oxide film on the reaction surface may have been another reason for the observed results.

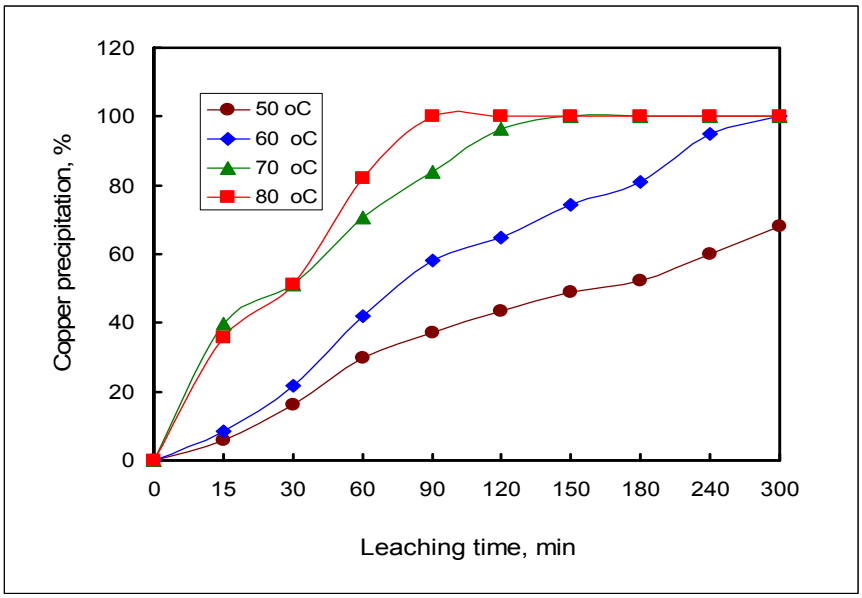

Figure 6.8: Copper precipitation as a function of time during atmospheric leaching of the matte at different temperatures (stirring rate: 205 rpm, pulp density: 1.7 kg/L)

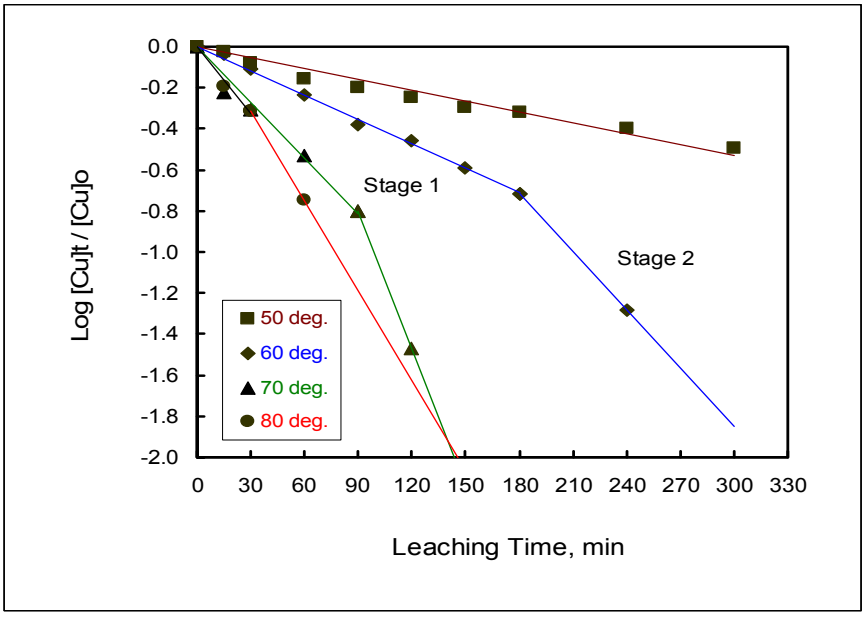

Figure 6.9a: Variation of $\log[Cu^{2+}]_t$ $/[Cu^{2+}]_0$ ratio with time at different temperatures, (205 rpm, 90g/L initial acid, 25g/L initial Cu concentration, 1.7 kg/L density).

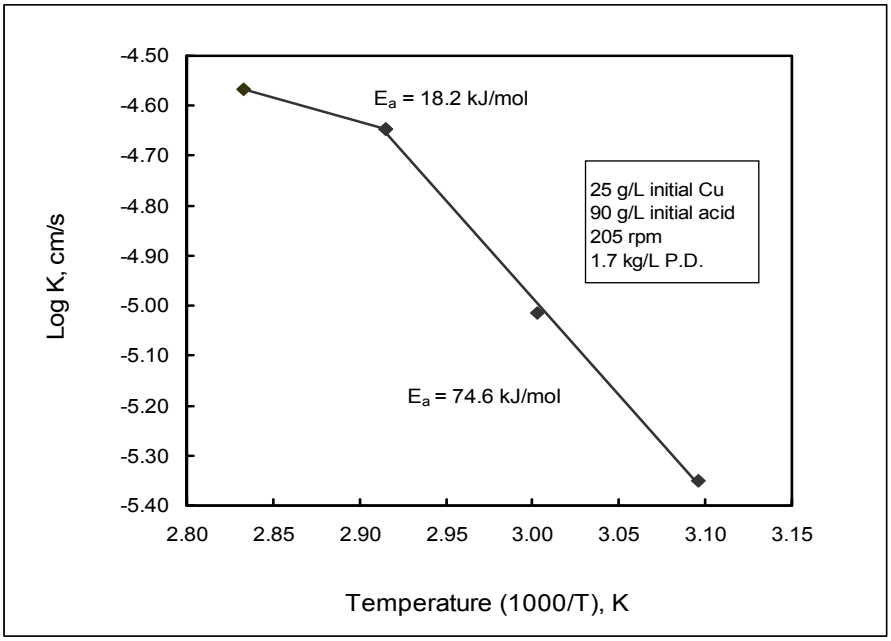

Figure 6.9b: Variation of cementation rate constant (K) with temperature

6.2 Effect of stirring rate on the leaching behaviour of the Ni-Cu matte

6.2.1 Effect of stirring rate on nickel, cobalt and iron dissolution

To investigate the effect of stirring rate on the leaching behaviour of the matte experiments were conducted at three different stirring rates, namely 145, 205 and 400 rpm; while keeping the temperature at 60 ^{o}C, pulp density at 1.7 kg/L and residence time of 5 hours. As mentioned in section 6.1.1, the interactions between the variables were not evaluated as the aim was not to optimise the process. The results obtained are shown in Table 6.2 and in Figures 6.10 – 6.13. Detailed information on the calculations of metal concentrations and extractions are illustrated in Appendix A2. Figure 6.14 is a typical example of results obtained in the tests that were done in duplicate to check reproducibility of the results.

The results indicated that nickel dissolution was lower at the stirring rate of 145 rpm; however, it increased gradually when the stirring rate was increased from

145 to 205 rpm and then to 400 rpm. The observed increase in nickel dissolution was accompanied by transformation in the mineral Ni_3S_2, which transformed to NiS, implying that more nickel was dissolved at the stirring rates of 205 and 400 rpm than at 145 rpm (see Table 7.2 in section 7.3.2). In the case of cobalt and iron the extractions were low at 145 rpm and 205rpm but increased when the stirring rate increased to 400 rpm (Figures 6.11 and 6.12). As in the other experiments, iron hydrolysed and subsequently precipitated when the pH was above 3. The fact that nickel dissolution rates were affected by stirring rates suggested that the leaching of this metal was probably influenced by transport processes; this was also in agreement with the calculated activation energy of 31 kJ/mol (see section 6.1.1).

The results suggested that the leaching of the metals from the matte did not entirely depend on the cementation process, but other mechanisms of leaching such as direct leaching with H_2SO_4 also played an important role (see chapter 5). Otherwise the rate of metal dissolution would not have increased when the stirring rate was increased from 205 rpm to 400 rpm, as the rate of cementation process was found to be independent of the stirring rate (see section 6.2.2).

Table 6.2: Ni, Co, and Fe extractions and final metal concentrations of the solution after atmospheric leaching of the matte at different stirring rates

Stirring rate rpm)	**Metal extraction (%)**			**Final solution concentration (g/L)**			
	Ni	**Co**	**Fe ***	**Ni**	**Co**	**Fe**	**Cu**
145	12.3	30.1	69.4	74.4	1.1	4.2	1.0
205	16.9	28.7	70.4	85.8	1.0	4.3	0.0
400	19.2	36.6	85.5	102.1	1.2	3.5	0.0

*The value shows maximum extraction attained prior to Fe precipitation.
Leaching conditions: temperature: 60 ^oC, pulp density: 1.7kg/L, residence time: 5 hours

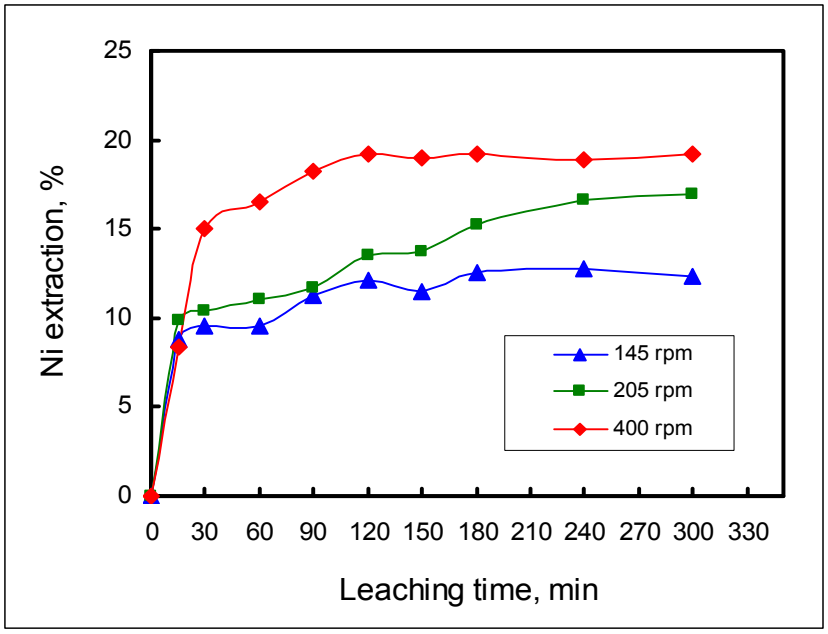

Figure 6.10: Nickel extraction as a function of leaching time at different stirring rate (Temperature: 60 ^{o}C, pulp density: 1.7kg/L)

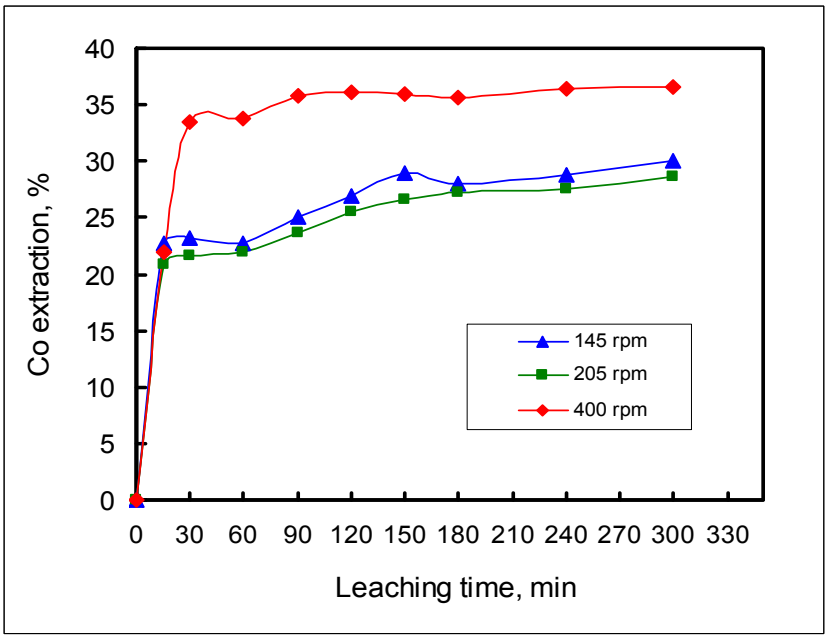

Figure 6.11: Cobalt extraction as a function of leaching time at different stirring rate (Temperature: 60 ^{o}C, pulp density: 1.7kg/L)

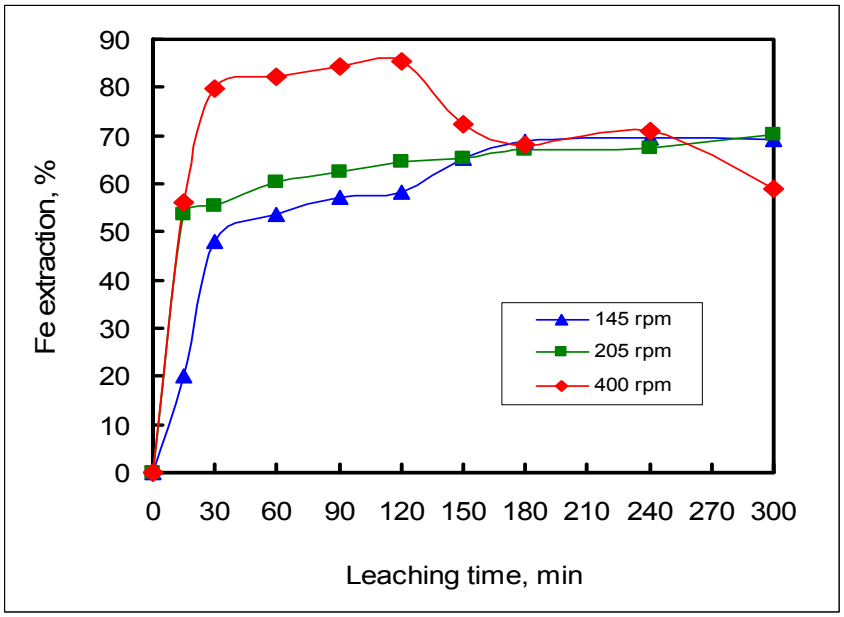

Figure 6.12: Iron extraction as a function of leaching time at different stirring rate (Temperature: 60 ^{o}C, pulp density: 1.7kg/L)

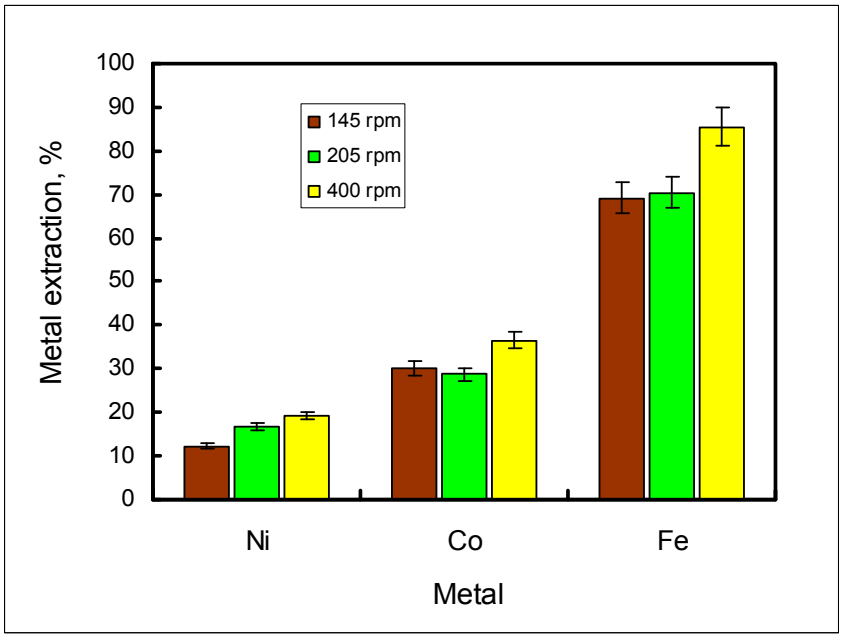

Figure 6.13: Metal extractions after atmospheric leaching of the matte at different stirring rates

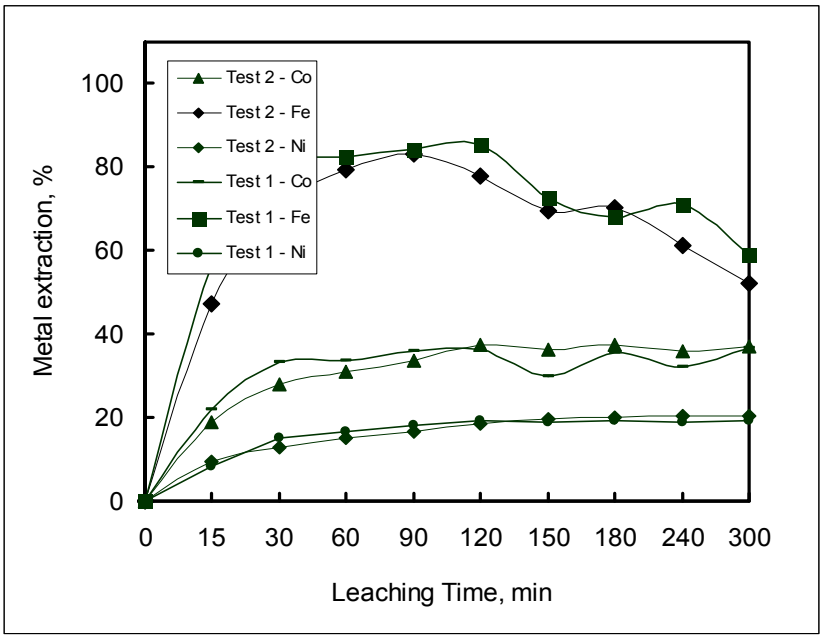

Figure 6.14: Comparison of metal extractions between two tests conducted at a stirring rate of 400 rpm (temperature: 60 ^{o}C, pulp density: 1.7kg/L).

6.2.2 Effect of stirring rate on copper cementation

The effect of stirring rate on copper cementation is illustrated in Figures 6.15 – 6.17. It can be seen that the rate of cementation of the aqueous copper was not affected by variations in the stirring rates. Figure 6.15 shows percent copper precipitation as a function of time. It can be seen that at all three stirring rates employed (145, 205 and 400 rpm) the rate of copper cementation was similar, with complete copper precipitation achieved after 5 hours of leaching at 205 and 400 rpm. The fact that the rate of copper cementation did not vary with varying stirring rates suggests that the copper cementation process is probably chemically controlled as discussed later. This implies that two different process controlling mechanisms are operative during the Ni-Cu matte pre-leaching process; i.e. the metal leaching process is diffusion controlled while the copper cementation process is chemically controlled.

The effect of stirring rate on copper cementation is presented in Figures 6.16 and 6.17. Figure 6.16 shows a graph of $\log[Cu^{2+}]_t / [Cu^{2+}]_0$ versus time for the investigated stirring rates, while Figure 6.17 is a plot of cementation rate constants as a function of stirring rates. The rate constants were derived from the slopes of plots in Figure 6.16. It can be seen that there was no increase in the cementation rate constant with increase in stirring rate. This result, together with the calculated activation energy of 74.6 kJ/mol (see Figure 6.9b), indicated that the rate of cementation was probably chemical reaction controlled under the employed leaching conditions. Nadkarni et al. (1967) reported similar results from a kinetic study of copper precipitation on iron.

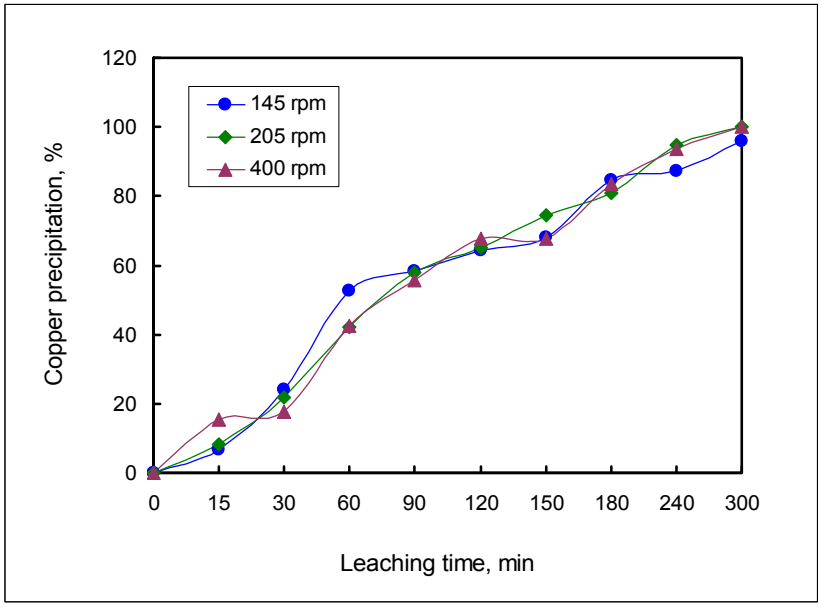

Figure 6.15: Copper precipitation as a function of time during atmospheric leaching of the matte at different stirring rates (temperature: 60 °C, pulp density: 1.7 kg/L)

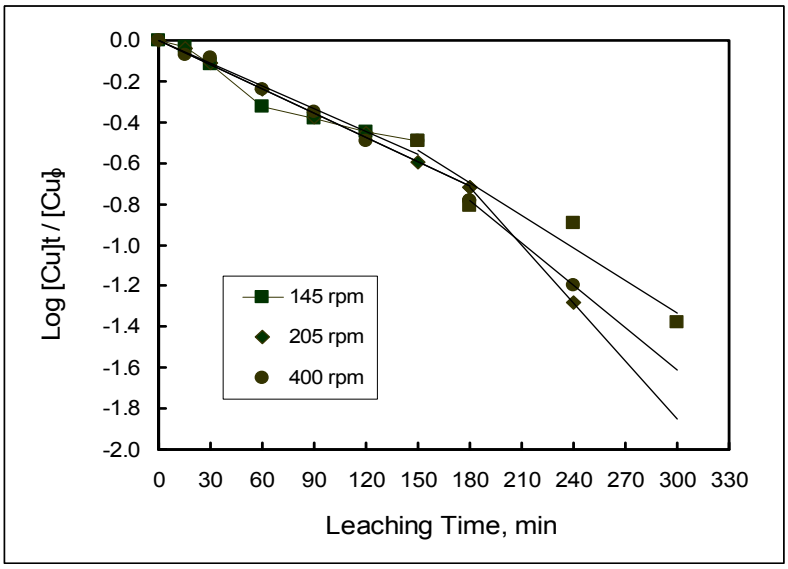

Figure 6.16: Variation of log[Cu $^{2+}]_t$ /[Cu $^{2+}]_0$ ratio with time at different stirring rates, (90g/L initial acid, 25g/L initial Cu concentration, 60 ^{o}C, 1.7 kg/L density).

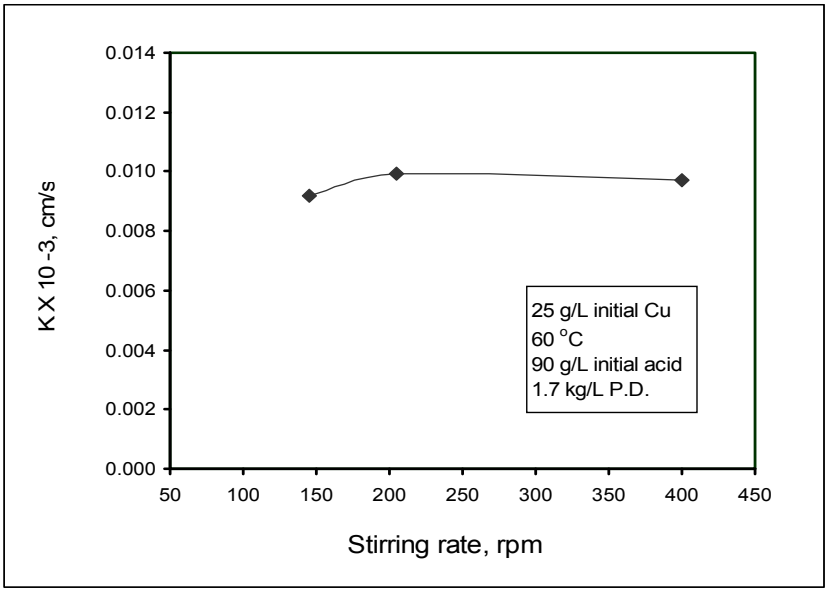

Figure 6.17: Variation of cementation rate constant (K) with stirring rate.

6.3 Effect of pulp density on the leaching behaviour of the Ni-Cu matte

6.3.1 Effect of pulp density on nickel, cobalt and iron dissolution

The effect of pulp density on the leaching behaviour of the Ni-Cu matte was investigated for three values, namely 1.6 kg/L, 1.7 kg/L and 1.75 kg/L. The results obtained are shown in Table 6.3 and Figures 6.18 – 6.21. Detailed information on the results can be found in Appendix A3. Figure 6.22 shows graphs of tests conducted in duplicate to check for reproducibility of the results. Results obtained indicated that nickel and cobalt extractions were not significantly affected by changes in the pulp density, as no clear trends were observed in their dissolution patterns; although slightly higher extractions were observed when the density was reduced from 1.7 kg/L to 1.6 kg/L. On the other hand, iron extraction was higher at a pulp density of 1.6 kg/L and was not affected at high pulp densities of 1.7 and 1.75 kg/L. (Figure 6.20).

Table 6.3: Ni, Co, and Fe extractions and final metal concentrations of the leach solution after atmospheric leaching of the matte at different pulp densities

Pulp density (kg/L)	Metal extraction (%)			Final solution concentration (g/L)			
	Ni	Co	Fe *	Ni	Co	Fe	Cu
1.6	19.9	40.5	90.2	86.52	1.1	4.0	8.2
1.7	16.9	28.7	70.3	85.84	1.0	4.3	0.0
1.75	17.1	34.9	69.4	100.5	1.2	4.3	0.3

*The value shows maximum extraction attained prior to Fe precipitation.
Leaching conditions: temperature: 60 ^{o}C, stirring rate: 205 rpm, residence time: 5 hours

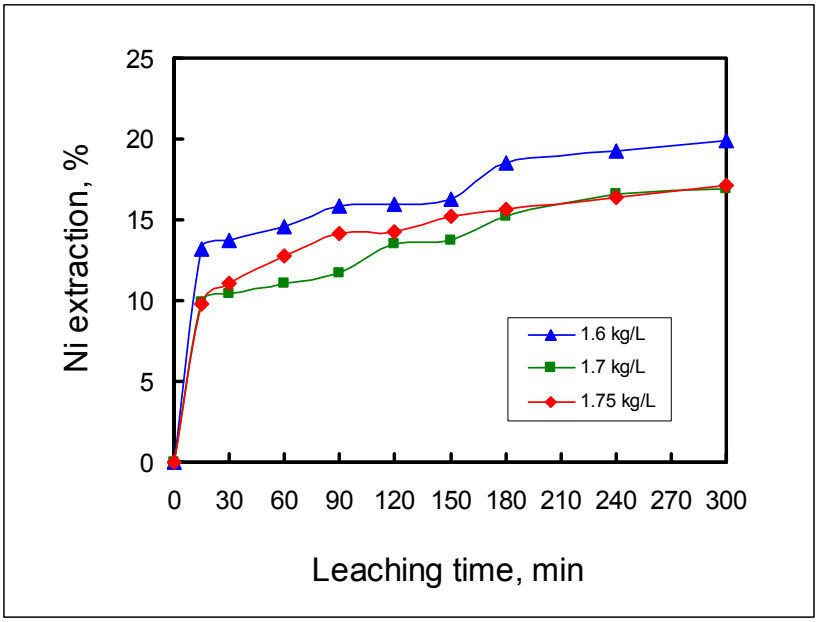

Figure 6.18: Nickel extraction as a function of leaching time at different pulp densities of matte (stirring rate: 205 rpm, temp. 60 ^{o}C).

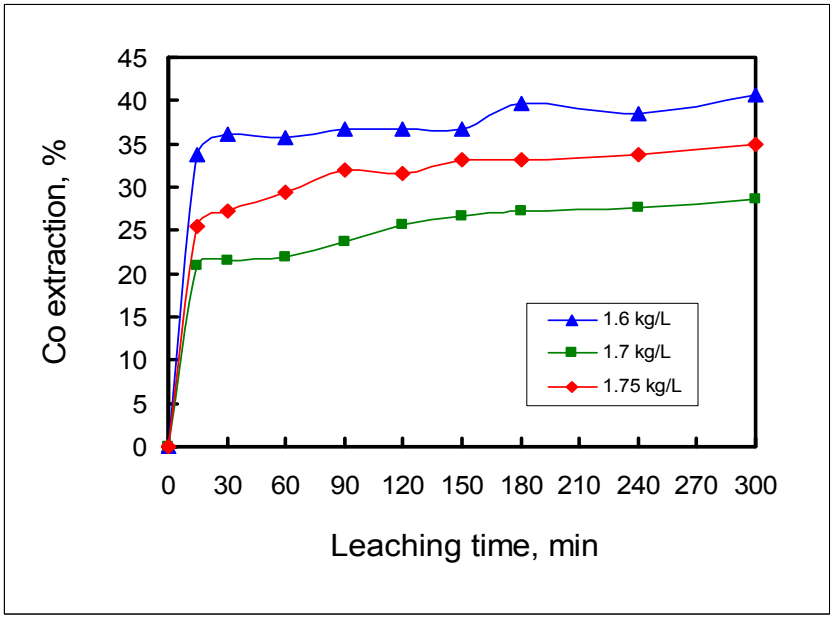

Figure 6.19: Cobalt extraction as a function of leaching time at different pulp densities of matte (stirring rate: 205 rpm, temp. 60 ^{o} C).

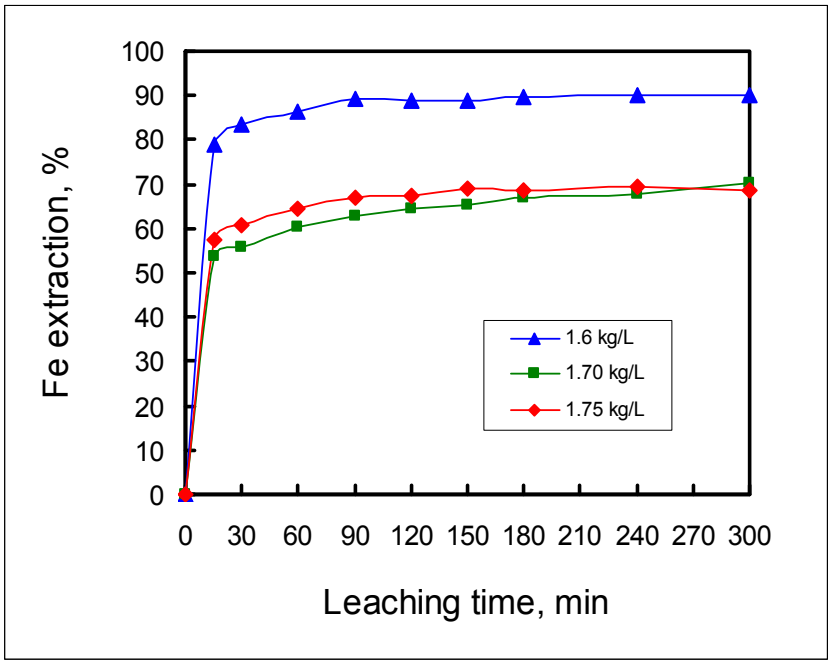

Figure 6.20: Iron extraction as a function of leaching time at different pulp densities of matte (stirring rate: 205 rpm, temp. 60 ° C).

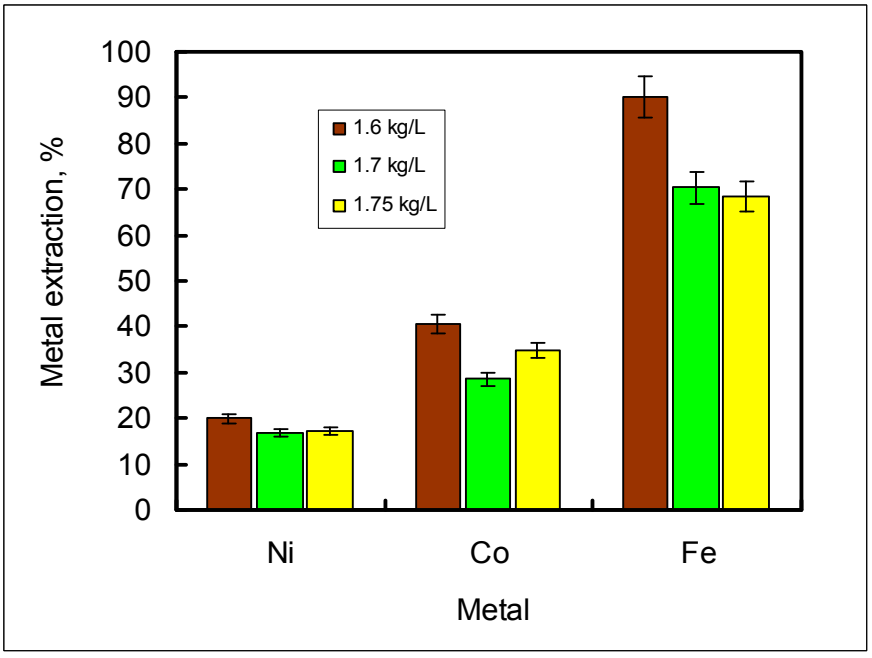

Figure 6.21: metal extractions after atmospheric leaching of the matte at different pulp densities.

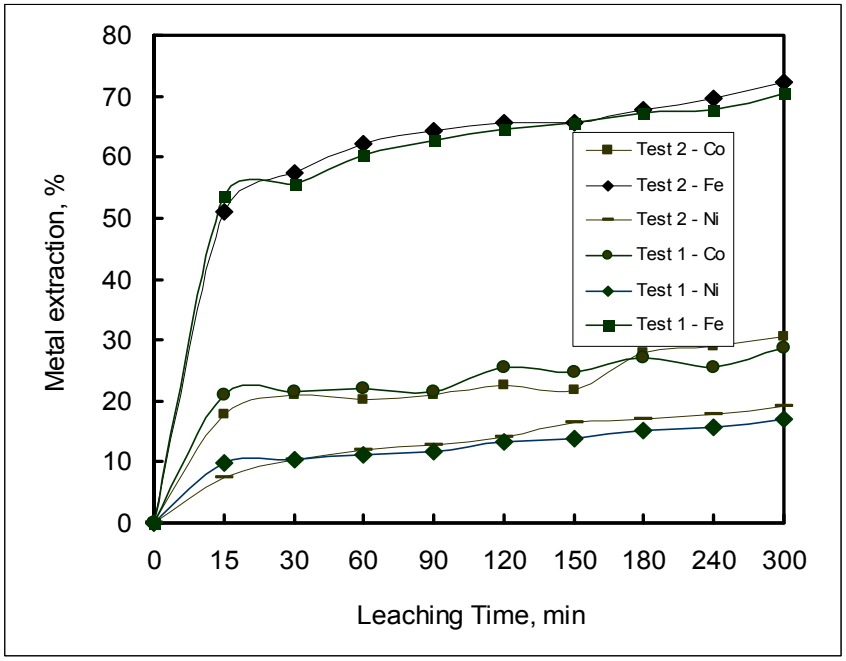

Figure 6.22: Comparison of metal extractions between two tests conducted at a pulp density of 1.7 kg/L (stirring rate: 205 rpm, temperature: 60 ^{o}C)

6.3.2 Effect of pulp density on copper cementation

The effect of variation in pulp density of the reaction mixture on copper cementation is illustrated in Figures 6.23 - 6.25. Figure 6.23 illustrates percent copper precipitation versus leaching time. The results indicated that copper precipitated faster at pulp densities above 1.6 kg/L, with complete copper precipitation achieved after 5 hours of leaching for pulp densities of 1.7 and 1.75 kg/L.

Figure 6.24 is a plot of $\log[Cu^{2+}]_t / [Cu^{2+}]_0$ versus leaching time. From the slopes of the graphs copper cementation rate constants were obtained, as explained earlier, and these were plotted as a function of pulp density (Figure 6.25). It can be seen from Figure 6.25 that the cementation rate constant increased as the pulp density increased from 1.6 to 1.7 kg/L and reached a maximum value at

about 1.7 kg/L. Above the pulp density of 1.7 kg/L copper cementation did not appear to be influenced by further increase in the pulp density. The increase in the rate of copper cementation when the pulp density was increased from 1.6 to 1.7 kg/L may be attributed to the increase in cathodic surface area of matte on which copper cementation takes place. At high pulp density values greater than 1.7kg/L low mass-transfer rates of reactants and products caused by the increase in the quantity of matte in the reaction mixture were probably responsible for slowing down the cementation process. The result indicates that pulp densities of above 1.6 kg/L are desirable in the pre-leach stage as the subsequent pressure leaching stage requires less dissolved copper. In the commercial plant the pulp density is kept at about 1.7 kg/L.

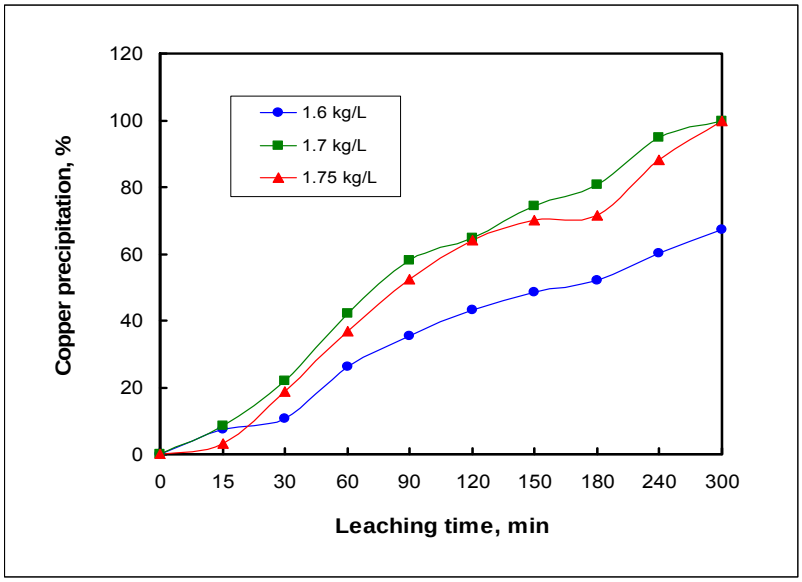

Figure 6.23: Copper precipitation as a function of time during atmospheric leaching of the matte at different pulp densities (stirring rate: 205 rpm, temperature: 60 ^{o}C)

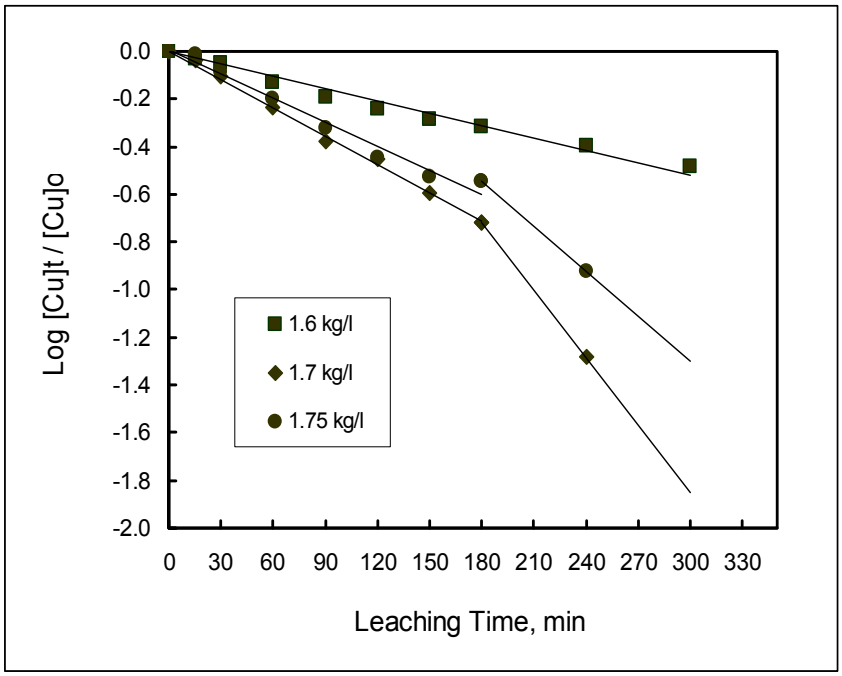

Figure 6.24: Variation of log[Cu $^{2+}]_t$ /[Cu $^{2+}]_0$ ratio with time at different pulp density values, (205 rpm, 90g/l initial acid, 60 ^oC, 25g/l initial Cu concentration).

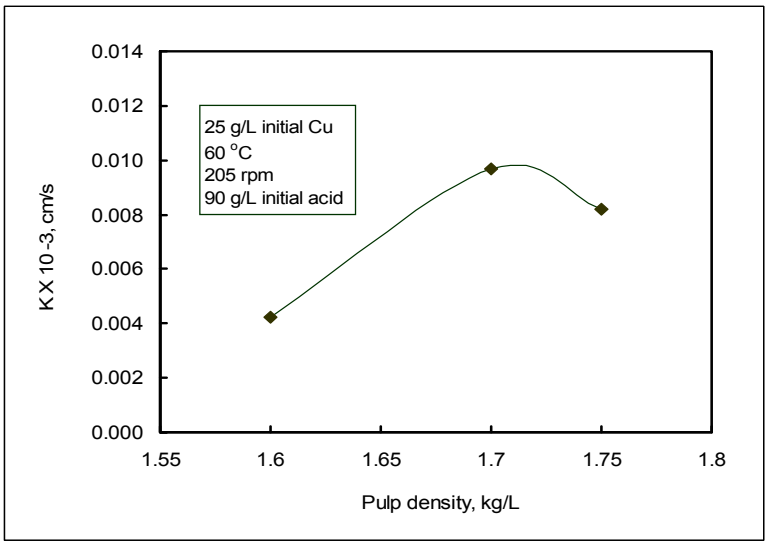

Figure 6.25: Variation of cementation rate constant (K) with pulp density of reaction mixture.

6.4 Effect of particle size on the leaching behaviour of the Ni-Cu matte

6.4.1 Effect of particle size on nickel, cobalt and iron dissolution

Results of leaching experiments conducted to investigate the influence of matte particle size on the leaching characteristics of the matte are shown in Table 6.4 and Figures 6.26 – 6.29. Three particle size fractions were investigated (–300+150 µm, -106+45µm, and -45 µm) at the temperature of 60 ^{o}C, stirring rate of 205 rpm and pulp density of 1.7 kg/L. Figure 6.30 serves to show reproducibility of the results. The results indicated that nickel extraction was not significantly affected by changes in the particle size, only a slight increase in the leaching rate was observed for the –45 µm size fraction (Figure 6.26). This indicates that in all the three particle sizes, the nickel alloy was liberated and hence exposed to the leaching solution. The leaching behaviour of cobalt was similar to that of nickel, although in this case the cobalt extractions for the –45 µm and -106+45µm size fractions were substantially higher than that of the 300+150 µm size fraction (Figure 6.27). The leaching behaviour of iron could not be determined accurately because of iron precipitation when the solution pH increased to above 3; this was especially so for smaller size fractions. It should be noted that small size fractions tend to have faster reaction kinetics due to the larger surface area of small particles that is exposed to the leaching solution.

Table 6.4: Ni, Co, and Fe extractions and final metal concentrations of the solution after atmospheric leaching of the matte at different particle sizes

Particle Size (µm)	Metal extraction (%)			Final solution concentration (g/L)			
	Ni	Co	Fe *	Ni	Co	Fe	Cu
-300+150	16.4	31.8	87.1	91.6	1.1	5.1	10.4
-106+45	17.0	39.3	76.7	94.7	1.31	4.5	0.0
-45	18.7	41.0	75.8	101.8	1.35	4.5	0.0

*The value shows maximum extraction attained prior to Fe precipitation.
Leaching conditions: temperature: 60 °C, stirring rate: 205 rpm, pulp density: 1.7kg/L, residence time: 5 hours.

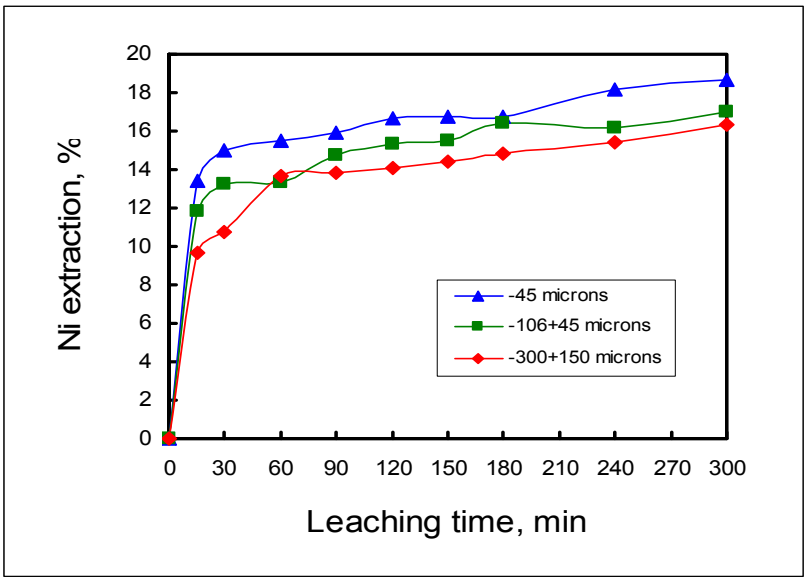

Figure 6.26: Nickel extraction as a function of leaching time at different particle sizes (temperature: 60 °C, stirring rate: 205 rpm, pulp density: 1.7 kg/L).

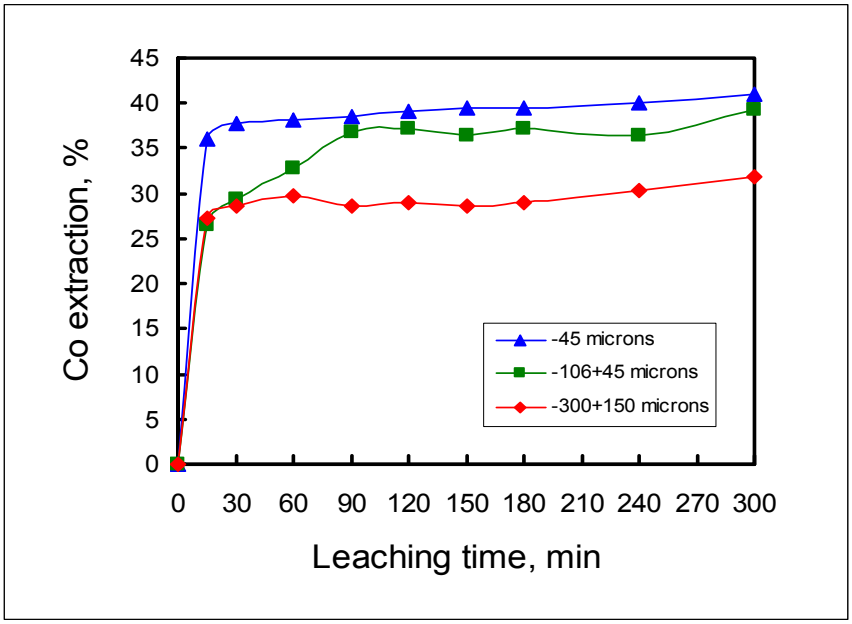

Figure 6.27: Cobalt extraction as a function of leaching time at different particle sizes (Temperature: 60 °C, stirring rate: 205 rpm, pulp density: 1.7 kg/L)

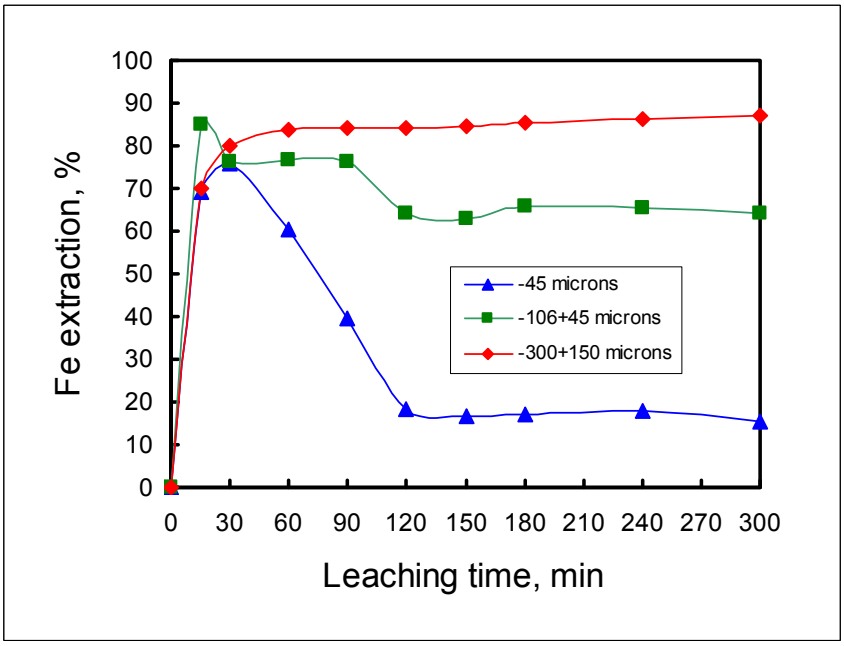

Figure 6.28: Iron extraction as a function of leaching time at different particle sizes (temperature: 60 °C, stirring rate: 205 rpm, pulp density: 1.7 kg/L).

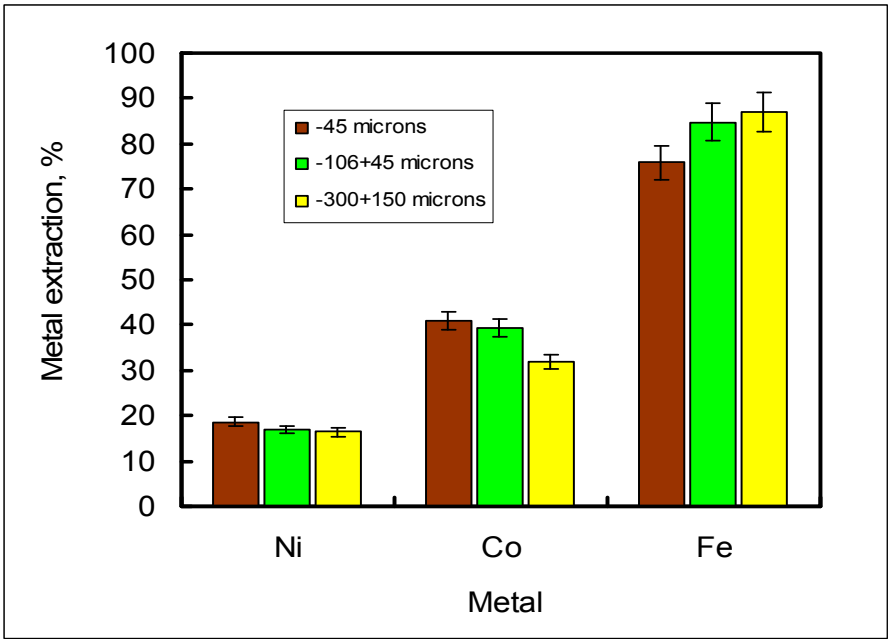

Figure 6.29: Metal extractions after atmospheric leaching of the matte at different particle sizes.

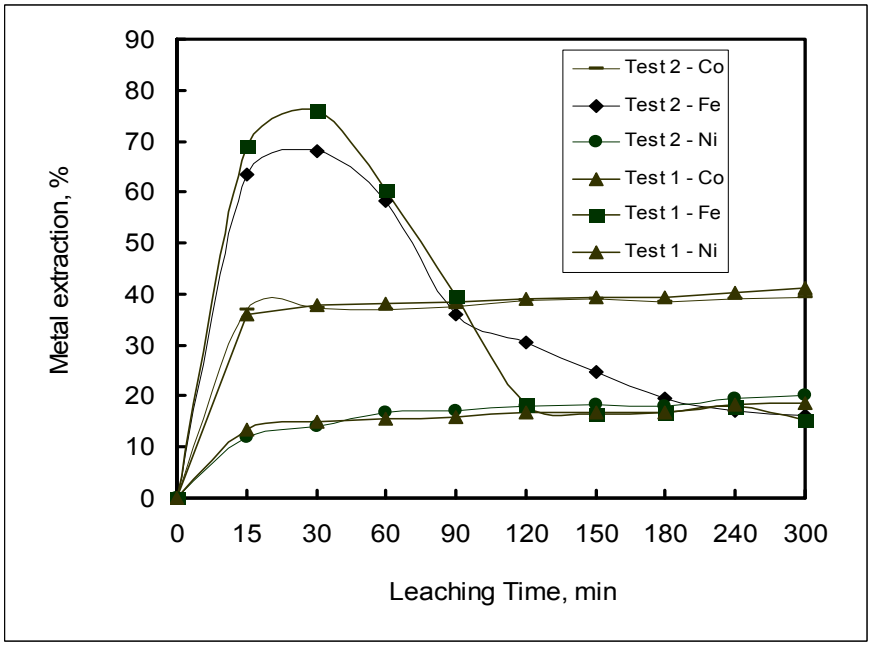

Figure 6.30: Comparison of metal extractions between two tests conducted at a particle size of –45 microns (stirring rate: 205 rpm, temp.: 60 ^{o}C, pulp density: 1.7 kg/L)

6.4.2 Effect of particle size on copper cementation

The effect of matte particle size on copper cementation is illustrated in Figures 6.31 - 6.33. Figure 6.31 shows percent copper precipitation versus time. It can be seen that the rate of copper cementation increased with decreasing particle size. At particle sizes of -45µm and -106+45 µm, all the aqueous copper was precipitated, whereas with the –300+150 µm particle size about 42% Cu precipitated after 5 hours of leaching. As noted with the metal dissolution rate, the faster rate of copper cementation observed with the finer size fractions was attributed to the increase in the surface area of fine particles.

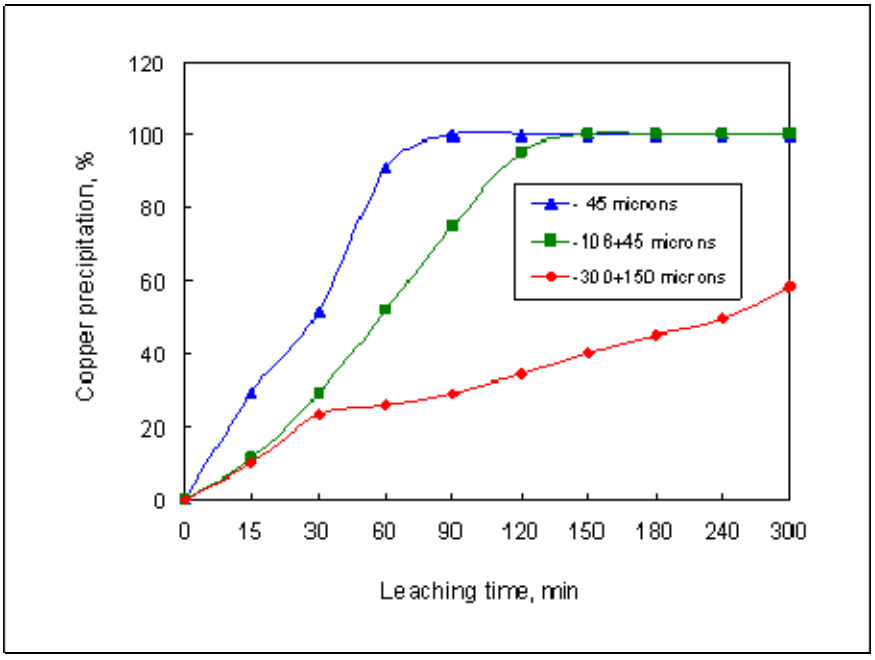

Figure 6.31: Copper precipitation as a function of time during atmospheric leaching of the matte at different particle sizes (stirring rate: 205 rpm, temperature: 60 ^{o}C, pulp density:1.7 kg/L).

Figures 6.32 and 6.33 illustrate the influence of matte particle size on the kinetics of copper cementation. The rate of copper cementation decreased with increasing particle size as illustrated in Figure 6.33, which shows a graph of cementation rate constants versus matte particle size. The copper cementation rate constants were obtained from Figure 6.32 using the same method as explained in the previous sections. It was found that the rate of cementation was more sensitive to particle size in the last period of the cementation reaction for the finer size fractions (-45 μm and –106+45 μm), as shown in Figure 6.32. This was probably due to the changes in the matte particle morphology and lattice structure, which opened up and exposed more Ni surface area to the solution. The morphology and structure of the cemented particles may also have an effect on the rate of cementation.

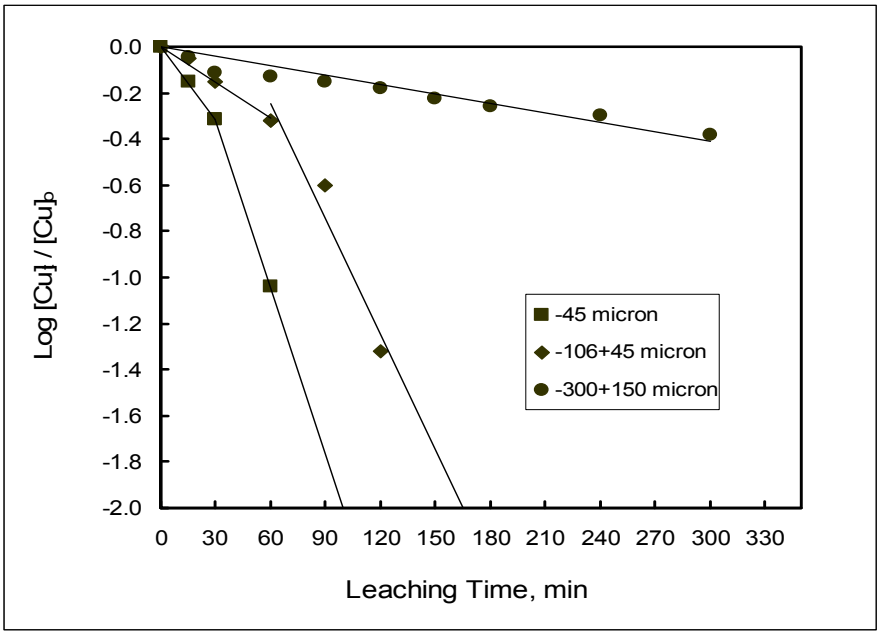

Figure 6.32: Variation of log[$Cu^{2+}]_t$ /[$Cu^{2+}]_0$ ratio with time at different matte particle sizes, (205 rpm, 90 g/L initial acid, 25 g/L initial Cu concentration, 60 ^oC, 1.7 kg/L density).

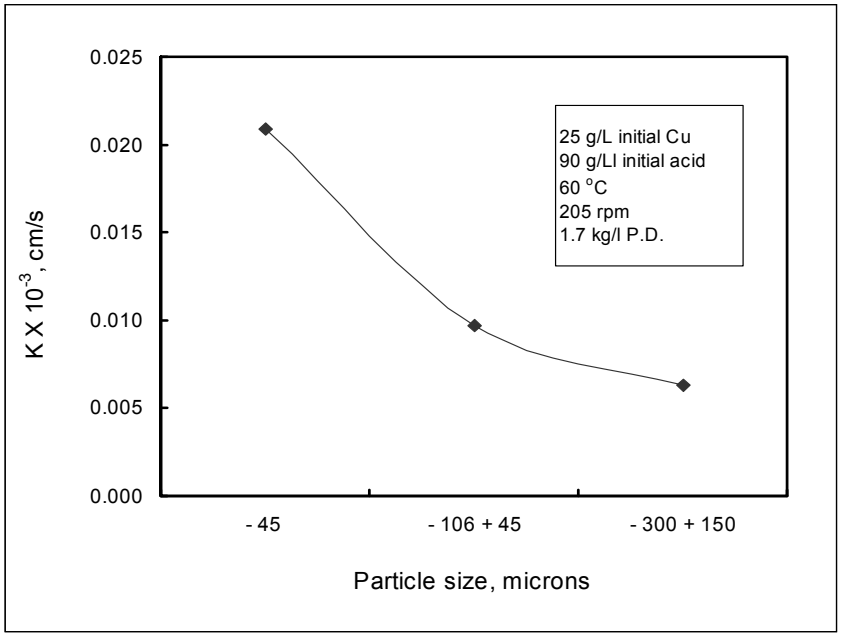

Figure 6.33: Variation of cementation rate constant (K) with matte particle size distribution.

6.5 Effect of initial copper concentration on the leaching behaviour of the Ni-Cu matte

6.5.1 Effect of initial copper concentration on nickel, cobalt and iron dissolution

Effect of initial copper concentration on the leaching behaviour of the Ni-Cu matte was investigated at initial copper concentrations of 25, 36 and 48 g/L, temperature of 60 ^{o}C, stirring rate of 205 rpm and pulp density of 1.7 kg/L. Results of metal dissolution are shown in Table 6.5 and Figures 6.34 – 6.37. Detailed data are presented in Appendix A5. Figures 6.34 – 6.36 indicate that generally the leaching of the metals did not depend on initial copper concentrations in the investigated copper concentration range of 25 - 48 g/L. The rate of leaching as well as the degree of leaching was not significantly different for the three copper concentrations, as can be seen from Figues 6.34 – 6.36. This

implies that copper concentration of the spent electrolyte does not have significant influence on the leaching of metals that occurs in the pre-leaching stage.

Table 6.5: Ni, Co and Fe extractions and final metal concentrations of the solution after atmospheric leaching of the matte at different initial copper concentrations.

Copper (g/L)	Metal extraction (%)			Final solution concentration (g/L)			
	Ni	Co	Fe *	Ni	Co	Fe	Cu
25	16.9	28.7	70.4	85.8	1.0	4.3	0.0
36	17.5	35.0	76.3	97.7	1.2	4.5	12.1
48	16.3	33.6	69.4	93.0	1.2	4.2	20.1

*The value shows maximum extraction attained prior to Fe precipitation.
Leaching conditions: temperature: 60 °C, stirring rate: 205 rpm, pulp density: 1.7kg/L, residence time: 5 hours.

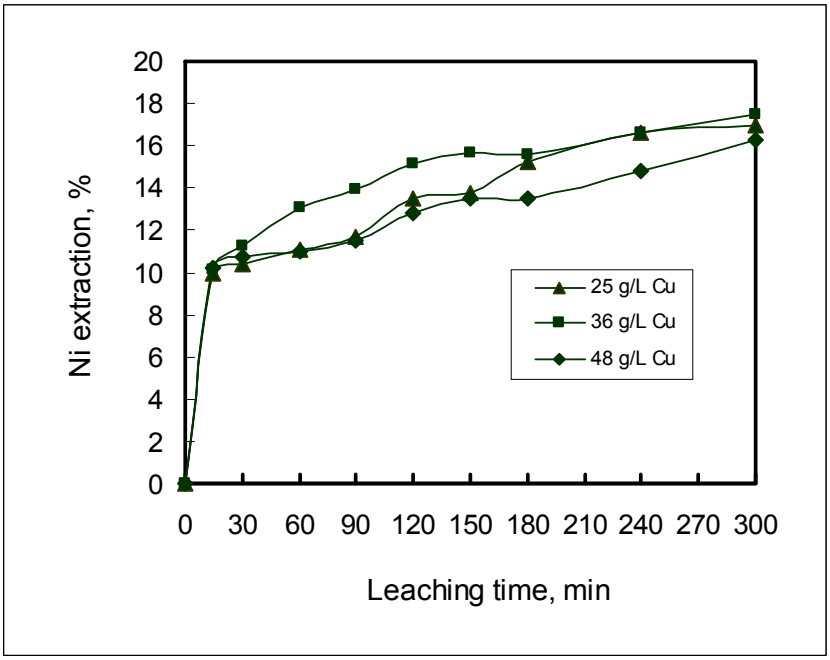

Figure 6.34: Nickel extraction as a function of leaching time at different initial copper concentrations (temperature: 60 °C, stirring rate: 205 rpm, pulp density: 1.7 kg/L).

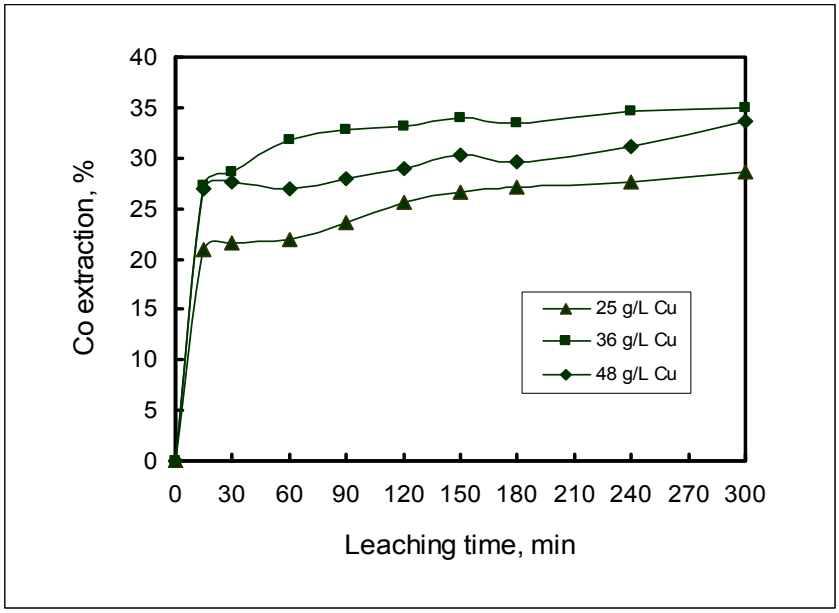

Figure 6.35: Cobalt extraction as a function of leaching time at different initial copper concentrations (Temperature: 60 °C, stirring rate: 205 rpm,pulp density: 1.7 kg/L)

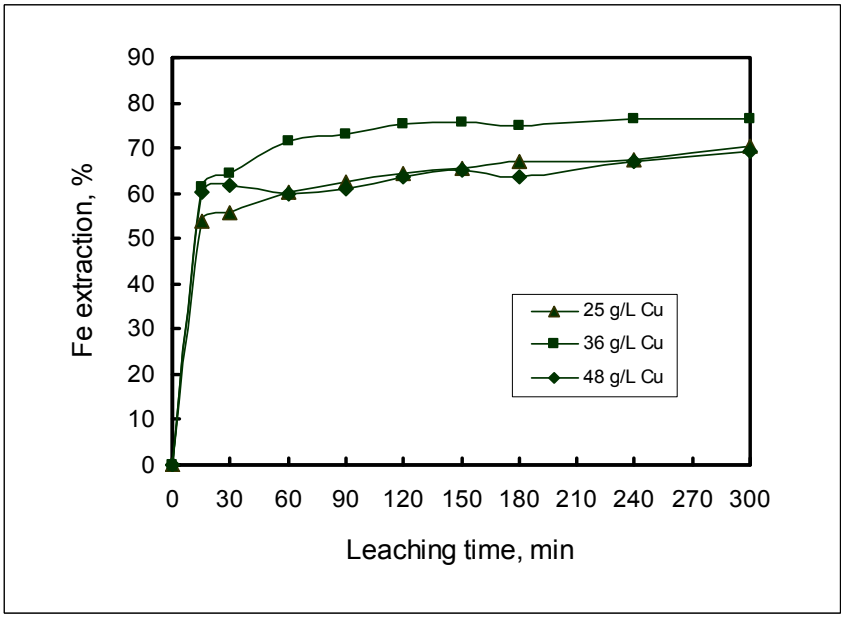

Figure 6.36: Iron extraction as a function of leaching time at different initial copper concentration (temperature: 60 °C, stirring rate: 205 rpm, pulp density: 1.7 kg/L).

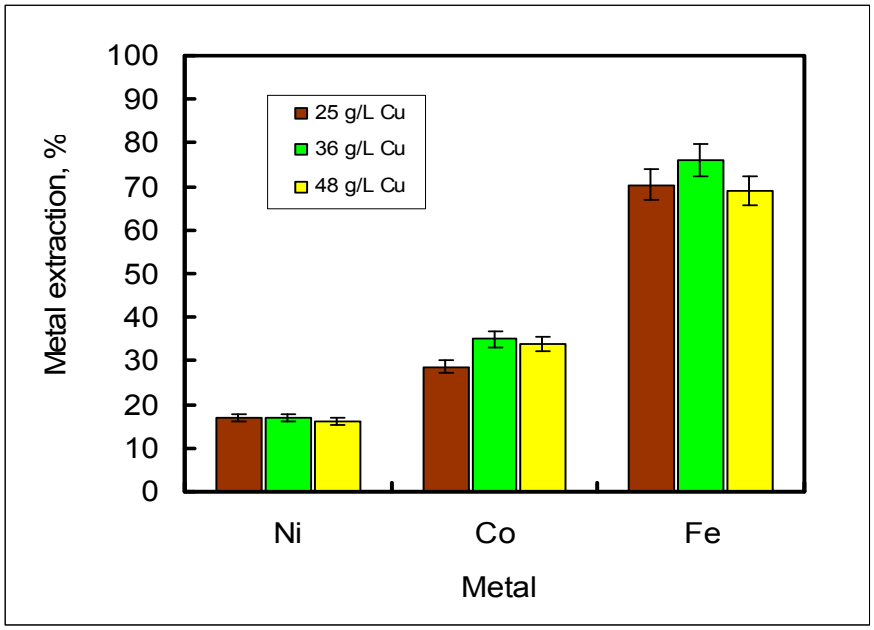

Figure 6.37: Overall metal extractions after atmospheric leaching of the matte at different initial copper concentrations (temperature: 60 ^{o}C, stirring rate: 205 rpm, pulp density: 1.7 kg/L).

6.5.2 Effect of initial copper concentration on copper cementation

The effect of varying the initial copper concentration of solution on the kinetics of copper cementation onto suspended particles of the matte was investigated at three different values, namely 25, 36 and 48 g/L Cu. The other variables were kept constant. The results obtained are depicted in Figures 6.38 - 6.40. Figure 6.38 shows percent copper precipitation as a function of leaching time. The results have shown that the rate as well as the degree of copper cementation was higher for the experiment conducted with lower initial copper concentrations (25 g/L). However, both the rate and degree of copper cementation decreased when the initial copper concentration increased to 36 g/L.

Figure 6.39 shows the first order kinetic plot of log ($[Cu^{2+}]_t/[Cu^{2+}]_0$) vs time, and Figure 6.40 presents a plot of rate constants as a function of the initial copper concentration. The values of the cementation rate constant (K) were determined

from the slopes of the plots in Figure 6.39. The cementation rate constant was found to decrease with increasing copper ion concentration until a value of about 36 g/L was reached, and then the rate constant became almost independent of the initial copper ion concentration (Figure 6.40). MacKinnon and Ingraham (1970) observed similar results for cementation of copper on rotating aluminium disc. The decrease in the cementation rate has been attributed to the following factors:

- changes of activity brought about by the increase in copper ion concentration,
- the rise in solution viscosity, and
- the decrease in the diffusivity of copper ions as a result of the increase of initial copper concentration in solution.

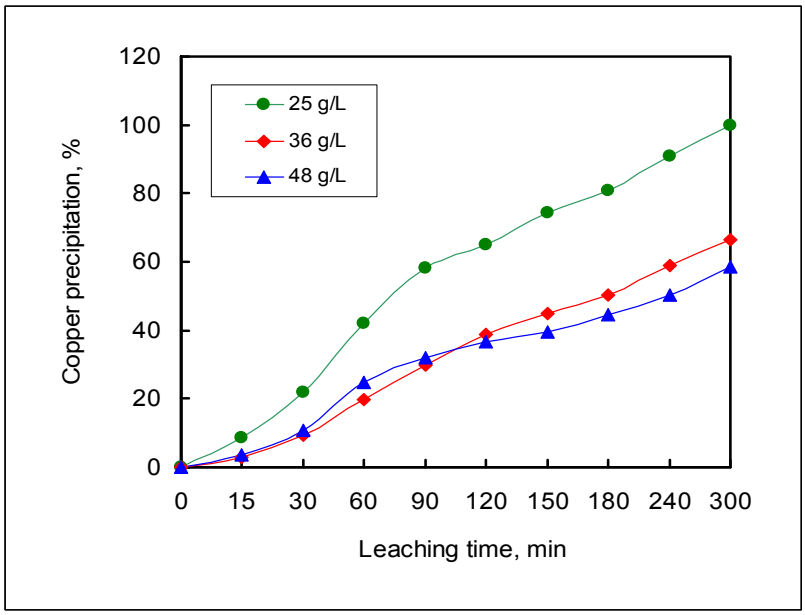

Figure 6.38: Copper precipitation as a function of time during atmospheric leaching of the matte at different initial copper concentrations (stirring rate: 205 rpm, temperature: 60 ^{o}C).

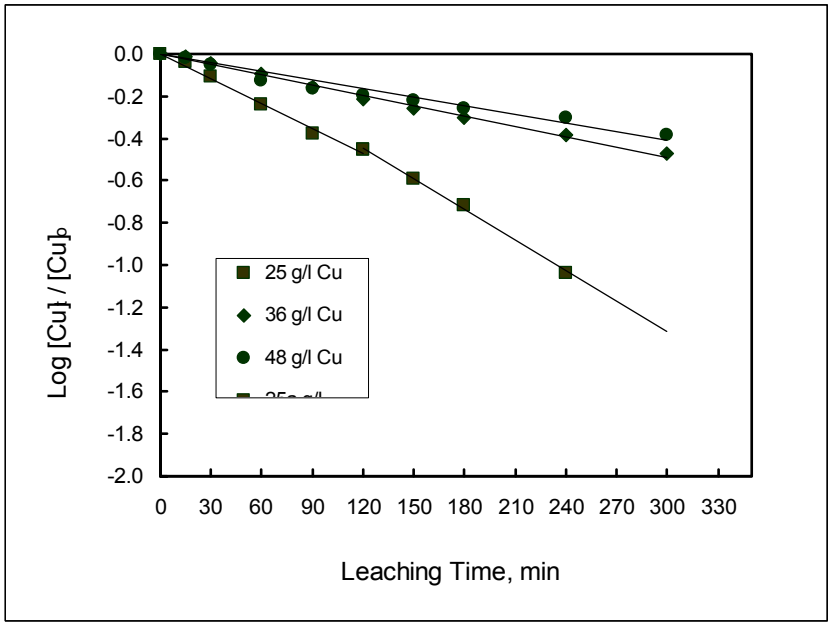

Figure 6.39: Variation of log[Cu $^{2+}$]$_t$ /[Cu $^{2+}$]$_0$ ratio with time at different initial Cu concentrations, (205 rpm, 90 g/L initial acid, 60 ^{o}C, 1.7 kg/L density).

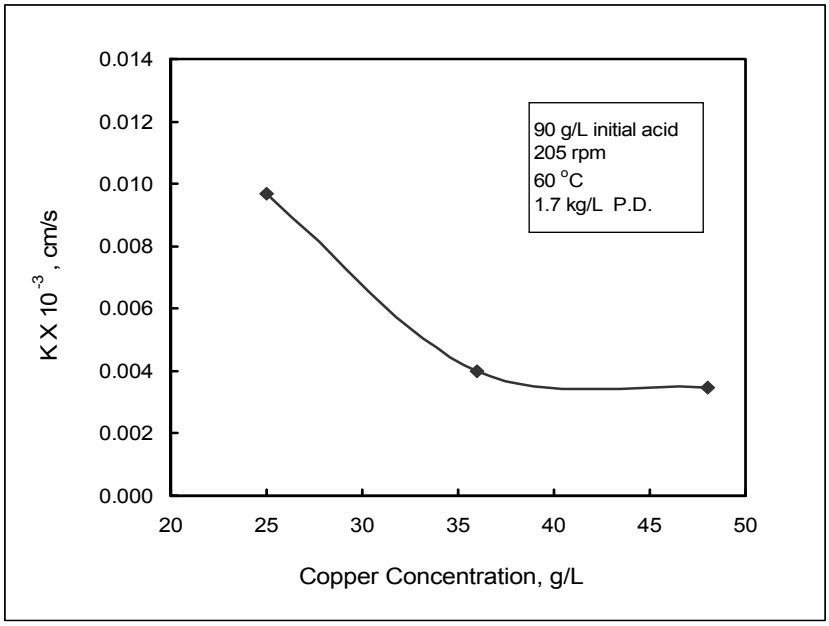

Figure 6.40: Variation of cementation rate constant (K) with initial Cu concentration.

6.6 Effect of initial acid concentration on the leaching behaviour of the Ni-Cu matte

6.6.1 Effect of initial acid concentration on nickel, cobalt and iron dissolution

Results of experiments conducted to investigate the effect of initial H_2SO_4 concentration on the dissolution behaviour of nickel cobalt and iron are presented in Table 6.6 and Figures 6.41 – 6.44. More data on the experiments and results are given in Appendix A6. The results indicate that variations in the initial acid concentration did not have effect on nickel extraction as no changes in the nickel extractions were observed (Figure 6.41). The observed leaching behaviour of nickel can probably be attributed to the fact that most of the nickel was leached by the process of cementation. Dissolution of the nickel by direct attack by acid was probably most prominent when the aquoues copper precipitated, as noted in section 5.2.2. On the other hand, cobalt and iron extractions were affected by variations in the initial acid concentration as shown in Figures 6.42 and 6.43, respectively. The rate of extraction of both metals increased when the acid increased from 90 g/L to 110 g/L. However, further increase in the initial acid concentration had no effect on both cobalt and iron extraction.

The observed leaching behaviour of cobalt and iron may be attributed to the fact that when the acid concentration was increased, the rate of leaching by acid (reactions 5.7 - 5.13) increased due to increased strength of the acid. However, when the acid strength was increased further metal dissolution did not increase further probably because almost all the metal that could be leached under the applied conditions had been dissolved.

Table 6.6: Ni, Co, and Fe extractions and final metal concentrations of the solution after atmospheric leaching of the matte at different initial H_2SO_4 concentrations.

H_2SO_4 (g/L)	Metal extraction (%)			Final solution concentration (g/L)			
	Ni	Co	Fe *	Ni	Co	Fe	Cu
90	16.9	28.7	70.4	85.84	1.01	4.34	0.0
110	17.17	34.8	86.5	96.39	1.18	5.04	2.57
125	17.55	36.2	89.9	98.05	1.22	5.22	1.93

*The value shows maximum extraction attained prior to Fe precipitation.
Leaching conditions: temperature: 60 °C, stirring rate: 205 rpm, pulp density: 1.7kg/L, residence time: 5 hours.

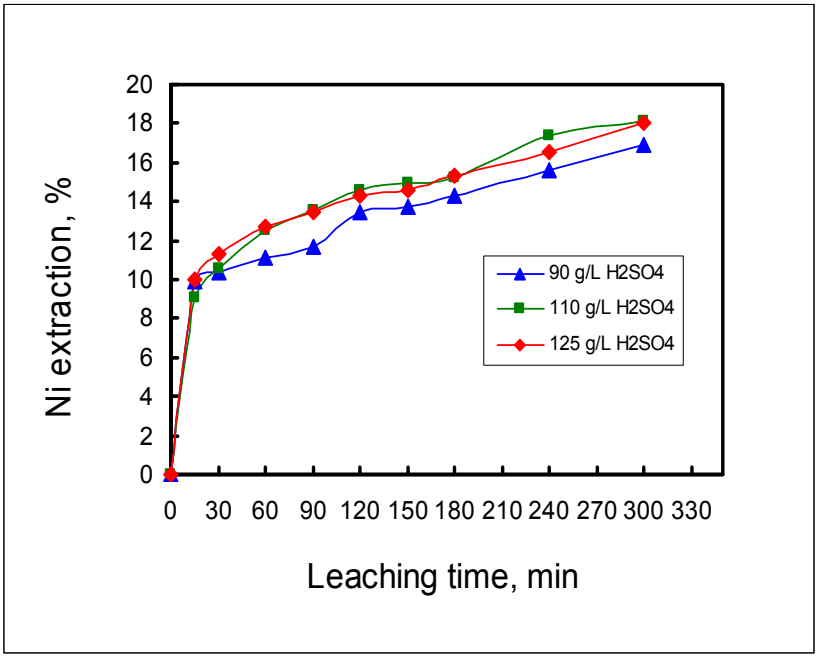

Figure 6.41: Nickel extraction as a function of leaching time at different initial H_2SO_4 concentrations (temperature: 60 °C, stirring rate: 205 rpm, pulp density: 1.7 kg/L).

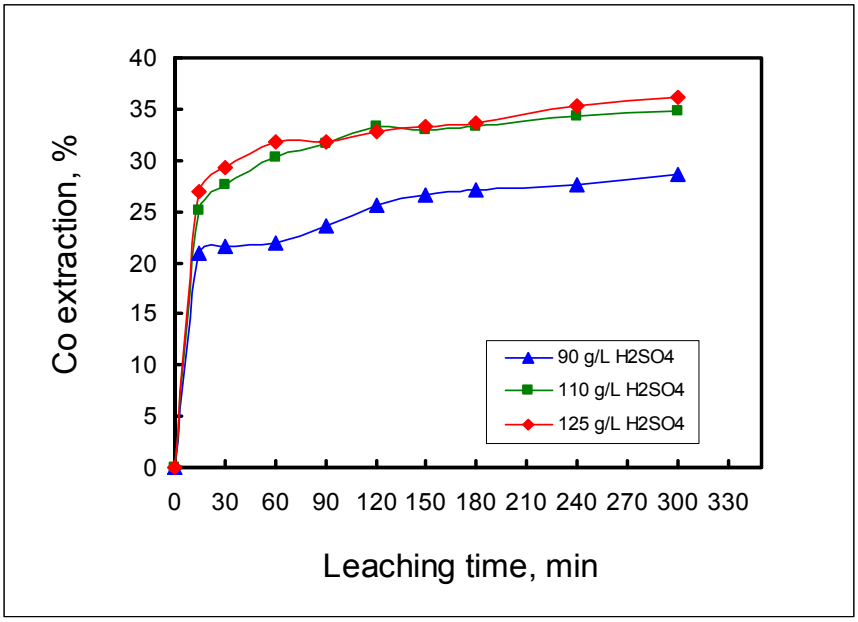

Figure 6.42: Cobalt extraction as a function of leaching time at different initial H_2SO_4 concentrations (Temperature: 60 °C, pulp density: 1.7 kg/L)

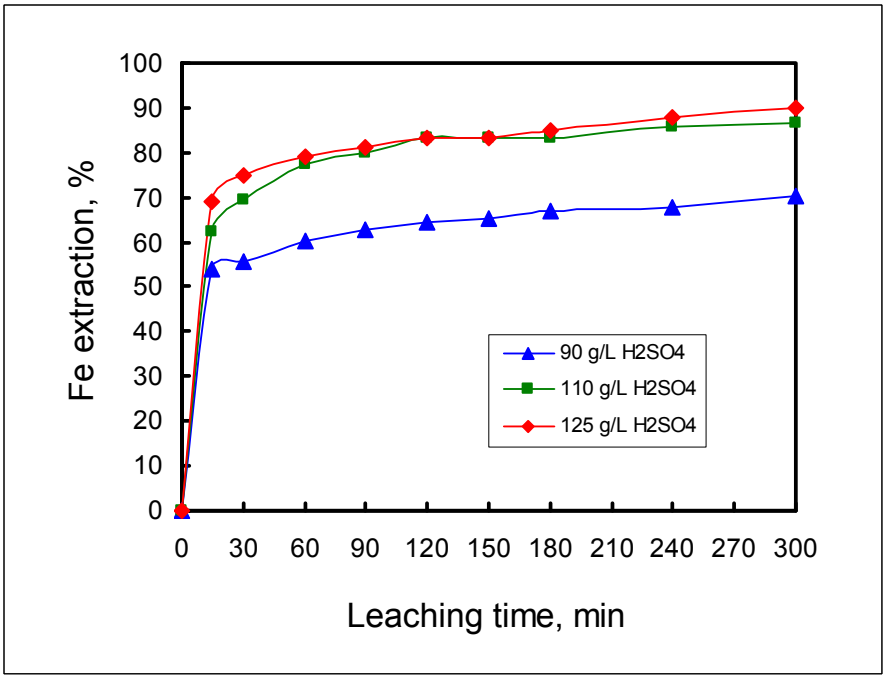

Figure 6.43: Iron extraction as a function of leaching time at different initial H_2SO_4 concentration (temperature: 60 °C, stirring rate: 205 rpm, pulp density: 1.7 kg/L).

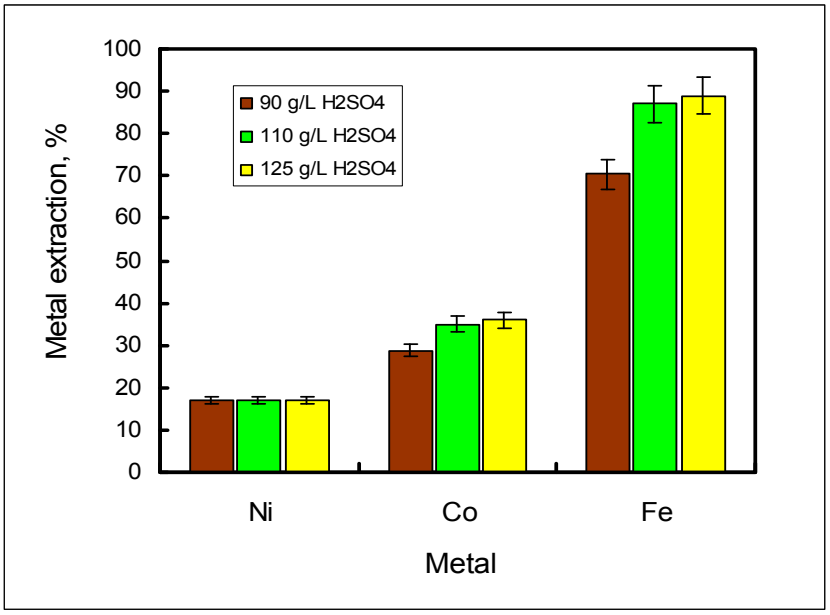

Figure 6.44: Metal extractions after atmospheric leaching of the matte at different initial H_2SO_4 concentrations

6.6.2 Effect of initial acid concentration on copper cementation

The effect of initial H_2SO_4 concentrations of the solution on the cementation of copper during the leaching of the Ni-Cu matte is illustrated in Figures 6.45 – 6.47. Figure 6.45 shows percent copper precipitation versus time, while Figure 6.46 is a plot of log ($[Cu^{2+}]_t/[Cu^{2+}]_0$) versus time. From the slopes of these graphs copper cementation rate constants were obtained and plotted as a function of H_2SO_4 concentration (Figure 6.47). It can be seen that the rate of copper cementation decreased slightly when acid was increased from 90 to 110 g/L, then the rate became insensitive to the initial acid concentration. At 90g/L H_2SO_4 all the copper was precipitated from the solution. The decrease in the rate of copper cementation when the acid concentration was increased to 110 g/L may be attributed to redissolution of some of the precipitated copper due to increase in the acidity of the solution. Figure 6.47 shows that beyond acid concentration of about 110g/L the rate constants did not vary with acid strength, probably because the rate of copper cementation was almost the same as the rate of copper redissolution.

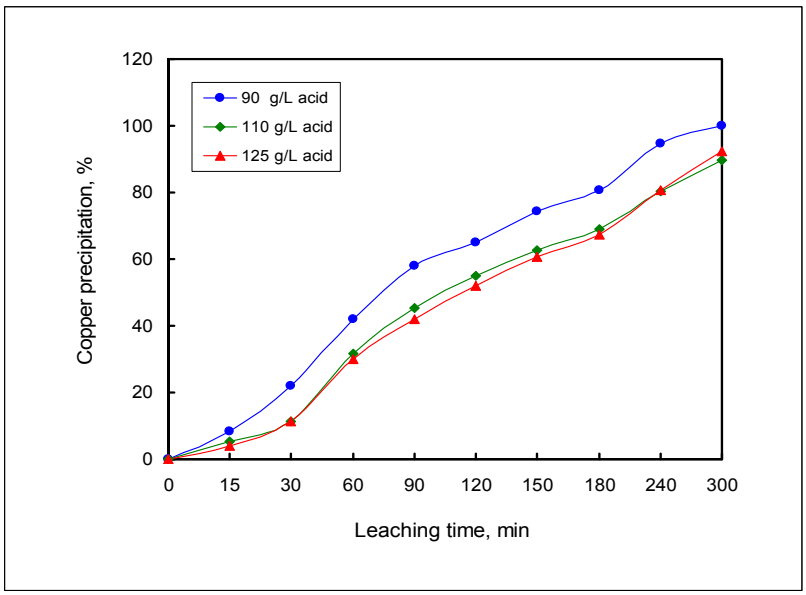

Figure 6.45: Copper precipitation as a function of time during atmospheric leaching of the matte at different initial H_2SO_4 concentrations (stirring rate: 205 rpm, temperature: 60 ^oC)

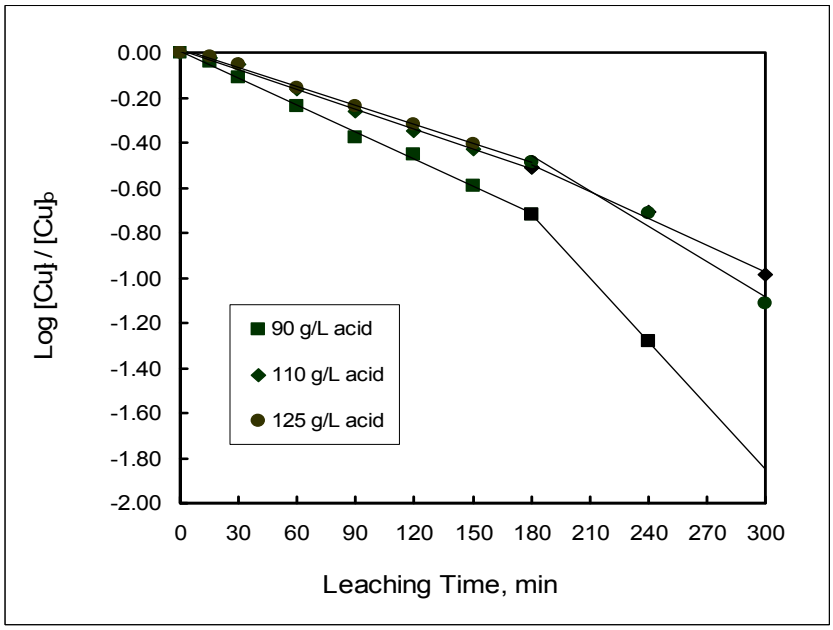

Figure 6.46 Variation of log[Cu $^{2+}]_t$ /[Cu $^{2+}]_0$ ratio with time at different initial acid strength, (205 rpm, 25 g/L initial Cu concentration, 60 ^oC, 1.7 kg/L density).

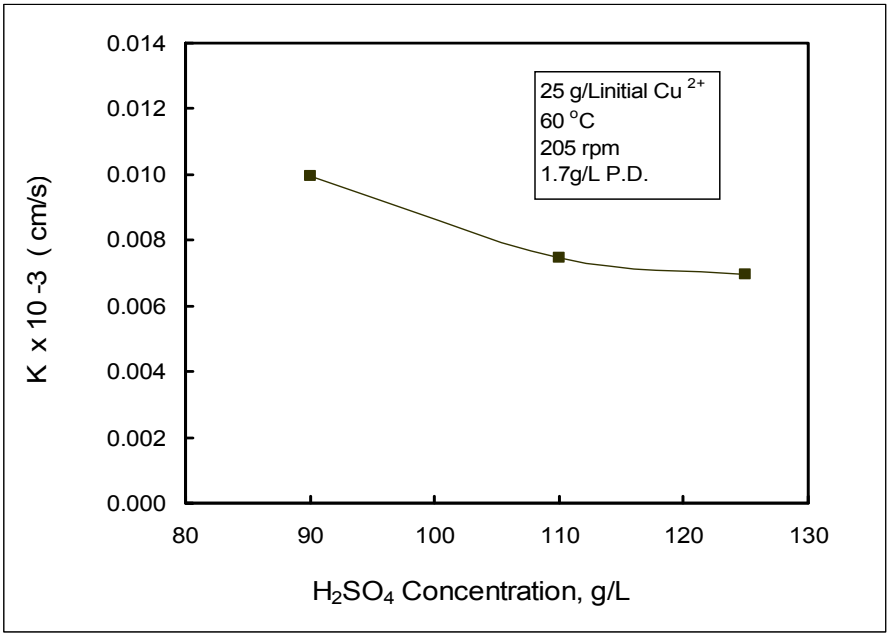

Figure 6.47: Variation of cementation rate constant (K) with initial acid strength.

6.7 Effect of residence time on the leaching behaviour of the Ni-Cu matte

6.7.1 Effect of residence time on nickel, cobalt and iron dissolution

To investigate the effect of residence time on the dissolution of nickel, cobalt and iron as well as copper cementation, the matte was leached for longer residence times of 7 and 9 hours; as opposed to a leaching time of 5 hours that was employed in the other experiments. The results obtained are presented in Table 6.7 and graphically illustrated in Figures 6.48 – 6.51 (see also Appendix A7). The results show that nickel extraction did not increase with increasing residence time for leaching times of more than 5 hrs, as no increase in the extractions was observed when the residence time was increased from 5 to 9 hours. Figure 6.48 shows that the degree of nickel extraction was similar for the residence times of 7 and 9 hours, and Figure 6.49 shows that the degree of cobalt dissolution was

also similar at the investigated residence times of 7 and 9 hours. The same leaching behaviour was observed for iron (Figure 6.50).

The observed leaching behaviour of the matte for different residence times indicated that a leaching time of 5 hours was enough to dissolve almost all the leachable metals under the applied conditions. It was also noted that for leaching times of more than 3 hrs, the mineral Ni_3S_2 was transformed to NiS indicating that the times were enough to dissolve most of the leacheable nickel.

6.7.2: Effect of residence time on copper cementation

Results obtained have shown that the aqueous copper was completely precipitated after 5 hours of leaching. For residence times of less than 5 hours, the copper did not precipitate completely, as can be seen from Tables A7.1 and A7.3 in Appendix A7.

Table 6.7: Ni, Co, and Fe extractions and final metal concentrations of the leach solution after atmospheric leaching of the matte for 5, 7 and 9 hours.

Time (hrs)	Metal extraction (%)			Final solution concentration (g/L)			
	Ni	Co	Fe *	Ni	Co	Fe	Cu
5	16. 9	28.7	70. 4	85.8	1.0	4.3	0.00
7	20.5	29.1	69.3	106.9	0.8	4.1	0.00
9	20.5	29.7	67.6	105.0	0.9	3.9	0.00

*The value shows maximum extraction attained prior to Fe precipitation.
Leaching conditions: stirring rate: temperature: 60 ^oC, 205 rpm, pulp density: 1.7kg/L,

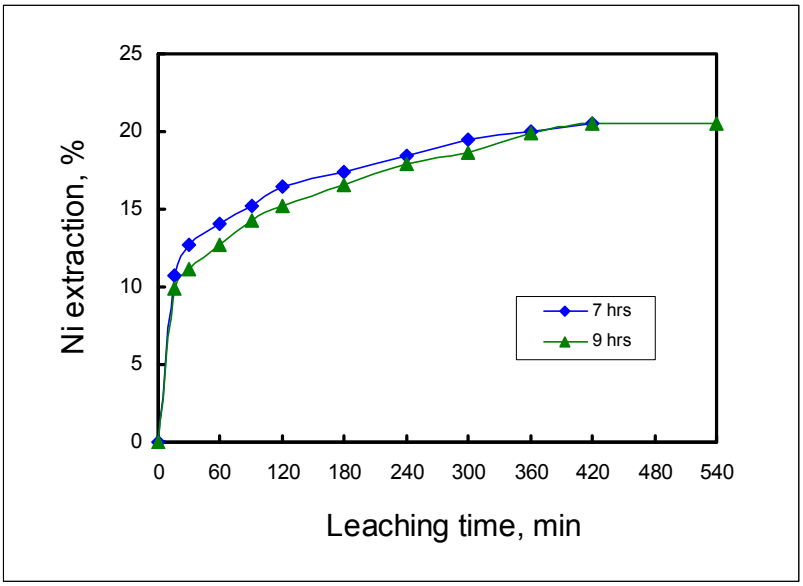

Figure 6.48: Nickel extraction as a function of leaching time at residence times of 7 and 9 hrs (temperature: 60 °C, stirring rate: 205 rpm, pulp density: 1.7 kg/L).

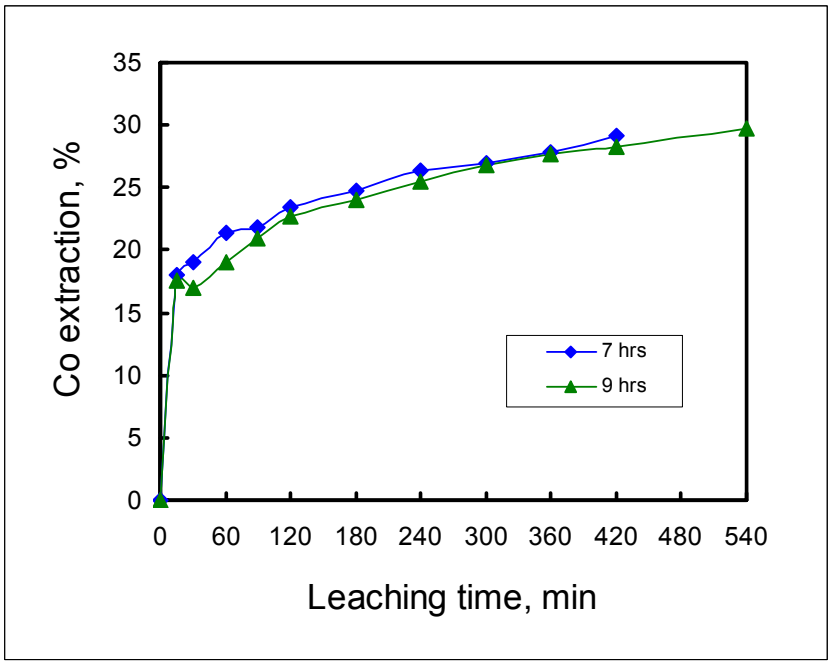

Figure 6.49: Cobalt extraction as a function of leaching time at residence times of 7 and 9 hours (Temperature: 60 °C, 205 rpm, pulp density: 1.7 kg/L)

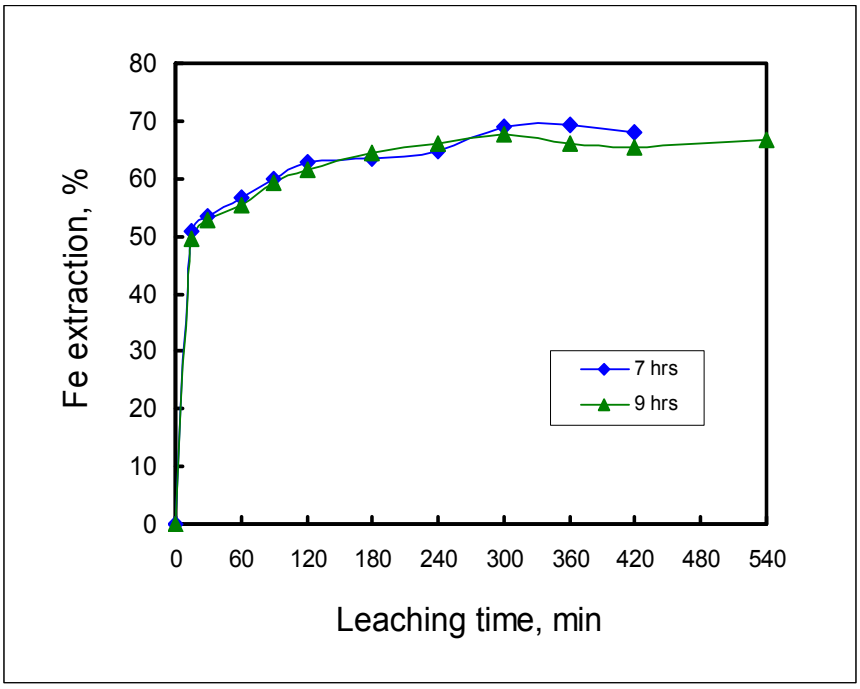

Figure 6.50: Iron extraction as a function of leaching time at residence times of 7 and 9 hours (temperature: 60 ^{o}C, stirring rate: 205 rpm, pulp density: 1.7 kg/L).

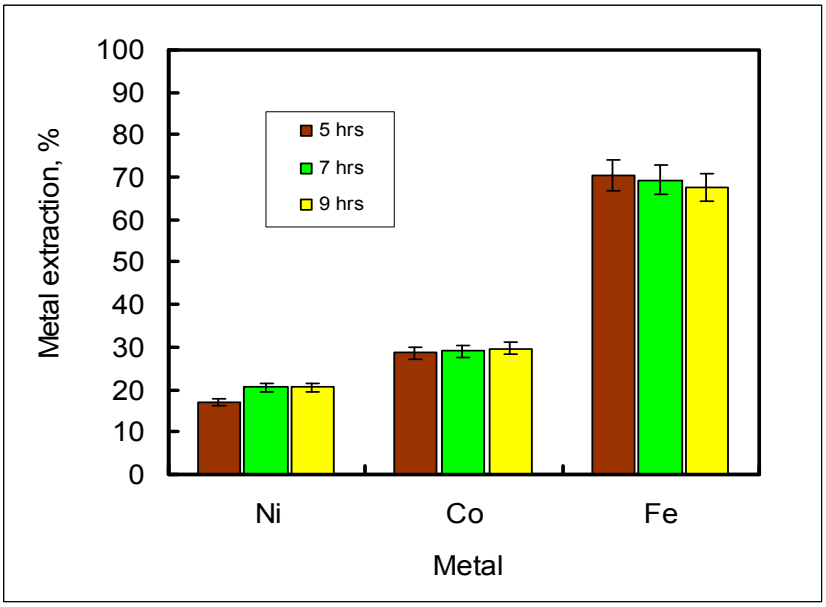

Figure 6.51: Metal extractions after atmospheric leaching of the matte for residence times of 7 and 9 hours.

6.8 Summary

This chapter has presented and discussed results of the atmospheric leaching experiments, which were conducted to investigate the effects of variations in the process variables. The variables studied were temperature, stirring rate, pulp density, matte particle size, residence time, initial copper and acid concentrations of the leaching solution. The dissolution kinetics of the metals was characterized with the shrinking core model using nickel dissolution kinetics data. The equation describing reaction controlled by diffusion through surface layer gave the best fit. An activation energy of 31 kJ/mol was obtained, which suggested a diffusion-controlled leaching process.

The results indicated that increasing the temperature from 50 ^{o}C to 60 ^{o}C slightly increased nickel extraction; but no significant increase in the extraction was achieved for the temperature range 60 – 80 ^{o}C. In the case of cobalt, no clear trend was observed as both the rate and degree of leaching appeared to be insensitive to temperature changes; although there was a slightly increase at 80 ^{o}C. At the low temperature of 50 ^{o}C relatively low iron extraction was achieved, however at 60 ^{o}C it increased but became insensitive at 80 ^{o}C. It was observed that nickel extraction increased gradually with increasing stirring rate for the investigated values of 145, 205 and 400 rpm. In the case of cobalt and iron the extractions were low at 145 rpm and 205 rpm but increased when the stirring rate increased to 400 rpm. Nickel and cobalt extractions did not appear to be affected by changes in the pulp density. On the other hand, iron extraction was higher at a pulp density of 1.6 kg/L and was not affected at higher pulp densities of 1.7 and 1.75 kg/L. It was found that nickel and cobalt extractions were not significantly affected by changes in the particle size. Iron extraction could not be determined accurately because of iron precipitation when the solution pH increased to above 3. Generally the leaching of the metals did not depend on initial copper concentrations in the investigated copper concentration range of 25 - 48 g/L. Metal extractions were not significantly different for the three copper concentrations. It was observed that variations in the initial acid concentration

did not have effect on nickel extraction, probably due to the fact that most of the nickel was leached by the process of cementation. However, cobalt and iron extractions increased when the acid increased from 90 g/L to 110 g/L, although further increase in the initial acid concentration had no effect on both cobalt and iron extraction. A residence time of 5 hours was found to be adequate as there was no significant increase in metal extractions when the residence time was increased beyond 5 hours.

The rate of copper cementation increased with increasing temperature. At 80 ^{o}C all the aqueous copper precipitated, whereas about 68% precipitated at 50 ^{o}C. The cementation reaction followed a mixed control mechanism, with two distinct activation energies namely 18.2 kJ/mol at 70 – 80 ^{o}C and 74.6 kJ/mol at 50 – 70 ^{o}C. This suggested that the rate of cementation reaction was probably controlled by a boundary layer diffusion mechanism at higher temperatures, and a surface reaction mechanism at low temperatures. The rate of copper cementation was not affected by variations in the stirring rate, suggesting a chemical reaction controlled process as indicated by the activation energy (74.6 kJ/mol). It was noted that copper precipitated faster as the pulp density increased from 1.6 to 1.7 kg/L and reached a maximum value at about 1.7 kg/L, probably due to the increase in cathodic surface area of matte. It was observed also that copper cementation increased with decreasing particles size, probably due to the increase in the surface area of fine particles. The effect of initial copper concentration of the leaching solution was that the rate of copper cementation decreased with increase in the initial copper concentration, until a value of about 36 g/L was reached. Thereafter it became almost independent of the initial copper concentration. It was found that copper cementation decreased with increase in the initial acid concentration up to a value of 110 g/L H_2SO_4, then it become almost insensitive to the acid concentration of the solution. The results showed that all the aqueous copper precipitated within 5 hours of leaching.

CHAPTER 7

7.0 PRESSURE LEACHING OF PRE-LEACHED Ni-Cu MATTE

The pressure leaching experiments were aimed at investigating the response of atmospheric pre-leached matte to the subsequent pressure leaching process, as practiced at Impala's Base Metal Refinery (BMR). Thus, it was important to simulate the leaching conditions employed on the plant, especially those of the first stage pressure leach. All the pressure leaching experiments were performed under the same conditions, which were within the conditions that are employed in the commercial plant at Impala, namely temperature of 145 ± 3 ^{o}C, pulp density of 1.4 kg/L, total pressure of ± 500 kPa and residence time of 3 hours. The material used was the pre-leached matte samples, which were the leach residues from the atmospheric leach experiments. The atmospheric leaching experiments were conducted under different leaching conditions as shown in Table 4.7 in section 4.4.2.

7.1 Thermodynamics of the Ni-Cu matte-H_2SO_4 pressure leaching system

The Eh-pH diagrams of the Ni-Cu matte-H_2SO_4 pressure leaching system are presented Figures 7.1 – 7.3. Figure 7.1 shows the stability regions of nickel species in the Ni-S-H_2O system; Figure 7.2 illustrates the stability regions of copper species in the Cu-S-H_2O system, while Figure 7.3 shows the stability regions of iron species in the Fe-S-H_2O system. As the experiments were conducted at one temperature value (±145 ^{o}C), all the Eh-pH diagrams were generated for the temperature of 145 ^{o}C . Figure 7.1 shows that the most stable nickel species under the investigated conditions (temperature of ±145 ^{o}C, pressure of ± 500 kPa and pH < 3) are the aqueous nickel (Ni^{2+}), millerite (NiS),

heazlewoodite (Ni_3S_2) and metallic nickel (Ni^o), depending on the potential of the system. Under oxidizing conditions (potential of more than zero) nickel can be leached from the matte. Figure 7.1 shows also that at pH values of greater than 4 and a potential of above zero, aqueous nickel can form NiO. At higher potential values (above 1.0 V) and pH of above 1.0 aqueous nickel can hydrolyse to form $Ni(OH)_3$. It should be noted that species such Ni^{2+}, NiS and Ni_3S_2 were observed in the leaching system under study, as predicted in Figure 7.1.

Figure 7.2 shows stability regions of the copper species in the system Cu-S-H_2O. The most stable species in the investigated pH values of less than 3 are aqueous copper (Cu^{2+}) Cu_2S, CuS and metallic copper, depending on the potential of the system. However, no CuS was observed in the leach solids, probably due to the fact that very small amounts were formed and the pH of the system was never less than zero as CuS is shown to form at pH of less than zero (Figure 7.2). Figure 7.2 shows also that at pH >3 and potential greater than 0.5V, aqueous copper can form basic copper sulphate ($Cu_3(OH)_4SO_4$. However, no $Cu_3(OH)_4SO_4$ was observed in the leaching system, probably due to the fact that all the aqueous copper precipitated before a pH of 3 was attained (Appendix B).

Figure 7.3 shows that the possible iron species in the system investigated are aqueous ferric iron (Fe^{3+}), ferrous iron (Fe^{2+}), metallic iron (Fe), and iron oxides (Fe_2O_3 and Fe_3O_4). In the system under study, no iron compounds were detected in the leach solids by XRD and SEM-EDS, probably due to the small amount of iron present in the matte (0.6 %) and in the leaching solution (0.67g/L).

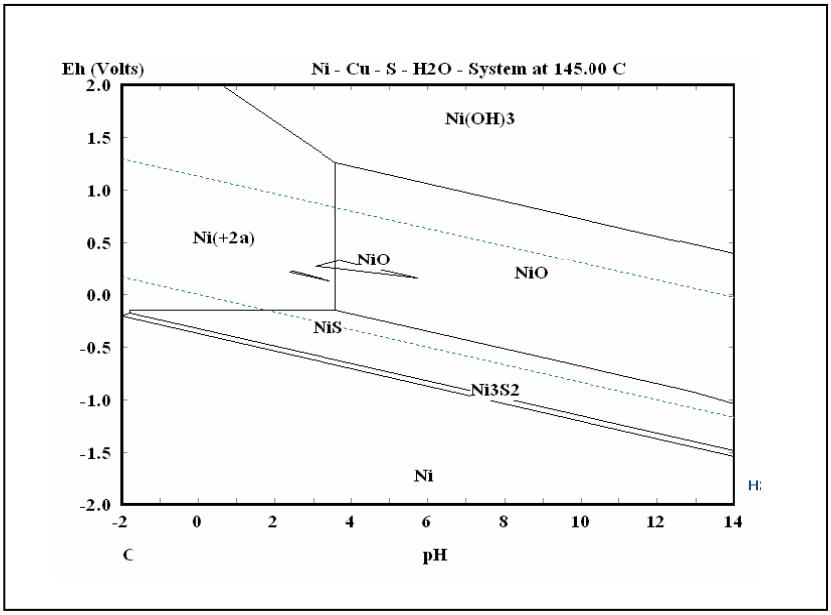

Figure 7.1: Eh-pH diagrams for the Ni-S-H_2O system at 145 ^oC and 5 bar pressure; [Ni] = 2.00 M, [S] = 2.00 M (M = molality)

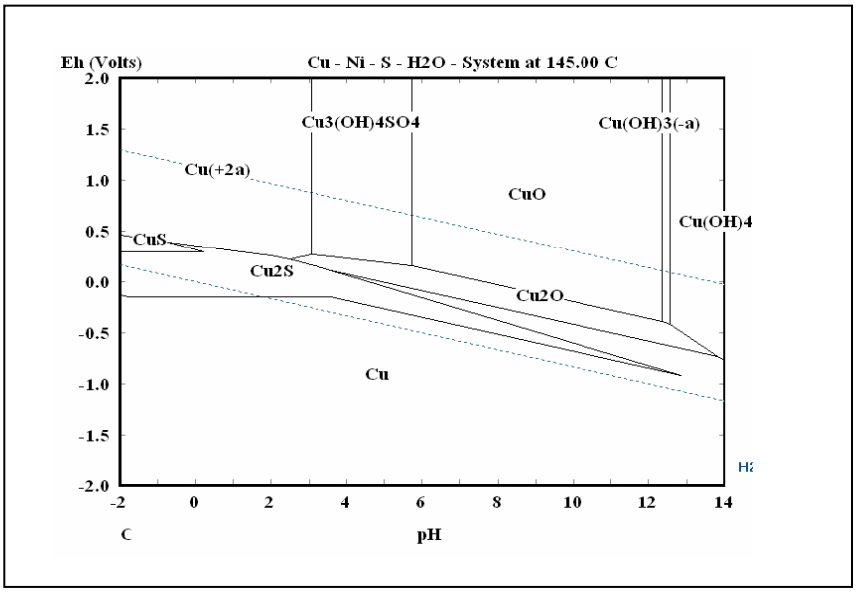

Figure 7.2: Eh-pH diagrams for the Cu-S-H_2O system at 145 ^oC and 5 bar pressure; [Cu] = 1.50 M, [S] = 2.00 M (M = molality)

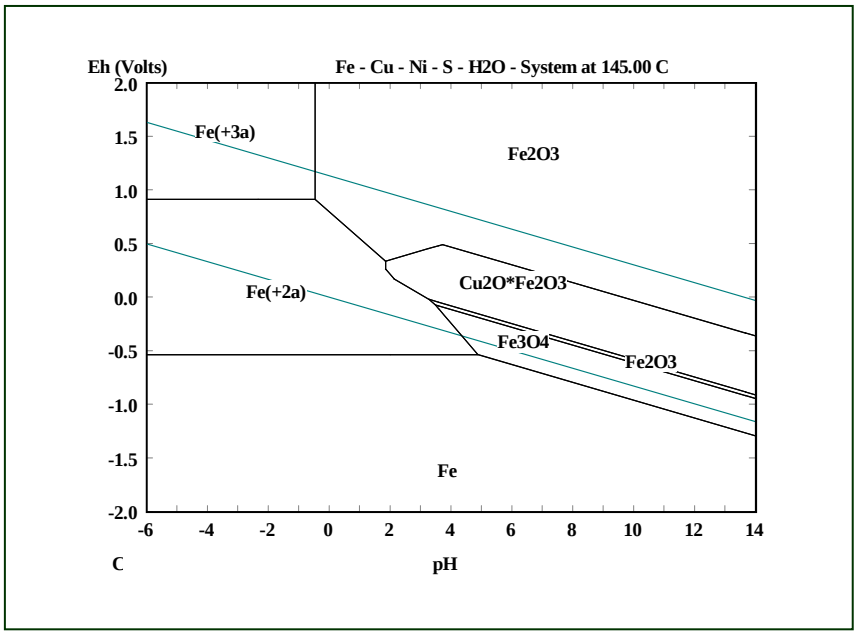

Figure 7.3: Eh-pH diagrams for the Fe-S-H_2O system at 145 ^oC and 5 bar pressure; [Fe] = 0.50 M, [S] = 2.00 M (M = molality)

7.2 Mechanism of pressure leaching of Ni-Cu matte

Although some pressure leaching experiments were conducted to investigate the response of pre-leached matte to the subsequent pressure leaching operations, no detailed study of the pressure leaching process has been done in the present study. This is because the main aim of the present study was to investigate the atmospheric leaching process, and not the pressure leaching process. Hence, the mechanism of Ni-Cu matte pressure leaching process was not investigated in detail in the present study. Pressure leaching mechanism of the Ni-Cu matte has been studied and published by many researchers, of which include the work of Rademan et al. (1999), who carried out an extensive study of the pressure leaching operation at Impala Base Metals Refinery (BMR). Plasket and Romanchuk (1978) also published the Ni-Cu refining process at Impala's BMR. Among the other workers who have investigated pressure leaching of the Ni-Cu

matte are Dutrizac and Chen (1987), Hofirek and Kerfoot (1992), Hofirek and Nofal (1995), and Steenekamp and Dunn (1999). According to Rademan (1995) the leaching mechanism for the acid-oxygen pressure leaching of Ni-Cu matte entails the following leaching sequences: the nickel sulphides leach from heazlewoodite (Ni_3S_2) to millerite (NiS), with godlevskite (Ni_7S_6) forming as an intermediate product. The millerite leaches further to form polydymite (Ni_3S_4) before it is completely leached. The mechanism for leaching the copper sulphides is slightly more complex with chalcocite (Cu_2S) being leached and formed in the beginning of the process. The chalcocite is then leached to form digenite ($Cu_{1.8}S$), with djurleite ($Cu_{31}S_{16}$) forming as an intermediate product. The digenite leaches further to form covellite (CuS), which is subsequently dissolved. The nickel in the alloy phase leaches out of the matte within the first 40 minutes and no mineral changes were detected in the alloy phase.

7.3 Results and discussion of Pressure Leaching Experiments

7.3.1 Effect of pre-leaching the matte at different temperatures

Results of pressure leaching experiments that were conducted to investigate the effect of pre-leaching the matte at different temperatures prior to the subsequent pressure leach stage are presented in Table 7.1 and Figures 7.4 – 7.6. The starting time, which is indicated as -25 minutes, on the horizontal axis of these graphs and all other metal extraction graphs in this chapter represents the 25 minutes of slurry heating time. The pressure leaching process was considered to have started at the point when the desired temperature was attained and O_2 added to the reactor, i.e 25 minutes after commencement of the experiment. The results are also presented in more detail in Appendix B. Table 7.1 shows results of the atmospheric and the pressure leaching stages for the investigated temperatures. It was found that the leaching behaviour was similar for the matte pre-leached at 50, 60 and 80 ^oC as similar leaching rates were observed during the pressure leaching stage.

Table 7.1: Metal extractions from matte pre-leached at temperatures of 50, 60 and 80 °C, and minerals present in the leach solids.

	Leaching stage	Extraction (%) and minerals in leach solids		
		50 °C	**60 °C**	**80 °C**
Nickel	Pre-leach	13	17	20
	Pres. Leach	64	67	66
	Overall	69	73	72
Cobalt	Pre-leach	28	29	35
	Pres. Leach	100	100	100
	Overall	100	100	100
Iron	Pre-leach	46	70	66
	Pres. Leach	100	100	100
	Overall	100	100	100
Mineral in leach solids	Pre-leach stage (Atm. Leach)	Ni_3S_2, $Cu_{1.96}S$, Cu_2S, Ni alloy	Ni_3S_2, NiS, $Cu_{1.96}S$, Cu_2S, Ni alloy	Ni_3S_2, NiS, $Cu_{1.96}S$, Cu_2S, Ni alloy
	Pressure leach stage	Ni_3S_2, NiS, $Cu_{1.8}S$, Cu_2S	Ni_3S_2, NiS, $Cu_{1.8}S$, Cu_2S	Ni_3S_2, NiS, $Cu_{1.8}S$, Cu_2S

- Pre-leach conditions: Pulp density 1.7 kg/L; stirring 205 rpm; residence time 5 hrs
- Pressure leach conditions: temp 145 °C; pulp density 1.4 kg/L; stirring 900 rpm; residence time 3 hrs; total pressure 500 kPa

It is understood that for matte pre-leached at 60 and 80 °C heazlewoodite (Ni_3S_2) transformed into millerite (NiS), which was easier to leach in the subsequent pressure leach stage, hence higher metal extractions would be expected. However, because of the conditions prevailing in the pressure leaching stage, all the nickel minerals appeared to be leached at the same rate regardless of the temperature at which the matte was pre-leached. The advantage that would be gained in pre-leaching the matte at a higher temperature would be that it would take less time to pressure leach nickel as more Ni_3S_2 would have transformed into NiS in the pre-leach stage.

The nickel alloy present in the pre-leached matte is leached within 90 minutes of the pressure leach stage (Rademan et al., 1999), and was therefore not present in

the final leach residue. The copper minerals (Cu_2S and $Cu_{1.96}S$) transformed into Cu_2S and $Cu_{1.8}S$, and were not leached under the applied conditions. The aqueous copper present in the leaching solution precipitated too. It has been found that, in the system under study, copper starts to leach after a leaching time of about 3 hours (Rademan, 1995). The sequence of mineral transformation occurring during the leaching of Ni-Cu matte has been described in sections 5.2 and 7.2. Rademan et al. (1999), Dutrizac and Chen (1987) and Hofirek and Kerfoot (1992) have presented detailed studies of phases formed during the leaching of Ni-Cu matte.

It was found that pre-leaching of the matte at different temperature values prior to pressure leaching did not have any effect on cobalt and iron extractions as both cobalt and iron were completely leached in the pressure leach stage. Figures 7.5 and 7.6 show the rates of cobalt and iron extractions, respectively. It can be seen that the rate of metal extraction was also independent of temperature at which the matte was pre-leached prior to pressure leaching.

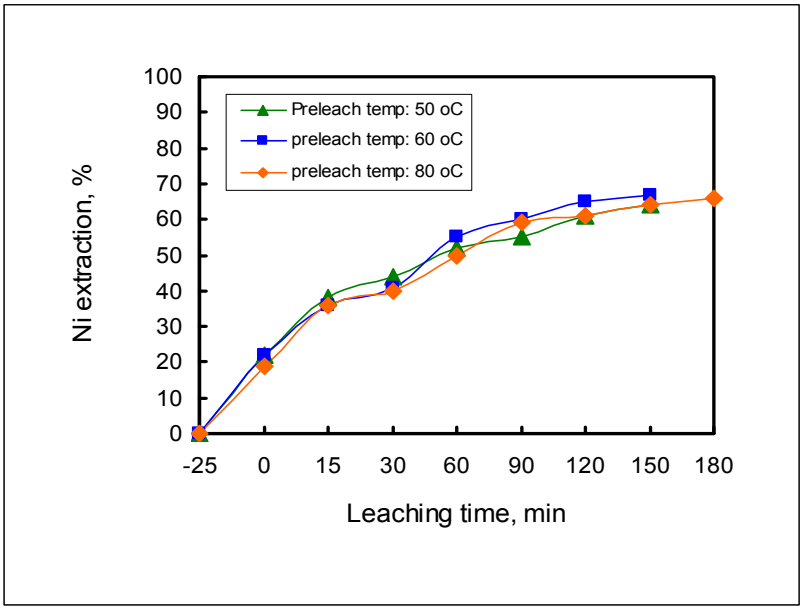

Figure 7.4: Ni extraction from matte pre-leached at different temperatures versus leaching time (Leaching conditions as in Table 7.1, starting time indicated as -25 minutes represents the 25 minutes of slurry heating time)

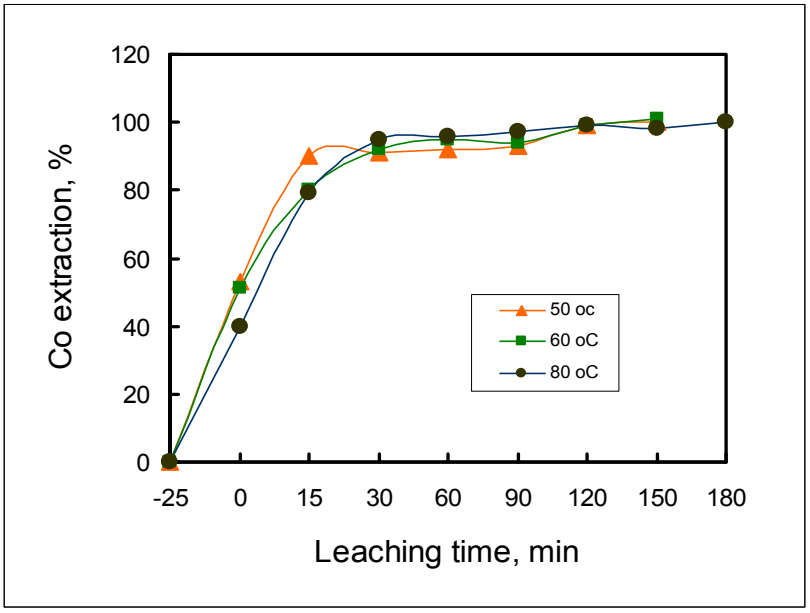

Figure 7.5: Cobalt extraction from matte pre-leached at different temperatures versus leaching time (Leaching conditions as in Table 7.1, starting time indicated as -25 minutes represents the 25 minutes of slurry heating time)

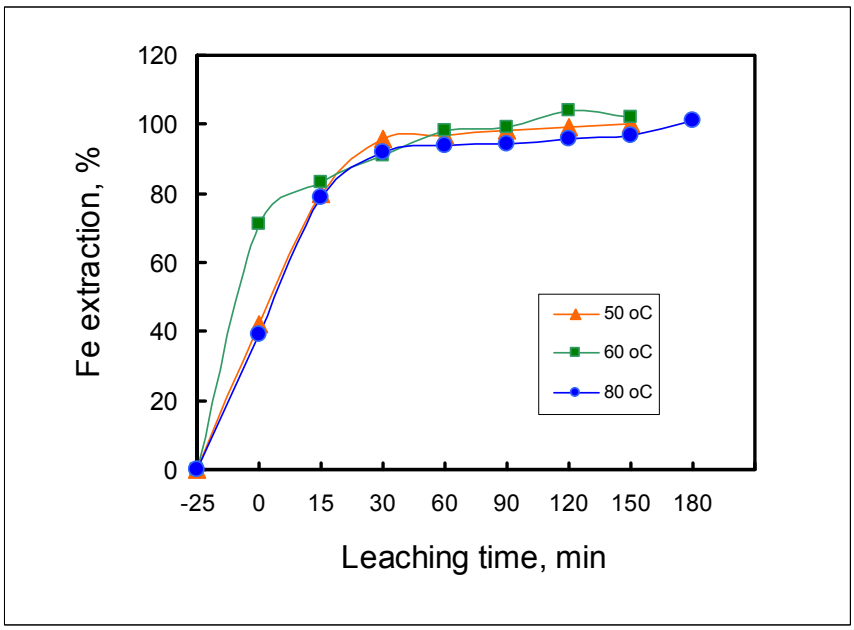

Figure 7.6: Iron extraction from matte pre-leached at different temperatures versus leaching time (Leaching conditions as in Table 7.1, starting time indicated as -25 minutes represents the 25 minutes of slurry heating time)

7.3.2 Effect of pre-leaching the matte at different stirring rates

The effect of pre-leaching the matte at different stirring rates on the subsequent pressure leaching stage is presented in Table 7.2 and Figures 7.7 – 7.9 (see Appendix B for more data). For the investigated stirring rates of 145, 205 and 400 rpm, it was found that the rate of nickel extraction was similar. The overall nickel extraction, which is the quantity of nickel leached during the atmospheric leach plus that leached during the pressure leach were also comparable.

Table 7.2: Metal extractions from matte pre-leached at stirring rates of 145, 205 and 400 rpm, and minerals present in the leach solids.

	Leaching stage	**Extraction (%) and minerals in leach solids**		
		145 rpm	**205 rpm**	**400 rpm**
Nickel	Pre-leach	12	17	19
	Pres. Leach	62	67	66
	Overall	67	73	73
Cobalt	Pre-leach	30	29	37
	Pres. Leach	100	100	100
	Overall	100	100	100
Iron	Pre-leach	69	70	59
	Pres. Leach	100	100	100
	Overall	100	100	100
Mineral in leach solids	Pre-leach stage (Atm. Leach)	Ni_3S_2, $Cu_{1.96}S$, Cu_2S, Ni alloy	Ni_3S_2, NiS, $Cu_{1.96}S$, Cu_2S, Ni alloy	Ni_3S_2, NiS, $Cu_{1.96}S$, Cu_2S, Ni alloy
	Pressure leach stage	Ni_3S_2, NiS, $Cu_{1.8}S$, Cu_2S	Ni_3S_2, NiS, $Cu_{1.8}S$, Cu_2S	Ni_3S_2, NiS, $Cu_{1.8}S$, Cu_2S

- Pre-leach conditions: Pulp density 1.7 kg/L; temp. 60 ^oC; residence time 5 hrs
- Pressure leach conditions: temp 145 ^oC; pulp density 1.4 kg/L; stirring 900 rpm; residence time 3 hrs; total pressure 500 kPa

It was noted that heazlewoodite (Ni_3S_2) transformed into millerite (NiS) at higher stirring rates of 205 and 400 rpm, and no millerite formed in the experiment conducted at 145 rpm. As noted in the previous section, one would expect higher

metal extractions in cases where there was Ni_3S_2 transformation but because of more aggressive conditions prevailing in the pressure leaching stage, all the nickel minerals were leached at about the same rate. Again the advantage of pre-leaching the matte at higher stirring rates would be that less time would be needed to pressure leach nickel as more Ni_3S_2 would have transformed into NiS in the pre-leach stage.

The nickel alloy and copper mineral leaching characteristics were the same as noted in the previous section: the alloy leached within 90 minutes of the pressure leach stage, and the copper minerals (Cu_2S and $Cu_{1.96}S$) transformed into Cu_2S and $Cu_{1.8}S$ with aqueous copper being precipitated. The degree and rate of cobalt and iron extractions were not affected by the stirring rates of the matte pre-leach stage, as 100% of cobalt and iron extraction was achieved (Table 7.2). The kinetics of cobalt and iron extractions were also independent of pre-leach stage stirring rates as illustrated in Figures 7.8 and 7.9, respectively.

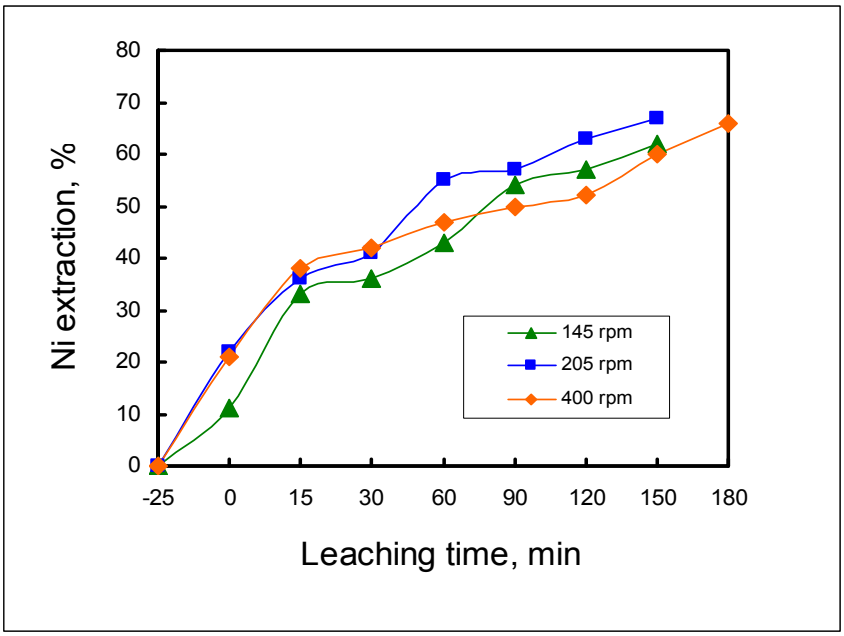

Figure 7.7: Nickel extraction from matte pre-leached at different stirring rates versus leaching time (Leaching conditions as in Table 7.2, starting time indicated as -25 minutes represents the 25 minutes of slurry heating time)

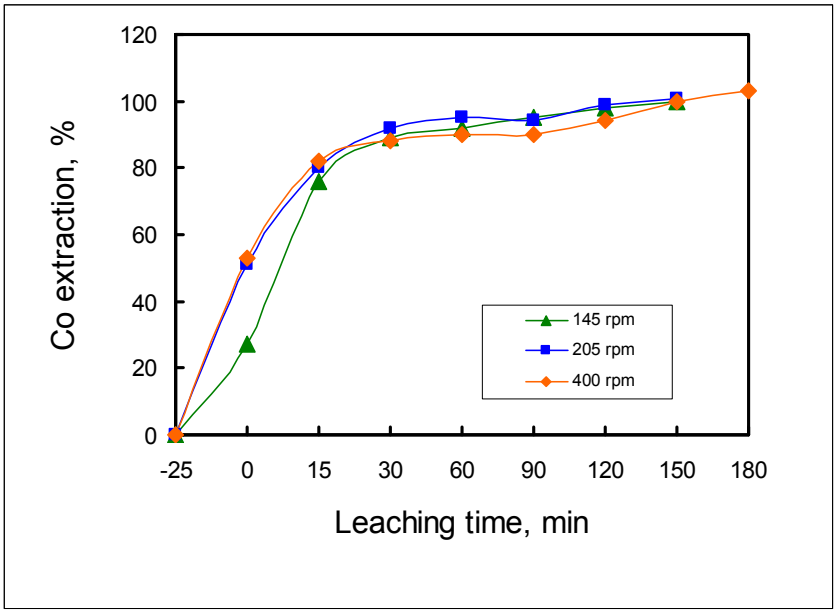

Figure 7.8: Cobalt extraction from matte pre-leached at different stirring rates versus leaching time (Leaching conditions as in Table 7.2, starting time indicated as -25 minutes represents the 25 minutes of slurry heating time)

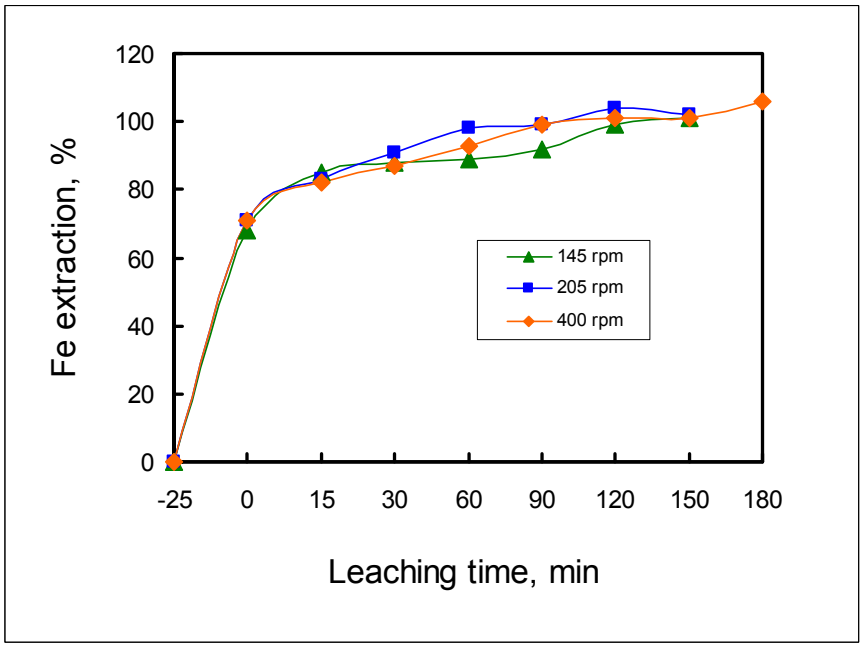

Figure 7.9: Iron extraction from matte pre-leached at different stirring rates versus leaching time (Leaching conditions as in Table 7.2, starting time indicated as -25 minutes represents the 25 minutes of slurry heating time)

7.3.3 Effect of pre-leaching the matte at different pulp density values

Results of experiments conducted to investigate the influence of pulp density of the atmospheric leach on the subsequent pressure leaching of the pre-leached matte are given in Table 7.3 and illustrated in Figures 7.10 – 7.12. More information is given in Appendix B. It was found that there was no clear trend in the leaching behaviour of the matte pre-leached at different pulp density values. The overall nickel extraction, as well as the leaching rates did not seem to be influenced by the fact that the matte was pre-leached at different pulp densities. Cobalt and iron extractions were 100% for all the investigated pulp density values.

Table 7.3: Metal extractions from matte pre-leached at Pulp density values of 1.6, 1.7 and 1.75 kg/L, and minerals present in the leach solids.

	Leaching stage	**Extraction (%) and minerals in leach solids**		
		1.6 kg/L	**1.7 kg/L**	**1.75 kg/L**
Nickel	Pre-leach	20	17	17
	Pres. Leach	63	67	65
	Overall	70	73	71
Cobalt	Pre-leach	41	29	35
	Pres. Leach	100	100	100
	Overall	100	100	100
Iron	Pre-leach	90	70	68
	Pres. Leach	100	100	100
	Overall	100	100	100
Mineral in leach solids	Pre-leach stage (Atm. Leach)	Ni_3S_2, NiS, $Cu_{1.96}S$, Cu_2S, Ni alloy	Ni_3S_2, NiS, $Cu_{1.96}S$, Cu_2S, Ni alloy	Ni_3S_2, NiS, $Cu_{1.96}S$, Cu_2S, Ni alloy
	Pressure leach stage	Ni_3S_2, NiS, $Cu_{1.8}S$, Cu_2S	Ni_3S_2, NiS, $Cu_{1.8}S$, Cu_2S	Ni_3S_2, NiS, $Cu_{1.8}S$, Cu_2S

- Pre-leach conditions: Stirring rate: 205 rpm; temp.: 60 ^oC; residence time: 5 hrs
- Pressure leach conditions : temp 145 ^oC; pulp density 1.4 kg/L; stirring 900 rpm; residence time 3 hrs; total pressure 500 kPag

The observed leaching behaviour of nickel can be attributed to the fact that nickel extractions as well as Ni_3S_2 transformation to NiS in the pre-leach stage were similar. The other contributing factor was the conditions prevailing in the pressure leaching stage, which allowed all the nickel minerals to be leached at about the same rate regardless of the pulp density at which the matte was pre-leached. Table 7.3 shows that at all three pulp density values millerite (NiS) was formed in the pre-leach stage. This implies that at the investigated pulp densities nickel leaching time is likely to be similar in the pressure leaching stage. The leaching behaviour of copper minerals and nickel alloy was the same as noted in section 7.3.1.

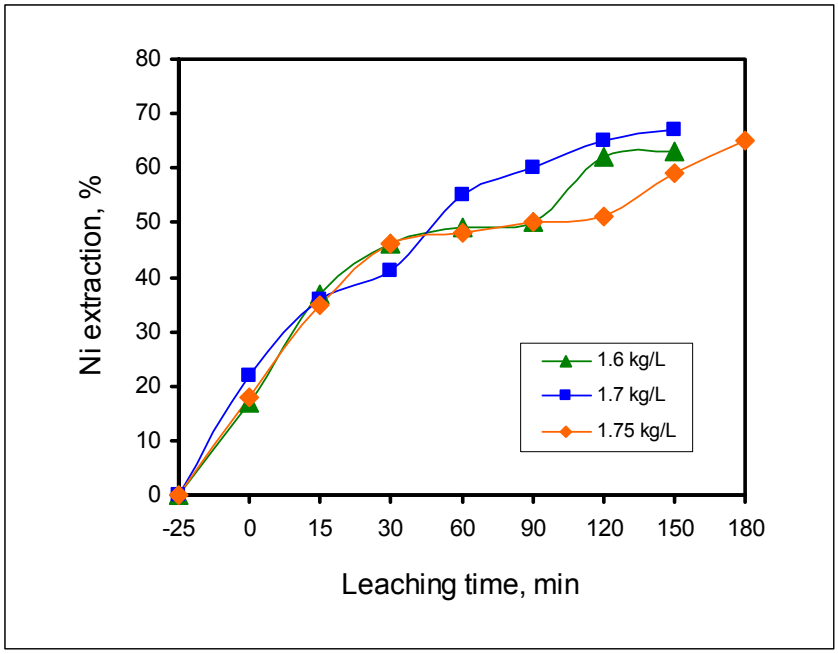

Figure 7.10: Nickel extraction from matte pre-leached at different pulp densities versus leaching time (Leaching conditions as in Table 7.3, starting time indicated as -25 minutes represents the 25 minutes of slurry heating time)

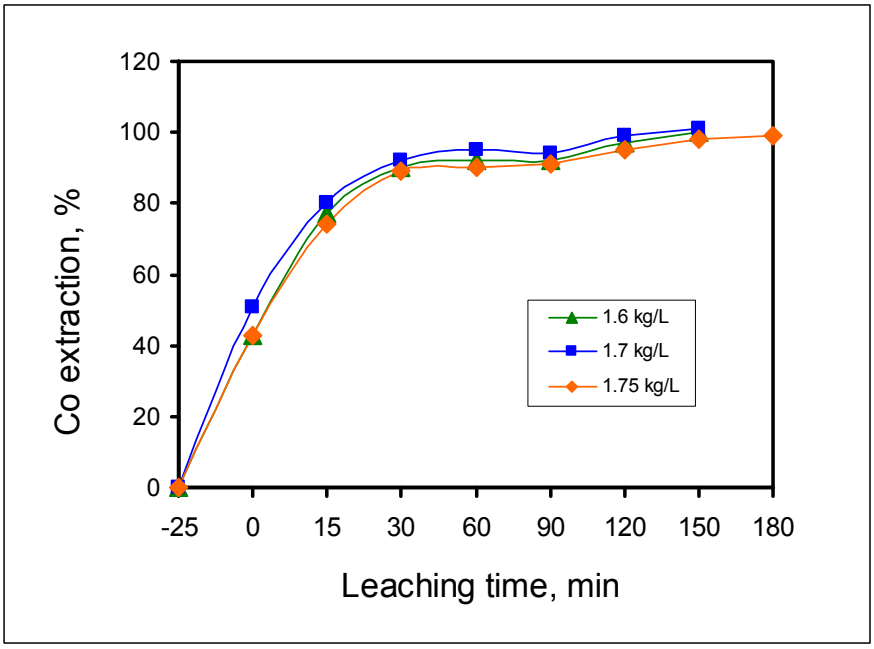

Figure 7.11: Cobalt extraction from matte pre-leached at different pulp densities versus leaching time (Leaching conditions as in Table 7.3, starting time indicated as -25 minutes represents the 25 minutes of slurry heating time).

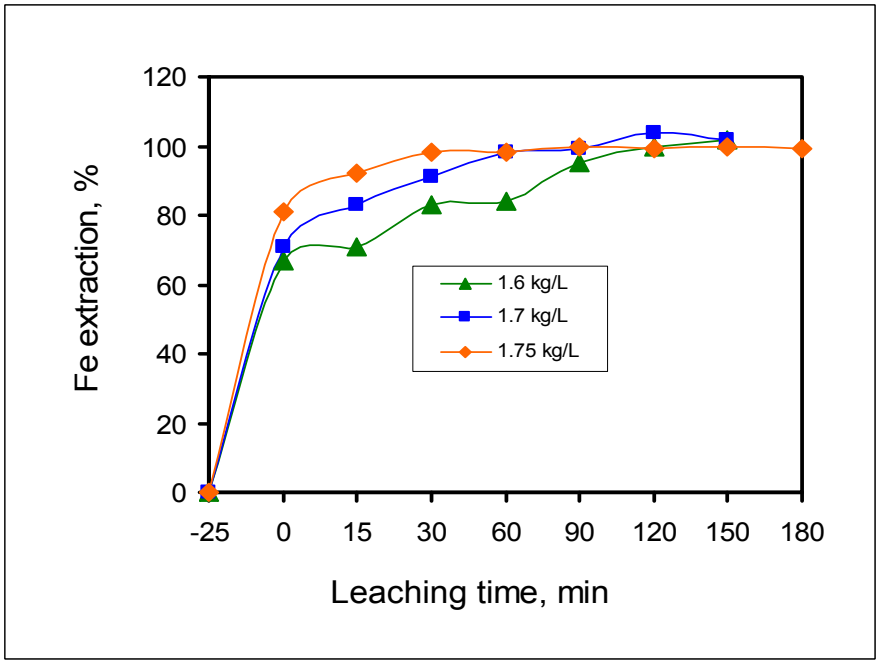

Figure 7.12: Iron extraction from matte pre-leached at different pulp densities versus leaching time (Leaching conditions as in Table 7.3, starting time indicated as -25 minutes represents the 25 minutes of slurry heating time)

7.3.4 Effect of pre-leaching the matte at different residence times

Results of experiments conducted to investigate the effect of varying residence time of the pre-leach stage on the subsequent pressure leaching stage are shown in Table 7.4 and Figures 7.13 – 7.15 (see Appendix B for more detail). The results indicated that pre-leaching of the matte at different residence times appeared to have effect on nickel extraction in the subsequent pressure leaching stage. Table 7.4 shows that the degree of nickel extraction increased with increasing residence time of the pre-leach stage.

Table 7.4: Metal extractions from matte pre-leached at residence times of 1, 3 and 9 hrs, and minerals present in the leach solids.

	Leaching stage	Extraction (%) and minerals in leach solids		
		1 hr	3 hrs	9 hrs
Nickel	Pre-leach	13	15	21
	Pres. Leach	41	57	65
	Overall	49	64	72
Cobalt	Pre-leach	30	27	30
	Pres. Leach	100	100	100
	Overall	100	100	100
Iron	Pre-leach	67	62	67
	Pres. Leach	100	100	100
	Overall	100	100	100
Mineral in leach solids	Pre-leach stage (Atm. Leach)	Ni_3S_2, $Cu_{1.96}S$, Cu_2S, Ni alloy	Ni_3S_2, NiS, $Cu_{1.96}S$, Cu_2S, Ni alloy	Ni_3S_2, NiS, $Cu_{1.96}S$, Cu_2S, Ni alloy
	Pressure leach stage	Ni_3S_2, NiS, $Cu_{1.8}S$, Cu_2S	Ni_3S_2, NiS, $Cu_{1.8}S$, Cu_2S	Ni_3S_2, NiS, $Cu_{1.8}S$, Cu_2S

- Pre-leach conditions: Pulp density 1.7 kg/L; stirring rate 205 rpm; temp. 60 ^oC;
- Pressure leach conditions : temp: 145 ^oC; pulp density: 1.4 kg/L; stirring rate: 900 rpm; residence time 3 hrs; total pressure 500 kPa

The rate of nickel extraction also increased with increasing residence time of the pre-leach stage, as illustrated in Figure 7.13. The reason for the observed nickel extraction results could probably be attributed to changes in the mineral phases of the matte as discussed in the preceding sections. The increase in nickel extraction when the matte was pre-leached for longer times was probably due to the presence of more NiS in the pre-leached solids, which is easily leached in the pressure leach stage. Table 7.4 shows that for a residence time of 1 hour no NiS was formed.

As discussed in the previous sections copper was never leached in the pressure leach stage due to shorter leaching time (3 hours). Cobalt and iron leaching behaviour was same as described in the previous sections. For all the three pre-leach stage residence times of 1, 3 and 9 hrs, cobalt and iron were completely leached (100 % extraction).

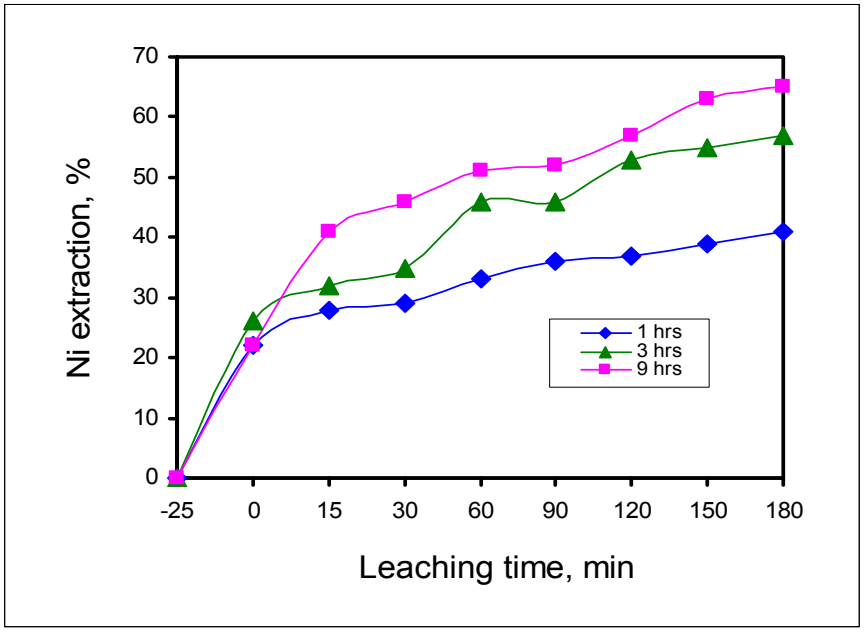

Figure 7.13: Nickel extraction from matte pre-leached at different residence times versus leaching time (Leaching conditions as in Table 7.4, starting time indicated as -25 minutes represents the 25 minutes of slurry heating time)

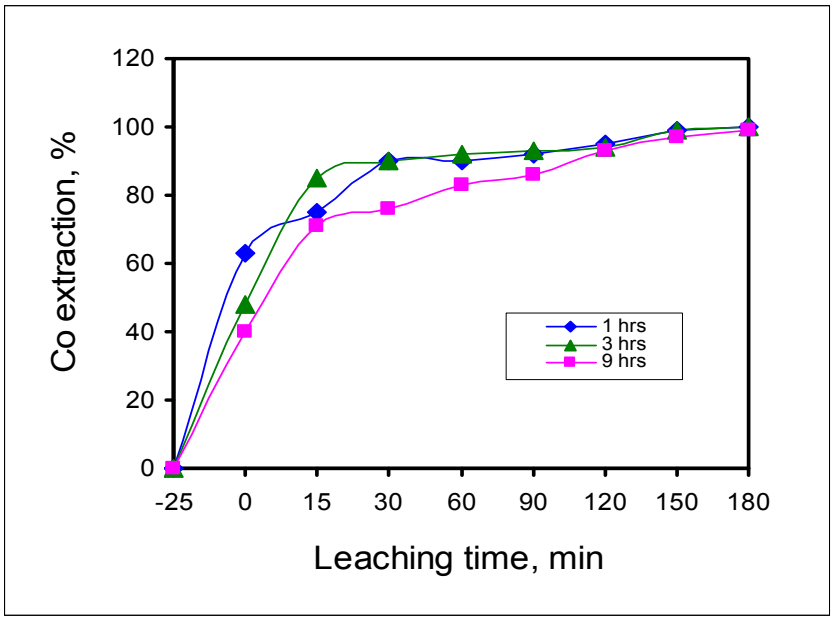

Figure 7.14: Cobalt extraction from matte pre-leached at different residence times versus leaching time (Leaching conditions as in Table 7.4, starting time indicated as -25 minutes represents the 25 minutes of slurry heating time)

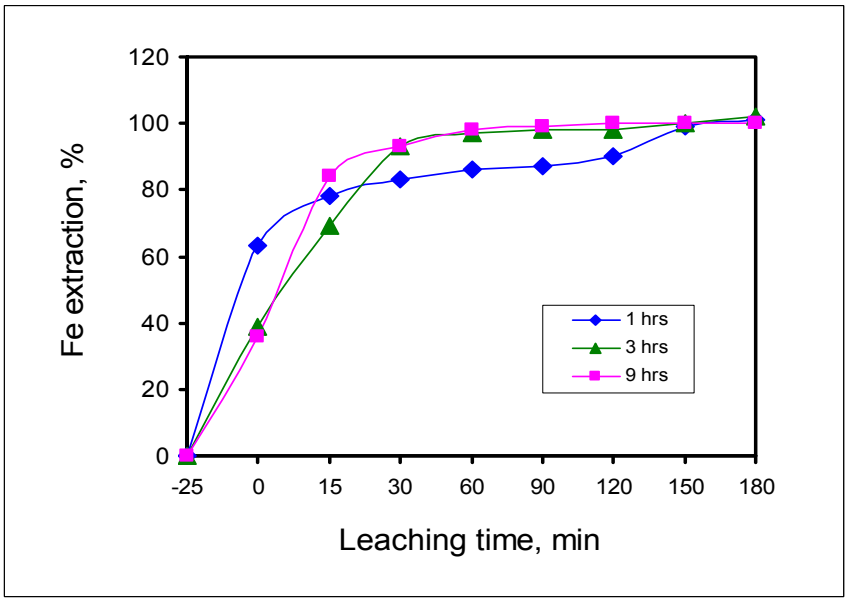

Figure 7.15: Iron extraction from matte pre-leached at different residence times versus leaching time (Leaching conditions as in Table 7.4, starting time indicated as -25 minutes represents the 25 minutes of slurry heating time)

7.4 Summary

In this chapter, results of the pressure leaching experiments are presented and discussed. In section 7.1 the thermodynamics of the Ni-Cu-H_2SO_4 pressure leaching system has been discussed using the Eh-pH diagrams. The diagrams showed that the thermodynamically possible stable species in the leaching system under investigation were Ni^{2+}, Cu^{2+}, NiS, Ni_3S_2, Cu_2S and CuS. However, Cu^{2+} easily precipitated, and CuS was not formed in the leaching conditions employed. In general, the species predicted by the Eh-pH diagrams were in agreement with what was observed in the leach samples. The results showed that similar nickel leaching rates were observed for the temperatures of 50, 60 and 80 ^oC. For matte pre-leached at 60 and 80 ^oC, Ni_3S_2 transformed into NiS which is easier to leach in the pressure leach stage, and no NiS was formed in the test conducted at 50 ^oC. However, because of the conditions prevailing in the pressure leaching stage, nickel was leached at the same rate regardless of the temperature at which the matte was pre-leached. The rate of nickel extraction was similar for the investigated stirring rates of 145, 205 and 400 rpm. At the stirring rates of 205 and 400 rpm, Ni_3S_2 transformed into NiS. No NiS formed in the experiment conducted at 145 rpm, though nickel minerals were leached at about the same rate due to the leaching conditions. Residence time of the pre-leaching stage had an effect on the nickel extraction in the pressure leaching stage. The nickel extraction increased with increasing residence time, due to the changes in the mineral phases of the matte as indicated above. In the case of pulp density, nickel extraction was comparable for the pulp densitiy range of 1.6 – 1.75 kg/L. This was probably due to the fact that the degree of mineral transformation in the pre-leach stage was similar. For all three pulp densities the Ni_3S_2 transformed to NiS. The copper minerals (Cu_2S and $Cu_{1.96}S$) transformed into Cu_2S and $Cu_{1.8}S$ with aqueous copper being precipitated, and were not leached under the applied conditions. All the cobalt and iron dissolved in the pressure leaching stage.

CHAPTER 8

8.0 KINETIC MODEL

This chapter presents a semi-empirical kinetic model which was developed on the basis of the leaching mechanism and chemical reactions presented in chapter 5. The model makes allowance for variations in the values of the leaching parameters such as initial copper concentration, temperature, particle size and initial acid concentration. As stated in chapter 5, under the leaching conditions employed in this study (where no oxidant was added) the sulphide minerals were not expected to leach to any significant degree. Therefore, the chemical reactions considered in the model are those that are most likely to occur to a significant degree during the leaching process.

8.1 Chemical reaction rates

The chemical reaction rates are presented in terms of the rate of change of the number of moles of the species in the reaction volume (Levenspiel, 1972 and Fogler, 1986), according to equation 8.1:

$$r_A = \frac{1}{V}\frac{dN_A}{dt} = \frac{moles}{(reaction\ volume)(time)}\ \frac{of}{}\ \frac{A}{}\ \frac{formed}{} \qquad (8.1)$$

$$Vr_A = \frac{dN_A}{dt} \qquad (8.2)$$

The actual volume of the reaction mixture decreased slightly during the experiments as samples were taken out for analysis. However, the volume taken out was considered insignificant in comparison to that which remained. Thus the

reaction volume term in equation 8.2 was taken as a constant, and was absorbed into the rate constants used in the model.
If we consider a single elementary homogeneous reaction with a stoichiometric equation given by

$$A + B \rightarrow D \qquad (8.3)$$

The rate of disappearance of A is given by:

$$-r_A = KC_AC_B \qquad (8.4)$$

Where K is the reaction rate constant and C_A and C_B are the concentrations of species A and B respectively. The negative sign indicates the disappearance of species A.

Combining equations 8.2 and 8.4, the reaction rate expression takes the form shown in equation 8.5:

$$\frac{dN_A}{dt} = KC_AC_B \qquad (8.5)$$

8.2 Reaction rate expressions

The reactions used in the mathematical model, and any assumptions made in developing the model are presented below. In chapter 5 it has been stated that the leaching mechanism can be divided into two categories namely

- Leaching of the matte via the cementation process and
- Leaching of the matte by direct acid attack

The two means of matte leaching occur simultaneously during the early part of the leaching process when aqueous copper is still present. Therefore, in

developing the mathematical model the chemical reactions were categorized into those that involve copper cementation and those that involve matte leaching by direct acid attack. The reactions and their reaction rate expressions are given below:

(i) Matte leaching by the cementation reaction

$$Ni^{o} + Cu^{2+} \rightarrow Cu^{o} + Ni^{2+} \quad (8.6)$$

$$Ni_3S_2 + Cu^{2+} \rightarrow Cu^{o} + 2NiS + Ni^{2+} \quad (8.7)$$

$$Ni_3S_2 + 2Cu^{2+} \rightarrow Cu_2S + NiS + 2Ni^{2+} \quad (8.8)$$

$$Ni_3S_2 + Ni^{o} + 4Cu^{2+} \rightarrow 2Cu_2S + 4Ni^{2+} \quad (8.9)$$

Under the leaching conditions employed in this study, in which no oxidant was added, the sulphide minerals were hardly leached. It was therefore deemed appropriate to consider the overall reaction for the leaching of nickel, as given by equation 8.10. This is the overall reaction of reactions 8.6 – 8.9:

$$3Ni_3S_2 + 2Ni^{o} + 8Cu^{2+} \rightarrow 3Cu_2S + 2Cu^{o} + 3NiS + 8Ni^{2+} \quad (8.10)$$

he reaction rate expression for equation 8.10 is given by:

$$\frac{dN_{A(8.10)}}{dt} = n_A K_{8.10} C_{Cu^{2+}} \quad (8.11)$$

where $\frac{dN_A}{dt}$ is the rate of production of species A, n_A is the stoichiometric coefficient of species A and K is a first-order rate constant incorporating the reaction volume term from equation 8.2.

Equation 8.11 was used to develop the reaction rate expressions for the dissolution and formation of various species during the leaching process, as a result of the cementation process (equations 8.10A – 8.10G).

$$\frac{d\,Ni^{2+}}{dt} = \frac{8}{3}k_{8.10}C_{Cu^{2+}} \qquad (8.10A)$$

$$\frac{d\,Cu^{2+}}{dt} = -\frac{8}{3}k_{8.10}C_{Cu^{2+}} \qquad (8.10B)$$

$$\frac{d\,Ni^{o}}{dt} = -\frac{2}{3}K_{8.10}C_{Cu^{2+}} \qquad (8.10C)$$

$$\frac{d\,Ni_3S_2}{dt} = -K_{8.10}C_{Cu^{2+}} \qquad (8.10D)$$

$$\frac{d\,Cu_2S}{dt} = K_{8.10}C_{Cu^{2+}} \qquad (8.10E)$$

$$\frac{d\,Ni\,S}{dt} = K_{8.10}C_{Cu^{2+}} \qquad (8.10F)$$

$$\frac{d\,Cu^{o}}{dt} = \frac{2}{3}K_{8.10}C_{Cu^{2+}} \qquad (8.10G)$$

The leaching of iron by the cementation process (equation 8.12) was assumed to be insignificant due to the presence of the iron alloy as small inclusions randomely distributed in the matte. The matte had to be attacked by the acid and penetrated to leach the iron grains embedded in the matte, besides the quantity of iron in the matte was very small (0.60%). It was therefore assumed that the iron was leached mainly by the acid according to reaction 8.15.

$$Fe^{o} + Cu^{2+} = Fe^{2+} + Cu^{o} \qquad (8.12)$$

(ii) Matte leaching by direct acid attack

The nickel alloy was leached by acid according to the following reaction:

$$Ni^{o} + 2H^{+} + 1/2O_2 \rightarrow Ni^{2+} + H_2O \quad (8.13)$$

The rate expression for reaction 8.13 is given by equation 8.14:

$$\frac{dN_{A(8.13)}}{dt} = n_A K_{8.13} C_{H^+} P_{O_2} \quad (8.14)$$

where $\frac{dN_A}{dt}$, n_A, and $K_{(8.13)}$ are as explained earlier for equation 8.11, C_{H^+} is the acid concentration and P_{O2} is the partial pressure of oxygen. But no oxygen was added to the system, so the O_2 partial pressure was taken to be the same as the atmospheric pressure and was assumed to be constant. Therefore, the oxygen partial pressure term in all the rate expressions for the dissolution and formation of species due to leaching by acid has been omitted. The rate expressions for reaction 8.13 are given by equations 8.13A – 8.13C:

$$\frac{d\,Ni^{2+}}{dt} = k_{8.13} C_{H^+} \quad (8.13A)$$

$$\frac{d\,H^{+}}{dt} = -2 k_{8.13} C_{H^+} \quad (8.13B)$$

$$\frac{d\,Ni^{o}}{dt} = -k_{8.13} C_{H^+} \quad (8.13C)$$

It should be noted that for modelling purposes, reactions of sulphide minerals with acid have not been considered due to the fact that the acid will mainly attack metal alloys, especially in this case where no oxidant was added.

The iron alloy present in the matte was leached according to reaction 8.15:

$Fe^{o} + 2H^{+} + 1/2O_2 \rightarrow Fe^{2+} + H_2O$ (8.15)

$Fe^{3+} + 3H_2O \rightarrow Fe(OH)_3 + 3H^{+}$ (8.16)

When the pH of the leaching system rose sufficiently, iron precipitated from the solution (see Figures 5.7 – 5.9). For modelling purposes, it has been assumed that the precipitation occurs via equation 8.16. The rate expressions for reaction 8.15 are represented by equations 8.15A – 8.15C, and again the O_2 partial pressure term has been assumed constant.

$$\frac{d\,Fe^{2+}}{dt} = k_{8.15} C_{H^+} \quad (8.15A)$$

$$\frac{d\,H^{+}}{dt} = -2 k_{8.15} C_{H^+} \quad (8.15B)$$

$$\frac{d\,Fe^{o}}{dt} = -k_{8.15} C_{H^+} \quad (8.15C)$$

The rate expressions for equation 8.16 are:

$$\frac{d\,Fe^{3+}}{dt} = -k_{8.16} C_{Fe^{3+}} \quad (8.16A)$$

$$\frac{d\,H^{+}}{dt} = 3 k_{8.16} C_{Fe^{3+}} \quad (8.16B)$$

$$\frac{d\,Fe(OH)_3}{dt} = k_{8.16} C_{Fe^{3+}} \quad (8.16C)$$

It was noted that any iron present as FeS would not have leached to a significant degree under the conditions employed in this study.

The cobalt alloy was leached according to reaction 8.17:

$$Co + 2H^+ + 1/2O_2 \rightarrow Co^{2+} + H_2O \qquad (8.17)$$

The reaction rate expressions for equation 8.17 are given below. As stated ealier, the oxygen partial pressure was constant (atmospheric pressure) and hence it was absorbed into the rate constant, $K_{8.17}$.

$$\frac{dCo^{2+}}{dt} = k_{8.17} C_{H^+} \qquad (8.17A)$$

$$\frac{dH^{+}}{dt} = -2k_{8.17} C_{H^+} \qquad (8.17B)$$

$$\frac{dCo^{o}}{dt} = -k_{8.17} C_{H^+} \qquad (8.17C)$$

8.3 Reaction rate constants

The empirical rate constants $K_{8.10}$, $K_{8.13}$, $K_{8.15}$, $K_{8.16}$ and $K_{8.17}$ were estimated and fine tuned to provide the best possible fit to the experimental data. A set of constants that enabled the model to accurately simulate the experimental data is presented in Table 8.1. The reaction rate constants incorporate expressions that can predict effect of variations in temperature, particle size, initial acid and copper concentrations. The leaching rate constants also incorporate a term for the shrinking core leaching effect. This is because the Ni alloy occurs as small inclusions randomly distributed in the matte particles. Hence, pores have to form for the leaching solution to reach the Ni alloy particles. In general the reaction rate constants are of the form:

$$K_i = A_s K_{H+/Cu+} K_{T,j} Z \qquad (8.18)$$

Where K_i is the reaction rate constant for reaction (i).

The terms in the reaction rate constant expression represent the following:

A_s is the surface area factor that accounts for the effect of variation in the effective surface area of the matte particles (Rademan, 1995).

K_{H^+/Cu^+} is the reaction rate constant that accounts for the effect of initial acid or copper concentration.

$K_{T,i}$ is the term that accounts for the effect of variations in the temperature. The effect of temperature is represented by the Arrhenius law, and may be written as:

$$K_{T,i} = A_i e^{\frac{-E_{a,i}}{RT}} \tag{8.19}$$

where A is the frequency factor of reaction (i), R is the gas constant and $E_{a,i}$ is the activation energy of the reaction (i).

Z is the term that accounts for the shrinking core leaching effect, and in this case applies to reactions where Ni alloy leaching takes place. This term is of the form (Rademan, 1995):

$$Z = \left(\frac{N_{Nialloy(t)}}{N_{Nialloy(t=0)}} \right)^{2/3} \tag{8.20}$$

where $N_{Ni\ alloy(t)}$ is the moles of the Ni alloy at time t, and $N_{Ni\ alloy(t=0)}$ is the initial moles of the alloy in the matte.

Table 8.1 Reaction rate constants used in the kinetic model

Process parameter		Reaction rate constant value				
		$K_{8.10}$	$K_{8.13}$	$K_{8.15}$	$K_{8.16}$	$K_{8.17}$
Temp. (°C)	60	0.298	0.679	0.0881	0.082	0.032
	80	1.728	0.979	o.0981	0.082	0.032
Stirring rate (rpm)	205	0.298	0.679	0.0881	0.082	0.032
	400	0.249	3.19	0.1109	2.02	0.032
Particle size (μm)	- 45	1.161	1.409	0.171	0.261	0.035
	-106+45	0.498	0.976	0.124	0.695	0.035
Initial acid (g/L)	90	0.298	0.679	0.0881	0.082	0.032
	125	0.173	1.532	0.086	-	0.024
Initial Cu (g/L)	25	0.298	0.679	0.0881	0.082	0.032
	48	0.0867	1.545	0.0881	0.082	0.032

8.4 Combined reaction expressions

The combined reaction rate expressions for the dissolution and formation of various species during the leaching process are represented by equations 8.21 - 8.31. These rate expressions were solved numerically by the 4th order Rung-Kutta method using the Excel spread sheet (see Appendix E), after values of the rate constants $K_{8.10}$, $K_{8.13}$, $K_{8.15}$, $K_{8.16}$ and $K_{8.17}$ were determined.

It should be noted that in the case of iron it was not possible to distinguish between Fe^{2+} and Fe^{3+}, hence they have been represented as total Fe concentration.

$$\frac{d\,Ni^{2+}}{dt} = \frac{8}{3}k_{8.10}C_{Cu^{2+}} + K_{8.13}C_{H^+} \tag{8.21}$$

$$\frac{d\,Cu^{2+}}{dt} = -\frac{8}{3}k_{8.10}C_{Cu^{2+}} \tag{8.22}$$

$$\frac{d\,Fe_{Total}}{dt} = -k_{8.15}C_{H^+} - K_{8.16}C_{Fe^{3+}} \tag{8.23}$$

$$\frac{d\,Co^{2+}}{dt} = k_{8.17}C_{H^+} \tag{8.24}$$

$$\frac{d\,H^{+}}{dt} = -2K_{8.13}C_{H^+} - 2K_{8.15}C_{H^+} + 3K_{8.16}C_{Fe^{3+}} - 2K_{8.17}C_{H^+} \tag{8.25}$$

$$\frac{d\,Ni^{o}}{dt} = -\frac{2}{3}K_{8.10}C_{Cu^{2+}} - K_{8.13}C_{H^+} \tag{8.26}$$

$$\frac{d\,Cu^{o}}{dt} = \frac{2}{3}K_{8.10}C_{Cu^{2+}} \tag{8.27}$$

$$\frac{d\,Cu_2S}{dt} = K_{8.10}C_{Cu^{2+}} \tag{8.28}$$

$$\frac{d\,Ni\,S}{dt} = K_{8.10}C_{Cu^{2+}} \tag{8.29}$$

$$\frac{d\,Fe^{o}}{dt} = -k_{8.15}C_{H^+} \tag{8.30}$$

$$\frac{d\,Co^{o}}{dt} = -k_{8.17}C_{H^+} \tag{8.31}$$

8.5 Evaluation of the kinetic model

The kinetic model was evaluated by comparing the model predictions to experimental data. The model was found to satisfactorily fit the trends in the leaching of the metals. Due to the fact that in most of the experiments only

solution samples were analysed for metal concentrations when determining the effect of variations in the leaching parameters, the accuracy of the model is mainly determined by how well its predictions fit the nickel, copper, cobalt, total iron and acid concentrations in the solution. It was not possible to analyse all the solid samples because of the difficult inherent in the analysis of large numbers of solid samples. The accuracy of analysis of solid samples was also a concern as the matte did not leach to a significant degree under the conditions employed in this study. Therefore, the rate of decrease and formation of solid species during the leaching of the matte were not evaluated. However, equations 8.26 – 8.31 could be used to predict the leaching and formation the solid species, since any transformation in the mineral phases are caused by the leaching process.

A comparison of the model predictions and experimental data for the dissolved species during the leaching process for different conditions is presented in Figures 8.1 - 8.7. It can be seen that the kinetic model was able to predict the leaching of the matte reasonably accurate. However, it should be mentioned that some of the model graphs could not fit the experimental data well probably due to the fact that a complex reaction mechanism takes place in the system where some metals dissolve and others precipitate. It is also understood that the model is basic and was indented to give a general trend in the leaching behaviour of the metals, and can be improved upon later.

8.6 Summary

A semi-empirical kinetic model was developed on the basis of the leaching mechanism and chemical reactions of the leaching system investigated. The kinetic model was evaluated by comparing the model predictions to experimental data. The model was found to satisfactorily fit the trends in the leaching of the metals.

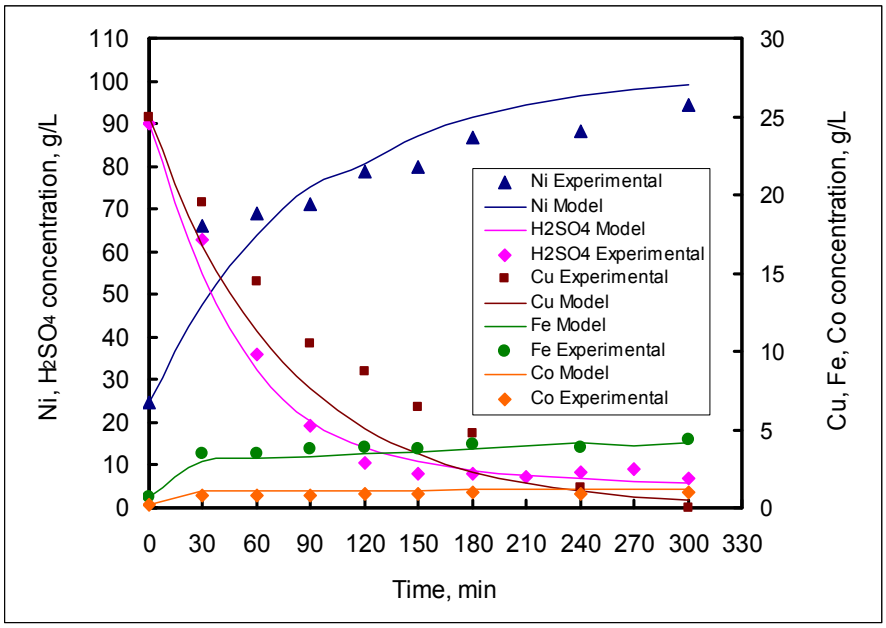

Figure 8.1: A comparison of the model predictions and experimental data for species in solution during the leaching of the matte at 60 ^{0}C (stirring rate: 205 rpm, pulp density: initial acid: 90 g/L, initial Cu: 25 g/L, Pulp density: 1.7 kg/L, residence time: 5 hours).

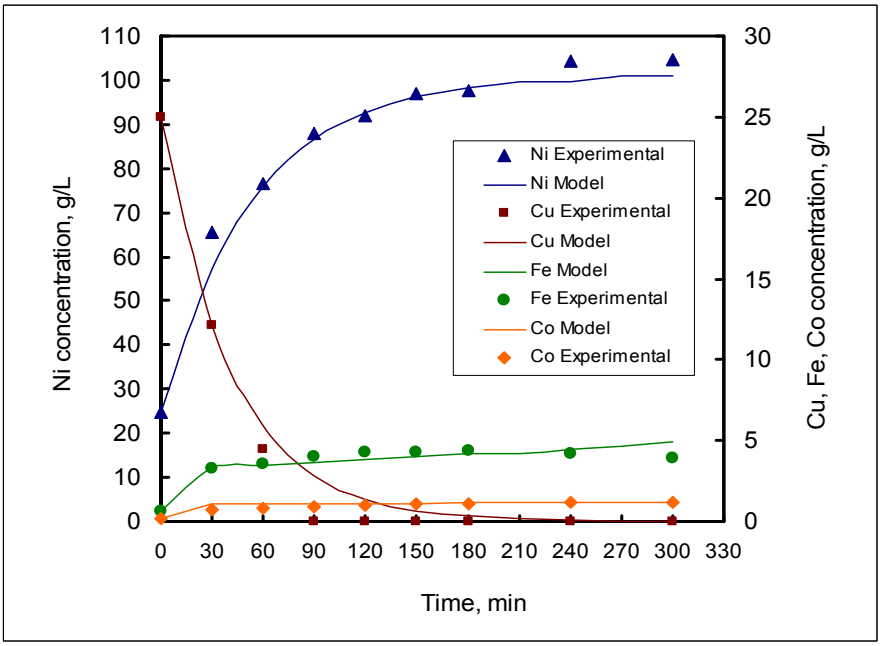

Figure 8.2: A comparison of the model predictions and experimental data for species in solution during the leaching of the matte at 80 ^{0}C (Stirring rate: 205 rpm, initial acid: 90 g/L, initial Cu: 25 g/L, pulp density: 1.7 kg/L, residence time: 5 hours).

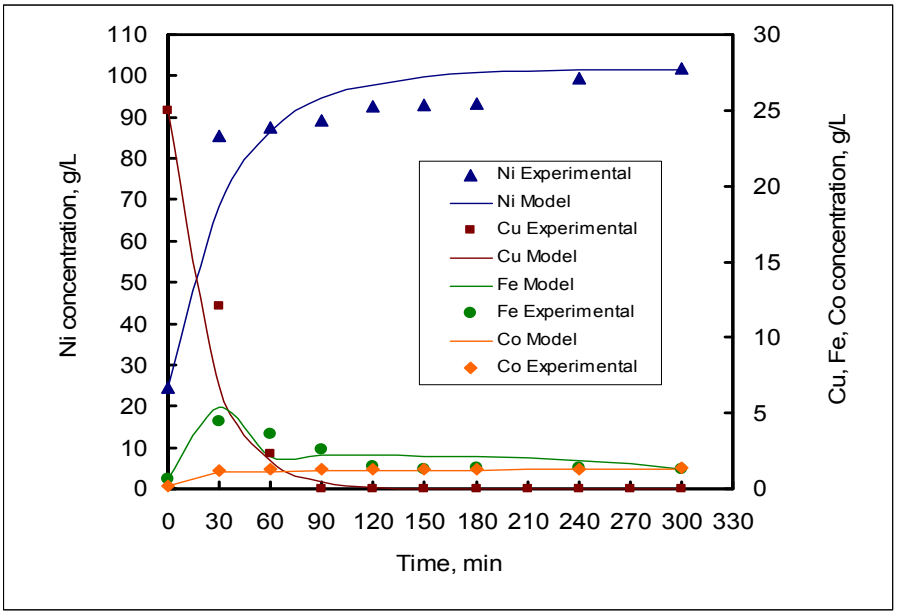

Figure 8.3: A comparison of the model predictions and experimental data for species in solution during the leaching of the matte at – 45 µm particle size (Temp.: 60 °C, stirring rate: 205 rpm, initial acid: 90 g/L, initial Cu: 25 g/L, pulp density: 1.7 kg/L, residence time: 5 hours).

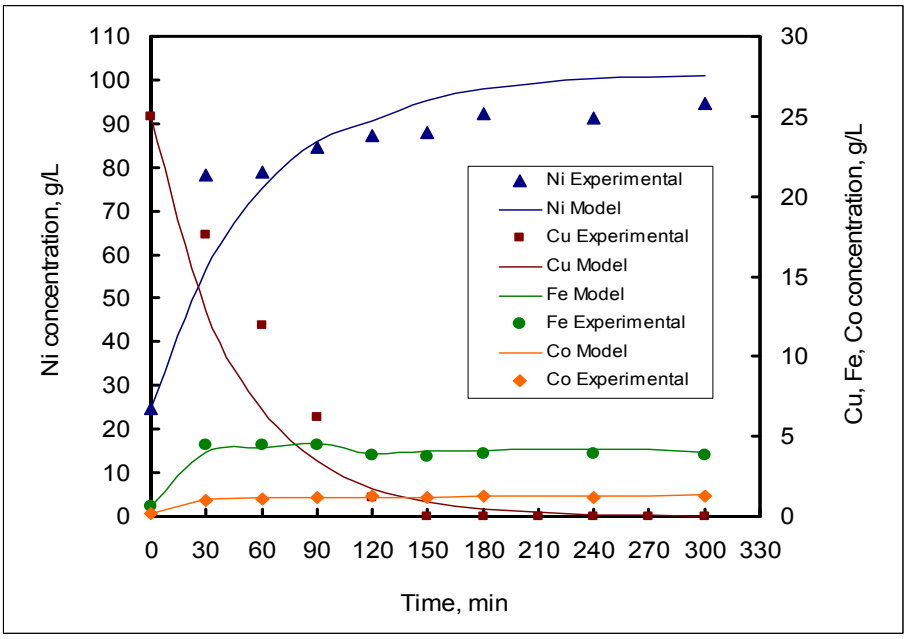

Figure 8.4: A comparison of the model predictions and experimental data for species in solution during the leaching of the matte at – 106+45 µm particle size (Temp.: 60 °C, stirring rate: 205 rpm, initial acid: 90 g/L, initial Cu: 25 g/L, pulp density: 1.7 kg/L, residence time: 5 hours).

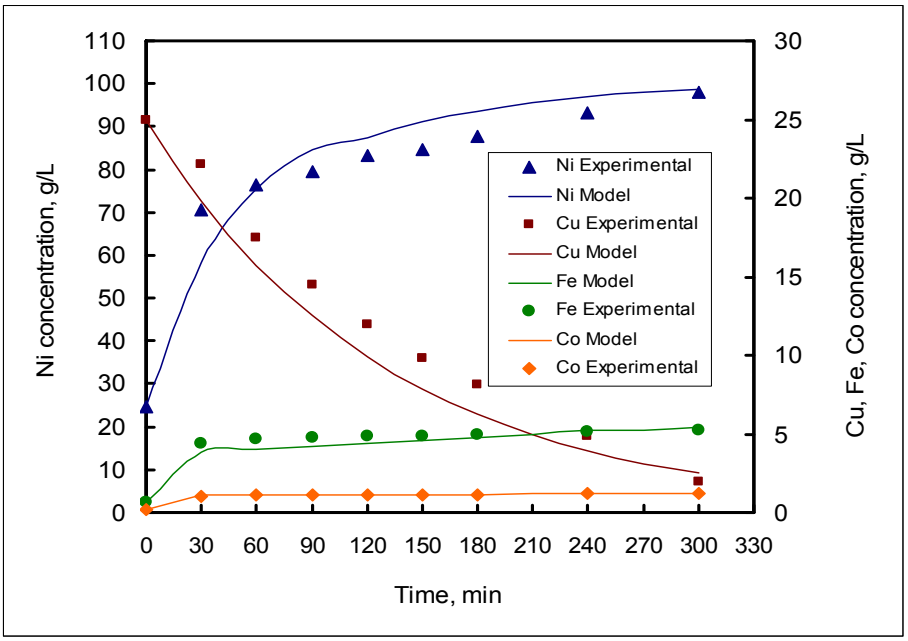

Figure 8.5: A comparison of the model predictions and experimental data for species in solution during the leaching of the matte at initial H_2SO_2 of 125g/L (Temp.: 60 °C, stirring rate: 205 rpm, initial Cu: 25 g/L, pulp density: 1.7 kg/L, residence time: 5 hours).

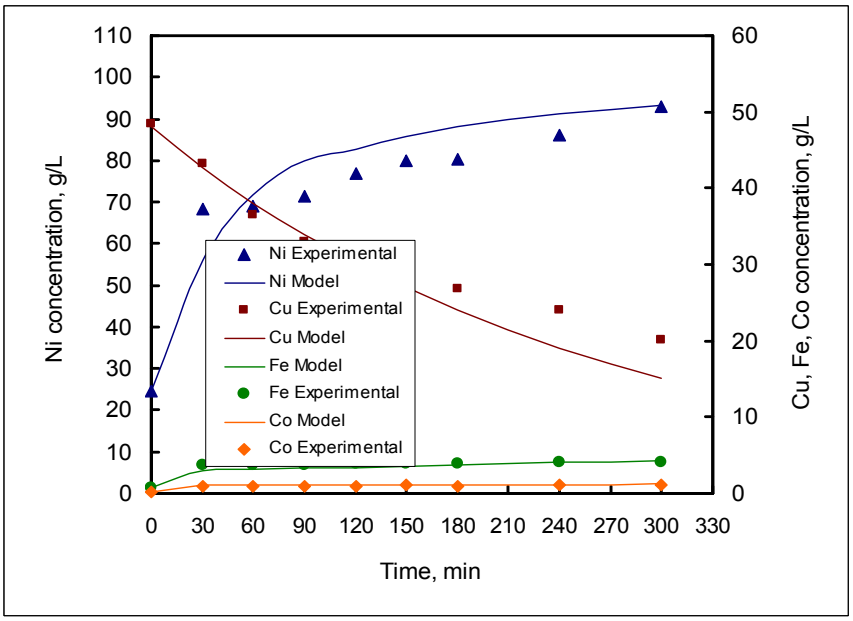

Figure 8.6: A comparison of the model predictions and experimental data for species in solution during the leaching of the matte at initial copper of 48 g/L (Temp.: 60 °C, stirring rate: 205 rpm, initial acid: 90 g/L, initial Cu: 25 g/L, pulp density: 1.7 kg/L, residence time: 5 hours).

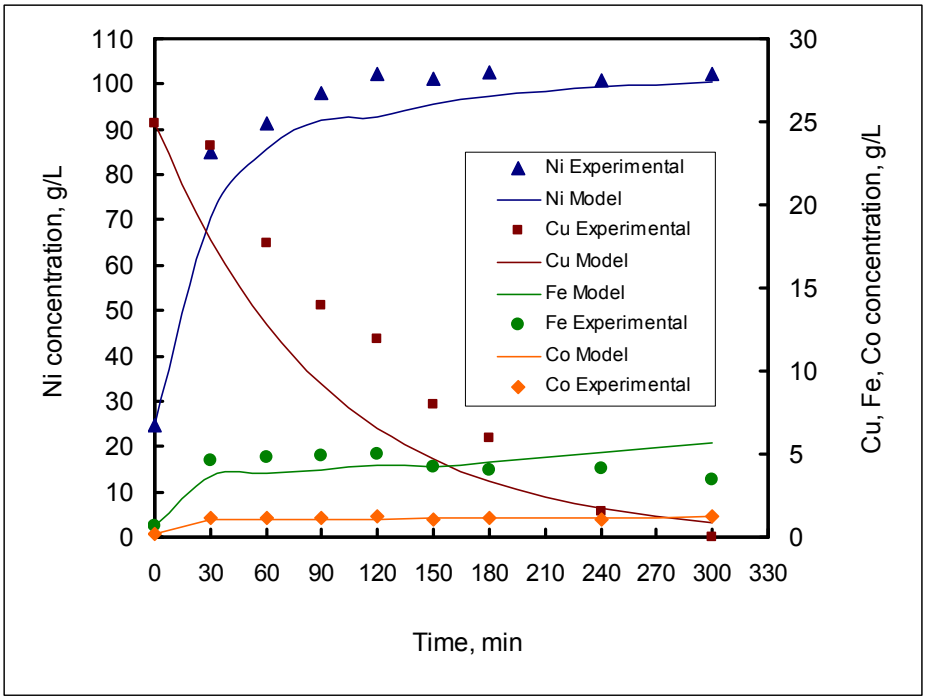

Figure 8.7: A comparison of the model predictions and experimental data for species in solution during the leaching of the matte at a stirring rate of 400 rpm (Temp.: 60 ^{o}C, acid: 90 g/L, initial acid: 90 g/L, initial Cu: 25 g/L, pulp density: 1.7 kg/L, residence time: 5 hours).

CHAPTER 9

9.0 CONCLUSIONS AND RECOMMENDATIONS

9.1 Conclusions

1) Atmospheric leaching experiments

Leaching behaviour of nickel-copper matte in H_2SO_4-$CuSO_4$ solution during the pre-leaching stage at Impala Base Metals Refinery has been studied to ascertain effects of variations in the key process variables such as temperature, stirring speed, particle size, pulp density, residence time, copper and acid concentrations. The leaching mechanism of the pre-leaching stage has been determined based on the mineralogical characterization and chemistry of the process. From the results obtained in the atmospheric leaching experiments, the following conclusions can be drawn:

1.1) Metal dissolution

- Potential - pH diagrams can be used to predict the thermodynamically stable species in the Ni-Cu matte-H_2SO_4 leaching system. The Eh-pH equilibrium diagrams showed that the possible thermodynamically stable species, under the investigated conditions (temperature 50 – 80 ^oC and pH <3) were Ni^{2+}, Cu^{2+}, Ni^o, Cu^o, Ni_3S_2 and Cu_2S. The species predicted by the Eh-pH diagrams were in agreement with the results obtained from the analysis of the leach solids and leach solutions.
- The leaching mechanism for the Ni-Cu matte entails dissolution of the metal alloy out of the matte particles without sulphide mineral disintegration. The nickel mineral sulphide (heazlewoodite) dissolves to

a lesser extent and transforms into millerite (NiS). Aqueous copper precipitates as metallic copper and as chalcocite.

- It was found that matte leaching occurs by the cementation process as well as direct attack by the acid. This is especially so in the early stages when the aqueous copper is still present. After the copper is completely precipitated, the leaching process occurs by direct reaction of the matte with the acid. This was supported by the sharp rise in the pH of the solution after the Cu^{2+} ions were precipitated.
- It has been postulated that because the Ni-Cu sulphide minerals and the Ni alloy are in intimate contact in the matte, they form a galvanic couple in which the Ni alloy has a lower rest potential and thus dissolve anodically. It is also possible that a galvanic couple between the copper and nickel sulphide minerals forms. In this case the nickel sulphide minerals dissolve anodically.
- The leaching kinetics of the matte can be characterized with the shrinking core model using Ni dissolution kinetics data. The Ni dissolution kinetics was characterized using the equation describing reaction controlled by diffusion through surface layer. An activation energy of 31 kJ/mol was obtained, which also suggested a diffusion controlled leaching reaction.
- It was found that increasing the temperature from 50 ^{o}C to 60 ^{o}C slightly increased nickel extraction; however no significant increase in nickel extraction was observed for temperatures above 60 ^{o}C, probably because the leaching process is diffusion controlled. The slight increase in nickel dissolution at higher temperatures (> 60 ^{o}C) may be attributed to the transformation of Ni_3S_2 to NiS, which is easier to leach. In the case of cobalt, no clear trend was observed as both the rate and degree of leaching appeared to be insensitive to temperature changes, only a slight increased at a higher temperature of 80 ^{o}C was noted. Relatively

low iron extraction was achieved (< 50 %) at 50 ^{o}C, but increased (> 65 %) when the temperature was raised to 60 - 80 ^{o}C.

- It was observed that nickel extraction was lower at the stirring rate of 145 rpm but increased gradually when the stirring rate was increased from 145 to 205 rpm and then to 400 rpm, probably due to increased mass transfer rate as the leaching process was found to be diffusion controlled. The leaching process was accompanied by transformation of Ni_3S_2 to NiS. In the case of cobalt and iron, the extractions increased significantly when the stirring rate increased from 145 to 205 - 400 rpm. At high pH of above 3 iron hydrolysed and subsequently precipitated.
- Nickel and cobalt extractions were not significantly affected by changes in the pulp density as only a slight increase in the extractions was observed when the density was reduced from 1.7 – 1.75 kg/L to 1.6 kg/L. On the other hand, iron extraction was higher at a pulp density of 1.6 kg/L but similar extraction rate was achieved at high pulp densities of 1.7 and 1.75 kg/L.
- It was found that nickel extraction was not significantly affected by changes in the particle size, probably because in all the three particle sizes the nickel alloy was liberated and hence exposed to the leaching solution. Cobalt extraction was similar to that of nickel, although cobalt extractions for the –45 μm and -106+45μm size fractions were relatively higher than that of the 300+150 μm size fraction. Iron extraction could not be determined accurately because of iron precipitation when the solution pH increased to above 3.
- Generally the leaching of the metals did not depend on initial copper concentrations in the investigated copper concentration range of 25 - 48 g/L. The rate of leaching as well as the degree of leaching was not significantly different for the three copper concentrations.

- It was observed that variations in the initial acid concentration did not have effect on nickel extraction. The observed leaching behaviour of nickel can probably be attributed to the fact that most of the nickel was leached by the process of cementation. Dissolution of the nickel by direct attack by acid was probably most prominent when the aquoues copper precipitated. However, cobalt and iron extractions increased when the acid increased from 90 g/L to 110 g/L, although further increase in the initial acid concentration had no effect on both cobalt and iron extraction.
- A residence time of 5 hours was found to be adequate as there was no significant increase in metal extractions when the residence time was increased beyond 5 hours.

1.2) Copper cementation

The kinetics of copper cementation onto Ni-Cu matte during the pre-leaching stage is influenced by process variables such as copper concentration, free acid concentration, temperature, particle size, and pulp density. Variations in the stirring rates appear to have little or no effect on the cementation kinetics, under the applied experimental conditions.

- It was found that the rate of copper cementation increased with increasing temperature. At 80 ^{o}C all the aqueous copper precipitated, whereas about 68% precipitated at a lower temperature of 50 ^{o}C. The cementation reaction followed a mixed control mechanism, with two distinct activation energies namely 18.2 kJ/mol at 70 – 80 ^{o}C and 74.6 kJ/mol at 50 – 70 ^{o}C. This suggested that the rate of cementation reaction was probably controlled by a boundary layer diffusion mechanism at higher temperatures. At low temperatures the rate was probably controlled by a surface reaction mechanism.

- The rate of copper cementation is not affected by variations in the stirring rate, under the investigated conditions, suggesting a chemical reaction controlled process as indicated by the activation energy (74.6 kJ/mol).
- It was noted that copper cementation increased as the pulp density increased from 1.6 to 1.7 kg/L and reached a maximum value at about 1.7 kg/L. Above the pulp density of 1.7 kg/L copper cementation did not appear to be influenced by increase in the pulp density. The increase in the rate of copper cementation when the pulp density was increased from 1.6 to 1.7 kg/L may be attributed to the increase in cathodic surface area of matte on which copper cementation takes place. At high pulp density values greater than 1.7kg/L low mass-transfer rates of reactants and products caused by the increase in the quantity of matte in the reaction mixture were probably responsible for slowing down the cementation process.
- Copper cementation increased with decreasing particles size, probably due to the increase in the surface area of fine particles. It was found that the rate of cementation was more sensitive to particle size in the last period of the cementation process for the finer size fractions (-45 μm and –106+45 μm). This was probably due to the changes in the matte particle morphology and lattice structure, which opened up and exposed more Ni surface area to the solution. The morphology and structure of the cemented particles may also have had an effect on the rate of cementation.
- The effect of initial copper concentration of the leaching solution was that the rate of copper cementation decreased with increase in the initial copper concentration, until a value of about 36 g/L was reached. Thereafter it became almost independent of the initial copper concentration. This behaviour can be attributed to changes in activity brought about by the increase in copper ion concentration, the rise in

solution viscosity and the decrease in the diffusivity of copper ions as a result of the increase of copper concentration in solution.

- It was found that copper cementation decreased with increase in the initial acid concentration up to a value of 110 g/L H_2SO_4, then copper cementation become almost insensitive to the acid concentration of the solution. The decrease in the rate of copper cementation with increasing acidity may be attributed to redissolution of some of the precipitated copper due to increase in the acidity of the solution.

- Aqueous copper can be precipitated from the leach solution within 90 minutes of the pre-leaching process, if the temperature is raised to 80 ^oC. However, under the present pre-leaching temperature of about 60 ^oC complete copper cementation can only be achieved after about 5 hours.

2) Pressure Leaching experiments

The pressure leaching experiments were aimed at investigating the response of atmospheric pre-leached matte to the subsequent pressure leaching process, as practiced at Impala's Base Metal Refinery. Thus, it was important to simulate the leaching conditions employed on the plant, especially those of the first stage pressure leach.

- Eh-pH diagrams were used to predict the thermodynamically stable species in the Ni-Cu matte – H_2SO_4 leaching system. The diagrams showed that the possible thermodynamically stable species in the leaching system under investigation were Ni^{2+}, Cu^{2+}, NiS, Ni_3S_2, Cu_2S and CuS. However, Cu^{2+} easily precipitated, and CuS was not formed in the leaching conditions employed. In general, the species predicted by the Eh-pH diagrams were in agreement with what was observed in the leach samples.

- It was found that nickel leaching behaviour was similar for the matte pre-leached at 50, 60 and 80 ^{o}C as similar leaching rates were observed during the pressure leaching stage. For matte pre-leached at 60 and 80 ^{o}C, heazlewoodite (Ni_3S_2) transformed into millerite (NiS) which is easier to leach in the subsequent pressure leach stage; no NiS was formed in the test conducted at 50 ^{o}C. However, because of the conditions prevailing in the pressure leaching stage, nickel was leached at the same rate regardless of the temperature at which the matte was pre-leached.
- It was found that the rate of nickel extraction was similar for the investigated stirring rates of 145, 205 and 400 rpm. At higher stirring rates of 205 and 400 rpm heazlewoodite (Ni_3S_2) transformed into millerite (NiS) which is earsier to leach, and no millerite formed in the experiment conducted at 145 rpm. However, as indicated above, because of the aggressive conditions prevailing in the pressure leaching stage, all the nickel minerals were leached at about the same rate.
- In the case of pulp density, it was found that nickel extraction was comparable for all the investigated pulp densities of the pre-leach stage. This was probably due to the fact that the degree of mineral transformation in the pre-leach stage was similar for the investigated pulp densities of 1.6, 1.7 and 1.75 kg/L. For all three pulp densities the heazlewoodite transformed to millerite. The conditions prevailing in the pressure leaching stage allowed all the nickel minerals to be leached at about the same rate regardless of the pulp density at which the matte was pre-leached.
- Residence time of the pre-leaching stage had an effect on the nickel extraction in the pressure leaching stage. The nickel extraction increased with increasing residence time, due to the changes in the mineral phases of the matte as indicated above.

- The copper minerals (Cu_2S and $Cu_{1.96}S$) transformed into Cu_2S and $Cu_{1.8}S$ with aqueous copper being precipitated, and were not leached under the applied conditions. All the cobalt and iron dissolved in the pressure leaching stage.

3) Kinetic Model

A semi-empirical kinetic model was developed on the basis of the leaching mechanism and chemical reactions of the leaching system investigated. The model makes allowance for variations in the values of the leaching parameters such as initial copper concentration, temperature, particle size and initial acid concentration. Under the leaching conditions employed in this study (where no oxidant was added) the sulphide minerals were not expected to leach to a significant degree. Therefore, the chemical reactions considered in the model are those that are most likely to occur to a significant degree during the leaching process. The kinetic model was evaluated by comparing the model predictions to experimental data. A comparison of the model predictions and the experimental data for the dissolved species during the leaching process showed that the model was able to satisfactorily fit the trends in the leaching of the metals.

9.2 Recommendations

- The findings of this study can be utilized to understand better the impact of conditions prevailing in the pre-leaching stage on the subsequent pressure leaching stage. In particular the nickel sulphide mineral transformations that take place in the pre-leaching stage, which may affect the rate of nickel dissolution in the pressure leaching stage.
- The findings on the behaviour of the copper cementation process can be of use in controlling copper levels in the copper cementantion section at

Impala Base Metals Refinery. In this plant the residual copper is removed from the nickel rich solution by cementation with matte, $NiSO_4$ powder or NaHS.

- The galvanic interaction between the mineral species of the matte can be investigated to quantify its influence on the degree and rate of base metal leaching.
- The rate of decrease and formation of solid species during the pre-leaching of the matte were not evaluated by the semi-empirical kinetic model, this may be worth considering if more tests were to be done on the pre-leaching process. Furthermore, the model can be improved upon so as to increase the accuracy of the predictions.
- It may be worthwhile to conduct more tests to measure the redox potential of the investigated leaching system in order to establish more accurate potential-pH diagrams (Pourbaix diagrams) of the species that may be thermodynamically stable in the leaching system investigated in this study.
- Future work should consider conducting factorial design experiments. This will help in determining the interrelationships between variables, which can help in modelling studies.

REFERENCES

Adam, K., Natarajan, K.A. and Iwasaki, I., 1984. Grinding media wear and its effect on the flotation of sulphide minerals. *International Journal of Mineral Processing*, 12, pp. 39-54.

Addy, s and Fletcher, A.J., 1987. The deposition of cobalt on iron powder by means of the cementation reaction. *Hydrometallurgy,* 17, 1987, pp. 269 – 280.

Ahmed, I.B., Gbor P.K. and Jia, C.Q., 2000. Aqueous sulphur dioxide leaching of Cu, Ni, Co, Zn and Fe from smelter slag in absence of oxygen. The *Canadian Journal of Chemical Engineering,* vol. 78, pp. 694 – 703.

Alcock, C.B., 1976. *Principles of pyrometallurgy*. Academic Press, London, 348 pp.

Annamalai, V. and Murr, L.E., 1979. Influence of deposit morphology on the kinetics of copper cementation on pure iron. *Hydrometallurgy,* 4, pp. 57 – 82.

Annamalai, V. and Hiskey, J.B., 1978. A kinetic study of copper cementation on pure aluminum. *Society of Mining Engineers*, pp. 650 – 659.

Anacleto, A.L. and Carvalho, R.J., 1996. Mercury cementation from chloride solutions using iron, zinc and aluminium. *Minerals Engineering*, vol 9, No.4, pp. 385 – 397.

Anonymous, 1981. Matthey Rustenburg Refiners. *Journal of SAIMM*, October, pp 11-14.

Barton, P.B. Jr, 1973. Solid solutions in the system Cu-Fe-S. Part I: The Cu-S and CuFe-S joins. *Economic Geology*, Vol 68, pp 455 – 465.

Berezowsky, R., 2003. Impala Platinum Limited, Base Metals Refinery, Review of process chemistry and mineralogy. *Dynatec Corporation, Metallurgical Technologies Division*, Fort Saskatchewan, Alberta, Canada, unpublished.

Berry, V.K., Murr, L.E. and Hiskey, J.B., 1978. Galvanic interaction between chalcopyrite and pyrite during bacterial leaching of low-grade waste. *Hydrometallurgy,* 3, pp. 309 – 326.

Biswas, A.K. and Davenport, W.G., 1976. *Extractive Metallurgy of Copper*. Pergamon Press, Oxford, pp. 80 – 155.

Boerst, K.D., 2001**.** *Geochemistry of the Merensky reef on Impala platinum mine, Western bushveld complex*. MSc Thesis, University of the Witwatersrand, South Africa, pp 1-19.

Boldt, J.R. Jr. and Queneau, P., 1967a. *The Winning of Nickel: Its Geology, Mining and Extractive Metallurgy*. Methuen and Co. Ltd, London, pp. 299 - 314.

Boldt, J.R. Jr. and Queneau, P., 1967b. *The winning of nickel: Its geology, mining and extractive metallurgy*. Methuen and Co. Ltd, London, pp. 228 – 288.

Brynard, H.J., de Villiers, J.P.R. and Viljoen, E.A., 1976. A mineralogical investigation of the Merensky Reef at the Western Platinum Mine, near Marikana, South Africa. *Economic Geology*, Vol. 71, pp 1299 – 1307.

Bryson, M.A.W, 2004a. Mineralogical control of minerals processing circuit design. *Journal of SAIMM*, vol. 104, No.6, July, pp 307-310.

Bryson, M.A.W, 2004b. New technologies in the concentration of PGM values from UG-2 ores. *Journal of SAIMM*, vol. 104, No.6, July, pp 311-313.

Brugman, C.F., and Kerfoot, D.G., 1986. Traetment of nickel-copper matte at Western Platinum by the Sherritt Acid Leach Process. In: *Proceedings of Nickel Metallurgy*, Vol. I, Extraction and Refining of Nickel. Ed. Ozberk, E. and Marcuson, S.W. CIM, August, Toronto, pp. 512 - 531.

Burkin, A.R., 1987. *Extractive Metallurgy of Nickel*. John Wiley & Sons, Chichester, pp. 99 – 113.

Burkin, A.R., 1966. *The Chemistry of Hydrometallurgical Processes*. E. & F.N. Spon Ltd, London, 157 pp.

Cabri, L.J., 1981. Relationship of Mineralogy to the recovery of Platinum-group elements from ores. In: Platinum-Group Elements: Mineralogy, Geology, Recovery, CIM special volume 23,. Ed. Cabri, L.J. *The Canadian Institute of Mining and Metallurgy,* pp. 233 – 249.

Celmer, R.S., Kaiura, G.H. and Toguri, J.M., 1987. Chemical reactions during the electric smelting of nickel-copper calcines. *Canadian Metallurgical Quarterly*, vol. 26, No. 4, pp. 277 - 284

Corrans, L.J., Dunne, R.C. and Allison, S.A., 1982. The recovery of platinum-group metals from the chromite reefs of the Bushveld Complex. *XIV International Mineral Processing Congress*, Toronto. CIM, October, pp. II-10.1 – II-10.21.

Colussi, I, Meriani, S. and Monte, U., 1983. Kinetic models for the leaching with sulphuric acid of zinc-containing slag. *Hydrometallurgy*, 10, pp. 61 – 67.

Colak, S., Alkan, M. and Kocakerim, M.M., 1987. Dissolution kinetics of chalcopyrite containing pyrite in water saturated with chlorine. *Hydrometallurgy*, 18, pp. 183 – 193.

Corrans, L.J. and Scholtz, M.T., 1976. A kinetic study of the leaching of pentlandite in acidic ferric sulphate solutions. *Journal of SAIMM*, May, pp. 403 - 411.

Crundwell, F.K. and Verbaan, B., 1987. Kinetics and mechanism of the non-oxidative dissolution of sphalerite (zinc sulphide). *Hydrometallurgy*, 17, pp. 369 – 384.

Deers, W.A., Howie, R.A. and Zussman, J., 1978. *Rock-forming minerals, vol. 2A, single-chain silicates*. Longman, 668 pp.

Donmez, B., Sevim, F. and Sarac, H., 1999. A kinetic study of the cementation of copper from sulphate solutions onto a rotating aluminium disc. *Hydrometallurgy*, 53, pp. 145 – 154.

Dry, M.J. and Bryson, A.W., 1987. Kinetics of leaching of a low-grade Fe-Ni-Cu-Co matte I ferric sulphate solution. *Hydrometallurgy*, 18, pp. 155 – 181.

Dutrizac, J.E. and Chen, T.T., 1987. A mineralogical study of the phases formed during the $CuSO_4$-H_2SO_4-O_2 leaching of nickel-copper matte. *Canadian Metallurgical Quarterly*, Vol. 26 (4), pp.265-276.

Dutrizac, J.E. and Chen, T.T., 1995. The leaching of galena in ferric sulphate media. *Metallurgical and Materials Transactions B*, vol. 26B, April, pp. 219 – 227.

Edwards, R.I., 1976. Refining of the platinum-group metals. *Journal of Metals*, August, pp 4 – 9.

Edwards, R.I., 1984. Metallurgical flowsheet II. The treatment of Merensky Reef ore – a complex metallurgical flowsheet. In: Metallurgy for geologists. *Mineralogical Association of South africa*, Johannesburg, pp 365 – 379.

Ferreira, R.C.H., 1975. High-temperature E-pH diagrams for the systems S-H_2O, Cu-S-H_2O and Fe-S-H_2O. In: Leaching and reduction in hydrometallurgy, Ed. Burkin, A.R. *The Institute of Mining and Metallurgy*, London, pp. 67- 83.

Filmer, A.O., 1981. The non-oxidative dissolution of nickel mattes in aqueous acidic solution. *Journal of SAIMM*, March, pp.74-84.

Filippou, D. and Demopoulos, G.P., 1992. A reaction kinetic model for the leaching of industrial zinc ferrite particulates in sulphuric acid media. *Canadian Metallurgical Quarterly,* vol 31, No. 1, pp. 41 – 54.

Forbes, P.B.C., 1999. *The use of life cycle assessment in the evaluation of environmental performance in the base metal refining industry*. MSc Dissertation, University of Cape Town, South Africa.

Fogler, H. S., 1986. *Elements of Chemical Reaction engineering*. Prentice-Hall, Inc., New Jersey, 769 pp.

Fugleberg, S., Hultholm, S.E., Rosenback, L. and Holohan, T., 1995. Development of the Hartley Platinum leaching process. Hydrometallurgy, 39, pp.1-10.

Gbor, P.K, Ahmed, I.B., and Jia, C.Q., 2000. Behaviour of Co and Ni during aqueous sulphur dioxide leaching of nickel smelter slag. *Hydrometallurgy*, 57, pp. 13 - 22.

Green, B.R., Smit, D.M.C., Maumela H. and Coetzer,G., 2004; Leaching and recovery of platinum group metals from UG-2 concentrates, *Journal of SAIMM*, vol. 104, No.6, July, pp 323-331.

Herreros, O. Quiroz, R. Hernandez, M.C. and Vinals, J., 2002. Dissolution kinetics of enargite in dilute Cl_2/Cl^- media. *Hydrometallurgy*, 64, pp. 153- 160.

Hiskey, J.B. and Wadsworth, M.E., 1981. Electrochemical processes in the leaching of metal sulphides and oxides. In: Process and fundamental considerations of selected hydrometallurgical systems. Ed. Kuhn, M.C. Society of Mining Engineers of *American Institute of Mining, Metallurgical, and Petroleum Engineers*, New York, pp. 359-369

Hochreiter, R.C., Kennedy, D.C., Muir, W. and Woods, A.I., 1985. Platinum in South Africa (Metal review series no. 3). *Journal of SAIMM*, vol. 85, No.6, June, pp 165-185.

Hofirek, Z. and Kerfoot, D.G.E., 1992. The chemistry of the nickel-copper matte leach and its application to process control and optimisation. *Hydrometallurgy*, 29, pp. 357-381.

Hofirek, Z. and Nofal, P.J, 1995. Pressure leach capacity expansion using oxygen-enriched air at RBMR (Pty) Ltd. *Hydrometallurgy*, 39, pp. 91-116.

Hofirek, Z. and Halton, P., 1990. Production of high quality electrowon nickel at Rustenburg Base Metals Refiners (Pty) Ltd. In: *Electrometallurgical Plant Practice*, Ed. Claessens, P.L and Harris G.B. New York, pp. 233 - 251.

Holmes, P.R. and Crundwell, F.K., 1995. Kinetic aspects of galvanic interactions between minerals during dissolution. *Hydrometallurgy*, 39, pp. 353- 375.

Hsu, Y.J. and Tran, T., 1996. Selective removal of gold from copper-gold cyanide liquors by cementation using zinc. *Minerals Engineering*, vol 9, No.1, pp. 1 – 13.

Hulbert, L.J. and von Gruenewaldt, G., 1982. Nickel, copper and platinum mineralization in the lower zone of the Bushveld Complex, south of Potgietersrus. *Economic Geology*, vol. 77, pp. 1296 – 1306.

Impala reports, 2003 – 2005, Weekly feedback reports on production, Impala platinum refineries, Johannesburg, unpublished.

Jayasekera, S., 1995. Pressure leaching of reduced ilmenite: electrochemical aspects. *Hydrometallurgy*, 39, pp. 183 -199.

Kellogg, H.H., 1986. Thermochemistry of nickel-matte converting. In: Proceedings of Nickel Metallurgy, Vol. I, Extraction and Refining of Nickel. Ed. Ozberk, E. and Marcuson, S.W. CIM, August, Toronto, pp. 95 - 128.

Kinloch, E.D., 1982. Regional trends in the platinum-group mineralogy of the critical Zone of the Bushveld Complex, South Africa. *Economic Geology*, vol. 77, pp. 1328 – 1347.

Kingston, G.A. and El-Dosuky, B.T., 1982. A contribution on the platinum-group mineralogy of the Merensky Reef at the Rustenburg Platinum Mine. *Economic Geology*, vol. 77, pp. 1367 – 1384.

Knuutila, K. Hultholm, S. Saxen, B. and Rosenback, L., 1997. New nickel process increasing production at Outokumpu harjavalta Metals Oy, Finland. *ALTA Nickel/Cobalt Pressure Leaching & Hydrometallurgy Forum*, Perth. W. Australia.

Levenspiel, O., 1972. *Chemical Reaction Engineering*. John Wiley & Sons, New York, 578 pp.

Lindsay, N.M., 1988. *The processing and recovery of the Platinum-group elements*. PhD Thesis, University of the Witwatersrand, Johannesburg, South Africa, pp. 9 – 59.

Long, H. and Dixon, D.G., 2004. Pressure oxidation of pyrite in sulphuric acid media: a kinetic study. *Hydrometallurgy*, 73, pp. 335 - 349.

Lorenzen, L. and van Deventer, J.S.J., 1992. Electrochemical interactions between gold and its associated minerals during cyanidation. *Hydrometallurgy*, 30, pp. 177 - 194.

Llanos, Z.R., Queneau, P.B. and Rickard, R.S., 1974. Atmospheric Leaching of

Matte at the Port Nickel Refinery. *CIM Bulletin*, 64, pp. 74-81.

Ma, Z. and Ek, C., 1991. Rate processes and mathematical modeling of the acid leaching of a manganese carbonate ore. *Hydrometallurgy*, 27, pp. 125 - 139.

MacKinnon, D.J., Ingraham, T.R. and Kerby, R., 1971. Copper cementation on nickel discs. *Canadian Metallurgical Quarterly*, Vol. 10, no. 3, pp 165 - 169.

Mashanyane. H.S. and Storey, M.J., 1986. Problems associated with the processing of nickel ores. In: Proceedings of Nickel Metallurgy, Vol. I, Extraction and Refining of Nickel. Ed. Ozberk, E. and Marcuson, S.W. *CIM*, August, Toronto pp. 13-35.

McLaren, C.H., 1978. A mineralogical investigation of the platinum-group minerals in the UG-2 layer of the Bushveld Complex with special reference to the recovery of the minerals from the ores. *Metals and Minerals Processing*, vol, pp. 19 – 27.

McLaren, C.H. and De Villiers, J.P.R., 1982. The platinum-group chemistry and mineralogy of the UG-2 chromitite layer of the Bushveld Complex. Economic Geology, vol. 77, pp. 1348 – 1366.

McKinnon, D.J. and Ingraham, T.R., 1970. Kinetics of Cu(II) cementation on a pure aluminum disc in acidic sulphate solution. *Canadian Metallurgical Quarterly*, Vol. 9, no. 3, pp. 443- 448.

Mostert, A.B., Hofmeyer, P.K. and Potgieter, G.A., 1982. The platinum-group mineralogy of the Merensky Reef at the Impala Platinum Mines, Bophuthatswana. *Economic Geology*, vol. 77, pp. 1385 – 1394.

Mostert, J.C. and Roberts, P.N., 1973. Electric smelting at Rustenburg Platinum Mines Limited of nickel-copper concentrates containing platinum-group metals. *Journal of SAIMM*, April, pp 290-299.

Mulak, W., 1987. The catalytic action of cupric and ferric ions in nitric acid leaching of Ni_3S_2. *Hydrometallurgy*, 17, pp. 201 - 214

Mulak, W., 1985. Kinetics of dissolution of synthetic heazlewoodite (Ni3S2) in nitric acid solutions. *Hydrometallurgy*, 14, pp. 67 - 81.

Nagamori, M., 1974. Metal loss to slag I.Sulfidic and oxidic dissolution of copper in Fayalite slag from low grade matte. *Metallurgical Transactions*, vol. 5, March, pp.531 – 538.

Nadkarni, R.M., Jelden, C.E., Bowles, K.C., Flanders, H.E. and Wadsworth, M.E. A , 1967. kinetic study of copper precipitation on iron – Part I. *Transactions of the Metallurgical Society of AIME***,** Vol. 239, pp. 581-585.

Naldrett, A.J., 1981. Platinum-group elements deposits. In: Platinum-Group Elements: Mineralogy, Geology, Recovery, CIM special volume 23,. Ed. Cabri, L.J. *The Canadian Institute of Mining and Metallurgy*, pp. 197 – 231.

Newman, S.C., 1973. Platinum. *Bulletin of Institute of Mining and Metallurgy* (6B), vol 82, Sect. A, pp. 52 – 68.

Nicol, M.J., Needs, C.R.S. and Finkelstein, 1975. Electrochemical model for the leaching of uranium dioxide: 1 – acid media. In: Leaching and reduction in hydrometallurgy. Ed. Burkin, A.R. *The Institute of Mining and Metallurgy*, London, pp. 1 – 11.

Nicol, M.J., 1984. An electrochemical study of the interaction of copper (II) ions with sulphide minerals. *Electrochemistry in mineral and metal processing* (Proceedings of the international Symposium). Ed. Richardson, P.E., Srinivasan, S. and Woods, R. The Electrochemical Society, Inc., 152 – 168.

Nyman, B., Aaltonen, A., Hultholm, E.S. and Karpale, K., 1992. Application of new hydrometallurgical developments in the Outokumpu HIKO process. *Hydrometallurgy*, 29, pp. 461 - 478.

Osseo-Asare, K. and Fuerstenau, D.W., 1978. Application of activity-activity diagrams to ammonia hydrometallurgy: The systems Cu-NH_3-H_2O, Ni-NH_3-H_2O, Co-NH_3-H_2O at 25 oC. Fundamental Aspects of Hydrometallurgical processes. Ed. Chapman, T.W., et al . *AIChE Symposium series*, vol. 74, No. 173, pp. 1 – 13.

Osseo-Asare, K., (1981). Application of activity-activity diagrams to ammonia hydrometallurgy II. The copper-, nickel-, cobalt-ammonia-water systems at elevated temperatures. In: Process and fundamental considerations of selected hydrometallurgical systems. Ed. Kuhn, M.C. Society of Mining Engineers of

American Institute of Mining, Metallurgical, and Petroleum Engineers, New York, pp. 359-369

Paul, R.L., Nicol, M.J., Diggle, J.W. and Saunders, A.P., 1978. The electrochemical behaviour of galena (lead sulphide)- I. Anodic dissolution. *Electrochimica Acta*, vol. 23, pp. 625 – 633.

Peyerl, W., 1983. The metallurgical implications of the mode of occurrence of platinum-group metals in the Merensky Reef and UG-2 chromitite of the Bushveld Complex. *Geological Society of South Africa*, special publication, 7, pp. 295 – 300.

Plasket, R.P. and Dunn, G.M., 1986a. Iron rejection and impurity removal from nickel leach liquor at Impala Platinum Limited. In: *Iron control in hydrometallurgy*. Ed. Dutrizac, J.E. and Monhemiums, A.J. Ellis Horwood Limited, Chichester, pp. 695 - 718.

Plasket, R.P. and Dunn, G.M., 1986b. Commissioning experiences in the cobalt plant at Impala Platinum Ltd. *Minerals and Metallurgical Processing*, February, pp. 7 – 14.

Plasket, R.P. and Romanchuk, S., 1978. Recovery of nickel and copper from high-grade matte at Impala Platinum by the Sherritt process. *Hydrometallurgy*, 3, pp. 135-151.

Pourbaix, M., 1966. Atlas of Electrochemical Equilibria in Aqueous Solutions. Pergamon press, Oxford, 644 pp.

Puvvada, G. and Tran, T., 1995. The cementation of Ag (I) ions from sodium chloride solutions onto a rotating copper disc. *Hydrometallurgy*, 37, pp. 193-205.

Provis, J.L., van Deventer, J.S.J., Rademan, J.A.M. and Lorenzen, L., 2003. A kinetic model for the acid-oxygen pressure leaching of Ni-Cu matte. *Hydrometallurgy*, 70, pp. 83 - 99.

Rademan, J.A.M., Lorenzen, L. and van Deventer, J.S.J., 1999. The leaching Characteristics of Ni-Cu matte in the acid-oxygen pressure leach process at Impala platinum. *Hydrometallurgy*, 52, pp. 231-252.

Raschman, p., 2000. Leaching of calcined magnesite using ammonium chloride at constant pH. *Hydrometallurgy*, 56, pp. 109 - 123

Rademan, J.A.M., (1995). *The simulation of a transient leaching circuit*, PhD Dissertation, University of stellenbosch, South Africa, 423 pp.

Reddy, P.L.N., Venkatachalam, S. and Mallikarjunan, R., 1987. Electrochemical dissolution of a chalcopyrite concentrate. In: Proceedings of the *International Symposium on Electrochemistry in Mineral and Metal processing*. Ed. Richardson, P.E., Srinivasan, S. and Woods, R. The Electrochemical Society, pp. 447-468.

Robiette, A.G.E, 1973. *Electric smelting processes*. Charles Griffin & Company Limited, London, pp. 203 - 233.

Roine, A., 2002. *Outokump HSC Chemistry 5.11*. Outokumpu Research Oy, Pori, Finland.

Rosenqvist, T., 1974. *Principles of Extractive Metallurgy*. McGraw-Hill, Tokyo, pp. 354 – 373.

Sato, T. and Lawson, F., 1983, Dfferential leaching of some lead smelter slags with sulfurous acid and oxygen. *Hydrometallurgy*, 11, pp. 371 - 388.

Sahoo, P.K. and Srinivasa, K., 1982. Cementation of copper from complex sulphide leach liquor. *Hydrometallurgy*, 8, pp. 223 - 229.

Schwellnus, J.S.I., Hiemstra, S.A. and Gasparrini, E., 1976. The Merensky Reef at the Atok Platinum Mine and its environs. *Economic Geology*, vol. 71, pp. 249 – 260.

Sharpe, M. R., 1982. Noble metals in the marginal rocks of the Bushveld Complex**.** *Economic Geology*, Vol 77, pp 1286 – 1295.

Southwood, M.J. 1985. The acid leaching of nickel and copper from sulphidic ore in the presence of pyrite. *Journal of SAIMM*, vol. 85, No.11, November, pp 395-401.

Spandiel, T., 1996. The chemistry of Impala base metal refining operations and its application to modelling and simulation, *discussion document* (confidential), unpublished.

Sohn, H. Y. and Wadsworth, M. E., 1979. *Rate Processees of Extractive Metallurgy*. Plenum Press, New York, pp. 1 – 51.

Steenekamp, N. and Dunn, M.G., 1999. Operations of and improvements to the Lonrho Platinum Base Metal refinery. *EPD Congress*, Ed. Mishra, B., pp. 365-378.

Symens, R.D., Queneau, P.B., Chou, E.C. and Clark, F.F., 1979. Leaching of iron-containing copper-nickel matte at atmospheric pressure. *Canadian Metallurgical Quarterly*, Vol. 18, pp.145-153.

Szekely, J., Evans, J.W. and Sohn, H.Y., 1976. *Gas-Solid Reactions*. Academic Press, New York, pp. 109 -125.

Terry, B., 1987. Pyrometallurgy of sulphide ores of nickel to finished metal or mattes. Extractive Metallurgy of Nickel. Ed. Burkin, A.R., Critical reports on applied chemistry, vol. 17, *Society of Chemical Industry*, John Wiley & Sons, Chichester, 150 pp.

Vermaak, C.F. and Hendriks, L.P., 1976. A review of the mineralogy of the Merensky Reef, with specific reference to new data on the precious metal mineralogy. *Economic Geology*, vol. 71, pp. 1244 – 1269.

Von Gruenewaldt, G., 1977. The mineral resources of the Bushveld complex. *Minerals Science Engineering*, vol. 9, no. 2, April, pp 83 - 95

Wagner, P.A., 1973. *The Platinum Deposits and Mines of South Africa*. C. Struik (Pty) Ltd, Cape Town, 338 pp.

Webb, P.A. and Orr, C., 1997. Analytical Methods in Fine Particle Technology. *Micromeritics Instrument Corporation*, Norcross,USA, PP. 53 – 153.

Youzbashi, A.A. and Dixit, S.G., 1991. Leaching of nickel from supported nickel waste catalyst using aqueous sulphur dioxide solution. *Metallurgical Transactions B*, vol. 22B, December, pp. 775 – 781.

Yu, P.H., Hansen, C.K. and Wadsworth, M.E., 1973. A kinetic study of the leaching of chalcopyrite at elevated temperatures. In: *Proceedings of 2nd International Symposium on hydrometallurgy,* Ed. Evans, D.J.I. AIME, New York, pp. 375 – 402.

Yuhua, Y., and Xianxuan, M., 1990. Operating practice and technical developments in nickel refining and cobalt recovery at Jinchuan non-ferrous metal company. In: *Electrometallurgical plant practice*, Ed. Claessens, P.L. and Harris, G.B, Pergamon, New York, pp. 253 – 268.

TABLE A1.7: METAL SOLUTION CONCENTRATIONS DURING ATMOSPHERIC LEACHING OF THE MATTE AT A TEMPERATURE OF 80 ^{O} C

Leaching conditions:

Temperature:	80 ^{o}C
Agitation:	205 rpm
Pulp density:	1.7 kg/L

Leaching Time (min)	Co (g/l)	Fe (g/l)	Ni (g/l)	Cu (g/l)	pH
0	0.18	0.67	24.61	24.95	0.051
15	0.68	3.04	58.34	16.06	0.241
30	0.76	3.32	65.58	12.16	0.38
60	0.83	3.58	76.59	4.44	1.17
90	0.94	4.03	87.97	0.00	1.35
120	1.00	4.25	91.86	0.00	1.82
150	1.07	4.33	97.00	0.00	2.44
180	1.09	4.39	97.73	0.00	3.24
240	1.16	4.15	104.17	0.00	3.65
300	1.21	3.96	104.59	0.00	4.79

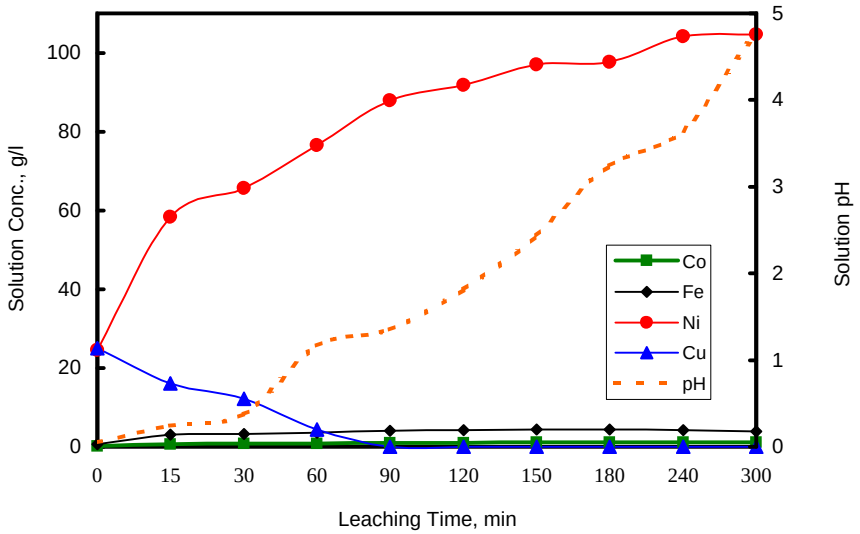

Fig. A1.7: Metal concentration as a function of leaching time at 80^{o}C.

TABLE A1.8: METAL EXTRACTIONS BASED ON SOLUTION CONCENTRATIONS DURING ATMOSPHERIC LEACHING OF THE MATTE AT A TEMPERATURE OF 80 ^{O} C

Leaching conditions:

Temperature:	80 ^{o}C	
Agitation:	205 rpm	
Pulp density:	1.7 kg/L	
Matte:	1.276	kg
Solution:	1.537	L

Metal content of matte

Ni	612.22 g	(47.98%)
Co	4.34 g	(0.34 %)
Fe	7.66 g	(0.60 %)

Leaching Time (min)	Ni (g/l)	Ni (g)	Ni Leach %	Co (g/l)	Co (g)	Co leach %	Fe (g/l)	Fe (g)	Fe %
0	24.61	37.83	0.00	0.18	0.28	0	0.67	1.03	0
15	58.34	89.67	8.47	0.68	1.05	17.71	3.04	4.67	47.58
30	65.58	100.62	10.26	0.76	1.17	20.50	3.32	5.10	53.11
60	76.59	117.26	12.98	0.83	1.27	22.90	3.58	5.48	58.16
90	87.97	134.18	15.74	0.94	1.43	26.61	4.03	6.14	66.75
120	91.86	139.77	16.65	1.00	1.52	28.60	4.25	6.46	70.88
150	97.00	147.03	17.84	1.07	1.62	30.87	4.33	6.57	72.36
180	97.73	148.04	18.00	1.09	1.64	31.51	4.39	6.65	73.44
240	104.17	156.82	19.44	1.16	1.74	33.71	4.15	6.33	69.17
300	104.59	157.38	19.53	1.21	1.81	35.25	3.96	6.07	65.86

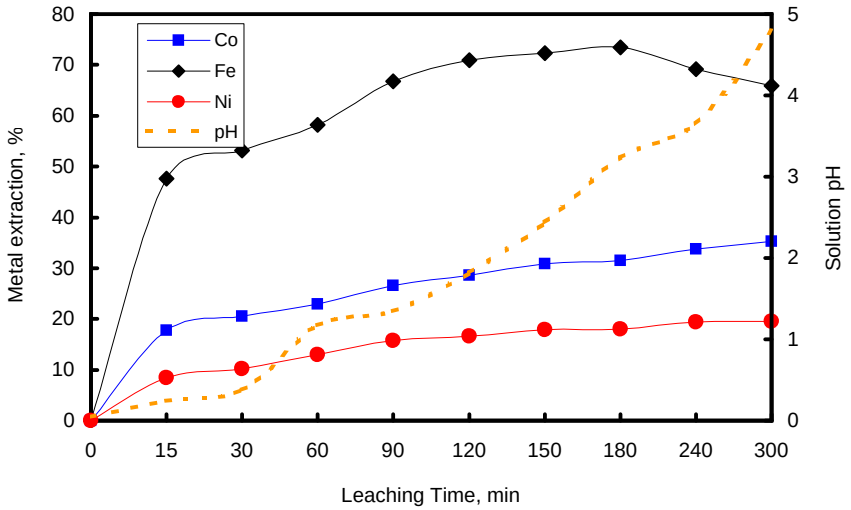

Figure A1.8: Metal extractions as a function of leaching time at 80^{o} C.

TABLE A1.7B: METAL SOLUTION CONCENTRATIONS DURING ATMOSPHERIC LEACHING OF THE MATTE AT A TEMPERATURE OF 80 ^{O} C - SECOND TEST

Leaching conditions:

Temperature:	80 ^{o}C
Agitation:	205 rpm
Pulp density:	1.7 kg/L

Leaching Time (min)	Co (g/L)	Fe (g/L)	Ni (g/L)	Cu (g/L)
0	0.18	0.67	24.61	24.95
15	0.74	3.14	61.03	15.17
30	0.79	3.3	68.18	10.26
60	0.86	4.01	79.43	3.96
90	0.91	4.06	85.67	0.00
120	1.02	4.45	93.36	0.00
150	1.08	4.31	96.89	0.00
180	1.09	4.02	99.23	0.00
240	1.19	4.05	102.67	0.00
300	1.25	3.61	107.09	0.00

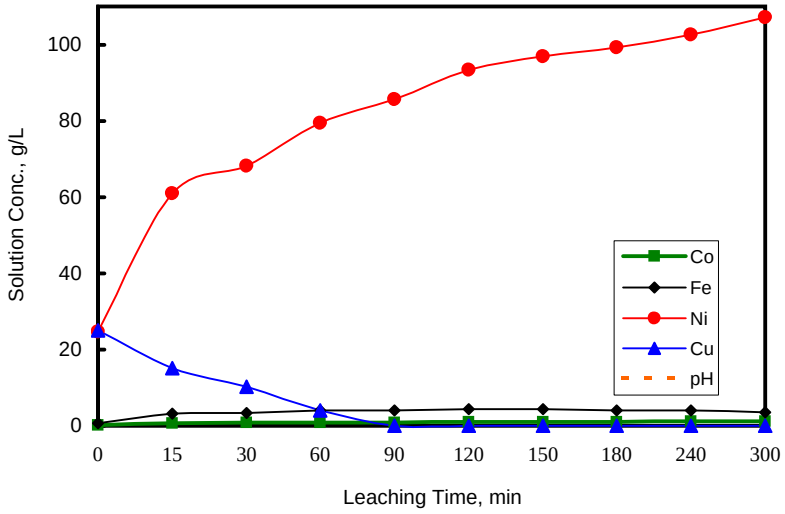

Fig. A1.7B: Metal concentration as a function of leaching time at 80 ^{O}c - second test

TABLE A1.8B: METAL EXTRACTIONS BASED ON SOLUTION CONCENTRATIONS DURING ATMOSPHERIC LEACHING OF THE MATTE AT A TEMPERATURE OF 80 ^{O} C - SECOND TEST

Leaching conditions:

Temperature:	80 ^{o}C	
Agitation:	205 rpm	
Pulp density:	1.7 kg/L	
Matte:	1.276	kg
Solution:	1.537	L

Metal content of matte

Ni	612.22 g	(47.98%)
Co	4.34 g	(0.34 %)
Fe	7.66 g	(0.60 %)

Leaching Time (min)	Ni (g/L)	Ni (g)	Ni Leach %	Co (g/L)	Co (g)	Co leach %	Fe (g/L)	Fe (g)	Fe %
0	24.61	37.83	0.00	0.18	0.28	0	0.67	1.03	0
15	61.03	93.80	9.14	0.74	1.14	19.84	3.14	4.83	49.59
30	68.18	104.61	10.91	0.79	1.21	21.58	3.3	5.07	52.75
60	79.43	121.62	13.69	0.86	1.32	23.98	4.01	6.12	66.54
90	85.67	130.90	15.20	0.91	1.39	25.67	4.06	6.20	67.49
120	93.36	141.95	17.01	1.02	1.55	29.31	4.45	6.76	74.81
150	96.89	146.94	17.82	1.08	1.63	31.26	4.31	6.56	72.23
180	99.23	150.18	18.35	1.09	1.65	31.58	4.02	6.16	66.98
240	102.67	154.87	19.12	1.19	1.78	34.72	4.05	6.20	67.51
300	107.09	160.78	20.08	1.25	1.86	36.57	3.61	5.61	59.83

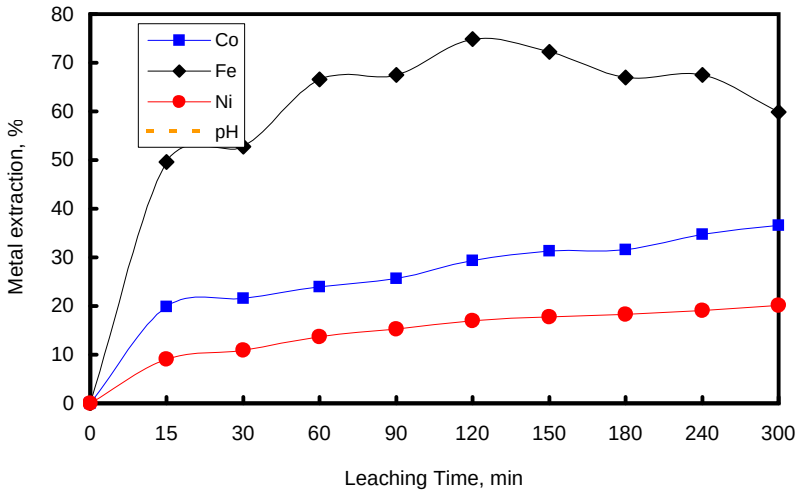

Figure A1.8B: Metal extractions as a function of leaching time at 80^{o} C - Second test.

TABLE A1.5: METAL SOLUTION CONCENTRATIONS DURING ATMOSPHERIC LEACHING OF THE MATTE AT A TEMPERATURE OF 70 ^{O} C

Leaching conditions Temperature: 70 ^{o}C
Agitation: 205 rpm
Pulp density: 1.7 kg/L

Leaching time (min)	Co (g/l)	Fe (g/l)	Ni (g/l)	Cu (g/l)	pH
0	0.18	0.67	24.61	24.95	1.10
15	0.73	3.09	59.60	15.03	1.03
30	0.77	3.3	65.88	12.23	1.06
60	0.79	3.29	67.80	7.35	1.10
90	0.88	3.61	77.59	3.97	1.14
120	0.89	3.63	79.13	0.85	1.18
150	0.96	3.95	86.36	0.00	1.29
180	1.01	4.05	92.39	0.00	1.61
240	1.08	4.28	97.99	0.00	2.12
300	1.06	3.62	101.60	0.00	4.51

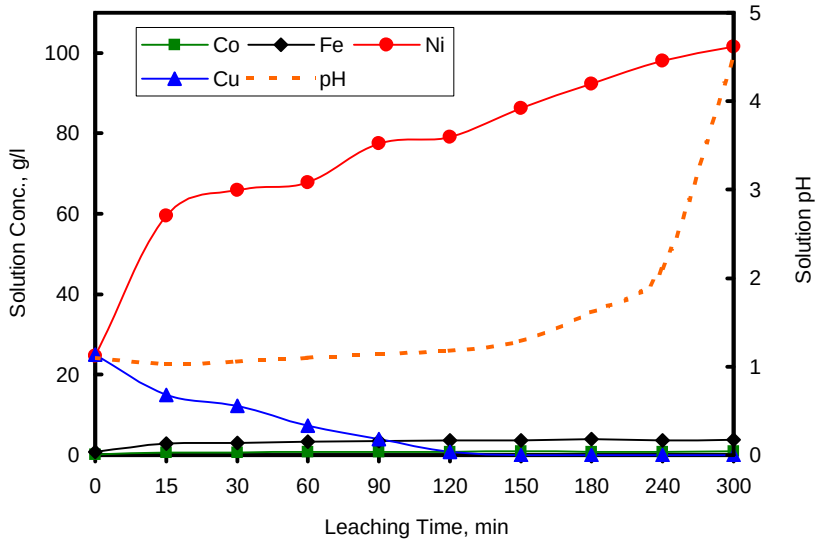

Fig. A1.5: Metal concentration as a function of leaching time at 70^{O}C

TABLE A1.6: METAL EXTRACTIONS BASED ON SOLUTION CONCENTRATIONS DURING ATMOSPHERIC LEACHING OF THE MATTE AT A TEMPERATURE OF 70 ^{O} C

Leaching conditions:	Temperature:	70 °C		Metal content of matte:	
	Agitation:	205 rpm		Ni	612.22 g (47.98%)
	Pulp density:	1.7 kg/L		Co	4.34 g (0.34 %)
	Matte:	1.276	kg	Fe	7.66 g (0.60 %)
	Solution:	1.537	L		

Leaching Time (min)	Ni (g/l)	Ni (g)	Ni Leach %	Co (g/l)	Co (g)	Co leach %	Fe (g/l)	Fe (g)	Fe %
0	24.61	37.83	0.00	0.18	0.28	0	0.67	1.03	0
15	59.60	91.61	8.78	0.73	1.12	19.49	3.09	4.75	48.58
30	65.88	101.10	10.34	0.77	1.18	20.88	3.3	5.07	52.73
60	67.80	103.96	10.80	0.79	1.21	21.56	3.29	5.05	52.54
90	77.59	118.27	13.14	0.88	1.34	24.60	3.61	5.52	58.65
120	79.13	120.48	13.50	0.89	1.36	24.93	3.63	5.55	59.02
150	86.36	130.69	15.17	0.96	1.46	27.21	3.95	6.00	64.92
180	92.39	139.05	16.53	1.01	1.53	28.81	4.05	6.14	66.74
240	97.99	146.68	17.78	1.08	1.62	31.00	4.28	6.45	70.83
300	101.60	151.51	18.57	1.06	1.59	30.39	3.62	5.57	59.30

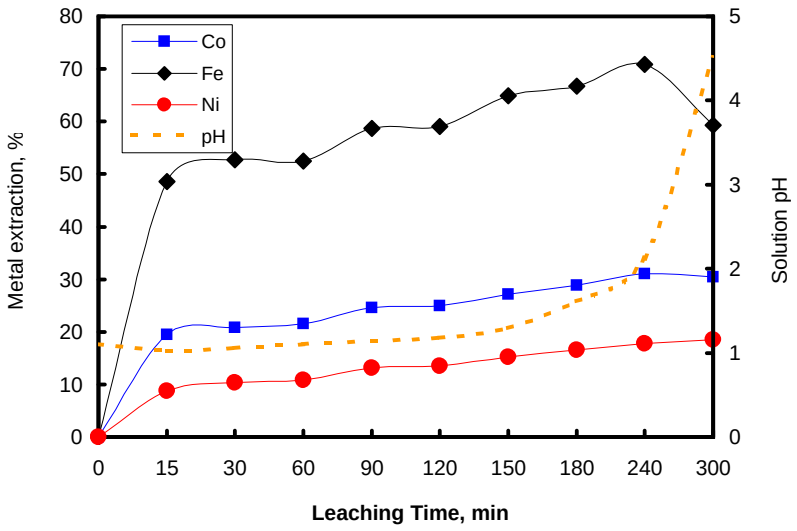

Fig. A1.6: Metal extraction as a function of leaching time at 70 °C

TABLE A1.3: METAL SOLUTION CONCENTRATIONS DURING ATMOSPHERIC LEACHING OF THE MATTE AT A TEMPERATURE OF 60 ^{O} C

Leaching conditions: Temperature: 60 ^{o}C
Agitation: 205 rpm
Pulp density: 1.7 kg/L

Leaching Time (min)	Co (g/l)	Fe (g/l)	Ni (g/l)	Cu (g/l)	pH
0	0.18	0.67	24.61	24.95	0.97
15	0.77	3.35	64.11	22.84	1.10
30	0.79	3.44	66.16	19.49	1.11
60	0.80	3.68	68.85	14.47	1.18
90	0.79	3.80	71.18	10.45	1.28
120	0.91	3.91	78.69	8.75	1.34
150	0.88	3.96	80.00	6.39	1.43
180	0.96	4.05	86.80	4.79	1.51
240	0.91	4.08	88.33	1.30	1.61
300	1.01	4.24	94.44	0.00	1.90

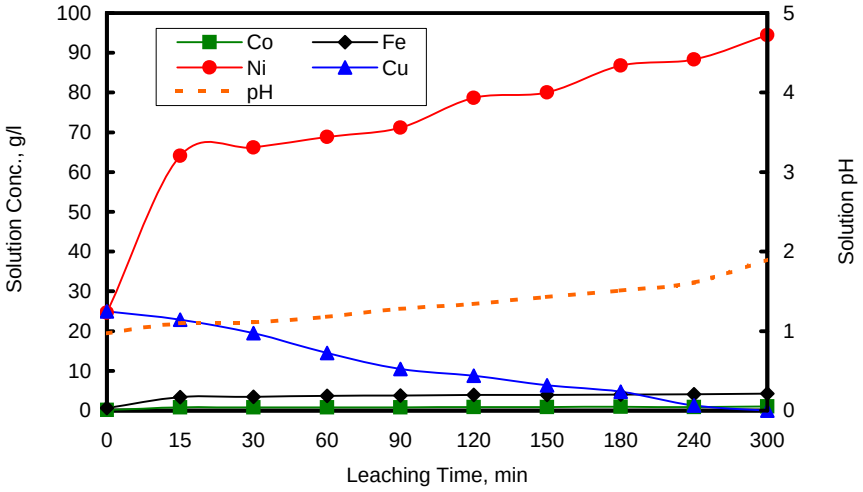

Fig. A1.3: Metal concentrations as a function of leaching time at 60 ^{o} C

TABLE A1.4: METAL EXTRACTIONS BASED ON SOLUTION CONCENTRATIONS DURING ATMOSPHERIC LEACHING OF THE MATTE AT A TEMPERATURE OF 60 ^{O} C

Leaching conditions:	Temperature:	60 oC		Metal content of matte:	
	Agitation:	205 rpm		Ni	612.22 g (47.98%)
	Pulp density:	1.7 kg/L		Co	4.34 g (0.34 %)
	Matte:	1.28	kg	Fe	7.66 g (0.60 %)
	Solution:	1.54	L		

Leaching Time (min)	**Ni (g/l)**	**Ni (g)**	**Ni Leach %**	**Co (g/l)**	**Co (g)**	**Co leach %**	**Fe (g/l)**	Fe (g)	Fe (%)
0	24.61	37.83	0.00	0.18	0.28	0	0.67	1.03	0
15	64.11	98.54	9.92	0.77	1.18	20.90	3.35	5.15	53.80
30	66.16	101.64	10.42	0.79	1.21	21.60	3.44	5.29	55.58
60	68.85	105.71	11.09	0.80	1.23	21.94	3.68	5.64	60.24
90	71.18	109.17	11.65	0.79	1.21	21.61	3.80	5.82	62.61
120	78.69	119.96	13.42	0.91	1.39	25.58	3.91	5.98	64.60
150	80.00	121.81	13.72	0.88	1.34	24.60	3.96	6.05	65.52
180	86.80	131.24	15.26	0.96	1.46	27.16	4.05	6.17	67.15
240	88.33	133.33	15.60	0.91	1.39	25.59	4.08	6.21	67.69
300	94.44	141.49	16.93	1.01	1.52	28.67	4.24	6.43	70.48
300									

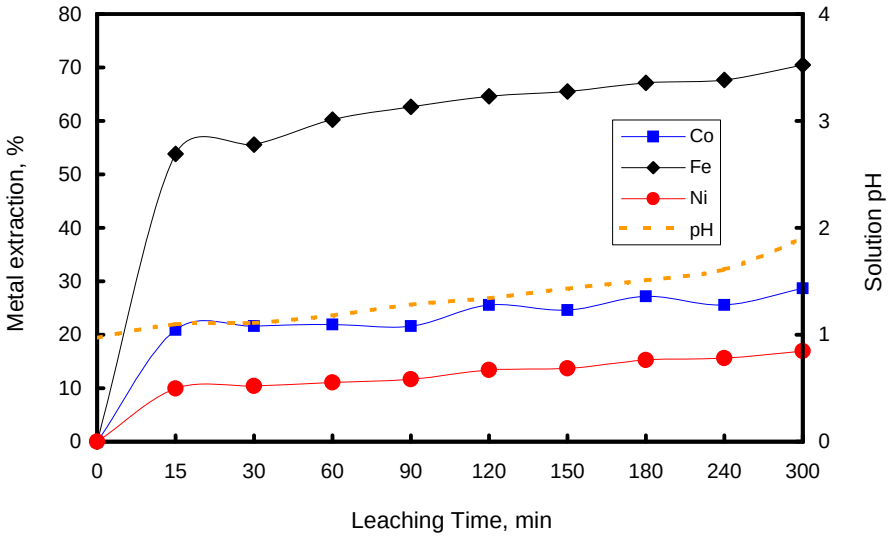

Figure A1.4: Metal extractions as a function of leaching time at 60 ^{o} C

TABLE A1.3B: METAL SOLUTION CONCENTRATIONS DURING ATMOSPHERIC LEACHING OF THE MATTE AT A TEMPERATURE OF 60 ^{O} C - SECOND TEST

Leaching conditions: Temperature: 60 ^{o}C
Agitation: 205 rpm
Pulp density: 1.7 kg/L

Leaching Time (min)	Co (g/L)	Fe (g/L)	Ni (g/L)	Cu (g/L)
0	0.17	0.67	24.61	24.95
15	0.67	3.21	54.21	21.14
30	0.76	3.54	69.75	19.58
60	0.79	3.78	70.85	16.57
90	0.76	3.89	74.16	12.25
120	0.81	3.96	77.61	8.15
150	0.79	3.96	82.16	5.87
180	0.98	4.08	88.68	4.09
240	0.97	4.18	89.32	0.92
300	1.06	4.34	99.69	0.00

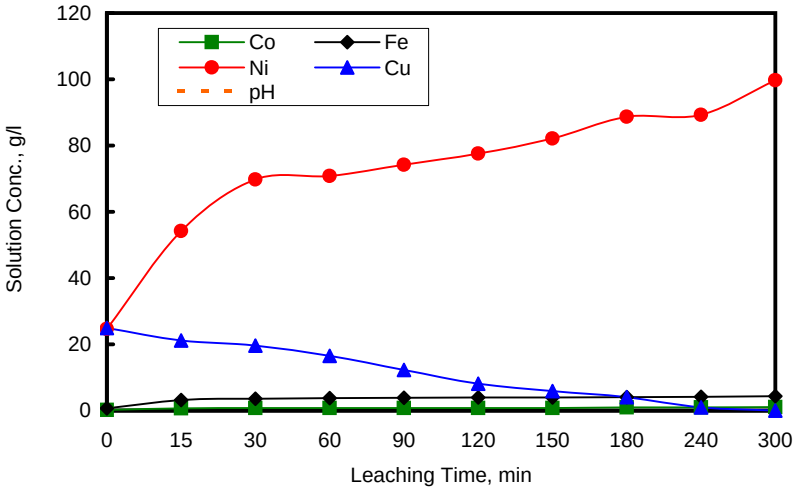

Fig. A1.3B: Metal concentrations as a function of leaching time at 60 ^{o} C - Second test

TABLE A1.4B: METAL EXTRACTIONS BASED ON SOLUTION CONCENTRATIONS DURING ATMOSPHERIC LEACHIN
OF THE MATTE AT A TEMPERATURE OF 60 ^{O} C

Leaching conditions:	Temperature:	60 oC		Metal content of matte:		
	Agitation:	205 rpm		Ni	612.22 g	(47.98%)
	Pulp density:	1.7 kg/L		Co	4.34 g	(0.34 %)
	Matte:	1.28	kg	Fe	7.66 g	(0.60 %)
	Solution:	1.54	L			

Leaching Time (min)	**Ni (g/L)**	**Ni (g)**	**Ni Leach %**	**Co (g/L)**	**Co (g)**	**Co leach %**	**Fe (g/L)**	Fe (g)	Fe (%)
0	24.61	37.83	0.00	0.17	0.26	0	0.67	1.03	0
15	54.21	83.32	7.43	0.67	1.03	17.78	3.21	4.93	50.99
30	69.75	106.82	11.27	0.76	1.17	20.92	3.54	5.43	57.51
60	70.85	108.48	11.54	0.79	1.21	21.95	3.78	5.79	62.17
90	74.16	113.41	12.35	0.76	1.17	20.90	3.89	5.95	64.27
120	77.61	118.36	13.15	0.81	1.24	22.59	3.96	6.05	65.59
150	82.16	124.78	14.20	0.79	1.21	21.94	3.96	6.05	65.59
180	88.68	133.83	15.68	0.98	1.47	28.02	4.08	6.22	67.76
240	89.32	134.70	15.82	0.97	1.46	27.70	4.18	6.35	69.54
300	99.69	148.56	18.09	1.06	1.58	30.48	4.34	6.57	72.33
Solid analysis									

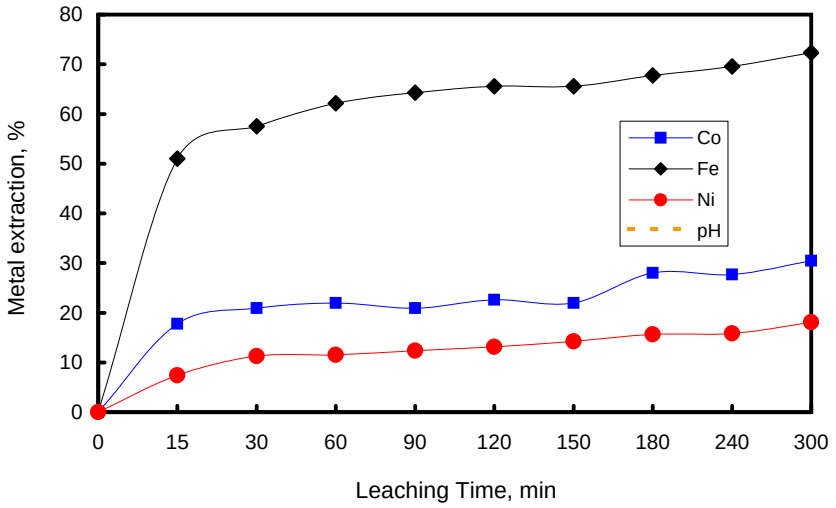

Figure A1.4B: Metal extractions as a function of leaching time at 60 ^{o} C - second test

TABLE A1.1: METAL SOLUTION CONCENTRATIONS DURING ATMOSPHERIC LEACHING OF THE MATTE AT A TEMPERATURE OF 50 ^{O} C

Leaching conditions:	Temperature:	50 ^{o}C
	Agitation:	205 rpm
	Pulp density:	1.7 kg/L

Leaching Time (min)	Co (g/l)	Fe (g/l)	Ni (g/l)	Cu (g/l)	pH
0	0.18	0.67	24.61	24.95	0.84
15	0.65	2.76	51.79	23.51	1.34
30	0.70	2.79	55.43	20.93	1.48
60	0.79	2.89	59.65	17.47	1.52
90	0.88	2.85	64.01	15.72	1.52
120	0.90	2.78	66.97	14.15	1.50
150	0.94	2.88	68.04	12.72	1.61
180	0.96	2.92	70.36	11.90	1.62
240	0.97	2.95	74.85	9.96	1.74
300	0.97	2.97	76.56	7.55	1.88

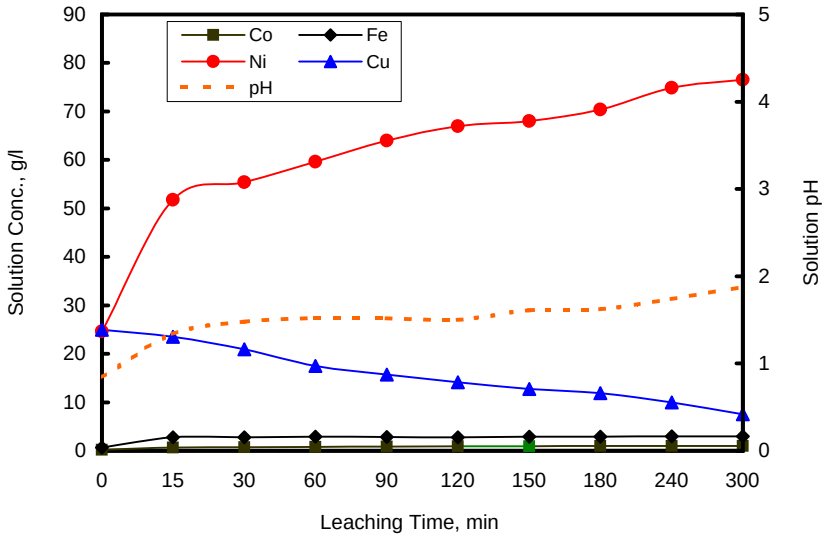

Fig. A.1.1: -Metal concentration as a function of leaching time at 50 ^{o}C

TABLE A1.2: METAL EXTRACTIONS BASED ON SOLUTION CONCENTRATIONS DURING ATMOSPHERIC LEACHING OF THE MATTE AT A TEMPERATURE OF 50 ^{O} C

Leaching conditions:	Temperature:	50 ^{o}C		Metal content of matte:		
	Agitation:	205 rpm		Ni	612.22 g	(47.98%)
	Pulp density:	1.7 kg/L		Co	4.34 g	(0.34 %)
	Matte:	1.28	kg	Fe	7.66 g	(0.60 %)
	Solution:	1.54	L			

Leaching Time (min)	**Ni (g/l)**	**Ni (g)**	**Ni Leach %**	**Co (g/l)**	**Co (g)**	**Co leach %**	**Fe (g/l)**	Fe (g)	Fe %
0	24.61	37.83	0.00	0.18	0.28	0.00	0.67	1.03	0
15	51.79	79.60	6.82	0.65	1.00	16.65	2.76	4.24	41.96
30	55.43	85.20	7.74	0.70	1.08	18.42	2.79	4.29	42.56
60	59.65	91.68	8.80	0.79	1.21	21.61	2.89	4.44	44.57
90	64.01	98.38	9.89	0.88	1.35	24.80	2.85	4.38	43.77
120	66.97	102.93	10.63	0.90	1.38	25.51	2.78	4.27	42.36
150	68.04	104.58	10.90	0.94	1.44	26.93	2.88	4.43	44.37
180	70.36	108.14	11.49	0.96	1.48	27.63	2.92	4.49	45.17
240	74.85	115.04	12.61	0.97	1.49	27.99	2.95	4.53	45.77
300	76.56	117.67	13.04	0.97	1.49	27.99	2.97	4.56	46.17

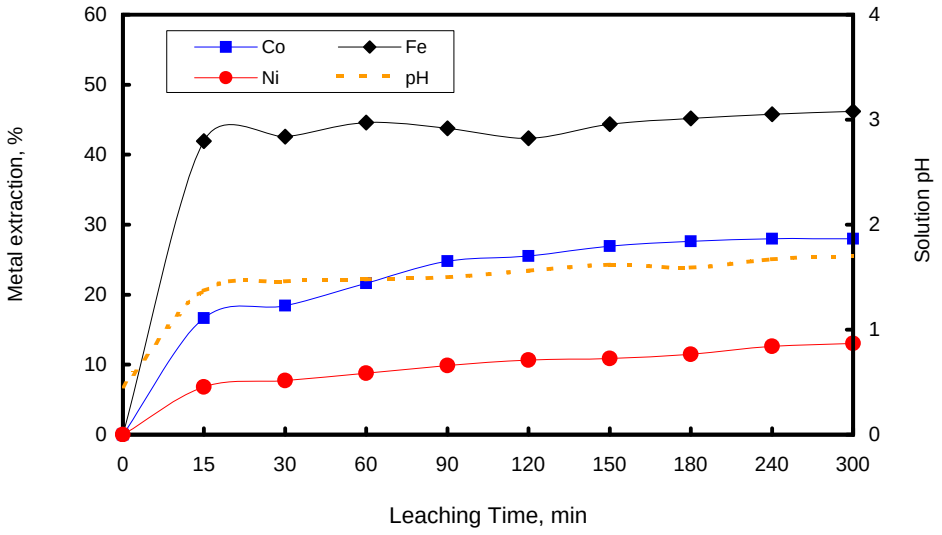

Fig. A1.2: Metal extraction as a function of leaching time at a temperature of 50 ^{o}C.

COMPARISON AT 80 oC

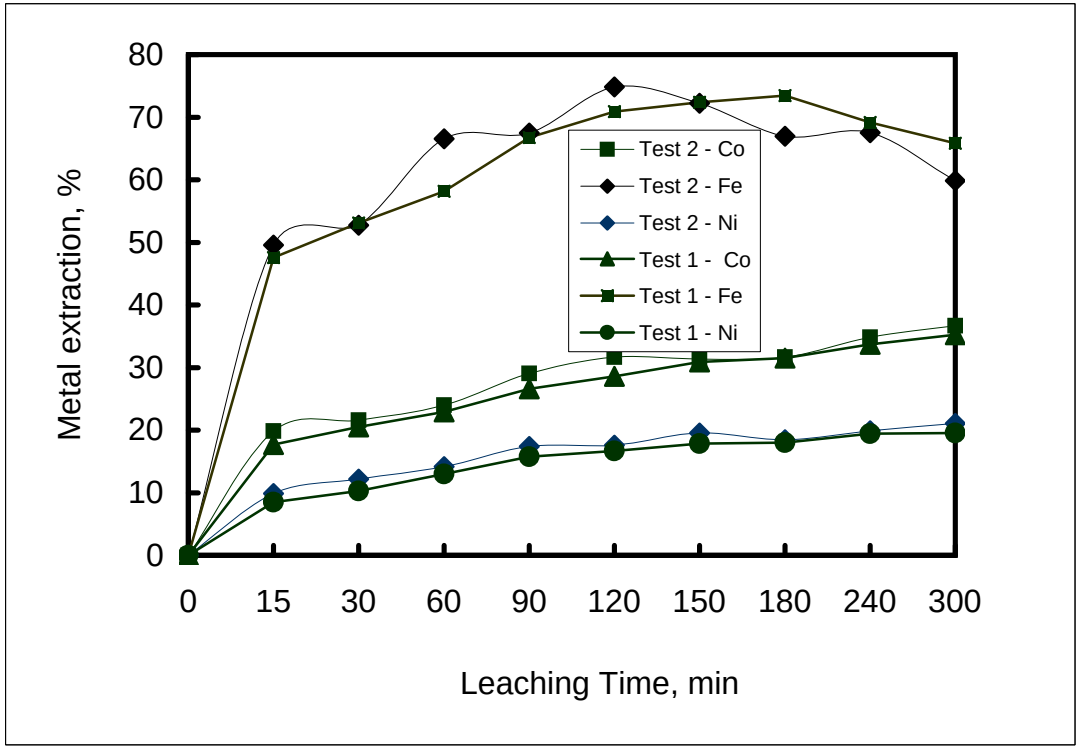

TABLE A1.10 : COPPER PRECIPITATION DURING ATMOSPHERIC LEACHING OF THE MATTE AT DIFFERENT TEMPERATURE VALUES

Leaching conditions		Feed matte		Feed solution	
Pulp density (kg/L)	1.7	Mass (kg)	1.28	Volume (mL)	1.54
Stirring rate (rpm):	205	Ni (%)	47.98%	Ni (g/L)	24.61
Leaching time (hr):	5 hrs	Cu (%)	31.31	Cu (g/L)	24.95
Matte (kg):	1.28	Co (%)	0.34%	Co (g/L)	0.18
		Fe (%)	0.6%	Fe (g/L)	0.67

Leaching Time (min)	Copper in leach solution, g				Copper precipitation, %			
	50 °C	60 °C	70 °C	80 °C	50 °C	60 °C	70 °C	80 °C
0	38.42	38.42	38.42	38.42	0.00	0.00	0.00	0.00
15	36.21	35.17	23.15	24.73	5.77	8.46	39.76	35.63
30	32.23	30.01	18.83	18.73	16.11	21.88	50.98	51.26
60	26.90	22.28	11.32	6.84	29.98	42.00	70.54	82.20
90	24.21	16.09	6.11	0.00	36.99	58.12	84.09	100.00
120	21.79	13.48	1.31	0.00	43.29	64.93	96.59	100.00
150	19.59	9.84	0.00	0.00	49.02	74.39	100.00	100.00
180	18.33	7.38	0.00	0.00	52.30	80.80	100.00	100.00
240	15.34	2.00	0.00	0.00	60.08	94.79	100.00	100.00
300	12.26	0.00	0.00	0.00	68.10	100.00	100.00	100.00

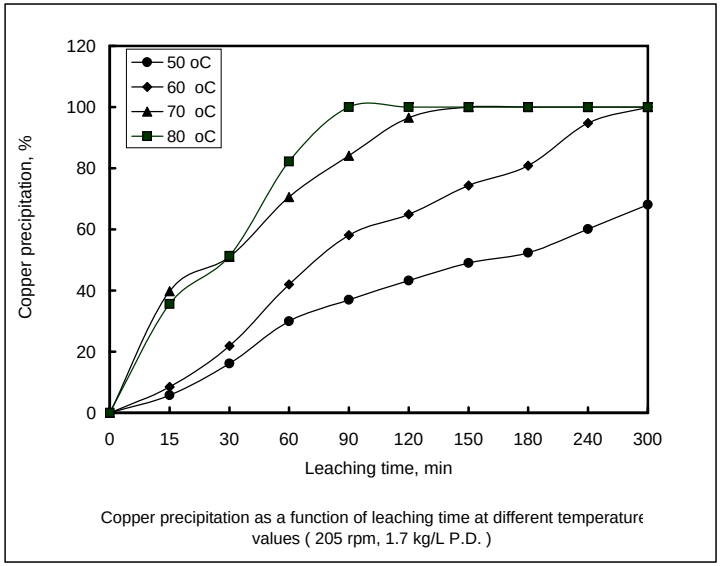

Copper precipitation as a function of leaching time at different temperature values (205 rpm, 1.7 kg/L P.D.)

TABLE A1.9: COPPER SOLUTION CONCENTRATION DURING ATMOSPHERIC LEACHING OF THE MATTE AT DIFFERENT TEMPERATURE VALUES

Leaching conditions		Feed matte		Feed solution	
Pulp density (kg/L)	1.7	Mass (kg)	1.28	/olume (mL	1.54
Stirring rate (rpm):	205	Ni (%)	47.98%	Ni	24.61
Leaching time (hr):	5 hrs	Cu (%)	31.31	Cu	24.95
Matte (kg):	1.28	Co (%)	0.34%	Co	??
		Fe (%)	0.6%	Fe	**??**

Leaching Time (min)	Copper Concentration, g/L				Log $[Cu^{2+}]_t / [Cu^{2+}]_0$			
	50 °C	60 °C	70 °C	80 °C	50 °C	60 °C	70 °C	80 °C
0	24.95	24.95	24.95	24.95	0.00	0.00	0.00	0.00
15	23.51	22.84	15.03	16.06	-0.03	-0.04	-0.22	-0.19
30	20.93	19.49	12.23	12.16	-0.08	-0.11	-0.31	-0.31
60	17.47	14.47	7.35	4.44	-0.15	-0.24	-0.53	-0.75
90	15.72	10.45	3.97	0.00	-0.20	-0.38	-0.80	
120	14.15	8.75	0.85	0.00	-0.25	-0.46	-1.47	
150	12.72	6.39	0.00	0.00	-0.29	-0.59		
180	11.9	4.79	0.00	0.00	-0.32	-0.72		
240	9.96	1.30	0.00	0.00	-0.40	-1.28		
300	7.96	0.00	0.00	0.00	-0.50			

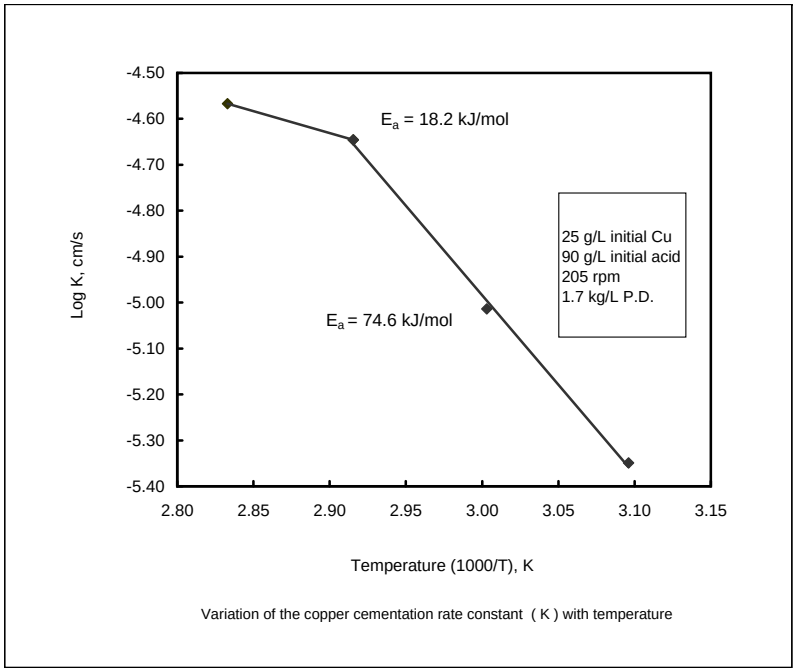

Variation of the copper cementation rate constant (K) with temperature

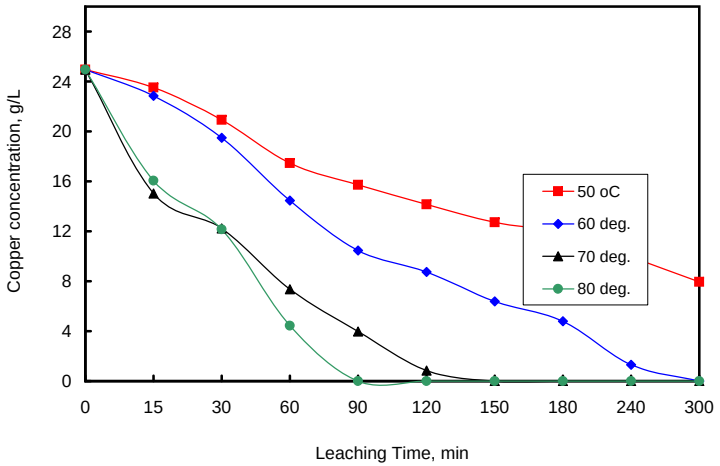

Figure A1.9: Copper concentration as a function of leaching time at different temperature values (205 rpm, 25g/L initial Cu, 90g/L initial acid, 1.7 kg/L pulp density)

TABLE A1.11: DETERMINATION OF COPPER CEMENTATION RATE CONSTANTS FOR STAGE 1 OF CEMENTATION REACTION AT DIFFERENT TEMPERATURE VALUES

Leaching conditions
Pulp densit 1.7
Stirring rate 205
Leaching tir 5 hrs
Matte (kg): 1.28

Specific surface area of matte (cm^2/g) 66982
Mass of matte (g): 1276
Volume of solution (cm^3) 1537

Temperature (T)			Slope of graph for reaction stage 1	rate constant K_1 X 10^{-3} (cm / s)	$K_{1/1000}$	Log K_1	TEMPERATURE Range (oC)	ACTIVATION ENERGY Ea (kJ/mol)
(^oC)	(^oK)	1000/T (^oK 0						
80	353	2.83	0.0018	0.02709	0.000027	-4.57	80 - 70	**18.2**
70	343	2.92	0.0039	0.02261	0.000023	-4.65	70 - 50	**74.6**
60	333	3.00	0.0091	0.00969	0.000010	-5.01		
50	323	3.10	0.0109	0.00447	0.000004	-5.35		

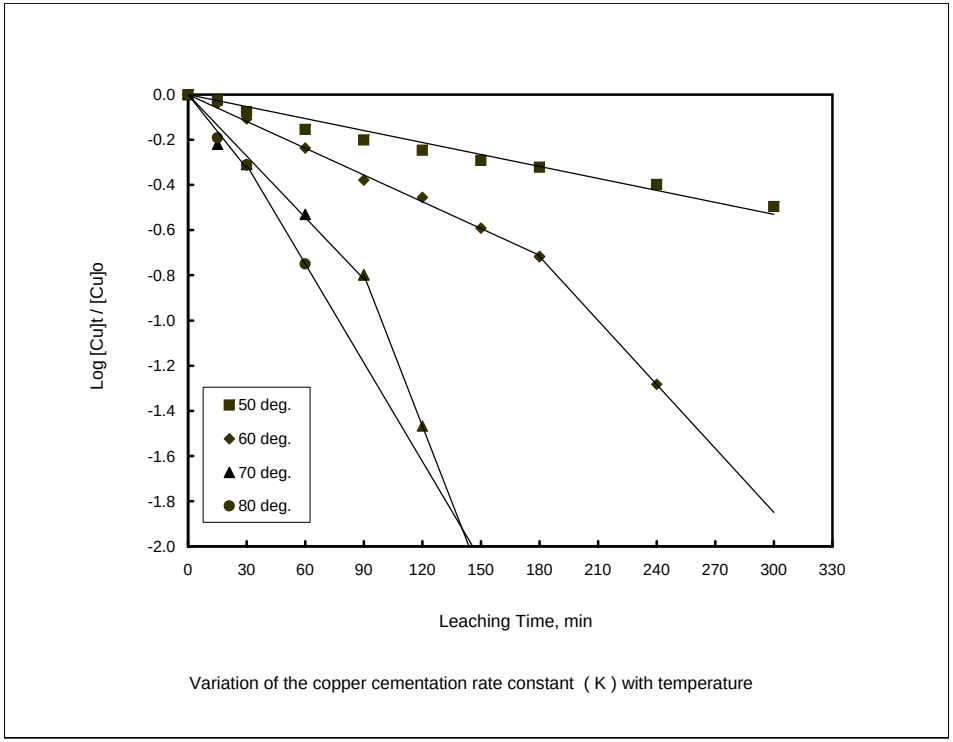

Variation of the copper cementation rate constant (K) with temperature

TABLE A2.1: METAL SOLUTION CONCENTRATIONS DURING ATMOSPHERIC LEACHING OF THE MATTE AT A STIRRING RATE OF 145 RPM

Leaching conditions:

Temperature: (^{o} C)	60
Mixing rate (rpm):	145
Pulp density (kg/L):	1.7
Leaching time (hrs):	5

Leaching Time (min)	Co (g/l)	Fe (g/l)	Ni (g/l)	Cu (g/l)	pH
0	0.18	0.67	24.61	24.95	0.46
15	0.82	1.68	59.55	19.25	1.37
30	0.83	3.09	62.67	18.99	1.46
60	0.82	3.37	62.90	11.83	1.48
90	0.89	3.56	69.78	10.40	1.50
120	0.95	3.62	73.41	7.92	1.56
150	1.01	4.01	70.61	8.00	1.62
180	0.98	4.19	75.56	3.85	1.59
240	0.91	4.23	76.18	3.18	1.67
300	1.05	4.22	74.39	1.04	1.70

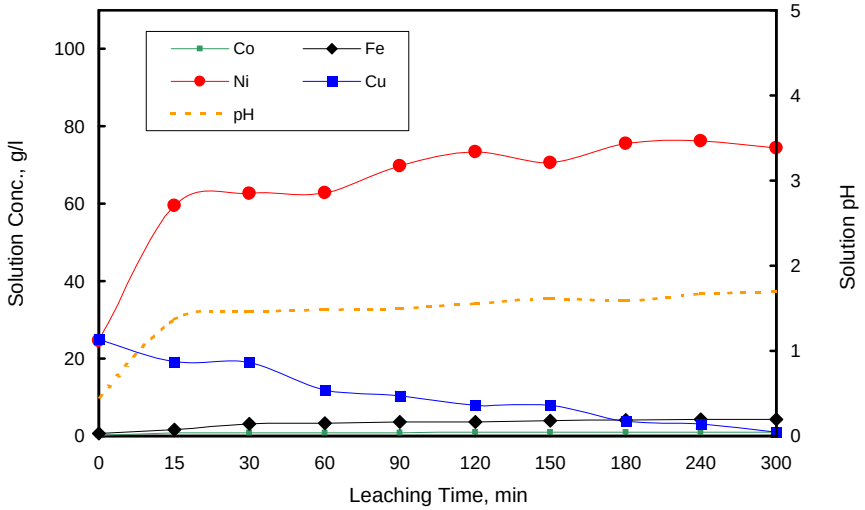

Figure A2.1: Metal concentrations as a function of leaching time at a stirring rate of 145 rpm

TABLE A2.2: METAL EXTRACTIONS BASED ON SOLUTION CONCENTRATIONS DURING ATMOSPHERIC LEACHNG OF THE MATTE AT A STIRRING RATE OF 145 RPM

Leaching conditions:	Temperature (o C):	60			
	Mixing rate (rpm):	145			
	Pulp density (kg/L):	1.7	Metal content of matte		
	Leaching time (hrs):	5	Ni	614.14 g	(47.98%)
	Matte (kg):	1.28	Co	4.35 g	(0.34%)
	Solution (L):	1.54	Fe	7.68 g	(0.6%)

Leaching Time (min)	Ni (g/l)	Ni (g)	Ni Leach %	Co (g/l)	Co (g)	Co leach %	Fe (g/l)	Fe (g)	Fe %
0	24.61	37.90	0.00	0.18	0.28	0	0.67	1.03	0
15	59.55	91.71	8.76	0.82	1.26	22.65	1.68	2.59	20.25
30	62.67	96.43	9.53	0.83	1.28	23.13	3.09	4.72	48.07
60	62.90	96.78	9.59	0.82	1.26	22.66	3.37	5.14	53.50
90	69.78	107.03	11.26	0.89	1.37	25.01	3.56	5.42	57.12
120	73.41	112.26	12.11	0.95	1.45	27.00	3.62	5.51	58.25
150	70.61	108.30	11.46	1.01	1.54	28.95	4.01	6.06	65.43
180	75.56	115.18	12.58	0.98	1.50	27.99	4.19	6.31	68.69
240	76.18	116.03	12.72	0.91	1.40	25.79	4.23	6.36	69.40
300	74.39	113.63	12.33	1.05	1.59	30.10	4.22	6.35	69.23

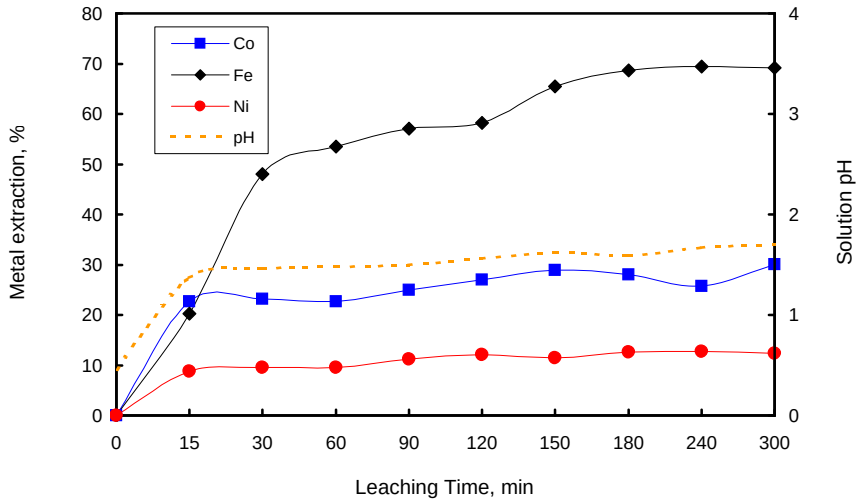

Fig.ure A2.2: Metal extraction as a function of leaching time at a stirring rate 145 rpm

TABLE A 2.5: METAL SOLUTION CONCENTRATIONS DURING ATMOSPHERIC LEACHING OF THE MATTE AT A STIRRING RATE OF 400 RPM

Leaching conditions:

Temperature: (° C)	60
Mixing rate (rpm):	400
Pulp density (kg/L):	1.7
Leaching time (hrs):	5

Leaching Time (min)	Co (g/l)	Fe (g/l)	Ni (g/l)	Cu (g/l)	pH
0	0.18	0.67	24.61	24.95	0.45
15	0.80	3.47	58.15	21.09	1.41
30	1.13	4.66	84.95	23.55	1.48
60	1.14	4.8	91.20	17.71	1.58
90	1.20	4.9	97.93	13.98	1.74
120	1.21	4.97	102.38	11.90	1.96
150	1.02	4.26	101.18	8.02	2.34
180	1.20	4.02	102.47	5.99	3.37
240	1.09	4.18	101.00	1.58	3.85
300	1.23	3.49	102.13	0.00	4.77

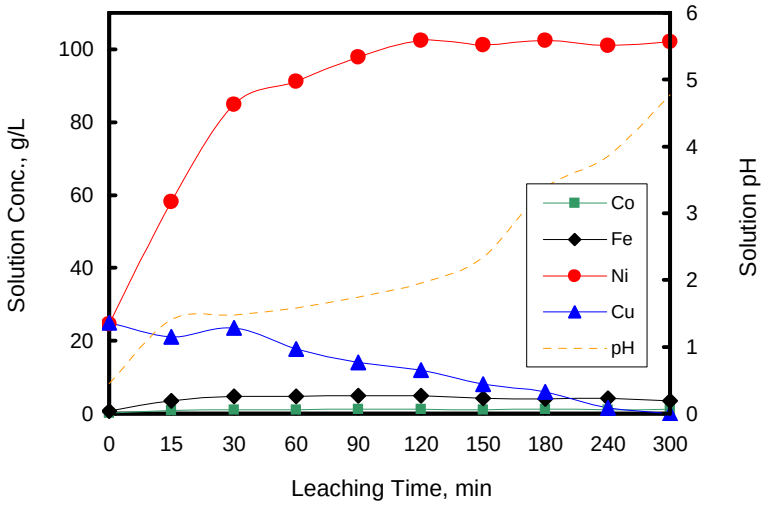

Figure A2.5: Metal concentrations as a function of leaching time at a stirring rate of 400 rpm

TABLE A2.6: METAL EXTRACTIONS BASED ON SOLUTION CONCENTRATIONS DURING ATMOSPHERIC LEACHNG OF THE MATTE AT A MIXING RATE OF 400 RPM

Leaching conditions:

Temperature (o C):	60
Mixing rate (rpm):	400
Pulp density (kg/L):	1.7
Leaching time (hrs):	5
Matte (kg):	1.28
Solution (L):	1.54

Metal content of matte

Ni	614.14 g	(47.98%)
Co	4.35 g	(0.34%)
Fe	7.68 g	(0.6%)

Leaching Time (min)	Ni (g/l)	Ni (g)	Ni Leach %	Co (g/l)	Co (g)	Co leach %	Fe (g/l)	Fe (g)	Fe leach %
0	24.61	37.90	0.00	0.18	0.28	0	0.67	1.03	0
15	58.15	89.55	8.41	0.80	1.23	21.94	3.47	5.34	56.15
30	84.95	130.15	15.02	1.13	1.73	33.43	4.66	7.15	79.62
60	91.20	139.62	16.56	1.14	1.75	33.77	4.8	7.36	82.34
90	97.93	149.65	18.20	1.20	1.83	35.79	4.9	7.50	84.24
120	102.38	156.06	19.24	1.21	1.85	36.12	4.97	7.60	85.56
150	101.18	154.36	18.96	1.02	1.58	29.94	4.26	6.60	72.48
180	102.47	156.15	19.25	1.20	1.83	35.69	4.02	6.26	68.13
240	101.00	154.15	18.93	1.09	1.68	32.24	4.18	6.48	70.98
300	102.13	155.66	19.17	1.23	1.87	36.55	3.49	5.56	58.94

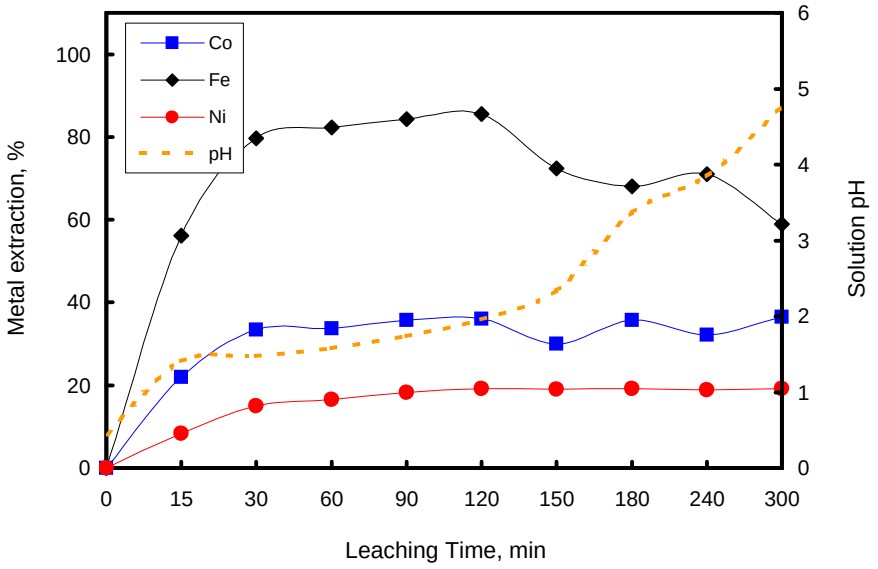

Figure A2.6: Metal extractions as a function of leaching time at a stirrin rate of 400 rpm

TABLE A 2.5B: METAL SOLUTION CONCENTRATIONS DURING ATMOSPHERIC LEACHING OF THE MATTE AT A STIRRING RATE OF 400 RPM - SECOND TEST

Leaching conditions:

Temperature: (°C)	60
Mixing rate (rpm):	400
Pulp density (kg/L):	1.7
Leaching time (hrs):	5

Leaching Time (min)	Co (g/L)	Fe (g/L)	Ni (g/L)	Cu (g/L)
0	0.18	0.67	24.61	24.95
15	0.71	3.02	62.55	20.48
30	0.98	4.18	76.65	18.57
60	1.06	4.67	85.97	15.05
90	1.14	4.86	91.03	12.03
120	1.26	4.57	98.87	9.64
150	1.12	4.12	102.23	5.78
180	1.86	4.16	101.98	6.09
240	1.21	3.07	102.55	3.18
300	1.25	3.13	101.96	0.00

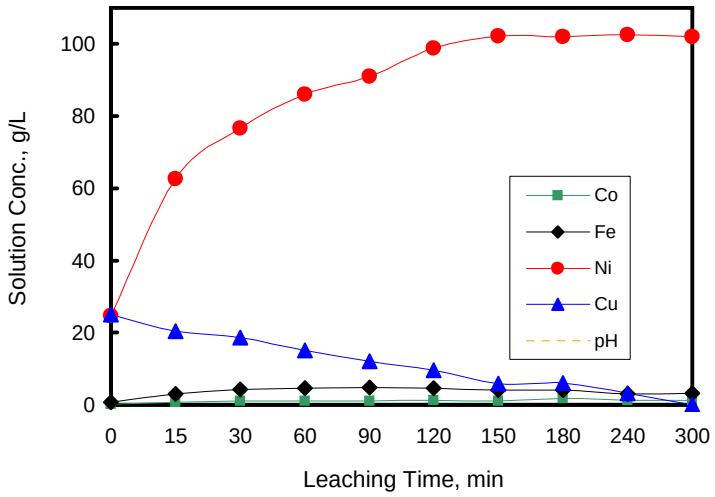

Figure A2.5B: Metal concentrations as a function of leaching time at a stirring rate of 400 rpm - second test

TABLE A2.6B: METAL EXTRACTIONS BASED ON SOLUTION CONCENTRATIONS DURING ATMOSPHERIC LEACHNG OF THE MATTE AT A MIXING RATE OF 400 RPM - SECOND TEST

Leaching conditions:

Temperature (o C):	60
Mixing rate (rpm):	400
Pulp density (kg/L):	1.7
Leaching time (hrs):	5
Matte (kg):	1.28
Solution (L):	1.54

Metal content of matte

Ni	614.14 g	(47.98%)
Co	4.35 g	(0.34%)
Fe	7.68 g	(0.6%)

Leaching Time (min)	Ni (g/L)	Ni (g)	Ni Leach %	Co (g/L)	Co (g)	Co leach %	Fe (g/L)	Fe (g)	Fe leach %
0	24.61	37.90	0.00	0.18	0.28	0	0.67	1.03	0
15	62.55	96.33	9.51	0.71	1.09	18.75	3.02	4.65	47.12
30	76.65	117.69	12.99	0.98	1.50	28.15	4.18	6.41	70.01
60	85.97	131.81	15.29	1.06	1.62	30.89	4.67	7.14	79.51
90	91.03	139.35	16.52	1.14	1.74	33.59	4.86	7.42	83.14
120	98.87	150.64	18.36	1.26	1.91	37.56	4.57	7.00	77.70
150	102.23	155.39	19.13	1.12	1.71	33.00	4.12	6.36	69.41
180	101.98	155.04	19.07	1.16	1.77	34.28	4.16	6.42	70.13
240	102.55	155.82	19.20	1.21	1.84	35.85	3.07	4.93	50.76
300	101.96	155.03	19.07	1.25	1.89	37.08	3.13	5.01	51.81

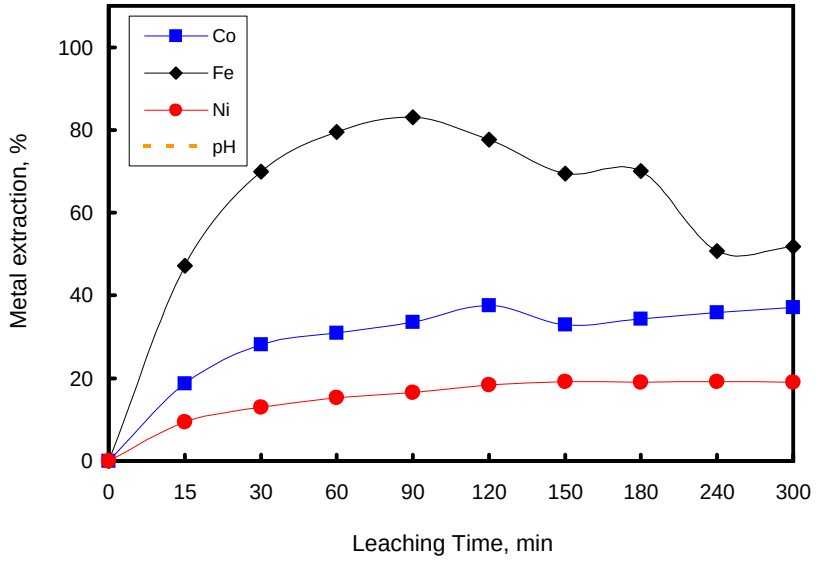

Figure A2.6B: Metal extractions as a function of leaching time at a stirring rate of 400 rpm - Second test

TABLE A2.3: METAL SOLUTION CONCENTRATIONS DURING ATMOSPHERIC LEACHING OF THE MATTE AT A STIRRING RATE OF 205 RPM

Leaching conditions: Temperature: 60 °C
Agitation: 205 rpm
Pulp density: 1.7 kg/L

Leaching Time (min)	Co (g/l)	Fe (g/l)	Ni (g/l)	Cu (g/l)	pH
0	0.18	0.67	24.61	24.95	0.97
15	0.77	3.35	64.11	22.84	1.10
30	0.79	3.44	66.16	19.49	1.11
60	0.80	3.68	68.85	14.47	1.18
90	0.79	3.80	71.18	10.45	1.28
120	0.91	3.91	78.69	8.75	1.34
150	0.88	3.96	80.00	6.39	1.43
180	0.96	4.05	86.80	4.79	1.51
240	0.91	4.08	88.33	1.30	1.61
300	1.01	4.24	94.44	0.00	1.90

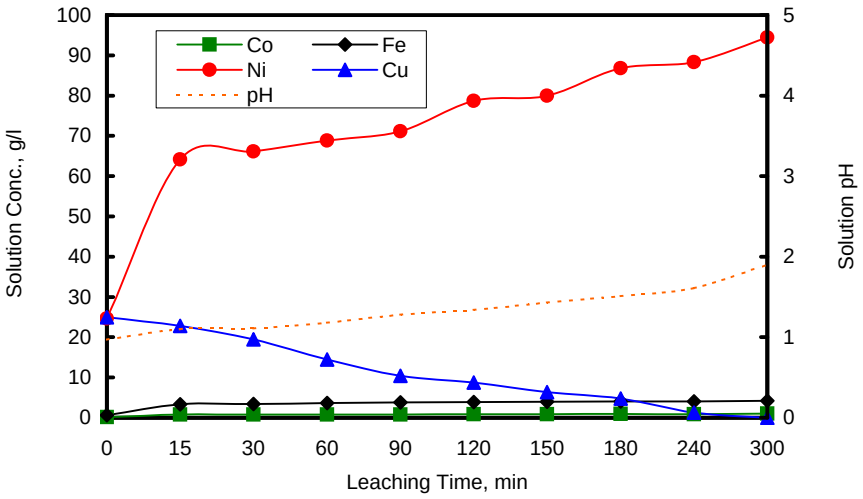

Fig. A2.3: Metal concentrations as a function of leaching time at stirring rate of 205 rpm

TABLE A2.4: METAL EXTRACTIONS BASED ON SOLUTION CONCENTRATIONS DURING ATMOSPHERIC LEACHING OF THE MATTE AT A STIRRING RATE OF 205 RPM

Leaching conditions:	Temperature:	60 oC		Metal content of matte:	
	Agitation:	205 rpm		Ni	612.22 g (47.98%)
	Pulp density:	1.7 kg/L		Co	4.34 g (0.34 %)
	Matte:	1.28	kg	Fe	7.66 g (0.60 %)
	Solution:	1.54	L		

Leaching Time (min)	**Ni (g/l)**	**Ni (g)**	**Ni Leach %**	**Co (g/l)**	**Co (g)**	**Co leach %**	**Fe (g/l)**	Fe (g)	Fe (%)
0	24.61	37.83	0.00	0.18	0.28	0	0.67	1.03	0
15	64.11	98.54	9.92	0.77	1.18	20.90	3.35	5.15	53.80
30	66.16	101.64	10.42	0.79	1.21	21.60	3.44	5.29	55.58
60	68.85	105.71	11.09	0.80	1.23	21.94	3.68	5.64	60.24
90	71.18	109.17	11.65	0.79	1.21	21.61	3.80	5.82	62.61
120	78.69	119.96	13.42	0.91	1.39	25.58	3.91	5.98	64.60
150	80.00	121.81	13.72	0.88	1.34	24.60	3.96	6.05	65.52
180	86.80	131.24	15.26	0.96	1.46	27.16	4.05	6.17	67.15
240	88.33	133.33	15.60	0.91	1.39	25.59	4.08	6.21	67.69
300	94.44	141.49	16.93	1.01	1.52	28.67	4.24	6.43	70.48
300									

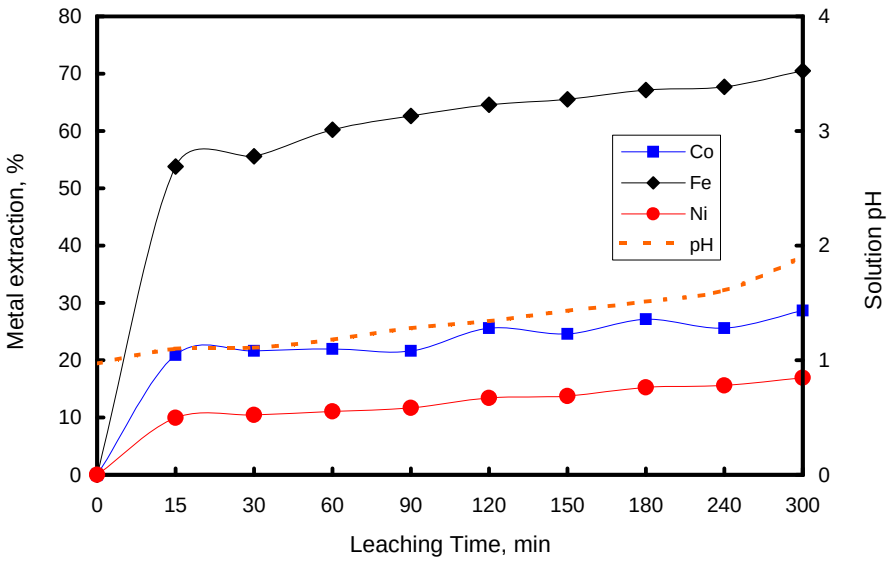

Figure A2.4: Metal extractions as a function of leaching time at stirring rate of 205 rpm

Comparison of leaching at 400 rpm

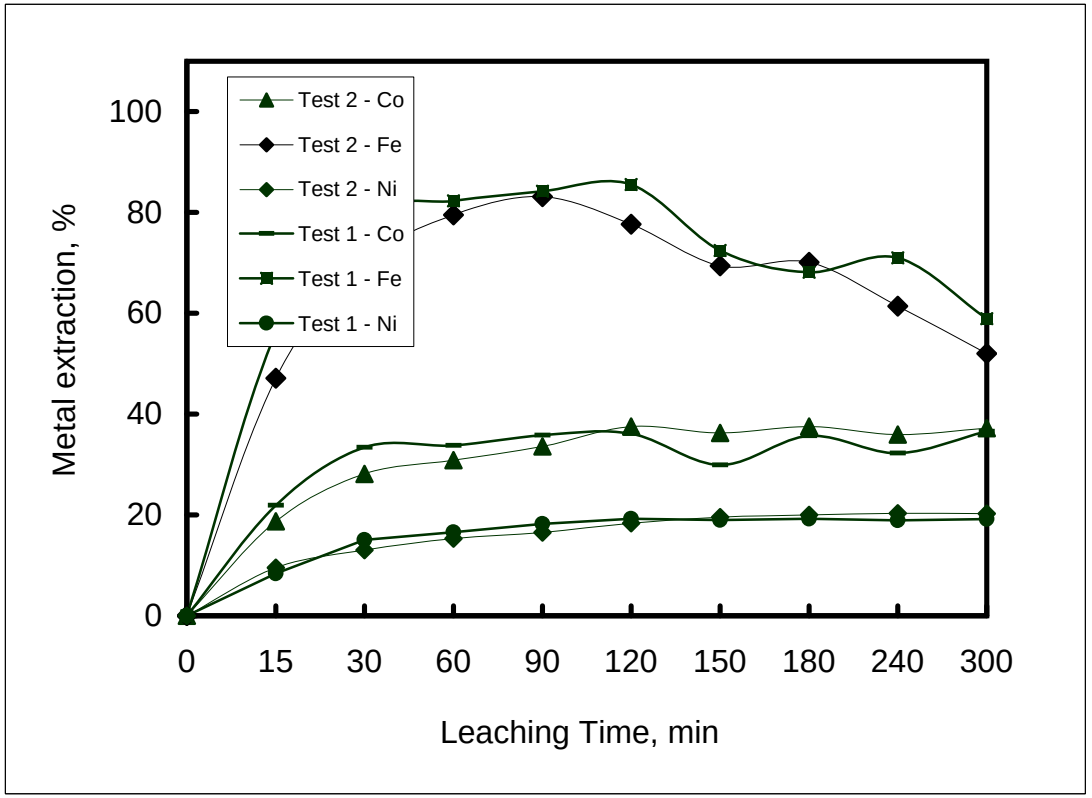

TABLE A2.8: COPPER PRECIPITATION DURING ATMOSPHERIC LEACHING OF THE MATTE AT DIFFERENT STIRRING RATES

Leaching conditions		Feed matte		Feed solution	
Pulp density (kg/L)	1.7	Mass (kg)	1.28	Volume (mL)	1.54
Stirring rate (rpm):	205	Ni (%)	47.98%	Ni (g/L)	24.61
Leaching time (hr):	5 hrs	Cu (%)	31.31	Cu (g/L)	24.95
Matte (kg):	1.28	Co (%)	0.34%	Co (g/L)	0.18
		Fe (%)	0.6%	Fe (g/L)	0.67

Leaching Time (min)	Copper in leach solution, g			Copper precipitation, %		
	145 rpm	205 rpm	400 rpm	145 rpm	205 rpm	400 rpm
0	38.42	38.42	38.42	0.00	0.00	0.00
15	35.81	35.17	32.48	6.81	8.46	15.47
30	29.24	30.01	31.65	23.89	21.88	17.64
60	18.22	22.28	22.05	52.59	42.00	42.61
90	16.02	16.09	17.06	58.32	58.12	55.59
120	13.74	13.48	12.40	64.25	64.93	67.74
150	12.32	9.78	12.35	67.94	74.55	67.86
180	5.93	7.38	6.34	84.57	80.80	83.49
240	4.90	2.00	2.43	87.25	94.79	93.67
300	1.60	0.00	0.00	95.83	100.00	100.00

TABLE A2.9: DETERMINATION OF COPPER CEMENTATION RATE CONSTANTS FOR CEMENTATION REACTION AT DIFFERENT STIRRING RATE VALUES

Leaching conditions			
Pulp density (kg/L)	1.7	Specific surface area of matte, A (cm^2/g)	66982
Stirring rate (rpm):	205	Mass of matte (g):	1276
Leaching time (hr):	5 hrs	Volume of solution (cm^3)	1537
Matte (kg):	1.28	Slope of graph = (KxA) / (2.303V)	

Stirring rate (rpm)	Slope (stage 1)	rate constant K_1 X 10^{-3} (cm / s)
145	0.0037	0.009
205	0.0040	0.010
400	0.0039	0.010

Note: Cementation rate constant obtained from slope of graph in Figure 6.15

TABLE A2.7: COPPER SOLUTION CONCENTRATION DURING ATMOSPHERIC LEACHING OF THE MATTE AT DIFFERENT STIRRING RATES

Leaching conditions		Feed matte		Feed solution	
Temperature (oC):	60	Mass (kg)	1.28	Volume (mL)	1.54
Stirring rate (rpm):	205	Ni (%)	47.98%	Ni	24.61
Pulp density (kg/L):	1.7	Cu (%)	31.31	Cu	24.95
Leaching time (hr):	5 hrs	Co (%)	0.34%	Co	0.18
Matte (kg):	1.28	Fe (%)	0.6%	Fe	0.67

Leaching Time (min)	Copper concentration, g/L			Log $[Cu^{2+}]_t / [Cu2+]_0$		
	145 rpm	205 rpm	400 rpm	145 rpm	205 rpm	400 rpm
0	24.95	24.95	24.95	0	0.00	0.00
15	23.25	22.84	21.09	-0.03	-0.04	-0.07
30	18.99	19.49	20.55	-0.12	-0.11	-0.08
60	11.83	14.47	14.32	-0.32	-0.24	-0.24
90	10.40	10.45	11.08	-0.38	-0.38	-0.35
120	8.92	8.75	8.05	-0.45	-0.46	-0.49
150	8.00	6.35	8.02	-0.49	-0.59	-0.49
180	3.85	4.79	4.12	-0.81	-0.72	-0.78
240	3.18	1.30	1.58	-0.89	-1.28	-1.20
300	1.04	0.00	0.00	-1.38		

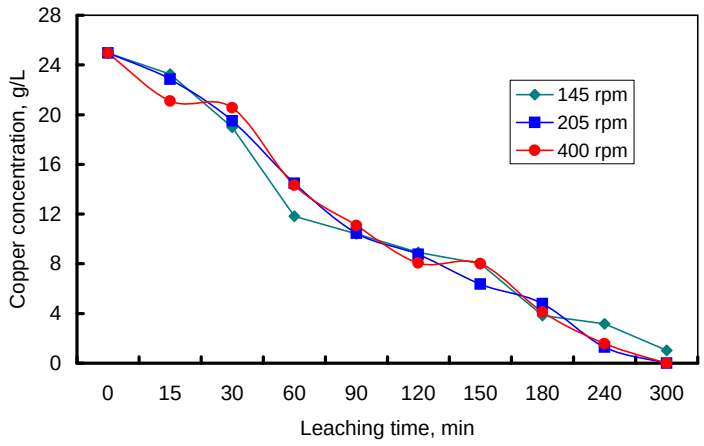

Figure A2.7: Copper concentration as a function of leaching time for the different stirring rates

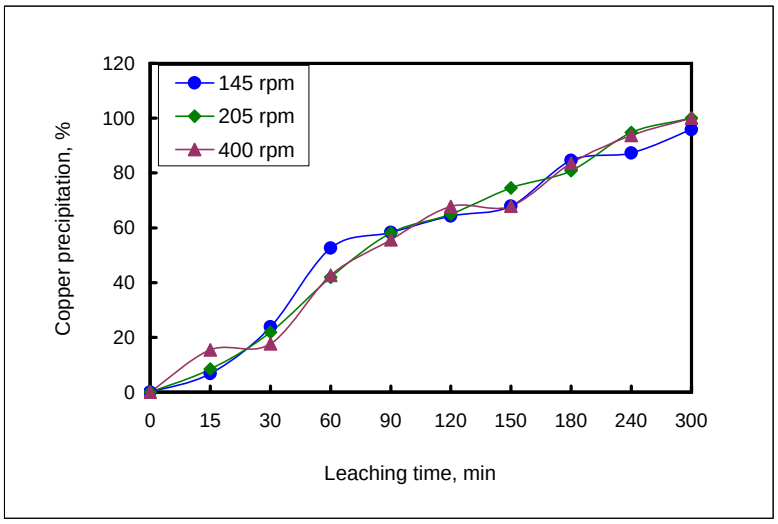
Copper precipitation, %
120
100
80
60
40
20
0
145 rpm
205 rpm
400 rpm
0
15
30
60
90
120
150
180
240
300
Leaching time, min

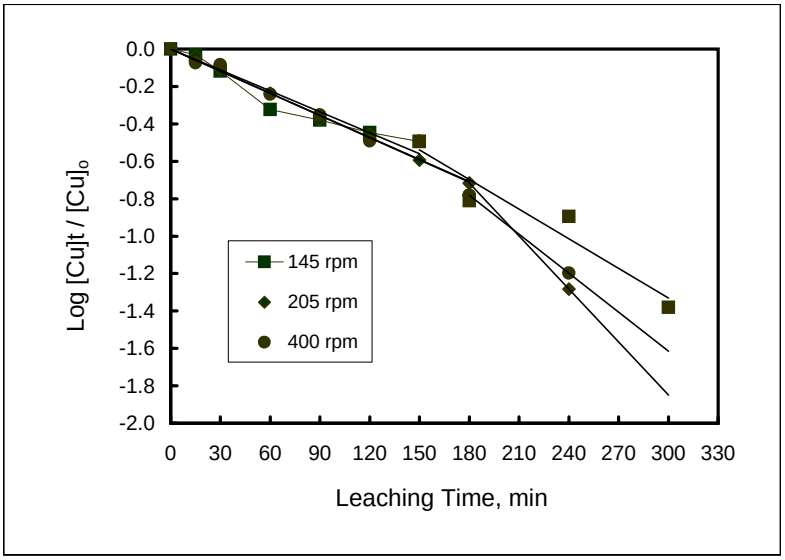
Log [Cu]t / [Cu]o
0.0
-0.2
-0.4
-0.6
-0.8
-1.0
-1.2
-1.4
-1.6
-1.8
-2.0
145 rpm
205 rpm
400 rpm
0
30
60
90
120
150
180
210
240
270
300
330
Leaching Time, min

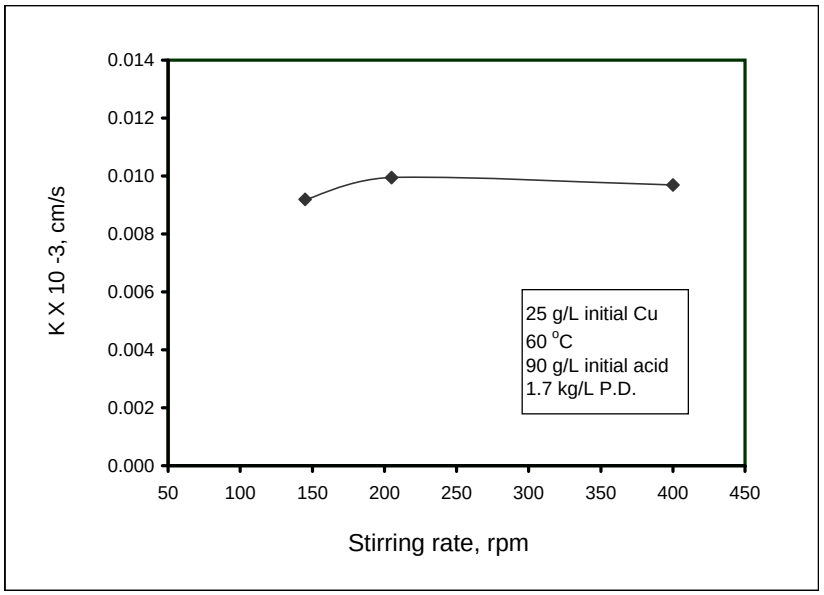
K X 10 -3, cm/s
0.014
0.012
0.010
0.008
0.006
0.004
0.002
0.000
25 g/L initial Cu
60 °C
90 g/L initial acid
1.7 kg/L P.D.
50
100
150
200
250
300
350
400
450
Stirring rate, rpm

TABLE A2.1: METAL SOLUTION CONCENTRATIONS DURING ATMOSPHERIC LEACHING OF THE MATTE AT A STIRRING RATE OF 145 RPM

Leaching conditions:

Temperature: (^{o} C)	60
Mixing rate (rpm):	145
Pulp density (kg/L):	1.7
Leaching time (hrs):	5

Leaching Time (min)	Co (g/l)	Fe (g/l)	Ni (g/l)	Cu (g/l)	pH
0	0.18	0.67	24.61	24.95	0.46
15	0.82	1.68	59.55	19.25	1.37
30	0.83	3.09	62.67	18.99	1.46
60	0.82	3.37	62.90	11.83	1.48
90	0.89	3.56	69.78	10.40	1.50
120	0.95	3.62	73.41	7.92	1.56
150	1.01	4.01	70.61	8.00	1.62
180	0.98	4.19	75.56	3.85	1.59
240	0.91	4.23	76.18	3.18	1.67
300	1.05	4.22	74.39	1.04	1.70

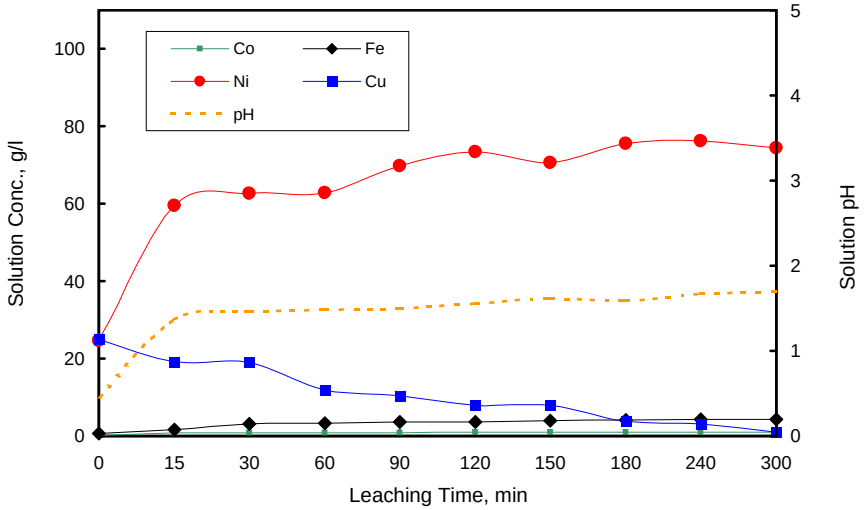

Figure A2.1: Metal concentrations as a function of leaching time at a stirring rate of 145 rpm

TABLE A2.2: METAL EXTRACTIONS BASED ON SOLUTION CONCENTRATIONS DURING ATMOSPHERIC LEACHNG OF THE MATTE AT A STIRRING RATE OF 145 RPM

Leaching conditions:	Temperature (o C):	60			
	Mixing rate (rpm):	145			
	Pulp density (kg/L):	1.7	Metal content of matte		
	Leaching time (hrs):	5	Ni	614.14 g	(47.98%)
	Matte (kg):	1.28	Co	4.35 g	(0.34%)
	Solution (L):	1.54	Fe	7.68 g	(0.6%)

Leaching Time (min)	Ni (g/l)	Ni (g)	Ni Leach %	Co (g/l)	Co (g)	Co leach %	Fe (g/l)	Fe (g)	Fe %
0	24.61	37.90	0.00	0.18	0.28	0	0.67	1.03	0
15	59.55	91.71	8.76	0.82	1.26	22.65	1.68	2.59	20.25
30	62.67	96.43	9.53	0.83	1.28	23.13	3.09	4.72	48.07
60	62.90	96.78	9.59	0.82	1.26	22.66	3.37	5.14	53.50
90	69.78	107.03	11.26	0.89	1.37	25.01	3.56	5.42	57.12
120	73.41	112.26	12.11	0.95	1.45	27.00	3.62	5.51	58.25
150	70.61	108.30	11.46	1.01	1.54	28.95	4.01	6.06	65.43
180	75.56	115.18	12.58	0.98	1.50	27.99	4.19	6.31	68.69
240	76.18	116.03	12.72	0.91	1.40	25.79	4.23	6.36	69.40
300	74.39	113.63	12.33	1.05	1.59	30.10	4.22	6.35	69.23

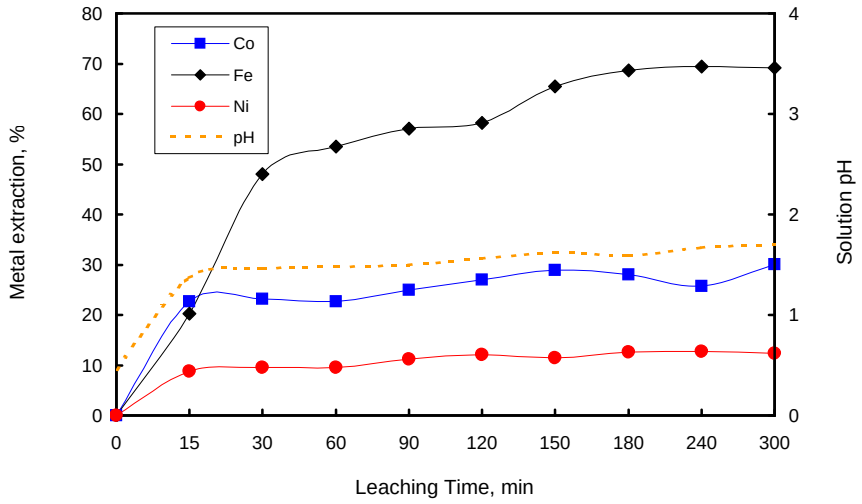

Fig.ure A2.2: Metal extraction as a function of leaching time at a stirring rate 145 rpm

TABLE A3.5: METAL SOLUTION CONCENTRATIONS DURING ATMOSPHERIC LEACHING OF THE MATTE AT A PULP DENSITY OF 1.75 kg/L

Leaching conditions:	Temperature: (o C)	60
	Mixing rate (rpm):	205
	Pulp density (kg/L):	1.75
	Leaching time (hrs):	5

Leaching Time (min)	Co (g/l)	Fe (g/l)	Ni (g/l)	Cu (g/l)	pH
0	0.18	0.67	24.61	24.95	0.75
15	0.95	3.72	66.27	24.16	1.75
30	1.00	3.90	72.58	20.31	1.78
60	1.07	4.11	79.87	15.75	1.90
90	1.15	4.35	86.34	11.90	2.26
120	1.14	4.26	87.00	8.94	2.34
150	1.19	4.36	91.11	7.44	2.40
180	1.19	4.35	93.53	5.12	2.74
240	1.21	4.39	96.98	2.98	3.31
300	1.25	4.33	100.51	0.25	5.09

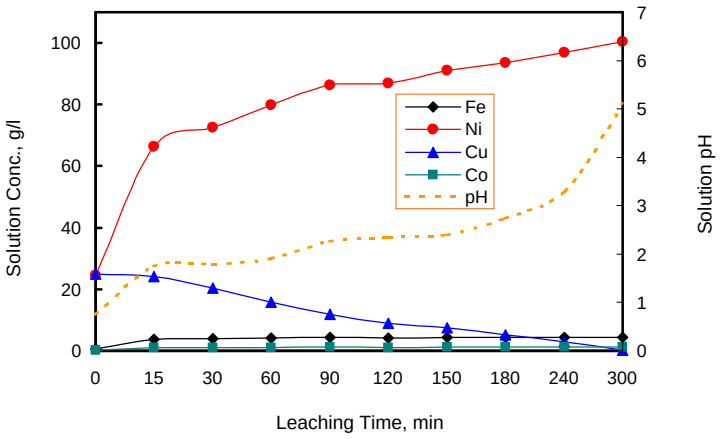

Figure A3.5: Metal concentration as a function of leaching tim at a pulp density of 1.75Kg/L

TABLE A3.6: METAL EXTRACTION BASED ON SOLUTION CONCENTRATIONS DURING ATMOSPHERIC LEACHING OF THE MATTE AT AT A PULP DENSITY OF 1.75 kg/L

Leaching conditions:			Metal content of matte:		
	Temperature (o C):	60			
	Mixing rate (rpm):	205	Ni	719.70 g	(47.98%)
	Pulp density (kg/L):	1.75	Co	5.10 g	(0.34%)
	Leaching time (hrs):	5	Fe	9.00 g	(0.6%)
	Matte (kg):	1.5			
	Solution (L):	1.69			

Leaching Time (min)	Ni (g/l)	Ni (g)	Ni Leach %	Co (g/l)	Co (g)	Co leach %	Fe (g/l)	Fe (g)	Fe Leach %
0	24.61	41.59	0.00	0.18	0.30	0	0.67	1.13	0
15	66.27	112.00	9.78	0.95	1.61	25.52	3.72	6.29	57.27
30	72.58	121.46	11.10	1.00	1.69	27.15	3.90	6.59	60.60
60	79.87	133.26	12.74	1.07	1.80	29.40	4.11	6.93	64.43
90	86.34	143.53	14.16	1.15	1.93	31.93	4.35	7.32	68.74
120	87.00	144.41	14.29	1.14	1.92	31.62	4.26	7.18	67.15
150	91.11	150.83	15.18	1.19	2.00	33.15	4.36	7.33	68.88
180	93.53	154.45	15.68	1.19	2.00	33.15	4.35	7.32	68.71
240	96.98	159.62	16.40	1.21	2.03	33.75	4.39	7.38	69.39
300	100.51	164.79	17.12	1.25	2.09	34.92	4.33	7.29	68.39

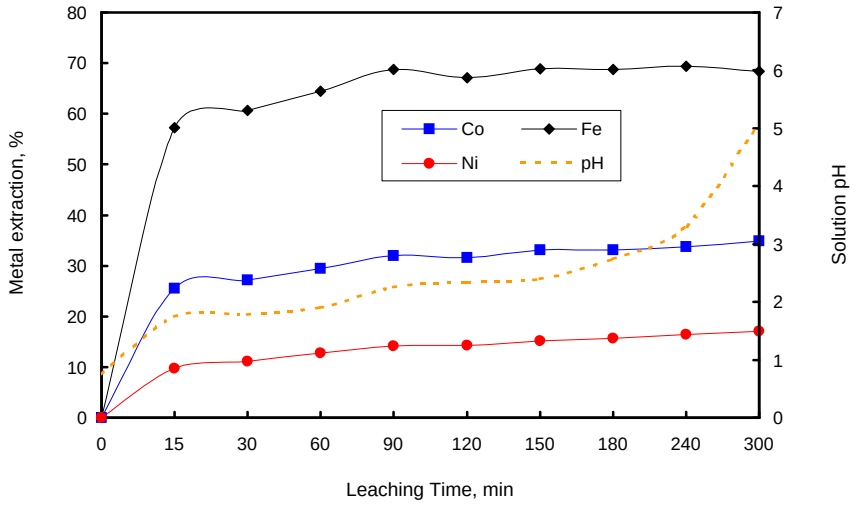

Figure A3.6: Metal extraction as a function of leaching time at a pulp density o 1.75 kg/L

TABLE A3.1: METAL SOLUTION CONCENTRATIONS DURING ATMOSPHERIC LEACHING OF THE MATTE AT A PULP DENSITY OF 1.6 kg/L

Leaching conditions:	Temperature: (o C)	60
	Mixing rate (rpm):	205
	Pulp density (kg/L):	1.6
	Leaching time (hrs):	5

Leaching Time (min)	Co (g/l)	Fe (g/l)	Ni (g/l)	Cu (g/l)	pH
0	0.18	0.67	24.61	24.95	0.75
15	0.88	3.62	64.13	26.11	1.32
30	0.96	3.79	66.22	22.33	1.32
60	0.94	3.90	69.05	18.42	1.36
90	0.96	4.02	72.90	16.12	1.40
120	0.96	4.01	73.46	14.21	1.34
150	0.96	4.01	74.46	12.87	1.37
180	1.03	4.03	81.89	11.98	1.39
240	1.00	4.05	84.17	9.97	1.40
300	1.05	4.06	86.52	8.15	1.45

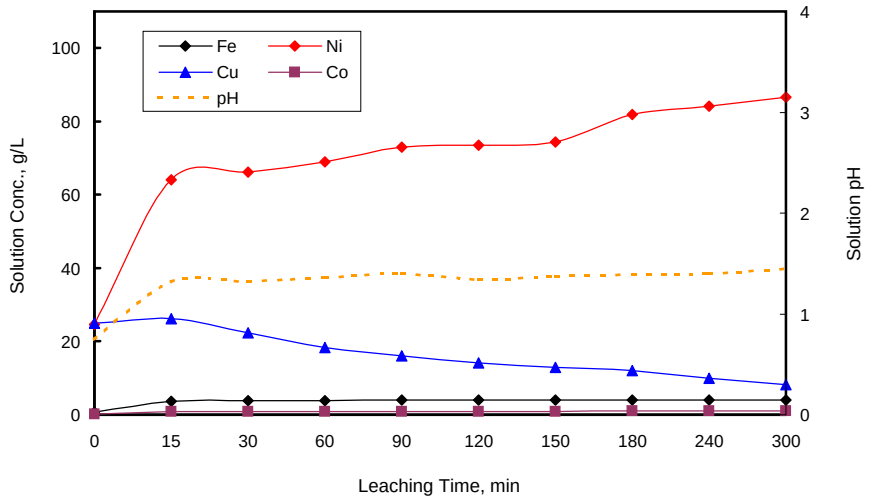

Figure A3.1: Metal concentration as a function of leaching time at a pulp density of 1.6Kg/L

TABLE A3.2: METAL EXTRACTION BASED ON SOLUTION CONCENTRATIONS DURING ATMOSPHERIC LEACHING OF THE MATTE AT A PULP DENSITY OF 1.6 kg/L

Leaching conditions:			Metal content of matte:		
	Temperature (o C):	60			
	Mixing rate (rpm):	205	Ni	532.58 g	(47.98%)
	Pulp density (kg/L):	1.6	Co	3.77 g	(0.34%)
	Leaching time (hrs):	5	Fe	6.66 g	(0.6%)
	Matte (kg):	1.11			
	Solution (L):	1.78			

Leaching Time (min)	Ni (g/l)	Ni (g)	Ni Leach %	Co (g/l)	Co (g)	Co leach %	Fe (g/l)	Fe (g)	Fe Leach %
0	24.61	43.81	0.00	0.18	0.32	0	0.67	1.19	0
15	64.13	114.15	13.21	0.88	1.57	33.02	3.62	6.44	78.84
30	66.22	116.83	13.71	0.96	1.71	36.74	3.79	6.74	83.32
60	69.05	121.68	14.62	0.94	1.67	35.82	3.90	6.93	86.18
90	72.90	128.17	15.84	0.96	1.71	36.72	4.02	7.14	89.25
120	73.46	129.01	16.00	0.96	1.71	36.72	4.01	7.12	89.00
150	74.46	130.65	16.31	0.96	1.71	36.72	4.01	7.12	89.00
180	81.89	142.74	18.58	1.03	1.82	39.75	4.03	7.15	89.52
240	84.17	146.21	19.23	1.00	1.77	38.47	4.05	7.19	90.01
300	86.52	149.87	19.92	1.05	1.85	40.56	4.06	7.20	90.21

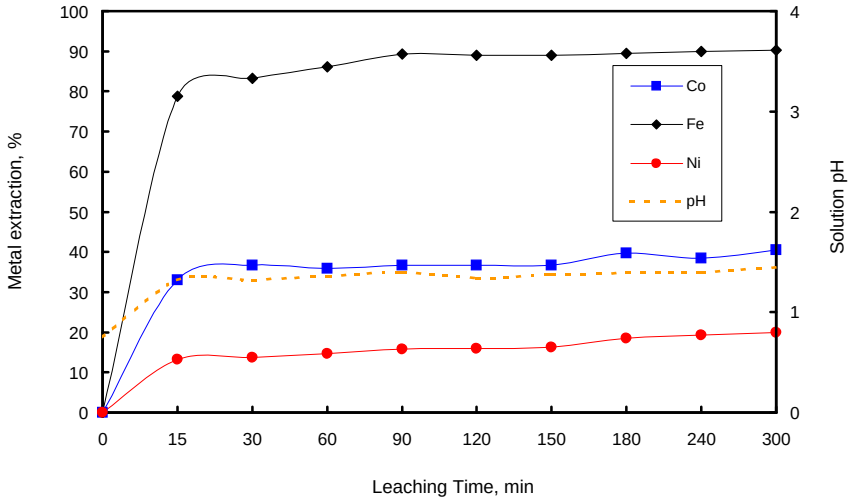

Figure A3.2: Metal extraction as a function of leaching time at a pulp density of 1.6 kg/L

TABLE A3.3: METAL SOLUTION CONCENTRATIONS DURING ATMOSPHERIC LEACHING OF THE MATTE AT A PULP DENSITY OF 1.7 kg/L

Leaching conditions: Temperature: 60 °C
Agitation: 205 rpm
Pulp density: 1.7 kg/L

Leaching Time (min)	Co (g/l)	Fe (g/l)	Ni (g/l)	Cu (g/l)	pH
0	0.18	0.67	24.61	0.67	0.97
15	0.77	3.35	64.11	3.35	1.10
30	0.79	3.44	66.16	3.44	1.11
60	0.80	3.68	68.85	3.68	1.18
90	0.79	3.80	71.18	3.80	1.28
120	0.91	3.91	78.69	3.91	1.34
150	0.88	3.96	80.00	3.96	1.43
180	0.96	4.05	86.80	4.05	1.51
240	0.91	4.08	88.33	4.08	1.61
300	1.01	4.24	94.44	4.24	1.90

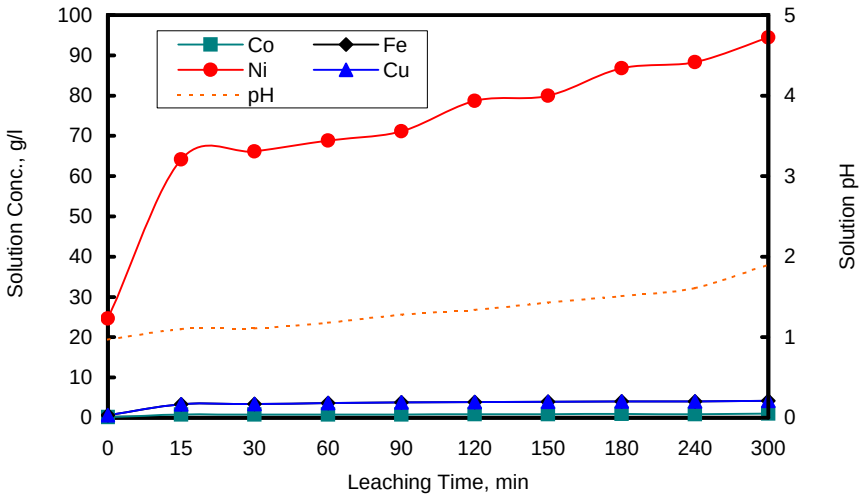

Fig. A3.3: Metal concentrations as a function of leaching time at pulp density of 1.7 kg/L

TABLE A3.4: METAL EXTRACTIONS BASED ON SOLUTION CONCENTRATIONS DURING ATMOSPHERIC LEACHING OF THE MATTE AT A PULP DENSITY OF 1.7 kg/L

Leaching conditions:	Temperature:	60 oC		Metal content of matte:		
	Agitation:	205 rpm		Ni	612.22 g	(47.98%)
	Pulp density:	1.7 kg/L		Co	4.34 g	(0.34 %)
	Matte:	1.28	kg	Fe	7.66 g	(0.60 %)
	Solution:	1.54	L			

Leaching Time (min)	**Ni (g/l)**	**Ni (g)**	**Ni Leach %**	**Co (g/l)**	**Co (g)**	**Co leach %**	**Fe (g/l)**	Fe (g)	Fe (%)
0	24.61	37.83	0.00	0.18	0.28	0	0.67	1.03	0
15	64.11	98.54	9.92	0.77	1.18	20.90	3.35	5.15	53.80
30	66.16	101.64	10.42	0.79	1.21	21.60	3.44	5.29	55.58
60	68.85	105.71	11.09	0.80	1.23	21.94	3.68	5.64	60.24
90	71.18	109.17	11.65	0.79	1.21	21.61	3.80	5.82	62.61
120	78.69	119.96	13.42	0.91	1.39	25.58	3.91	5.98	64.60
150	80.00	121.81	13.72	0.88	1.34	24.60	3.96	6.05	65.52
180	86.80	131.24	15.26	0.96	1.46	27.16	4.05	6.17	67.15
240	88.33	133.33	15.60	0.91	1.39	25.59	4.08	6.21	67.69
300	94.44	141.49	16.93	1.01	1.52	28.67	4.24	6.43	70.48
300									

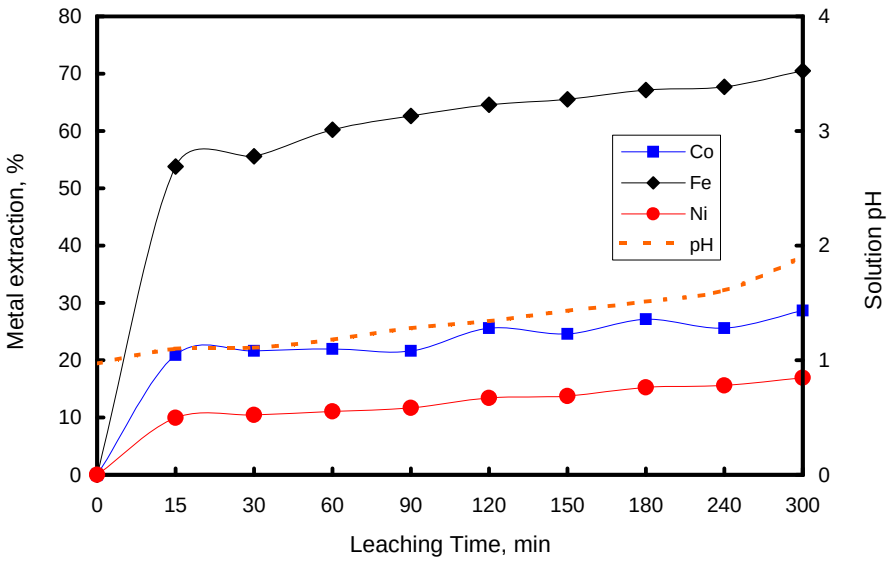

Figure A3.4: Metal extractions as a function of leaching time at pulp density of 1.7 kg/L

TABLE A1.3B: METAL SOLUTION CONCENTRATIONS DURING ATMOSPHERIC LEACHING OF THE MATTE AT A TEMPERATURE OF 60 ^{O} C - SECOND TEST

Leaching conditions: Temperature: 60 ^{o}C
Agitation: 205 rpm
Pulp density: 1.7 kg/L

Leaching Time (min)	Co (g/L)	Fe (g/L)	Ni (g/L)	Cu (g/L)
0	0.17	0.67	24.61	24.95
15	0.67	3.21	54.21	21.14
30	0.76	3.54	69.75	19.58
60	0.79	3.78	70.85	16.57
90	0.76	3.89	74.16	12.25
120	0.81	3.96	77.61	8.15
150	0.79	3.96	82.16	5.87
180	0.98	4.08	88.68	4.09
240	0.97	4.18	89.32	0.92
300	1.06	4.34	99.69	0.00

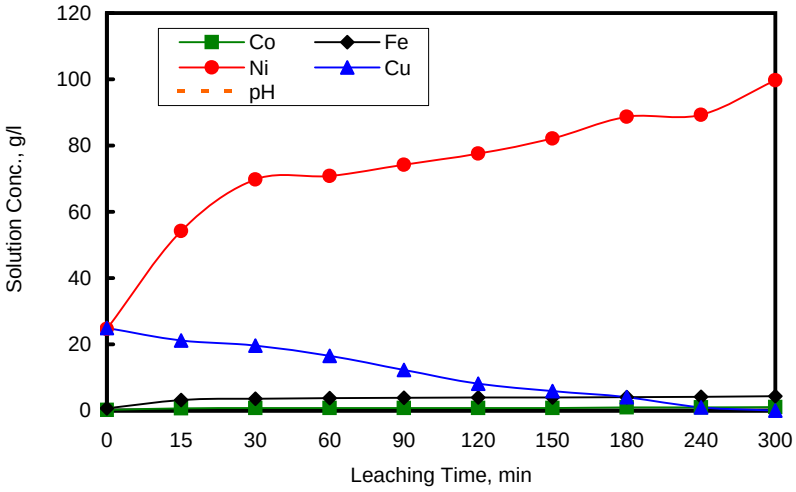

Fig. A1.3B: Metal concentrations as a function of leaching time at 60 ^{o} C - Second test

TABLE A1.4B: METAL EXTRACTIONS BASED ON SOLUTION CONCENTRATIONS DURING ATMOSPHERIC LEACHIN
OF THE MATTE AT A TEMPERATURE OF 60 ^{O} C

Leaching conditions:	Temperature:	60 oC		Metal content of matte:		
	Agitation:	205 rpm		Ni	612.22 g	(47.98%)
	Pulp density:	1.7 kg/L		Co	4.34 g	(0.34 %)
	Matte:	1.28	kg	Fe	7.66 g	(0.60 %)
	Solution:	1.54	L			

Leaching Time (min)	**Ni (g/L)**	**Ni (g)**	**Ni Leach %**	**Co (g/L)**	**Co (g)**	**Co leach %**	**Fe (g/L)**	Fe (g)	Fe (%)
0	24.61	37.83	0.00	0.17	0.26	0	0.67	1.03	0
15	54.21	83.32	7.43	0.67	1.03	17.78	3.21	4.93	50.99
30	69.75	106.82	11.27	0.76	1.17	20.92	3.54	5.43	57.51
60	70.85	108.48	11.54	0.79	1.21	21.95	3.78	5.79	62.17
90	74.16	113.41	12.35	0.76	1.17	20.90	3.89	5.95	64.27
120	77.61	118.36	13.15	0.81	1.24	22.59	3.96	6.05	65.59
150	82.16	124.78	14.20	0.79	1.21	21.94	3.96	6.05	65.59
180	88.68	133.83	15.68	0.98	1.47	28.02	4.08	6.22	67.76
240	89.32	134.70	15.82	0.97	1.46	27.70	4.18	6.35	69.54
300	99.69	148.56	18.09	1.06	1.58	30.48	4.34	6.57	72.33
Solid analysis									

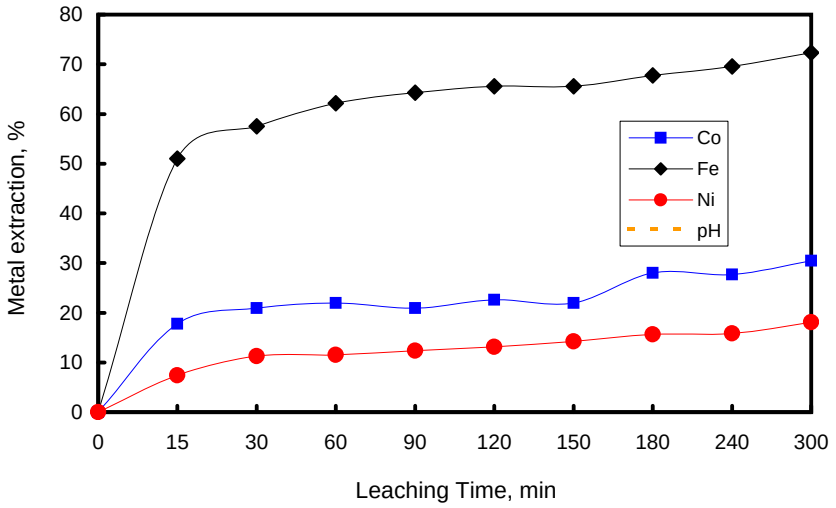

Figure A1.4B: Metal extractions as a function of leaching time at 60 ^{o} C - second test

Comparison of metal leaching at PD of 1.7 g/L

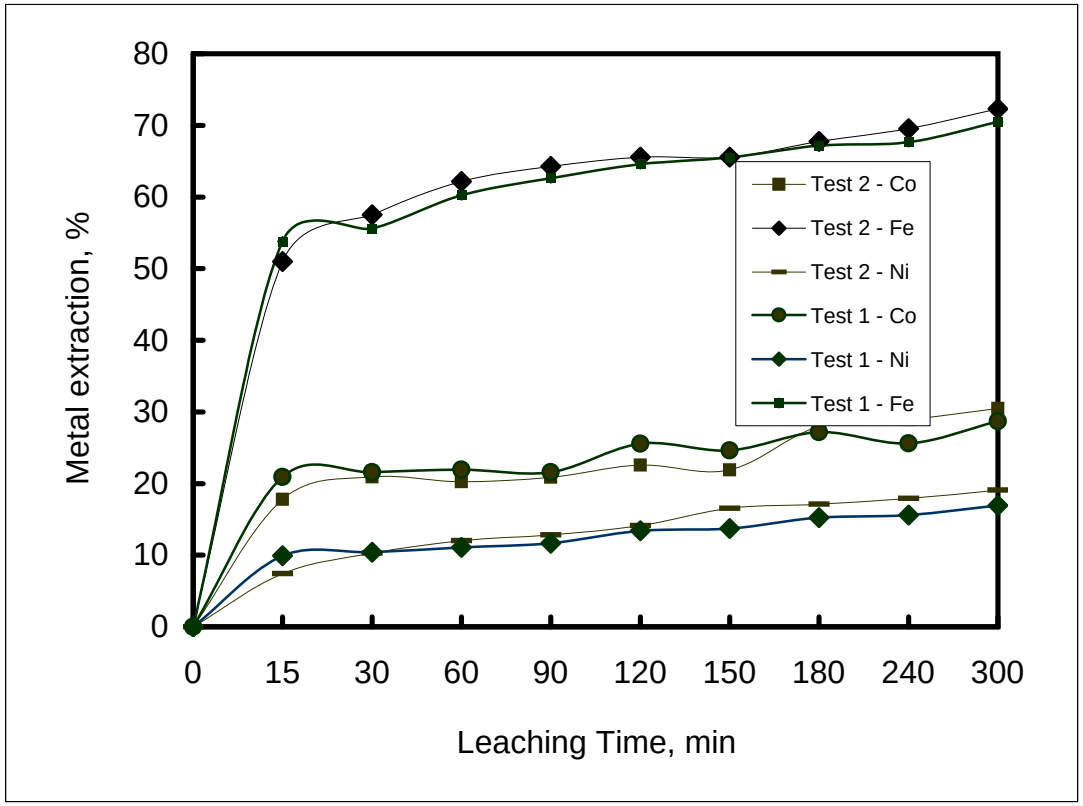

TABLE A3.8: COPPER SOLUTION CONCENTRATION DURING ATMOSPHERIC LEACHING OF THE MATTE AT DIFFERENT PULP DENSITIES

Leaching conditions		Feed matte		Feed solution	
Temperature (oC):	60	Mass (kg)	1.28	Volume (mL)	1.54
Stirring rate (rpm):	205	Ni (%)	47.98%	Ni (g/L)	24.61
Leaching time (hr):	5	Cu (%)	31.31	Cu (g/L)	24.95
Matte (kg):	1.28	Co (%)	0.34%	Co (g/L)	0.18
		Fe (%)	0.6%	Fe (g/L)	0.67

Leaching Time (min)	Copper in leach solution, g			Copper precipitation, %		
	1.6 kg/L P.D.	1.7 kg/L P.D.	1.75 kg/L P.D.	1.6 kg/L P.D.	1.7 kg/L P.D.	1.75 kg/L P.D.
0	38.42	38.42	38.42	0.00	0.00	0.00
15	35.59	35.17	37.21	7.37	8.46	3.17
30	34.39	30.01	31.28	10.50	21.88	18.60
60	28.37	22.28	24.32	26.17	42.00	36.71
90	24.82	16.09	18.33	35.39	58.12	52.30
120	21.88	13.48	13.77	43.05	64.93	64.17
150	19.82	9.84	11.46	48.42	74.39	70.18
180	18.45	7.38	10.96	51.98	80.80	71.46
240	15.35	2.00	4.59	60.04	94.79	88.06
300	12.55	0.00	0.00	67.33	100.00	100.00

TABLE A3.9: DETERMINATION OF COPPER CEMENTATION RATE CONSTANTS FOR CEMENTATION REACTION AT DIFFERENT PULP DENSITY VALUES

Leaching conditions

Temperature (oC):	60	Specific surface area of matte, A (cm^2/g)	66982
Stirring rate (rpm):	205	Mass of matte (g):	1276
Leaching time (hr):	5 hrs	Volume of solution (cm^3)	1537
Matte (kg):	1.28	Slope of graph = (KxA) / (2.303V)	

Pulp density (kg/L)	Slope (stage 1)	rate constant K_1 X 10^{-3} (cm / s)
1.6	0.0017	0.004
1.7	0.0039	0.010
1.75	0.0033	0.008

Note: Cementation rate constant obtained from slope of graph in Figure 6.22

TABLE A3.7: COPPER SOLUTION CONCENTRATION DURING ATMOSPHERIC LEACHING OF THE MATTE AT DIFFERENT PULP DENSITIES

Leaching conditions		Feed matte		Feed solution	
Temperature (oC):	60	Mass (kg)	1.28	Volume (mL)	1.54
Stirring rate (rpm):	205	Ni (%)	47.98%	Ni	24.61
Leaching time (hr):	5 hrs	Cu (%)	31.31	Cu	24.95
Matte (kg):	1.28	Co (%)	0.34%	Co	0.18
		Fe (%)	0.6%	Fe	0.67

Leaching Time (min)	Copper Concentration, g/L			Log $[Cu^{2+}]_t / [Cu2+]_0$		
	1.6 kg/L P.D.	1.7 kg/L P.D.	1.75 kg/L P.D.	1.6 kg/L P.D.	1.7 kg/L P.D.	1.75 kg/L P.D.
0	24.95	24.95	24.95	0.00	0.00	0.00
15	23.11	22.84	24.16	-0.03	-0.04	-0.01
30	22.33	19.49	20.31	-0.05	-0.11	-0.09
60	18.42	14.47	15.79	-0.13	-0.24	-0.20
90	16.12	10.45	11.90	-0.19	-0.38	-0.32
120	14.21	8.75	8.94	-0.24	-0.46	-0.45
150	12.87	6.39	7.44	-0.29	-0.59	-0.53
180	11.98	4.79	7.12	-0.32	-0.72	-0.54
240	9.97	1.30	2.98	-0.40	-1.28	-0.92
300	8.15	0.00	0.00	-0.49		

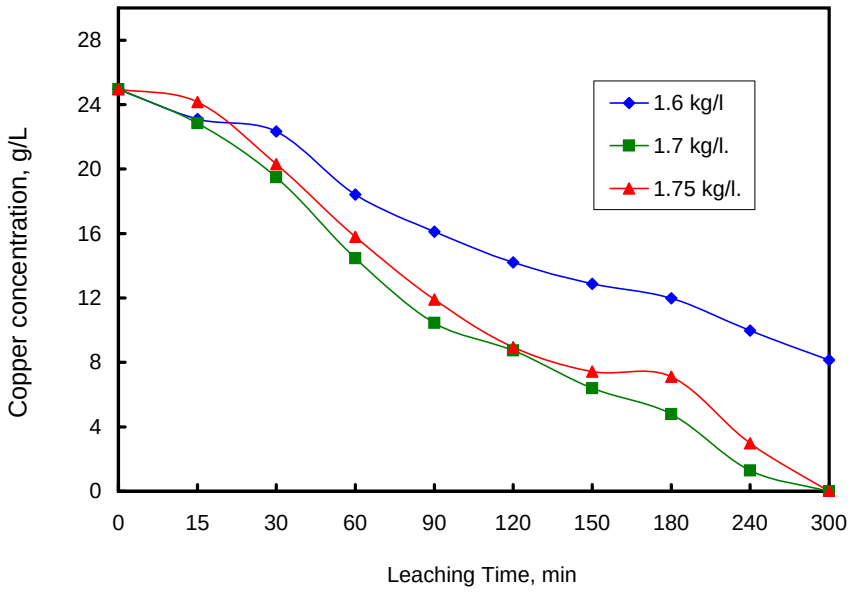

Figure A3.7 copper concentration as a function of leaching time for the different pulp densities (205 rpm, 25 g/L initial Cu, 90 g/L initial acid)

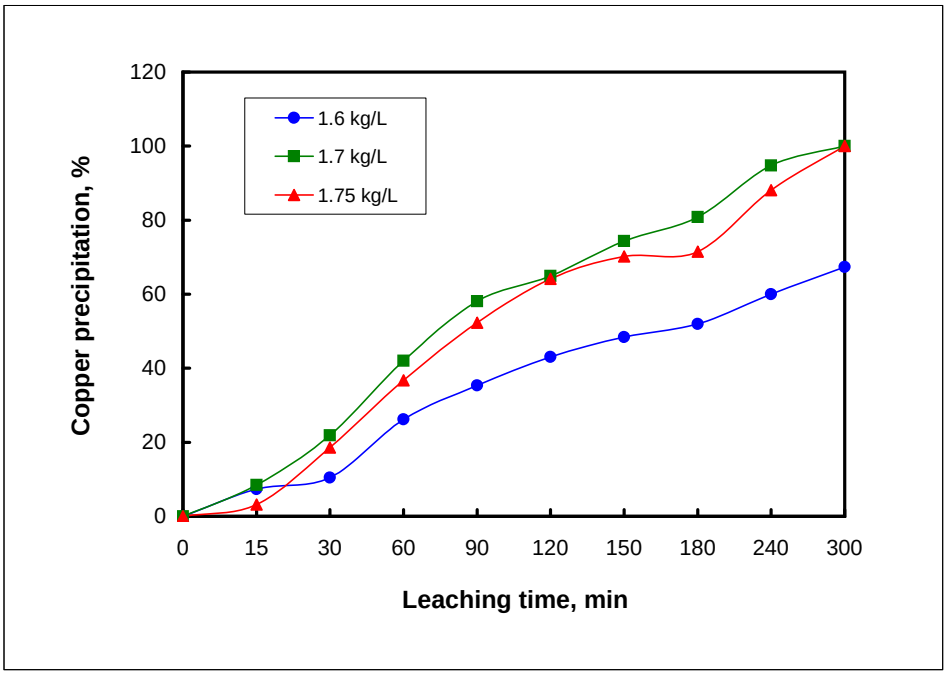
Copper precipitation, %
120
100
80
60
40
20
0
1.6 kg/L
1.7 kg/L
1.75 kg/L
0
15
30
60
90
120
150
180
240
300
Leaching time, min

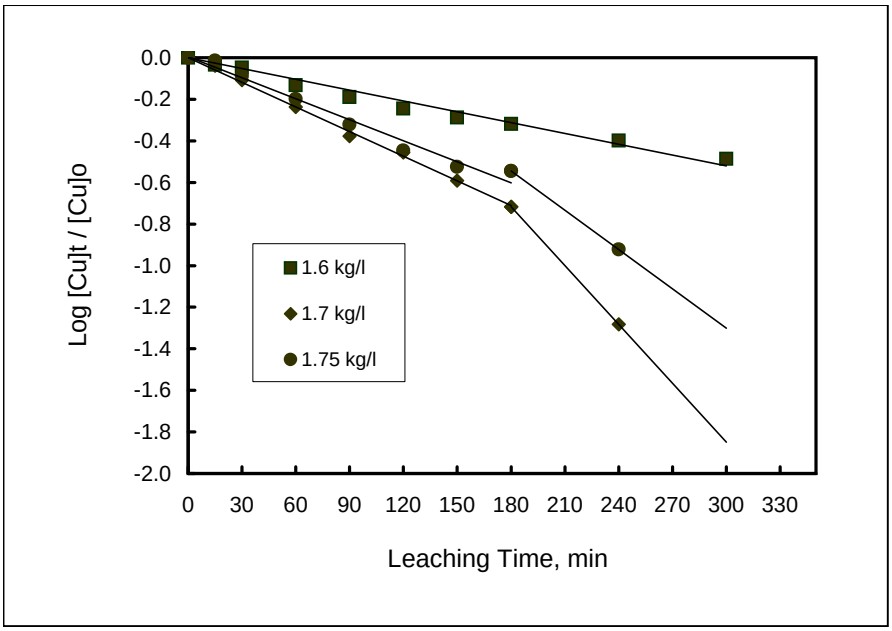
Log [Cu]t / [Cu]o
0.0
-0.2
-0.4
-0.6
-0.8
-1.0
-1.2
-1.4
-1.6
-1.8
-2.0
1.6 kg/l
1.7 kg/l
1.75 kg/l
0
30
60
90
120
150
180
210
240
270
300
330
Leaching Time, min

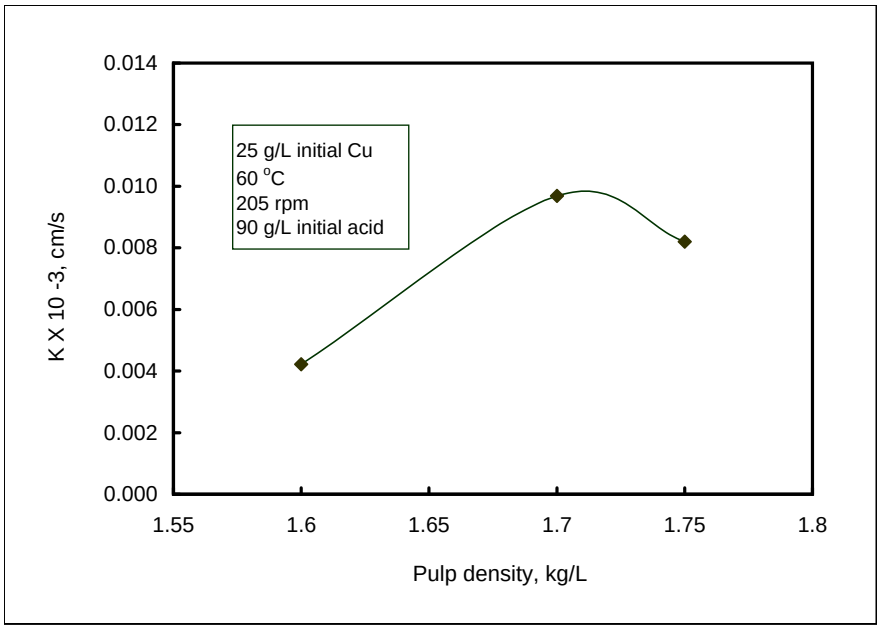
0.014
0.012
0.010
0.008
0.006
0.004
0.002
0.000
K X 10 -3, cm/s
25 g/L initial Cu
60 °C
205 rpm
90 g/L initial acid
1.55
1.6
1.65
1.7
1.75
1.8
Pulp density, kg/L

TABLE A 2.5B: METAL SOLUTION CONCENTRATIONS DURING ATMOSPHERIC LEACHING OF THE MATTE AT A STIRRING RATE OF 400 RPM - SECOND TEST

Leaching conditions:

Temperature: (°C)	60
Mixing rate (rpm):	400
Pulp density (kg/L):	1.7
Leaching time (hrs):	5

Leaching Time (min)	Co (g/L)	Fe (g/L)	Ni (g/L)	Cu (g/L)
0	0.18	0.67	24.61	24.95
15	0.71	3.02	62.55	20.48
30	0.98	4.18	76.65	18.57
60	1.06	4.67	85.97	15.05
90	1.14	4.86	91.03	12.03
120	1.26	4.57	98.87	9.64
150	1.12	4.12	102.23	5.78
180	1.86	4.16	101.98	6.09
240	1.21	3.07	102.55	3.18
300	1.25	3.13	101.96	0.00

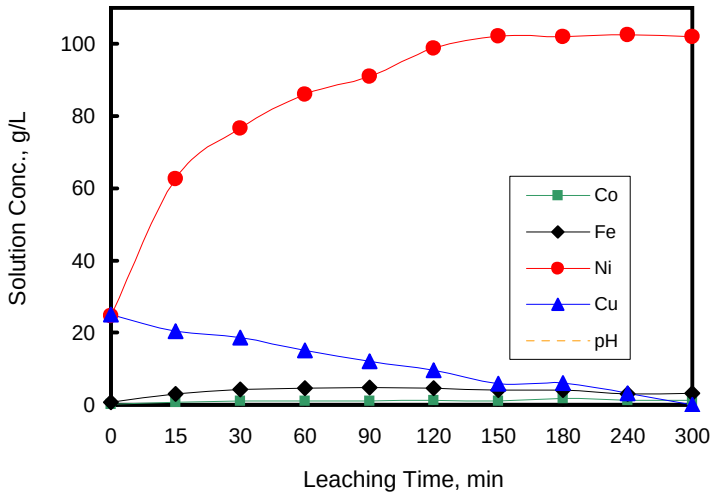

Figure A2.5B: Metal concentrations as a function of leaching time at a stirring rate of 400 rpm - second test

TABLE A2.6B: METAL EXTRACTIONS BASED ON SOLUTION CONCENTRATIONS DURING ATMOSPHERIC LEACHNG OF THE MATTE AT A MIXING RATE OF 400 RPM - SECOND TEST

Leaching conditions:

Temperature (o C):	60
Mixing rate (rpm):	400
Pulp density (kg/L):	1.7
Leaching time (hrs):	5
Matte (kg):	1.28
Solution (L):	1.54

Metal content of matte

Ni	614.14 g	(47.98%)
Co	4.35 g	(0.34%)
Fe	7.68 g	(0.6%)

Leaching Time (min)	Ni (g/L)	Ni (g)	Ni Leach %	Co (g/L)	Co (g)	Co leach %	Fe (g/L)	Fe (g)	Fe leach %
0	24.61	37.90	0.00	0.18	0.28	0	0.67	1.03	0
15	62.55	96.33	9.51	0.71	1.09	18.75	3.02	4.65	47.12
30	76.65	117.69	12.99	0.98	1.50	28.15	4.18	6.41	70.01
60	85.97	131.81	15.29	1.06	1.62	30.89	4.67	7.14	79.51
90	91.03	139.35	16.52	1.14	1.74	33.59	4.86	7.42	83.14
120	98.87	150.64	18.36	1.26	1.91	37.56	4.57	7.00	77.70
150	102.23	155.39	19.13	1.12	1.71	33.00	4.12	6.36	69.41
180	101.98	155.04	19.07	1.16	1.77	34.28	4.16	6.42	70.13
240	102.55	155.82	19.20	1.21	1.84	35.85	3.07	4.93	50.76
300	101.96	155.03	19.07	1.25	1.89	37.08	3.13	5.01	51.81

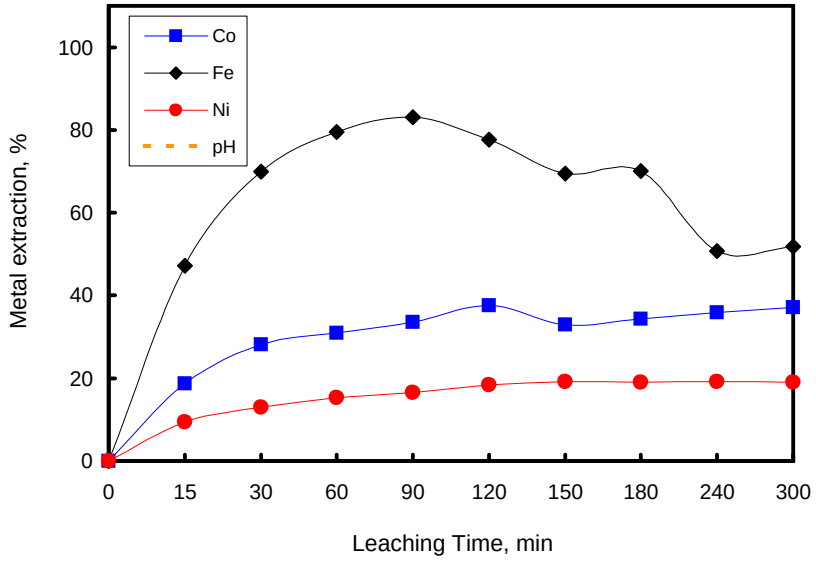

Figure A2.6B: Metal extractions as a function of leaching time at a stirring rate of 400 rpm - Second test

TABLE A4.5: METAL SOLUTION CONCENTRATIONS DURING ATMOSPHERIC LEACHING OF THE -300 +150 MICRONS SIZE FRACTION OF THE MATTE

Leaching conditions:	Temperature: (^{o} C)	60
	Mixing rate (rpm):	205
	Pulp density (kg/L):	1.7
	Leaching time (hrs):	5

Leaching Time (min)	Co (g/l)	Fe (g/l)	Ni (g/l)	Cu (g/l)	pH
0	0.18	0.67	24.61	24.95	0.25
15	0.95	4.17	63.20	22.46	0.60
30	0.99	4.66	67.73	19.15	0.63
60	1.02	4.86	79.68	18.53	0.64
90	0.99	4.88	80.18	17.65	0.66
120	1.00	4.89	81.35	16.42	0.68
150	0.99	4.91	82.77	14.90	0.70
180	1.00	4.95	84.69	13.70	0.71
240	1.04	5.00	87.13	12.56	0.74
300	1.09	5.05	91.57	10.38	0.75

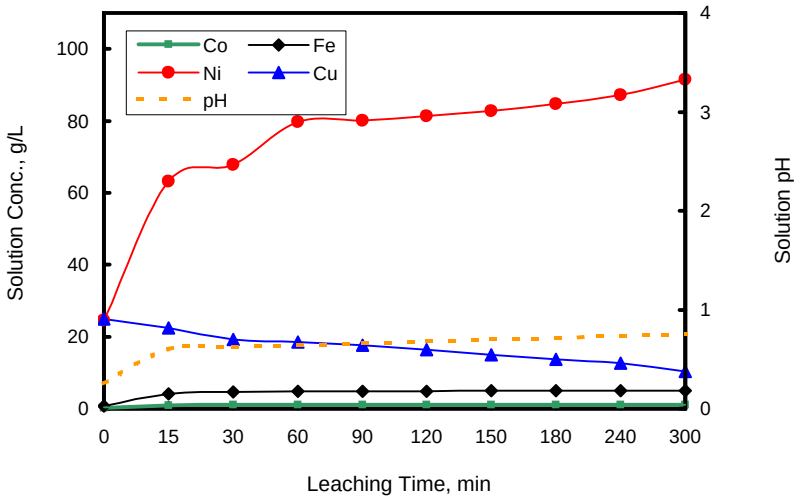

Figure A4.5: Metal concentrations as a function of leaching time fc
the -300 +150 microns size fraction of the matte

TABLE A4.6: METAL EXTRACTIONS BASED ON SOLUTION CONCENTRATIONS DURING ATMOSPHERIC LEACHNG OF THE -300+150 MICRONS SIZE FRACTION OF THE MATTE

Leaching conditions:

Temperature (o C):	60
Mixing rate (rpm):	205
Pulp density (kg/L):	1.7
Leaching time (hrs):	5
Matte (kg):	1.28
Solution (L):	1.54

Metal content of matte:

Ni	614.14 g	(47.98%)
Co	4.35 g	(0.34%)
Fe	7.68 g	(0.6%)

Leaching Time (min)	Ni (g/l)	Ni (g)	Ni Leach %	Co (g/l)	Co (g)	Co leach %	Fe (g/l)	Fe (g)	Fe Leach %
0	24.61	37.90	0.00	0.18	0.28	0	0.67	1.03	0
15	63.20	97.33	9.68	0.95	1.46	27.25	4.17	6.42	70.18
30	67.73	104.19	10.79	0.99	1.52	28.64	4.66	7.16	79.85
60	79.68	122.00	13.69	1.02	1.57	29.67	4.86	7.46	83.73
90	80.18	122.73	13.81	0.99	1.52	28.66	4.88	7.49	84.11
120	81.35	124.41	14.09	1.00	1.54	28.99	4.89	7.51	84.30
150	82.77	126.42	14.41	0.99	1.52	28.66	4.91	7.53	84.67
180	84.69	129.09	14.85	1.00	1.54	28.98	4.95	7.59	85.39
240	87.13	132.42	15.39	1.04	1.59	30.24	5.00	7.66	86.28
300	91.57	138.37	16.36	1.09	1.66	31.78	5.05	7.73	87.15

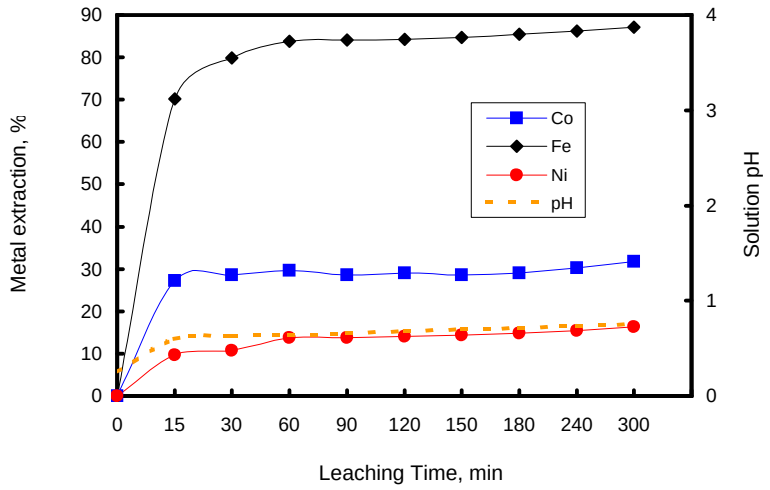

Figure A4.6: Metal extraction as a function of leaching time for the -300+150 micron size fraction of the matte

TABLE A4.3: METAL SOLUTION CONCENTRATIONS DURING ATMOSPHERIC LEACHING OF THE -106+45 MICRONS SIZE FRACTION OF THE MATTE

Leaching conditions:		
	Temperature: (^{o} C)	60
	Mixing rate (rpm):	205
	Pulp density (kg/L):	1.7
	Leaching time (hrs):	5

Leaching Time (min)	Co (g/l)	Fe (g/l)	Ni (g/l)	Cu (g/l)	pH
0	0.18	0.67	24.61	0.00	0.46
15	0.93	4.19	71.70	22.12	3.04
30	1.01	4.46	78.22	17.64	3.09
60	1.11	4.49	78.79	11.94	3.18
90	1.23	4.47	84.73	6.23	3.39
120	1.24	3.81	87.23	1.19	3.75
150	1.22	3.76	88.09	0.00	4.64
180	1.24	3.91	92.30	0.00	5.05
240	1.22	3.89	91.20	0.00	5.20
300	1.31	3.81	94.71	0.00	5.24

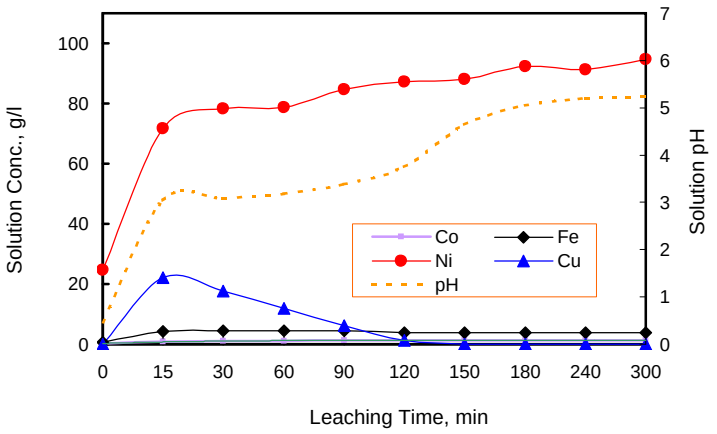

Figure A4.3: Metal concentrations as a function of leaching time for the -106+45 micron size fraction of the matte.

TABLE A4.4: METAL EXTRACTION BASED ON SOLUTION CONCENTRATIONS DURING ATMOSPHERIC LEACHING OF THE -106+45 MICRONS SIZE FRACTION OF THE MATTE

Leaching conditions

Temperature (o C):	60
Mixing rate (rpm):	205
Pulp density (kg/L):	1.7
Leaching time (hrs):	5
Matte (kg):	1.28
Solution (L):	1.54

Metal content of matte:

Ni	614.14 g	(47.98%)
Co	4.35 g	(0.34%)
Fe	7.68 g	(0.6%)

Leaching Time (min)	Ni (g/l)	Ni (g)	Ni Leach %	Co (g/l)	Co (g)	Co leach %	Fe (g/l)	Fe (g)	Fe leach %
0	24.61	37.90	0.00	0.18	0.28	0	0.67	1.03	0
15	71.70	110.42	11.81	0.93	1.43	26.54	4.19	6.45	70.50
30	78.22	119.12	13.22	1.01	1.55	29.32	4.46	6.86	75.91
60	78.79	119.80	13.34	1.11	1.70	32.75	4.49	6.91	76.49
90	84.73	128.49	14.75	1.23	1.88	36.79	4.47	6.88	76.11
120	87.23	131.94	15.31	1.24	1.89	37.12	3.81	5.93	63.73
150	88.09	133.10	15.50	1.22	1.86	36.47	3.76	5.86	62.81
180	92.30	138.93	16.45	1.24	1.89	37.11	3.91	6.06	65.53
240	91.20	137.32	16.19	1.22	1.86	36.48	3.89	6.04	65.17
300	94.71	142.05	16.96	1.31	1.99	39.25	3.81	5.93	63.78

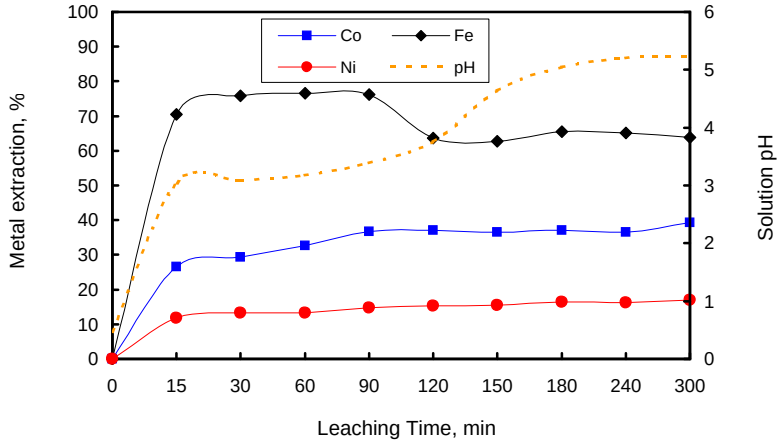

Figure A4.4: Metal extraction as a function of leaching time for the -106+45 microns particle size of the matte

TABLE A4.1: METAL SOLUTION CONCENTRATIONS DURING ATMOSPHERIC LEACHING OF THE - 45 MICRONS SIZE FRACTION OF THE MATTE

Leaching conditions:

Temperature: (^{o} C)	60
Mixing rate (rpm):	205
Pulp density (kg/L):	1.7
Leaching time (hrs):	5

Leaching Time (min)	Co (g/l)	Fe (g/l)	Ni (g/l)	Cu (g/l)	pH
0	0.18	0.67	24.61	24.95	0.46
15	1.20	4.11	78.26	17.59	3.38
30	1.25	4.46	85.38	12.08	3.6
60	1.26	3.66	87.58	2.28	3.65
90	1.27	2.58	89.29	0.00	4.37
120	1.29	1.44	92.55	0.00	4.51
150	1.30	1.34	93.10	0.00	4.71
180	1.30	1.36	93.18	0.00	5.17
240	1.32	1.42	99.45	0.00	5.42
300	1.35	1.27	101.84	0.00	5.53

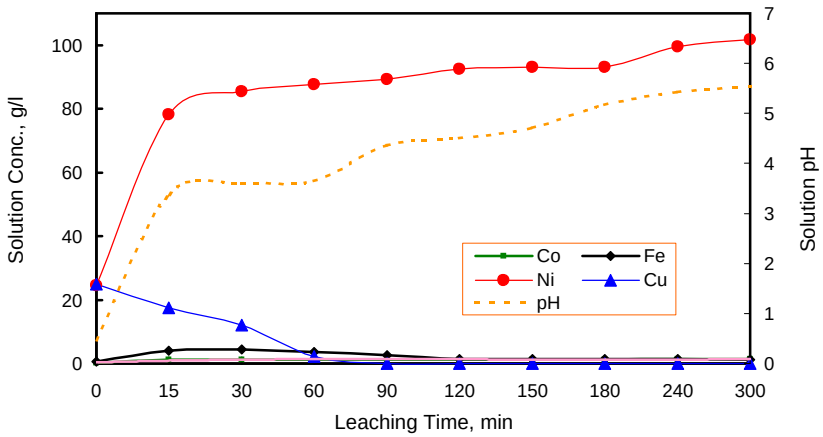

Figure A4 1: Metal concentrations as a function of leaching time for the -45 micron size fraction of the matte

TABLE A4.2: METAL EXTRACTION BASED ON SOLUTION CONCENTRATIONS DURING ATMOSPHERIC LEACHING OF THE -45 MICRONS SIZE FRACTION OF THE MATTE

Leaching conditions:

Temperature (o C):	60
Mixing rate (rpm):	205
Pulp density (kg/L):	1.7
Leaching time (hrs):	5
Matte (kg):	1.28
Solution (L):	1.54

Metal content of matte:

Ni	614.14 g	(47.98%)
Co	4.35 g	(0.34%)
Fe	7.68 g	(0.6%)

Leaching Time (min)	Ni (g/l)	Ni (g)	Ni Leach %	Co (g/l)	Co (g)	Co leach %	Fe (g/l)	Fe (g)	Fe leach %
0	24.61	37.90	0.00	0.18	0.28	0	0.67	1.03	0
15	78.26	120.52	13.45	1.20	1.85	36.09	4.11	6.33	68.98
30	85.38	129.97	14.99	1.25	1.92	37.83	4.46	6.86	75.88
60	87.58	133.07	15.50	1.26	1.94	38.18	3.66	5.67	60.36
90	89.29	135.52	15.89	1.27	1.95	38.51	2.58	4.09	39.76
120	92.55	140.17	16.65	1.29	1.98	39.18	1.44	2.44	18.39
150	93.10	140.86	16.77	1.30	2.00	39.50	1.34	2.30	16.54
180	93.18	140.96	16.78	1.30	2.00	39.50	1.36	2.33	16.91
240	99.45	149.52	18.17	1.32	2.02	40.13	1.42	2.41	17.97
300	101.84	152.56	18.67	1.35	2.06	41.05	1.27	2.21	15.35

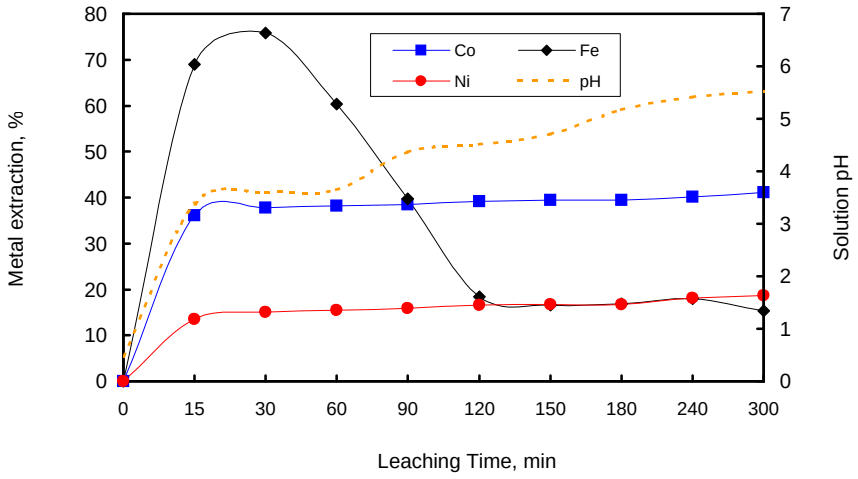

Figure A4.2: Metal extraction as a function of leaching time for the - 45 microns size fraction of the matte

Comparison of metal leaching at a particle size of -45 microns

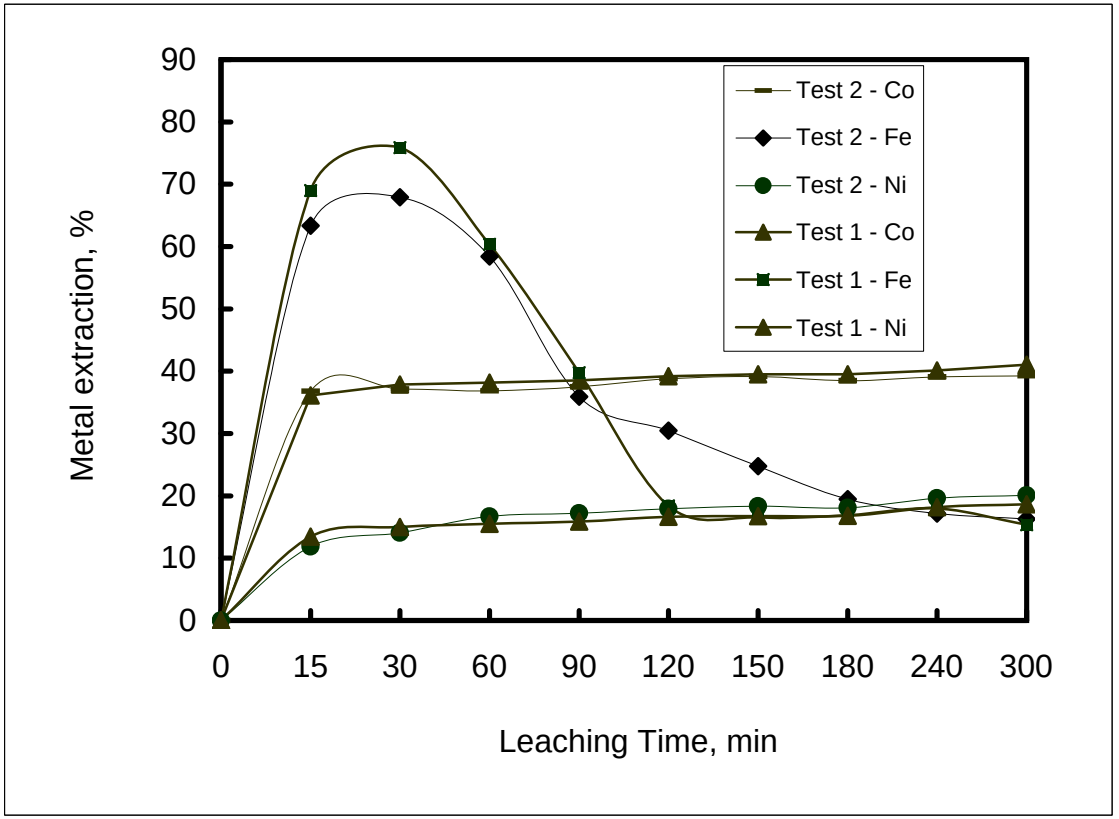

TABLE A4.8: COPPER SOLUTION CONCENTRATION DURING ATMOSPHERIC LEACHING OF THE MATTE AT DIFFERENT PARTICLE SIZE FRACTIONS

Leaching conditions		Feed matte		Feed solution	
Temperature (oC):	60	Mass (kg)	1.28	Volume (mL)	1.54
Stirring rate (rpm):	205	Ni (%)	47.98%	Ni (g/L)	24.61
Pulp density (kg/L):	1.7	Cu (%)	31.31	Cu (g/L)	24.95
Leaching time (hr):	5 hrs	Co (%)	0.34%	Co (g/L)	0.18
Matte (kg):	1.28	Fe (%)	0.6%	Fe (g/L)	0.67

Leaching Time (min)	Copper in leach solution, g			Copper precipitation, %		
	- 300 + 150 (micron)	- 106 + 45 (micron)	- 45 (micron)	- 300 + 150 (micron)	- 106 + 45 (micron)	- 45 (micron)
0	38.42	38.42	38.42	0.00	0.00	0.00
15	34.59	34.06	27.09	9.98	11.34	29.50
30	29.49	27.17	18.60	23.25	29.30	51.58
60	28.54	18.39	3.51	25.73	52.14	90.86
90	27.18	9.59	0.00	29.26	75.03	100.00
120	25.29	1.83	0.00	34.19	95.23	100.00
150	22.95	0.00	0.00	40.28	100.00	100.00
180	21.10	0.00	0.00	45.09	100.00	100.00
240	19.34	0.00	0.00	49.66	100.00	100.00
300	15.99	0.00	0.00	58.40	100.00	100.00

TABLE A4.9: DETERMINATION OF COPPER CEMENTATION RATE CONSTANTS FOR CEMENTATION REACTION AT DIFFERENT PARTICLE SIZE FRACTIONS

Leaching conditions

Temperature (oC):	60	Specific surface area of original matte (cm^2/g)	66982
Stirring rate (rpm):	205	Mass of matte (g):	1276
Leaching time (hr):	5	Volume of solution (cm^3)	1537
Matte (kg):	1.28	Slope of graph = (KxA) / (2.303V)	

Particle size (microns)	Surface area (cm^2/g)	Slope (stage 1)	rate constant $K_1 \times 10^{-3}$ (cm / s)
- 45	82846	0.0104	0.021
- 106 + 45	89247	0.0052	0.010
- 300 + 150	36868	0.0014	0.006

Note: Cementation rate constant obtained from slope of graph in Figure 6.29

TABLE A4.7: COPPER SOLUTION CONCENTRATION DURING ATMOSPHERIC LEACHING OF THE MATTE AT DIFFERENT PARTICLE SIZE FRACTIONS

Leaching conditions		Feed matte		Feed solution	
Temperature (oC):	60	Mass (kg)	1.28	Volume (mL)	1.54
Stirring rate (rpm):	205	Ni (%)	47.98%	Ni (g/L)	24.61
Pulp density (kg/L):	1.7	Cu (%)	31.31	Cu (g/L)	24.95
Leaching time (hr):	5 hrs	Co (%)	0.34%	Co (g/L)	0.18
Matte (kg):	1.28	Fe (%)	0.6%	Fe (g/L)	0.67

Leaching Time (min)	Copper concentration, g/L			Log $[Cu^{2+}]_t$ / $[Cu2+]_0$		
	- 300 + 150 (micron)	- 106 + 45 (micron)	- 45 (micron)	- 300 + 150' um	- 106 + 45 um	'- 45 ' um
0	24.95	24.95	24.95	0.00	0.00	0.00
15	22.46	22.12	17.59	-0.05	-0.05	-0.15
30	19.15	17.64	12.08	-0.11	-0.15	-0.32
60	18.53	11.94	2.28	-0.13	-0.32	-1.04
90	17.65	6.23	0.00	-0.15	-0.60	
120	16.42	1.19	0.00	-0.18	-1.32	
150	14.90	0.00	0.00	-0.22		
180	13.70	0.00	0.00	-0.26		
240	12.56	0.00	0.00	-0.30		
300	10.38	0.00	0.00	-0.38		

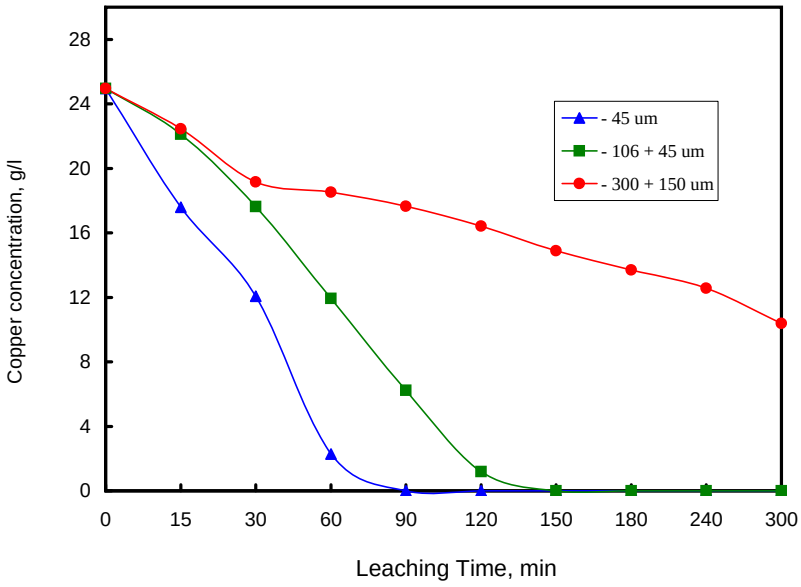

Figure A4.7: Copper concentration as a function of leaching time for the different particle size fractions (205 rpm, 25 g/L initial Cu, 90 g/L initial acid, 1.7 kg/L P.D.

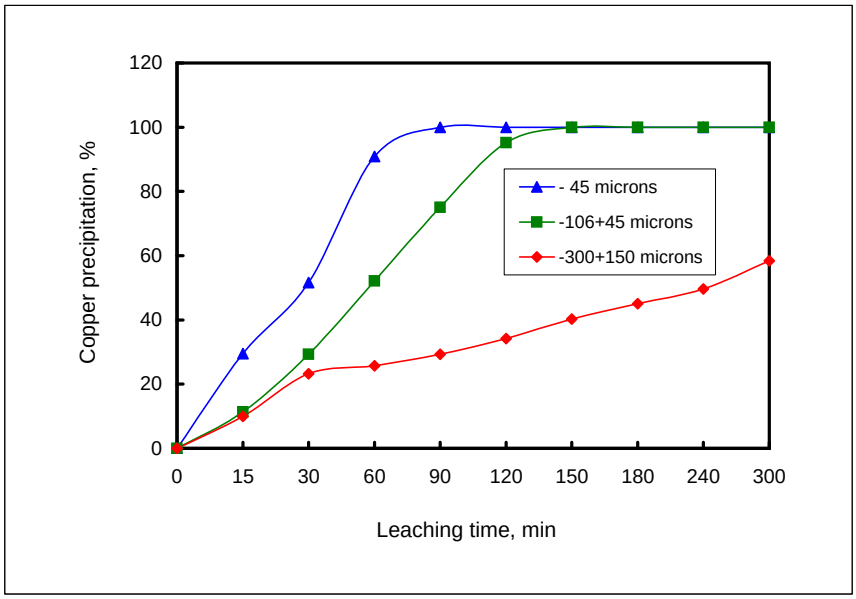
Copper precipitation, %
120
100
80
60
40
20
0
0
15
30
60
90
120
150
180
240
300
Leaching time, min
- 45 microns
-106+45 microns
-300+150 microns

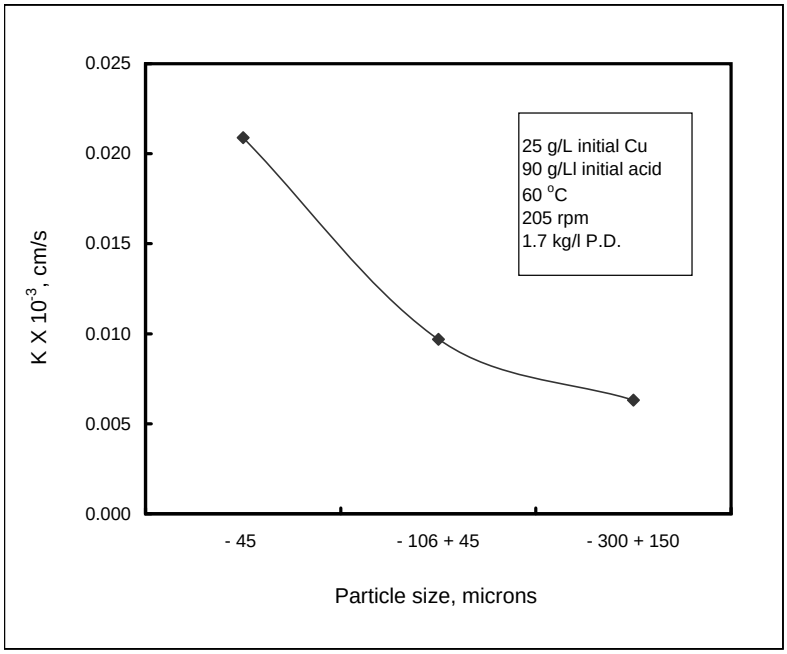
K X 10-3, cm/s
0.025
0.020
0.015
0.010
0.005
0.000
- 45
- 106 + 45
- 300 + 150
Particle size, microns
25 g/L initial Cu
90 g/Ll initial acid
60 °C
205 rpm
1.7 kg/l P.D.

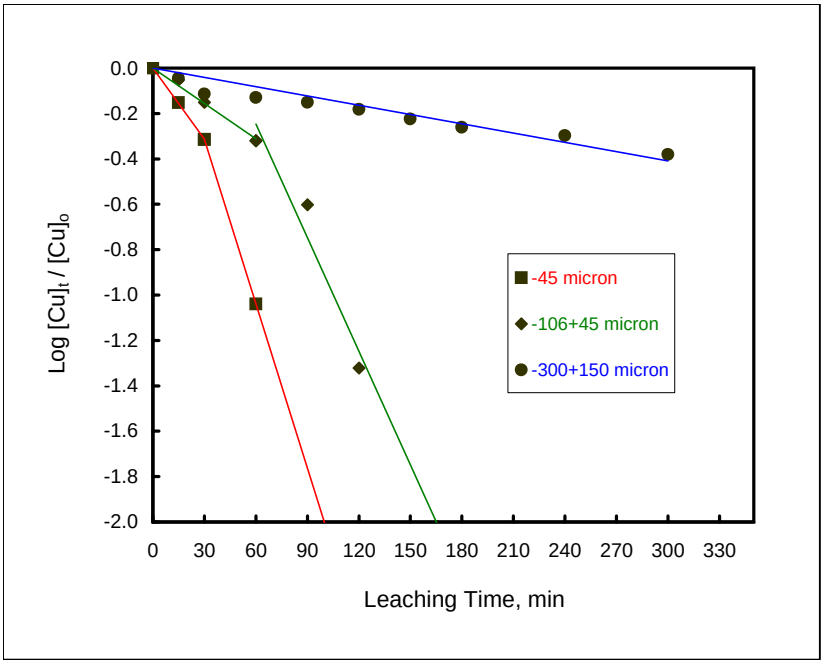
0.0
-0.2
-0.4
-0.6
-0.8
-1.0
-1.2
-1.4
-1.6
-1.8
-2.0
Log [Cu]t / [Cu]o
0
30
60
90
120
150
180
210
240
270
300
330
Leaching Time, min
-45 micron
-106+45 micron
-300+150 micron

TABLE A5.3: METAL SOLUTION CONCENTRATIONS DURING ATMOSPHERIC LEACHING OF THE MATTE AT INITIAL COPPER CONCENTRATION OF 36 g/L

Leaching conditions:		
	Temperature: (o C)	60
	Mixing rate (rpm):	205
	Pulp density (kg/L):	1.7
	Leaching time (hrs):	5

Leaching Time (min)	Co (g/l)	Fe (g/l)	Ni (g/l)	Cu (g/l)	pH
0	0.18	0.67	24.61	36.03	0.74
15	0.95	3.74	65.00	35.93	1.56
30	0.99	3.88	70.10	32.63	1.62
60	1.08	4.25	77.97	28.90	1.64
90	1.11	4.33	81.59	25.26	1.75
120	1.12	4.46	86.65	21.99	1.84
150	1.15	4.48	89.02	19.91	1.94
180	1.13	4.44	88.98	17.87	2.03
240	1.17	4.51	93.42	14.84	2.25
300	1.18	4.51	97.73	12.14	2.68

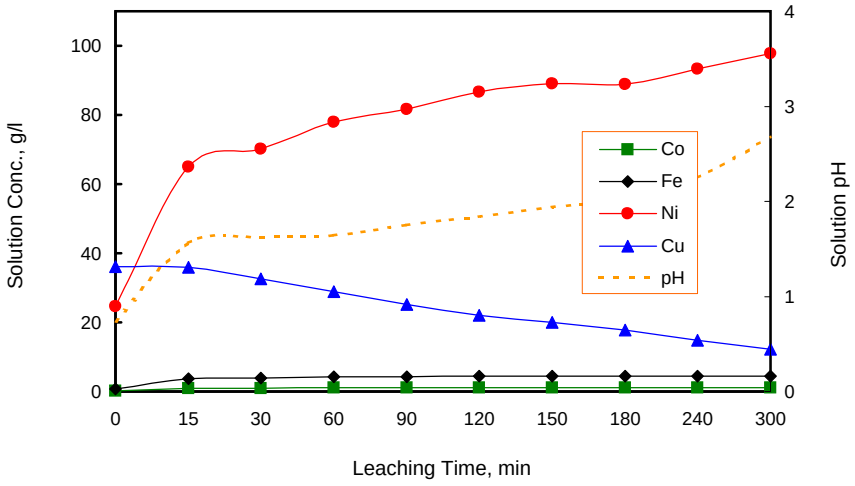

Figure A5.3: Metal concentration as a function of leaching time at initial copper concentration of 36g/l

TABLE A5.4: METAL EXTRACTION BASED ON SOLUTION CONCENTRATIONS DURING ATMOSPHERIC LEACHING OF THE MATTE AT INITIAL COPPER CONCENTRATION OF 36 g/L

Leaching conditions:		
	Temperature (o C):	60
	Mixing rate (rpm):	205
	Pulp density (kg/L):	1.7
	Leaching time (hrs):	5
	Matte (kg):	1.28
	Solution (L):	1.54

Metal content of matte:		
Ni	614.14 g	(47.98%)
Co	4.35 g	(0.34%)
Fe	7.68 g	(0.6%)

Leaching Time (min)	Ni (g/l)	Ni (g)	Ni Leach %	Co (g/l)	Co (g)	Co leach %	Fe (g/l)	Fe (g)	Fe Leach %
0	24.61	37.90	0.00	0.18	0.28	0	0.67	1.03	0
15	65.00	100.10	10.13	0.95	1.46	27.25	3.74	5.76	61.56
30	70.10	106.82	11.22	0.99	1.52	28.64	3.88	5.97	64.32
60	77.97	118.42	13.11	1.08	1.66	31.72	4.25	6.52	71.50
90	81.59	123.52	13.94	1.11	1.70	32.73	4.33	6.64	73.03
120	86.65	130.72	15.11	1.12	1.72	33.06	4.46	6.83	75.46
150	89.02	133.95	15.64	1.15	1.76	34.04	4.48	6.86	75.83
180	88.98	133.83	15.62	1.13	1.73	33.40	4.44	6.80	75.11
240	93.42	139.89	16.61	1.17	1.79	34.65	4.51	6.90	76.35
300	97.73	145.56	17.53	1.18	1.80	34.96	4.51	6.90	76.35

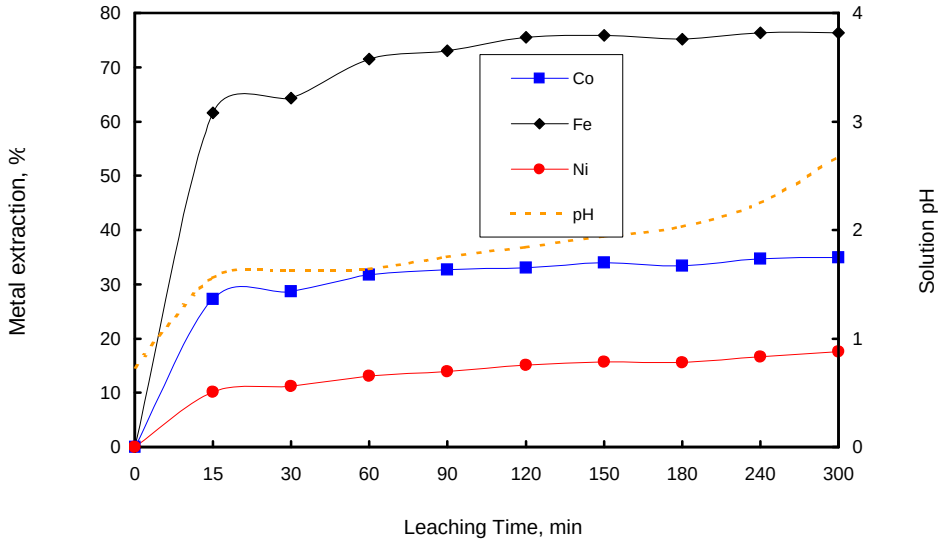

Figure A5.4: Metal extraction as a function of leaching time at an initial copper concetration of 36 g/L

TABLE A5.5: METAL SOLUTION CONCENTRATIONS DURING ATMOSPHERIC LEACHING OF THE MATTE AT INITIAL COPPER CONCENTRATION OF 48 g/L

Leaching conditions:		
	Temperature: (o C)	60
	Mixing rate (rpm):	205
	Pulp density (kg/L):	1.7
	Leaching time (hrs):	5

Leaching Time (min)	Co (g/l)	Fe (g/l)	Ni (g/l)	Cu (g/l)	pH
0	0.18	0.67	24.61	48.43	0.78
15	0.94	3.67	65.45	48.43	1.58
30	0.96	3.75	68.25	43.25	1.63
60	0.94	3.66	69.17	36.43	1.67
90	0.97	3.71	71.47	33.01	1.63
120	1.00	3.85	77.02	30.73	1.76
150	1.04	3.94	79.99	29.37	1.85
180	1.02	3.86	80.16	26.80	1.92
240	1.07	4.04	86.15	24.06	2.07
300	1.15	4.18	92.97	20.11	2.46

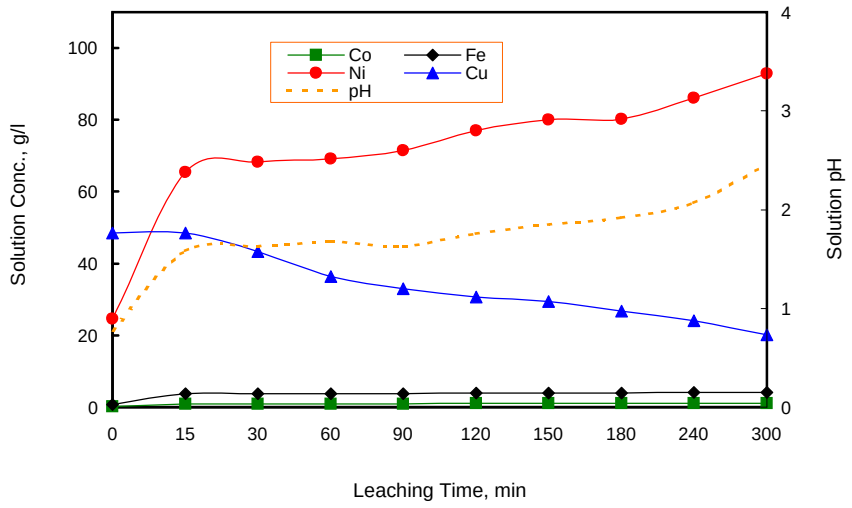

Figure A5.5: Metal concentration as a function of leaching time at initia copper concentration of 48g/L

TABLE A5.6: METAL EXTRACTION BASED ON SOLUTION CONCENTRATIONS DURING ATMOSPHERIC LEACHING OF THE MATTE AT INITIAL COPPER CONCENTRATION OF 48 g/L

Leaching conditions:			Metal content of matte:		
	Temperature (o C):	60	Ni	614.14 g	(47.98%)
	Mixing rate (rpm):	205	Co	4.35 g	(0.34%)
	Pulp density (kg/L):	1.7	Fe	7.68 g	(0.6%)
	Leaching time (hrs):	5			
	Matte (kg):	1.28			
	Solution (L):	1.54			

Leaching Time (min)	Ni (g/l)	Ni (g)	Ni Leach %	Co (g/l)	Co (g)	Co leach %	Fe (g/l)	Fe (g)	Fe Leach %
0	24.61	37.90	0.00	0.18	0.28	0	0.67	1.03	0
15	65.45	100.79	10.24	0.94	1.45	26.89	3.67	5.65	60.16
30	68.25	104.01	10.77	0.96	1.48	27.59	3.75	5.77	61.73
60	69.17	105.31	10.98	0.94	1.45	26.90	3.66	5.64	59.99
90	71.47	108.66	11.52	0.97	1.49	27.91	3.71	5.71	60.94
120	77.02	116.60	12.81	1.00	1.54	28.91	3.85	5.91	63.57
150	79.99	120.66	13.48	1.04	1.59	30.21	3.94	6.04	65.23
180	80.16	120.82	13.50	1.02	1.56	29.57	3.86	5.93	63.78
240	86.15	128.99	14.83	1.07	1.63	31.14	4.04	6.18	66.98
300	92.97	137.98	16.30	1.15	1.74	33.60	4.18	6.36	69.42

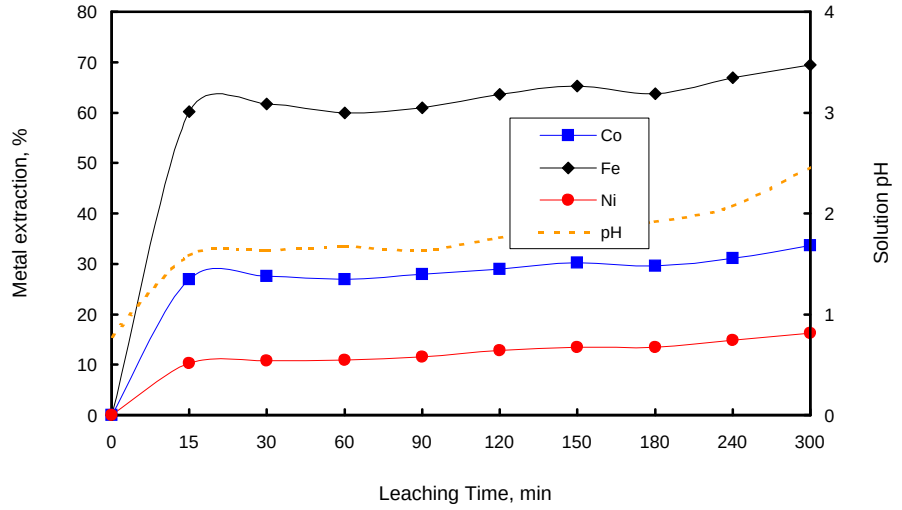

Figure A5.6: Metal extraction as a function of leaching time at an initial Coppe concetration of 48 g/L

TABLE A5.1: METAL SOLUTION CONCENTRATIONS DURING ATMOSPHERIC LEACHING OF THE MATTE AT INITIAL Cu CONCENTRATION OF 25 g/L

Leaching conditions: Temperature: 60 °C
Agitation: 205 rpm
Pulp density: 1.7 kg/L

Leaching Time (min)	Co (g/l)	Fe (g/l)	Ni (g/l)	Cu (g/l)	pH
0	0.18	0.67	24.61	24.95	0.97
15	0.77	3.35	64.11	22.84	1.10
30	0.79	3.44	66.16	19.49	1.11
60	0.80	3.68	68.85	14.47	1.18
90	0.79	3.80	71.18	10.45	1.28
120	0.91	3.91	78.69	8.75	1.34
150	0.88	3.96	80.00	6.39	1.43
180	0.96	4.05	86.80	4.79	1.51
240	0.91	4.08	88.33	1.30	1.61
300	1.01	4.24	94.44	0.00	1.90

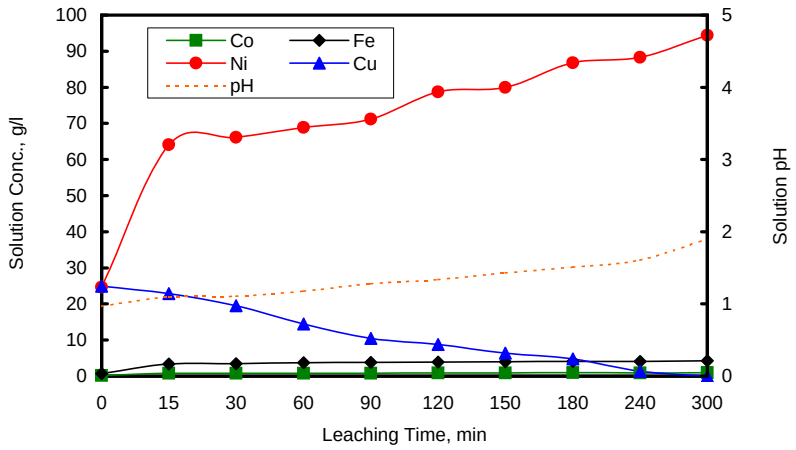

Fig. A5.1: Metal concentrations as a function of leaching time at initial Cu concentration of 25 g/L

TABLE A5.2: METAL EXTRACTIONS BASED ON SOLUTION CONCENTRATIONS DURING ATMOSPHERIC LEACHING OF THE MATTE AT INITIAL Cu CONCENTRATION OF 25 g/L

Leaching conditions:	Temperature:	60 oC		Metal content of matte:	
	Agitation:	205 rpm		Ni	612.22 g (47.98%)
	Pulp density:	1.7 kg/L		Co	4.34 g (0.34 %)
	Matte:	1.28	kg	Fe	7.66 g (0.60 %)
	Solution:	1.54	L		

Leaching Time (min)	**Ni (g/l)**	**Ni (g)**	**Ni Leach %**	**Co (g/l)**	**Co (g)**	**Co leach %**	**Fe (g/l)**	Fe (g)	Fe (%)
0	24.61	37.83	0.00	0.18	0.28	0	0.67	1.03	0
15	64.11	98.54	9.92	0.77	1.18	20.90	3.35	5.15	53.80
30	66.16	101.64	10.42	0.79	1.21	21.60	3.44	5.29	55.58
60	68.85	105.71	11.09	0.80	1.23	21.94	3.68	5.64	60.24
90	71.18	109.17	11.65	0.79	1.21	21.61	3.80	5.82	62.61
120	78.69	119.96	13.42	0.91	1.39	25.58	3.91	5.98	64.60
150	80.00	121.81	13.72	0.88	1.34	24.60	3.96	6.05	65.52
180	86.80	131.24	15.26	0.96	1.46	27.16	4.05	6.17	67.15
240	88.33	133.33	15.60	0.91	1.39	25.59	4.08	6.21	67.69
300	94.44	141.49	16.93	1.01	1.52	28.67	4.24	6.43	70.48
300									

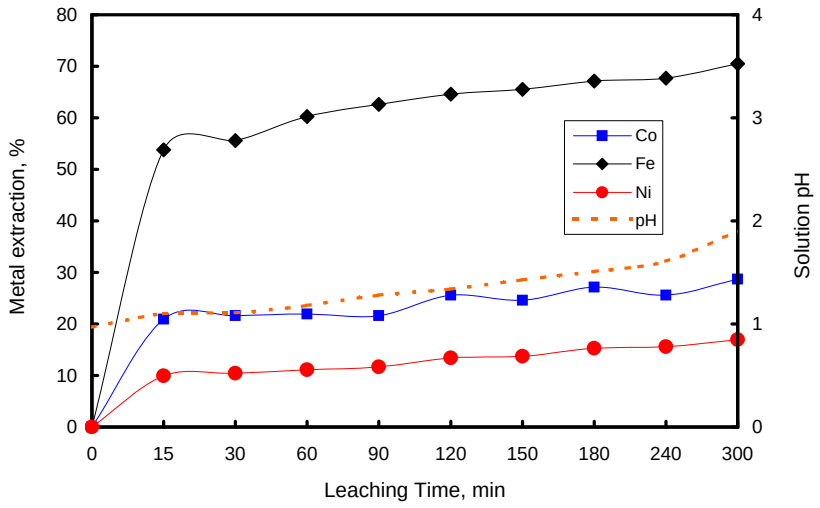

Figure A5.2: Metal extractions as a function of leaching time at initial Cu concentration of 25 g/L

TABLE A6.3: METAL SOLUTION CONCENTRATIONS DURING ATMOSPHERIC LEACHING OF THE MATTE AT INITIAL H_2SO_4 CONCENTRATION OF 110 g/L

Leaching conditions:		
	Temperature: (o C)	60
	Mixing rate (rpm):	205
	Pulp density (kg/L):	1.7
	Leaching time (hrs):	5

Leaching Time (min)	Co (g/l)	Fe (g/l)	Ni (g/l)	Cu (g/l)	pH
0	0.18	0.67	24.61	0.00	0.61
15	0.89	3.77	60.68	26.60	1.04
30	0.96	4.15	67.35	22.12	0.98
60	1.04	4.55	75.51	17.07	1.09
90	1.08	4.69	79.96	13.65	1.14
120	1.13	4.86	84.58	11.23	1.18
150	1.12	4.86	86.35	9.23	1.19
180	1.13	4.85	87.40	7.72	1.25
240	1.16	5.01	92.65	4.87	1.27
300	1.18	5.04	96.39	2.57	1.32

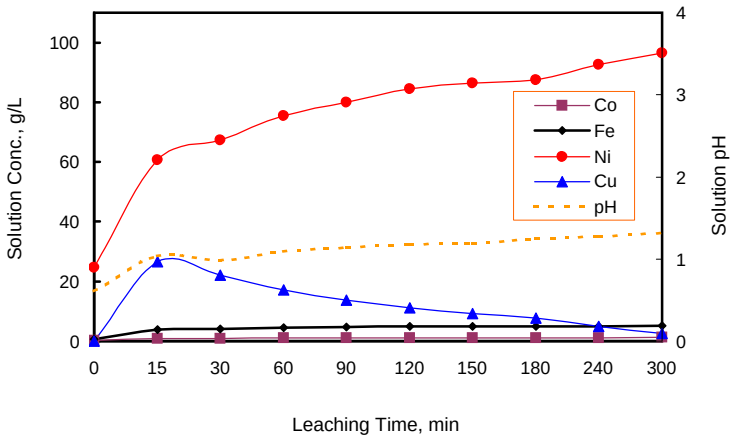

Figure A6.3: Metal concentration as a function of leaching time at initia H_2SO_4 concentration of 110g/L

TABLE A6.4: METAL EXTRACTION BASED ON SOLUTION CONCENTRATIONS DURING ATMOSPHERIC LEACHING OF THE MATTE AT INITIAL H_2SO_4 CONCENTRATION OF 110 g/L

Leaching conditions:			Metal content of matte:		
	Temperature (o C):	60			
	Mixing rate (rpm):	205	Ni	614.14 g	(47.98%)
	Pulp density (kg/L):	1.7	Co	4.35 g	(0.34%)
	Leaching time (hrs):	5	Fe	7.68 g	(0.6%)
	Matte (kg):	1.28			
	Solution (L):	1.54			

Leaching Time (min)	Ni (g/l)	Ni (g)	Ni Leach %	Co (g/l)	Co (g)	Co leach %	Fe (g/l)	Fe (g)	Fe Leach %
0	24.61	37.90	0.00	0.18	0.28	0	0.67	1.03	0
15	60.68	93.45	9.04	0.89	1.37	25.12	3.77	5.81	62.16
30	67.35	102.65	10.54	0.96	1.48	27.56	4.15	6.38	69.66
60	75.51	114.64	12.50	1.04	1.60	30.30	4.55	6.98	77.42
90	79.96	120.96	13.52	1.08	1.65	31.65	4.69	7.18	80.09
120	84.58	127.50	14.59	1.13	1.73	33.30	4.86	7.43	83.28
150	86.35	129.89	14.98	1.12	1.71	32.98	4.86	7.43	83.28
180	87.40	131.30	15.21	1.13	1.73	33.30	4.85	7.41	83.10
240	92.65	138.44	16.37	1.16	1.77	34.24	5.01	7.63	85.94
300	96.39	143.32	17.17	1.18	1.79	34.85	5.04	7.67	86.46

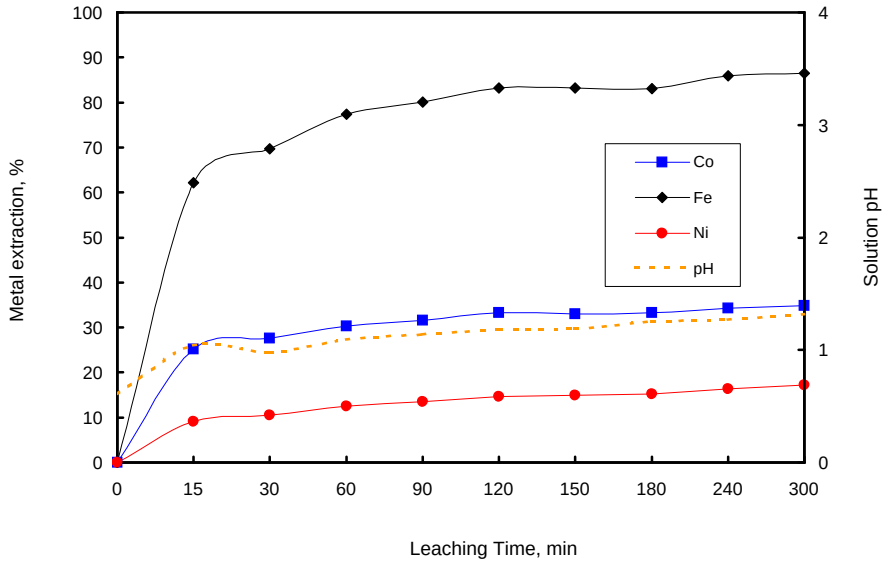

Figure A6.4: Metal extraction as a function of leaching time at initial H2SO4 concentration of 110 g/L

TABLE A6.5: METAL SOLUTION CONCENTRATIONS DURING ATMOSPHERIC LEACHING OF THE MATTE AT INITIAL H_2SO_4 CONCENTRATION OF 125 g/L

Leaching conditions:

Temperature: (o C)	60
Mixing rate (rpm):	205
Pulp density (kg/L):	1.7
Leaching time (hrs):	5

Leaching Time (min)	Co (g/l)	Fe (g/l)	Ni (g/l)	Cu (g/l)	pH
0	0.18	0.67	24.61	24.95	0.57
15	0.94	4.11	64.66	25.99	0.92
30	1.01	4.40	70.58	22.16	0.87
60	1.08	4.63	76.40	17.46	0.95
90	1.08	4.74	79.58	14.48	0.98
120	1.11	4.85	83.22	11.95	1.01
150	1.13	4.84	84.66	9.81	0.91
180	1.14	4.93	87.63	8.12	1.01
240	1.19	5.11	93.38	4.86	0.90
300	1.22	5.22	98.05	1.93	1.17

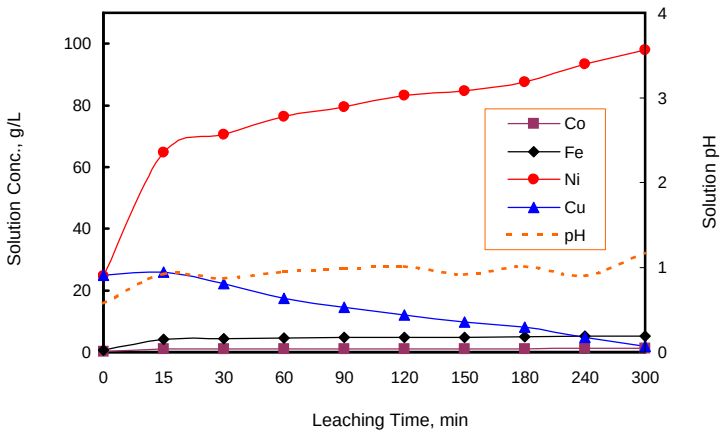

Figure A6.5: Metal concentration as a function of leaching time at initial H_2SO_4 concentration of 125g/lL.

TABLE A6.6: METAL EXTRACTION BASED ON SOLUTION CONCENTRATIONS DURING ATMOSPHERIC LEACHING OF THE MATTE AT INITIAL H_2SO_4 CONCENTRATION OF 125 g/L

Leaching conditions:			Metal content of matte:		
	Temperature (o C):	60	Ni	614.14 g	(47.98%)
	Mixing rate (rpm):	205	Co	4.35 g	(0.34%)
	Pulp density (kg/L):	1.7	Fe	7.68 g	(0.6%)
	Leaching time (hrs):	5			
	Matte (kg):	1.28			
	Solution (L):	1.54			

Leaching Time (min)	Ni (g/l)	Ni (g)	Ni Leach %	Co (g/l)	Co (g)	Co leach %	Fe (g/l)	Fe (g)	Fe Leach %
0	24.61	37.90	0.00	0.18	0.28	0	0.67	1.03	0
15	64.66	99.58	10.04	0.94	1.45	26.89	4.11	6.33	68.98
30	70.58	107.54	11.34	1.01	1.55	29.33	4.40	6.77	74.70
60	76.40	116.07	12.73	1.08	1.66	31.73	4.63	7.11	79.16
90	79.58	120.58	13.46	1.08	1.66	31.73	4.74	7.27	81.26
120	83.22	125.74	14.30	1.11	1.70	32.72	4.85	7.43	83.32
150	84.66	127.69	14.62	1.13	1.73	33.37	4.84	7.42	83.14
180	87.63	131.78	15.29	1.14	1.74	33.69	4.93	7.54	84.77
240	93.38	139.56	16.55	1.19	1.81	35.26	5.11	7.79	87.97
300	98.05	145.67	17.55	1.22	1.85	36.18	5.22	7.94	89.89

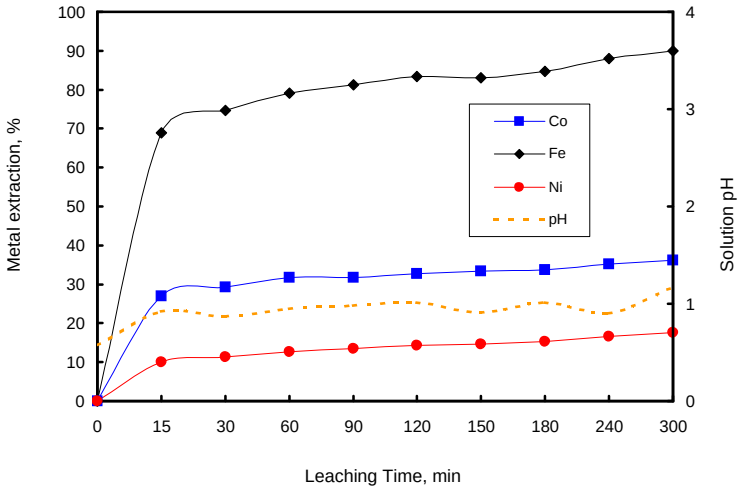

Figure A6.6: Metal extraction as a function of leaching time at initial H_2SO_4 concentration of 125 g/L

TABLE A6.1: METAL SOLUTION CONCENTRATIONS DURING ATMOSPHERIC LEACHING OF THE MATTE AT INITIAL H_2SO_4 CONCENTRATION OF 90 g/L

Leaching conditions: Temperature: 60 °C
Agitation: 205 rpm
Pulp density: 1.7 kg/L

Leaching Time (min)	Co (g/l)	Fe (g/l)	Ni (g/l)	Cu (g/l)	pH
0	0.18	0.67	24.61	24.95	0.97
15	0.77	3.35	64.11	22.84	1.10
30	0.79	3.44	66.16	19.49	1.11
60	0.80	3.68	68.85	14.47	1.18
90	0.79	3.80	71.18	10.45	1.28
120	0.91	3.91	78.69	8.75	1.34
150	0.88	3.96	80.00	6.39	1.43
180	0.96	4.05	86.80	4.79	1.51
240	0.91	4.08	88.33	1.30	1.61
300	1.01	4.24	94.44	0.00	1.90

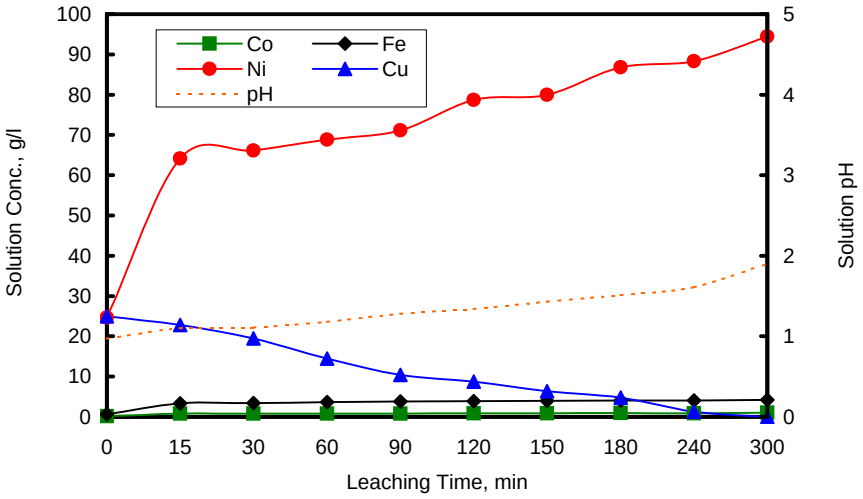

Fig. A6.1: Metal concentrations as a function of leaching time at initial H_2SO_4 concentration of 90 g/L

TABLE A6.2: METAL EXTRACTIONS BASED ON SOLUTION CONCENTRATIONS DURING ATMOSPHERIC LEACHING OF THE MATTE AT INITIAL H_2SO_4 CONCENTRATION OF 90 g/L

Leaching conditions:	Temperature:	60 oC		Metal content of matte:	
	Agitation:	205 rpm		Ni	612.22 g (47.98%)
	Pulp density:	1.7 kg/L		Co	4.34 g (0.34 %)
	Matte:	1.28	kg	Fe	7.66 g (0.60 %)
	Solution:	1.54	L		

Leaching Time (min)	**Ni (g/l)**	**Ni (g)**	**Ni Leach %**	**Co (g/l)**	**Co (g)**	**Co leach %**	**Fe (g/l)**	Fe (g)	Fe (%)
0	24.61	37.83	0.00	0.18	0.28	0	0.67	1.03	0
15	64.11	98.54	9.92	0.77	1.18	20.90	3.35	5.15	53.80
30	66.16	101.64	10.42	0.79	1.21	21.60	3.44	5.29	55.58
60	68.85	105.71	11.09	0.80	1.23	21.94	3.68	5.64	60.24
90	71.18	109.17	11.65	0.79	1.21	21.61	3.80	5.82	62.61
120	78.69	119.96	13.42	0.91	1.39	25.58	3.91	5.98	64.60
150	80.00	121.81	13.72	0.88	1.34	24.60	3.96	6.05	65.52
180	86.80	131.24	15.26	0.96	1.46	27.16	4.05	6.17	67.15
240	88.33	133.33	15.60	0.91	1.39	25.59	4.08	6.21	67.69
300	94.44	141.49	16.93	1.01	1.52	28.67	4.24	6.43	70.48
300									

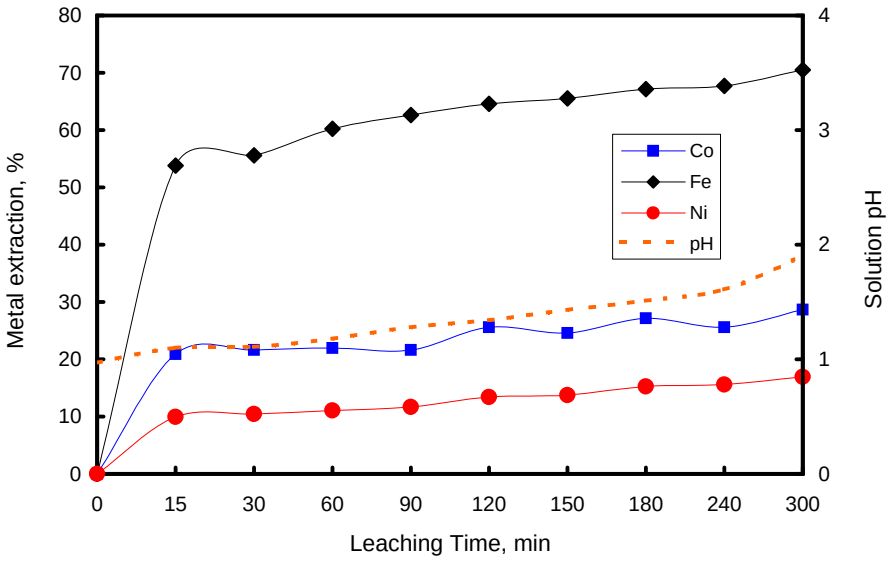

Figure A6.2: Metal extractions as a function of leaching time at initial H_2SO_4 concentration of 90 g/L

TABLE A6.8: COPPER SOLUTION CONCENTRATION DURING ATMOSPHERIC LEACHING OF THE MATTE AT DIFFERENT INITIAL H_2SO_4 CONCENTRATIONS OF THE LEACHING SOLUTION

Leaching conditions		Feed matte		Feed solution	
Temperature (^oC):	60	Mass (kg)	1.28	Volume (mL)	1.54
Stirring rate (rpm):	205	Ni (%)	47.98%	Ni (g/L)	24.61
Pulp density (kg/L):	1.7	Cu (%)	31.31	Cu (g/L)	24.95
Leaching time (hr):	5 hrs	Co (%)	0.34%	Co (g/L)	0.18
Matte (kg):	1.28	Fe (%)	0.6%	Fe (g/L)	0.67

Leaching Time (min)	Copper in leach solution, g			Copper precipitation, %		
	90 g/L H_2SO_4	110 g/L H_2SO_4	125 g/L H_2SO_4	90 g/L H_2SO_4	110 g/L H_2SO_4	125 g/L H_2SO_4
0	38.42	38.42	38.42	0.00	0.00	0.00
15	35.17	36.34	36.94	8.46	5.41	3.85
30	30.01	34.06	34.13	21.88	11.34	11.18
60	22.28	26.29	26.89	42.00	31.58	30.02
90	16.09	21.02	22.30	58.12	45.29	41.96
120	13.48	17.29	18.40	64.93	54.99	52.10
150	9.84	14.29	15.11	74.39	62.81	60.68
180	7.38	11.89	12.50	80.80	69.06	67.45
240	2.00	7.50	7.48	94.79	80.48	80.52
300	0.00	3.96	2.97	100.00	89.70	92.26

TABLE A6.9: DETERMINATION OF COPPER CEMENTATION RATE CONSTANTS FOR CEMENTATION REACTION AT DIFFERENT INITIAL H_2SO_4 CONCENTRATION

Leaching conditions

Temperature (oC):	60	Specific surface area of matte (cm^2/g)	66982
Stirring rate (rpm):	205	Mass of matte (g):	1276
Leaching time (hr):	5	Volume of solution (cm^3)	1537
Matte (kg):	1.28	Slope of graph = (KxA) / (2.303V)	

H_2SO_4 (g/L)	Slope (stage 1)	Rate constant K_1 X 10^{-3} (cm / s)
90	0.0040	0.010
110	0.0030	0.007
125	0.0028	0.007

Note: Cementation rate constant obtained from slope of graph in Figure 6.43

TABLE A6.7: COPPER SOLUTION CONCENTRATION DURING ATMOSPHERIC LEACHING OF THE MATTE AT DIFFERENT INITIAL H_2SO_4 CONCENTRATIONS OF THE LEACHING SOLUTION

Leaching conditions		Feed matte		Feed solution	
Temperature (^oC):	60	Mass (kg)	1.28	Volume (mL)	1.54
Stirring rate (rpm):	205	Ni (%)	47.98%	Ni (g/L)	24.61
Pulp density (kg/L):	1.7	Cu (%)	31.31	Cu (g/L)	24.95
Leaching time (hr):	5 hrs	Co (%)	0.34%	Co (g/L)	0.18
Matte (kg):	1.28	Fe (%)	0.6%	Fe (g/L)	0.67

Leaching Time (min)	Copper concentration, g/L			Log $[Cu^{2+}]_t / [Cu^{2+}]_0$		
	90 g/L H_2SO_4	110 g/L H_2SO_4	125 g/L H_2SO_4	90 g/L H_2SO_4	110 g/L H_2SO_4	125 g/L H_2SO_4
0	24.95	24.95	24.95	0.000	0.000	0.000
15	22.84	23.60	23.99	-0.038	-0.024	-0.017
30	19.49	22.12	22.16	-0.107	-0.052	-0.052
60	14.47	17.07	17.46	-0.237	-0.165	-0.155
90	10.45	13.65	14.48	-0.378	-0.262	-0.236
120	8.75	11.23	11.95	-0.455	-0.347	-0.320
150	6.39	9.28	9.81	-0.592	-0.430	-0.405
180	4.79	7.72	8.12	-0.717	-0.509	-0.488
240	1.30	4.87	4.86	-1.283	-0.710	-0.710
300	0.00	2.57	1.93		-0.987	-1.112

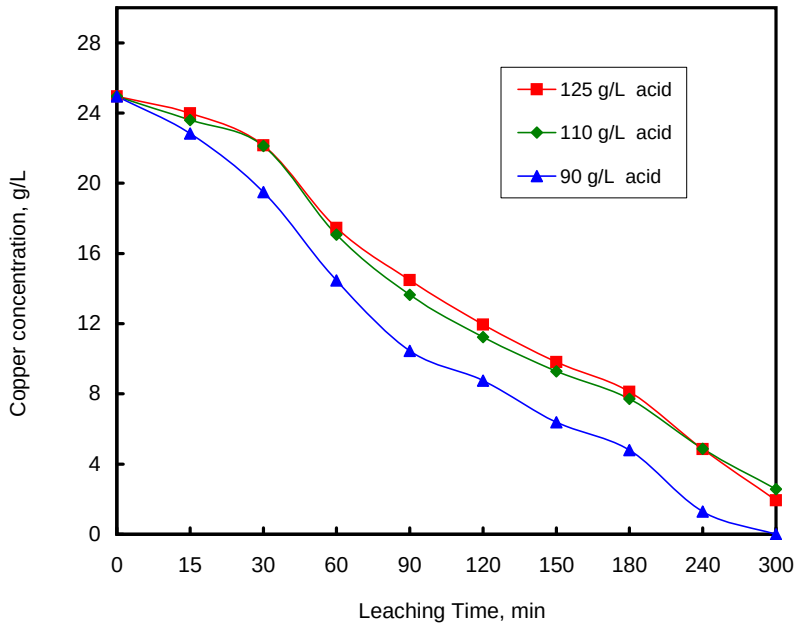

Figure A6.7: Acid concentration as a function of leaching time for different initial H_2SO_4 concentration of leaching solution (205 rpm, 25 g/L initial Cu, 1.7 gk/L P.D.)

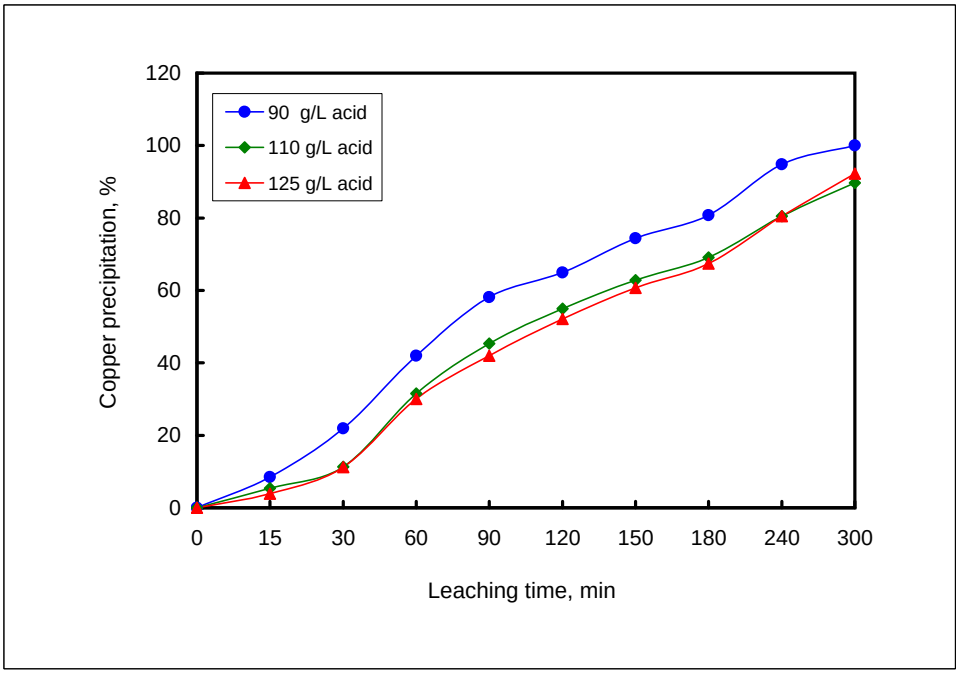
Copper precipitation, %
120
100
80
60
40
20
0
90 g/L acid
110 g/L acid
125 g/L acid
0
15
30
60
90
120
150
180
240
300
Leaching time, min

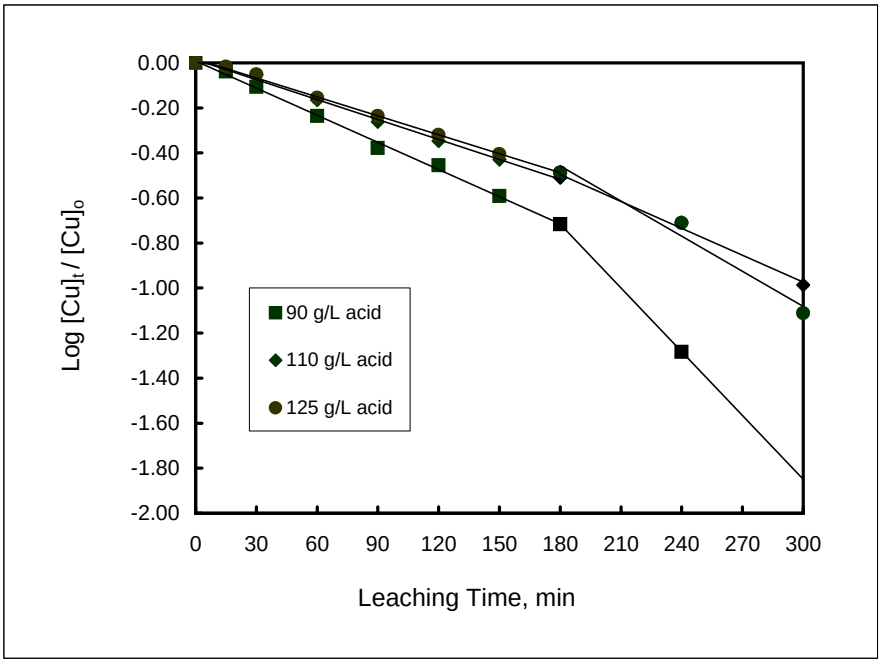
Log [Cu]t / [Cu]o
0.00
-0.20
-0.40
-0.60
-0.80
-1.00
-1.20
-1.40
-1.60
-1.80
-2.00
90 g/L acid
110 g/L acid
125 g/L acid
0
30
60
90
120
150
180
210
240
270
300
Leaching Time, min

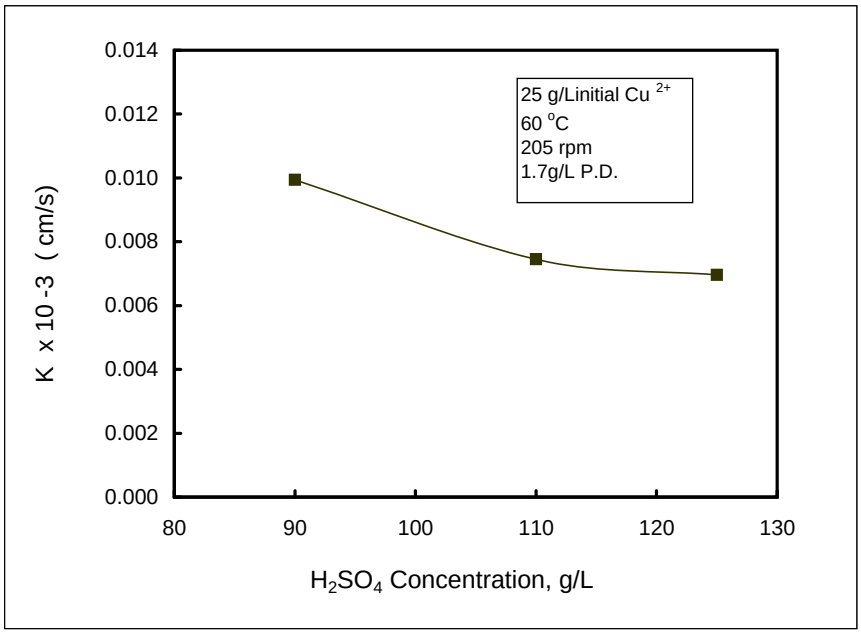
0.014
0.012
0.010
0.008
0.006
0.004
0.002
0.000
K x 10 -3 (cm/s)
80
90
100
110
120
130
H2SO4 Concentration, g/L
25 g/Linitial Cu 2+
60 oC
205 rpm
1.7g/L P.D.

TABLE A7.1: METAL SOLUTION CONCENTRATIONS DURING ATMOSPHERIC LEACHING OF THE MATTE FOR A RESIDENCE TIME OF 5 HOURS

Leaching conditions: Temperature: 60 °C
Agitation: 205 rpm
Pulp density: 1.7 kg/L

Leaching Time (min)	Co (g/l)	Fe (g/l)	Ni (g/l)	Cu (g/l)	pH
0	0.18	0.67	24.61	24.95	0.97
15	0.77	3.35	60.14	22.84	1.10
30	0.79	3.44	62.18	19.49	1.11
60	0.80	3.68	64.86	14.47	1.18
90	0.79	3.49	67.18	10.45	1.28
120	0.91	3.91	74.94	8.75	1.34
150	0.88	3.96	76.05	6.39	1.43
180	0.96	4.05	82.83	4.79	1.51
240	0.91	4.08	84.33	1.30	1.61
300	1.01	4.24	85.84	0.00	1.90

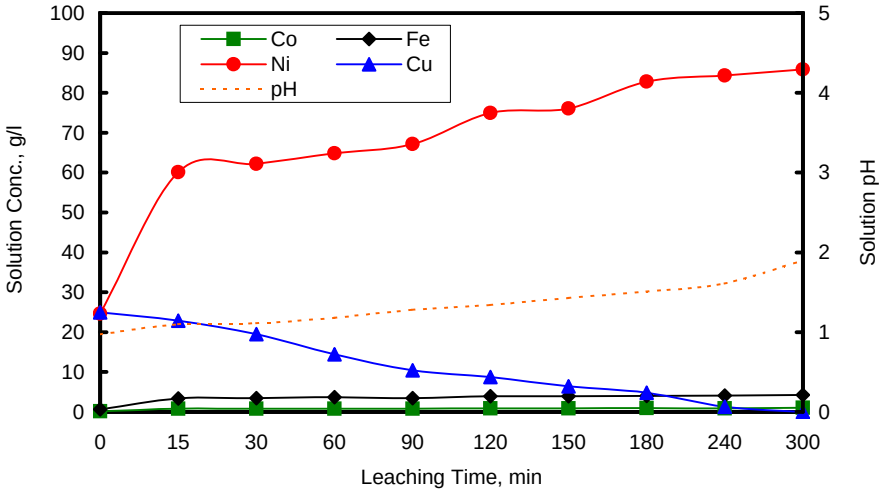

Figure A7.1: Metal concentrations as a function of leaching time for a residence time of 5 hours

TABLE A7.2: METAL EXTRACTIONS BASED ON SOLUTION CONCENTRATIONS DURING ATMOSPHERIC LEACHING OF THE MATTE FOR A RESIDENCE TIME OF 5 HOURS

Leaching conditions:				**Metal content of matte:**	
	Temperature:	60 oC		**Ni**	**612.22** g (47.98%)
	Agitation:	205 rpm		**Co**	**4.34** g (0.34 %)
	Pulp density:	1.7 kg/L		**Fe**	**7.66** g (0.60 %)
	Matte:	1.28	kg		
	Solution:	1.54	L		

Leaching Time (min)	**Ni (g/l)**	**Ni (g)**	**Ni Leach %**	**Co (g/l)**	**Co (g)**	**Co leach %**	**Fe (g/l)**	Fe (g)	Fe (%)
0	24.61	37.83	0.00	0.18	0.28	0	0.67	1.03	0
15	60.14	92.44	8.92	0.77	1.18	20.90	3.35	5.15	53.80
30	62.18	95.52	9.42	0.79	1.21	21.60	3.44	5.29	55.58
60	64.86	99.57	10.09	0.80	1.23	21.94	3.68	5.64	60.24
90	67.18	103.02	10.65	0.79	1.21	21.61	3.49	5.36	56.61
120	74.94	114.17	12.47	0.91	1.39	25.58	3.91	5.97	64.50
150	76.05	115.74	12.73	0.88	1.34	24.60	3.96	6.04	65.42
180	82.83	125.14	14.26	0.96	1.46	27.16	4.05	6.16	67.05
240	84.33	127.19	14.60	0.91	1.39	25.59	4.08	6.20	67.58
300	85.84	129.21	14.93	1.01	1.52	28.67	4.24	6.42	70.38
300									

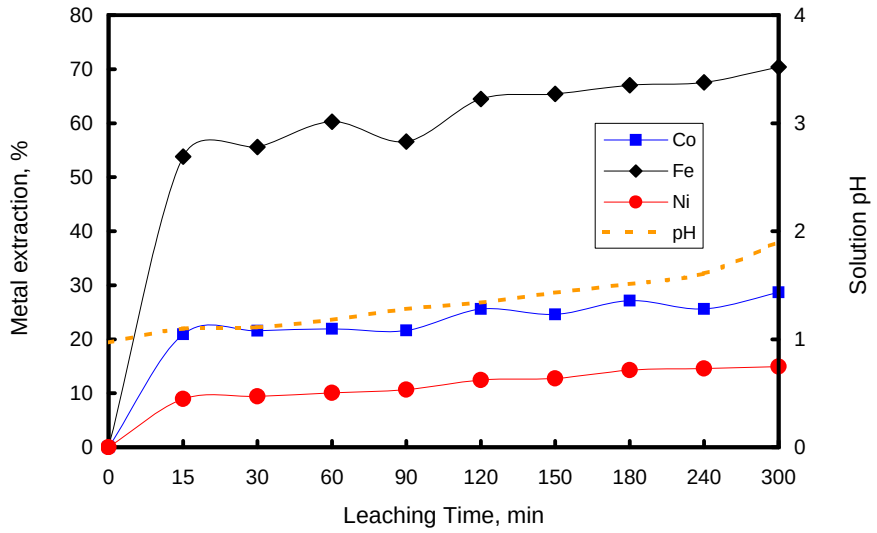

Figure A7.2: Metal extractions as a function of leaching time for a residence time of 5 hours

TABLE A7.3: METAL SOLUTION CONCENTRATIONS DURING ATMOSPHERIC LEACHING OF THE MATTE FOR A RESIDENCE TIME OF 7 HOURS

Leaching conditions:	Temperature: (^{o} C)	60
	Mixing rate (rpm):	205
	Pulp density (kg/L):	1.7
	Leaching time (hrs):	7

Leaching Time (min)	Co (g/l)	Fe (g/l)	Ni (g/l)	Cu (g/l)	pH
0	0.18	0.67	24.61	24.95	0.51
15	0.49	3.20	69.46	20.70	1.43
30	0.52	3.34	73.15	18.00	1.45
60	0.59	3.50	78.78	14.28	1.50
90	0.60	3.67	83.71	10.70	1.55
120	0.65	3.83	88.78	8.59	1.60
180	0.69	3.87	93.10	5.32	1.68
240	0.74	3.94	97.41	2.02	1.80
300	0.76	4.18	102.23	0.00	2.00
360	0.79	4.19	104.73	0.00	2.76
420	0.83	4.11	106.89	0.00	3.22

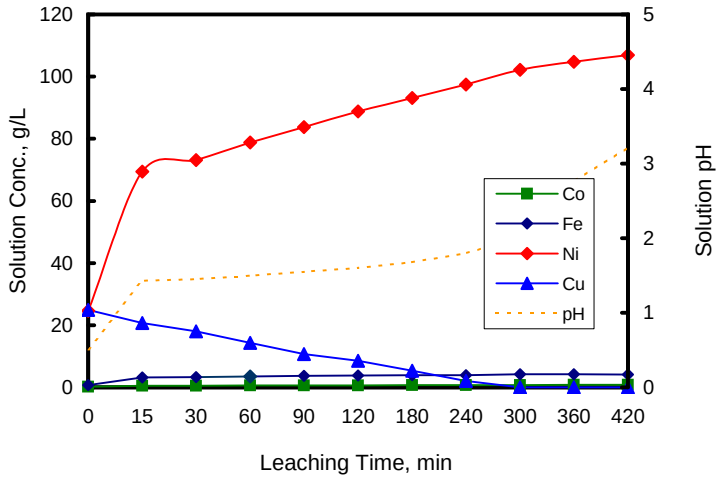

Figure A7.3: Metal concentrations as a function of leaching time for a residence time of 7 hours

TABLE A7.4: METAL EXTRACTIONS BASED ON SOLUTION CONCENTRATIONS DURING ATMOSPHERIC LEACHNG OF THE MATTE FOR A RESIDENCE TIME OF 7 HOURS

Leaching conditions:	Temperature (o C):	60				
	Mixing rate (rpm):	205				
	Pulp density (kg/L):	1.7	**Metal content of matte**			
	Leaching time (hrs):	7	Ni	614.14	g	(47.98%)
	Matte (kg):	1.28	Co	4.35	g	(0.34%)
	Solution (L):	1.54	Fe	7.68	g	(0.6%)

Leaching Time (min)	Ni (g/l)	Ni (g)	Ni Leach %	Co (g/l)	Co (g)	Co leach %	Fe (g/l)	Fe (g)	Fe %
0	24.61	37.90	0.00	0.18	0.28	0	0.67	1.03	0
15	69.46	106.97	11.25	0.49	0.75	10.97	3.20	4.93	50.73
30	73.15	112.56	12.16	0.52	0.80	12.01	3.34	5.14	53.49
60	78.78	121.09	13.55	0.59	0.90	14.41	3.50	5.38	56.60
90	83.71	128.43	14.74	0.60	0.92	14.75	3.67	5.63	59.84
120	88.78	135.73	15.93	0.65	0.99	16.40	3.83	5.86	62.84
180	93.10	141.85	16.93	0.69	1.05	17.70	3.87	5.91	63.58
240	97.41	147.84	17.90	0.74	1.12	19.30	3.94	6.01	64.84
300	102.23	154.42	18.97	0.76	1.14	19.93	4.18	6.34	69.11
360	104.73	157.77	19.52	0.79	1.18	20.85	4.19	6.35	69.28
420	106.89	160.61	19.98	0.83	1.24	22.06	4.11	6.25	67.91

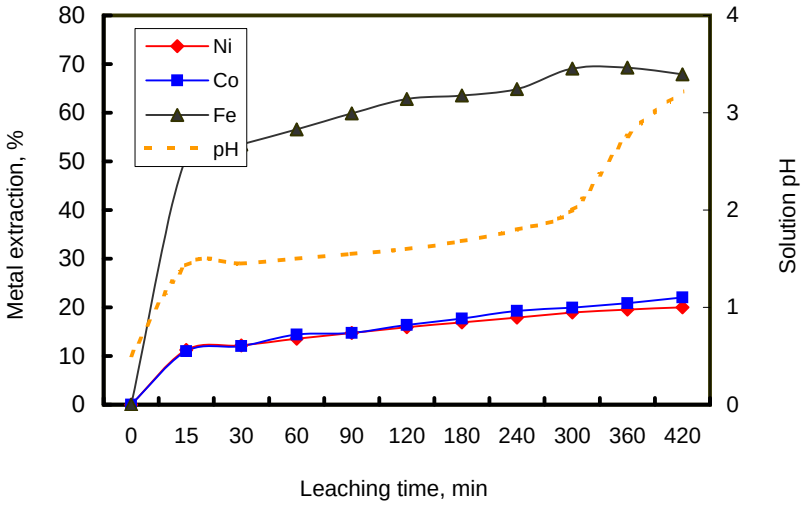

Figure A7.4: Metal extractions as a function of leaching time for a residence time of 7 hours

TABLE A7.5: METAL SOLUTION CONCENTRATIONS DURING ATMOSPHERIC LEACHING OF THE MATTE FOR A RESIDENCE TIME OF 9 HOURS

Leaching conditions:	Temperature: (^{o} C)	60
	Mixing rate (rpm):	205
	Pulp density (kg/L):	1.7
	Leaching time (hrs):	9

Leaching Time (min)	Co (g/l)	Fe (g/l)	Ni (g/l)	Cu (g/l)	pH
0	0.18	0.67	24.61	24.95	0.44
15	0.48	3.14	64.03	24.79	1.33
30	0.46	3.3	69.32	21.01	1.36
60	0.52	3.44	75.68	15.80	1.42
90	0.58	3.64	82.03	11.71	1.46
120	0.63	3.76	85.98	9.31	1.58
180	0.67	3.93	91.91	5.26	1.69
240	0.72	4.02	97.56	2.04	1.80
300	0.76	4.1	101.12	0.00	1.93
360	0.79	4.01	102.28	0.00	2.68
420	0.81	3.98	104.87	0.00	3.28
540	0.89	3.92	105.04	0.00	4.92

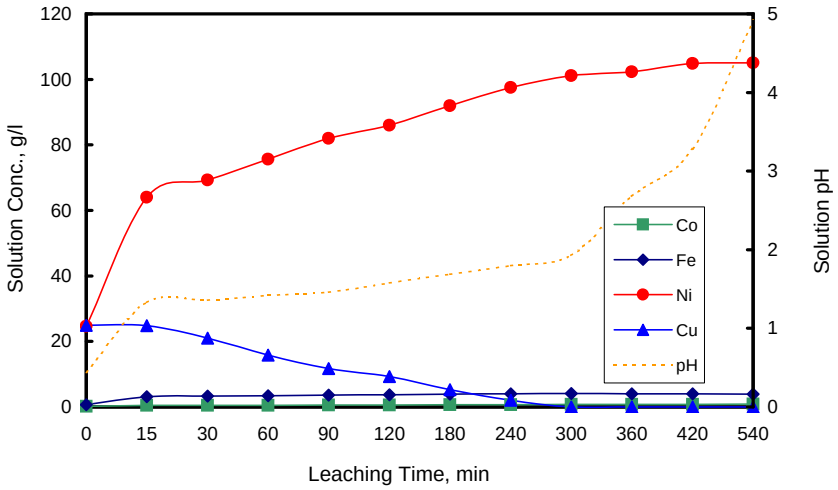

Figure A7.5: Metal concentrations as a function of leaching time for a residence time of 9 hrs

TABLE A7.6: METAL EXTRACTIONS BASED ON SOLUTION CONCENTRATIONS DURING ATMOSPHERIC LEACHNG OF THE MATTE FOR A RESIDENCE TIME OF 9 HOURS

Leaching conditions:

Temperature (o C):	60
Mixing rate (rpm):	205
Pulp density (kg/L):	1.7
Leaching time (hrs):	9
Matte (kg):	1.28
Solution (L):	1.54

Metal content of matte

Ni	**614.14 g**	(47.98%)
Co	**4.35 g**	(0.34%)
Fe	**7.68 g**	(0.6%)

Leaching Time (min)	Ni (g/l)	Ni (g)	Ni Leach %	Co (g/l)	Co (g)	Co leach %	Fe (g/l)	Fe (g)	Fe %
0	24.61	37.90	0.00	0.18	0.28	0	0.67	1.03	0
15	64.03	98.61	9.88	0.48	0.74	10.62	3.14	4.84	49.53
30	69.32	106.62	11.19	0.46	0.71	9.92	3.3	5.08	52.68
60	75.68	116.26	12.76	0.52	0.80	11.97	3.44	5.29	55.40
90	82.03	125.72	14.30	0.58	0.89	13.99	3.64	5.58	59.22
120	85.98	131.41	15.23	0.63	0.96	15.65	3.76	5.75	61.47
180	91.91	139.80	16.59	0.67	1.01	16.95	3.93	5.99	64.60
240	97.56	147.65	17.87	0.72	1.08	18.55	4.02	6.12	66.23
300	101.12	152.51	18.66	0.76	1.14	19.80	4.1	6.23	67.65
360	102.28	154.06	18.91	0.79	1.18	20.72	4.01	6.11	66.08
420	104.87	157.47	19.47	0.81	1.21	21.33	3.98	6.07	65.57
540	105.04	157.69	19.51	0.89	1.31	23.70	3.92	5.99	64.56

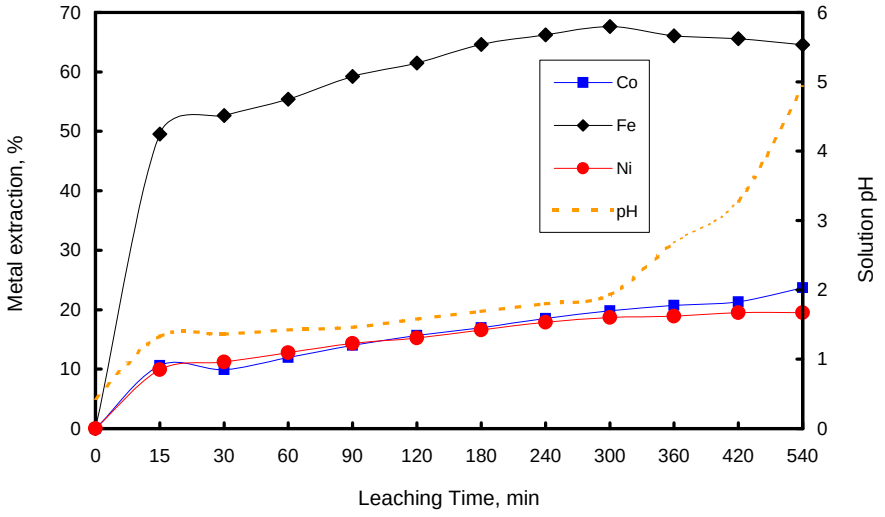

Fig.ure A7.6: Metal extractions as a function of leaching time for a residance time of 9 hrs

TABLE A7.5B: METAL SOLUTION CONCENTRATIONS DURING ATMOSPHERIC LEACHING OF THE MATTE FOR A RESIDENCE TIME OF 9 HOURS - SECOND TEST

Leaching conditions:

Temperature: (^{o} C)	60
Mixing rate (rpm):	205
Pulp density (kg/L):	1.7
Leaching time (hrs):	9

Leaching Time (min)	Co (g/L)	Fe (g/L)	Ni (g/L)	Cu (g/L)
0	0.18	0.67	24.61	24.95
15	0.41	2.25	58.73	22.15
30	0.51	2.84	67.51	18.08
60	0.54	3.41	76.18	13.26
90	0.59	3.57	80.42	11.01
120	0.65	3.84	88.36	7.91
180	0.70	4.05	94.11	5.39
240	0.74	4.01	100.12	1.54
300	0.78	4.15	102.78	0.00
360	0.79	4.11	102.89	0.00
420	0.86	3.95	105.62	0.00
540	0.87	3.79	104.16	0.00

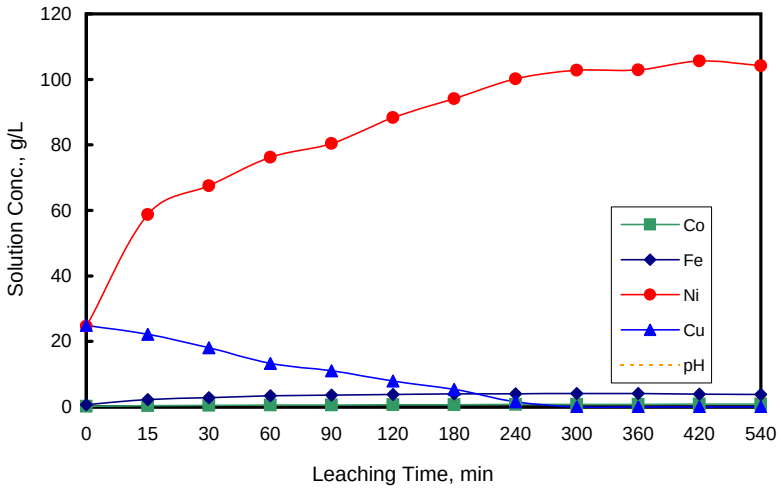

Figure A7.5B: Metal concentrations as a function of leaching time for a residence time of 9 hrs - second test

TABLE A7.6: METAL EXTRACTIONS BASED ON SOLUTION CONCENTRATIONS DURING ATMOSPHERIC LEACHNG OF THE MATTE FOR A RESIDENCE TIME OF 9 HOURS - SECOND TEST

Leaching conditions:

Temperature (o C):	60
Mixing rate (rpm):	205
Pulp density (kg/L):	1.7
Leaching time (hrs):	9
Matte (kg):	1.28
Solution (L):	1.54

Metal content of matte

Ni	**614.14 g**	(47.98%)
Co	**4.35 g**	(0.34%)
Fe	**7.68 g**	(0.6%)

Leaching Time (min)	Ni (g/L)	Ni (g)	Ni Leach %	Co (g/L)	Co (g)	Co leach %	Fe (g/L)	Fe (g)	Fe %
0	24.61	37.90	0.00	0.18	0.28	0.00	0.67	1.03	0.00
15	58.73	90.44	8.56	0.41	0.63	8.14	2.25	3.47	31.68
30	67.51	103.75	10.72	0.51	0.78	11.62	2.84	4.36	43.32
60	76.18	116.88	12.86	0.54	0.83	12.65	3.41	5.21	54.38
90	80.42	123.20	13.89	0.59	0.90	14.33	3.57	5.44	57.43
120	88.36	134.63	15.75	0.65	0.99	16.32	3.84	5.83	62.49
180	94.11	142.77	17.08	0.70	1.06	17.94	4.05	6.13	66.36
240	100.12	151.12	18.44	0.74	1.11	19.22	4.01	6.07	65.64
300	102.78	154.75	19.03	0.78	1.17	20.47	4.15	6.26	68.13
360	102.89	154.90	19.05	0.79	1.18	20.78	4.11	6.21	67.43
420	105.62	158.49	19.64	0.86	1.27	22.90	3.95	6.00	64.69
540	104.16	156.61	19.33	0.87	1.29	23.19	3.79	5.79	62.00

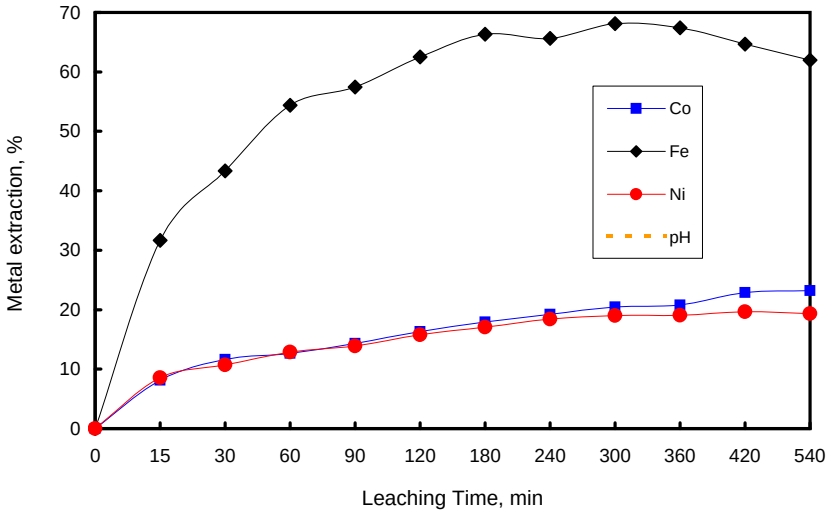

Fig.ure A7.6B: Metal extractions as a function of leaching time for a residance time of 9 hrs - Second test

TABLE A7.1: METAL SOLUTION CONCENTRATIONS DURING ATMOSPHERIC LEACHING OF THE MATTE FOR A RESIDENCE TIME OF 5 HOURS

Leaching conditions: Temperature: 60 °C
Agitation: 205 rpm
Pulp density: 1.7 kg/L

Leaching Time (min)	Co (g/l)	Fe (g/l)	Ni (g/l)	Cu (g/l)	pH
0	0.18	0.67	24.61	24.95	0.97
15	0.77	3.35	60.14	22.84	1.10
30	0.79	3.44	62.18	19.49	1.11
60	0.80	3.68	64.86	14.47	1.18
90	0.79	3.49	67.18	10.45	1.28
120	0.91	3.91	74.94	8.75	1.34
150	0.88	3.96	76.05	6.39	1.43
180	0.96	4.05	82.83	4.79	1.51
240	0.91	4.08	84.33	1.30	1.61
300	1.01	4.24	85.84	0.00	1.90

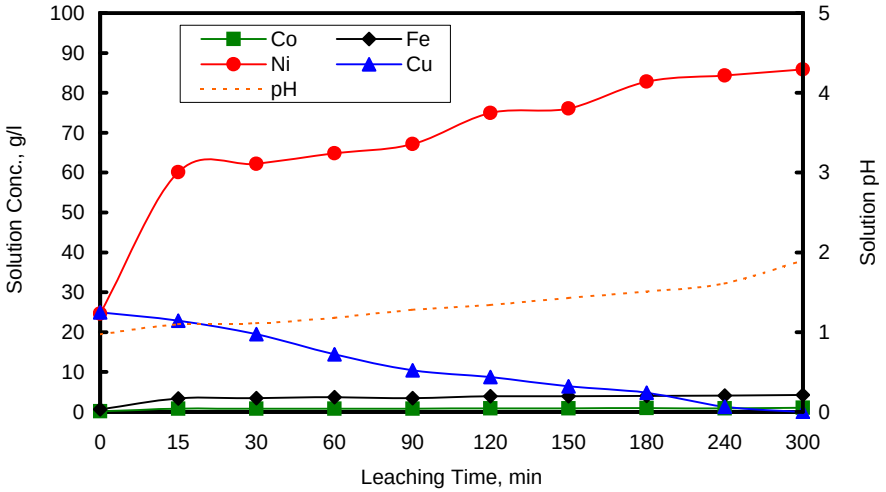

Figure A7.1: Metal concentrations as a function of leaching time for a residence time of 5 hours

TABLE A7.2: METAL EXTRACTIONS BASED ON SOLUTION CONCENTRATIONS DURING ATMOSPHERIC LEACHING OF THE MATTE FOR A RESIDENCE TIME OF 5 HOURS

Leaching conditions:				**Metal content of matte:**	
	Temperature:	60 oC		**Ni**	**612.22** g (47.98%)
	Agitation:	205 rpm		**Co**	**4.34** g (0.34 %)
	Pulp density:	1.7 kg/L		**Fe**	**7.66** g (0.60 %)
	Matte:	1.28	kg		
	Solution:	1.54	L		

Leaching Time (min)	**Ni (g/l)**	**Ni (g)**	**Ni Leach %**	**Co (g/l)**	**Co (g)**	**Co leach %**	**Fe (g/l)**	Fe (g)	Fe (%)
0	24.61	37.83	0.00	0.18	0.28	0	0.67	1.03	0
15	60.14	92.44	8.92	0.77	1.18	20.90	3.35	5.15	53.80
30	62.18	95.52	9.42	0.79	1.21	21.60	3.44	5.29	55.58
60	64.86	99.57	10.09	0.80	1.23	21.94	3.68	5.64	60.24
90	67.18	103.02	10.65	0.79	1.21	21.61	3.49	5.36	56.61
120	74.94	114.17	12.47	0.91	1.39	25.58	3.91	5.97	64.50
150	76.05	115.74	12.73	0.88	1.34	24.60	3.96	6.04	65.42
180	82.83	125.14	14.26	0.96	1.46	27.16	4.05	6.16	67.05
240	84.33	127.19	14.60	0.91	1.39	25.59	4.08	6.20	67.58
300	85.84	129.21	14.93	1.01	1.52	28.67	4.24	6.42	70.38
300									

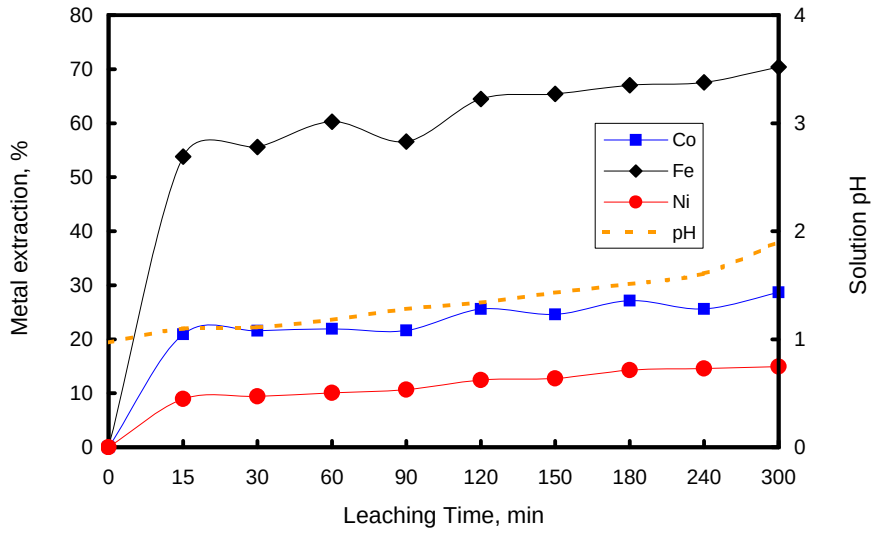

Figure A7.2: Metal extractions as a function of leaching time for a residence time of 5 hours

TABLE A8: METAL EXTRACTIONS BASED ON XRF ANALYSIS OF SOLID RESIDUE FROM ATMOSPHERIC LEACHING EXPERIMENTS

Feed matte

Ni (%) 47.98 Co (%) 0.34

Cu (%) 31.31 Fe (%) 0.60

Fixed Variable	Wt of matte (g)	Wt of residue (g)	Metal in leach residue (%)				Metal extraction (%)		
			Ni	Co	Fe	Cu	Ni	Co	Fe
Temp: 80 ^{o}C	1276	1143	41.3	0.25	0.19	42.00	22.89	34.13	71.63
Temp: 70^{o}C	1276	1172	42.9	0.26	0.17	42.00	17.88	29.76	73.98
Temp: 60^{o}C	1276	1181	43.7	0.27	0.18	41.00	15.70	27.04	72.23
Temp: 50^{o}C	1276	1199	43.5	0.26	0.29	40.00	14.81	27.31	54.58
Time: 5 hrs	1276	1181	43.7	0.27	0.18	41.00	15.70	27.04	72.23
Time: 7 hrs	1276	1178	42.3	0.26	0.19	41.00	18.61	30.49	70.77
Time: 9 hrs	1276	1174	41.9	0.26	0.19	41.00	19.65	29.91	70.86
Stirring rate: 145 rpm	1276	1195	44.9	0.25	0.20	41.00	12.36	31.14	68.94
Stirring rate: 205 rpm	1276	1181	43.7	0.27	0.18	41.00	15.70	27.04	72.23
Stirring rate: 400 rpm	1276	1178	41.4	0.24	0.13	40.00	20.34	35.10	80.46
Particle size: -300+150 µm	1276	1182	43.2	0.25	0.10	36.00	16.60	31.89	84.25
Particle size: -106+45 µm	1276	1139	43.7	0.24	0.17	39.00	18.70	36.99	74.71
Particle size: -45 um	1276	1136	43.2	0.24	0.16	38.00	19.84	38.47	76.26
SCM: temp: 70^{o}C	1276	1176	41.3	0.25	0.13	39.00	20.67	-	-
SCM: temp: 60^{o}C	1276	1181	42.9	0.25	0.12	36.00	17.24	-	-
SCM: temp: 50^{o}C	1276	1186	43.2	0.25	0.15	35.00	16.31	-	-
PD: 1.75 kg/L	1276	1179	43.3	0.23	0.112	40.00	16.61	38.85	82.75
PD: 1.7 kg/L	1276	1181	43.7	0.27	0.18	41.00	15.70	27.04	72.23
PD: 1.6 kg/L	1276	1174	41.8	0.24	0.19	41.00	19.84	34.51	70.86
H_2SO_4: 90 kg/L	1276	1181	43.7	0.27	0.18	41.00	15.70	27.04	72.23
H_2SO_4: 110 kg/L	1276	1176	42.5	0.25	0.08	41.00	18.36	33.59	87.71
H_2SO_4: 125 kg/L	1276	1161	42.4	0.23	0.08	41.00	19.59	38.18	87.87
Cu: 25 kg/L	1276	1181	43.7	0.27	0.18	41.00	15.70	27.04	72.23
Cu: 36 kg/L	1276	1180	42.4	0.24	0.16	40.00	18.28	34.45	75.34
Cu: 48 kg/L	1276	1185	43.8	0.25	0.19	40.00	15.22	32.26	70.59

SCM = Shrinking Core Model (data for shrinking core model tests)

TABLE A8B: METAL EXTRACTIONS BASED ON XRF ANALYSIS OF SOLID RESIDUE FROM ATMOSPHERIC LEACHING EXPERIMENTS - REPEAT TESTS

Feed matte

Ni (%)	47.98	Co (%)	0.34
Cu (%)	31.31	Fe (%)	0.6

Fixed Variable	Wt of matte (g)	Wt of residue (g)	Metal in leach residue (%)				Metal extraction (%)		
			Ni	Co	Fe	Cu	Ni	Co	Fe
Temp: 80 ^{o}C	1276	1146	41.9	0.24	0.18	42	21.57	36.6	73.06
Temp: 60 ^{o}C	1276	1183	42.8	0.26	0.19	41	17.3	29.1	70.64
Time: 5 hrs	1276	1183	42.8	0.26	0.19	41	17.3	29.1	70.64
Time: 9 hrs	1276	1176	42.5	0.26	0.18	41	18.36	30.06	72.66
Stirring rate: 205 rpm	1276	1183	42.8	0.26	0.19	41	17.3	29.1	70.64
Stirring rate: 400 rpm	1276	1183	40.3	0.23	0.12	42	22.13	36.19	81.15
Particle size: -300+150 µm	1276	1175	44.2	0.26	0.11	36	15.17	29.58	83.27
Particle size: -45 µm	1276	1141	41.9	0.24	0.17	42	21.91	36.88	74.66
PD: 1.7 kg/L	1276	1183	42.8	0.26	0.19	41	17.3	29.1	70.64
PD: 1.6 kg/L	1276	1174	42.3	0.25	0.18	41	18.89	32.35	72.4
H_2SO_4: 90 kg/L	1276	1183	42.8	0.26	0.19	41	17.3	29.1	70.64
H_2SO_4: 125 kg/L	1276	1161	43.3	0.24	0.09	41	17.89	35.77	86.35
Cu: 25 kg/L	1276	1183	42.8	0.26	0.19	41	17.3	29.1	70.64
Cu: 48 kg/L	1276	1185	43.1	0.25	0.18	40	16.58	30.62	72.14

SHRINKING CORE MODELS

PARTICLE SIZE: -300 + 150 UM

Leaching Time (hrs)	Ni extraction %			Fraction Leached (X) Ni (50 deg)	Fraction Leached (X) Ni (60 deg)	Fraction Leached (X) Ni (70 deg)	Diffusion controlled $1-3(1-X)^{2/3}+2(1-X)$			Chemical reaction controlled $1-(1-X)^{1/3}$			Mixed controlled $[1-3(1-X)^{2/3}+2(1-X)]+\alpha_{[1-(1-X)^{1/3}]}$		
	50	60	70				(50 deg)	(60 deg)	(70 deg)	(50 deg)	(60 deg)	(70 deg)	(50 deg)	(60 deg)	(70 deg)
0	0.00	0	0	0.000	0.000	0.000	0.000	0.000	0.000	0.000	0.000	0.000	0.000	0.000	0.000
15	5.91	6.24	7.71	0.059	0.062	0.077	0.001	0.001	0.002	0.020	0.021	0.026	0.002	0.002	0.003
30	6.99	9.62	9.61	0.070	0.096	0.096	0.002	0.003	0.003	0.024	0.033	0.033	0.003	0.005	0.005
60	9.72	10.8	12.26	0.097	0.108	0.123	0.003	0.004	0.005	0.034	0.037	0.043	0.005	0.006	0.007
90	10.20	12.5	15.04	0.102	0.125	0.150	0.004	0.006	0.008	0.035	0.044	0.053	0.005	0.007	0.011
120	12.10	13.6	15.86	0.121	0.136	0.159	0.005	0.007	0.009	0.042	0.048	0.056	0.007	0.009	0.012
180	13.01	16.45	18.22	0.130	0.165	0.182	0.006	0.010	0.012	0.045	0.058	0.065	0.008	0.012	0.015
240	14.21	17.5	19.89	0.142	0.175	0.199	0.007	0.011	0.015	0.050	0.062	0.071	0.009	0.014	0.018

DIFFUSION CONTROL

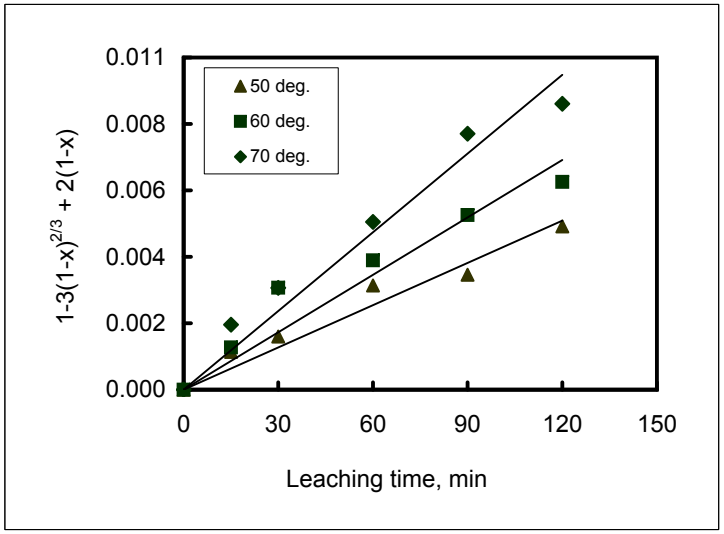

CHEMICAL CONTROL

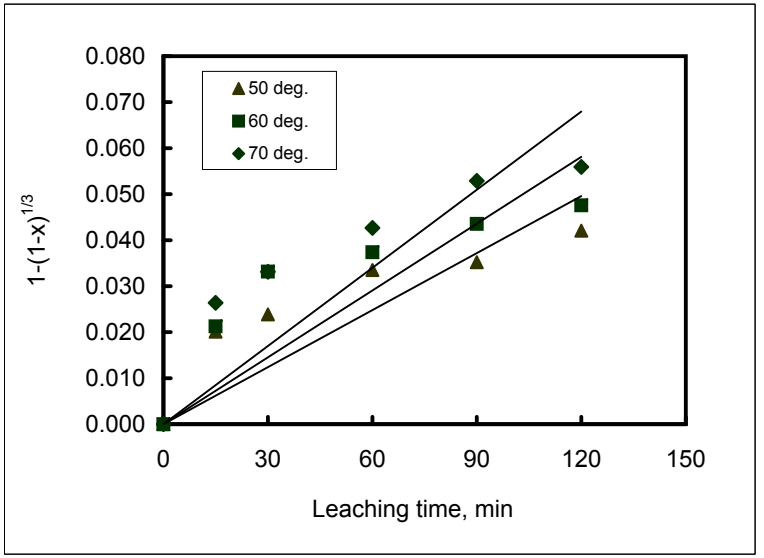

50 oC		60 oC		70 oC	
$[1-3(1-X)^{2/3} + 2(1-X)]/t$	$[1-(1-X)^{1/3}]/t$	$[1-3(1-X)^{2/3} + 2(1-X)]/t$	$[1-(1-X)^{1/3}]/t$	$[1-3(1-X)^{2/3} + 2(1-X)]/t$	$[1-(1-X)^{1/3}]/t$
#DIV/0!	#DIV/0!	#DIV/0!	#DIV/0!	#DIV/0!	#DIV/0!
0.0797	1.3401	0.0890	1.4166	0.1368	1.7594
0.0560	0.7955	0.1075	1.1051	0.1073	1.1039
0.0549	0.5585	0.0681	0.6230	0.0884	0.7110
0.0404	0.3914	0.0613	0.4837	0.0899	0.5876
0.0430	0.3507	0.0548	0.3963	0.0753	0.4661
0.0333	0.2522	0.0542	0.3231	0.0671	0.3603
0.0300	0.2075	0.0462	0.2588	0.0605	0.2969

MIXED CONTROL

ESTIMATION OF KINETIC CONSTANT α

Temp. (^{o} C)	α
50	0.0417
60	0.0449
70	0.0497

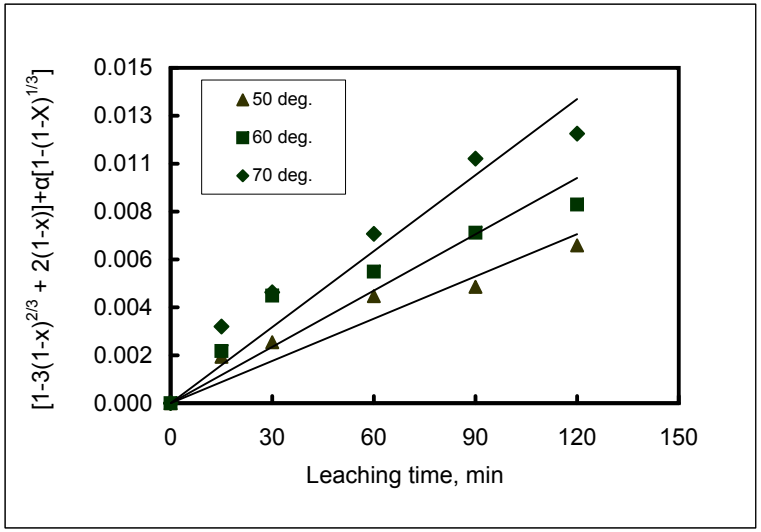

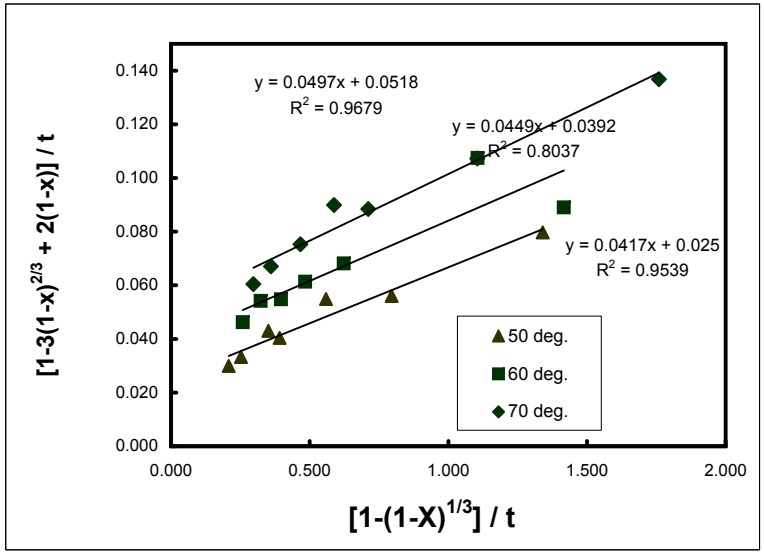

TABLE B1.1: METAL CONCENTRATIONS DURING PRESSURE LEACHING OF MATTE PRE-LEACHED AT 80 oC

Leaching conditions:

Temperature (^{o}C):	145
Total pressure (kPa):	500
Initial P.D. (kg/L):	1.4
Leaching time (hrs):	3
Mixing rate (rpm):	900
Oxidant :	O_2

Leaching Time (min)	Co (g/l)	Fe (g/l)	Ni (g/l)	Cu (g/l)	pH
*					
-25	0.17	0.75	21.90	26.20	0.41
0	0.32	1.00	44.20	14.80	0.46
15	0.47	1.28	64.50	0.79	0.5
30	0.53	1.35	68.70	0.20	0.52
60	0.54	1.37	81.10	0.19	0.72
90	0.54	1.37	93.20	0.22	0.82
120	0.55	1.39	96.50	0.12	0.89
150	0.54	1.39	99.80	0.12	0.95
180	0.55	1.43	103.00	0.06	1.01

* First 25 minutes was solution pre-heating time

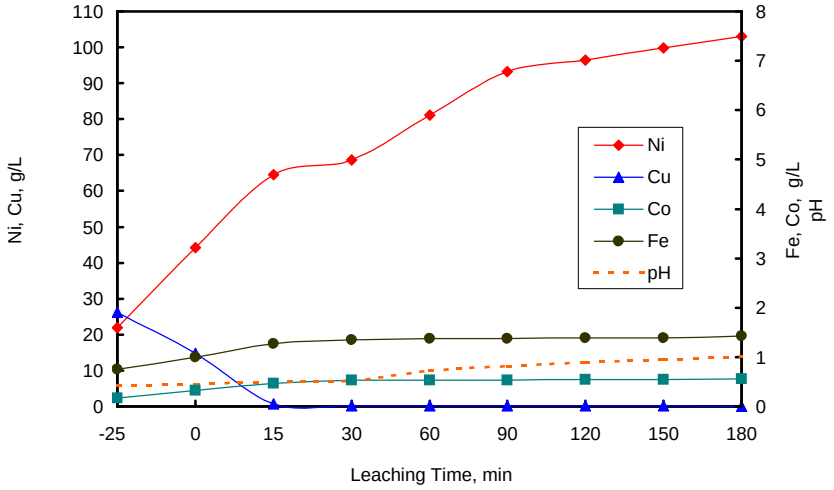

Figure B1.1: Metal concentrations as a function of leaching time for the matte pre-leached at 80 ^{o}C

TABLE B1.2: METAL EXTRACTIONS BASED ON SOLUTION CONCENTRATIONS DURING PRESSURE LEACHING OF MATTE PRE-LEACHED AT 80°C

Feed matte:		**Feed solution:**		**Leaching conditions:**	
Wt	397 g	Volume	1.167 L	Temperature:	145 °C
Ni	34.30 %	Ni	21.9 g/L	Total pressure:	500 kPa
Co	0.11 %	Co	0.17 g/L	Initial P.D. :	1.4 kg/L
Fe	0.19 %	Fe	0.75 g/L	Oxidant:	O_2

Leaching Time (min)	Ni (g/l)	Ni (g)	Ni Leach %	Co (g/l)	Co (g)	Co leach %	Fe (g/l)	Fe (g)	Fe %	H2SO4 (g/l)
- 25	21.90	25.56	0	0.17	0.20	0	0.75	0.88	0	99.40
0	44.20	51.58	19	0.32	0.37	40	1.00	1.17	39	73.60
15	64.50	74.76	36	0.47	0.54	79	1.28	1.48	80	68.20
30	68.70	79.46	40	0.53	0.61	95	1.35	1.57	92	48.60
60	81.10	93.00	50	0.54	0.62	96	1.37	1.59	94	28.50
90	93.20	105.91	59	0.54	0.62	97	1.37	1.59	94	24.20
120	96.50	109.35	62	0.55	0.63	99	1.39	1.60	97	21.10
150	99.80	112.70	64	0.54	0.63	98	1.39	1.61	97	14.50
180	103.00	115.88	66	0.55	0.63	100	1.43	1.65	102	13.40

* First 25 minutes was solution pre-heating time

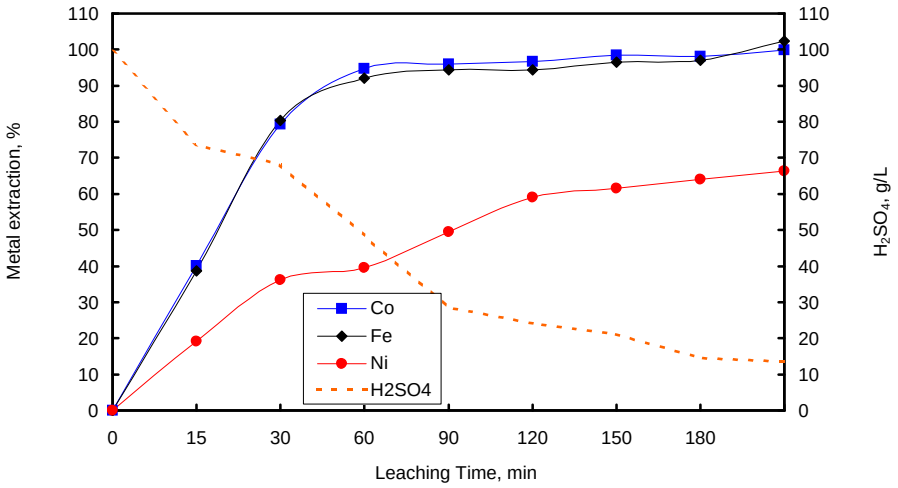

Figure B1.2.: Metal extraction as a function of leaching time for matte pre-leached at 80 oC

TABLE B1.3: METAL CONCENTRATIONS DURING PRESSURE LEACHING OF MATTE PRE-LEACHED AT 60 oC

Leaching conditions:	Temperature (^{o}C):	145
	Total pressure (kPa):	500
	Initial P.D. (kg/L):	1.4
	Leaching time (hrs):	3
	Mixing rate (rpm)	900
	Oxidant :	O_2

Leaching Time (min)	Co (g/l)	Fe (g/l)	Ni (g/l)	Cu (g/l)	pH
*					
-25	0.17	0.75	21.90	26.20	0.41
0	0.38	1.16	47.20	10.60	0.5
15	0.50	1.23	64.30	0.18	0.53
30	0.55	1.28	71.00	0.30	0.63
60	0.56	1.32	88.00	0.87	1.34
90	0.56	1.33	91.20	0.13	3.19
120	0.58	1.00	99.90	0.01	3.45
180	0.59	0.99	104.00	0.00	4.28

*First 25 minutes were solution pre-heating time

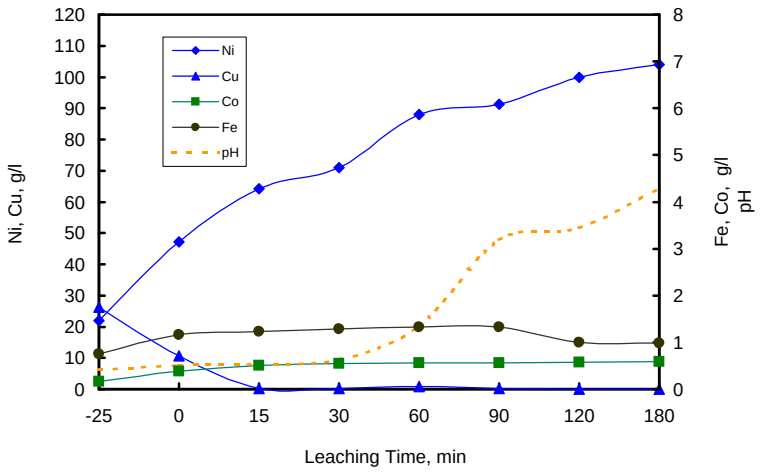

Figure B1.3: Metal concentrations as a function of time for the matte pre-leached a 60 ^{o}C

TABLE B1.4: METAL EXTRACTIONS BASED ON SOLUTION CONCENTRATIONS DURING PRESSURE LEACHING OF MATTE PRE-LEACHED AT 60°C

Feed matte:		**Feed solution:**		**Leaching conditions:**	
Wt	397 g	Volume	1.167 L	Temperature:	145 °C
Ni	34.50 %	Ni	21.9 g/L	Total pressure:	500 kPa
Co	0.12 %	Co	0.17 g/L	Initial P.D. :	1.4 kg/L
Fe	0.17 %	Fe	0.75 g/L	Oxidant:	O_2

Leaching Time (min)	Ni (g/l)	Ni (g)	Ni Leach %	Co (g/l)	Co (g)	Co leach %	Fe (g/l)	Fe (g)	Fe %	H2SO4 (g/l)
*										
-25	21.90	25.56	0	0.17	0.20	0	0.75	0.88	0	99.40
0	47.20	55.08	22	0.38	0.44	51	1.16	1.35	71	57.20
15	64.30	74.61	36	0.50	0.58	80	1.23	1.43	83	47.60
30	71.00	82.09	41	0.55	0.64	92	1.28	1.49	91	32.10
60	88.00	100.66	55	0.56	0.65	95	1.32	1.53	98	31.60
90	91.20	104.07	57	0.56	0.65	94	1.33	1.54	99	30.10
120	99.90	113.14	64	0.58	0.67	99	1.36	1.58	104	21.60
180	104.00	117.31	67	0.59	0.68	101	1.35	1.56	102	12.10

* First 25 minutes was solution pre-heating time

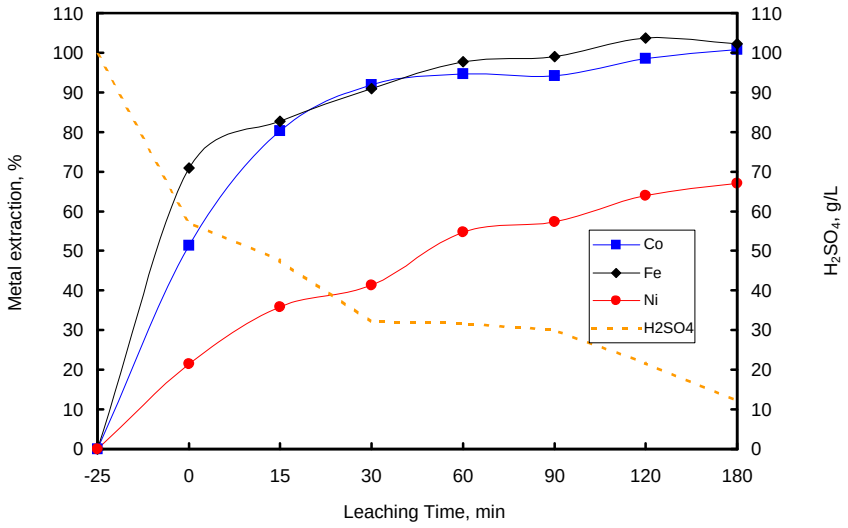

Figure B1.4: Metal extraction as a function of leaching time for matte pre-leached at 60 °C)

TABLE B1.5: METAL CONCENTRATIONS DURING PRESSURE LEACHING OF MATTE PRE-LEACHED AT 50°C

Leaching conditions:

Temperature (°C):	145
Total pressure (kPa)	500
Initial P.D. (kg/L):	1.4
Leaching time (hrs):	2.5
Mixing rate (rpm)	900
Oxidant :	O_2

Leaching Time (min)	Co (g/l)	Fe (g/l)	Ni (g/l)	Cu (g/l)	pH
*					
-25	0.17	0.75	21.90	26.20	0.41
0	0.37	1.02	47.40	11.90	0.52
15	0.51	1.27	66.10	0.84	0.55
30	0.51	1.38	73.90	0.13	0.64
60	0.52	1.39	83.90	0.13	0.90
90	0.52	1.40	87.70	0.04	0.99
120	0.55	1.40	96.10	0.03	1.03
150	0.55	1.41	99.30	0.07	1.12
180					

* First 25 minutes were solution pre-heating time

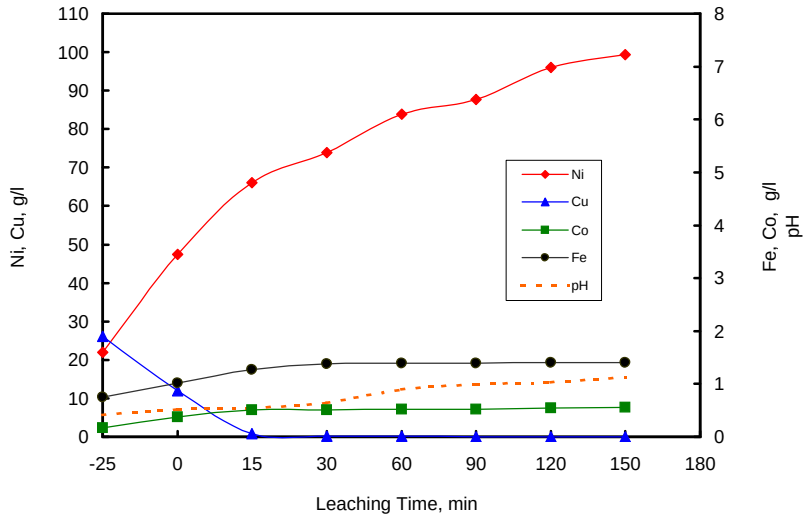

Figure B1.5: Metal concentrations as a function of leaching time for the matte pre-leache at 50 oC

TABLE B1.6: METAL EXTRACTIONS BASED ON SOLUTION CONCENTRATIONS DURING PRESSURE LEACHING OF MATTE PRE-LEACHED AT 50°C

Feed matte:		**Feed solution:**		**Leaching conditions:**	
Wt	397 g	Volume	1.167 L	Temperature:	145 °C
Ni	34.30 %	Ni	21.9 g/L	Total pressure:	500 kPa
Co	0.11 %	Co	0.17 g/L	Initial P.D. :	1.4 kg/L
Fe	0.19 %	Fe	0.75 g/L	Oxidant:	O_2

Leaching Time (min)	Ni (g/l)	Ni (g)	Ni Leach %	Co (g/l)	Co (g)	Co leach %	Fe (g/l)	Fe (g)	Fe %	H2SO4 (g/l)
*										
-25	21.90	25.56	0	0.17	0.20	0	0.75	0.88	0	99.40
0	47.40	55.32	22	0.37	0.43	53	1.02	1.19	42	64.30
15	66.10	76.67	38	0.51	0.59	90	1.27	1.48	80	53.40
30	73.90	85.38	44	0.51	0.59	91	1.38	1.60	96	32.30
60	83.90	96.30	52	0.52	0.60	92	1.39	1.61	97	22.40
90	87.70	100.36	55	0.52	0.61	93	1.40	1.61	98	21.40
120	96.10	109.11	61	0.55	0.63	99	1.40	1.62	99	15.50
150	99.30	112.37	64	0.55	0.63	100	1.41	1.63	100	13.10
180										

* First 25 minutes were solution pre-heating time

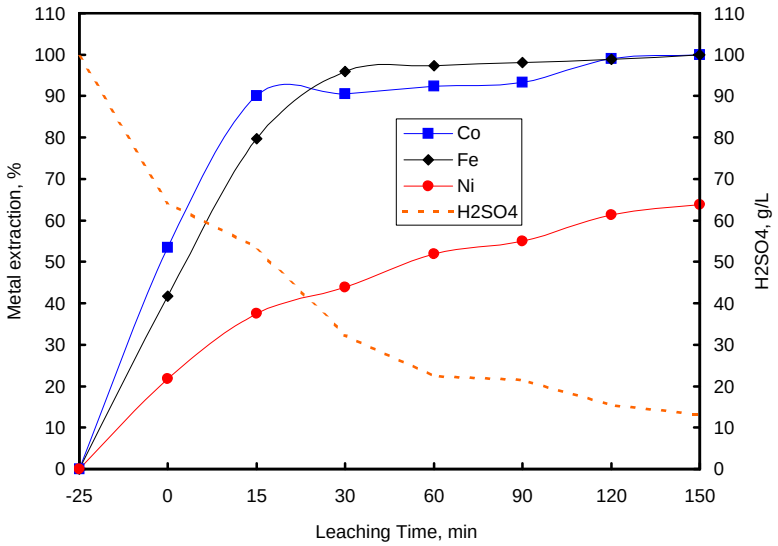

Figure B1.6: Metal extraction as a function of leaching time for matte pre-leached at 50 °C

TABLE B2.3: METAL CONCENTRATIONS DURING PRESSURE LEACHING OF MATTE PRE-LEACHED AT STIRRING RATE OF 205 RPM

Leaching conditions:	Temperature (^{o}C):	145
	Total pressure (kPag):	500
	Initial P.D. (kg/L):	1.4
	Leaching time (hrs):	3
	Mixing rate (rpm)	900
	Oxidant :	O_2

Leaching Time (min)	Co (g/l)	Fe (g/l)	Ni (g/l)	Cu (g/l)	pH
*					
-25	0.17	0.75	21.90	26.20	0.41
0	0.38	1.16	47.20	10.60	0.5
15	0.50	1.23	64.30	0.18	0.53
30	0.55	1.28	71.00	0.30	0.63
60	0.56	1.32	88.00	0.87	1.34
90	0.56	1.33	91.20	0.13	3.19
120	0.58	1.00	98.60	0.01	3.45
180	0.59	0.99	104.00	0.00	4.28

*First 25 minutes were solution pre-heating time

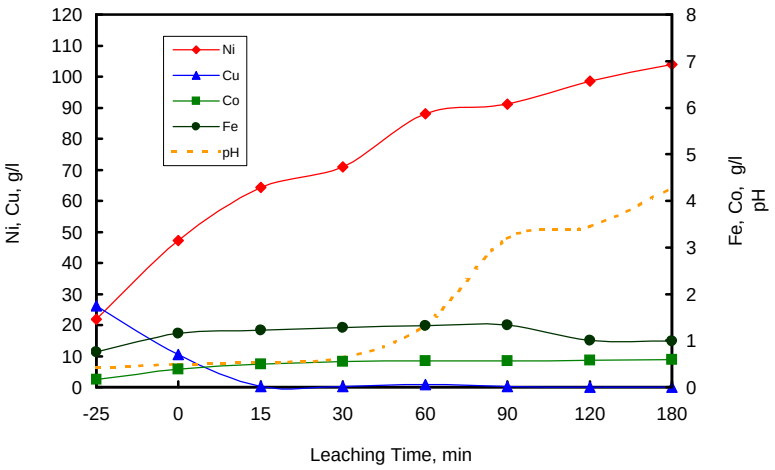

Figure B2.3: Metal concentration as a function of time for the matte pre-leached a stirring rate of 205 rpm

TABLE B2.4: METAL EXTRACTIONS BASED ON SOLUTION CONCENTRATIONS DURING PRESSURE LEACHING OF MATTE PRE-LEACHED AT STIRRING RATE OF 205 RPM

Feed matte:		**Feed solution:**		**Leaching conditions:**	
Wt	397 g	Volume	1.167 L	Temperature:	145 ^{o}C
Ni	34.50 %	Ni	21.9 g/L	Total pressure:	500 kPag
Co	0.12 %	Co	0.17 g/L	Initial P.D. :	1.4 kg/L
Fe	0.17 %	Fe	0.75 g/L	Oxidant:	O_2

Leaching Time (min)	Ni (g/l)	Ni (g)	Ni Leach %	Co (g/l)	Co (g)	Co leach %	Fe (g/l)	Fe (g)	Fe %	H2SO4 (g/l)
*										
-25	21.90	25.56	0	0.17	0.20	0	0.75	0.88	0	99.40
0	47.20	55.08	22	0.38	0.44	51	1.16	1.35	71	57.20
15	64.30	74.61	36	0.50	0.58	80	1.23	1.43	83	47.60
30	71.00	82.09	41	0.55	0.64	92	1.28	1.49	91	32.10
60	88.00	100.66	55	0.56	0.65	95	1.32	1.53	98	31.60
90	91.20	104.07	57	0.56	0.65	94	1.33	1.54	99	30.10
120	98.60	111.78	63	0.58	0.67	99	1.36	1.58	104	21.60
180	104.00	117.28	67	0.59	0.68	101	1.35	1.56	102	12.10

* First 25 minutes was solution pre-heating time

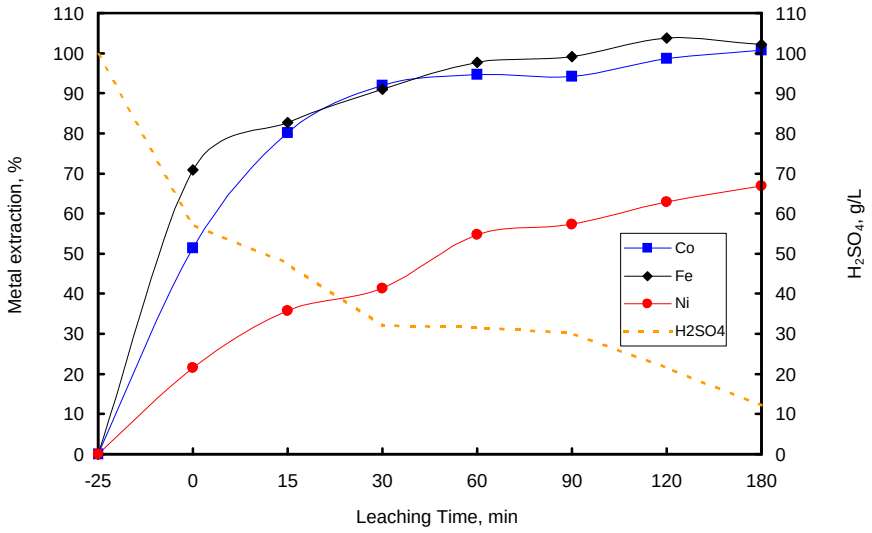

Figure B2.4: Metal extraction as a function of leaching time for matte pre-leached at stirring rat of 205 rpm

TABLE B2.1: METAL CONCENTRATIONS DURING PRESSURE LEACHING OF MATTE PRE-LEACHED AT STIRRING RATE OF 145 RPM

Leaching conditions	Temperature (^{o}C):	145
	Total pressure (kPag)	500
	Initial P.D. (kg/L):	1.4
	Leaching time (hrs):	3
	Mixing rate (rpm)	900
	Oxidant :	O_2

Leaching Time (min)	Co (g/l)	Fe (g/l)	Ni (g/l)	Cu (g/l)	H2SO4 (g/l)	pH
*						
-25	0.17	0.75	21.90	26.20	994.00	0.41
0	0.27	1.19	34.70	0.00	711.00	0.49
15	0.46	1.30	60.80	0.04	575.00	0.59
30	0.51	1.32	64.60	0.02	415.00	0.65
60	0.52	1.33	72.80	0.14	366.00	0.72
90	0.53	1.35	86.80	0.04	290.00	0.77
120	0.55	1.40	91.20	0.00	231.00	0.82
150	0.56	1.42	98.50	0.01	211.00	0.84
180						

* First 25 minutes were solution pre-heating time

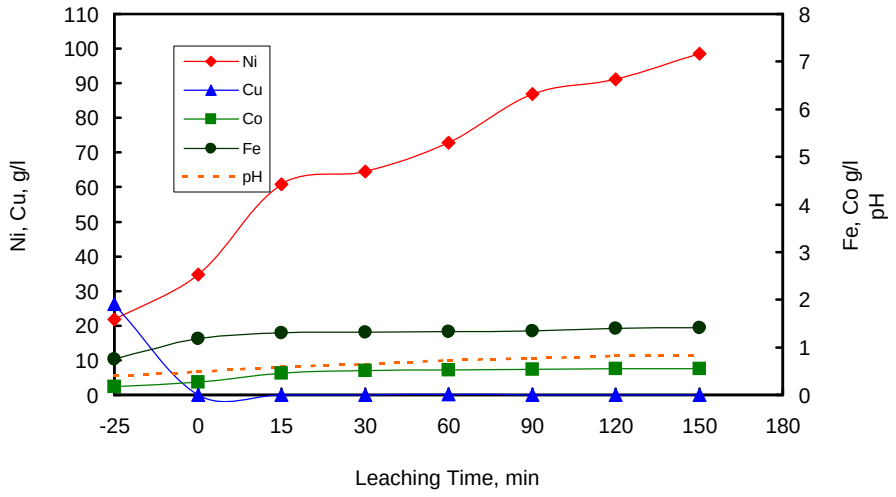

Figure B2.1: Metal concentration as a function of time for matte pre-leached a stirring rate 145 rpm

TABLE B2.2: METAL EXTRACTIONS BASED ON SOLUTION CONCENTRATIONS DURING PRESSURE LEACHING OF MATTE PRE-LEACHED AT STIRRING RATE OF 145 RPM

Feed matte:		**Feed solution:**		**Leaching conditions:**	
Wt	397 g	Volume	1.167 L	Temperature:	145 °C
Ni	34.30 %	Ni	21.9 g/L	Total pressure:	500 kPa
Co	0.11 %	Co	0.17 g/L	Initial P.D. :	1.4 kg/L
Fe	0.19 %	Fe	0.75 g/L	Oxidant:	O_2

Leaching Time (min)	Ni (g/l)	Ni (g)	Ni Leach %	Co (g/l)	Co (g)	Co leach %	Fe (g/l)	Fe (g)	Fe %	H2SO4 (g/l)
*										
-25	21.90	25.56	0	0.17	0.20	0	0.75	0.88	0	99.40
0	34.70	40.49	11	0.27	0.32	27	1.19	1.39	68	71.10
15	60.80	70.30	33	0.46	0.53	76	1.30	1.51	85	57.50
30	64.60	74.55	36	0.51	0.59	89	1.32	1.54	88	41.50
60	72.80	83.50	43	0.52	0.60	92	1.33	1.55	89	36.60
90	86.80	98.44	54	0.53	0.61	95	1.35	1.57	92	29.00
120	91.20	103.02	57	0.55	0.63	98	1.40	1.62	99	23.10
150	98.50	110.45	62	0.56	0.64	100	1.42	1.64	101	21.10
180										

*First 25 minutes were solution pre-heating time

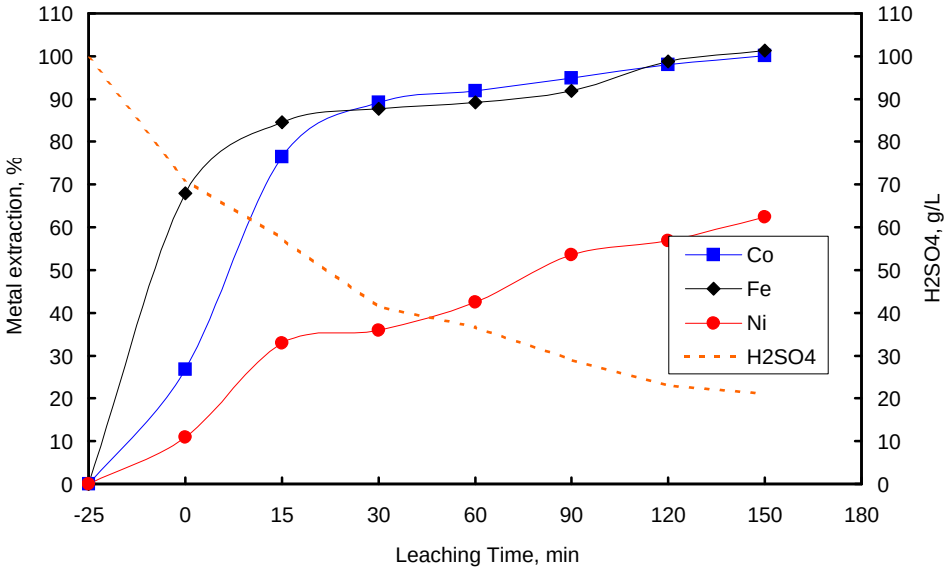

Figure B2.2: Metal extraction as a function of leaching time for matte pre-leached at stirring rate o 145 rpm

TABLE B2.5: METAL CONCENTRATIONS DURING PRESSURE LEACHING OF MATTE PRE-LEACHED AT STIRRING RATE OF 400 RPM

Leaching conditior	Temperature (^{o}C):	145
	Total pressure (kPag	500
	Initial P.D. (kg/L):	1.4
	Leaching time (hrs):	3
	Mixing rate (rpm)	900
	Oxidant :	O_2

Leaching Time (min)	Co (g/l)	Fe (g/l)	Ni (g/l)	Cu (g/l)	H2SO4 (g/l)	pH
*						
-25	0.17	0.75	21.90	26.20	994.00	0.41
0	0.37	1.21	46.40	0.00	662.00	0.5
15	0.48	1.28	66.80	0.05	563.00	0.53
30	0.50	1.31	71.00	0.01	484.00	0.57
60	0.51	1.36	78.40	0.03	432.00	0.63
90	0.51	1.40	81.20	0.01	422.00	0.65
120	0.53	1.41	83.70	0.04	403.00	0.68
150	0.55	1.41	95.30	0.17	421.00	0.70
180	0.55	1.41	100.80	0.79	316.00	0.74

* First 25 minutes were solution pre-heating time

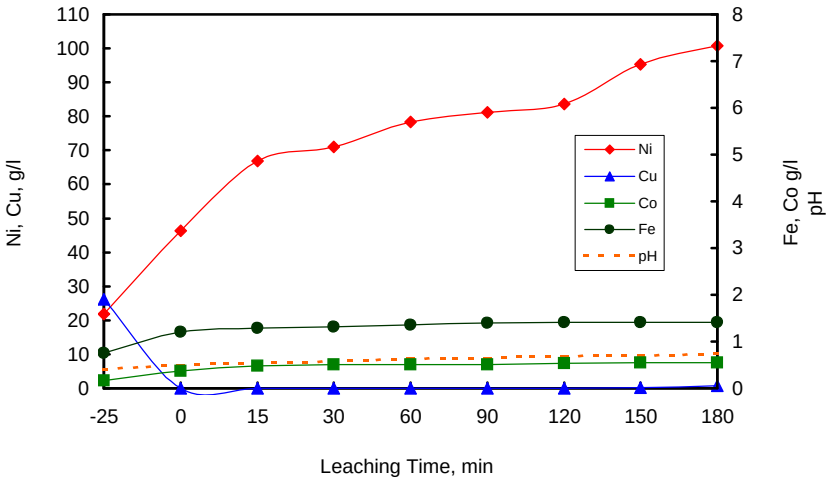

Figure B2.5: Metal concentration as a function of time for matte pre-leached at stirring rate of 400 rpm

TABLE B2.6: METAL EXTRACTIONS BASED ON SOLUTION CONCENTRATIONS DURING PRESSURE LEACHING OF MATTE PRE-LEACHED AT STIRRING RATE OF 400 RPM

Feed matte:		**Feed solution:**		**Leaching conditions:**	
Wt	397 g	Volume	1.167 L	Temperature:	145 ^{o}C
Ni	34.30 %	Ni	21.9 g/L	Total pressure:	500 kPa
Co	0.11 %	Co	0.17 g/L	Initial P.D. :	1.4 kg/L
Fe	0.19 %	Fe	0.75 g/L	Oxidant:	O_2

Leaching Time (min)	Ni (g/l)	Ni (g)	Ni Leach %	Co (g/l)	Co (g)	Co leach %	Fe (g/l)	Fe (g)	Fe %	H2SO4 (g/l)
*										
-25	21.90	25.56	0	0.17	0.20	0	0.75	0.88	0	99.40
0	46.40	54.15	21	0.37	0.43	53	1.21	1.41	71	66.20
15	66.80	77.45	38	0.48	0.56	82	1.28	1.49	82	56.30
30	71.00	82.14	42	0.50	0.58	88	1.31	1.53	87	48.40
60	78.40	90.22	47	0.51	0.59	90	1.36	1.57	93	43.20
90	81.20	93.21	50	0.51	0.59	90	1.40	1.62	99	42.20
120	83.70	95.81	52	0.53	0.61	94	1.41	1.63	100	40.30
150	95.30	107.61	60	0.55	0.63	100	1.41	1.63	100	42.10
180	100.80	115.58	66	0.55	0.65	103	1.41	1.67	105	31.60

* First 25 minutes were solution pre-heating time

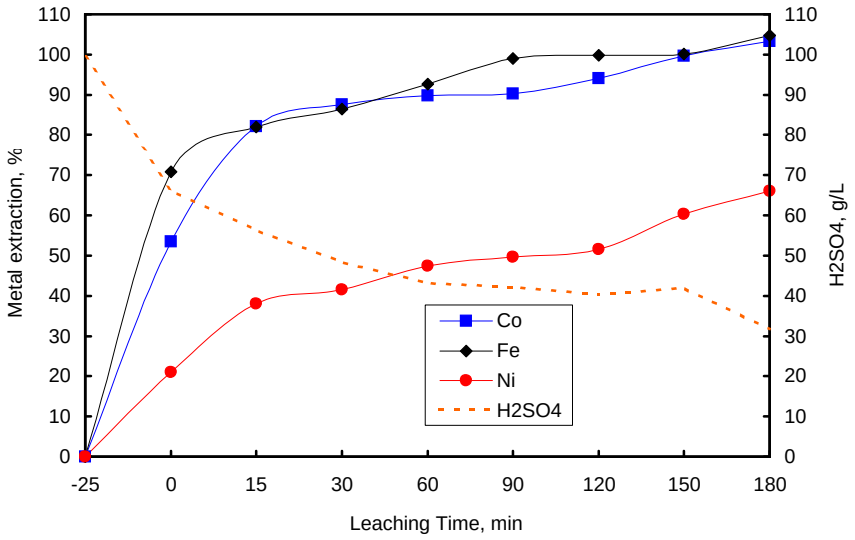

Fig.ure B2.6: Metal extraction as a function of leaching time for matte pre-leached at stirring rate of 400 rpm

TABLE B3.3: METAL CONCENTRATIONS DURING PRESSURE LEACHING OF MATTE PRE-LEACHED AT PULP DENSITY OF 1.7 kg/L

Leaching conditions:

Temperature (^{o}C):	145
Total pressure (kPa):	500
Initial P.D. (kg/L):	1.4
Leaching time (hrs):	3
Mixing rate (rpm)	900
Oxidant :	O_2

Leaching Time (min)	Co (g/l)	Fe (g/l)	Ni (g/l)	Cu (g/l)	pH
*					
-25	0.17	0.75	21.90	26.20	0.41
0	0.38	1.16	47.20	10.60	0.5
15	0.50	1.23	64.30	0.18	0.53
30	0.55	1.28	71.00	0.30	0.63
60	0.56	1.32	88.00	0.87	1.34
90	0.56	1.33	91.20	0.13	3.19
120	0.58	1.00	98.60	0.01	3.45
180	0.59	0.99	104.00	0.00	4.28

*First 25 minutes were solution pre-heating time

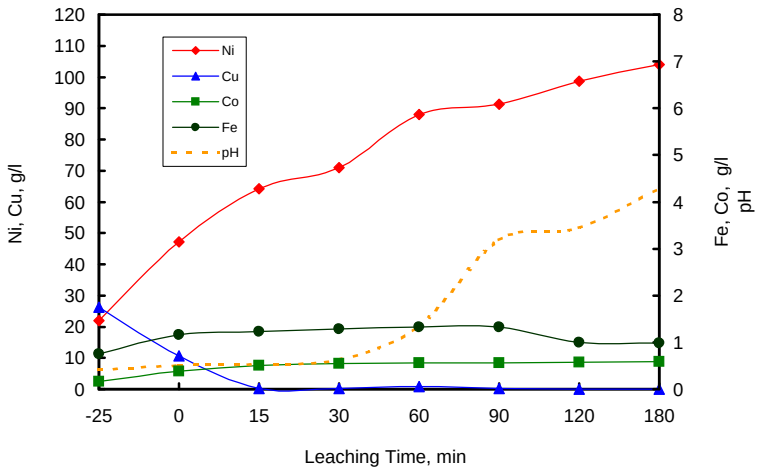

Figure B3.3: Metal concentrations as a function of time for the matte pre-leached a pulp density of 1.7 kg/L

TABLE B3.4: METAL EXTRACTIONS BASED ON SOLUTION CONCENTRATIONS DURING PRESSURE LEACHING OF MATTE PRE-LEACHED AT PULP DENSITY OF 1.7 kg/L

Feed matte:		**Feed solution:**		**Leaching conditions:**	
Wt	397 g	Volume	1.167 L	Temperature:	145 ^{o}C
Ni	34.50 %	Ni	21.9 g/L	Total pressure:	500 kPa
Co	0.12 %	Co	0.17 g/L	Initial P.D. :	1.4 kg/L
Fe	0.17 %	Fe	0.75 g/L	Oxidant:	O_2

Leaching Time (min)	Ni (g/l)	Ni (g)	Ni Leach %	Co (g/l)	Co (g)	Co leach %	Fe (g/l)	Fe (g)	Fe %	H2SO4 (g/l)
*										
-25	21.90	25.56	0	0.17	0.20	0	0.75	0.88	0	99.40
0	47.20	55.08	22	0.38	0.44	51	1.16	1.35	71	57.20
15	64.30	74.61	36	0.50	0.58	80	1.23	1.43	83	47.60
30	71.00	82.09	41	0.55	0.64	92	1.28	1.49	91	32.10
60	88.00	100.66	55	0.56	0.65	95	1.32	1.53	98	31.60
90	91.20	104.07	57	0.56	0.65	94	1.33	1.54	99	30.10
120	98.60	111.78	63	0.58	0.67	99	1.36	1.58	104	21.60
180	104.00	117.28	67	0.59	0.68	101	1.35	1.56	102	12.10

* First 25 minutes was solution pre-heating time

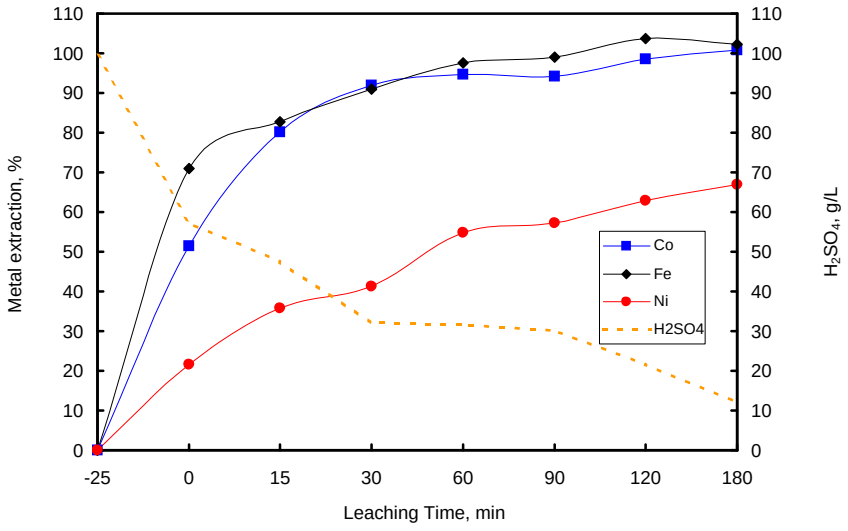

Figure B3.4: Metal extraction as a function of leaching time for matte pre-leached at pulp density of 1.7 kg/L

TABLE B3.1 METAL CONCENTRATIONS DURING PRESSURE LEACHING OF MATTE PRE-LEACHED AT PULP DENSITY OF 1.6 kg/L

Leaching conditior	Temperature (^{o}C):	145
	Total pressure (kPa):	500
	Initial P.D. (kg/L):	1.4
	Leaching time (hrs):	3
	Mixing rate (rpm)	900
	Oxidant :	O_2

Leaching Time (min)	Co (g/l)	Fe (g/l)	Ni (g/l)	Cu (g/l)	H2SO4 (g/l)	pH
*						
-25	0.17	0.75	21.90	26.20	994.00	0.41
0	0.33	1.18	41.30	15.90	516.00	0.58
15	0.46	1.21	65.20	0.04	369.00	0.62
30	0.51	1.29	76.50	0.00	254.00	0.68
60	0.52	1.30	80.20	0.00	223.00	0.87
90	0.52	1.38	81.60	0.01	222.00	0.97
120	0.54	1.42	96.70	0.02	269.00	1.02
150	0.55	1.43	98.80	0.47	265.00	1.05
180						

* First 25 minutes were solution pre-heating time

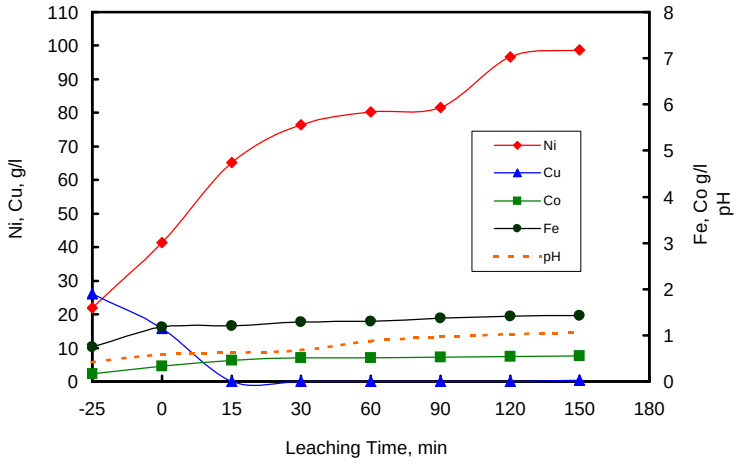

Figure B3.1 Metal concentration as a function of time for matte pre-leached at a pulp density of 1.6 kg/L

TABLE B3.2: METAL EXTRACTIONS BASED ON SOLUTION CONCENTRATIONS DURING PRESSURE LEACHING OF MATTE PRE-LEACHED AT PULP DENSITY OF 1.6 kg/L

Feed matte:		**Feed solution:**		**Leaching conditions:**	
Wt	397 g	Volume	1.167 L	Temperature:	145 °C
Ni	34.30 %	Ni	21.9 g/L	Total pressure:	500 kPa
Co	0.11 %	Co	0.17 g/L	Initial P.D. :	1.4 kg/L
Fe	0.19 %	Fe	0.75 g/L	Oxidant:	O_2

Leaching Time (min)	Ni (g/l)	Ni (g)	Ni Leach %	Co (g/l)	Co (g)	Co leach %	Fe (g/l)	Fe (g)	Fe %	H2SO4 (g/l)
*										
-25	21.90	25.56	0	0.17	0.20	0	0.75	0.88	0	99.40
0	41.30	48.20	17	0.33	0.39	43	1.18	1.38	67	51.60
15	65.20	75.49	37	0.46	0.53	77	1.21	1.41	71	36.90
30	76.50	88.11	46	0.51	0.59	90	1.29	1.50	83	25.40
60	80.20	92.15	49	0.52	0.60	92	1.30	1.51	84	22.30
90	81.60	93.65	50	0.52	0.60	92	1.38	1.60	96	22.20
120	96.70	109.38	62	0.54	0.62	97	1.42	1.63	101	26.90
150	98.80	111.52	63	0.55	0.63	100	1.43	1.65	103	26.50
180										

* First 25 minutes were solution pre-heating time

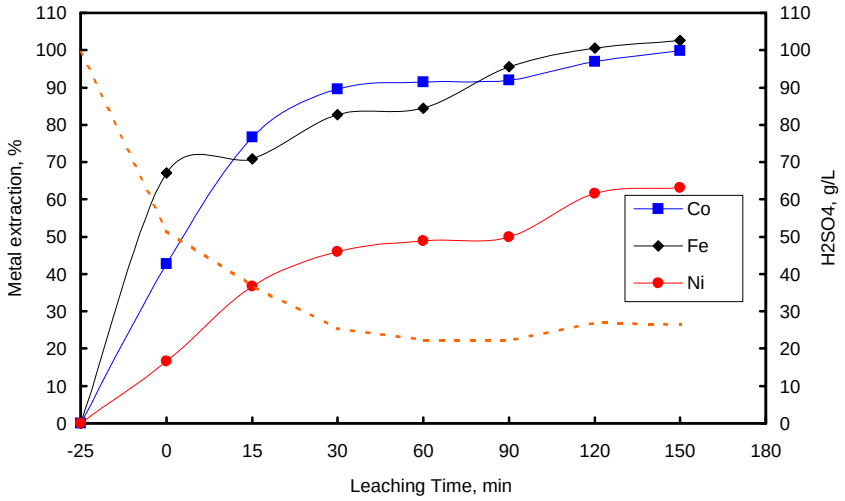

Figure B3.2: Metal extraction as a function of leaching time for the matte pre-leached at pul density of 1.6 kg/L

TABLE B3.5 METAL CONCENTRATIONS DURING PRESSURE LEACHING OF MATTE PRE-LEACHED AT PULP DENSITY OF 1.75 kg/L

Leaching conditions:		
	Temperature (^{o}C):	145
	Total pressure (kPa):	500
	Initial P.D. (kg/L):	1.4
	Leaching time (hrs):	3
	Mixing rate (rpm)	900
	Oxidant :	O_2

Leaching Time (min)	Co (g/l)	Fe (g/l)	Ni (g/l)	Cu (g/l)	H2SO4 (g/l)	pH
*						
-25	0.17	0.75	21.90	26.20	994.00	0.41
0	0.33	1.00	43.20	17.20	582.00	0.46
15	0.45	1.03	64.00	0.01	509.00	0.5
30	0.51	1.05	77.30	0.01	375.00	0.52
60	0.51	1.05	79.60	0.01	262.00	0.72
90	0.52	1.06	82.80	0.00	227.00	0.82
120	0.53	1.05	84.50	0.06	221.00	0.89
150	0.55	1.06	95.40	0.03	211.00	0.95
180	0.55	1.05	100.20	0.00	206.00	1.01

* First 25 minutes were solution pre-heating time

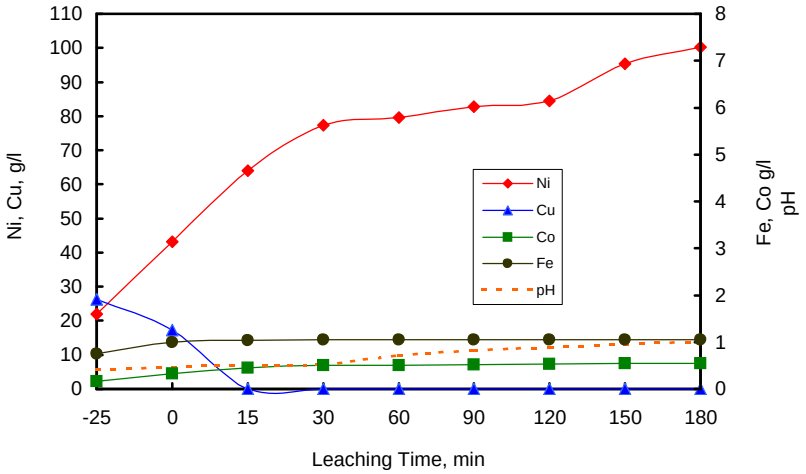

Figure B3.5: Metal concentration as a function of time for matte pre-leached at pulp density of 1.75 kg/L

TABLE B3.6: METAL EXTRACTIONS BASED ON SOLUTION CONCENTRATIONS DURING PRESSURE LEACHING OF MATTE PRE-LEACHED AT PULP DENSITY OF 1.75 kg/L

Feed matte:		**Feed solution:**		**Leaching conditions:**	
Wt	397 g	Volume	1.167 L	Temperature:	145 ^{o}C
Ni	34.80 %	Ni	21.9 g/L	Total pressure:	500 kPa
Co	0.11 %	Co	0.17 g/L	Initial P.D. :	1.4 kg/L
Fe	0.09 %	Fe	0.75 g/L	Oxidant:	O_2

Leaching Time (min)	Ni (g/l)	Ni (g)	Ni Leach %	Co (g/l)	Co (g)	Co leach %	Fe (g/l)	Fe (g)	Fe %	H2SO4 (g/l)
-25	21.90	25.56	0	0.17	0.20	0	0.75	0.88	0	99.40
0	43.20	50.41	18	0.33	0.39	43	1.00	1.16	81	58.20
15	64.00	74.17	35	0.45	0.52	74	1.03	1.20	92	50.90
30	77.30	89.02	46	0.51	0.59	89	1.05	1.22	97	37.50
60	79.60	91.54	48	0.51	0.59	90	1.05	1.22	98	26.20
90	82.80	94.95	50	0.52	0.60	91	1.06	1.23	99	22.70
120	84.50	96.72	52	0.53	0.61	95	1.05	1.23	99	22.10
150	95.40	107.81	60	0.55	0.63	98	1.06	1.23	99	21.10
180	100.20	115.07	65	0.55	0.63	99	1.05	1.23	98	20.60

* Fisrt 25 minutes were solution pre-heating time

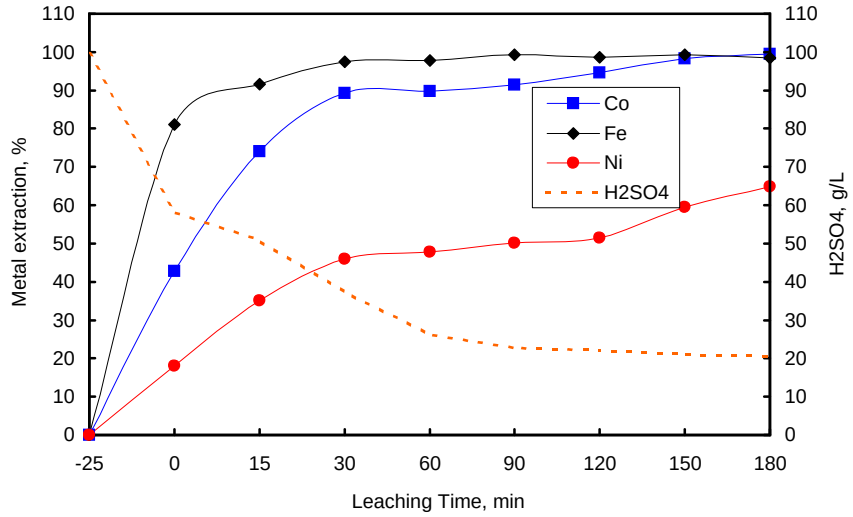

Fig.ure B3.6: Metal extraction as a function of leaching time for matte pre-leached at pulp density of 1.75 kg/L

TABLE B4.3: METAL CONCENTRATIONS DURING PRESSURE LEACHING OF MATTE PRE-LEACHED FOR 3 HOURS

Leaching conditions	Temperature (^{o}C):	145
	Total pressure (kPa):	500
	Initial P.D. (kg/L):	1.4
	Leaching time (hrs):	3
	Mixing rate (rpm):	900
	Oxidant :	O_2

Leaching Time (min)	Co (g/l)	Fe (g/l)	Ni (g/l)	Cu (g/l)	H2SO4 (g/l)	pH
-25	0.17	0.75	21.90	26.20	99.40	
0	0.35	0.95	52.40	2.98	65.40	0.51
15	0.49	1.20	59.10	0.25	51.80	0.55
30	0.51	1.36	62.80	0.01	47.40	0.58
60	0.52	1.39	76.20	0.01	41.40	0.76
90	0.52	1.39	76.80	0.01	37.30	0.83
120	0.53	1.40	85.50	0.01	29.20	0.90
150	0.55	1.41	88.30	0.01	31.20	0.91
180	0.55	1.43	91.60	0.01	28.90	0.94

* First 25 minutes was solution pre-heating time

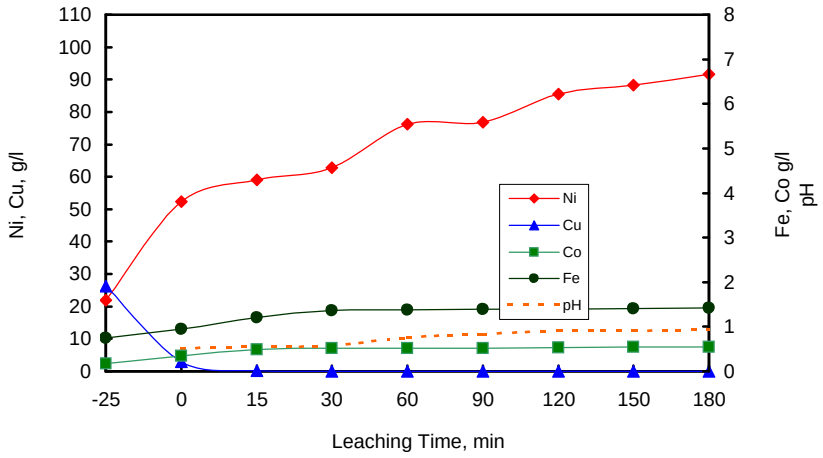

Figure B4.3: Metal concentration as a function of time for matte pre-leached for a residence time of 3 hours

TABLE B4.4: METAL EXTRACTIONS BASED ON SOLUTION CONCENTRATIONS DURING PRESSURE LEACHING OF MATTE PRE-LEACHED FOR A RESIDENCE TIME OF 3 HOURS

Feed matte:		**Feed solution:**		**Leaching conditions:**	
Wt	397 g	Volume	1.167 L	Temperature:	145 °C
Ni	34.30 %	Ni	21.9 g/L	Total pressure:	500 kPa
Co	0.11 %	Co	0.17 g/L	Initial P.D. :	1.4 kg/L
Fe	0.19 %	Fe	0.75 g/L	Oxidant:	O_2

Leaching Time (min)	Ni (g/l)	Ni (g)	Ni Leach %	Co (g/l)	Co (g)	Co leach %	Fe (g/l)	Fe (g)	Fe %	H2SO4 (g/l)
-25	21.90	25.56	0	0.17	0.20	0	0.75	0.88	0	99.40
0	52.40	61.15	26	0.35	0.41	48	0.95	1.11	31	65.40
15	59.10	68.80	32	0.49	0.57	85	1.20	1.40	69	51.80
30	62.80	72.94	35	0.51	0.59	90	1.36	1.57	92	47.40
60	76.20	87.57	46	0.52	0.60	92	1.39	1.60	96	41.40
90	76.80	88.21	46	0.52	0.60	93	1.39	1.61	97	37.30
120	85.50	97.27	53	0.53	0.61	94	1.40	1.61	98	29.20
150	88.30	100.12	55	0.55	0.63	99	1.41	1.63	99	31.20
180	91.60	103.39	57	0.55	0.63	100	1.43	1.64	102	28.90

* First 25 minutes was solution pre-heating time

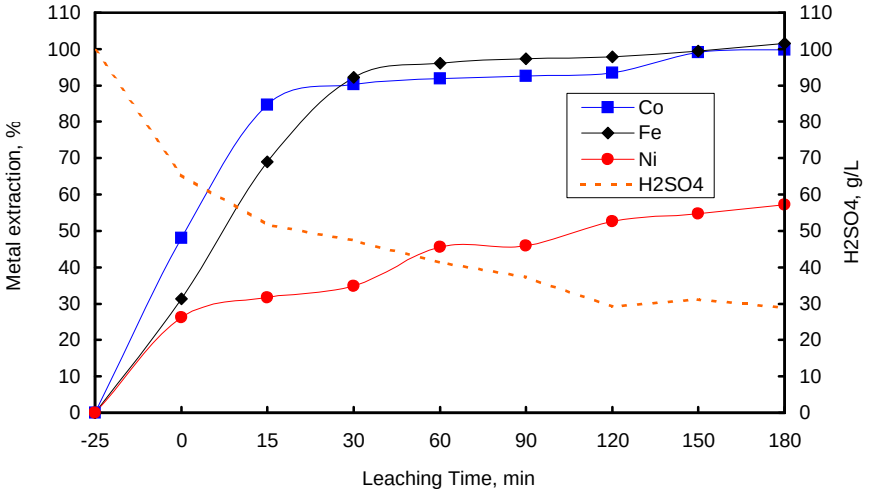

Figure B4.4: Metal extraction as a function of leaching time for matte pre-leached for a residence time of 3 hours.

TABLE B4.3: METAL CONCENTRATIONS DURING PRESSURE LEACHING OF MATTE PRE-LEACHED FOR 9 HOURS

Leaching conditions:

Temperature (^{o}C):	145
Total pressure (kPa):	500
Initial P.D. (kg/L):	1.4
Leaching time (hrs):	3
Mixing rate (rpm):	900
Oxidant :	O_2

Leaching Time (min)	Co (g/l)	Fe (g/l)	Ni (g/l)	Cu (g/l)	H2SO4 (g/l)	pH
*						
-25	0.17	0.75	21.90	26.20	99.40	0.41
0	0.32	0.98	47.40	7.72	72.80	0.52
15	0.44	1.30	70.20	0.00	53.30	0.56
30	0.46	1.36	76.30	0.01	42.60	0.67
60	0.49	1.39	82.80	0.10	26.10	1.05
90	0.50	1.41	84.30	0.01	24.60	1.18
120	0.53	1.41	89.90	0.05	18.60	1.28
150	0.55	1.41	98.60	0.06	15.60	1.34
180	0.55	1.41	101.10	0.02	14.80	1.41

* First 25 minutes were solution pre-heating time

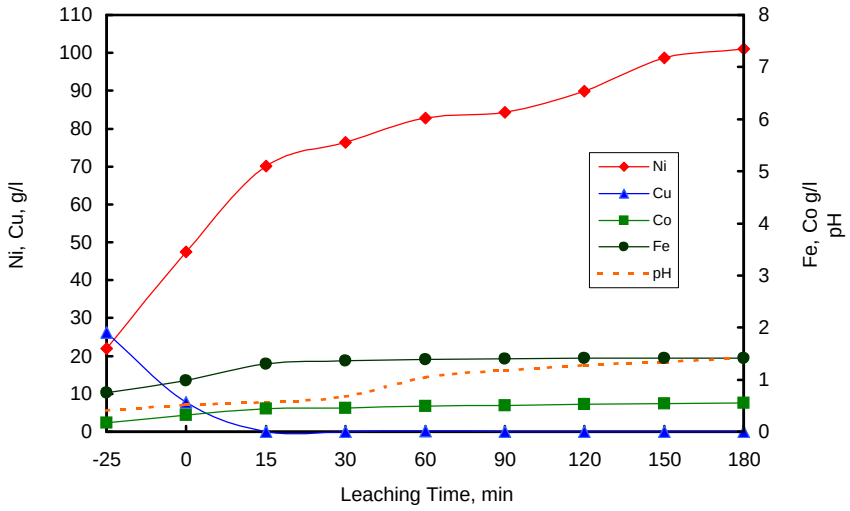

Figure B4.3: Metal concentration as a function of leaching time for matte pre-leached for 9 hours

TABLE B4.4: METAL EXTRACTIONS BASED ON SOLUTION CONCENTRATIONS DURING PRESSURE LEACHING OF MATTE PRE-LEACHED FOR 9 HOURS

Feed matte:		**Feed solution:**		**Leaching conditions:**	
Wt	397 g	Volume	1.167 L	Temperature:	145 ^{o}C
Ni	34.30 %	Ni	21.9 g/L	Total pressure:	500 kPa
Co	0.11 %	Co	0.17 g/L	Initial P.D. :	1.4 kg/L
Fe	0.19 %	Fe	0.75 g/L	Oxidant:	O_2

Leaching Time (min)	Ni (g/l)	Ni (g)	Ni Leach %	Co (g/l)	Co (g)	Co leach %	Fe (g/l)	Fe (g)	Fe %	H2SO4 (g/l)
*										
-25	21.90	25.56	0	0.17	0.20	0	0.75	0.88	0	99.40
0	47.40	55.32	22	0.32	0.37	40	0.98	1.14	36	72.80
15	70.20	81.35	41	0.44	0.51	71	1.30	1.51	84	53.30
30	76.30	88.17	46	0.46	0.53	76	1.36	1.58	93	42.60
60	82.80	95.27	51	0.49	0.56	83	1.39	1.61	98	26.10
90	84.30	96.87	52	0.50	0.57	86	1.41	1.63	99	24.60
120	89.90	102.70	57	0.53	0.61	93	1.41	1.63	100	18.60
150	98.60	111.55	63	0.55	0.62	97	1.41	1.63	100	15.60
180	101.10	114.03	65	0.55	0.63	99	1.41	1.63	100	14.80

* First 25 minutes were solution pre-heating time

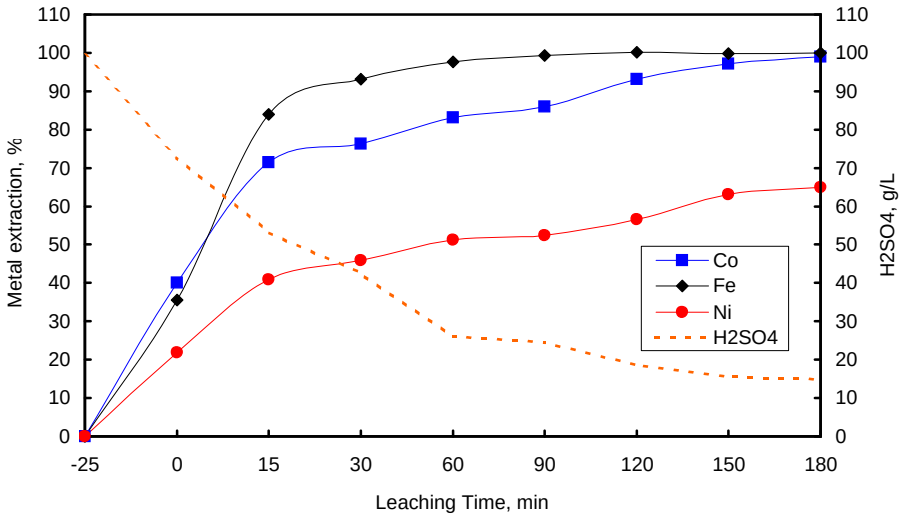

Figure B4.4: Metal extraction as a function of leaching time for matte pre-leached for 9 hours

TABLE B4.5: METAL CONCENTRATIONS DURING PRESSURE LEACHING OF MATTE PRE-LEACHED FOR 1 HOURS

Leaching conditions:

Temperature (^{o}C):	145
Total pressure (kPa):	500
Initial P.D. (kg/L):	1.4
Leaching time (hrs):	3
Mixing rate (rpm):	900
Oxidant :	O_2

Leaching Time (min)	Co (g/l)	Fe (g/l)	Ni (g/l)	Cu (g/l)	H2SO4 (g/l)	pH
*						
-25	0.17	0.75	21.90	26.20	99.40	0.41
0	0.40	1.03	47.20	9.14	62.40	0.43
15	0.45	1.10	54.90	0.01	56.30	0.44
30	0.51	1.12	56.40	0.01	53.60	0.47
60	0.51	1.13	60.40	0.02	46.20	0.52
90	0.52	1.14	64.80	0.01	45.70	0.54
120	0.53	1.15	66.60	0.02	42.60	0.55
150	0.55	1.20	68.60	0.14	41.30	0.58
180	0.55	1.22	70.90	0.00	32.70	0.59

* First 25 minutes were solution pre-heating time

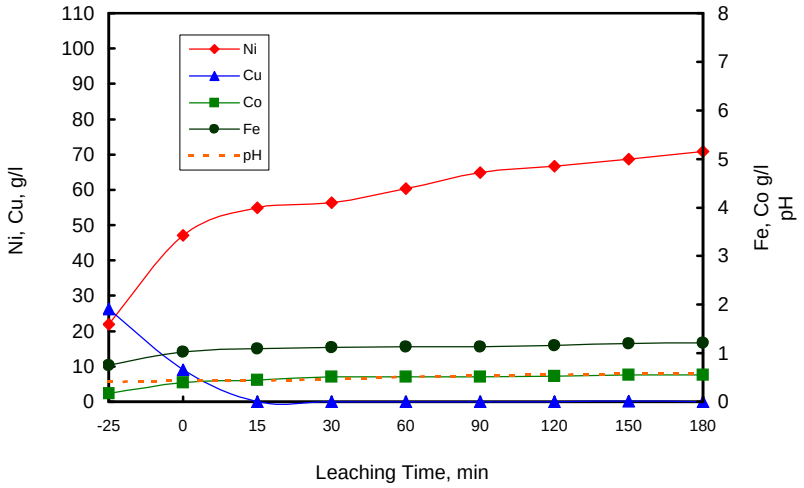

Figure B4.5: Metal concentration as a function of leaching time for matte pre-leached for 1 hour

TABLE B4.6: METAL EXTRACTIONS BASED ON SOLUTION CONCENTRATIONS DURING PRESSURE LEACHING OF MATTE PRE-LEACHED FOR 1 HOURS

Feed matte:		**Feed solution:**		**Leaching conditions:**	
Wt	397 g	Volume	1.167 L	Temperature:	145 ^{o}C
Ni	34.30 %	Ni	21.9 g/L	Total pressure:	500 kPa
Co	0.11 %	Co	0.17 g/L	Initial P.D. :	1.4 kg/L
Fe	0.13 %	Fe	0.75 g/L	Oxidant:	O_2

Leaching Time (min)	Ni (g/l)	Ni (g)	Ni Leach %	Co (g/l)	Co (g)	Co leach %	Fe (g/l)	Fe (g)	Fe %	H2SO4 (g/l)
*										
-25	21.90	25.56	0	0.17	0.20	0	0.75	0.88	0	99.40
0	47.20	55.08	22	0.40	0.47	61	1.03	1.20	63	62.40
15	54.90	63.88	28	0.45	0.52	75	1.10	1.28	78	56.30
30	56.40	65.55	29	0.51	0.59	90	1.12	1.31	83	53.60
60	60.40	69.92	33	0.51	0.59	90	1.13	1.32	86	46.20
90	64.80	74.61	36	0.52	0.60	92	1.14	1.32	87	45.70
120	66.60	76.49	37	0.53	0.61	95	1.15	1.34	90	42.60
150	68.60	78.52	39	0.55	0.63	99	1.20	1.39	99	41.30
180	70.90	80.81	41	0.55	0.63	100	1.22	1.40	102	32.70

* First 25 minutes were solution pre-heating time

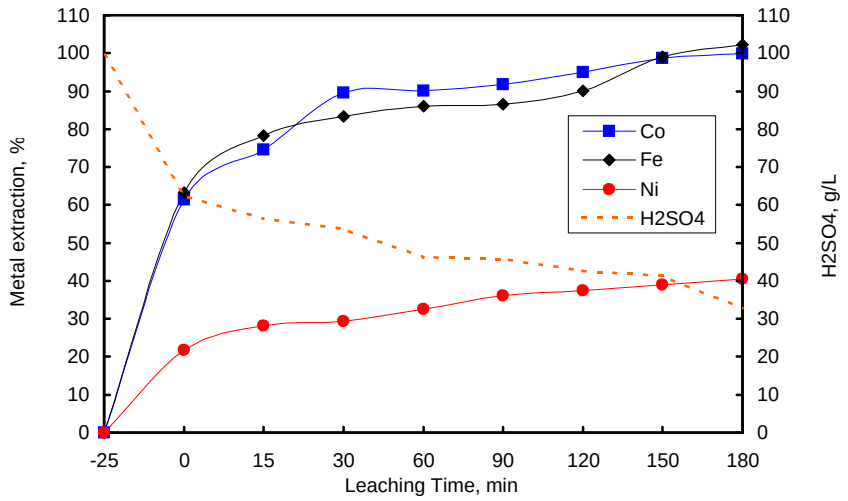

Fig.ure B4.6: Metal extraction as a function of leaching time for the matte pre-leached for 1 hour

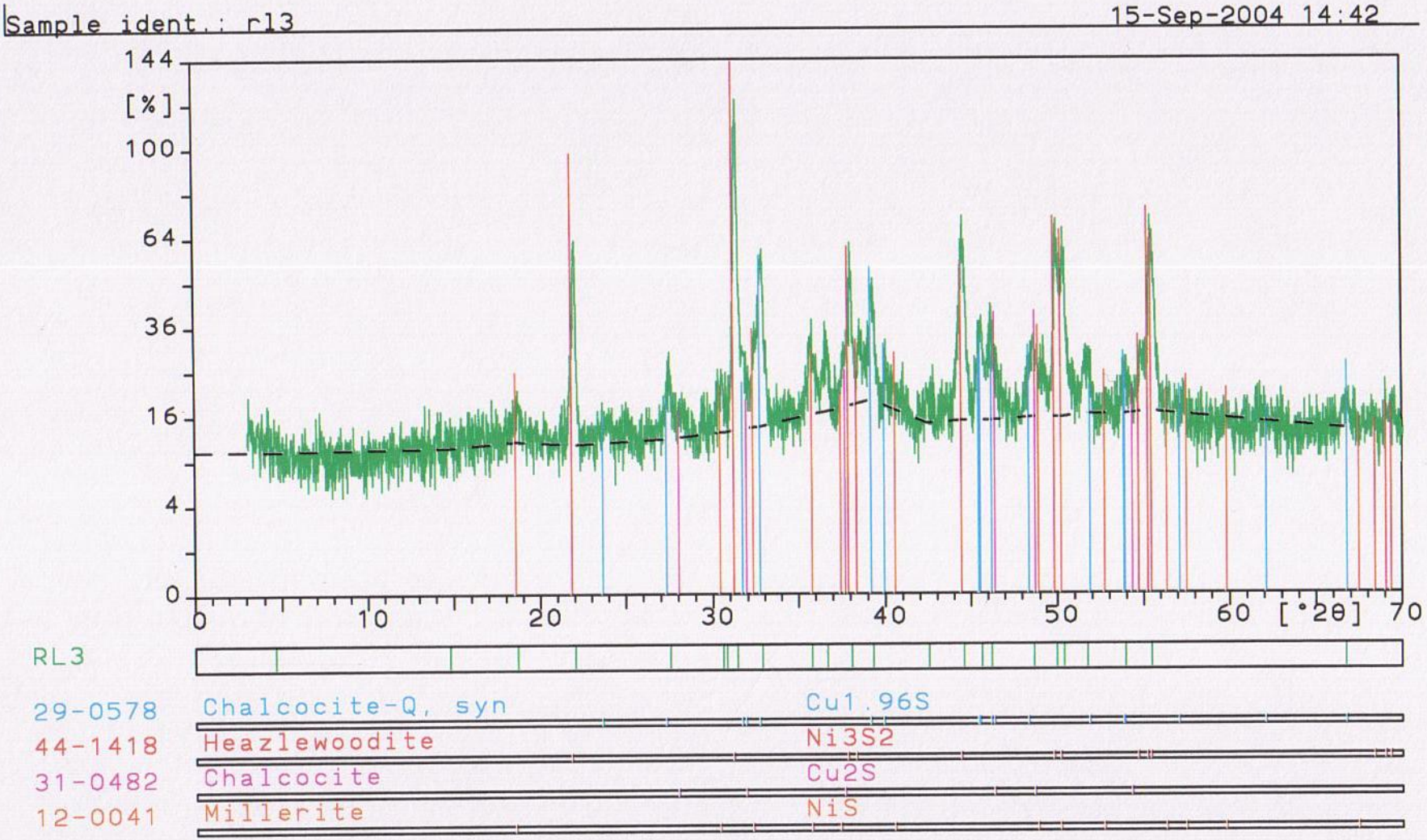
Sample ident.: rl3
15-Sep-2004 14:42
144
[%]
100
64
36
16
4
0
0
10
20
30
40
50
60
[°2θ]
70
RL3
29-0578 Chalcocite-Q, syn Cu1.96S
44-1418 Heazlewoodite Ni3S2
31-0482 Chalcocite Cu2S
12-0041 Millerite NiS

Sample ident.: rl1a

20-Aug-2004 11:08

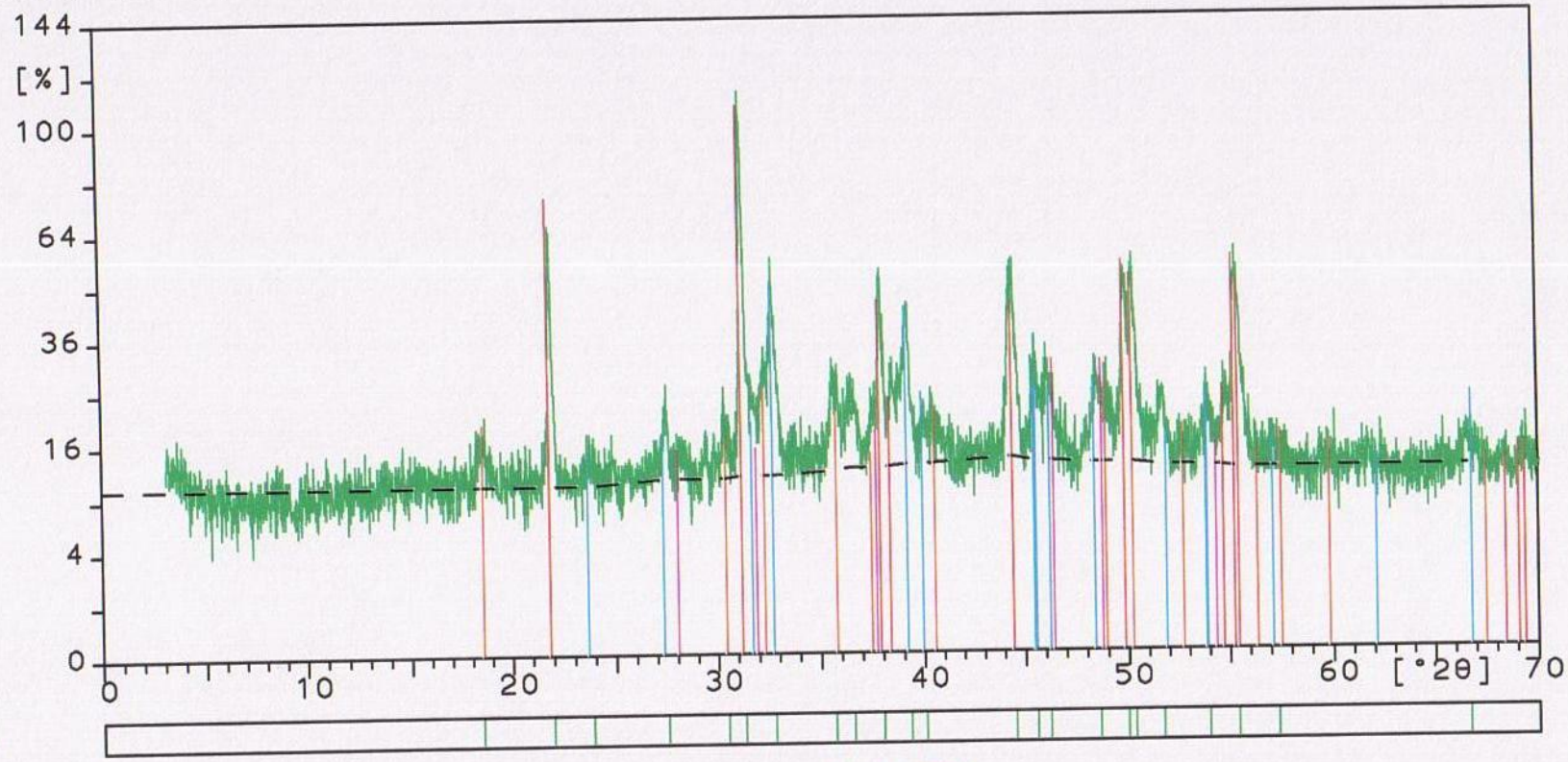

RL1A

29-0578	Chalcocite-Q, syn	Cu1.96S
44-1418	Heazlewoodite	Ni3S2
31-0482	Chalcocite	Cu2S
12-0041	Millerite	NiS

Sample ident.: rl9 15-Sep-2004 16:02

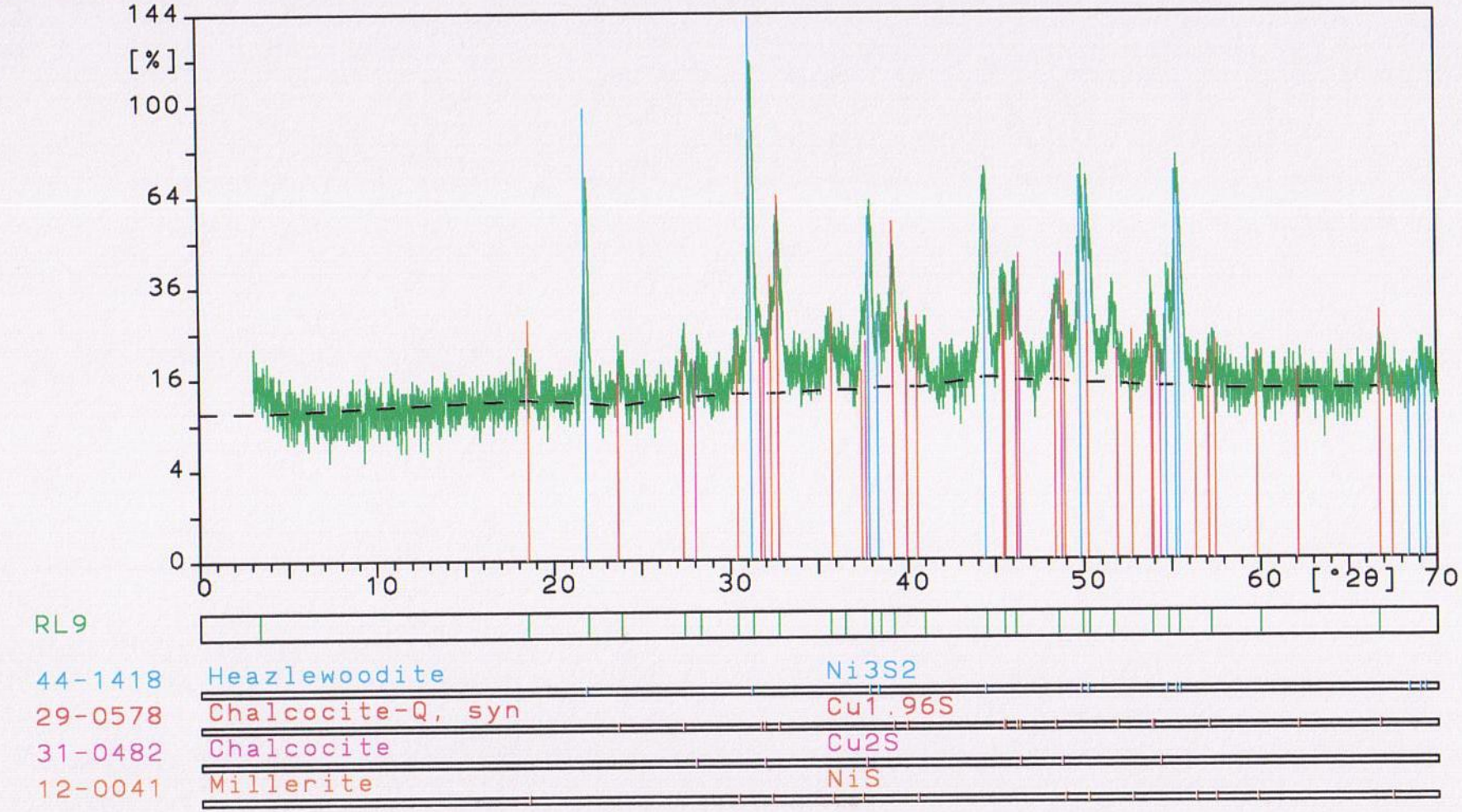

Sample ident.: rl16 15-Sep-2004 15:58

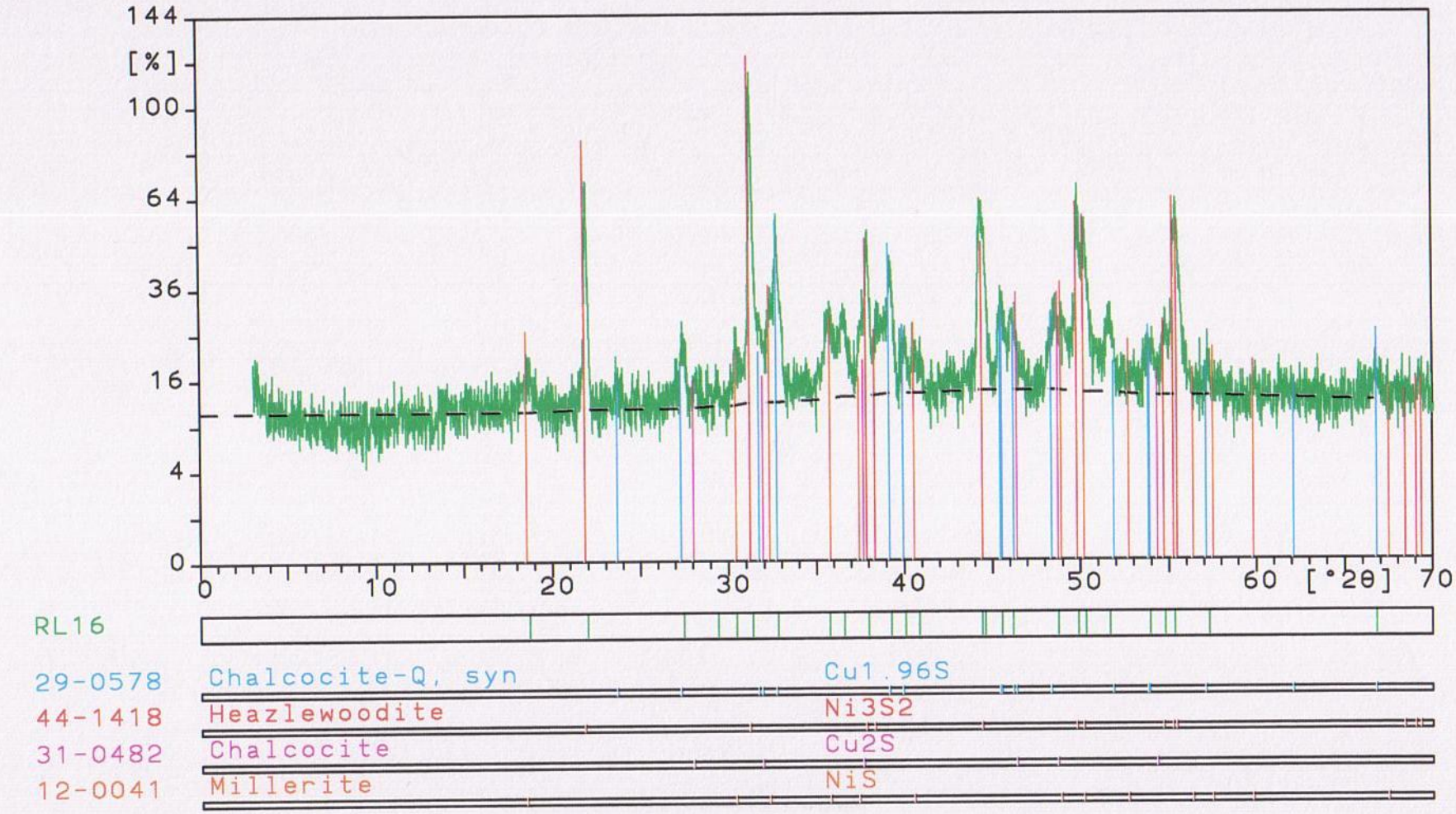

Sample ident.: rl/5

15-Sep-2004 15:44

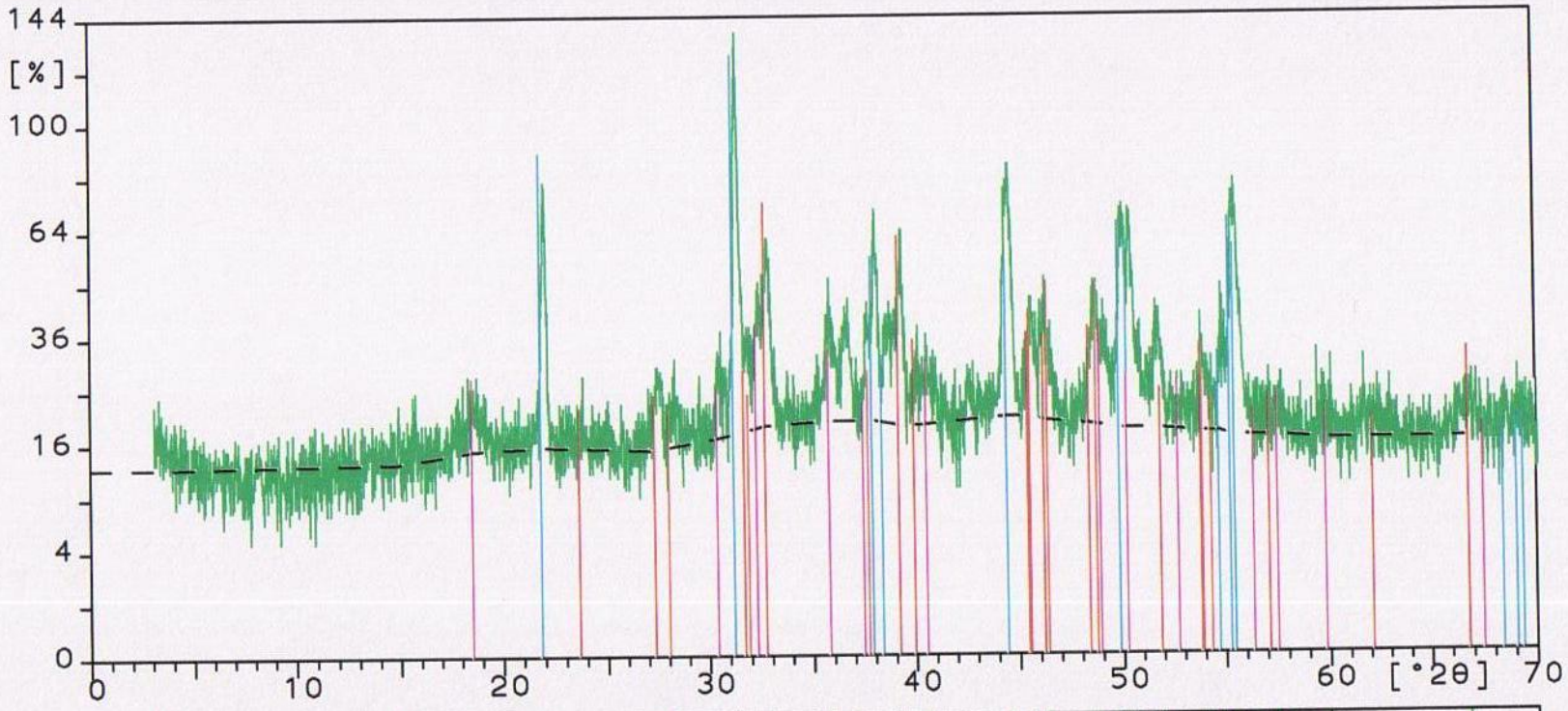

RL5

44-1418	Heazlewoodite	Ni3S2
29-0578	Chalcocite-Q, syn	Cu1.96S
12-0041	Millerite	NiS
31-0482	Chalcocite	Cu2S

Sample ident.: r1/7

15-Sep-2004 15:06

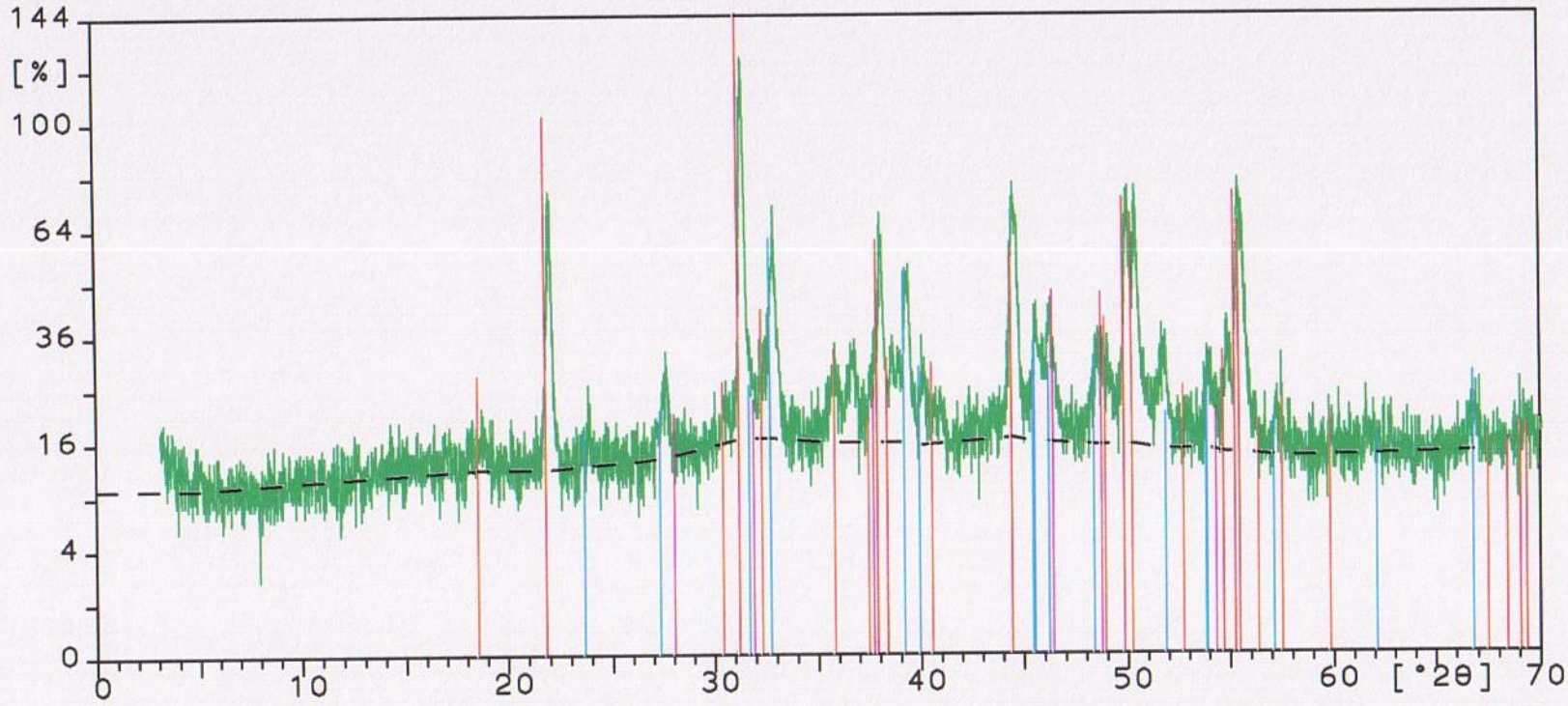

RL7

29-0578	Chalcocite-Q, syn	Cu1.96S
44-1418	Heazlewoodite	Ni3S2
31-0482	Chalcocite	Cu2S
12-0041	Millerite	NiS

Sample ident.: 22h

14-Sep-2004 13:56

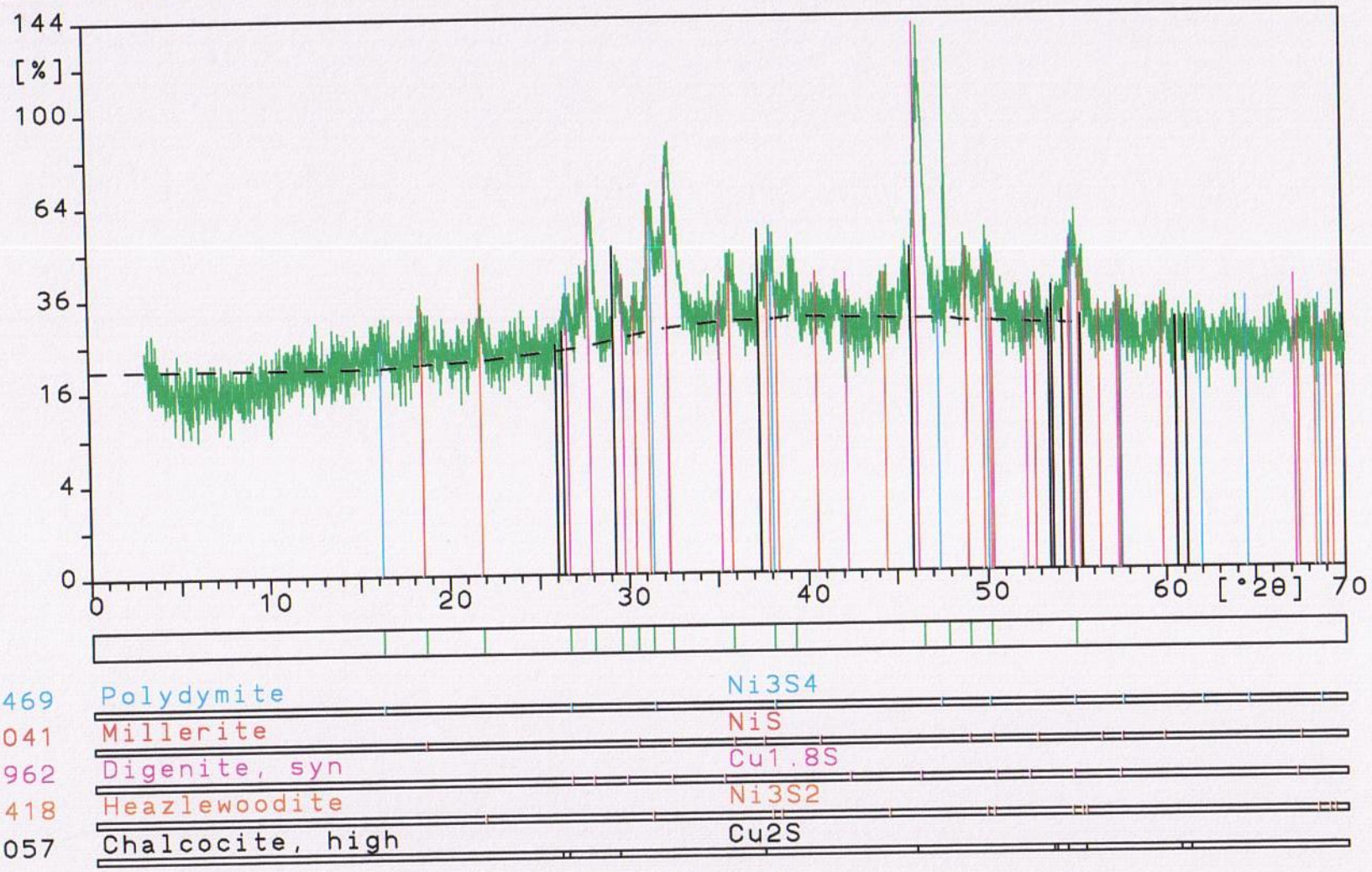

Sample ident.: rl21h 14-Sep-2004 13:08

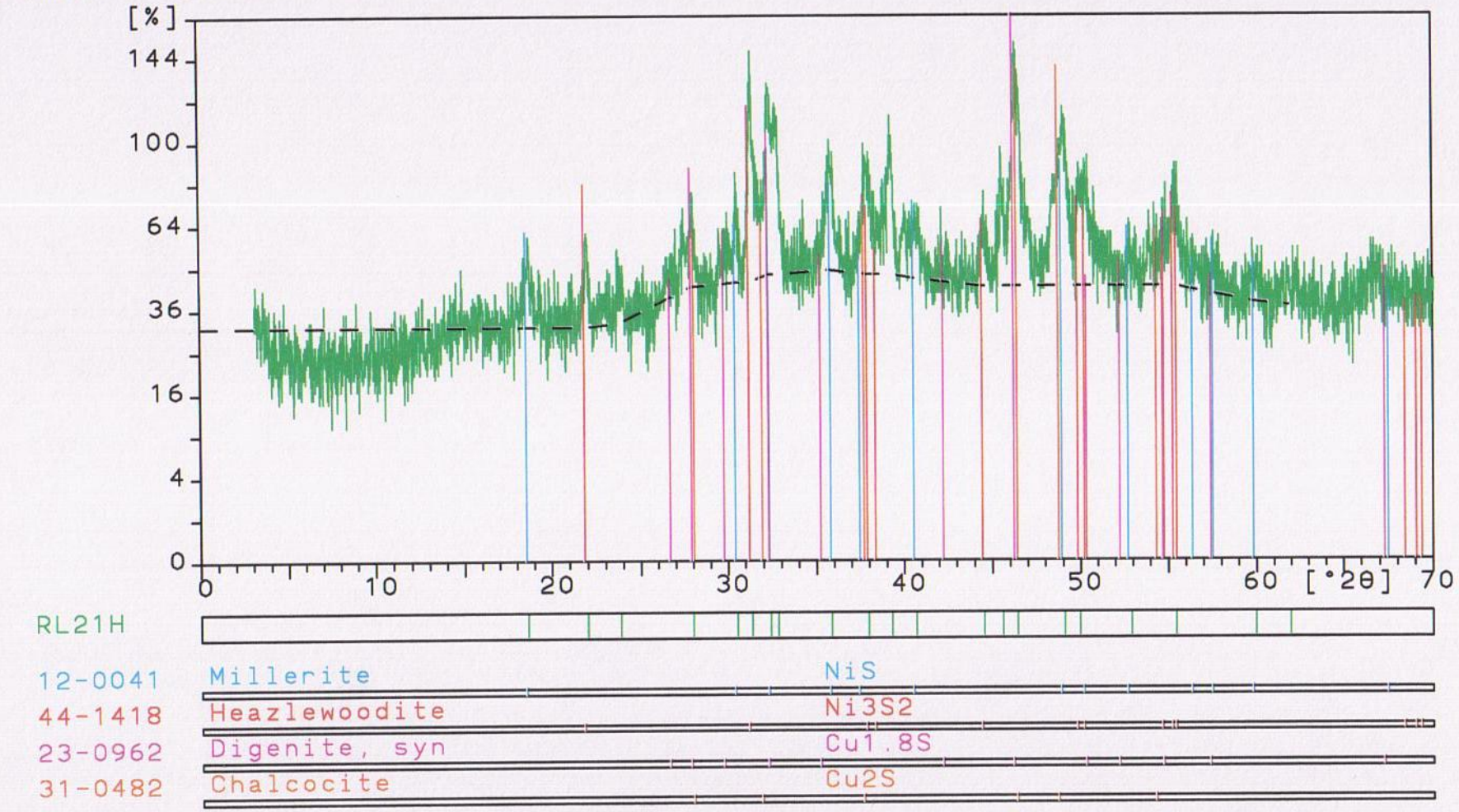

Sample ident.: rl27h

14-Sep-2004 14:29

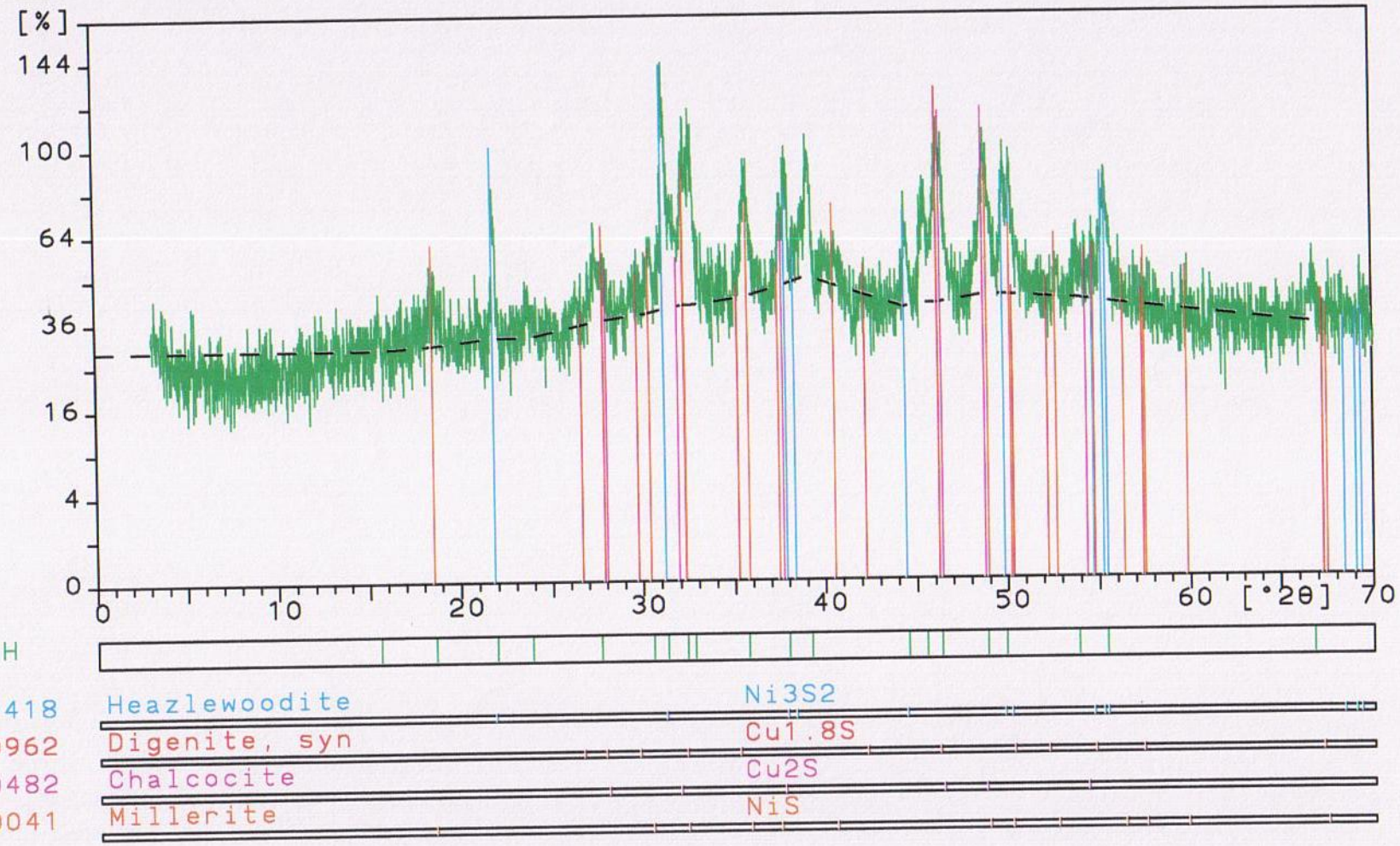

Sample ident.: rl25h

14-Sep-2004 15:04

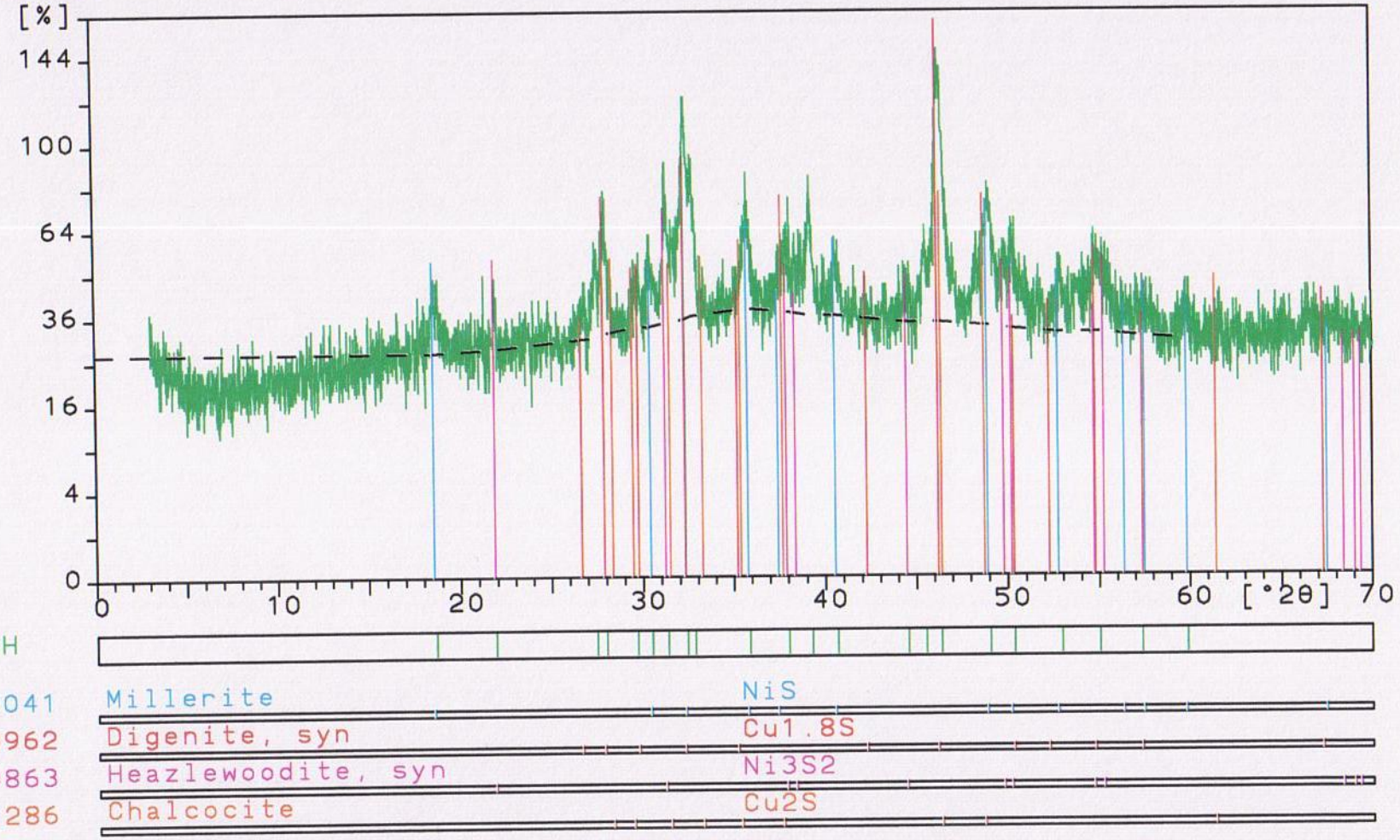

RL25H

12-0041	Millerite	NiS
23-0962	Digenite, syn	Cu1.8S
30-0863	Heazlewoodite, syn	Ni3S2
02-1286	Chalcocite	Cu2S

APPENDIX D

DETERMINATION OF MINERAL COMPOSITION OF THE MATTE AND PREPARATION OF THE LEACHING SOLUTION

APPENDIX D1

DETERMINATION OF APPROXIMATE MINERAL COMPOSITION OF THE MATTE

The matte consisted of 47% Ni, 30% Cu and 21% S with small amounts of Co and Fe. The balance (2 %) constituted cobalt, iron, PGMs and other chemical elements in the matte. The major mineral phases in the matte were Ni_3S_2, Cu_2S, $Cu_{1.9}S$ and a nickel-rich alloy. The quantities of these mineral phases were not known; hence it was necessary to determine the approximate mineral composition of the matte. In the calculations it was assumed that all of the copper in the matte was present as Cu_2S; and that the quantities of cobalt and iron minerals / alloys were insignificant, and hence were not considered in the calculations. The ratio of copper to nickel in the Ni alloy is assumed to be 1: 2, as reported by Dynatec Corporation (2003)*.

The calculations involved are illustrated below; please note that the calculations are based on 100 g of matte sample:

Total moles of nickel in matte

Amount of Ni in the matte = 47%, for 100g of matte there is 47g of Ni
Moles of Ni in the matte = 47/58.69 = **0.801**, where 58.69 is the molecular weight of Ni

Let moles of Ni_3S_2 = X (D1.1)

therefore, moles of Ni in Ni_3S_2 = 3X (D1.2)

let moles of Ni in the alloy = Z (D1.3)

therefore, mass of Ni in the alloy = 58.69Z (D1.4)

Total moles of Ni in the matte = 3X + Z = 0.801 **(D1.5)**

Total moles of copper in matte

Amount of copper in the matte = 30%, for 100g of matte there is 30g of Cu
Moles of Cu in the matte = 30/63.55 = **0.472**, where 63.55 is the molecular weight of Cu

Let moles of Cu_2S = Y (D1.6)

therefore, moles of Cu in Cu_2S = 2Y (D1.7)

moles of Cu in the alloy = (58.69Z/2) / 63.55 = 0.4618Z (D1.8)

where 58.69Z is mass of Ni in the alloy (equation D1.4), and ratio of mass of Ni to Cu in the alloy is 2:1

Total moles of Cu in the matte = 2Y + 0.4618Z = 0.472 (D1.9)

Total moles of sulphur in matte

Amount of sulphur in the matte = 21%, for 100g of matte there is 21g of S

Moles of S in the matte = 21/32.06 = **0.655**, where 32.o6 is the molecular weight of S

From equation (D1.1), moles of S in Ni_3S_2 = 2X (D1.10)

From equation (D1.6), moles of S in Cu_2S = Y (D1.11)

Total moles of S in the matte = 2X + Y = 0.655 (D1.12)

Equations (D1.5), (D1.9) and (D1.12) can now be solved for X, Y and Z:

Solving for Z in equation (D1.5) gives:

Z = 0.801 – 3X (D1.13)

Substituting equation (D1.13) into (D1.9) gives:

2Y – 1.3854X = 0.1021 (D1.14)

solving equations (D1.12) and (D1.14) simultaneously by multiplying (D1.12) by 2 and subtracting (D1.14) from (D1.12) gives:

X = 0.2243 (D1.15)

Substituting value of X into equation (D1.12):

2(0.2243) + Y = 0.655

Y = 0.2064 **(D1.16)**

Substituting values of X and Z into equation (D1.5) gives:

3(0.2243) + Z = 0.801

Z = 0.1281 **(D1.17)**

Compostion of the matte

<u>Heazlewoodite (Ni_3S_2)</u>

Moles of Ni_3S_2 in the matte = X = 0.2243

mass of Ni_3S_2 in the matte = 0.2243 x 240.19 = 53.87 g, where 240.19 is molecular wt of Ni_3S_2.

Therefore Percent composition in matte = **53.87 % Ni_3S_2**

Ni in Ni_3S_2

From equation (D1.2), moles of Ni in Ni_3S_2 = 3X = 3 x 0.2243 = 0.6729
mass of Ni in Ni_3S_2 = 0.6729 x 58.69 = 39.49 g = **39.49 %**

S in Ni_3S_2

From equation (D1.10), moles of S in Ni_3S_2 = 2X = 2 x 0.2243 = 0.4486
mass of Ni in Ni_3S_2 = 0.4486 x 32.06 = 14.38 g = **14.38 %**

<u>Chalcocite (Cu_2S)</u> **-** other copper sulphides assumed to be in the form of Cu_2S

Moles of Cu_2S in the matte = Y = 0.2064

mass of Cu_2S in the matte = 0.2064 x 159.2 = 32.86 g, where 159.2 is molecular wt of Cu_2S.

Therefore Percent composition in matte = **32.86 % Cu_2S**

Cu in Cu_2S

From equation (D1.7), moles of Cu in Cu_2S = 2Y = 2 x 0.2064 = 0.4128

mass of Cu in Cu_2S = 0.4128 x 63.55 = 26.23 g = **26.23 %**

S in Cu_2S

From equation (D1.11), moles of S in Cu_2S = Y = 0.2064

mass of S in Cu_2S = 0.2064 x 32.06 = 6.62 g = **6.62 %**

Alloy – any Fe and Co in the alloy assumed to be negligible

Ni in alloy

Moles of Ni in the alloy = Z = 0.1281

mass of Ni in the alloy = 0.1281 x 58.69 = 7.52 g

Percent composition of Ni in the alloy is = **7.52 % Ni**

Cu in alloy

Moles of Cu in the alloy = (58.69Z/2) / 63.55 = 0.4618Z = 0.0592; (from equation (D1.8))

mass of Cu in the alloy = 0.0592 x 63.55 = 3.76 g

Percent composition of Cu in the alloy = **3.76 % Cu**

Therefore Percent composition of Ni-Cu alloy in the matte = **11.28 % alloy**

Table D1: Summary of mineral composition of the matte

Mineral phase	Mineral composition (%)			
	Ni	Cu	S	Total
Ni2S2	39.49	-	14.38	53.87
Cu2S	-	26.24	6.62	32.86
Ni alloy	7.52	3.76	-	11.28
Total	47.0	30.0	21.0	98.0

N.B. Other minerals in the matte account for 2%

APPENDIX D2

DETERMINATION OF QUANTITY OF MATTE, SPENT ELECTROLYTE SOLUTION AND DEMINERALIZED WATER TO BE MIXED FOR THE VARIATION IN THE PULP DENSITY REACTION MIXTURE

D2.1 ATMOSPHERIC LEACHING EXPERIMENTS

To simulate the pre-leach conditions it was necessary to determine the quantities of matte, spent electrolyte solution and demineralised water to be mixed for the variation in the pulp density of the reaction mixture. On the commercial plant the pulp density in the atmospheric (pre-leach) stage is controlled by the addition of copper spent electrolyte to

the matte pulp. The matte pulp is a mixture of matte and water coming from the ball milling section. The pre-leach experiments were performed at a pulp density of 1.7 kg/L, so to determine how much matte, spent electrolyte and demineralised water were needed to achieve this pulp density the following calculations were performed:

The variables considered were:
Volume of spent electrolyte, V_{se} (mL)
Volume of demineralised water, V_{dw} (mL)
Volume of matte, V_m (mL)
Volume of pulp from the milling section, V_{ms} (mL)
Volume of pulp in the pre-leach stage, V_{pL} (mL)
Density of spent electrolyte, D_{se} (g/mL)
Density of demineralised water, D_{dw} (g/mL)
Density of matte, D_m (g/mL)
Density of pulp from the milling section, D_{ms} (g/mL)
Density of pulp in the pre-leach stage, D_{pL} (g/mL)

Values of the densities were known, and were as follows:
$D_{se} = 1.17, D_{dw} = 1, D_m = 5.8, D_{ms} = 2.4, D_{pL} = 1.7$

From the relationship of density, volume and mass (density = mass/volume) the following equations were derived, which were then solved for volumes of demineralised water and spent electrolyte as well as mass of matte required for the atmospheric experiments.

$$D_{pL} = \frac{D_{dw}V_{dw} + D_{se}V_{se} + D_mV_m}{V_{dw} + V_{se} + V_m} \quad \text{(D2.1)}$$

$$D_{ms} = \frac{D_{dw}V_{dw} + D_mV_m}{V_{dw} + V_m} \quad \text{(D2.2)}$$

Where

$D_{dw}V_{dw}$ = mass of demineralised water
$D_{se}V_{se}$ = mass of spent electrolyte solution
D_mV_m = mass of matte
$V_{dw} + V_{se} + V_m$ = volume of pulp in the pre-leach stage, V_{pL} (mL)
$V_{dw} + V_m$ = volume of pulp from the milling section, V_{ms} (mL)

Substituting the values of densities into equation D2.1

$$1.7 = \frac{1V_{dw} + 1.17V_{se} + 5.8V_m}{V_{dw} + V_{se} + V_m} \quad \text{(D2.3)}$$

Simplifying and rearranging equation D2.3 gives:

$$V_{dw} + 1.17V_{se} + 5.8V_m = 1.7\left(V_{dw} + V_{se} + V_m\right)$$

$$4.1V_m - 0.7V_{dw} = 0.53V_{se} \quad \text{(D2.4)}$$

Substituting the values of densities into equation D2.2

$$2.4 = \frac{1V_{dw} + 5.8V_m}{V_{dw} + V_m} \quad \text{(D2.5)}$$

Simplifying and rearranging equation D2.5 gives:

$$V_{dw} + 5.8V_m = 2.4\left(V_{dw} + V_m\right)$$

$$3.4V_m = 1.4V_{dw}$$

$$\boxed{V_m = 0.4118V_{dw}} \quad \text{(D2.6)}$$

Substituting equation D2.6 into equation D2.4

$$4.1\left(0.4118V_{dw}\right) - 0.7V_{dw} = 0.53V_{se} \quad \text{(D2.7)}$$

Simplifying equation D2.7 gives:

$$V_{se} = 1.864 V_{dw} \qquad \text{(D2.8)}$$

The volumes of spent electrolyte and demineralised water were thus calculated using the relationship given in equation D2.8. Volume of the matte was calculated from equation D2.6. Then the mass was found by using the relationship:

mass $= D_m \times V_m$

D2.2 PRESSURE LEACHING EXPERIMENTS

To simulate the pressure leaching conditions the quantities of matte, spent electrolyte solution and demineralised water to be mixed were again calculated, using the same approach as illustrated in D2.1 above. It was assumed that changes in the density of the matte from the pre-leach stage were insignificant. On the commercial plant the pulp density in the pressure leaching stage is controlled by the addition of copper spent electrolyte to the matte pulp from the pre-leach stage. The pressure leaching experiments were performed at a pulp density of 1.4 kg/L, so to determine how much matte, spent electrolyte and demineralised water were needed to achieve this pulp density the following calculations were performed:

For pressure leaching conditions, equation D2.3 becomes:

$$1.4 = \frac{1V_{dw} + 1.17V_{se} + 5.8V_m}{V_{dw} + V_{se} + V_m} \qquad \text{(D2.9)}$$

Simplifying and rearranging equation D2.9 gives

$$V_{dw} + 1.17V_{se} + 5.8V_m = 1.4(V_{dw} + V_{se} + V_m)$$

$$4.4V_m - 0.4V_{dw} = 0.23V_{se} \qquad \text{(D2.10)}$$

Equation D2.6 is true for both the atmospheric leach and pressure leach.

Substituting equation D2.6 into equation D2.10:

$$4.4(0.4118V_{dw}) - 0.4V_{dw} = 0.23V_{se} \qquad \text{(D2.11)}$$

Simplifying equation D2.11 gives

$$\boxed{V_{se} = 6.14V_{dw}} \qquad \text{(D2.12)}$$

Like explained in D2.1 above, the volumes of spent electrolyte and demineralised water were calculated using the relationship given in equation D2.12. Volume of the matte was calculated from equation D2.6. Then the mass was found by using the relationship:

mass $= D_m \times V_m$

* *Dynatec Corporation, 2003. Impala Platinum Ltd, Base Metals Refinery diagnosis of plant samples. Confidential report, Dynatec Corporation, Fort Saskatchewan, Alberta, Canada, unpublished.*

INCREASE IN Ni CONCENTRATION DUE TO LEACHING BY CEMENTATION AND ACID AT 60 oC

RUNGE-KUTTA FOURTH-ORDER METHOD

Overall rate equation: $dNi^{2+}/dt = 8/3K_{8.10}Cu^{2+} + K_{8.13}C_{H+}$

Temp. = 60 oC

$dNi^{2+}/dt = 8/3K_{8.10}Cu^{2+}$ Initial Ni = 24.61 g/L 0.419 moles $dNi^{2+}/dt = K_{8.13}C_{H+}$

$K_{8.10}$ = 0.298 Initial Cu = 24.95 g/L 0.393 moles

$K_{8.10}$ = -0.795 Initial H2SO4 = 90 g/L 0.918 moles $K_{8.13}$ = -0.679

EXPERIMENTAL VALUES		MODEL VALUES										
Time	$[Ni^{2+}]$	$[Ni^{2+}]$	$[Ni^{2+}]$	Copper contribution					Acid contribution				
(min)	(g/L)	(g/L)	(mol)	(mol)	K1	K2	K3	K4	(moles)	K1	K2	K3	K4
0	24.61	24.61	0.419	0.393					0.918				
30	66.16	47.68	0.812	0.264	-0.16	-0.13	-0.13	-0.10	0.65	-0.31	-0.26	-0.27	-0.22
60	68.85	63.80	1.087	0.177	-0.10	-0.08	-0.09	-0.07	0.47	-0.22	-0.18	-0.19	-0.16
90	71.18	75.08	1.279	0.119	-0.07	-0.06	-0.06	-0.05	0.33	-0.16	-0.13	-0.14	-0.11
120	78.69	80.69	1.375	0.119	-0.05	-0.04	-0.04	-0.03	0.24	-0.11	-0.09	-0.10	-0.08
150	80.00	86.97	1.482	0.080	-0.05	-0.04	-0.04	-0.03	0.17	-0.08	-0.07	-0.07	-0.06
180	86.80	91.36	1.557	0.054	-0.03	-0.03	-0.03	-0.02	0.12	-0.06	-0.05	-0.05	-0.04
210		94.42	1.609	0.036	-0.02	-0.02	-0.02	-0.01	0.09	-0.04	-0.03	-0.03	-0.03
240	88.33	96.56	1.645	0.024	-0.01	-0.01	-0.01	-0.01	0.06	-0.03	-0.02	-0.02	-0.02
270		98.05	1.671	0.016	-0.01	-0.01	-0.01	-0.01	0.04	-0.02	-0.02	-0.02	-0.01
300	94.44	99.10	1.688	0.011	-0.01	-0.01	-0.01	0.00	0.03	-0.01	-0.01	-0.01	-0.01

INCREASE IN Fe CONCENTRATION DUE TO LEACHING BY ACID AT 60 oC

RUNGE-KUTTA FOURTH-ORDER METHOD

Overall rate equation: $dFe_{(total)}/dt = K_{8.15}C_{H+} - K_{8.16}CFe^{3+}$

Temp. = 60 oC

Initial H2SO4 = 90 g/L 0.918367 moles

Initial Fe = 0.67 g/L 0.012055 moles

H2SO4 after 180 min = 20 g/L 0.204 moles

$dFe^{2+}/dt = K_{8.15}C_{H+}$ Total Fe after 180 min = 4.39 g/L 0.079 moles $dFe^{3+}/dt = -K_{8.15}C_{H+}$

$K_{8.15}$ = 0.0881 $K_{8.16}$ = -0.082

EXPERIMENTAL VALUES		MODEL VALUES											
Time	Fe	Fe	Fe	Fe2+ contribution					Fe3+ contribution				
(min)	(g/L)	(g/L)	(mol)	(mol)	K1	K2	K3	K4	(mol)	K1	K2	K3	K4
0	0.67	0.67	0.012	0.012									
30	3.44	3.01	0.05	0.05	0.040	0.041	0.041	0.042					
60	3.45	3.15	0.06	0.06	0.002	0.002	0.002	0.002					
90	3.8	3.29	0.06	0.06	0.002	0.003	0.003	0.003					
120	3.91	3.44	0.06	0.06	0.003	0.003	0.003	0.003					
150	3.76	3.60	0.06	0.06	0.003	0.003	0.003	0.003					
180	4.05	3.76	0.07	0.07	0.003	0.003	0.003	0.003					
210		3.93	0.07	0.07	0.003	0.003	0.003	0.003					
240	3.86	4.11	0.07	0.07	0.003	0.003	0.003	0.003	0.07				
270		3.94	0.07	0.08	0.003	0.003	0.003	0.003	0.07	-0.0031	-0.0030	-0.0030	-0.0030
300	4.34	4.13	0.07	0.08	0.003	0.003	0.003	0.004	0.07	-0.0030	-0.0029	-0.0029	-0.0028

INCREASE IN Co CONCENTRATION DUE TO LEACHING BY ACID AT 60 oC

RUNGE-KUTTA FOURTH-ORDER METHOD

$dCo^{2+}/dt = K_{8.16}C_{H+}$ **Temp. = 60 oC**

Initial H2SO4 = 90 g/L 0.918 moles

$K_{8.17}$ = 0.0320 Initial Co = 0.18 g/L 0.003 moles

EXPERIMENTAL VALUES		MODEL VALUES					
Time (min)	Co (g/L)	Co (g/L)	Co (mol)	K1	K2	K3	K4
0	0.18	0.18	0.003				
30	0.79	1.05	0.02	0.0147	0.0148	0.0148	0.0149
60	0.8	1.07	0.02	0.0003	0.0003	0.0003	0.0003
90	0.79	1.09	0.02	0.0003	0.0003	0.0003	0.0003
120	0.91	1.10	0.02	0.0003	0.0003	0.0003	0.0003
150	0.88	1.12	0.02	0.0003	0.0003	0.0003	0.0003
180	0.96	1.14	0.02	0.0003	0.0003	0.0003	0.0003
210		1.16	0.02	0.0003	0.0003	0.0003	0.0003
240	0.91	1.18	0.02	0.0003	0.0003	0.0003	0.0003
270		1.20	0.02	0.0003	0.0003	0.0003	0.0003
300	1.01	1.22	0.02	0.0003	0.0003	0.0003	0.0003

DECREASE IN Cu CONCENTRATION DUE TO LEACHING BY ACID AT 60 oC

RUNGE-KUTTA FOURTH-ORDER METHOD

$dCu^{2+}/dt = -8/3K_{8.10}Cu^{2+}$ **Temp. = 60 oC**

$K_{8.10}$ = 0.298 Initial Cu = 24.95 g/L 0.393 moles

$-8/3K_{8.10}$ = -0.795 Initial H2SO4 = 90 g/L 0.918 moles

EXPERIMENTAL VALUES		MODEL VALUES					
Time (min)	Cu (g/L)	Cu (g/L)	Cu (mol)	K1	K2	K3	K4
0	24.95	24.95	0.393				
30	19.49	16.77	0.26	-0.1560	-0.1250	-0.1312	-0.1039
60	14.47	11.27	0.18	-0.1049	-0.0840	-0.0882	-0.0698
90	10.45	7.58	0.12	-0.0705	-0.0565	-0.0593	-0.0469
120	8.75	5.09	0.08	-0.0474	-0.0380	-0.0398	-0.0316
150	6.39	3.42	0.05	-0.0318	-0.0255	-0.0268	-0.0212
180	4.79	2.30	0.04	-0.0214	-0.0172	-0.0180	-0.0143
210		1.55	0.02	-0.0144	-0.0115	-0.0121	-0.0096
240	1.30	1.04	0.02	-0.0097	-0.0078	-0.0081	-0.0064
270		0.70	0.01	-0.0065	-0.0052	-0.0055	-0.0043
300	0.00	0.47	0.01	-0.0044	-0.0035	-0.0037	-0.0029

DECREASE IN ACID CONCENTRATION DUE TO LEACHING BY CEMENTATION AND ACID AT 60 oC (Eqns 8B1,8B2,8B3 &8B4)

RUNGE-KUTTA FOURTH-ORDER METHOD

Overall rate equation: $dH^+/dt = -2K_{8.13}C_{H+} -2K_{8.14}C_{H+} -2K_{8.16} + 3K_{8.15}C_{Fe3+}$

Temp. = 60 oC

Initial Ni = 24.61 g/L	0.419	moles	$dH^+/dt = -2K_{8.13}C_{H+}$	$dH^+/dt = -2K_{8.14}C_{H+}$	$dH^+/dt = 2K_{8.16}C_{H+}$	$dH^+/dt = 3K_{8.15}C_{Fe3+}$
Initial Cu = 24.95 g/L	0.393	moles	$K_{8.13}$ = 0.679	$K_{8.15}$ = 0.0881	$K_{8.17}$ = 0.032	$K_{8.16}$ = 0.0820
Initial H2SO4 = 90 g/L	0.918	moles	$2K_{8.13}$ = -1.358	$2K_{8.15}$ = -0.1762	$2K_{8.17}$ = -0.064	$3K_{8.16}$ = 0.246

EXPERIMENTAL VALUES		MODEL VALUES																				
Time	[H2SO4]	[H2SO4]	[H2SO4]	Acid contribution from equation 8.13					Acid contribution from equation 8.14					Acid contribution from equation 8.16					Acid contribution from equation 8.15				
(min)	(g/L)	(g/L)	(mol)	(mol)	K1	K2	K3	K4	(moles)	K1	K2	K3	K4	(mol)	K1	K2	K3	K4	(moles)	K1	K2	K3	K4
0	90.00	90.00	0.918	0.918					0.918					0.918									
30	62.87	54.69	0.558	0.467	-0.62	-0.41	-0.48	-0.30	0.84	-0.08	-0.08	-0.08	-0.07	0.889	-0.03	-0.03	-0.03	-0.03					
60	36.04	32.19	0.328	0.237	-0.32	-0.21	-0.25	-0.15	0.77	-0.07	-0.07	-0.07	-0.07	0.861	-0.03	-0.03	-0.03	-0.03					
90	19.23	20.45	0.209	0.121	-0.16	-0.11	-0.12	-0.08	0.71	-0.07	-0.06	-0.06	-0.06	0.834	-0.03	-0.03	-0.03	-0.03					
120	10.68	14.21	0.145	0.061	-0.08	-0.05	-0.06	-0.04	0.65	-0.06	-0.06	-0.06	-0.06	0.808	-0.03	-0.03	-0.03	-0.03					
150	7.96	10.78	0.110	0.031	-0.04	-0.03	-0.03	-0.02	0.59	-0.06	-0.05	-0.05	-0.05	0.783	-0.03	-0.03	-0.03	-0.03					
180	8.03	8.80	0.090	0.016	-0.02	-0.01	-0.02	-0.01	0.54	-0.05	-0.05	-0.05	-0.05	0.758	-0.03	-0.02	-0.02	-0.02					
210	7.43	7.58	0.077	0.008	-0.01	-0.01	-0.01	-0.01	0.50	-0.05	-0.05	-0.05	-0.04	0.734	-0.02	-0.02	-0.02	-0.02					
240	8.29	6.75	0.069	0.004	-0.01	0.00	0.00	0.00	0.45	-0.04	-0.04	-0.04	-0.04	0.711	-0.02	-0.02	-0.02	-0.02	0.00				
270	8.97	6.14	0.063	0.002	0.00	0.00	0.00	0.00	0.42	-0.04	-0.04	-0.04	-0.04	0.689	-0.02	-0.02	-0.02	-0.02	0.00	0.11	0.12	0.12	0.13
300	7.05	5.66	0.058	0.001	0.00	0.00	0.00	0.00	0.38	-0.04	-0.04	-0.04	-0.03	0.667	-0.02	-0.02	-0.02	-0.02	0.00	0.00	0.00	0.00	0.00

KINETIC MODEL OF METAL CONCENTRATIONS DURING ATMOSPHERIC LEACHING OF THE MATTE AT A TEMPERATURE OF 60 oC

Conditions
Temp. = 60 oC
Initial copper = 25 g/L
Initial nickel = 25 g/L
Initial H2SO4 = 90 g/L
Stirring rate = 205 rpm
PD = 1.7 kg/L

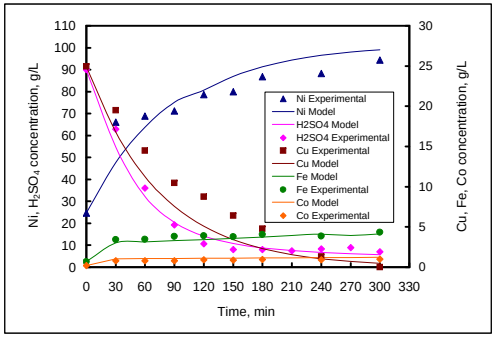

INCREASE IN Ni CONCENTRATION DUE TO LEACHING BY CEMENTATION AND ACID AT STIRRING RATE OF 400 RPM

RUNGE-KUTTA FOURTH-ORDER METHOD

Overall rate equation: $dNi^{2+}/dt = 8/3K_{8.10}Cu^{2+} + K_{8.13}C_{H+}$

Temp. = 60 oC

$dNi^{2+}/dt = 8/3K_{8.10}Cu^{2+}$ — Initial Ni = 24.61 g/L — 0.419 moles — $dNi^{2+}/dt = K_{8.13}C_{H+}$

$K_{8.10}$ = **0.2498** — Initial Cu = 24.95 g/L — 0.393 moles

$K_{8.10}$ = **-0.666** — Initial H2SO4 = 90 g/L — 0.918 moles — $K_{8.13}$ = **-3.19**

EXPERIMENTAL VALUES		MODEL VALUES												
Time	$[Ni^{2+}]$	$[Ni^{2+}]$	$[Ni^{2+}]$	Copper contribution					Acid contribution					
(min)	(g/L)	(g/L)	(mol)	(mol)	K1	K2	K3	K4	(moles)	K1	K2	K3	K4	
0	24.61	24.61	0.419	0.393					0.918					
30	84.95	70.46	1.201	0.281	-0.13	-0.11	-0.11	-0.09	0.25	-1.46	-0.30	-1.23	0.49	
60	91.20	85.77	1.461	0.202	-0.09	-0.08	-0.08	-0.07	0.07	-0.40	-0.08	-0.33	0.13	
90	97.93	92.00	1.568	0.145	-0.07	-0.06	-0.06	-0.05	0.02	-0.11	-0.02	-0.09	0.04	
120	102.38	92.78	1.581	0.145	-0.05	-0.04	-0.04	-0.03	0.00	-0.03	-0.01	-0.02	0.01	
150	101.18	95.39	1.625	0.104	-0.05	-0.04	-0.04	-0.03	0.00	-0.01	0.00	-0.01	0.00	
180	102.47	97.17	1.656	0.074	-0.03	-0.03	-0.03	-0.02	0.00	0.00	0.00	0.00	0.00	
210		98.42	1.677	0.053	-0.02	-0.02	-0.02	-0.02	0.00	0.00	0.00	0.00	0.00	
240	101.00	99.31	1.692	0.038	-0.02	-0.01	-0.02	-0.01	0.00	0.00	0.00	0.00	0.00	
270		99.95	1.703	0.027	-0.01	-0.01	-0.01	-0.01	0.00	0.00	0.00	0.00	0.00	
300	102.13	100.40	1.711	0.020	-0.01	-0.01	-0.01	-0.01	0.00	0.00	0.00	0.00	0.00	

INCREASE IN Fe CONCENTRATION DUE TO LEACHING BY ACID AT STIRRING RATE OF 400 RPM

RUNGE-KUTTA FOURTH-ORDER METHOD

Overall rate equation: $d(Fe^{2+}/Fe^{3+})/dt = K_{8.15}C_{H+} - K_{8.16}CFe^{3+}$

Temp. = 60 oC

Initial H2SO4 = 90 g/L — 0.918367 moles

Initial Fe = 0.67 g/L — 0.012055 moles (assumed to Fe^{2+})

H2SO4after 180 min = 20 g/L — 0.204 moles

$dFe^{2+}/dt = K_{8.15}C_{H+}$ — Assume 10%Fe oxidised to Fe^{3+} after 150 min = 0.0024109 moles — $dFe^{3+}/dt = -K_{8.16}CFe^{3+}$

$K_{8.15}$ = **0.1109** — K8.16 = **-2.02**

EXPERIMENTAL VALUES		MODEL VALUES											
Time	Fe	Fe	Fe	Fe2+ (rate of increase)					Fe3+ contribution				
(min)	(g/L)	(g/L)	(mol)	(mol)	K1	K2	K3	K4	(mol)	K1	K2	K3	K4
0	0.67	0.67	0.012	0.012									
30	4.66	3.64	0.07	0.07	0.051	0.052	0.052	0.054					
60	4.8	3.85	0.07	0.07	0.004	0.004	0.004	0.004					
90	4.9	4.07	0.07	0.07	0.004	0.004	0.004	0.004					
120	4.97	4.31	0.08	0.08	0.004	0.004	0.004	0.004	0.0024				
150	4.26	4.22	0.08	0.08	0.004	0.004	0.004	0.005	0.0009	-0.0024	-0.0012	-0.0018	-0.0006
180	4.02	4.52	0.08	0.09	0.005	0.005	0.005	0.005	0.0003	-0.0009	-0.0004	-0.0007	-0.0002
210		4.81	0.09	0.09	0.005	0.005	0.005	0.005	0.0001	-0.0003	-0.0002	-0.0003	-0.0001
240	4.18	5.09	0.09	0.10	0.005	0.005	0.005	0.005	0.0000	-0.0001	-0.0001	-0.0001	0.0000
270		5.39	0.10	0.10	0.005	0.006	0.006	0.006	0.0000	0.0000	0.0000	0.0000	0.0000
300	3.49	5.70	0.10	0.11	0.006	0.006	0.006	0.006	0.0000	0.0000	0.0000	0.0000	0.0000

KINETIC MODEL OF METAL CONCENTRATIONS DURING ATMOSPHERIC LEACHING OF THE MATTE AT STIRRING RATE OF 400 RPM

Conditions

Temp. = 60 oC

Initial copper = 25 g/L

Initial nickel = 25 g/L

Initial H2SO4 = 90 g/L

Stirring rate = 400 rpm

PD = 1.7 kg/L

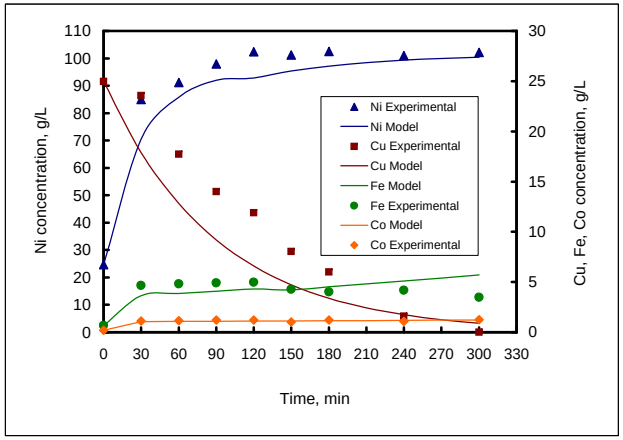

INCREASE IN Co CONCENTRATION DUE TO LEACHING BY ACID AT STIRRING RATE OF 400 RPM

RUNGE-KUTTA FOURTH-ORDER METHOD

$dCo^{2+}/dt = K_{8.17}C_{H+}$ **Temp. = 60 oC**

Initial H2SO4 = 90 g/L 0.918 moles

$K_{8.17}$ = **0.0320** Initial Co = 0.18 g/L 0.003 moles

EXPERIMENTAL VALUES				MODEL VALUES			
Time (min)	**Co (g/L)**	**Co (g/L)**	**Co (mol)**	**K1**	**K2**	**K3**	**K4**
0	0.18	0.18	0.003				
30	1.13	1.05	0.02	0.0147	0.0148	0.0148	0.0149
60	1.14	1.07	0.02	0.0003	0.0003	0.0003	0.0003
90	1.2	1.09	0.02	0.0003	0.0003	0.0003	0.0003
120	1.21	1.10	0.02	0.0003	0.0003	0.0003	0.0003
150	1.02	1.12	0.02	0.0003	0.0003	0.0003	0.0003
180	1.2	1.14	0.02	0.0003	0.0003	0.0003	0.0003
210		1.16	0.02	0.0003	0.0003	0.0003	0.0003
240	1.09	1.18	0.02	0.0003	0.0003	0.0003	0.0003
270		1.20	0.02	0.0003	0.0003	0.0003	0.0003
300	1.23	1.22	0.02	0.0003	0.0003	0.0003	0.0003

DECREASE IN Cu CONCENTRATION DUE TO LEACHING BY ACID AT STIRRING RATE OF 400 RPM

RUNGE-KUTTA FOURTH-ORDER METHOD

$dCu^{2+}/dt = -8/3K_{8.10}Cu^{2+}$ **Temp. = 60 oC**

$K_{8.10}$ = 0.2498 Initial Cu = 24.95 g/L 0.393 moles

$-8/3K_{8.10}$ = -0.666 Initial H2SO4 = 90 g/l 0.918 moles

EXPERIMENTAL VALUES				MODEL VALUES			
Time (min)	**Cu (g/L)**	**Cu (g/L)**	**Cu (mol)**	**K1**	**K2**	**K3**	**K4**
0	24.95	24.95	0.393				
30	23.55	17.88	0.28	-0.1308	-0.1090	-0.1126	-0.0933
60	17.71	12.82	0.20	-0.0937	-0.0781	-0.0807	-0.0668
90	13.98	9.19	0.14	-0.0672	-0.0560	-0.0579	-0.0479
120	11.90	6.58	0.10	-0.0482	-0.0401	-0.0415	-0.0343
150	8.02	4.72	0.07	-0.0345	-0.0288	-0.0297	-0.0246
180	5.99	3.38	0.05	-0.0247	-0.0206	-0.0213	-0.0176
210		2.42	0.04	-0.0177	-0.0148	-0.0153	-0.0126
240	1.58	1.74	0.03	-0.0127	-0.0106	-0.0109	-0.0091
270		1.25	0.02	-0.0091	-0.0076	-0.0078	-0.0065
300	0.00	0.89	0.01	-0.0065	-0.0054	-0.0056	-0.0047

INCREASE IN Ni CONCENTRATION DUE TO LEACHING BY CEMENTATION AND ACID AT 48 g/L INITIAL COPPER

RUNGE-KUTTA FOURTH-ORDER METHOD

Overall rate equation: $dNi^{2+}/dt = 8/3K_{8.10}Cu^{2+} + K_{8.13}C_{H+}$

Temp. = 60 oC

$dNi^{2+}/dt = 8/3K_{8.10}Cu^{2+}$	Initial Ni = 24.61 g/L	0.419	moles	$dNi^{2+}/dt = K_{8.13}C_{H+}$
$K_{8.10}$ = **0.0867**	Initial Cu = 24.95 g/L	0.393	moles	$K_{8.13}$ = **1.545**
$K_{8.10}$ = **-0.231**	Initial H2SO4 = 90 g/L	0.918	moles	$K_{8.13}$ = **-1.545**

EXPERIMENTAL VALUES		MODEL VALUES											
Time	$[Ni^{2+}]$	$[Ni^{2+}]$	$[Ni^{2+}]$	Copper contribution					Acid contribution				
(min)	(g/L)	(g/L)	(mol)	(mol)	K1	K2	K3	K4	(moles)	K1	K2	K3	K4
0	24.61	24.61	0.419	0.393					0.918				
30	68.25	56.02	0.955	0.350	-0.05	-0.04	-0.04	-0.04	0.43	-0.71	-0.44	-0.54	-0.29
60	69.17	71.67	1.221	0.312	-0.04	-0.04	-0.04	-0.04	0.20	-0.33	-0.20	-0.25	-0.14
90	71.47	79.88	1.361	0.278	-0.04	-0.03	-0.03	-0.03	0.09	-0.15	-0.09	-0.12	-0.06
120	77.02	82.77	1.410	0.278	-0.03	-0.03	-0.03	-0.03	0.04	-0.07	-0.04	-0.05	-0.03
150	79.99	85.88	1.463	0.247	-0.03	-0.03	-0.03	-0.03	0.02	-0.03	-0.02	-0.03	-0.01
180	80.16	88.09	1.501	0.220	-0.03	-0.03	-0.03	-0.03	0.01	-0.02	-0.01	-0.01	-0.01
210		89.79	1.530	0.196	-0.03	-0.02	-0.02	-0.02	0.00	-0.01	0.00	-0.01	0.00
240	86.15	91.18	1.554	0.175	-0.02	-0.02	-0.02	-0.02	0.00	0.00	0.00	0.00	0.00
270		92.36	1.574	0.156	-0.02	-0.02	-0.02	-0.02	0.00	0.00	0.00	0.00	0.00
300	92.97	93.39	1.591	0.139	-0.02	-0.02	-0.02	-0.02	0.00	0.00	0.00	0.00	0.00

INCREASE IN Fe CONCENTRATION DUE TO LEACHING BY ACID AT 48 g/L COPPER

RUNGE-KUTTA FOURTH-ORDER METHOD

Overall rate equation: $dFe_{(total)}/dt = K_{8.15}C_{H+} - K_{8.16}C_{Fe3+}$

Temp. = 60 oC

Initial H2SO4 = 90 g/L	0.918367	moles
Initial Fe = 0.67 g/L	0.012055	moles

$dFe^{2+}/dt = K_{8.15}C_{H+}$ $K_{8.15}$ = **0.0881**

$dFe^{3+}/dt = -K_{8.16}C_{Fe3+}$ $K_{8.16}$ = **-0.082**

EXPERIMENTAL VALUES		MODEL VALUES											
Time	Fe	Fe	Fe	Fe2+ contribution					Fe3+ contribution				
(min)	(g/L)	(g/L)	(mol)	(mol)	K1	K2	K3	K4	(mol)	K1	K2	K3	K4
0	0.67	0.67	0.012	0.012									
30	3.75	3.01	0.05	0.05	0.040	0.041	0.041	0.042					
60	3.66	3.15	0.06	0.06	0.002	0.002	0.002	0.002					
90	3.71	3.29	0.06	0.06	0.002	0.003	0.003	0.003					
120	3.85	3.44	0.06	0.06	0.003	0.003	0.003	0.003					
150	3.94	3.60	0.06	0.06	0.003	0.003	0.003	0.003					
180	3.86	3.76	0.07	0.07	0.003	0.003	0.003	0.003					
210		3.93	0.07	0.07	0.003	0.003	0.003	0.003					
240	4.04	4.11	0.07	0.07	0.003	0.003	0.003	0.003	0.00				
270		4.11	0.07	0.08	0.003	0.003	0.003	0.003	0.00	0.0000	0.0000	0.0000	0.0000
300	4.18	4.30	0.08	0.08	0.003	0.003	0.003	0.004	0.00	0.0000	0.0000	0.0000	0.0000

INCREASE IN Co CONCENTRATION DUE TO LEACHING BY ACID AT 48 g/L COPPER

RUNGE-KUTTA FOURTH-ORDER METHOD

$dCo^{2+}/dt = K_{8.17}C_{H+}$ **Temp. = 60 oC**

Initial H2SO4 = 90 g 0.918 moles

$K_{8.17}$ = **0.0320** Initial Co = 0.18 g/L 0.003 moles

EXPERIMENTAL VALUES		MODEL VALUES					
Time (min)	Co (g/L)	Co (g/L)	Co (mol)	K1	K2	K3	K4
0	0.18	0.18	0.003				
30	0.96	1.05	0.02	0.0147	0.0148	0.0148	0.0149
60	0.94	1.07	0.02	0.0003	0.0003	0.0003	0.0003
90	0.97	1.09	0.02	0.0003	0.0003	0.0003	0.0003
120	1.00	1.10	0.02	0.0003	0.0003	0.0003	0.0003
150	1.04	1.12	0.02	0.0003	0.0003	0.0003	0.0003
180	1.02	1.14	0.02	0.0003	0.0003	0.0003	0.0003
210		1.16	0.02	0.0003	0.0003	0.0003	0.0003
240	1.07	1.18	0.02	0.0003	0.0003	0.0003	0.0003
270		1.20	0.02	0.0003	0.0003	0.0003	0.0003
300	1.15	1.22	0.02	0.0003	0.0003	0.0003	0.0003

DECREASE IN Cu CONCENTRATION DUE TO LEACHING BY ACID AT 48 g/L COPPER

RUNGE-KUTTA FOURTH-ORDER METHOD

$dCu^{2+}/dt = -7/3K_{8A}Cu^{2+}$ **Temp. = 60 oC**

$K_{8.10}$ = **0.0867** Initial Cu = 48.00 g/L 0.755 moles

$-8/3K_{8.10}$= -0.231 Initial H2SO4 = 90 g/L 0.918 moles

EXPERIMENTAL VALUES		MODEL VALUES					
Time (min)	Cu (g/L)	Cu (g/L)	Cu (mol)	K1	K2	K3	K4
0	48.43	48.00	0.755				
30	43.25	42.76	0.67	-0.0873	-0.0823	-0.0826	-0.0778
60	36.43	38.09	0.60	-0.0778	-0.0733	-0.0735	-0.0693
90	33.01	33.93	0.53	-0.0693	-0.0653	-0.0655	-0.0617
120	30.73	30.23	0.48	-0.0617	-0.0582	-0.0584	-0.0550
150	29.37	26.93	0.42	-0.0550	-0.0518	-0.0520	-0.0490
180	26.80	23.99	0.38	-0.0490	-0.0462	-0.0463	-0.0436
210		21.37	0.34	-0.0436	-0.0411	-0.0413	-0.0389
240	24.06	19.04	0.30	-0.0389	-0.0366	-0.0368	-0.0346
270		16.96	0.27	-0.0346	-0.0326	-0.0327	-0.0308
300	20.11	15.11	0.24	-0.0308	-0.0291	-0.0292	-0.0275

KINETIC MODEL OF METAL CONCENTRATIONS DURING ATMOSPHERIC LEACHING OF THE MATTE AT 48 g/L INITIAL COPPER

Conditions
Temp. = 60 oC
Initial copper = 48 g/L
Initial nickel = 25 g/L
Initial H2SO4 = 90 g/L
Stirring rate = 205 rpm
PD = 1.7 kg/L

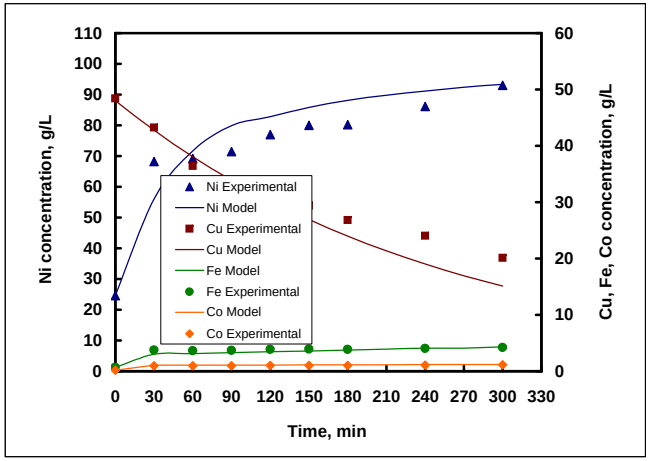

INCREASE IN Ni CONCENTRATION DUE TO LEACHING BY CEMENTATION AND ACID AT 80 oC

RUNGE-KUTTA FOURTH-ORDER METHOD

Overall rate equation: $dNi^{2+}/dt = 8/3K_{8.10}Cu^{2+} + K_{8.13}C_{H+}$

Temp. = 80 oC

$dNi^{2+}/dt = 8/3\ K_{8.10}Cu^{2+}$ — Initial Ni = 24.61 g/L — 0.419 moles — $dNi2^{+}/dt = K_{8.13}C_{H+}$

$K_{8.10}$ = 1.728 — Initial Cu = 24.95 g/L — 0.393 moles

$8/3K_{8.10}$ = -4.608 — Initial H2SO4 = 90 g/L — 0.918 moles — K8.13 = -0.979

EXPERIMENTAL VALUES		MODEL VALUES												
Time	$[Ni^{2+}]$	$[Ni^{2+}]$	$[Ni^{2+}]$	Copper contribution					Acid contribution					
(min)	(g/L)	(g/L)	(mol)	(mol)	K1	K2	K3	K4	(moles)	K1	K2	K3	K4
0	24.61	24.61	0.419	0.393					0.918				
30	65.58	57.31	0.976	0.191	-0.90	0.14	-1.06	1.54	0.56	-0.45	-0.34	-0.37	-0.27
60	76.59	75.85	1.292	0.093	-0.44	0.07	-0.52	0.75	0.35	-0.28	-0.21	-0.22	-0.17
90	87.97	86.48	1.474	0.045	-0.21	0.03	-0.25	0.36	0.21	-0.17	-0.13	-0.14	-0.10
120	91.86	92.65	1.579	0.022	-0.10	0.02	-0.12	0.18	0.13	-0.10	-0.08	-0.08	-0.06
150	97.00	96.26	1.640	0.011	-0.05	0.01	-0.06	0.09	0.08	-0.06	-0.05	-0.05	-0.04
180	97.73	98.38	1.676	0.005	-0.02	0.00	-0.03	0.04	0.05	-0.04	-0.03	-0.03	-0.02
210		99.65	1.698	0.003	-0.01	0.00	-0.01	0.02	0.03	-0.02	-0.02	-0.02	-0.01
240	104.17	99.645	1.711	0.001	-0.01	0.00	-0.01	0.01	0.02	-0.01	-0.01	-0.01	-0.01
270		100.86	1.718	0.001	0.00	0.00	0.00	0.00	0.01	-0.01	-0.01	-0.01	-0.01
300	104.59	101.13	1.723	0.000	0.00	0.00	0.00	0.00	0.01	-0.01	0.00	0.00	0.00

INCREASE IN Fe CONCENTRATION DUE TO LEACHING BY ACID AT 80 oC

RUNGE-KUTTA FOURTH-ORDER METHOD

Overall rate equation: $dFe_{(total)}/dt = K_{8.15}C_{H+} - K_{8.16}CFe^{3+}$

Temp. = 80 oC

Initial H2SO4 = 90 g/L — 0.918367 moles

Initial Fe = 0.67 g/L — 0.012055 moles

H2SO4after 180 min = 20 g/L — 0.204 moles

$dFe^{2+}/dt = K_{8.15}C_{H+}$ — Total Fe after 180 min = 4.39 g/L — 0.079 moles — $dFe^{3+}/dt = -K_{8.16}C_{H+}$

$K_{8.15}$ = 0.0981 — $K_{8.16}$ = -0.082

EXPERIMENTAL VALUES		MODEL VALUES												
Time	Fe	Fe	Fe	Fe2+ contribution					Fe3+ contribution					
(min)	(g/L)	(g/L)	(mol)	(mol)	K1	K2	K3	K4	(mol)	K1	K2	K3	K4
0	0.67	0.67	0.012	0.012									
30	3.32	3.28	0.06	0.059	0.045	0.046	0.046	0.047					
60	3.58	3.45	0.06	0.062	0.003	0.003	0.003	0.003					
90	4.03	3.63	0.06	0.065	0.003	0.003	0.003	0.003					
120	4.25	3.81	0.07	0.068	0.003	0.003	0.003	0.003					
150	4.33	4.00	0.07	0.072	0.003	0.003	0.003	0.004					
180	4.39	4.21	0.08	0.075	0.004	0.004	0.004	0.004	0.00				
210		4.21	0.08	0.079	0.004	0.004	0.004	0.004	0.00	0.0000	0.0000	0.0000	0.0000
240	4.15	4.42	0.08	0.083	0.004	0.004	0.004	0.004	0.00	0.0000	0.0000	0.0000	0.0000
270		4.65	0.08	0.087	0.004	0.004	0.004	0.004	0.00	0.0000	0.0000	0.0000	0.0000
300	3.96	4.88	0.09	0.092	0.004	0.004	0.004	0.005	0.00	0.0000	0.0000	0.0000	0.0000

KINETIC MODEL OF METAL CONCENTRATIONS DURING ATMOSPHERIC LEACHING OF THE MATTE AT A TEMPERATURE OF 80 oC

Conditions

Temp. = 80 °C

Initial copper = 25 g/L

Initial nickel = 25 g/L

Initial H2SO4 = 90 g/L

Stirring rate = 205 rpm

PD = 1.7 kg/L

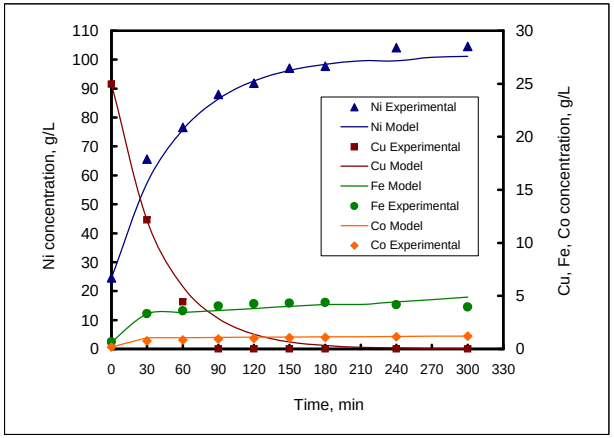

INCREASE IN Co CONCENTRATION DUE TO LEACHING BY ACID AT 80 oC

RUNGE-KUTTA FOURTH-ORDER METHOD

$dCo^{2+}/dt = K_{8.17}C_{H+}$ **Temp. = 80 oC**

Initial H2SO4 = 90 g/L 0.918 moles

$K_{8.17}$ = 0.0320 Initial Co = 0.18 g/L 0.003 moles

EXPERIMENTAL VALUES		MODEL VALUES					
Time (min)	Co (g/L)	Co (g/L)	Co (mol)	K1	K2	K3	K4
0	0.18	0.18	0.003				
30	0.76	1.05	0.02	0.0147	0.0148	0.0148	0.0149
60	0.83	1.07	0.02	0.0003	0.0003	0.0003	0.0003
90	0.94	1.09	0.02	0.0003	0.0003	0.0003	0.0003
120	1.00	1.10	0.02	0.0003	0.0003	0.0003	0.0003
150	1.07	1.12	0.02	0.0003	0.0003	0.0003	0.0003
180	1.09	1.14	0.02	0.0003	0.0003	0.0003	0.0003
210		1.16	0.02	0.0003	0.0003	0.0003	0.0003
240	1.16	1.18	0.02	0.0003	0.0003	0.0003	0.0003
270		1.20	0.02	0.0003	0.0003	0.0003	0.0003
300	1.21	1.22	0.02	0.0003	0.0003	0.0003	0.0003

DECREASE IN Cu CONCENTRATION DUE TO LEACHING BY ACID AT 80 oC

RUNGE-KUTTA FOURTH-ORDER METHOD

$dCu^{2+}/dt = -8/3K_{8.10}Cu^{2+}$ **Temp. = 80 oC**

$K_{8.10}$ = -1.728 Initial Cu = 24.95 g/L 0.393 moles

$-8/3K_{8.10}$ = -4.608 Initial H2SO4 = 90 g/L 0.918 moles

EXPERIMENTAL VALUES		MODEL VALUES					
Time (min)	Cu (g/L)	Cu (g/L)	Cu (mol)	K1	K2	K3	K4
0	24.95	24.95	0.393				
30	12.16	12.12	0.19	-0.9046	0.1375	-1.0630	1.5445
60	4.44	5.89	0.09	-0.4395	0.0668	-0.5165	0.7505
90	0.00	2.86	0.05	-0.2136	0.0325	-0.2510	0.3647
120	0.00	1.39	0.02	-0.1038	0.0158	-0.1220	0.1772
150	0.00	0.68	0.01	-0.0504	0.0077	-0.0593	0.0861
180	0.00	0.33	0.01	-0.0245	0.0037	-0.0288	0.0418
210		0.16	0.00	-0.0119	0.0018	-0.0140	0.0203
240	0.00	0.08	0.00	-0.0058	0.0009	-0.0068	0.0099
270		0.04	0.00	-0.0028	0.0004	-0.0033	0.0048
300	0.00	0.02	0.00	-0.0014	0.0002	-0.0016	0.0023

INCREASE IN Ni CONCENTRATION DUE TO LEACHING BY CEMENTATION AND ACID AT 125 g/L ACI

RUNGE-KUTTA FOURTH-ORDER METHOD

Overall rate equation: $dNi^{2+}/dt = 8/3K_{8.10}Cu^{2+} + K_{8.13}C_{H+}$

Temp. = 60 oC

$dNi^{2+}/dt = 8/3K_{8.10}Cu^{2+}$

$K_{8.10}$ = **0.173**

$K_{8.10}$ = **-0.461**

Initial Ni = 24.61 g/L 0.419 moles

Initial Cu = 24.95 g/L 0.393 moles

Initial H2SO4 = 125 g/L 1.276 moles

$dNi^{2+}/dt = K_{8.13}C_{H+}$

$K_{8.13}$ = **-1.532**

EXPERIMENTAL VALUES		MODEL VALUES												
Time	$[Ni^{2+}]$	$[Ni^{2+}]$	$[Ni^{2+}]$	Copper contribution					Acid contribution					
(min)	(g/L)	(g/L)	(mol)	(mol)	K1	K2	K3	K4	(moles)	K1	K2	K3	K4
0	24.61	24.61	0.419	0.393					0.918				
30	70.58	58.09	0.990	0.312	-0.09	-0.08	-0.08	-0.07	0.43	-0.70	-0.43	-0.54	-0.29
60	76.40	75.28	1.283	0.248	-0.07	-0.06	-0.06	-0.06	0.20	-0.33	-0.20	-0.25	-0.14
90	79.58	84.53	1.440	0.197	-0.06	-0.05	-0.05	-0.05	0.09	-0.15	-0.09	-0.12	-0.06
120	83.22	87.46	1.490	0.197	-0.05	-0.04	-0.04	-0.04	0.04	-0.07	-0.04	-0.05	-0.03
150	84.66	91.20	1.554	0.156	-0.05	-0.04	-0.04	-0.04	0.02	-0.03	-0.02	-0.03	-0.01
180	87.63	93.72	1.597	0.124	-0.04	-0.03	-0.03	-0.03	0.01	-0.02	-0.01	-0.01	-0.01
210		95.52	1.627	0.098	-0.03	-0.03	-0.03	-0.02	0.00	-0.01	0.00	-0.01	0.00
240	93.38	96.84	1.650	0.078	-0.02	-0.02	-0.02	-0.02	0.00	0.00	0.00	0.00	0.00
270		97.85	1.667	0.062	-0.02	-0.02	-0.02	-0.01	0.00	0.00	0.00	0.00	0.00
300	98.05	98.63	1.681	0.049	-0.01	-0.01	-0.01	-0.01	0.00	0.00	0.00	0.00	0.00

INCREASE IN Fe CONCENTRATION DUE TO LEACHING BY ACID AT 125 g/L CI

RUNGE-KUTTA FOURTH-ORDER METHOD

Overall rate equation: $dFe_{(total)}/dt = K_{8.15}C_{H+} - K_{8.16}C_{Fe3+}$

Temp. = 60 oC

Initial H2SO4 = 125 g/L 1.27551 moles

Initial Fe = 0.67 g/L 0.012055 moles

$dFe^{2+}/dt = K_{8.15}C_{H+}$

$K_{8.15}$ = **0.086**

$dFe^{3+}/dt = -K_{8.16}C_{Fe3+}$

$K_{8.16}$ = **0.00**

EXPERIMENTAL VALUES		MODEL VALUES												
Time	Fe	Fe	Fe	Fe^{2+} contribution					Fe^{3+} contribution					
(min)	(g/L)	(g/L)	(mol)	(mol)	K1	K2	K3	K4	(mol)	K1	K2	K3	K4
0	0.67	0.67	0.012	0.012									
30	4.40	3.84	0.07	0.07	0.055	0.056	0.056	0.057					
60	4.63	4.01	0.07	0.07	0.003	0.003	0.003	0.003					
90	4.74	4.19	0.07	0.07	0.003	0.003	0.003	0.003					
120	4.85	4.37	0.08	0.08	0.003	0.003	0.003	0.003					
150	4.84	4.57	0.08	0.08	0.003	0.003	0.003	0.004					
180	4.93	4.77	0.09	0.09	0.004	0.004	0.004	0.004					
210		4.98	0.09	0.09	0.004	0.004	0.004	0.004					
240	5.11	5.20	0.09	0.09	0.004	0.004	0.004	0.004	0.00				
270		5.20	0.09	0.10	0.004	0.004	0.004	0.004	0.00	0.0000	0.0000	0.0000	0.0000
300	5.22	5.43	0.10	0.10	0.004	0.004	0.004	0.004	0.00	0.0000	0.0000	0.0000	0.0000

KINETIC MODEL OF METAL CONCENTRATIONS DURING ATMOSPHERIC LEACHING OF THE MATTE AT 125 g/L INITIAL ACID TEMPERATURE OF 60 o

Conditions

Temp. = 60 oC

Initial copper = 24.95 g/L

Initial nickel = 25 g/L

Initial H2SO4 = 125 g/L

Stirring rate = 205 rpm

PD = 1.7 kg/L

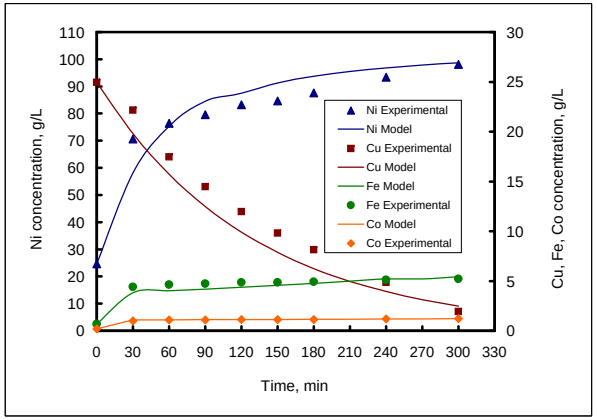

INCREASE IN Co CONCENTRATION DUE TO LEACHING BY ACID AT 125 g/L ACII

RUNGE-KUTTA FOURTH-ORDER METHOD

$dCo^{2+}/dt = K_{8.17}C_{H+}$ **Temp. = 60 oC**

Initial H2SO4 = 125 g/L 1.276 moles

$K_{8.17}$ = **0.0240** Initial Co = 0.18 g/L 0.003 moles

EXPERIMENTAL VALUES		MODEL VALUES					
Time (min)	Co (g/L)	Co (g/L)	Co (mol)	K1	K2	K3	K4
0	0.18	0.18	0.003				
30	1.01	1.09	0.02	0.0153	0.0154	0.0154	0.0155
60	1.08	1.10	0.02	0.0002	0.0002	0.0002	0.0002
90	1.08	1.11	0.02	0.0002	0.0002	0.0002	0.0002
120	1.11	1.13	0.02	0.0002	0.0002	0.0002	0.0002
150	1.13	1.14	0.02	0.0002	0.0002	0.0002	0.0002
180	1.14	1.15	0.02	0.0002	0.0002	0.0002	0.0002
210		1.17	0.02	0.0002	0.0002	0.0002	0.0002
240	1.19	1.18	0.02	0.0002	0.0002	0.0002	0.0002
270		1.20	0.02	0.0002	0.0002	0.0002	0.0002
300	1.22	1.21	0.02	0.0002	0.0002	0.0002	0.0002

DECREASE IN Cu CONCENTRATION DUE TO LEACHING BY ACID AT 125 g/L ACIC

RUNGE-KUTTA FOURTH-ORDER METHOD

$dCu^{2+}/dt = -8/3K_{8A}Cu^{2+}$ **Temp. = 60 oC**

$K_{8.10}$ = **0.173** Initial Cu = 24.95 g/L 0.393 moles

$-8/3K_{8.10}$= -0.461 Initial H2SO4 = 125 g/L 1.276 moles

EXPERIMENTAL VALUES		MODEL VALUES					
Time (min)	Cu (g/L)	Cu (g/L)	Cu (mol)	K1	K2	K3	K4
0	24.95	24.95	0.393				
30	22.16	19.81	0.31	-0.0906	-0.0801	-0.0813	-0.0718
60	17.46	15.73	0.25	-0.0719	-0.0636	-0.0646	-0.0570
90	14.48	12.49	0.20	-0.0571	-0.0505	-0.0513	-0.0453
120	11.95	9.92	0.16	-0.0453	-0.0401	-0.0407	-0.0359
150	9.81	7.87	0.12	-0.0360	-0.0318	-0.0323	-0.0285
180	8.12	6.25	0.10	-0.0286	-0.0253	-0.0257	-0.0227
210		4.96	0.08	-0.0227	-0.0201	-0.0204	-0.0180
240	4.86	3.94	0.06	-0.0180	-0.0159	-0.0162	-0.0143
270		3.13	0.05	-0.0143	-0.0127	-0.0128	-0.0113
300	1.93	2.49	0.04	-0.0114	-0.0100	-0.0102	-0.0090

INCREASE IN Ni CONCENTRATION DUE TO LEACHING BY CEMENTATION AND ACID At -45um PARTICLE SIZ

RUNGE-KUTTA FOURTH-ORDER METHOD

Overall rate equation: $dNi^{2+}/dt = 8/3K_{8.10}Cu^{2+} + K_{8.13}C_{H+}$

Temp. = 60 oC

$dNi^{2+}/dt = 8/3K_{8.10}Cu^{2+}$ Initial Ni = 24.61 g/L 0.419 moles $dNi^{2+}/dt = K_{8.13}C_{H+}$

$K_{8.10}$ = **1.161** Initial Cu = 24.95 g/L 0.393 moles

$K_{8.10}$ = **-3.096** Initial H2SO4 = 90 g/L 0.918 moles K8.13 = **-1.409**

EXPERIMENTAL VALUES		MODEL VALUES											
Time	$[Ni^{2+}]$	$[Ni^{2+}]$	$[Ni^{2+}]$	Copper contribution					Acid contribution				
(min)	(g/L)	(g/L)	(mol)	(mol)	K1	K2	K3	K4	(moles)	K1	K2	K3	K4
0	24.61	24.61	0.419	0.393					0.918				
30	85.38	68.59	1.169	0.106	-0.61	-0.14	-0.50	0.17	0.46	-0.65	-0.42	-0.50	-0.30
60	87.58	86.62	1.476	0.029	-0.16	-0.04	-0.14	0.05	0.23	-0.32	-0.21	-0.25	-0.15
90	89.29	94.53	1.611	0.008	-0.04	-0.01	-0.04	0.01	0.11	-0.16	-0.10	-0.12	-0.07
120	92.55	97.84	1.667	0.008	-0.01	0.00	-0.01	0.00	0.06	-0.08	-0.05	-0.06	-0.04
150	93.10	99.81	1.701	0.002	-0.01	0.00	-0.01	0.00	0.03	-0.04	-0.03	-0.03	-0.02
180	93.18	100.72	1.716	0.001	0.00	0.00	0.00	0.00	0.01	-0.02	-0.01	-0.01	-0.01
210		101.15	1.723	0.000	0.00	0.00	0.00	0.00	0.01	-0.01	-0.01	-0.01	0.00
240	99.45	101.35	1.727	0.000	0.00	0.00	0.00	0.00	0.00	0.00	0.00	0.00	0.00
270		101.45	1.729	0.000	0.00	0.00	0.00	0.00	0.00	0.00	0.00	0.00	0.00
300	101.84	101.50	1.729	0.000	0.00	0.00	0.00	0.00	0.00	0.00	0.00	0.00	0.00

INCREASE IN Fe CONCENTRATION DUE TO LEACHING BY ACID AT - 45 um PARTICLE SIZ

RUNGE-KUTTA FOURTH-ORDER METHOD

Overall rate equation: $dFe_{(total)}/dt = K_{8.15}C_{H+} - K_{8.16}CFe^{3+}$

Temp. = 60 oC

Initial H2SO4 = 90 g/L 0.918367 moles

Initial Fe = 0.67 g/L 0.012055 moles

H2SO4after 180 min = 20 g/L 0.204 moles

$dFe^{2+}/dt = K_{8.15}C_{H+}$ Total Fe after 180 min = 4.39 g/L 0.079 moles $dFe^{3+}/dt = -K_{8.16}C_{Fe3+}$

$K_{8.15}$ = 0.171 $K_{8.16}$ = 0.261

EXPERIMENTAL VALUES		MODEL VALUES											
Time	Fe	Fe	Fe	Fe2+ contribution					Fe3+ contribution				
(min)	(g/L)	(g/L)	(mol)	(mol)	K1	K2	K3	K4	(mol)	K1	K2	K3	K4
0	0.67	0.67	0.012	0.012									
30	4.46	5.35	0.10	0.10	0.079	0.082	0.082	0.086					
60	3.66	2.18	0.04	0.10	0.008	0.009	0.009	0.009	0.07				
90	2.58	2.20	0.04	0.11	0.009	0.009	0.009	0.010	0.07	0.0086	0.0091	0.0091	0.0097
120	1.44	2.20	0.04	0.12	0.010	0.010	0.010	0.011	0.09	0.0097	0.0104	0.0104	0.0111
150	1.34	2.17	0.04	0.14	0.011	0.011	0.011	0.012	0.10	0.0111	0.0118	0.0119	0.0127
180	1.36	2.11	0.04	0.15	0.012	0.012	0.012	0.013	0.11	0.0127	0.0135	0.0135	0.0144
210		2.00	0.04	0.16	0.013	0.013	0.013	0.014	0.13	0.0144	0.0154	0.0154	0.0164
240	1.42	1.85	0.03	0.18	0.014	0.014	0.014	0.015	0.14	0.0164	0.0175	0.0176	0.0187
270		1.63	0.03	0.19	0.015	0.016	0.016	0.016	0.16	0.0187	0.0199	0.0200	0.0213
300	1.27	1.34	0.02	0.21	0.016	0.017	0.017	0.018	0.19	0.0213	0.0227	0.0228	0.0243

KINETIC MODEL OF METAL CONCENTRATIONS DURING ATMOSPHERIC LEACHING OF THE MATTE AT -45 um PARTICLE SIZE

Conditions

Particle size = - 45µm

Temp. = 60 oC

Initial copper = 25 g/L

Initial nickel = 25 g/L

Initial H2SO4 = 90 g/L

Stirring rate = 205 rpm

PD = 1.7 kg/L

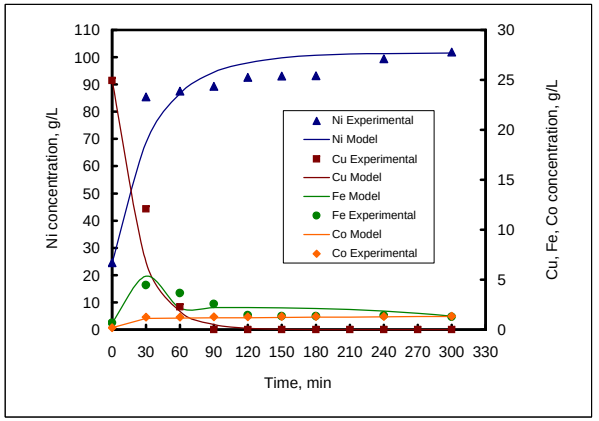

INCREASE IN Co CONCENTRATION DUE TO LEACHING BY ACID AT -45um PARTICLE SIZI

RUNGE-KUTTA FOURTH-ORDER METHOD

$dCo^{2+}/dt = K_{8.17}C_{H+}$ Temp. = 60 oC

Initial H2SO4 = 90 g/L 0.918 moles

$K_{8.17}$ = 0.0350 Initial Co = 0.18 g/L 0.003 moles

EXPERIMENTAL VALUES		MODEL VALUES					
Time (min)	Co (g/L)	Co (g/L)	Co (mol)	K1	K2	K3	K4
0	0.18	0.18	0.003				
30	1.25	1.14	0.02	0.0161	0.0162	0.0162	0.0164
60	1.26	1.16	0.02	0.0003	0.0003	0.0003	0.0003
90	1.27	1.18	0.02	0.0003	0.0003	0.0003	0.0003
120	1.29	1.20	0.02	0.0003	0.0004	0.0004	0.0004
150	1.30	1.22	0.02	0.0004	0.0004	0.0004	0.0004
180	1.30	1.24	0.02	0.0004	0.0004	0.0004	0.0004
210		1.26	0.02	0.0004	0.0004	0.0004	0.0004
240	1.32	1.28	0.02	0.0004	0.0004	0.0004	0.0004
270		1.31	0.02	0.0004	0.0004	0.0004	0.0004
300	1.35	1.33	0.02	0.0004	0.0004	0.0004	0.0004

DECREASE IN Cu CONCENTRATION DUE TO LEACHING BY ACID AT -45 um ARTICLE SIZI

RUNGE-KUTTA FOURTH-ORDER METHOD

$dCu^{2+}/dt = -8/3K_{8.10}Cu^{2+}$ **Temp. = 60 oC**

$K_{8.10}$ = **1.161** Initial Cu = 24.95 g/L 0.393 moles

$-8/3K_{810}$ = -3.096 Initial H2SO4 = 90 g/L 0.918 moles

EXPERIMENTAL VALUES		MODEL VALUES					
Time (min)	Cu (g/L)	Cu (g/L)	Cu (mol)	K1	K2	K3	K4
0	24.95	24.95	0.393				
30	12.08	6.77	0.11	-0.6078	-0.1374	-0.5014	0.1685
60	2.28	1.83	0.03	-0.1648	-0.0372	-0.1360	0.0457
90	0	0.50	0.01	-0.0447	-0.0101	-0.0369	0.0124
120	0	0.13	0.00	-0.0121	-0.0027	-0.0100	0.0034
150	0	0.04	0.00	-0.0033	-0.0007	-0.0027	0.0009
180	0	0.01	0.00	-0.0009	-0.0002	-0.0007	0.0002
210	0	0.00	0.00	-0.0002	-0.0001	-0.0002	0.0001
240	0	0.00	0.00	-0.0001	0.0000	-0.0001	0.0000
270	0	0.00	0.00	0.0000	0.0000	0.0000	0.0000
300	0	0.00	0.00	0.0000	0.0000	0.0000	0.0000

INCREASE IN Ni CONCENTRATION DUE TO LEACHING BY CEMENTATION AND ACID AT - 106+45 um PARTICLE SIZE

RUNGE-KUTTA FOURTH-ORDER METHOD

Overall rate equation: $dNi^{2+}/dt = 8/3K_{8.10}Cu^{2+} + K_{8.13}C_{H+}$

Temp. = 60 oC

$dNi^{2+}/dt = 8/3K_{8.10}Cu^{2+}$ — Initial Ni = 24.61 g/L 0.419 moles — $dNi^{2+}/dt = K_{8.13}C_{H+}$

$K_{8.10}$ = **0.498** — Initial Cu = 24.95 g/L 0.393 moles

$K_{8.10}$ = **-1.328** — Initial H2SO4 = 90 g/L 0.918 moles — $K_{8.13}$ = **-0.976**

EXPERIMENTAL VALUES		MODEL VALUES												
Time	$[Ni^{2+}]$	$[Ni^{2+}]$	$[Ni^{2+}]$	Copper contribution					Acid contribution					
(min)	(g/L)	(g/L)	(mol)	(mol)	K1	K2	K3	K4	(moles)	K1	K2	K3	K4
0	24.61	24.61	0.419	0.393					0.918				
30	78.22	56.57	0.964	0.202	-0.26	-0.17	-0.20	-0.13	0.56	-0.45	-0.34	-0.37	-0.27
60	78.79	75.10	1.280	0.104	-0.13	-0.09	-0.10	-0.06	0.35	-0.28	-0.21	-0.22	-0.17
90	84.73	85.91	1.464	0.054	-0.07	-0.05	-0.05	-0.03	0.21	-0.17	-0.13	-0.14	-0.10
120	87.23	90.73	1.546	0.054	-0.04	-0.02	-0.03	-0.02	0.13	-0.10	-0.08	-0.08	-0.06
150	88.09	95.21	1.622	0.028	-0.04	-0.02	-0.03	-0.02	0.08	-0.06	-0.05	-0.05	-0.04
180	92.30	97.82	1.667	0.014	-0.02	-0.01	-0.01	-0.01	0.05	-0.04	-0.03	-0.03	-0.02
210		99.34	1.693	0.007	-0.01	-0.01	-0.01	0.00	0.03	-0.02	-0.02	-0.02	-0.01
240	91.20	100.24	1.708	0.004	0.00	0.00	0.00	0.00	0.02	-0.01	-0.01	-0.01	-0.01
270		100.77	1.717	0.002	0.00	0.00	0.00	0.00	0.01	-0.01	-0.01	-0.01	-0.01
300	94.71	101.08	1.722	0.001	0.00	0.00	0.00	0.00	0.01	-0.01	0.00	0.00	0.00

INCREASE IN Fe CONCENTRATION DUE TO LEACHING BY ACID AT - 106+45 um PARTICLE SIZE

RUNGE-KUTTA FOURTH-ORDER METHOD

Overall rate equation: $d(Fe^{2+}/Fe^{3+})/dt = K_{8.15}C_{H+} - K_{8.16}CFe^{3+}$

Temp. = 60 oC

Initial H2SO4 = 90 g/L 0.918 moles

Initial Fe = 0.67 g/L 0.012 moles

H2SO4after 180 min = 20 g/L 0.204 moles

$dFe^{2+}/dt = K_{8.15}C_{H+}$ — Total Fe after 180 min = 4.39 g/L 0.079 moles — $dFe^{3+}/dt = -K_{8.16}C_{Fe3+}$

$K_{8.15}$ = **0.124** — $K_{8.16}$ = **0.695**

EXPERIMENTAL VALUES		MODEL VALUES												
Time	Fe	Fe	Fe	Fe2+ contribution					Fe^{3+} contribution					
(min)	(g/L)	(g/L)	(mol)	(mol)	K1	K2	K3	K4	(mol)	K1	K2	K3	K4
0	0.67	0.67	0.012	0.012									
30	4.46	4.01	0.07	0.07	0.057	0.059	0.059	0.061					
60	4.49	4.27	0.08	0.08	0.004	0.005	0.005	0.005					
90	4.47	4.54	0.08	0.08	0.005	0.005	0.005	0.005	0.012				
120	3.81	3.90	0.07	0.09	0.005	0.005	0.005	0.005	0.017	0.0041	0.0048	0.0049	0.0058
150	3.76	4.10	0.07	0.09	0.005	0.006	0.006	0.006	0.019	0.0058	0.0068	0.0070	0.0082
180	3.91	4.12	0.07	0.10	0.006	0.006	0.006	0.006	0.025	0.0065	0.0077	0.0079	0.0093
210		4.23	0.08	0.10	0.006	0.006	0.006	0.006	0.029	0.0085	0.0100	0.0103	0.0121
240	3.89	4.18	0.07	0.11	0.006	0.007	0.007	0.007	0.037	0.0101	0.0118	0.0121	0.0143
270		4.16	0.07	0.12	0.007	0.007	0.007	0.007	0.044	0.0127	0.0149	0.0153	0.0180
300	3.81	3.99	0.07	0.13	0.007	0.008	0.008	0.008	0.05	0.0153	0.0180	0.0185	0.0218

KINETIC MODEL OF METAL CONCENTRATIONS DURING ATMOSPHERIC
LEACHING OF THE MATTE AT - 106+45 um PARTICLE SIZE

Conditions
Particle size: - 106+45
Temp. = 60 oC
Initial copper = 25 g/L
Initial nickel = 25 g/L
Initial H2SO4 = 90 g/L
Stirring rate = 205 rpm
PD = 1.7 kg/L

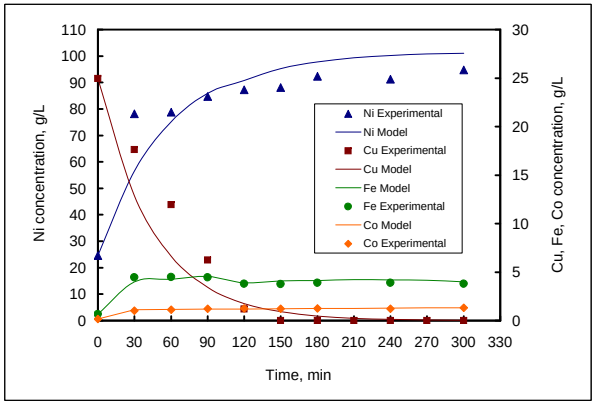

INCREASE IN Co CONCENTRATION DUE TO LEACHING BY ACID AT - 106+45 um PARTICLE SIZE

RUNGE-KUTTA FOURTH-ORDER METHOD

$dCo^{2+}/dt = K_{8.17}C_{H+}$ **Temp. = 60 oC**

Initial H2SO4 = 90 g 0.918 moles

$K_{8.17}$ = **0.0350** Initial Co = 0.18 g/L 0.003 moles

EXPERIMENTAL VALUES		MODEL VALUES					
Time (min)	Co (g/L)	Co (g/L)	Co (mol)	K1	K2	K3	K4
0	0.18	0.18	0.003				
30	1.01	1.14	0.02	0.0161	0.0162	0.0162	0.0164
60	1.11	1.16	0.02	0.0003	0.0003	0.0003	0.0003
90	1.23	1.18	0.02	0.0003	0.0003	0.0003	0.0003
120	1.24	1.20	0.02	0.0003	0.0004	0.0004	0.0004
150	1.22	1.22	0.02	0.0004	0.0004	0.0004	0.0004
180	1.24	1.24	0.02	0.0004	0.0004	0.0004	0.0004
210		1.26	0.02	0.0004	0.0004	0.0004	0.0004
240	1.22	1.28	0.02	0.0004	0.0004	0.0004	0.0004
270		1.31	0.02	0.0004	0.0004	0.0004	0.0004
300	1.31	1.33	0.02	0.0004	0.0004	0.0004	0.0004

DECREASE IN Cu CONCENTRATION DUE TO LEACHING BY ACID AT - 106+45 um PARTICLE SIZE

RUNGE-KUTTA FOURTH-ORDER METHOD

$dCu^{2+}/dt = -8/3K_{8.10}Cu^{2+}$ **Temp. = 60 oC**

$K_{8.10}$ = **0.498** Initial Cu = 24.95 g/L 0.393 moles

$-8/3K_{8.10}$ = -1.328 Initial H2SO4 = 90 g/L 0.918 moles

EXPERIMENTAL VALUES		MODEL VALUES					
Time (min)	Cu (g/L)	Cu (g/L)	Cu (mol)	K1	K2	K3	K4
0	24.95	24.95	0.393				
30	17.64	12.87	0.20	-0.2607	-0.1741	-0.2029	-0.1260
60	11.94	6.64	0.10	-0.1345	-0.0898	-0.1046	-0.0650
90	6.23	3.42	0.05	-0.0693	-0.0463	-0.0540	-0.0335
120	1.19	1.77	0.03	-0.0358	-0.0239	-0.0278	-0.0173
150	0.00	0.91	0.01	-0.0184	-0.0123	-0.0144	-0.0089
180	0.00	0.47	0.01	-0.0095	-0.0064	-0.0074	-0.0046
210	0.00	0.24	0.00	-0.0049	-0.0033	-0.0038	-0.0024
240	0.00	0.12	0.00	-0.0025	-0.0017	-0.0020	-0.0012
270	0.00	0.06	0.00	-0.0013	-0.0009	-0.0010	-0.0006
300	0.00	0.03	0.00	-0.0007	-0.0004	-0.0005	-0.0003

APPENDIX F

PAPERS BASED ON THIS DISSERTATION

Lamya, R.M. and Lorenzen, L., 2005. A study of the factors influencing the kinetics of copper cementation during atmospheric leaching of converter matte. Journal of SAIMM, January, pp. 21 – 27.

Lamya, R.M., Orellana, E.A., Fox, M. and Lorenzen, L., 2004. A study of factors influencing the kinetics of atmospheric leaching of nickel-copper matte in copper spent electrolyte. SAIMM colloquium – Innovations in leaching technology, 18 – 19 May.

Lamya, R.M. and Lorenzen, L., Atmospheric acid leaching of nickel-copper matte from Impala Platinum Refineries. Journal of SAIMM, (submitted for publication).